

University of Montana

## ScholarWorks at University of Montana

---

Graduate Student Theses, Dissertations, &  
Professional Papers

Graduate School

---

2014

### Synthesis and Biological Evaluation of a Library of Polyacetylene Compounds based on an Antiprotozoal Natural Product from *Cussonia zimmermannii*

John Hoody  
*The University of Montana*

Follow this and additional works at: <https://scholarworks.umt.edu/etd>

**Let us know how access to this document benefits you.**

---

#### Recommended Citation

Hoody, John, "Synthesis and Biological Evaluation of a Library of Polyacetylene Compounds based on an Antiprotozoal Natural Product from *Cussonia zimmermannii*" (2014). *Graduate Student Theses, Dissertations, & Professional Papers*. 4609.  
<https://scholarworks.umt.edu/etd/4609>

This Dissertation is brought to you for free and open access by the Graduate School at ScholarWorks at University of Montana. It has been accepted for inclusion in Graduate Student Theses, Dissertations, & Professional Papers by an authorized administrator of ScholarWorks at University of Montana. For more information, please contact [scholarworks@mso.umt.edu](mailto:scholarworks@mso.umt.edu).

SYNTHESIS AND BIOLOGICAL EVALUATION OF A LIBRARY OF  
POLYACETYLENE COMPOUNDS BASED ON AN ANTIPROTOZOAL NATURAL  
PRODUCT FROM *CUSSONIA ZIMMERMANNII*

By

JOHN HOWARD HOODY

B.A. Biology, University of Saint Thomas, Saint Paul, MN, 2000

Dissertation

presented in partial fulfillment of the requirements  
for the degree of

Doctor of Philosophy in Chemistry

The University of Montana  
Missoula, MT

June 2014

Approved by:

Sandy Ross, Dean of the Graduate School  
Graduate School

Dr. Christopher P. Palmer, Department Chair and Committee Chair  
Department of Chemistry and Biochemistry

Dr. Holly Thompson  
Department of Chemistry and Biochemistry

Dr. Andrea Stierle  
Department of Biomedical and Pharmaceutical Sciences

Dr. Nigel D. Priestley  
Department of Chemistry and Biochemistry

Dr. Nicholas Natale  
Department of Biomedical and Pharmaceutical Sciences

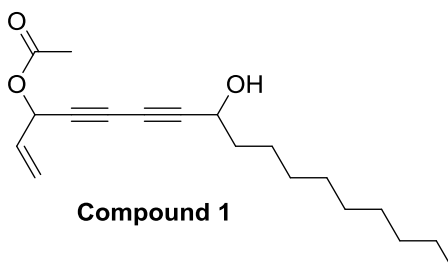
Synthesis and Biological Evaluation of a Library of Polyacetylene Compounds based on an Antiprotozoal Natural Product from *Cussonia zimmermannii*

Advisor: Dr. David B. Bolstad

Committee Chair: Dr. Christopher P. Palmer

Leishmaniasis is one of several tropical diseases classified as a “neglected tropical disease”. Its global prevalence is 12 million people with an estimated at-risk population of 350 million people.<sup>1</sup> Current treatments include antimonials, amphotericin B, pentamidine, and miltefosine. Access to these medications is often limited in the impoverished nations that Leishmaniasis predominantly affects. Drug resistance and toxicity are also significant drawbacks to the current treatments.<sup>3</sup> Therefore, there is an immediate need for the research and development of novel therapeutic molecules and strategies to combat Leishmaniasis.

In 2007, Senn and coworkers reported the isolation of four polyacetylene compounds from the Tanzanian medicinal plant *Cussonia zimmermannii*.<sup>124</sup> Three of the four compounds displayed activity against *Trypanosoma brucei rhodesiense*, *Trypanosoma cruzi*, *Plasmodium falciparum*, and *Leishmania donovani*. Of these four compounds, Compound **1** had the lowest IC<sub>50</sub> (0.32 $\mu$ M) and the highest selectivity index (37; IC<sub>50</sub> for rat skeletal myoblasts/IC<sub>50</sub> for *L. donovani*) when screened against *Leishmania donovani* in infected macrophages.<sup>124</sup>



We herein report the total synthesis and *in vitro* antileishmanial activity of the four diastereomers of **1** as well as thirty-four analogues of **1**. *In vitro* antileishmanial testing yielded numerous compounds that possessed increased antileishmanial activity as compared to the natural product including one compound that displayed over a 100-fold increase in activity. We also report the results of three of our compounds that were evaluated in an *in vivo* mouse model of Leishmaniasis.

As there are numerous reported examples of antileishmanial compounds that also possess significant anticancer activity, twenty-four of our compounds were submitted to the National Cancer Institute (NCI) to evaluate their anticancer activity. Several of our compounds possessed potent anticancer activity in the NCI60 one-dose screen and are currently being evaluated in advanced staging of testing at the NCI.

## Acknowledgements

Thank you to Dr. David Bolstad for taking me on as his first graduate student and providing me with a great environment to development my skills as a synthetic organic chemist. His enthusiasm for organic synthesis was evident right from the start of my working in his lab. I am especially grateful for his guidance in research as well as allowing time and space to develop independent strategies and tactics to accomplish research goals.

Thank you to all of the members on my committee: Dr. David Bolstad, Dr. Chris Palmer, Dr. Holly Thompson, Dr. Nigel Priestley, Dr. Andrea Stierle, and Dr. Nick Natale. I am very grateful for all the time and guidance you provided me with over the years.

Thank you to all of my fellow graduate students and other colleagues I worked with during my years here. You all provided a great amount of help with my studies and a lot of fun times. I would like to especially thank Sheryl Akagi, Katherine Harris, Ofuka Ichire, James Ormord, Lilly Matti, Teri Jo Lanoue, Patrick Barney, Whitney Swain, Jeremy Alverson, and Adrienne Sochia. Your help and comradery was truly invaluable.

Thank you to my family for all of your love and support over the years. Mom, Dad, Maggie, Katie, Betsy and Dan, you have all been true inspirations to me and have given me so much support through the good times and tough times that we have traveled through together.

# Table of Contents

Chapter 1: Leishmaniasis Epidemiology, Pathology, Treatment, and Prevention.....	1
1.1 Introduction to protozoal disease and epidemiology.....	2
1.2 <i>Leishmania</i> biology and transmission.....	3
1.3 <i>Leishmania</i> treatment.....	6
1.4 Drug mechanisms and validated targets .....	11
1.4.1 Proposed antileishmanial mechanism of pentavalent antimonials .....	11
1.4.1.1 Prodrug model of pentavalent antimonials.....	12
1.4.1.2 Intrinsic activity model of pentavalent antimonials .....	16
1.4.2 Proposed antileishmanial mechanism of amphotericin B.....	19
1.4.3 Proposed antileishmanial mechanism of pentamidine .....	20
1.4.4 Proposed antileishmanial mechanism of Miltefosine .....	21
1.4.5 Proposed antileishmanial mechanism of Paromomycin .....	26
1.4.6 Proposed antileishmanial mechanism of sitamaquine.....	27
1.5 Preventative strategies for control of <i>Leishmania</i> .....	28
1.5.1 Vaccine development .....	28
1.5.2 Vector and reservoir control.....	32
1.6 Concluding remarks .....	35
Chapter 2: Natural product library synthesis and antileishmanial biological activity.....	36
2.1 Antiprotozoal polyacetylene compounds discovered by Senn and colleagues ....	37
2.2 First Round of SAR studies – Evaluating Stereochemistry.....	37
2.3 Second Round of SAR studies – Lipophilicity and Hansch Cluster Analysis.....	44
2.4 Third Round of SAR studies.....	48
2.4.1 Synthesis of Third Round SAR Compounds.....	48
2.4.2 Antileishmanial Activity of Third Round SAR Compounds.....	52
2.5 Fourth Round of SAR studies .....	54
2.5.1 Synthesis of fourth round SAR compounds.....	54
2.5.2 Antileishmanial activity of fourth round SAR compounds .....	56
2.6 Fifth round of SAR studies.....	59
2.6.1 Synthesis of fifth round SAR compounds .....	59
2.6.2 Antileishmanial activity of fifth round SAR compounds.....	62
2.7 <i>In Vivo</i> evaluation.....	63

2.8 Cytotoxicity .....	64
Chapter 3: Anticancer evaluation of natural product analogues .....	67
3.1 Compounds possessing antiprotozoal and anticancer activity .....	68
3.2 Stereochemistry .....	70
3.3 Lipophilicity .....	72
3.4 Isothiocyanate.....	73
3.5 Analysis of different cell line categories .....	73
Chapter 4: Breast Cancer .....	74
4.1 Overview .....	75
4.2 Hansch Cluster Analysis on Breast Cancer Cell Lines Data .....	77
4.3 Breast Cancer SAR Analysis of Amide Compounds.....	78
Chapter 5: Prostate Cancer .....	83
5.1 Overview .....	84
5.2 Hansch Cluster Analysis on Prostate Cancer Cell Lines Data .....	88
5.3 Prostate Cancer SAR Analysis of Amide Compounds .....	90
Chapter 6: Renal Cancer.....	93
6.1 Renal Cancer Overview .....	94
6.2 Hansch Cluster Analysis on Renal Cancer Cell Lines Data.....	96
6.3 Renal Cancer SAR Analysis of Amide Compounds .....	97
Chapter 7: Ovarian Cancer .....	101
7.1 Ovarian Cancer Overview.....	102
7.2 Hansch Cluster Analysis on Ovarian Cancer Cell Lines Data .....	104
7.3 SAR Analysis of Amide Compounds against Ovarian Cancer Cell Lines .....	105
Chapter 8: CNS Cancer .....	111
8.1 CNS Cancer Overview.....	112
8.2 Hansch Cluster Analysis on CNS Cancer Cell Lines Data .....	113
Chapter 9: Melanoma .....	118
9.1 Melanoma Overview.....	119
9.2 Hansch Cluster Analysis on Lung Cancer Cell Lines Data .....	120
9.3 SAR Analysis of Amide Compounds against Melanoma Cell Lines .....	121
Chapter 10: Lung Cancer.....	126
10.1 Lung Cancer Overview .....	127
10.2 Hansch Cluster Analysis on Lung Cancer Cell Lines Data.....	128

10.3 SAR Analysis of Amide Compounds against Lung Cancer Cell Lines .....	129
Chapter 11: Leukemia .....	134
11.1 Leukemia Overview .....	135
11.2 Hansch Cluster Analysis on Leukemia Cell Lines Data .....	136
11.3 SAR Analysis of Amide Compounds against Leukemia Cell Lines .....	137
Chapter 12: Colon Cancer .....	141
12.1 Colon Cancer Overview .....	142
12.2 Hansch Cluster Analysis on Colon Cancer Cell Lines Data .....	143
12.3 SAR Analysis of Amide Compounds against Colon Cancer Cell Lines .....	144
Chapter 13: Experimentals .....	149
Appendix A: Selected NMR spectra from synthesized compounds .....	239
Appendix B: National Cancer Institute One Dose Screening Results .....	279

## List of Abbreviations

<b><sup>13</sup>C NMR</b>	Carbon nuclear magnetic resonance spectrum
<b><sup>1</sup>H NMR</b>	Proton nuclear magnetic resonance spectrum
<b>AAH</b>	adenine aminohydrolase
<b>Ac<sub>2</sub>O</b>	Acetic Anhydride
<b>ACR2</b>	antimoniate reductase
<b>AdCMV</b>	adenovirus vector cytomegalovirus
<b>ADE</b>	adenine
<b>ADO</b>	adenosine
<b>ADSS</b>	adenylosuccinate synthetase
<b>AgF</b>	silver fluoride
<b>AgNO<sub>3</sub></b>	silver nitrate
<b>AI</b>	androgen insensitive
<b>AIDS</b>	acquired immunodeficiency syndrome
<b>AK</b>	adenosine kinase
<b>Akt</b>	protein kinase B
<b>AmB</b>	amphotericin B
<b>AMP</b>	adenosine monophosphate
<b>AMPDA</b>	adenosine monophosphate deaminase
<b>APC</b>	adenomatous polyposis coli
<b>APRT</b>	adenine phosphoribosyltransferase
<b>ASL</b>	adenylosuccinate lyase
<b>ATP</b>	adenosine triphosphate
<b>BCG</b>	Bacillus Calmette-Guerin
<b>br</b>	broad
<b>BRAF</b>	v-raf murine sarcoma viral oncogene homologue β1
<b>BRCA2</b>	familial breast/ovarian cancer gene 2
<b>calcd.</b>	calculated
<b>CDC</b>	Center for Disease Control
<b>CDKN2A</b>	cyclin-dependent kinase inhibitor 2A
<b>CDP</b>	cytidine diphosphate
<b>CH<sub>2</sub>Cl<sub>2</sub></b>	dichloromethane
<b>CH<sub>3</sub>CN</b>	acetonitrile
<b>CHCl<sub>3</sub></b>	chloroform
<b>CHCl<sub>3</sub></b>	chloroform
<b>CK</b>	cytokeratin
<b>CNAs</b>	copy number alterations
<b>CTNNB1</b>	catenin (cadherin associated protein) β1
<b>CTP</b>	cytidine triphosphate
<b>CuCl</b>	copper (I) chloride
<b>d</b>	doublet
<b>DCC</b>	<i>N,N'</i> -dicyclohexylcarbodiimide
<b>DCL</b>	diffuse cutaneous Leishmaniasis
<b>DCM</b>	dichloromethane
<b>dd</b>	doublet of doublets



<b>ddd</b>	doublet of doublets of doublets
<b>dddd</b>	doublet of doublets of doublets of doublets
<b>DHFR-TS</b>	dihydrofolate reductase-thymidylate synthase
<b>DIAD</b>	diisopropyl azodicarboxylate
<b>DMAP</b>	4-dimethylaminopyridine
<b>DMF</b>	N,N-dimethylformamide
<b>DMSO</b>	dimethylsulfoxide
<b>DNA</b>	deoxyribonucleic acid
<b>dt</b>	doublet of triplets
<b>ED<sub>50</sub></b>	effective dose for 50% of people receiving drug
<b>ee</b>	enantiomeric excess
<b>EGF</b>	epidermal growth factor
<b>EGFR</b>	epidermal growth factor receptor
<b>EI</b>	electron impact
<b>eq</b>	equivalent
<b>ER</b>	estrogen receptor
<b>ERBB2</b>	v-erb-b2 erythroblastic leukemia viral oncogene homologue 2
<b>ESI</b>	electrospray ionization
<b>Et</b>	ethyl
<b>Et<sub>2</sub>O</b>	diethyl ether
<b>Et<sub>2</sub>O</b>	diethyl ether
<b>Et<sub>3</sub>N</b>	triethylamine
<b>EtOAc</b>	ethyl acetate
<b>EtOH</b>	ethanol
<b>FAD</b>	flavin adenine dinucleotide
<b>FLT3</b>	fms-related tyrosine kinase 3
<b>g</b>	gram(s)
<b>GC/MS</b>	gas chromatography/mass spectroscopy
<b>GDA</b>	guanine deaminase
<b>GDP</b>	guanosine diphosphate
<b>GI</b>	gastro-intestinal
<b>GIPL</b>	glycoinositol phospholipids
<b>GMP</b>	guanosine monophosphate
<b>GMPR</b>	guanosine monophosphate reductase
<b>GMPS</b>	guanosine monophosphate synthase
<b>GP</b>	growth percent
<b>GP63</b>	<i>Leishmania</i> surface protease
<b>GPI</b>	glycosylphosphatidylinositol
<b>GR</b>	glutathione reductase
<b>GSH</b>	glutathione
<b>GSSG</b>	glutathione disulfide
<b>GUA</b>	guanine
<b>GUO</b>	guanosine
<b>h</b>	hour(s)
<b>h</b>	hour(s)
<b>HER2</b>	human epidermal growth factor receptor 2

<b>HEXBP</b>	hexamer-binding protein
<b>HGPRT</b>	hypoxanthine-guanine phosphoribosyltransferase
<b>HIV</b>	human immunodeficiency virus
<b>HRMS</b>	high resolution mass spectrum
<b>HYP</b>	hypoxanthine
<b>Hz</b>	Hertz
<b>IC<sub>50</sub></b>	drug concentration which inhibits activity (or growth) by 50 percent
<b>IFN</b>	interferon
<b>IM</b>	intramuscular
<b>IMPDH</b>	inosine monophosphate dehydrogenase
<b>INO</b>	inosine
<b>IR</b>	infrared spectroscopy
<b>IV</b>	intravenous
<b>J</b>	coupling constant
<b>JACS</b>	Journal of the American Chemical Society
<b>K<sub>2</sub>CO<sub>3</sub></b>	potassium carbonate
<b>kg</b>	kilogram(s)
<b>KRAS</b>	vi-Ki-ras2 Kirsten rat sarcoma viral oncogene homologue
<b>LAH</b>	lithium aluminum hydride
<b>LCL</b>	localized cutaneous Leishmaniasis
<b>LdNT1</b>	<i>Leishmania donovani</i> nucleoside transporter 1
<b>LdNT2</b>	<i>Leishmania donovani</i> nucleoside transporter 2
<b>LDU</b>	Leishman Donovan Units
<b>LeIF</b>	<i>Leishmania</i> elongation and initiation factor
<b>LmSTI1</b>	<i>L. major</i> homolog of eukaryotic stress-inducible protein-1
<b>LPG</b>	lipophosphoglycans
<b>m</b>	multiplet
<b>M</b>	molar
<b>m/z</b>	mass to charge ratio
<b>MCL</b>	mucocutaneous Leishmaniasis
<b>MeOH</b>	methanol
<b>mg</b>	milligram(s)
<b>MHz</b>	megahertz
<b>mL</b>	milliliter(s)
<b>mM</b>	millimolar
<b>mmol</b>	millimol
<b>MOI</b>	multiplicity of infection
<b>mRNA</b>	messenger ribonucleic acid
<b>N/A</b>	not available
<b>N<sub>2</sub>H<sub>4</sub>.H<sub>2</sub>O</b>	hydrazine monohydrate
<b>Na<sub>2</sub>SO<sub>4</sub></b>	sodium sulfate
<b>NaBH<sub>4</sub></b>	sodium borohydride
<b>NADPH</b>	nicotinamide adenine dinucleotide phosphate
<b>NaH</b>	sodium hydride
<b>NaHCO<sub>3</sub></b>	sodium bicarbonate

<b>NaOH</b>	sodium hydroxide
<b>NBS</b>	<i>N</i> -bromosuccinimide
<b><i>n</i>-BuLi</b>	<i>n</i> -butyllithium
<b>ND</b>	not determined
<b>NH</b>	nucleoside hydrolase
<b>NH<sub>2</sub>OH.HCl</b>	hydroxylamine hydrochloride
<b>NH<sub>4</sub>Cl</b>	ammonium chloride
<b>NMR</b>	nuclear magnetic resonance
<b>NRAS</b>	neuroblastoma RAS viral (v-ras) oncogene homologue
<b>NT</b>	not tested
<b>PC</b>	phosphatidylcholine
<b>PDGFRA</b>	platelet-derived growth factor receptor, $\alpha$ polypeptide
<b>PE</b>	phosphatidylethanolamine
<b>PEMT</b>	phosphatidylethanolamine- <i>N</i> -methyltransferase
<b>PGR</b>	progesterone receptor
<b>PI3K</b>	phosphatidylinositol-4,5-bisphosphate 3-kinase
<b>PIK3CA</b>	phosphoinositide-3-kinase, catalytic, $\alpha$ polypeptide
<b>PPh<sub>3</sub></b>	triphenylphosphine
<b>PP<sub>i</sub></b>	pyrophosphate
<b>ppm</b>	parts per million
<b>PSA</b>	prostate-specific antigen
<b>PSP</b>	promastigote surface protease
<b>PTEN</b>	phosphatase and tensin homologue
<b>RB1</b>	retinoblastoma 1
<b>R<sub>f</sub></b>	retention factor
<b>ROS</b>	reactive oxygen species
<b>s</b>	singlet
<b>SAH</b>	<i>S</i> -adenosyl homocysteine
<b>SAM</b>	<i>S</i> -adenosyl methionine
<b>SAR</b>	structure activity relationship
<b>SD</b>	succinate dehydrogenase
<b>SMAD4</b>	SMAD, mothers against DPP homologue 4 (MADH4)
<b>SOCl<sub>2</sub></b>	thionyl chloride
<b>STK11</b>	serine/threonine kinase 11/LKB1
<b>t</b>	triplet
<b>T(SH)<sub>2</sub></b>	trypanothione
<b>TBAF</b>	tetrabutylammonium fluoride
<b>TDR1</b>	thiol-dependent reductase
<b>TEA</b>	triethylamine
<b>TGF-<math>\alpha</math></b>	transforming growth factor alpha
<b>Th1</b>	T helper cell type 1
<b>Th2</b>	T helper cell type 2
<b>THF</b>	tetrahydrofuran
<b>THF</b>	tetrahydrofuran
<b>TLC</b>	thin layer chromatography
<b>TMS</b>	trimethylsilyl

<b>TOF</b>	time of flight
<b>TP53</b>	tumor protein p53
<b>TR</b>	trypanothione reductase
<b>TRAIL</b>	tumor necrosis factor related apoptosis inducing ligand
<b>Ts</b>	p-toluenesulfonyl
<b>TS<sub>2</sub></b>	trypanothione disulfide
<b>TSA</b>	thiol-specific antioxidant
<b>UV</b>	ultraviolet
<b>VHL</b>	von Hippel-Lindau tumor suppressor
<b>VL</b>	visceral Leishmaniasis
<b>WHO</b>	World Health Organization
<b>XAN</b>	xanthine
<b>XAO</b>	xanthosine
<b>XPRT</b>	xanthine phosphoribosyltransferase
<b>δ</b>	chemical shifts in parts per million (ppm)
<b>μg</b>	microgram(s)
<b>μM</b>	micromolar

***Chapter 1: Leishmaniasis Epidemiology, Pathology, Treatment, and Prevention***

## **1.1 Introduction to protozoal disease and epidemiology**

Protozoal infections are endemic in many parts of the world leading to hundreds of thousands of deaths each year. According to the World Health Organization (WHO), malaria alone caused an estimated 655,000 deaths in 2010.<sup>1</sup> In addition to the high mortality rates, protozoal infections lead to significant decreases in quality of life for millions of others. Protozoal infections are most common in impoverished nations and for this reason, there has been less money invested in discovering new treatments to combat protozoal diseases. Due to this lack of research, many protozoal diseases such as Leishmaniasis and trypanosomiasis are often classified under the category of “neglected diseases”. The main focus of our research was to develop novel antileishmanial agents in an attempt to add to the chemotherapeutic arsenal to help combat the morbidity and mortality associated with Leishmaniasis.

According to WHO, Leishmaniasis causes approximately 60,000 deaths per year.<sup>2</sup> The overall prevalence of Leishmaniasis is estimated at 12 million people with an annual incidence of 2 million.<sup>3</sup> Leishmaniasis is endemic in 88 countries with a worldwide distribution as shown in Figure 1.1.<sup>4</sup> In these endemic countries, an estimated 350 million people are at risk of contracting Leishmaniasis. There are four main clinical forms of the disease: 1) visceral Leishmaniasis (VL, also known as kala-azar), 2) localized cutaneous Leishmaniasis (LCL), 3) mucocutaneous Leishmaniasis (MCL), and 4) diffuse cutaneous Leishmaniasis (DCL). VL and LCL are the most common forms. Nearly all of the deaths due to Leishmaniasis are caused by VL which is typically fatal if left untreated. VL is characterized by an insidious onset and is particularly lethal to children and immuno-compromised individuals such as those with HIV.<sup>5</sup> Although not

usually lethal, the cutaneous forms are characterized by large skin ulcers which can lead to permanent disfigurement due to scarring of infected areas of the body.<sup>3</sup>

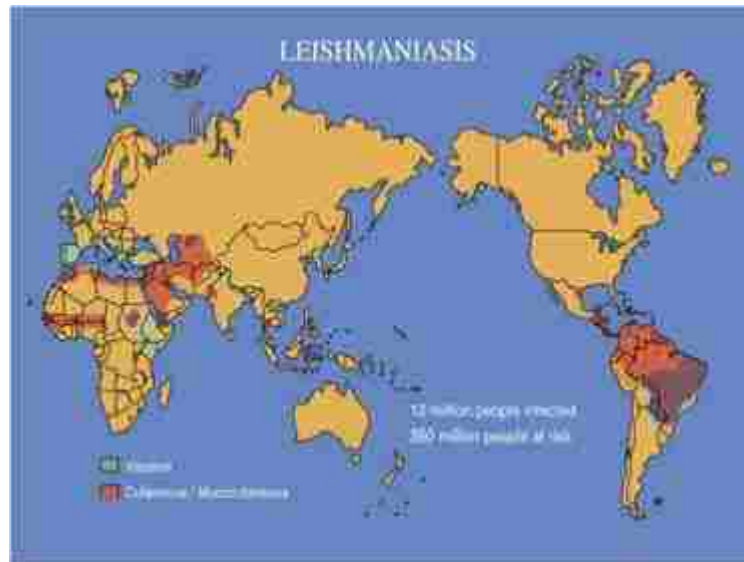


Figure 1.1: Distribution map showing Leishmaniasis endemicity<sup>4</sup> (Image reprinted with permission).

## 1.2 *Leishmania* biology and transmission

There are 21 species of the genus *Leishmania* that can cause Leishmaniasis.<sup>3</sup> The genus *Leishmania* falls under the class of Kinetoplastida (single-cell flagellate protozoa) and the order of Trypanosomatida (single flagellum Kinetoplastids). Members of the Kinetoplastida class are characterized by a single large

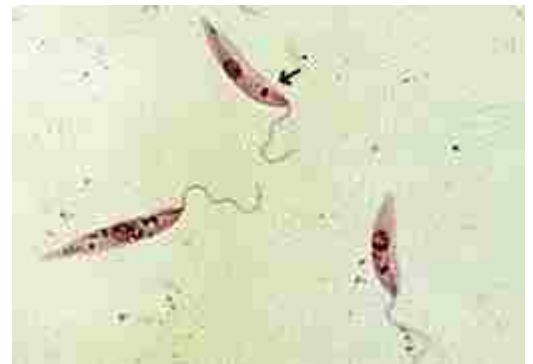


Figure 1.2: Promastigotes of *Leishmania donovani*. Arrow points to kinetoplast.<sup>123</sup> (Image reprinted with permission).

mitochondrion within which resides a dark staining mass of DNA called a kinetoplast (Figure 1.2).<sup>6</sup> Members of the genus *Leishmania* are obligate intramacrophage protozoa and can infect a variety of hosts including humans, rodents, and dogs.<sup>7</sup> The vector for transmission of *Leishmania* from host to host is typically the sandfly of which there are at least 30 species capable of serving as the vector. Although rare, transmission can also

occur from the sharing of dirty needles and blood transfusions.<sup>8</sup> Both the sandfly and the host (e.g. human) are essential to the life cycle of *Leishmania* (Figure 1.3).<sup>9</sup>

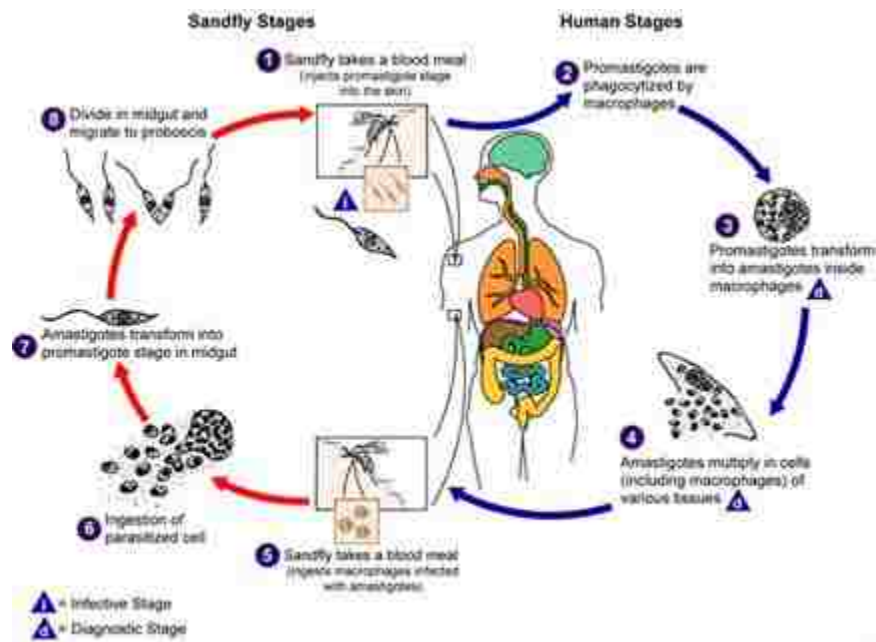


Figure 1.3: Life cycle of *Leishmania*<sup>9</sup> (Image reprinted with permission).

As is shown in Figure 1.3, the disease is transmitted to humans when an infected sandfly takes a blood meal from a human and injects the promastigote form of the protozoa into the skin. Once in the human, the promastigotes are taken up by macrophages and then morph into the amastigote form (Figure 1.4). Rapid multiplication of the amastigotes leads to cell lysis causing the release of the amastigotes into the blood stream. When another sandfly takes a blood meal from an infected human (or other host), it can ingest the amastigote infected macrophages. The amastigotes can morph into



Figure 1.4: Macrophage infected with amastigotes from *Leishmania donovani*.<sup>123</sup> (Image reprinted with permission).



promastigotes and multiply in the gut. These promastigotes migrate to the proboscis and are then ready to be injected into another human completing the life cycle.

Once a human is infected, there are a myriad of pathological processes that determine which of the four main forms (VL, LCL, MCL, or DCL) of Leishmaniasis evolves. A full discussion of these pathological processes is beyond the scope of this dissertation. However, it is worth noting that the specific species of *Leishmania* involved in the infection plays a significant role in the resulting disease form. For example, VL is typically caused by *L. donovani*, *L. infantum*, or *L. tropica* in the Old World and *L. donovani chagasi* in the New World (Table 1.1).<sup>10</sup> As evidence that more than just the species is involved in determining disease progression, some species can cause more than one form of the disease. For example, *L. donovani chagasi* can lead to both VL and LCL.

Form of Disease	New World Parasite*	Old World Parasite*	Geography
<b>VL</b>	<i>L. donovani chagasi</i>	<i>L. donovani</i>	China, India, Bangladesh, Asia, Sudan, Africa, East Russia, Mediterranean, South America
		<i>L. infantum</i>	
		<i>L. tropica</i>	
<b>LCL</b>	<i>L. b. braziliensis</i>	<i>L. major</i>	North Africa, India, Middle East, China, South Russia, Pakistan, Mediterranean, Central and South America, Texas, Caribbean
	<i>L. b. guyanensis</i>	<i>L. tropica</i>	
	<i>L. b. panamensis</i>	<i>L. aethiopica</i>	
	<i>L. m. mexicana</i>	<i>L. infantum</i>	
	<i>L. m. amazonensis</i>		
<b>MCL</b>	<i>L. b. braziliensis</i>	N/A	Brazil, Venezuela, Peru, Ecuador, Colombia
	<i>L. b. panamensis</i>		
<b>DCL</b>	<i>L. m. amazonensis</i>	<i>L. aethiopica</i>	Venezuela, Bolivia, Mexico, Dominican Republic, Brazil, Ethiopia
	<i>L. mexicana</i>		
	<i>L. m. pifanoi</i>		

\*Old World parasites typically have a species name, whereas New World organisms are divided into species and subspecies complexes.

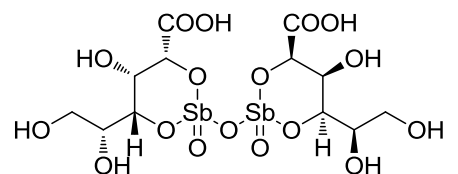
Figure 1.5: Clinical forms of Leishmaniasis, associated parasites, and geographic location.<sup>10</sup>

### 1.3 *Leishmania* treatment

Despite the devastating effects that *Leishmania* inflicts worldwide, treatment options remain relatively limited and expensive. Seven treatment options will be discussed below; three primary drugs (pentavalent antimonials, amphotericin B, and pentamidine) that are approved worldwide and four other promising drugs (Miltefosine, Paromomycin, Sitamaquine, and Imiquimod) that are approved only in certain countries or are in various phases of clinical trials.

Pentavalent antimonials (such as sodium stibogluconate) are the main first-line treatment option for most forms of Leishmaniasis worldwide. Their first reported use for treatment of VL dates all the way back to 1937 in

China and India.<sup>11</sup> The fact that pentavalent antimonials remain the primary first-line treatment option despite being discovered over 70 years ago

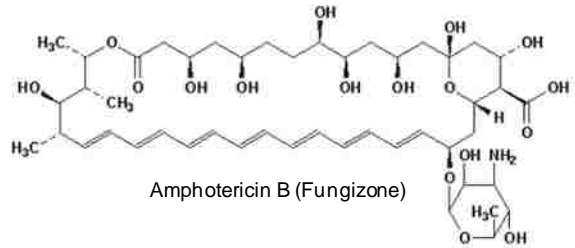


Sodium stibogluconate (Pentostam)

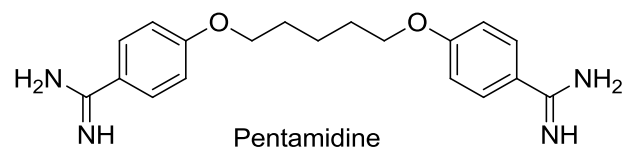
shows the paucity of advancement in antileishmanial therapeutics. Pentavalent antimonials are hampered by toxicity, dosing regimen, cost, and resistance. Side-effects include cardiotoxicity, arthralgias, and pancreatitis. Furthermore, patients with both Leishmaniasis and HIV-infection are particularly prone to chemical pancreatitis.

Pentavalent antimonials are only administered IV and typically require inpatient hospital treatment for 20-40 days.<sup>11</sup> This leads to high cost and often an inability for patients to maintain their employment, family responsibilities, and other obligations during this time. Resistance to antimonials is increasing worldwide and is especially prevalent in regions of India where up to 65% of new patients do not respond to antimonial treatment.<sup>12</sup> This antimonial resistance has been confirmed by *in vitro* analysis of *Leishmania* strains cultured from these patients.<sup>13</sup>

If antimonial treatment is unsuccessful, the main second-line treatment is Amphotericin B (Fungizone).<sup>11</sup> Amphotericin B treatment is hampered by many of the same problems that antimonials have. It is expensive, requires 3-week inpatient stay for IV administration, and has a myriad of side effects including numerous acute phase reactions such as vomiting, blood pressure abnormalities, and rigors in addition to chronic effects such as nephrotoxicity and electrolyte imbalances.<sup>14</sup> A relatively new liposomal formulation of Amphotericin B (AmBisome) has been shown to be less toxic than the standard formulation. However, AmBisome is over ten times more expensive than the antimonials and the standard Amphotericin B formulation and costs \$1000-\$2500 to treat one patient. This high cost is often an insurmountable hurdle for impoverished patients to overcome without charitable assistance. Thus far, there is limited evidence of resistance of *Leishmania* species to Amphotericin B.<sup>15</sup> However, AmBisome has a significantly longer half-life as compared to the standard formulation which increases the likelihood of the development of resistant strains.<sup>16</sup>



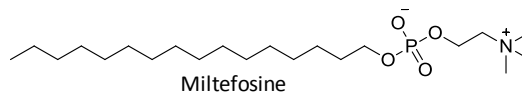
In addition to Amphotericin B, Pentamidine is also used as a second-line treatment if antimonials are unsuccessful. Pentamidine has been utilized as an anti-*Leishmania* agent for over 40 years but is not widely used today.<sup>16</sup> Apparent pentamidine resistant strains have evolved in India although this has not been confirmed by *in vitro* studies. However, resistance is likely as



cure rates resulting from pentamidine use in India were greater than 95% in 1980 and less than 70% ten years later.<sup>17,18</sup> Pentamidine is also plagued by the necessity of IV or IM administration and significant side effects including hyperglycemia with the development of a permanent “diabetes-like syndrome” and fatal cardiac arrhythmias.<sup>19</sup>

In addition to the approved treatments described above, there are numerous anti-Leishmanial candidates in various stages of clinical trials. Perhaps the most promising candidate is Miltefosine

(hexadecylphosphocholine) which is currently



approved for use in India, Colombia, and Germany.<sup>20</sup> Miltefosine marks a significant advancement in antileishmanial treatment as it is the first oral medication licensed for use. Miltefosine was originally developed as an oral anti-neoplastic agent for the

treatment of breast cancer and other solid tumors. However, it fell out of clinical trials due to gastro-intestinal (GI) toxicity.<sup>21</sup> Miltefosine’s antileishmanial activity was

serendipitously discovered in 1987.<sup>22</sup> In clinical trials as an antileishmanial treatment, Miltefosine still caused significant GI disturbances (nausea, vomiting, and diarrhea) in

most patients. The GI side-effects typically lasted one day or less and most patients were able to complete the therapeutic regimen. Other common side effects of Miltefosine

include reversible nephrotoxicity and reversible hepatotoxicity.<sup>21</sup> In Phase III clinical trials, Miltefosine cured 94% of the 299 enrolled patients with VL. Only 8 (2.7%) of the

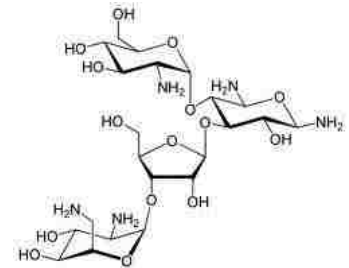
299 patients had to discontinue Miltefosine treatment due to its side-effects. A

significant drawback to Miltefosine is that it was shown to be teratogenic in rats and is thus unavailable to pregnant women and extra caution must be taken to avoid becoming

pregnant during treatment and the two months after treatment completion. Another

shortcoming of Miltefosine is that some species of *Leishmania* are not as responsive as others. For example, in Guatemala, the most prevalent strains of *Leishmania* are *L. braziliensis* and *L. mexicana*. In one Guatemalan study, the cure rate of LCL with Miltefosine was only 53%.<sup>16</sup> As far as resistance is concerned, there is little field evidence supporting the existence of Miltefosine resistant strains. However, Miltefosine resistant strains of *L. donovani* have been grown in the lab and resistance is likely to be an issue as Miltefosine has a very long half-life (~150 hours). The long half-life causes days of sub-therapeutic drug levels at the completion of treatment which is a fertile environment for the evolution of resistant strains.<sup>23</sup>

Another antileishmanial drug in the development pipeline is the aminoglycoside Paromomycin (also known as aminosidine). In a Phase III clinical trial completed in 2004, Paromomycin efficacy was compared to amphotericin B for treating VL. Paromomycin showed an effective cure rate of 95% (501 total patients) compared to amphotericin B which had a cure rate of 99% (165 total patients). Common side effects from Paromomycin were liver enzyme increases, pain at injection site (IM), and reversible ototoxicity. Only 1% of patients in the Paromomycin group suffered any level of renal dysfunction as compared to 25% of patients in the amphotericin B group. Only 5 patients (1%) in the Paromomycin group had to discontinue treatment before finishing the dosing regimen. For these 5 patients, it was not clear if Paromomycin was actually culpable in causing the side effects that resulted in discontinued treatment.<sup>24</sup> Paromomycin has had limited use thus far and there is little field evidence of Paromomycin resistant strains. Evidence of resistance is limited to a

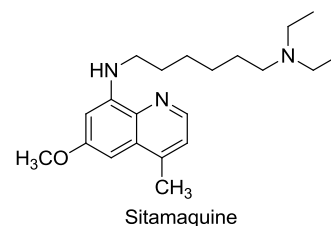


Paromomycin (aminosidine)

1992 study on Paromomycin use for the treatment of DCL. Two of the patients in this study initially were infected with an *L. aethiopica* strain which had an average *in vitro* ED<sub>50</sub> value of 5.6 ug/mL. After 60 days of treatment with Paromomycin, these patients were still infected with *L. aethiopica* and *in vitro* analysis showed a significant decrease in sensitivity to Paromomycin as the ED<sub>50</sub> values rose to an average of 21.6 ug/mL.<sup>25</sup> Resistance is a legitimate concern for Paromomycin as there are numerous aminoglycoside resistant strains of several bacterial species including strains of *E. coli* and *P. aeruginosa*.<sup>26</sup>

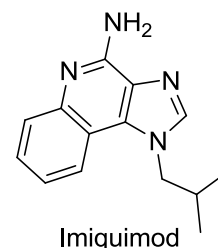
Another antileishmanial drug in clinical trials is Sitamaquine which belongs to the 8-aminoquinoline family of drugs and is administered orally.

In a Phase II dose-ranging study, sitamaquine had a cure rate of 87% (106 total patients) for patients with VL.<sup>27</sup> Four different doses were tested and sitamaquine had a 100% cure rate (23



patients) at a dose of 2.0 mg/kg. Interestingly, when the dose was raised to 2.5 mg/kg, the cure rate fell to 80% (25 patients). Vomiting and dyspepsia were the most common side effects with each occurring in 8% of the patients. Nine patients had to discontinue the treatment before completion due to nephrotoxicity. Likely due to its limited clinical use, there are no published reports of *Leishmania* resistance to Sitamaquine in the field though Sitamaquine resistant strains of *L. donovani* have been produced in the lab.<sup>28</sup>

The last drug to be discussed in detail in this section is the immunomodulator Imiquimod (Aldara). Imiquimod is a topical cream which is currently licensed for the treatment of several diseases including basal cell carcinoma, actinic keratosis, and genital warts.<sup>29</sup> By itself, Imiquimod



failed in treating cases of LCL in a small study involving ten patients. Only four patients were able to complete the dosing regimen and only one patient showed significant improvement.<sup>30</sup> A later study involved the use of Imiquimod as a supplemental treatment along with the pentavalent antimonial meglumine antimonite. This study involved twelve patients whose LCL infection was unresponsive to treatment by meglumine antimonite alone. When treated with Imiquimod and meglumine antimonite together for 20 days, a 90% cure rate was achieved.<sup>30</sup> Although this study only had 12 patients, it provides hope that supplemental Imiquimod could be efficacious in areas where antimonial resistant strains are endemic.

#### **1.4 Drug mechanisms and validated targets**

In addition to there being relatively few treatment options for *Leishmania*, the actual mechanisms of action for all of these drugs is still unclear. As stated by Kouni, “The rational design of a drug is usually based on biochemical and physiological differences between pathogens and host.”<sup>43</sup> The nebulousness of the mechanisms of action has made it more difficult to rationally design new antileishmanial compounds.

##### **1.4.1 Proposed antileishmanial mechanism of pentavalent antimonials**

Despite being used for over 70 years to treat Leishmaniasis, the mechanism of action for pentavalent antimonials is still largely debated. Furthermore, there is not even consensus on whether the active form of the drug is Sb (V) or Sb(III). Two main models are proposed for their mechanism of action: 1) the prodrug model; and 2) the intrinsic activity model (also known as Active Sb(V) model).<sup>40</sup>

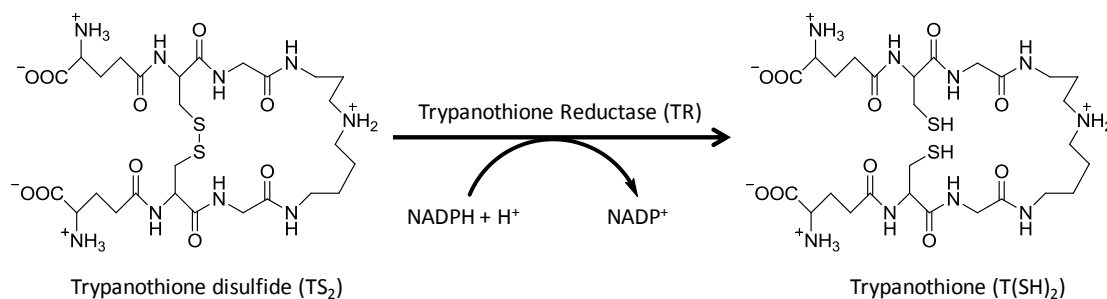
#### 1.4.1.1 Prodrug model of pentavalent antimonials

In the prodrug model, Sb(V) is biologically reduced to Sb(III) which then possesses the antileishmanial activity. Studies have shown that this reduction likely takes place in the amastigote life stage of Leishmanial species and not in the promastigote form. This is in congruence with experimental evidence which shows that amastigotes are much more susceptible to Sb(V) treatment as compared to promastigotes.<sup>32</sup> In another study, strains of *L. infantum* were produced with different levels of Sb(III) resistance. When treated with the Sb(V) compound meglumine, the observed Sb(V) resistance levels directly correlated with the Sb(III) resistance levels induced in the different strains of *L. infantum*.<sup>33</sup> This supports the idea that the level of Sb(III) is the determining factor in the susceptibility of *Leishmania* species to antimonial therapy. Another postulation is that it could be the macrophage itself that reduces Sb(V) to Sb(III). However, this is unlikely as macrophages have been shown to be extremely sensitive to Sb(III) levels and tolerant to Sb(V) levels.<sup>34</sup> In other words, if the macrophage itself was responsible for the reducing activity, it would be susceptible to both Sb(III) and Sb(V) compounds. It is possible that macrophages can reduce a certain level of Sb(V) to Sb(III), but unlikely that macrophages are responsible for producing the Sb(III) levels necessary for antiLeishmanial activity.

The prodrug model is further supported by a 2009 study which disclosed the crystal structure of the enzyme trypanothione reductase (TR) from *L. infantum* with an Sb(III) atom coordinated to the active site of TR.<sup>35</sup> TR is essential to the survival of protozoal species as it is responsible for maintaining the intracellular reducing



environment of protozoa. More specifically, TR is an FAD-dependent NADPH oxidoreductase enzyme that catalyzes the reduction of trypanothione disulfide (TS<sub>2</sub>) to trypanothione (T(SH)<sub>2</sub>) (Figures 1.6 and 1.7).<sup>36</sup> Trypanothione can then reduce potentially damaging species such as peroxides. If TR function is reduced, protozoal species are subjected to increased oxidative stress which can damage DNA, proteins, and lipids and lead to cell death.<sup>37</sup> Sb(III) is capable of binding to TR in its reduced state and preventing TR from delivering a hydride to TS<sub>2</sub> thereby inhibiting the production of T(SH)<sub>2</sub> (Figure 1.8). Instead of a trypanothione based system, mammalian cells use a glutathione based system to maintain their reducing environment. Thus, mammalian cells possess the enzyme glutathione reductase (GR) instead of TR (See Figure 1.9). This makes TR a valuable drug target for anti-protozoal therapeutics.



**Figure 1.6: Reduction of trypanothione disulfide to trypanothione.**

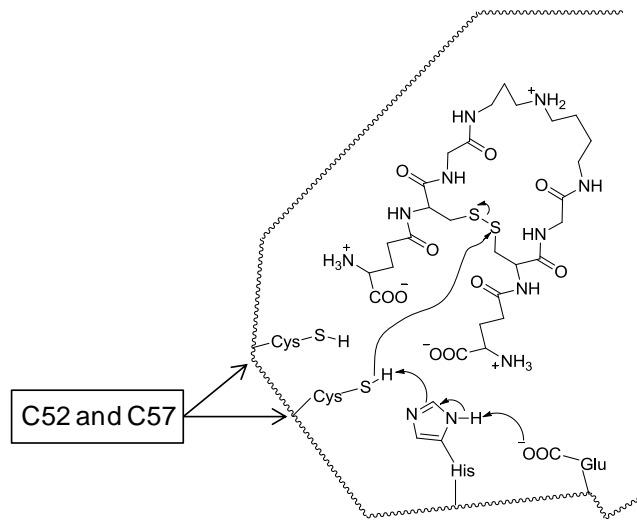


Figure 1.7: Catalytic triad mechanism of reduction of trypanothione disulfide.

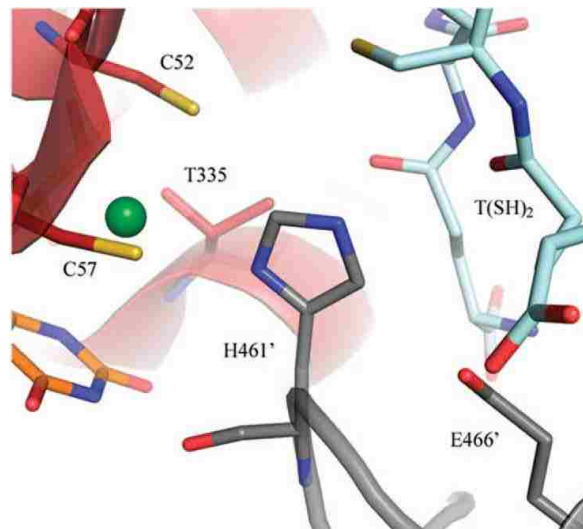


Figure 1.8: Sb (III) atom (green sphere) occupying catalytic site of trypanothione reductase.<sup>35</sup>

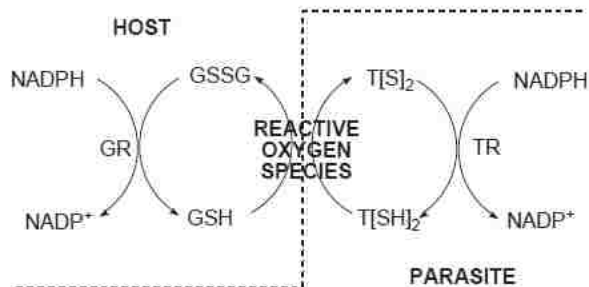


Figure 1.9: Mammals (host) use a glutathione based system to handle reactive oxygen species (ROS) whereas protozoa (parasite) use trypanothione based system.<sup>36</sup>

Another proposed mechanism of action for Sb(III) is via the displacement of Zn(II) from zinc-finger proteins. The Zn(II) atoms normally coordinate to amino acid residues (typically cysteines and histidines) and help stabilize the zinc-finger protein's structure. Therefore, when Zn(II) atoms are displaced by Sb(III) atoms, the structure of the protein is altered which can lead to altered protein function as well. The zinc-finger proteins in *Leishmania* are implicated in DNA replication, structure, and repair.<sup>31</sup> In the proposed mechanism of action, the Sb(III) atom coordinates to three cysteine residues and one histidine which is referred to as a CX<sub>2</sub>CX<sub>4</sub>HX<sub>4</sub>C (X = any other amino acid) or a CCHC domain. A study on the HEXBP (hexamer-binding protein) zinc-finger protein found in *L. major* showed that it has nine CCHC domains. HEXBP binds to DNA in the region that encodes the gene for GP63 which is a major surface glycoprotein found in *Leishmania*.<sup>38,39</sup> Although the exact mechanism is yet unknown, if Sb(III) displaces Zn(II) in HEXBP, it could alter the structure and function of HEXBP and inhibit the ability of the protozoa to produce GP63.

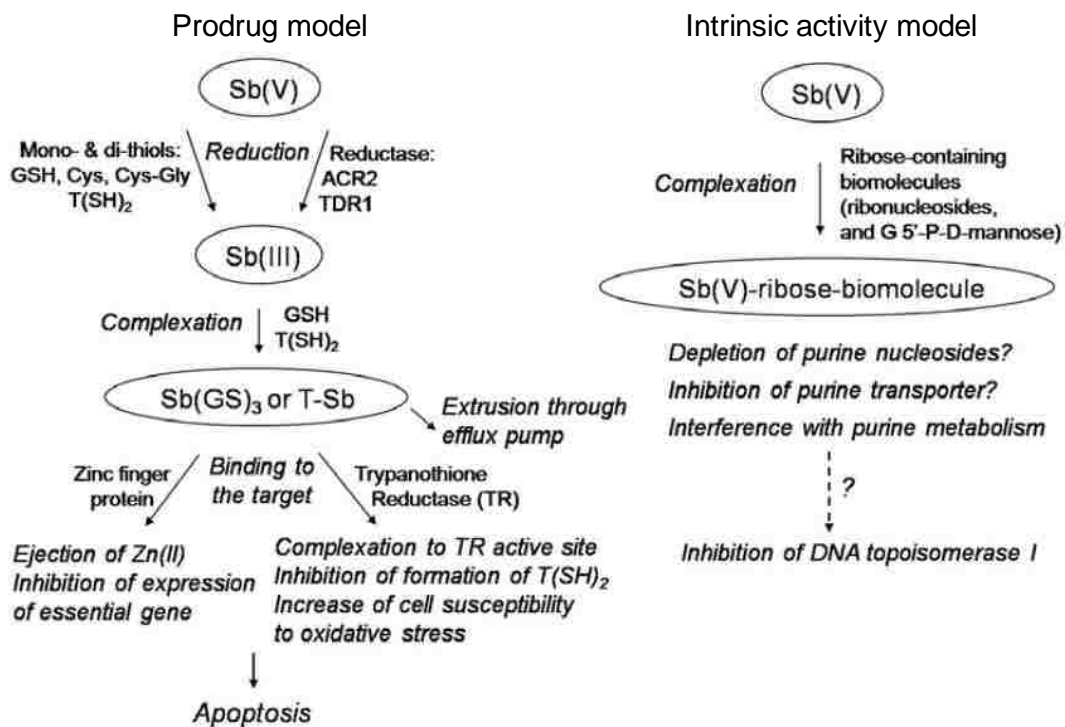


Figure 1.10: Prodrug model and intrinsic activity model describing the different possible mechanisms of action for antimonial treatments .<sup>40</sup> (Image reprinted with permission).

#### 1.4.1.2 Intrinsic activity model of pentavalent antimonials

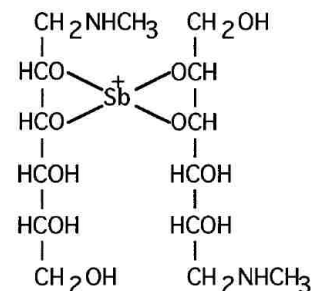
The intrinsic activity model (Figure 1.10) proposes that it is Sb(V) itself that is responsible for the antileishmanial activity of pentavalent antimonials. Sb(V) was shown to inhibit DNA topoisomerase type I in *L. donovani* whereas Sb(III) did not show inhibition activity. Furthermore, a level selectivity for *L. donovani* topoisomerase type I was observed as Sb(V) did not inhibit the activity of calf-thymus topoisomerase type I or DNA gyrase (a type II topoisomerase) from *E. coli*.<sup>41</sup> Topoisomerases relieve supercoiling of DNA during replication and transcription and their function is vital to these processes.

There is also evidence that Sb(V) disrupts protozoal purine metabolism and transport. All known protozoal species are unable to produce purines and rely on salvaging purine compounds from their host.<sup>42</sup> Purines are an essential component to many physiological processes including DNA synthesis and energy-requiring reactions in both parasite and host.<sup>43</sup> Therefore, selective disruption of the parasites' purine salvage pathway is a potential target for antileishmanial drugs. For a parasite's salvage pathway to be functional, it requires correct recognition of the purine substrate, transport of the substrate, and conversion of the substrate into the desired product. Figure 1.X shows the proposed purine salvage biochemical pathways in *Leishmania*.<sup>44</sup>

Sb(V) has been shown to form complexes with many purine based compounds including adenosine, adenosine monophosphate (AMP), guanosine 5'-monophosphate (5'-GMP), and guanosine 5'-disphospho-D-mannose (5'-GDP-mannose).<sup>45,46</sup> Demicheli showed that the Sb(V) atom in meglumine antimoniate will trade its original ligand for adenosine or AMP in aqueous solution at acidic pH (pH = 5).

Interestingly, this transfer did not readily occur at neutral pH (pH = 7.2) and also did not occur with deoxyadenosine.<sup>45</sup> A later study showed that Sb(V) complexation with GMP is also faster at

acidic pH.<sup>48</sup> The preference for transfer at acidic pH is important as *Leishmania* amastigotes reside in the acidic environment of the phagolysosome (pH ~ 5) of macrophages.<sup>49</sup> It is hypothesized that the antileishmanial activity of Sb(V) could be due to the inhibition of the two known nucleoside transport proteins (*LdNT1* and *LdNT2*) of *L. donovani* by the Sb(V)-nucleoside complexes.<sup>42,48,50</sup> Another hypothesis is that the



**Figure 1.11: Proposed meglumine antimoniate structure. Meglumine antimoniate has been shown to exist in numerous different Sb(V)-ligand complexes with the major moiety being the structure shown.<sup>47</sup>**

Sb(V)-nucleoside complexes are formed in the acidic environment and then transported across the protozoal plasma membrane encountering the neutral pH of the cytosol where they then interfere with the purine salvage pathway. This idea is plausible as it was shown that once formed, the Sb(V)-nucleoside complexes are slow to dissociate even at neutral pH.<sup>48</sup>

The activity level of the enzymes shown in Figure 1.12 is not the same in all parasites.

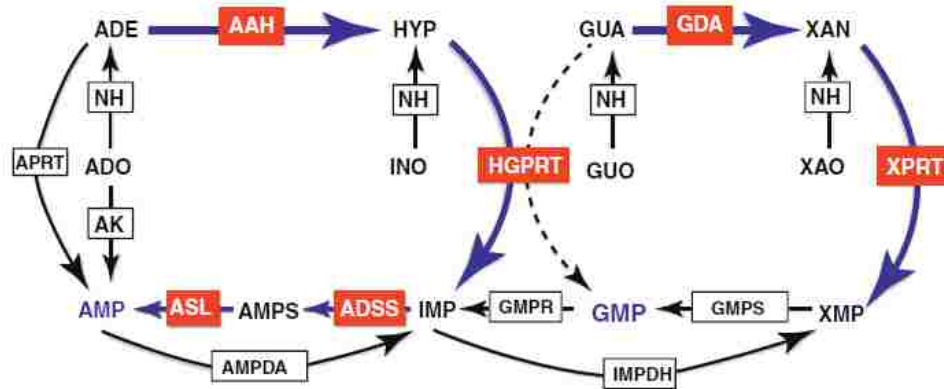


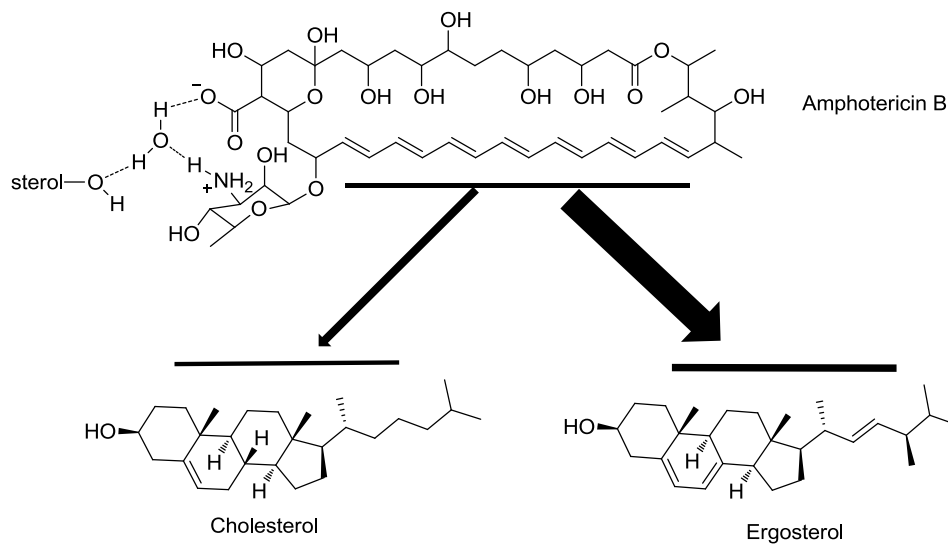
Figure 1.12: Proposed purine salvage pathway of *Leishmania*.<sup>44</sup> Heavy blue arrows indicate major flux pathways. Minor flux pathways indicated by black arrows. Dashed line indicates unlikely pathway under normal physiological conditions in *Leishmania*. Abbreviations: APRT, adenine phosphoribosyltransferase; HGPRT, hypoxanthine-guanine phosphoribosyltransferase; XPRT, xanthine phosphoribosyltransferase; AK, adenosine kinase; AAH, adenine aminohydrolase; GDA, guanine deaminase; ADSS, adenylosuccinate synthetase; ASL, adenylosuccinate lyase; AMPDA, AMP deaminase; IMPDH, inosine monophosphate dehydrogenase; GMPS, GMP synthase; GMPR, GMP reductase; NH, nucleoside hydrolase; ADO, adenosine; ADE, adenine; INO, inosine; HYP, hypoxanthine; GUO, guanosine; GUA, guanine; XAO, xanthosine; XAN, xanthine. (Image reprinted with permission).

#### 1.4.2 Proposed antileishmanial mechanism of amphotericin B

Amphotericin B (AmB) is believed to exert its antileishmanial (and antifungal) activity by binding to ergosterol in the protozoal membrane which leads to disruption of membrane integrity and an increase in membrane permeability.<sup>51,52</sup> One consequence of the increased permeability is that monovalent cations and anions such as  $K^+$  and  $Na^+$  can freely flow across the cell membrane which depolarizes the membrane and can lead to cell death.<sup>53</sup> Selectivity in membrane disruption is possible as mammalian cells use the sterol cholesterol in their cell membranes instead of ergosterol. It is proposed that the selectivity is due to the increased van der Waals interactions between the conjugated region of AmB and ergosterol as compared to cholesterol. This increase in attraction is believed to be due to one of the double bonds (on the right side of the ergosterol molecule as shown in Figure 1.13) in ergosterol which is absent in cholesterol. As confirmed by conformational studies, this double bond causes this region of ergosterol to be much flatter than the corresponding region in cholesterol. This leads to more favorable interaction with the flat polyene region of AmB.<sup>52</sup> Both sterols can also bind to AmB via the hydroxyl group of the sterol and the carboxylate and ammonium ions of AmB with incorporation of a water molecule. This hydrogen bonding interaction is equally likely for both sterols and thus does not lead to any selectivity between the two.<sup>52</sup>

Although the binding of AmB and cholesterol likely leads to side-effects, this interaction also has been shown to inhibit the entry of *Leishmania* promastigotes into macrophages. Pucadyil and coworkers showed that cholesterol is required for entry of non-opsonized *L. donovani* into macrophages. They used methyl- $\beta$ -cyclodextrin to extract cholesterol from J774A.1 macrophage membranes which resulted in a marked decrease in *L. donovani* virulence. Virulence was restored when these cells were

replenished with cholesterol.<sup>54</sup> It is proposed that since AmB binds to cholesterol, it reduces the amount of free cholesterol available for *Leishmania* promastigotes to use as attachment points for entry.<sup>55</sup>



**Figure 1.13: Interactions of cholesterol and ergosterol with Amphotericin B.** Larger arrow indicates the stronger interaction between Amphotericin B with ergosterol as compared to cholesterol. The left side of the Amphotericin B molecule also shows where either sterol can bind to Amphotericin B via hydrogen bonds with incorporation of a water molecule.<sup>52</sup>

### 1.4.3 Proposed antileishmanial mechanism of pentamidine

Pentamidine is believed to exert its antileishmanial effects by disruption of protozoal mitochondrial structure and function. Though its exact mechanism is unknown, several studies have shown significant morphological changes in the kinetoplast and mitochondrial membranes. One study showed that the normal tightly bound DNA of the kinetoplast of *L. tropica* is broken into “a filamentous network” when exposed to pentamidine. In addition, dilatation of the mitochondria was observed along with abnormal or absent cristae formation. Pentamidine is a lipophilic cationic drug which can be concentrated in the mitochondria via electrophoresis due to its inside-



negative membrane potential.<sup>56</sup> Fluorescent analogues of pentamidine have been shown to accumulate in protozoal mitochondria and bind to kinetoplast DNA.<sup>57</sup> Vercesi and coworkers propose that once inside the mitochondria, pentamidine can disrupt the mitochondrial membranes resulting in decreased membrane potentials and an uncoupling of oxidative phosphorylation.<sup>56</sup>

#### **1.4.4 Proposed antileishmanial mechanism of Miltefosine**

The antiprotozoal mechanism of Miltefosine is still unknown but there are several hypotheses including: 1) flagellar membrane damage, 2) interference with alkyl-lipid metabolism and ether-lipid remodeling, and 3) inhibiting phosphatidylcholine synthesis.<sup>58</sup> Some mechanisms appear to be more damaging to promastigotes and others to amastigotes. Interestingly, there is significant evidence that Miltefosine can trigger apoptosis (programmed cell death) in *Leishmania* species which certainly seems to be a counter-productive process for unicellular organisms.<sup>51,58,59</sup> Moreira observed that, “The reason apoptosis is not expected to occur in unicellular organisms is that it may lead to the extinction of a species in which this type of death is part of a developmental program.”<sup>60</sup> Though seemingly counter-intuitive in unicellular organisms, Verma states that, “apoptosis could be a useful mechanism to avoid killing of the entire population.”<sup>59</sup> Common features of apoptosis are compared to the features of necrosis (non-programmed cell death) in Figure 1.14.<sup>61</sup>

<b>Apoptosis</b>	<b>Necrosis</b>
Single cells or small clusters of cells	Often contiguous cells
Cell shrinkage and convolution	Cell swelling
Pyknosis and karyorrhexis	Karyolysis, pyknosis, and karyorrhexis
Intact cell membrane	Disrupted cell membrane
Cytoplasm retained in apoptotic bodies	Cytoplasm released
No inflammation	Inflammation usually present

Figure 1.14: Common features of apoptosis and necrosis.<sup>61</sup>

When studying the effects of Miltefosine on *Leishmania donovani* promastigotes, Paris and coworkers observed characteristics of apoptotic promastigote cell death including karyorrhexis (nuclear fragmentation), cell shrinkage, and maintenance of cell membrane integrity. In addition, they observed the translocation of phosphatidylserine residues from the inside to the outside of the plasma membrane which is also a common apoptotic feature. When present on the cell surface, phosphatidylserine attracts phagocytes which will eventually digest the apoptotic cell remnants. Paris and coworkers also tested the effects of caspase inhibitors on miltefosine treated promastigotes. In mammalian, caspases activate enzymes such as endonucleases which perform the DNA digesting aspect of apoptosis. Paris observed that caspase inhibitors do inhibit DNA digestion in promastigotes further supporting the postulation of an apoptotic death.<sup>58</sup> Verma and coworkers studied Miltefosine's effects on amastigotes as well as promastigotes. They observed karyorrhexis in both extracellular and intra-macrophage *L. donovani* amastigotes which supports the apoptotic hypothesis for this life stage as well.<sup>59</sup>

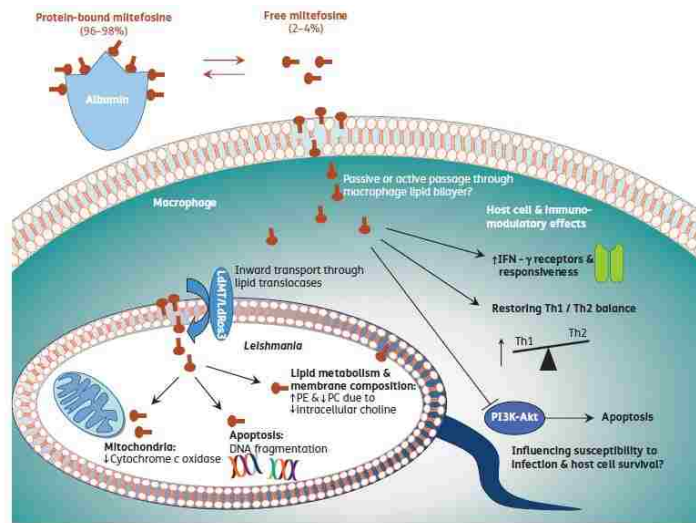


Figure 1.15: Proposed mechanisms of action of Miltefosine against *Leishmania*.<sup>71</sup> (Image reprinted with permission)

In addition to the apoptosis hypothesis, there is evidence of several other drug targets for miltefosine. It is possible that these other drug targets also play some role in the complex apoptotic pathway. One such target is interference with lipid metabolism and remodeling. For *Leishmania donovani* promastigotes, phosphatidylcholine (PC) is the primary phospholipid and makes up approximately 45-52% of the total cell phospholipid content.<sup>62,63</sup> Following exposure to miltefosine, total cell PC content dropped by 42% and was accompanied by a 19% increase in phosphatidylethanolamine (PE) content.<sup>63</sup> Rakotomanga and coworkers proposed that this decrease in PC content was due to miltefosine inhibiting the CTP-phosphocholine-

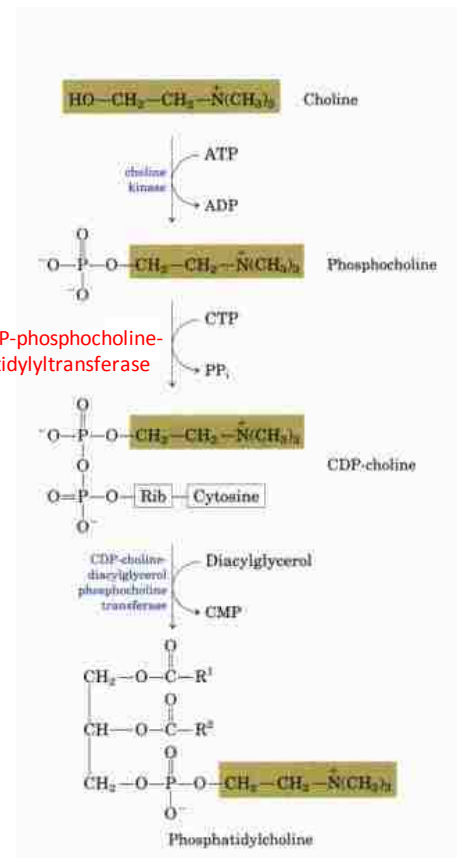
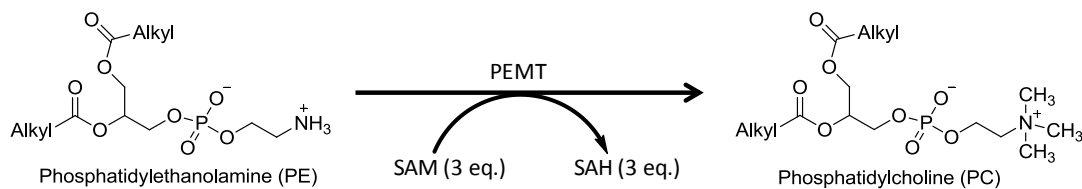
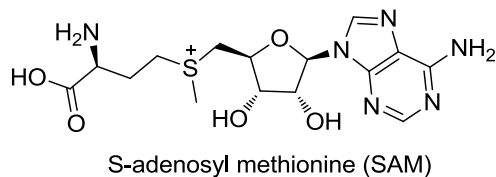


Figure 1.16: General phosphatidylcholine synthetic pathway in eukaryotes.<sup>64</sup>

cytidyltransferase enzyme activity in the synthesis of phosphatidylcholine (See Figure 1.16).<sup>63</sup> Croft postulates that miltefosine prevents CTP-phosphocholine-cytidyltransferase from convert from its inactive form in the cytosol to its active form in the membrane.<sup>66</sup> Inhibition of this same enzyme is also hypothesized to contribute to the anti-neoplastic activity of miltefosine.<sup>65</sup> Rakotomanga also postulates that the CTP-PE cytidyltransferase enzyme could be stimulated by miltefosine along with inhibition of PE-N-methyltransferase (PEMT). Stimulation of CTP-PE cytidyltransferase could obviously lead to increased PE as this enzyme is in the PE synthetic pathway. Inhibition of PEMT would lead to a decrease in PC and an increase in PE as PEMT catalyzes the transfer of 3 methyl groups from 3 equivalents of S-adenosyl methionine (SAM) converting PE to PC (Figure 1.17).<sup>67</sup> Inhibition of PEMT is an intriguing target as protozoal cells utilize the PEMT pathway as their primary method of PC synthesis whereas mammalian cells primarily use the CDP-choline pathway.<sup>68</sup>



**Figure 1.17: Conversion of PE to PC by the enzyme Phosphatidylethanolamine-N-methyltransferase (PEMT). SAM = S-adenosyl methionine; SAH = S-adenosyl homocysteine**



In addition to changes in PC and PE content, it has also been hypothesized that miltefosine interferes with synthesis of glycoinositol phospholipids (GIPLs), lipophosphoglycans (LPGs), and glycosylphosphatidylinositol (GPI) anchored proteins.

These compounds are abundant on *Leishmania* cell surfaces and play a significant role in the virulence of the parasite.<sup>70</sup> Figure 1.18 shows the size and abundance of these surface lipids in *Leishmania* promastigotes.<sup>72</sup> Mammalian cells do not use GPIs and LPGs at all and use significantly less GPI-anchored proteins. Therefore, interference with the synthesis and functions of these molecules should selectively disrupt protozoal cell functions without disturbance of mammalian cell functions.<sup>70</sup>

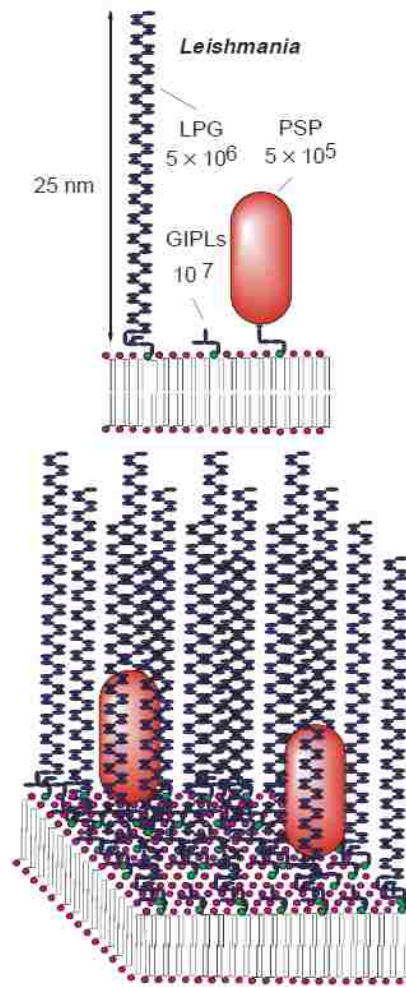


Figure 1.18: Surface Lipids of *Leishmania*<sup>72</sup>

#### 1.4.5 Proposed antileishmanial mechanism of Paromomycin

Akin to the aminoglycoside inhibition of bacterial protein synthesis, paromomycin's antileishmanial effect is attributed to selective perturbation of protozoal protein synthesis.<sup>73,74</sup> Fernandez and coworkers showed that Paromomycin significantly interferes with translation of mRNA in *in vitro* analysis of protein synthesis using ribosomes from *Leishmania* promastigotes. In the same analysis using mammalian cells, there was only minimal perturbation of translation indicating a high degree of selectivity for protozoal ribosomes over mammalian ribosomes (Figure 1.19). With the *Leishmania* ribosomes, they observed a decrease in protein synthesis as well as a less accurate translation of mRNA. They also analyzed binding activity of Paromomycin to ribosomes which showed strong binding of Paromomycin to Leishmanial ribosomes and minimal binding to mammalian ribosomes. In addition to the *in vitro* analysis, *in vivo* studies also showed that Paromomycin significantly inhibits protein synthesis in *Leishmania* promastigotes. Furthermore, they showed that Paromomycin is vastly superior in inhibiting protozoal protein synthesis when compared to streptomycin and neomycin which are also aminoglycosides.<sup>74</sup>

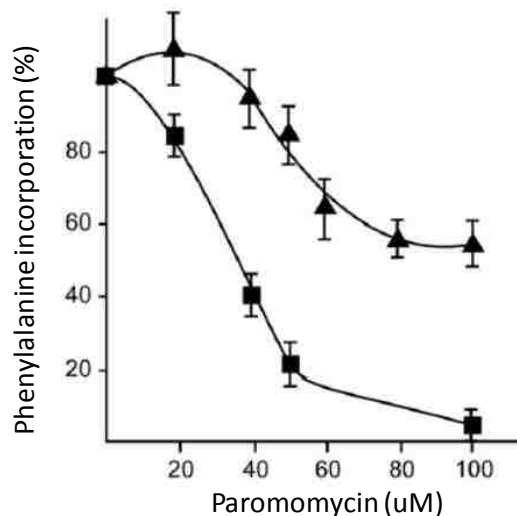
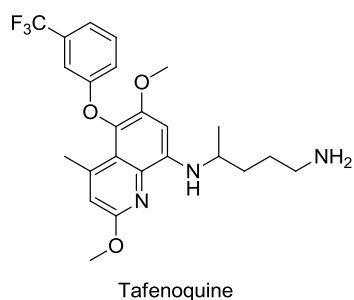


Figure 1.19: Paromomycin effect on protein translation with *Leishmania mexicana* ribosomes (squares) and mammalian (rat liver) ribosomes (triangles).<sup>74</sup>

#### 1.4.6 Proposed antileishmanial mechanism of sitamaquine

Based on their studies with *L. donovani* promastigotes, Carvalho and coworkers propose that the orally active sitamaquine exerts its antileishmanial activity via inhibition of succinate dehydrogenase (SD, also known as respiratory complex II) which is a key enzyme in both the citric acid cycle and the electron transport chain.<sup>75,76</sup> Carvalho postulates that sitamaquine “induces a fast and significant decrease of intracellular free ATP levels, thus leading to a bio-energetic collapse of the parasite”.<sup>75</sup> Inhibition of SD has been shown to result in increased reactive oxygen species (ROS) causing oxidative stress which can lead to apoptosis.<sup>77</sup> Whereas sitamaquine interferes with respiratory complex II, Tafenoquine (which is also an 8-aminoquinoline analogue) was shown to inhibit respiratory complex III which also led to apoptosis in *Leishmania* promastigotes.<sup>78</sup>



## 1.5 Preventative strategies for control of *Leishmania*

### 1.5.1 Vaccine development

The ultimate goal for the treatment of Leishmaniasis is the development of a successful vaccine to decrease the incidence and prevalence of Leishmaniasis with an accompanied decrease in morbidity and mortality. Due to the “simple life cycle” of *Leishmania*, Davies and coauthors stated, “Of all the parasitic diseases, Leishmaniasis is considered the most likely to succumb to vaccination.”<sup>79</sup> Despite the relative success seen in mouse model *Leishmania* vaccination studies, success in human trials has remained elusive.<sup>80</sup>

The belief that a Leishmaniasis vaccine is an attainable goal stems from the fact that patients who have recovered from LCL are usually immune to new infections.<sup>81</sup> To date, the only successful vaccination strategy in humans has been through the direct inoculation of subjects with virulent *L. major*.<sup>82</sup> This strategy has been termed “leishmanization” and has been used for over 60 years.<sup>83</sup> In the most primitive form of leishmanization, “scratched tissue from active lesions of patients with [LCL] was applied to, or sandflies were allowed to bite, the skin of healthy individuals.”<sup>81</sup> When it works, leishmanization results in a small, self-healing lesion which confers immunity to the



individual. However, some individuals develop severe lesions which in certain cases never fully resolve.<sup>81</sup> For this reason, leishmanization has been deemed unethical and discontinued by most countries worldwide with the exception of its current use in Uzbekistan and Iran.<sup>83</sup>

Many vaccination studies have been completed using first-generation vaccines composed of either live attenuated parasites or whole-killed parasites. The live attenuated vaccines have had varying degrees of success in conferring immunity to *Leishmania*. Titus and coworkers deleted the gene encoding for dihydrofolate reductase-thymidylate synthase (*DHFR-TS*) from a strain of *L. major* and evaluated its immunogenicity in mice. This altered strain did not cause Leishmaniasis and the inoculated mice were markedly more resistant to disease when challenged with wild-type *L. major*.<sup>84</sup> However, when this same *DHFR-TS* deficient strain was evaluated in a primate model using Rhesus monkeys, protective immunity did not result as the inoculated monkeys developed LCL when challenged with virulent *L. major*.<sup>85</sup> In both the mouse and monkey studies, parasites of the *DHFR-TS* deficient strain persisted at low levels in the animals for up to 2-3 months. The persistence of parasites in subjects without disease has been shown in numerous studies. In one murine study with *L. major* infected mice, all 23 mice in the study recovered from the experimentally induced LCL and yet all 23 had persistent parasites after 12 months. The most common location of the persistent parasites was in lymph node near the original inoculation site.<sup>86</sup> There is debate as to whether the persistent parasites (subclinical infection) are beneficial or detrimental to the host. In a study done by Uzonna and colleagues, persistent parasites were necessary to maintain immunity in mice.<sup>87</sup> If parasites were completely cleared

from the mice, they lost their resistance to subsequent infection. Uzonna postulated that the persistent parasites provided a continuous low level of antigen presentation to T-memory cells specific for the parasite which confers immunity. Furthermore, they hypothesized that when the parasites are completely cleared, the specific T-memory cells die out leaving the host once again susceptible to Leishmaniasis. The problem with subclinical infections is that the host may become immunocompromised from a different disease state (such as AIDS) which can result in parasite proliferation and a condition known as reactivation Leishmaniasis.<sup>87,88,89</sup> In addition, with a long lasting subclinical infection, it is possible that a live attenuated non-disease causing parasite may mutate into a disease causing strain.<sup>83,90</sup>

The literature on whole killed parasites for use in vaccination exhibits a similar history to the live attenuated parasite vaccine in that success has been seen in animal models but it has not translated to success in humans.<sup>83</sup> Misra and coworkers used a monkey model to evaluate an autoclaved *L. major* vaccine with alum and Bacillus Calmette-Guerin (BCG) as adjuvants. All four monkeys in the unvaccinated group died from VL within 180 days whereas 7 of the 8 monkeys in the vaccinated group survived.<sup>91</sup> Mohebbi and colleagues later showed that this same vaccine preparation was efficacious for canine VL as well.<sup>92</sup> However, when tested in a clinical trial in Iran, the vaccine was shown to be safe but vaccine efficacy results were inconclusive. There are plans to re-evaluate this vaccine in humans with an “improved study design” in hope of more conclusive results.<sup>93</sup> Several other first generation vaccines have been shown to have acceptable safety profiles but “reproducible evidence of protective efficacy has not emerged from clinical trials of first generation Leishmaniasis vaccines”.<sup>93</sup> As

summarized by Coler and Reed, “the results from several clinical trials using whole parasite antigens vary from 0-75% efficacy against [LCL] and little (<6%) or no protection against VL.”<sup>94</sup>

Numerous second generation antileishmanial vaccines have also been developed though few have been evaluated in humans. Second generation vaccines utilize subunits of *Leishmania* which can administered in several different ways including being conjugated to bacteria or viruses.<sup>83</sup> Numerous studies describe success with second generation vaccines in murine and canine models.<sup>95-100</sup> A vaccine known as Leish-111f is the only second generation antileishmanial vaccine that has advanced to human clinical trials.<sup>80</sup> Leish-111f is a polyprotein composed of three proteins that were each initially assessed individually as potential vaccine candidate antigens.<sup>101-103</sup> The three proteins linked together are: 1) thiol-specific antioxidant (TSA) from *L. major*, 2) stress-inducible protein 1 (LeSTI1) from *L. major*, and 3) elongation and initiation factor (LeIF) from *L. braziliensis*.<sup>83</sup> When evaluated in BALB/c mice, Leish-111f formulations elicited an equal or greater immunogenic response as compared with any of the single proteins used alone.<sup>104</sup> Despite the success in mice, Leish-111f was unsuccessful in curbing Leishmanial infections in a canine Phase III field trial.<sup>105</sup> A later canine study evaluated a modified version of Leish-111f known as Leish-110f. There are two slight differences between Leish-111f and Leish-110f. Leish-111f has a tag of six histidine residues at one end of the polyprotein whereas Leish-110f does not and the lysine<sub>274</sub> residue of Leish-111f has been change to glutamine in Leish-110f.<sup>106</sup> When a Leish-110f formulation was evaluated in dogs as a combination therapy with pentavalent antimonials, the group receiving Leish-110f and antimonial treatment showed significantly less mortality as

compared to the groups receiving only antimonial treatment or no treatment.<sup>107</sup> Leish-111f formulations have been evaluated in humans in Phase I and II clinical trials and have been deemed both safe and immunogenic though human vaccine efficacy remains to be assessed.<sup>108</sup>

Third generation DNA vaccines are also being evaluated for their potential utility as antileishmanial agents. As stated by Nagill, “DNA vaccines are advantageous as they are relatively simple to produce, stable, easy to administer and often very immunogenic”.<sup>83</sup> DNA vaccines involve direct injection of DNA which encodes for specific Leishmanial proteins. Immunogenic responses can occur to the DNA itself and/or to the antigenic protein synthesized from the DNA by the host.<sup>109</sup> In what is known as the “prime-boost vaccine strategy”, a recombinant virus is injected within days or weeks of the DNA vaccine. The recombinant virus is engineered to express the same protein that the DNA in the vaccine encodes for. Numerous studies have shown protective immunogenic responses to antileishmanial DNA vaccines and prime-boost DNA vaccines in mice and dogs.<sup>83,110-115</sup> To the best of my knowledge, there are no publications evaluating antileishmanial DNA vaccine use in humans.

Overall, it is evident that progress has been made in vaccine development for Leishmaniasis yet it is also evident that an efficacious human vaccine is likely several years off and possibly decades away.

### **1.5.2 Vector and reservoir control**

The phlebotomine sand fly is the only known vector for *Leishmania*. Therefore, there has been extensive research on methods to control sand fly populations and

prevention of sand fly bites. Common control and preventative measures include spraying houses with insecticide, use of insecticide impregnated bed nets and clothing, topical repellents, and insecticide application to animal burrows which are common breeding grounds for sand flies.<sup>79,116</sup> The efficacy of these methods is often difficult to accurately assess. In a 2003 study in Iraq during Operation Iraqi Freedom, members of the United States Theater Army Medical Laboratory unit directed Leishmaniasis control measures and attempted to evaluate their efficacy at Tallil Air Base. Their control and preventative measures included insecticide impregnated uniforms and bed nets, spraying shelters with pesticides (lambda cyhalothrin, cypermethrin, and cyfluthrin), area spraying with pesticides (resmethrin and malathion), and removal of sand fly habitat. From May to October, they captured 19,454 sand flies using light traps in twelve different locations (10 traps in pesticide treated areas and 2 traps in untreated control areas). In the first two months, similar amounts of sand flies were trapped in both treated areas and control areas. After the first two months, the treated areas showed significant reductions in the number of trapped sand flies indicating some efficacy in the pesticide treatment. Removal of habitat measures were not efficacious as “hundreds of sand flies were often captured in a single light trap placed in the middle of heavily compacted and completely denuded tent cities with no apparent ‘normal’ habitat for hundreds of meters in all directions.” The study authors further pointed out that “although it was encouraging that we could reduce the [sand fly] numbers over time, it is unclear whether these gradual reductions translated into fewer cases of Leishmaniasis in the soldiers stationed at Tallil Air Base.”<sup>117</sup> Unfortunately, the majority of vector control studies fail to develop any clear conclusions on the efficacy of the control measures in preventing cases of

Leishmaniasis. It is often difficult to control the variables in this type of study which can cloud conclusions. Despite the nebulous results, Claborn states that “vector control remains a key component of many anti-Leishmaniasis programs and probably will remain so until an effective vaccine becomes available.”<sup>116</sup>

In addition to vector control, reservoir control has also received much attention. There are many animal reservoirs for Leishmanial species including dogs, sloths, rats, and gerbils.<sup>117</sup> As dogs are the reservoir that most commonly live in close proximity with humans, most reservoir control studies have evaluated methods to decrease dog to human parasite transmission via the sand fly vector. These control methods include treating or killing seropositive dogs, spraying dogs with insecticide, and using insecticide-impregnated dog collars.<sup>79,120-122</sup> A dog culling study in a city (Jacobina) in Brazil from 1989-1993 showed that pediatric cases of VL decreased significantly in the years that seropositive dogs were killed. From 1986-1989, there were an average of 10 cases of VL per 1000 children in Jacobina. This number dropped down to an average of 2 cases per 1000 children from 1990-1993. This was paralleled by a drop in the number of seropositive dogs which was 36% of dogs tested in 1989 and down to 14% in 1993. The authors of the study point out that it is impossible to say if this drop in pediatric VL is directly due to the dog culling as there are many other variables at play.<sup>121</sup> For instance, these types of studies typically involve an increase in information dissemination concerning the dangers of Leishmaniasis which can lead to the population taking more personal protective measures such as using bed nets and insecticides which may be the actual cause of the decrease in disease incidence. Although clear conclusions from dog

control studies are difficult to achieve, dog control measures are still widely used and studied.

## **1.6 Concluding remarks**

As shown in the preceding sections, considerable efforts have been made to develop numerous therapeutic strategies to combat Leishmaniasis. However, Leishmaniasis continues to plague many regions of the world and still has high rates of morbidity and mortality associated with it. For this reason, it is important that research continues in the search for novel therapeutic strategies to combat this disease. Our efforts in the endeavor to develop new pharmacological molecules to treat Leishmaniasis are detailed in the following chapter.

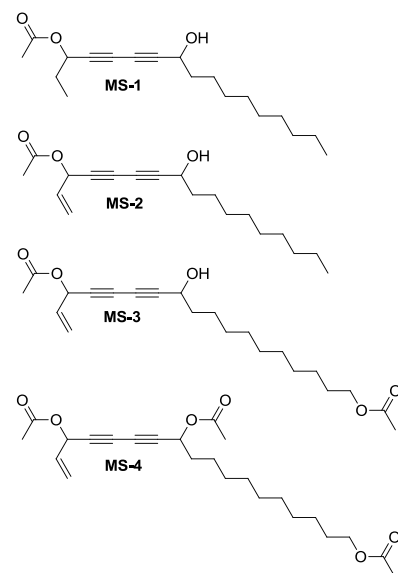
***Chapter 2: Natural product library synthesis and antileishmanial biological activity***



## Chapter 2: Natural product library synthesis and antileishmanial biological activity

### 2.1 Antiprotozoal polyacetylene compounds discovered by Senn and colleagues

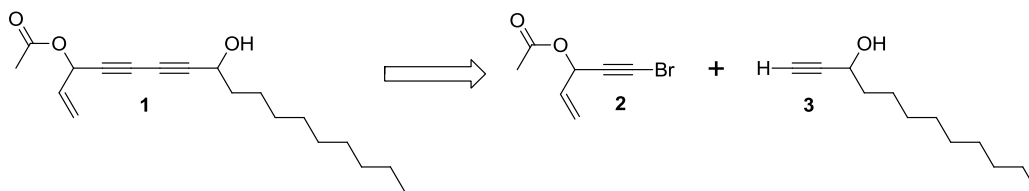
In 2007, Martin Senn and coworkers reported the isolation of four polyacetylene compounds (**MS-1** through **MS-4**) from the Tanzanian medicinal plant *Cussonia zimmermannii*.<sup>124</sup> **MS-1**, **MS-2**, and **MS-3** were tested for biological activity against *Trypanosoma brucei rhodesiense*, *Trypanosoma cruzi*, *Plasmodium falciparum*, and *Leishmania donovani*. **MS-4** was not tested as not enough was isolated for biological activity assays. Of the three compounds assayed, **MS-2** had the lowest IC<sub>50</sub> (0.32 μM) and the highest selectivity index (37; IC<sub>50</sub> for rat skeletal myoblasts/IC<sub>50</sub> for *L. donovani*) when screened against *Leishmania donovani* in infected macrophages. As our goal was to develop antileishmanial agents, we started with **MS-2** as our lead compound to investigate. As **MS-2** was our first synthetic target, it will from here forward be referred to as compound **1**.



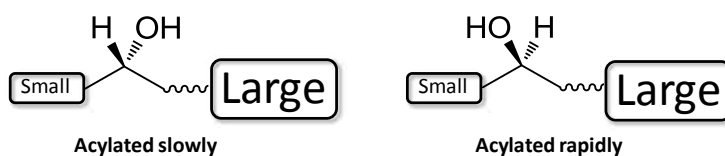
### 2.2 First Round of SAR studies – Evaluating Stereochemistry

Senn and coworkers did not determine the absolute or relative stereochemistry of the two stereocenters in **1**. As **1** has two stereocenters, there are four stereoisomers of the molecule and our initial SAR goal was to synthesize all four stereoisomers and evaluate their biological activity. Retrosynthetic analysis (Figure 2.1) showed that **1** and its

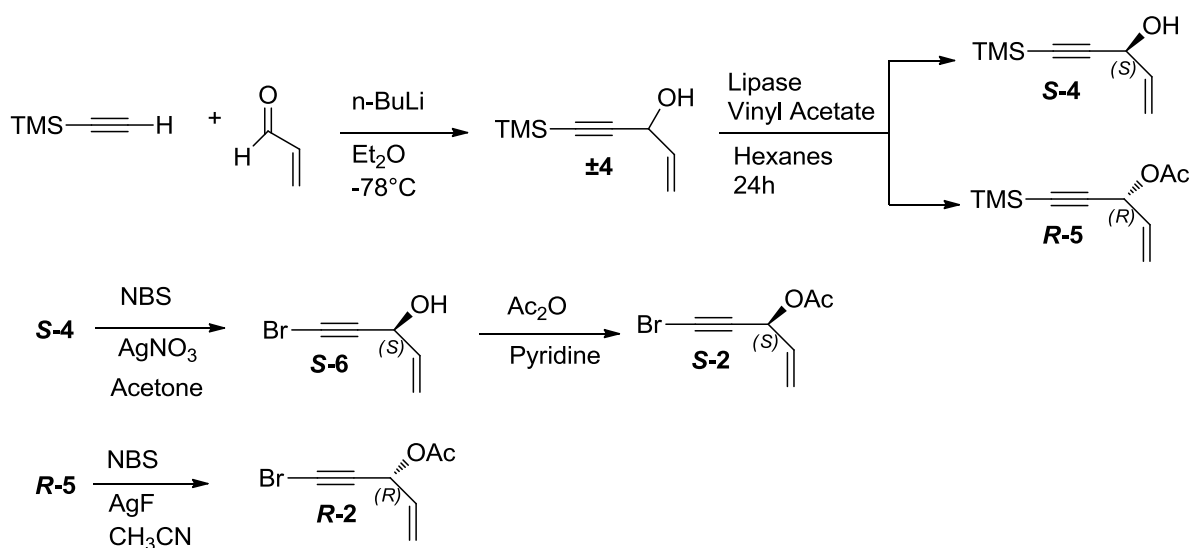
stereoisomers could be synthesized by the Cadiot-Chodkiewicz coupling of the respective enantiomers of **2** and **3**.<sup>125</sup> We set both stereocenters by resolving the respective propargylic alcohols via enantioselective esterification using Lipase AK from *Pseudomonas fluorescens*.<sup>126</sup> In their 1991 JACS publication, Burgess and Jennings described the utility of *Pseudomonas sp.* Lipase AK in resolving a wide variety of alcohol substrates including allyl alcohols, propargyl alcohols, and homopropargylic alcohols. Adapted Figure 2.2 from Burgess and Jennings' article shows their "simple model for predicting which substrates will be resolved effectively via biocatalytic acylations mediated by crude lipase from *Pseudomonas sp.* (Amano AK), and the sense of the enantioselection."<sup>126</sup>



**Figure 2.1: Retrosynthetic analysis for compound 1.**



**Figure 2.2: Enantioselective esterification model for *Pseudomonas sp.* lipase Amano AK.<sup>126</sup>**

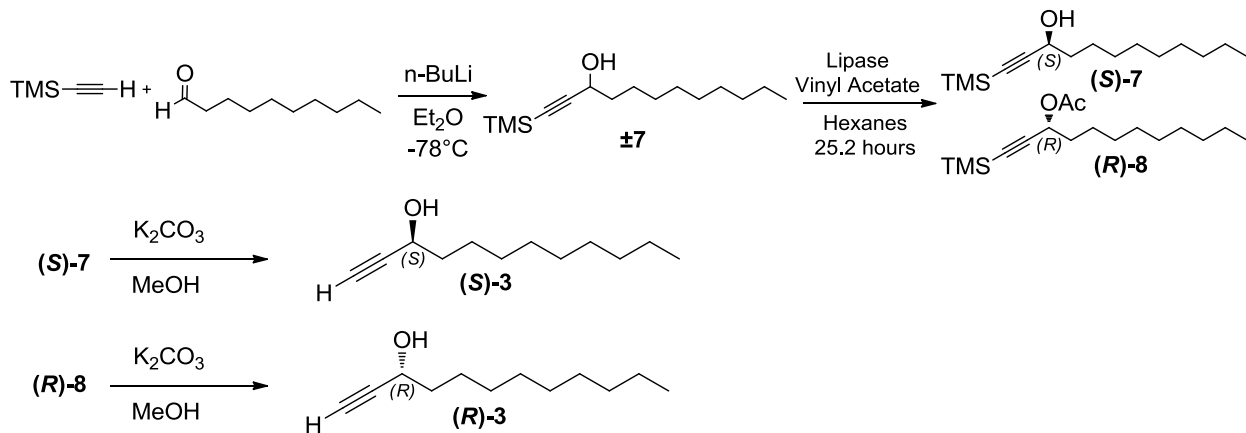


**Scheme 2.1**

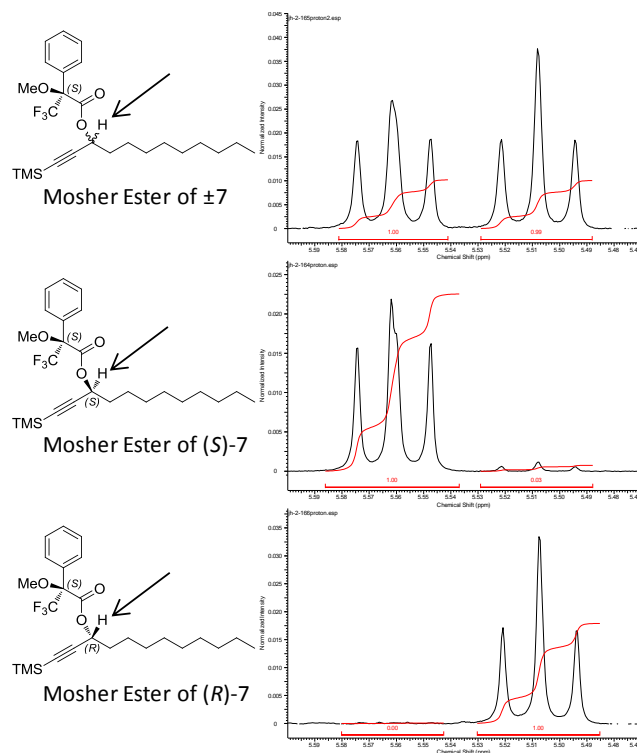
The enantiomers of 1-bromoalkyne **2** were prepared as shown in Scheme 2.1. **±4** was obtained by the reaction of lithium trimethylsilylacetylide with acrolein.<sup>127</sup> Enzymatic resolution of **±4** by Lipase AK from *Pseudomonas fluorescens* yielded **(S)-4** and **(R)-5**. Enantiomeric excess was determined by Mosher ester preparation.<sup>128,129</sup> The *ee* value for **(S)-4** was greater than 99%. To determine the *ee* value of **(R)-5**, it was first converted to **(R)-4** with LAH and then the Mosher ester was prepared which showed an *ee* value of 97%. **(S)-4** was converted to 1-bromoalkyne **(S)-6** with NBS and AgNO<sub>3</sub>.<sup>130</sup> **(S)-6** was subsequently acylated with acetic anhydride in pyridine to obtain **(S)-2**. **(R)-2** was obtained by brominating **(R)-5** at the acetylenic position with NBS and AgF.<sup>131</sup>

The enantiomers of propargyl alcohol **3** were synthesized as outlined in Scheme 2.2. **±7** was obtained by the reaction of lithium trimethylsilylacetylide with decanal.<sup>127</sup> Enzymatic resolution of **±7** by Lipase AK from *Pseudomonas fluorescens* yielded **(S)-7** and **(R)-8**.<sup>126</sup> **(S)-3** and **(R)-3** were obtained by treating **(S)-7** and **(R)-8** respectively with potassium carbonate in methanol.<sup>132</sup> Enantiomeric excess was determined by Mosher ester preparation.<sup>128,129</sup> The *ee* value of **(S)-7** was 94%. To determine the *ee* value of **(R)-**

**8**, it was first converted to **(R)**-**7** with LAH and then the Mosher ester was prepared which showed an *ee* value greater than 99%. Figure 2.3 shows zoomed in areas of the spectra of the Mosher esters obtained from  $\pm$ **7**, **(S)**-**7**, and **(R)**-**7**. The resonance from the methine proton in each compound is shown in the zoomed in area and the integration values from the methine proton were used to determine *ee* values.

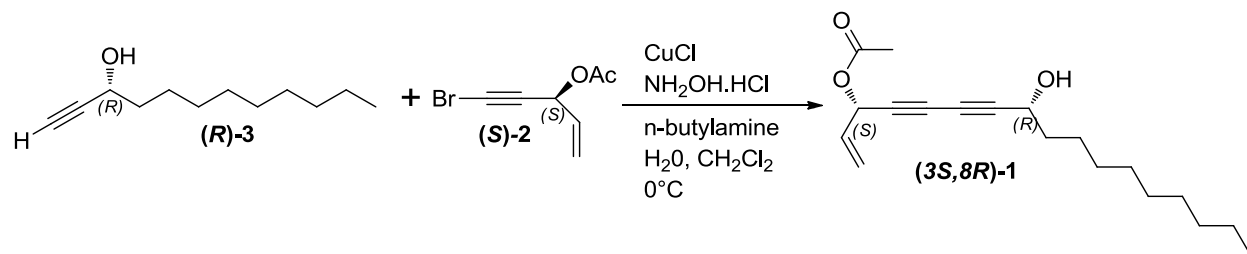


Scheme 2.2



**Figure 2.3:**  $^1\text{H}$  NMR spectra of Mosher esters prepared from racemic **7** and following enzymatic resolution via *Pseudomonas fluorescens* lipase.

The four diastereomers of **1** were then afforded by the Cadiot-Chodkiewicz coupling of (*S*)-**2** and (*S*)-**3**, (*R*)-**2** and (*R*)-**3**, (*R*)-**2** and (*S*)-**3**, and (*S*)-**2** and (*R*)-**3** respectively.<sup>133</sup> The reaction scheme for (*3S,8R*)-**1** is shown below in Scheme 2.3. The other 3 stereoisomers were prepared in an analogous fashion by substituting the respective reagent enantiomers for each compound. Our measured optical rotation (Table 2.1) of the (*3S,8S*)-**1** stereoisomer was consistent with the optical rotation of the natural product reported by Senn and in agreement with the optical rotation and absolute stereochemistry assignment reported by Trost and coworkers in their synthesis of the natural product.<sup>124,134</sup> Our  $^1\text{H}$  NMR (Table 2.1) and  $^{13}\text{C}$  NMR (Table 2.3) data also closely matched the data reported by Senn.



Scheme 2.3

	Specific Rotation ( $^\circ$ )	Concentration (grams/100 mL)	Temperature ( $^\circ\text{C}$ )
Senn Product	-28.0	0.85	20
Trost Product	-24.3	1.02	23
<b>(3S,8S)-1</b>	-29.1	0.59	17
<b>(3R,8R)-1</b>	31.7	0.90	18
<b>(3R,8S)-1</b>	44.6	1.19	17
<b>(3S,8R)-1</b>	-46.0	0.67	17

The solvent used for all testing was 0.75% ethanol in chloroform.

The wavelength used for all testing was the sodium D line.

Table 2.1: Comparison of optical rotation data recorded in Bolstad lab to that reported by Senn and Trost.

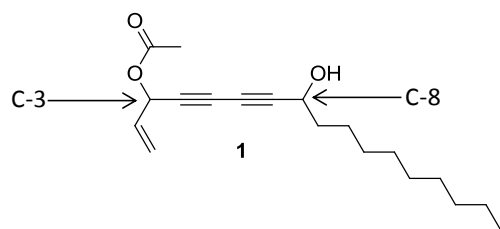
MS-2 $^1\text{H}$ NMR Data (Senn publication)			<b>(3S,8S)-1</b> $^1\text{H}$ NMR Data (Bolstad Lab)		
MS-2 $^1\text{H}$ $\delta_{\text{H}}$ (ppm)	Splitting ( $J$ in Hz)	Integration (# of H atoms)	<b>(3S,8S)-1</b> $^1\text{H}$ $\delta_{\text{H}}$ (ppm)	Splitting ( $J$ in Hz)	Integration (# of H atoms)
0.88	t (7.0)	3	0.88	t (6.97)	3
1.22 - 1.31	m	12	1.22 - 1.34	m	12
1.43	br, quint. (7.5)	2	1.44	quint. (7.58)	2
1.70	m	2	1.71	m	2
1.81	br, s	1	1.91	d (4.40)	1
2.11	s	3	2.11	s	3
4.43	br, t (6.5)	1	4.43	m	1
5.35	d (10.0)	1	5.36	dd (1.10, 10.03)	1
5.55	d (16.8)	1	5.55	dd (1.22, 16.63)	1
5.86	m	1	5.84 - 5.94	m	2
5.91	m	1			

Table 2.2: Comparison of  $^1\text{H}$  NMR data.

<b>MS-2</b> <sup>13</sup> C NMR Data	<b>(3<i>S</i>,8<i>S</i>)-1</b> <sup>13</sup> C NMR Data
Senn publication	Bolstad Lab
$\delta_c$ (ppm)	$\delta_c$ (ppm)
14.1	14.1
20.9	20.9
22.7	22.7
25.0	25.0
29.2	29.2
29.3	29.3
29.48	29.45
29.51	29.48
31.9	31.9
37.4	37.4
62.9	62.9
64.5	64.4
68.6	68.6
70.8	70.8
74.4	74.3
81.3	81.3
119.8	119.7
131.9	131.9
169.5	169.5

**Table 2.3: Comparison of <sup>13</sup>C NMR data.**

The four diastereomers were analyzed for biological activity against *Leishmania amazonensis* which showed the **(3*S*,8*R*)-1** stereoisomer had the lowest IC<sub>50</sub> of 0.63uM while the **(3*S*,8*S*)-1** stereoisomer had an IC<sub>50</sub> of 1.28uM (Table 2.4). The **(3*R*,8*S*)-1** and **(3*R*,8*R*)-1** stereoisomers displayed no antileishmanial activity at 10uM indicating the stereochemistry plays a significant role in the antileishmanial action of the compounds. More specifically, it appeared that the stereochemistry at C-3 was more important than C-8 since the only active compounds had the (*S*)-configuration at C-3.



Compound	IC <sub>50</sub> <i>L. amazonensis</i> in infected macrophages [uM]
(3 <i>S</i> ,8 <i>R</i> )-1	0.63
<sup>a</sup> (3 <i>S</i> ,8 <i>S</i> )-1	1.28
(3 <i>R</i> ,8 <i>R</i> )-1	>10
(3 <i>R</i> ,8 <i>S</i> )-1	>10
<sup>a</sup> stereochemistry of natural product	

**Table 2.4:** Biological activity of the four diastereomers of compound **1** against *L. amazonensis* in infected macrophages.

### 2.3 Second Round of SAR studies – Lipophilicity and Hansch Cluster Analysis

Since the (3*S*,8*R*)-**1** stereoisomer had the lowest IC<sub>50</sub>, several analogues (Figure 1) were synthesized with the same stereochemistry. Analogue selection was based on cluster analysis theory (Table 2.5)<sup>135,136</sup> as described by Hansch and coworkers and on the simplicity of synthesis. The initial analogues set consisted of compounds **9-16** (Figure 2.4) which all had the (3*S*,8*R*) configuration. Compounds **9** and **10** were synthesized to assess the significance of the length of the lipophilic side chain. Compounds **11-15** are analogues of (3*S*,8*R*)-**1** with different functional groups at the C-8 position. Compound **16** has replaced the C-3 acetate with an alcohol.



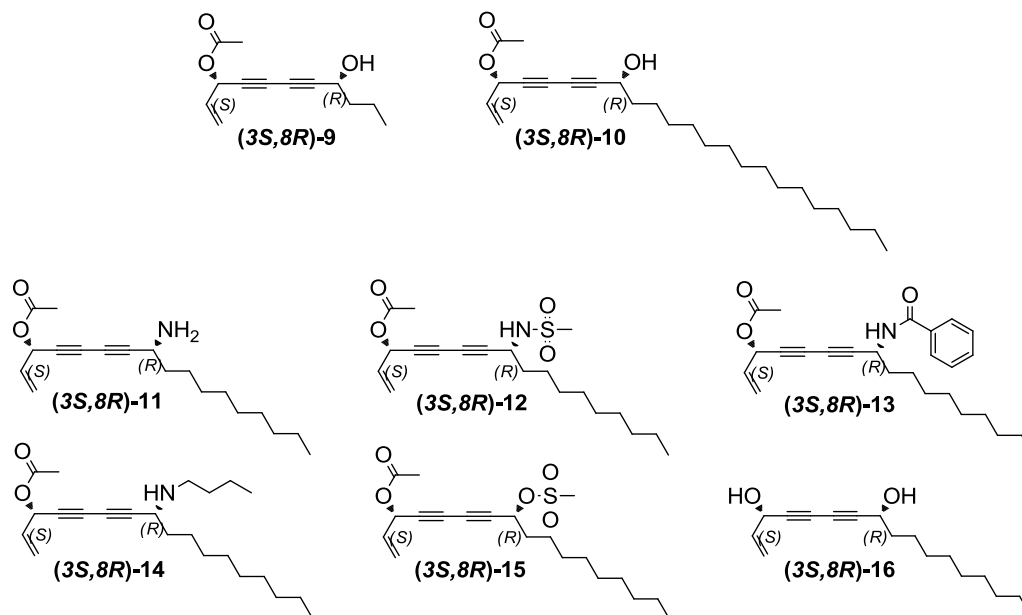


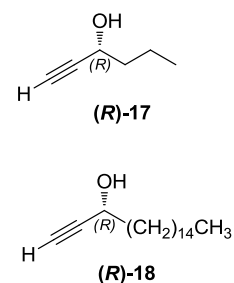
Figure 2.4: Second-round SAR study structures.

Hansch Cluster Analysis Table	
Cluster Number	Typical Members
1	Me, H, 3,4-(OCH <sub>2</sub> O), CH <sub>2</sub> CH <sub>2</sub> COOH, CH=CH <sub>2</sub> , Et, CH <sub>2</sub> OH
2	CH=CHCOOH
3a	CN, NO <sub>2</sub> , CHO, COOH, COMe
3b	C + CH, CH <sub>2</sub> Cl, Cl, NNN, SH, SMe, CH=NOH, CH <sub>2</sub> CN, <b>OCOMe</b> , SCOMe, COOMe, SCN
4a	CONH <sub>2</sub> , CONHMe, SO <sub>2</sub> NH <sub>2</sub> , SO <sub>2</sub> Me, SOMe
4b	NHCHO, NHCOMe, NHCONH <sub>2</sub> , NHCSNH <sub>2</sub> , <b>NHSO<sub>2</sub>Me</b>
5	F, OMe, <b>NH<sub>2</sub></b> , NHNH <sub>2</sub> , OH, NHMe, NHet, NMe <sub>2</sub>
6	Br, OCF <sub>3</sub> , CF <sub>3</sub> , <b>NCS</b> , I, SF <sub>5</sub> , SO <sub>2</sub> F
7	CH <sub>2</sub> Br, SeMe, NHCO <sub>2</sub> Et, SO <sub>2</sub> Ph, <b>OSO<sub>2</sub>Me</b>
8	<b>NHCOPh</b> , NHSO <sub>2</sub> Ph, OSO <sub>2</sub> Ph, COPh, N=NPh, OCOPh, PO <sub>2</sub> Ph
9	3,4-(CH <sub>2</sub> ) <sub>3</sub> , 3,4-(CH <sub>2</sub> ) <sub>4</sub> , Pr, <i>i</i> -Pr, 3,4-(CH) <sub>4</sub> , <b>NHBu</b> , Ph, CH <sub>2</sub> Ph, <i>t</i> -Bu, OPh
10	Ferrocenyl, adamantyl

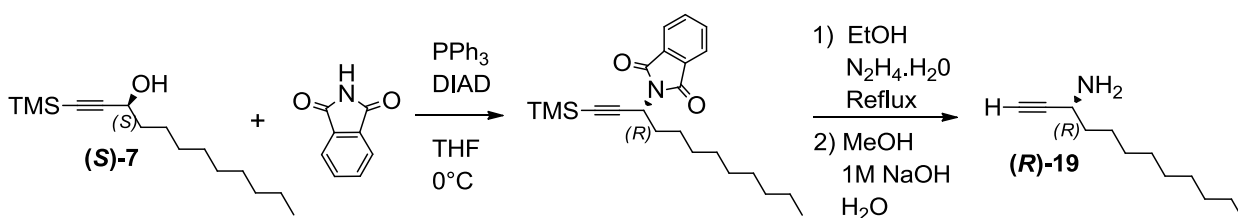
Table 2.5: Substituents shown in bold represent the first substituent we chose to use in our analogues from each cluster. Table adapted from Silverman.<sup>136</sup>

Compound **9**, **10**, and **11** were obtained by the Cadiot-Chodkiewicz coupling of (*S*)-**2** with terminal alkynes (*R*)-**17**, (*R*)-**18**, and (*R*)-**19** respectively.

Compounds (*R*)-**17** and (*R*)-**18** were prepared in an analogous fashion to (*R*)-**3** substituting butyraldehyde and palmitic aldehyde respectively for decanal as shown in Scheme 2.2. (*R*)-**19** was obtained via a Mitsunobu



reaction of (*S*)-**7** with phthalimide which inverted the stereochemistry followed by hydrazinolysis and removal of the TMS group via methanolysis (Scheme 2.4).<sup>137,138,139,140</sup>



Scheme 2.4

Compounds **12**, **13**, and **14** were all derived from Compound **11**. **12** was obtained by mesylation of **11**.<sup>141</sup> **13** was synthesized by the reaction of **11** and benzoic anhydride.<sup>142</sup> **14** was afforded by the reductive amination of **11** with butyraldehyde followed by NaBH<sub>4</sub>.<sup>143</sup> Compound **15** was obtained by the mesylation of (*3S,8R*)-**1**. Compound **16** was afforded via the Cadiot-Chodkiewicz coupling of (*S*)-**6** to (*R*)-**3**.

Compound	IC <sub>50</sub> <i>L. donovani</i> in infected macrophages [uM]
( <i>3S,8R</i> )- <b>9</b>	0.197
( <i>3S,8R</i> )- <b>10</b>	0.287
( <i>3S,8R</i> )- <b>12</b>	0.055
( <i>3S,8R</i> )- <b>13</b>	0.035
( <i>3S,8R</i> )- <b>14</b>	0.034
( <i>3S,8R</i> )- <b>15</b>	0.061
( <i>3S,8R</i> )- <b>16</b>	0.013

Table 2.6: Biological activity of compounds 9-10 and 12-16 against *L. donovani* in infected macrophages.

Compounds **9-10** and **12-16** were evaluated for antileishmanial activity by in vitro screening against *Leishmania donovani* (Table 2.6). Antileishmanial results for Compound **11** were not obtained due to a laboratory complication during the testing assay. All seven compounds tested showed increased antileishmanial activity as compared to the lead compound (**3S,8R**)-**1** though it should be noted that (**3S,8R**)-**1** was screened against *Leishmania amazonensis* while the seven analogues were screened against *Leishmania donovani*. Compounds **12-16** all showed over an order of magnitude increase in antileishmanial activity as compared to (**3S,8R**)-**1**. Compounds **12-15** were 11-fold to 18-fold more active than (**3S,8R**)-**1** and Compound **16** was 48-fold more active than (**3S,8R**)-**1**.

Compounds **9** and **10** had IC<sub>50</sub> values of 0.197uM and 0.287uM respectively which are both lower than the 0.63uM IC<sub>50</sub> of lead compound (**3S,8R**)-**1**. **9** and **10** were evaluated to assess the effects of altering the length of the lipophilic alkyl chain and although their IC<sub>50</sub> values were lower than (**3S,8R**)-**1**, the values were not low enough to warrant more exploration of alkyl chain length at this point in the study. If more analogues with different alkyl chain lengths were evaluated, it would allow us to determine the ideal length and one would expect a resultant parabolic curve in the potency versus carbon chain length graph such as that described by Silverman (Figure 2.5).<sup>136</sup> Dohme and coworkers reported this effect in their 1926 *JACS* article describing their studies on the antibacterial effects of 4-alkylresorcinols where they determined that the *n*-hexyl side chain had the highest potency (Figure 2.5).<sup>144</sup>

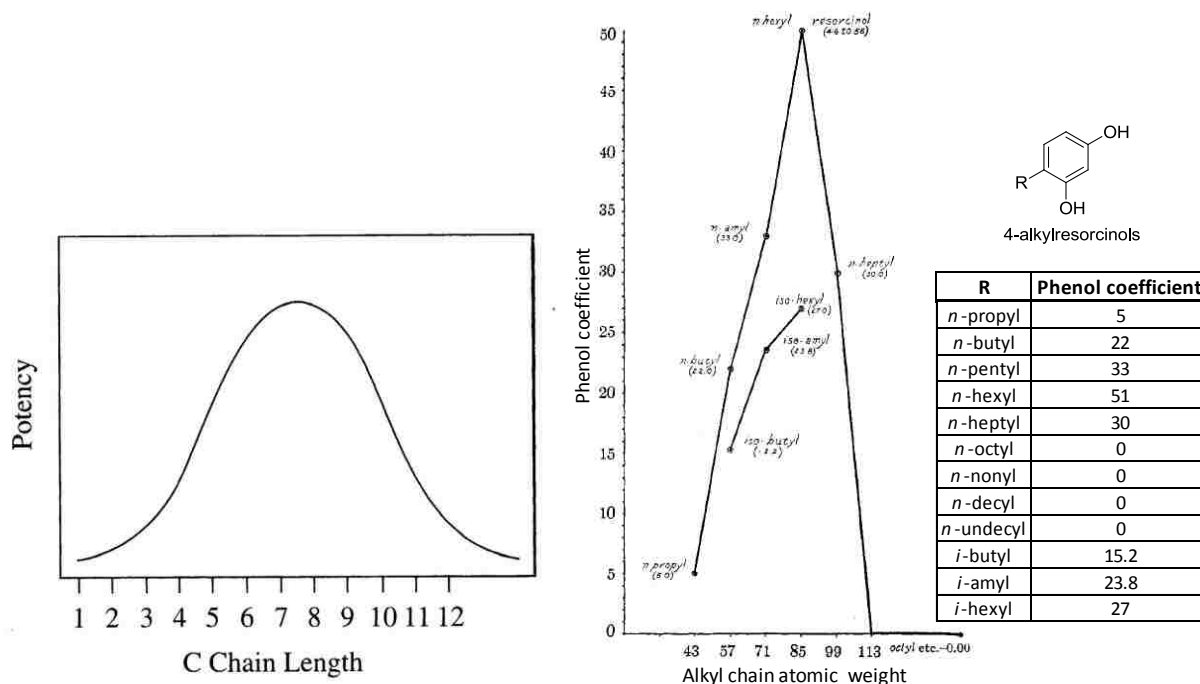


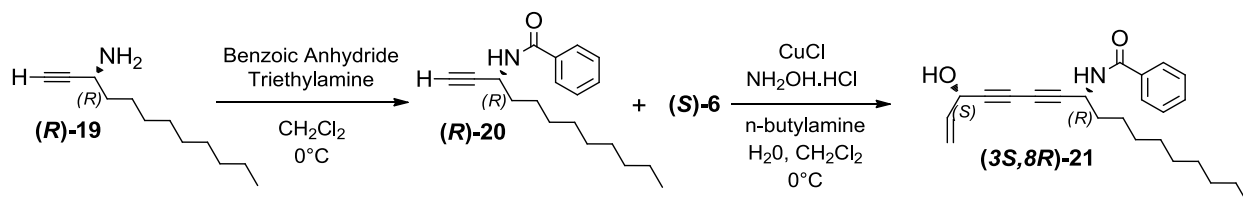
Figure 2.5: Effect of carbon chain length on biological activity.<sup>136,144</sup>

## 2.4 Third Round of SAR studies

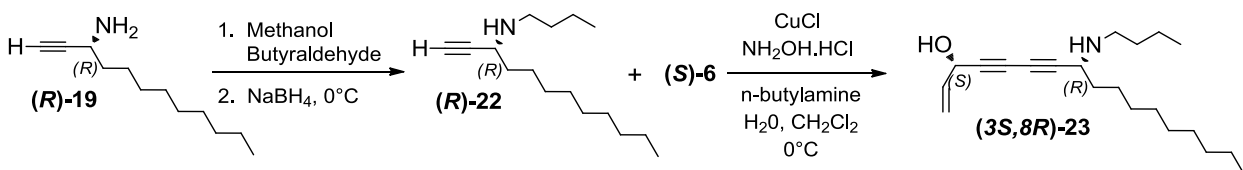
### 2.4.1 Synthesis of Third Round SAR Compounds

Since Compounds **13**, **14**, and **16** showed the most antileishmanial activity, eight analogues were prepared of these compounds for the next round of testing. The low  $IC_{50}$  of Compound **16** showed the positive impact of having a hydroxyl group at the C-3 position instead of an acetate group. Compounds **13** and **14** had the lowest  $IC_{50}$  values of the C-3 acetate compounds and we thus proposed making analogues of **13** and **14** with a hydroxyl group at C-3. Compound **21** was formed in two steps by first reacting (**R**)-**19** with benzoic anhydride to give (**R**)-**20**. (**R**)-**20** was then coupled to (**S**)-**6** to give Compound **21** (Scheme 2.6). Compound **23** was formed by the reductive amination of

(*R*)-**19** to give (*R*)-**22** which was then coupled to (*S*)-**6** to afford Compound **23** (Scheme 2.7).

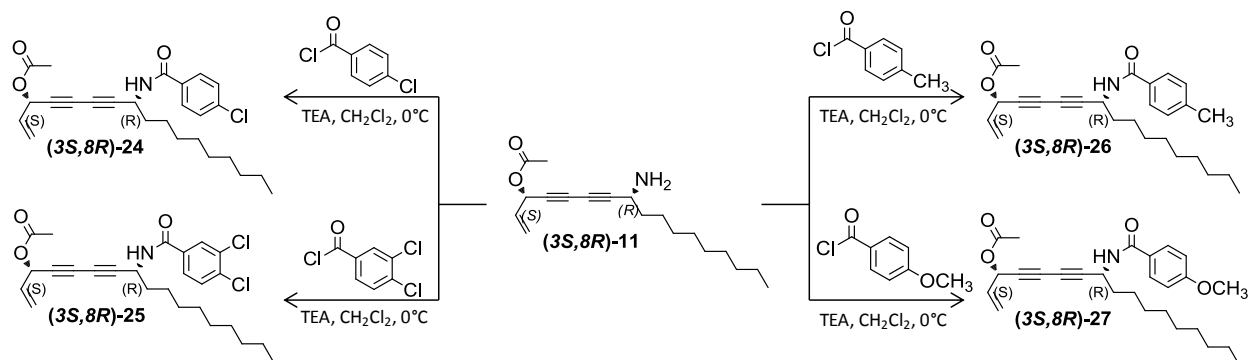


Scheme 2.6



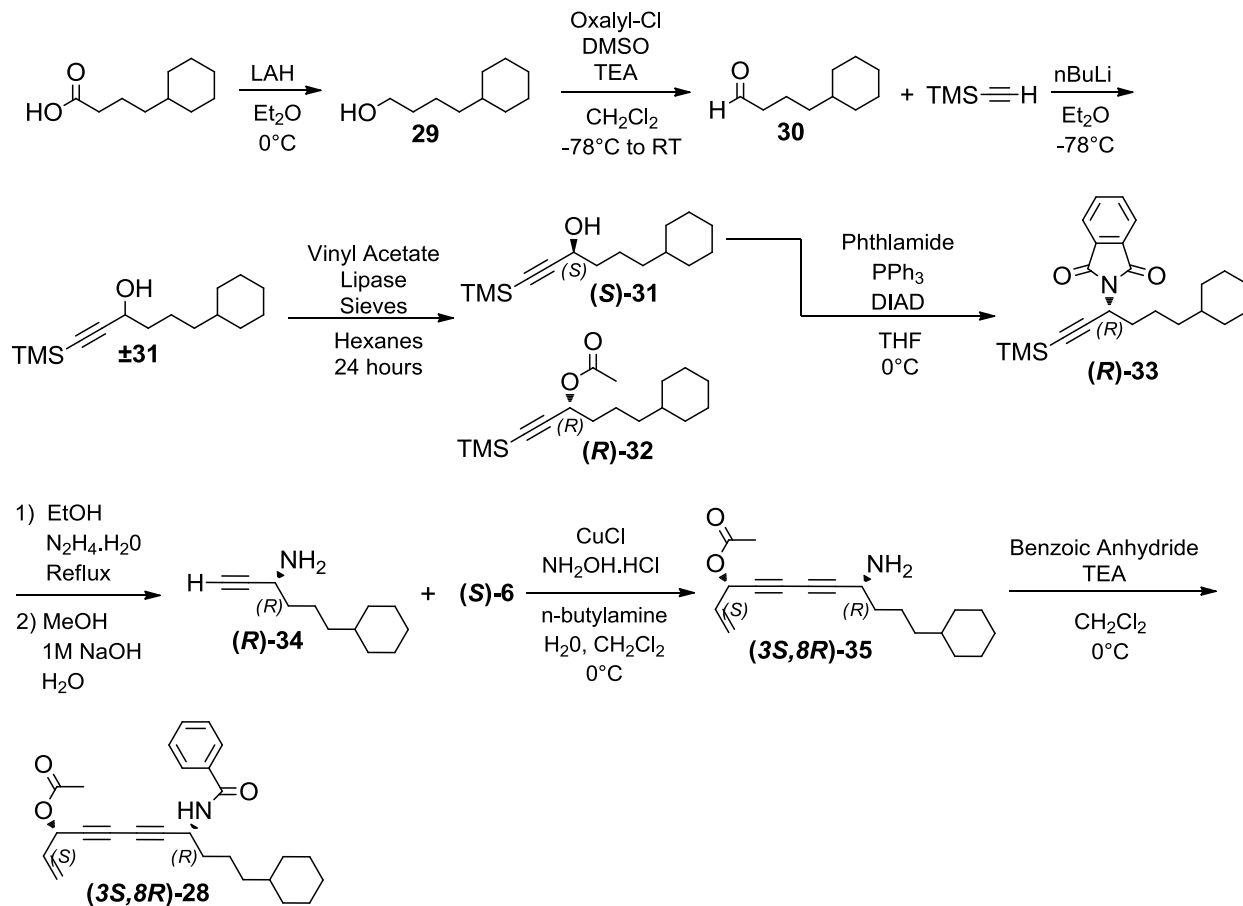
Scheme 2.7

With the presence of the phenyl ring in Compound **13**, it was amenable to analysis via the Topliss Operational Scheme in an effort to determine how the aromatic lipophilicity and electronic parameters affect antileishmanial potency. According to the first step of the Topliss Scheme, our goal was to synthesize the 4-chloro; 3,4-dichloro; 4-methyl; and 4-methoxy derivatives of Compound **13**.<sup>22</sup> This synthesis was straightforward as all four compounds could easily be synthesized via reaction of **11** with the appropriate aromatic acid chloride as shown in Scheme 2.8.



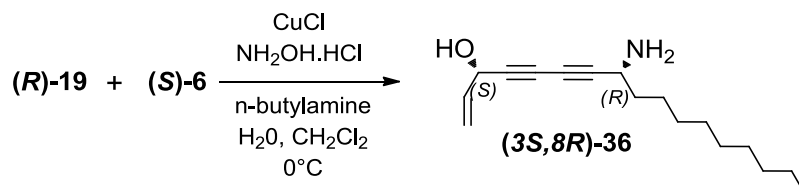
Scheme 2.8

Since previous studies<sup>146,147,148</sup> involving miltefosine analogues have shown that introducing cycloalkanes into the alkyl chain has resulted in an increase in antileishmanial potency, we decided to synthesize Compound **28** which is an analogue of Compound **13** with a cyclohexane ring in the lipophilic chain. To synthesize Compound **28** (Scheme 2.9), we started by converting cyclohexanebutyric acid into its aldehyde (**30**) form via LAH reduction followed by a Swern Oxidation. The TMS acetylene group was then added followed by enzymatic resolution of the resultant alcohol. The alcohol (*S*)-**31** was then subjected to a Mitsunobu reaction with phthalimide followed by hydrazinolysis and methanolysis to yield (*R*)-**34**. (*R*)-**34** was then coupled with (*S*)-**2** which afforded (*3S,8R*)-**35**. Treating (*3S,8R*)-**35** with benzoic anhydride and TEA in CH<sub>2</sub>Cl<sub>2</sub> yielded Compound **28**.



Scheme 2.9

The final compound included in our third round of SAR evaluation was Compound **36** which is an analogue of **16** in which the C-8 hydroxyl group of **16** is replaced by an amino group. This compound was readily available via the Cadiot-Chodkiewicz coupling of (*S*)-**6** and (*R*)-**19** (Scheme 2.10).



Scheme 2.10

### 2.4.2 Antileishmanial Activity of Third Round SAR Compounds

Compound	IC <sub>50</sub> <i>L. donovani</i> in infected macrophages [uM]
(3 <i>S</i> ,8 <i>R</i> )-21	0.005
(3 <i>S</i> ,8 <i>R</i> )-23	0.003
(3 <i>S</i> ,8 <i>R</i> )-24	0.112
(3 <i>S</i> ,8 <i>R</i> )-25	0.428
(3 <i>S</i> ,8 <i>R</i> )-26	0.126
(3 <i>S</i> ,8 <i>R</i> )-27	0.165
(3 <i>S</i> ,8 <i>R</i> )-28	0.027
(3 <i>S</i> ,8 <i>R</i> )-36	0.040

Table 2.7: Biological activity of third round SAR compounds against *L. donovani* in infected macrophages.

As shown in Table 2.7, antileishmanial activity was significantly increased in Compounds **21** and **23** as their IC<sub>50</sub> values were 0.005uM and 0.003uM respectively which represents 64-fold and 107-fold increases in potency respectively as compared to the 0.32uM IC<sub>50</sub> value of the natural product as reported by Senn.<sup>1</sup> Thus we were successful in increasing potency by combining the most potent functional groups from the second round SAR study at the C-3 and C-8 positions.

Potency Rank	Substituent	IC <sub>50</sub> <i>L. donovani</i> in infected macrophages [uM]	Compound
1	H	0.035	(3 <i>S</i> ,8 <i>R</i> )-13
2	4-Cl	0.112	(3 <i>S</i> ,8 <i>R</i> )-24
3	4-CH <sub>3</sub>	0.126	(3 <i>S</i> ,8 <i>R</i> )-26
4	4-OCH <sub>3</sub>	0.165	(3 <i>S</i> ,8 <i>R</i> )-27
5	3,4-dichloro	0.428	(3 <i>S</i> ,8 <i>R</i> )-25

Table 2.8: Biological activity of Topliss scheme compounds against *L. donovani* in infected macrophages.

The Topliss scheme compounds **24-27** all had higher IC<sub>50</sub> values (Table 2.8) than the parent compound **13**. This indicates that the hydrogen atom in the aromatic 4-position is superior to our four new analogues with functional groups in the 4-position. This could indicate that there is a negative steric interaction caused by substituents in the



4-position. The negative steric hindrance hypothesis is further supported by the fact that the 3,4-dichloro compound is significantly less active than the other compounds which could be the result of the increased steric hindrance by having a Cl atom in both the 3-position and 4-position. Unfortunately, as shown in Table 2.9 in the far right column, when the 4-hydrogen compound has the highest potency, the Topliss scheme does not provide detailed conclusions regarding the importance of the different electronic and lipophilic parameters of the aromatic ring. If the 4-hydrogen compound has the highest potency, Topliss recommends synthesizing a group of analogues with substituents in the 3-position. The 3-position compounds are discussed in Section 2.5.

Substituents	Parameters									$E_s^a$
	$\pi$	$2\pi - \pi^2$	$\sigma$	$-\sigma$	$\pi + \sigma$	$2\pi - \sigma$	$\pi - \sigma$	$\pi - 2\sigma$	$\pi - 3\sigma$	
3,4-Cl <sub>2</sub>	1	1-2	1	5	1	1	1-2	3-4	5	2-5
4-Cl	2	1-2	2	4	2	2-3	3	3-4	3-4	2-5
4-CH <sub>3</sub>	3	3	4	2	3	2-3	1-2	1	1	2-5
4-OCH <sub>3</sub>	4-5	4-5	5	1	5	4	4	2	2	2-5
H	4-5	4-5	3	3	4	5	5	5	3-4	1

<sup>a</sup> Unfavorable steric effect from 4 substitution.

Table 2.9: Potency order table for Topliss Scheme.<sup>145</sup>

The cyclohexane derivative **28** had an antileishmanial IC<sub>50</sub> value of 0.027uM as compared to 0.035uM IC<sub>50</sub> of the straight chain compound **13**. This represents a slight increase in potency with the introduction of the cyclohexane group yet the increase was not marked enough for us to explore more cycloalkane derivatives at this time. We are aware though that the analysis of one cycloalkane compound certainly does not provide conclusive evidence concerning the potency of straight chain versus cycloalkane derivatives.

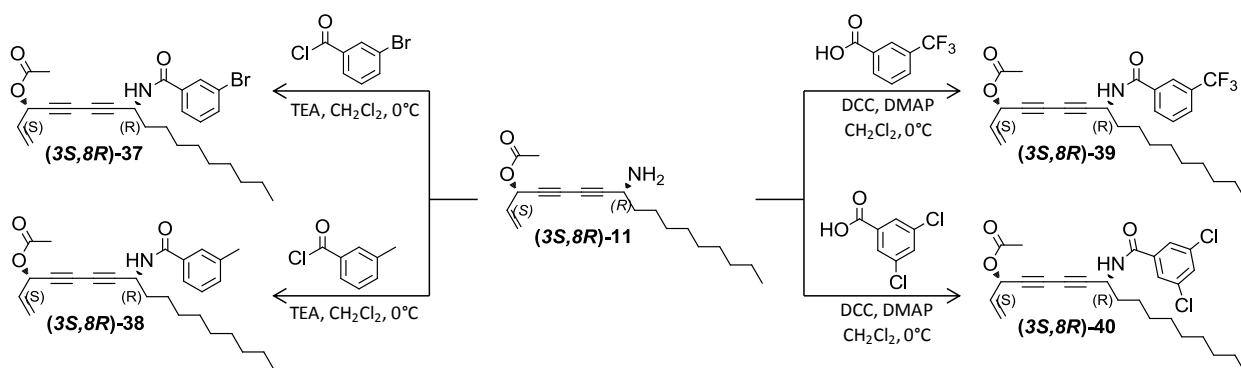
The C-8 amino compound **36** had an IC<sub>50</sub> value of 0.040uM which represent a decrease in potency as compared to the 0.013uM IC<sub>50</sub> value of the related C-8 alcohol compound **13**. Compound **36** is also closely related to compound **23** as compound **36** is

a primary amine whereas **23** is a secondary amine with an n-butyl group on the nitrogen atom. Compound **36** had a 13-fold decrease in potency as compared to **23**.

## 2.5 Fourth Round of SAR studies

### 2.5.1 Synthesis of fourth round SAR compounds

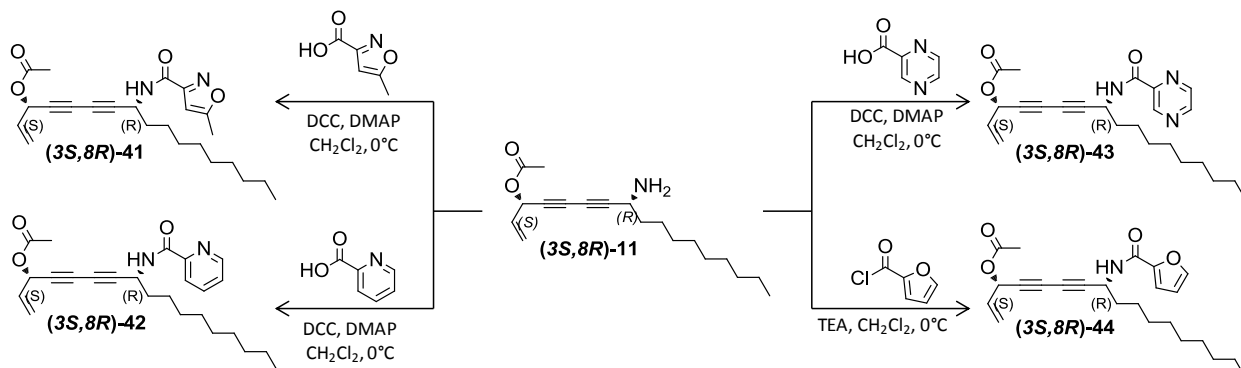
The first set of analogues from our fourth round were prepared in accordance with the second level of the Topliss scheme recommendations. Since the 4-hydrogen analogue of **13** had the most potency, the Topliss scheme calls for the following four compounds to be prepared: 3-Cl, 3-CH<sub>3</sub>, 3-CF<sub>3</sub>, and 3,5-Cl<sub>2</sub>. In addition, the scheme says the 3-Br and 3-NH<sub>2</sub> analogues may help provide insight as well. We started by preparing compounds **37-40** which are the 3-Br, 3-CH<sub>3</sub>, 3-CF<sub>3</sub>, and 3,5-Cl<sub>2</sub> analogues. Unfortunately, we had an error in our VWR chemical order and did not receive the acid chloride to prepare the 3-Cl analogue which can easily be prepared at a later date. The analogues we did prepare were readily available via amide bond formation between **11** and the appropriate aromatic acid chloride or carboxylic acid (Scheme 2.11).



Scheme 2.11

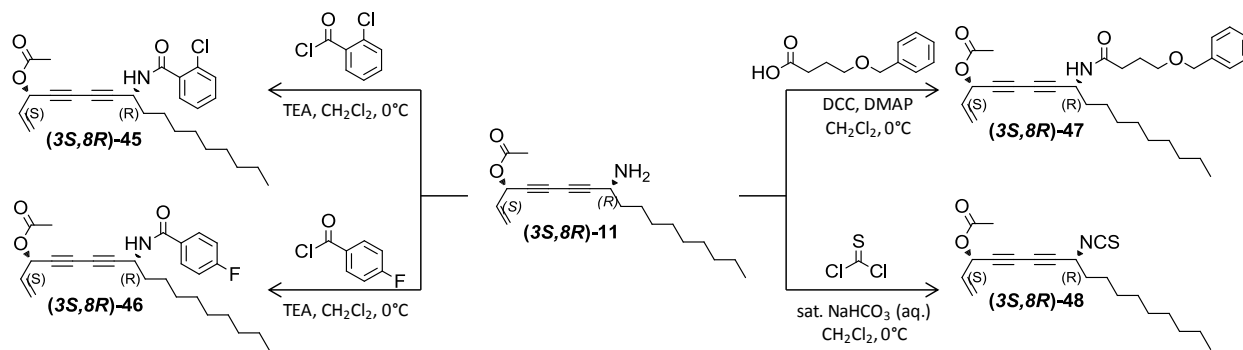
The second set of analogues from the fourth round consisted of compounds in which the phenyl ring in **13** was replaced with a heteroaromatic ring. In place of the

phenyl ring, Compounds **41-44** had a 5-methyl isoxazole ring, a 2-pyridine ring, a pyrazine ring, and a 2-furan ring respectively. Like Compounds **37-40**, Compounds **41-44** were readily available via amide bond formation between **11** and the appropriate aromatic acid chloride or carboxylic acid (Scheme 2.12).



**Scheme 2.12**

The final set of analogues from the fourth round consisted of three more amides and an isocyanate all derived from compound **11** (Scheme 2.13). Compound **45** was synthesized to assess the impact of a chlorine atom in the 2-position of the phenyl ring. Since the first set of Topliss structures discussed above in SAR Round 3 showed that there may be a negative steric impact by any substituent in the 4-position of the phenyl ring, we decided to synthesize Compound **46** with a fluorine atom in the 4-position as the fluorine atom is sterically smaller than the previous substituents. Compound **47** was synthesized to evaluate placing a four carbon ethereal linkage between the phenyl ring and the amide group. Compound **48** has an isocyanate group at the C-8 position. The isocyanate group is in Cluster 6 of the Hansch Cluster table shown above and Compound **48** was the first compound synthesized from this cluster.



Scheme 2.13

### 2.5.2 Antileishmanial activity of fourth round SAR compounds

Compound	IC <sub>50</sub> <i>L. donovani</i> in infected macrophages [uM]
(3 <i>S</i> ,8 <i>R</i> )-37	0.184
(3 <i>S</i> ,8 <i>R</i> )-38	0.120
(3 <i>S</i> ,8 <i>R</i> )-39	0.191
(3 <i>S</i> ,8 <i>R</i> )-40	0.252
(3 <i>S</i> ,8 <i>R</i> )-41	0.077
(3 <i>S</i> ,8 <i>R</i> )-42	0.089
(3 <i>S</i> ,8 <i>R</i> )-43	0.042
(3 <i>S</i> ,8 <i>R</i> )-44	0.050
(3 <i>S</i> ,8 <i>R</i> )-45	0.109
(3 <i>S</i> ,8 <i>R</i> )-46	0.072
(3 <i>S</i> ,8 <i>R</i> )-47	0.529
(3 <i>S</i> ,8 <i>R</i> )-48	21.65

Table 2.10: Biological activity of fourth-round SAR compounds against *L. donovani* in infected macrophages.

Table 2.10 shows the results of the anti-*Leishmania* testing done of the fourth-round SAR compounds. Analogous to the third round SAR Topliss scheme compounds, the four compounds prepared in the fourth round SAR for the Topliss scheme all had lower IC<sub>50</sub> values than the parent compound **13** (Table 2.11). Once again, this could

indicate a negative steric interaction due to the increased bulk of the substituents in the 3-position. A difference in activity is observed between the dichloro compounds as the 3,5-dichloro compound (Compound **40**) had an IC<sub>50</sub> value of 0.252 uM whereas the 3,4-dichloro compound (Compound **25**) had an IC<sub>50</sub> value of 0.428 uM. In contrast, the placement of the methyl group did not impact activity as the 3-CH<sub>3</sub> compound (Compound **38**) had an IC<sub>50</sub> value of 0.120 uM whereas the 4-CH<sub>3</sub> compound (Compound **26**) had an IC<sub>50</sub> value of 0.126 uM.

Potency Rank	Substituent	IC <sub>50</sub> <i>L. donovani</i> in infected macrophages [uM]	Compound
1	H	0.035	(3 <i>S</i> ,8 <i>R</i> )- <b>13</b>
2	3-CH <sub>3</sub>	0.120	(3 <i>S</i> ,8 <i>R</i> )- <b>38</b>
3	3-Br	0.184	(3 <i>S</i> ,8 <i>R</i> )- <b>37</b>
4	3-CF <sub>3</sub>	0.191	(3 <i>S</i> ,8 <i>R</i> )- <b>39</b>
5	3,5-dichloro	0.252	(3 <i>S</i> ,8 <i>R</i> )- <b>40</b>

**Table 2.11: Biological activity of Topliss scheme compounds against *L. donovani* in infected macrophages.**

The substitution of a heteroaromatic ring in place of the phenyl ring in **13** did not have a large impact on the antileishmanial activity of the compound as shown in Table 2.12. Compound **13** had the lowest IC<sub>50</sub> value of the five compounds tested and the IC<sub>50</sub> range of the five compounds was 0.035-0.089uM. Though the substitution of the phenyl ring for heteroaromatic rings did not improve antileishmanial activity, it also did not drastically reduce antileishmanial activity as evidenced by the narrow range of IC<sub>50</sub> values for the five compounds.

Potency Rank	Aromatic Ring	IC <sub>50</sub> <i>L. donovani</i> in infected macrophages [uM]	Compound
1	Phenyl	0.035	(3 <i>S</i> ,8 <i>R</i> )-13
2	Pyrazine	0.042	(3 <i>S</i> ,8 <i>R</i> )-43
3	2-furan	0.050	(3 <i>S</i> ,8 <i>R</i> )-44
4	5-methyl isoxazole	0.077	(3 <i>S</i> ,8 <i>R</i> )-41
5	2-pyridine	0.089	(3 <i>S</i> ,8 <i>R</i> )-42

**Table 2.12: Biological activity of heteroaromatic compounds against *L. donovani* in infected macrophages. Compound 13 is shown for comparison.**

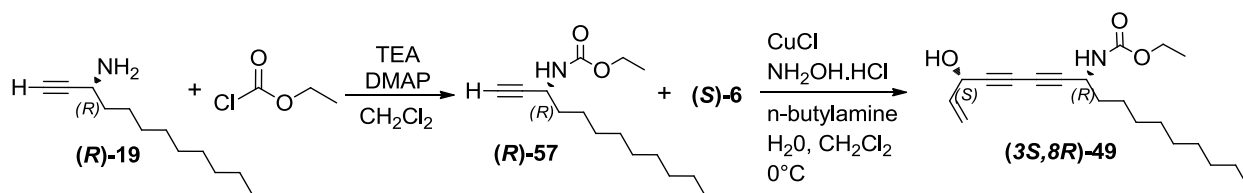
Although Compounds **45** and **46** were not part of the Topliss operational scheme at this point, their IC<sub>50</sub> values can be meaningfully compared to the Topliss structures prepared thus far. Compounds **45** and **46** both had higher IC<sub>50</sub> values than Compound **13** but Compounds **45** and **46** had lower IC<sub>50</sub> values than all of the other eight Topliss structures prepared. Compound **45** had an IC<sub>50</sub> value of 0.109 uM whereas Compound **46** had an IC<sub>50</sub> value of 0.072 uM. The IC<sub>50</sub> value of Compound **45** is very similar to the IC<sub>50</sub> value of 0.112 uM for Compound **24** which has the 4-chloro substituent. This indicates that replacing a hydrogen atom in Compound **13** with a chlorine atom at either the meta or para position has a similar negative impact on antileishmanial activity. The para fluorine atom of Compound **46** also caused an increase in IC<sub>50</sub> value as compared with Compound **13**. However, Compound **46** did retain more antileishmanial activity as compared to all of the other Topliss structures prepared. This supports the hypothesis that it could be a negative steric interaction at the para position that is causing the decrease in antileishmanial activity rather than the decrease being caused by other parameters such as lipophilicity or electronic effects.

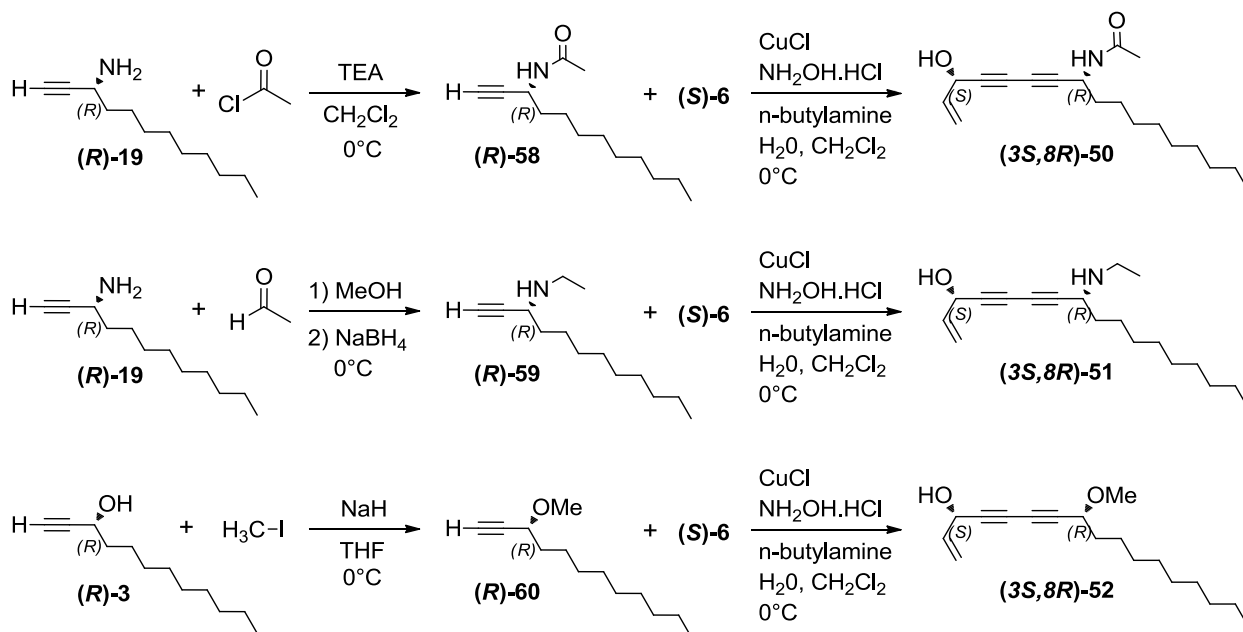
The ethereal linkage of Compound **47** caused a dramatic reduction in antileishmanial activity as Compound **47** had an IC<sub>50</sub> value that was 15-fold higher than Compound **13**. The introduction of the isothiocyanate group of Compound **48** caused an even more dramatic reduction in activity as its IC<sub>50</sub> value was over 600-fold higher than Compound **13**.

## 2.6 Fifth round of SAR studies

### 2.6.1 Synthesis of fifth round SAR compounds

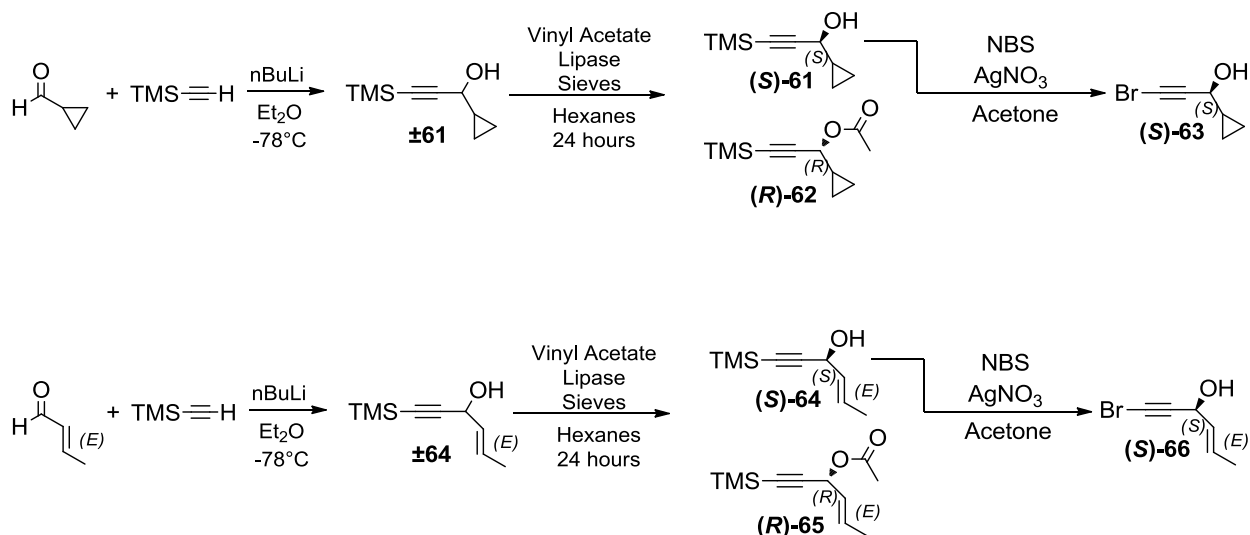
The fifth and final round of SAR compounds prepared involved the synthesis of four compounds with different C-8 substituents and four compounds with different groups at the alkene position of the natural product. The four groups installed at the C-8 position were the carbamate, the acetamide, the ethylamino, and the methyl ether groups of Compounds **49-52** respectively (Scheme 2.14). The alkene position was changed to a cyclopropyl group in Compound **53**, a methyl substituted alkene in Compound **54**, a phenyl group in Compound **55**, and a para-ethoxy phenyl group in Compound **56**. The synthetic routes to Compounds **49-52** were similar as they all involved the synthesis of their respective terminal alkyne right-hand portion of the molecule followed by the Cadiot-Chodkiewicz coupling to the previously prepared bromoalkyne **S-6**.



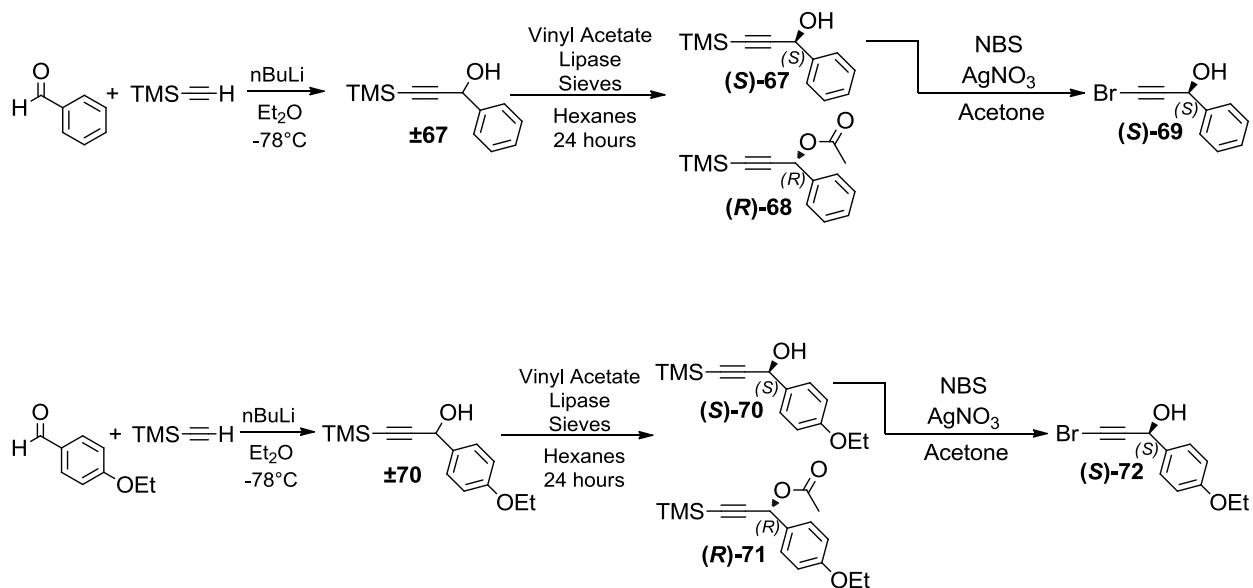


**Scheme 2.14**

The synthetic routes to Compounds **53-56** (Scheme 2.15) were also similar as they each involved the reaction of TMS-acetylene with the appropriate aldehyde followed by enzymatic resolution and bromination







Scheme 2.15

Cadiot-Chodkiewicz coupling of bromoalkynes (*S*)-63, (*S*)-66, (*S*)-69, and (*S*)-72 with the previously prepared (*R*)-22 yielded Compounds 53-56 respectively (Figure 2.6).

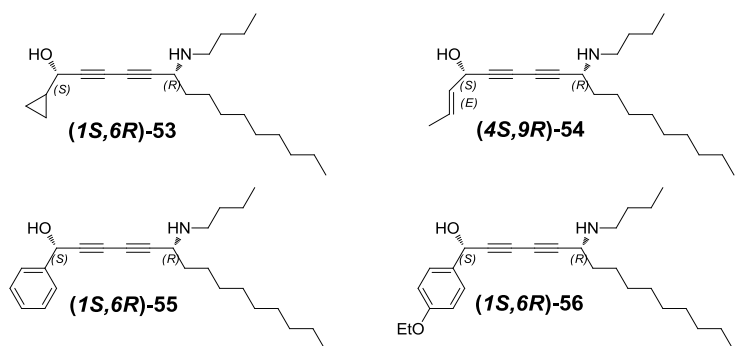


Figure 2.6: Structures of compounds 53-56.

### 2.6.2 Antileishmanial activity of fifth round SAR compounds

Compound	IC <sub>50</sub> <i>L. donovani</i> in infected macrophages [uM]
(3 <i>S</i> ,8 <i>R</i> )-49	0.010
(3 <i>S</i> ,8 <i>R</i> )-50	0.018
(3 <i>S</i> ,8 <i>R</i> )-51	0.030
(3 <i>S</i> ,8 <i>R</i> )-52	0.011
(1 <i>S</i> ,6 <i>R</i> )-53	0.722
(4 <i>S</i> ,9 <i>R</i> )-54	0.031
(1 <i>S</i> ,6 <i>R</i> )-55	0.113
(1 <i>S</i> ,6 <i>R</i> )-56	0.443

**Table 2.13: Biological activity of fifth-round SAR compounds against *L. donovani* in infected macrophages.**

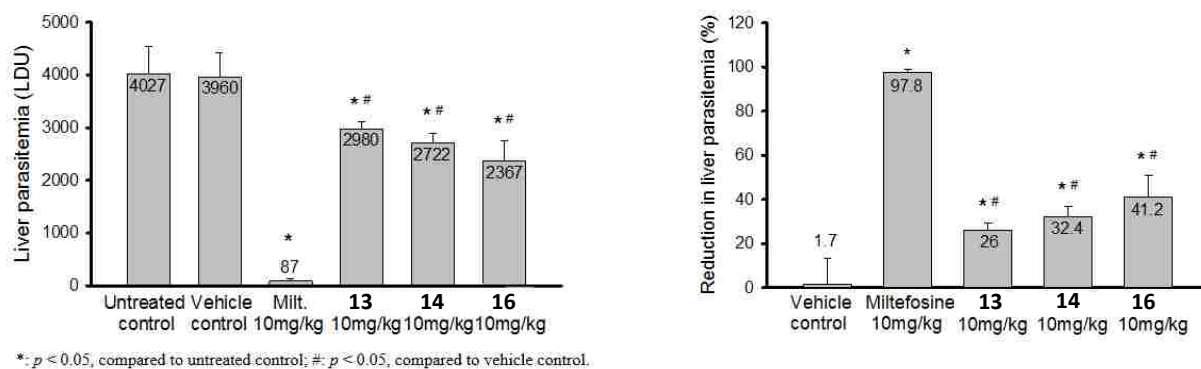
Table 2.13 shows the results of the anti-*Leishmania* testing done of the fifth-round SAR compounds. Compounds **49-52** all retained potent antileishmanial activity as the IC<sub>50</sub> values ranged from 0.010-0.030 uM. Although still potent, these IC<sub>50</sub> values represent a decrease in activity as compared with the closely related Compound **23** which had an IC<sub>50</sub> value of 0.003 uM. Changing the butylamino group of Compound **23** to the ethylamino group of Compound **51** caused a 10-fold reduction in antileishmanial activity. Compounds **50** and **51** have relatively similar IC<sub>50</sub> values indicating the interchanging of an amide for an amine at the C-8 position does not have a significant effect on antileishmanial activity.

Whereas Compounds **49-52** had a narrow range of IC<sub>50</sub> values, Compounds **53-56** had a wide range of antileishmanial activity with IC<sub>50</sub> values ranging from 0.031-0.722uM. All four compounds had higher IC<sub>50</sub> values than Compound **23**. The wide range indicates the importance of the functional group at the alkene position. The installation of the methyl group onto the alkene in Compound **54** caused a 10-fold

reduction in antileishmanial activity as compared to Compound **23**. Switching the alkene to a cyclopropyl group in Compound **53** caused a whopping 240-fold decrease in antileishmanial activity. Switching the alkene to a phenyl group (Compound **55**) caused a 38-fold decrease in activity whereas the inclusion of a para-ethoxy phenyl group (Compound **56**) caused a 148-fold decrease in activity. These data demonstrate the importance of the alkene position to the antileishmanial activity of the analogues. It was expected that changes at the alkene position could lead to dramatic changes in antiprotozoal activity as Senn and colleagues showed that Compound **MS-1** had significantly less antiprotozoal activity than **MS-2**. The only difference between **MS-1** and **MS-2** is the presence of the alkene in **MS-2** that is absent in **MS-1**.

## 2.7 *In Vivo* evaluation

Compounds **13**, **14**, and **16** were evaluated for *in vivo* efficacy in BALB/c mice infected with *Leishmania donovani*. As can be seen in Figure 2.6 below, all three compounds significantly reduced the liver parasite load as compared to the untreated control and the vehicle control. Miltefosine was evaluated in the same study for comparison purposes. Whereas Miltefosine treatment led to a 97.8% reduction in liver



**Figure 2.6** *In Vivo* results from testing of compounds **13**, **14**, and **16** in BALB/c mice infected with *Leishmania donovani*.

parasitemia, compounds **13**, **14**, and **16** led to reductions of 26.0%, 32.4%, and 41.2% respectively.

## 2.8 Cytotoxicity

Table 2.14 shows the antileishmanial testing results for all of the compounds we had tested. The table also shows IC<sub>50</sub> values for our compounds which were screened against non-infected J774 macrophages. The selectivity index value was calculated by dividing the IC<sub>50</sub> value against the J774 cell line by the IC<sub>50</sub> value against the *Leishmania* species assayed. When looking at a series of compounds, the ones with the higher selectivity index values often represent the more promising drug candidates as the high selectivity values indicate the ability of a compound to damage or destroy the parasite while having minimal impact on the healthy cells of the host. As can be seen in the table, compound **23** has the highest selectivity index value at 116.3. This is a marked improvement (greater than 1000-fold) as compared to the 0.1 selectivity index value for **(3*S*,8*R*)-1** which has the same stereochemistry as compound **23**. Another intriguing comparison is seen in the selectivity index values of compounds **9** and **10** which are 18.3 and 0.2 respectively. This signifies that compound **9** is more than 90 times more selective than compound **10**. The only difference in their structures is that compound **9** has an n-butyl side chain whereas compound **10** has an n-hexadecyl side chain. Interestingly, the IC<sub>50</sub> values of **9** and **10** against *Leishmania donovani* are similar with values of 0.197 uM and 0.287 uM respectively. The selectivity difference thus arises from their significantly differing IC<sub>50</sub> values against the non-infected J774 macrophage

cell line with values of 3.61  $\mu\text{M}$  and 0.05  $\mu\text{M}$  for compounds **9** and **10** respectively. This indicates the promising prospect that it could be possible to reduce the cytotoxicity of other compounds of ours without reducing their antileishmanial activity, thus increasing their selectivity index. For example, it would be interesting to modify compound **23** so that it contains an n-butyl side chain instead of the n-decyl side chain. Ideally, this change would result in decreased cytotoxicity against the J774 macrophage cell line while maintaining its potent activity against *Leishmania*.

Compound	<i>Leishmania sp.</i> IC <sub>50</sub> (uM) <sup>a</sup>	J774 IC <sub>50</sub> (uM)	Selectivity Index <sup>b</sup>
(3 <i>S</i> ,8 <i>R</i> )-1	0.63	0.056	0.1
(3 <i>S</i> ,8 <i>S</i> )-1	1.28	0.209	0.2
(3 <i>R</i> ,8 <i>R</i> )-1	>10	3.25	N/A
(3 <i>R</i> ,8 <i>S</i> )-1	>10	5.81	N/A
9	0.197	3.610	18.3
10	0.287	0.050	0.2
12	0.055	NT	N/A
13	0.035	NT	N/A
14	0.034	1.460	42.9
15	0.061	0.652	10.7
16	0.013	NT	N/A
21	0.005	0.131	26.2
23	0.003	0.349	116.3
24	0.112	0.983	8.8
25	0.428	1.220	2.9
26	0.126	1.486	11.8
27	0.165	1.327	8.0
28	0.027	0.393	14.6
37	0.184	0.676	3.7
38	0.120	0.596	5.0
39	0.191	0.700	3.7
40	0.252	0.721	2.9
41	0.077	0.515	6.7
42	0.089	0.673	7.6
43	0.042	0.359	8.5
44	0.050	0.388	7.8
45	0.109	0.674	6.2
46	0.072	0.805	11.2
47	0.529	1.113	2.1
48	21.65	NT	N/A
49	0.010	NT	N/A
50	0.018	NT	N/A
51	0.030	NT	N/A
52	0.011	NT	N/A
53	0.722	NT	N/A
54	0.031	NT	N/A
55	0.113	NT	N/A
56	0.443	NT	N/A
<sup>a</sup> The four stereoisomers of compound <b>1</b> were screened against <i>Leishmania amazonensis</i> . All other compounds were screened against <i>Leishmania donovani</i> .			
<sup>b</sup> Selectivity Index = IC <sub>50</sub> J744 / IC <sub>50</sub> <i>Leishmania sp.</i>			
NT = Not tested			
N/A = Not available			

**Table 2.14 Results from antileishmanial and cytotoxicity assays.**

**Chapter 3:** *Anticancer evaluation of natural product analogues*

### 3.1 Compounds possessing antiprotozoal and anticancer activity

There are many reported examples of antileishmanial compounds that also possess significant anticancer activity. As discussed in chapter 1, Miltefosine was originally developed as an anticancer compound before its antileishmanial activity was serendipitously discovered. Another example is Kahalalide F (Figure 3.1) which is currently in Phase II clinical trials for treatment of prostate cancer and has also shown potent antileishmanial activity.<sup>149</sup> A third example is the series of dihydroartemisinin acetal dimers synthesized by Slade and colleagues. Their compound shown in Figure 3.2 had an  $IC_{50}$  value of 2.5  $\mu$ M against *L. donovani* and  $IC_{50}$  values of 0.24  $\mu$ M, 0.16  $\mu$ M, and 0.08  $\mu$ M against cancer cell lines SK-MEL (human malignant melanoma), KB (human epidermal carcinoma), and BT-549 (human ductal breast carcinoma) respectively.<sup>150</sup>

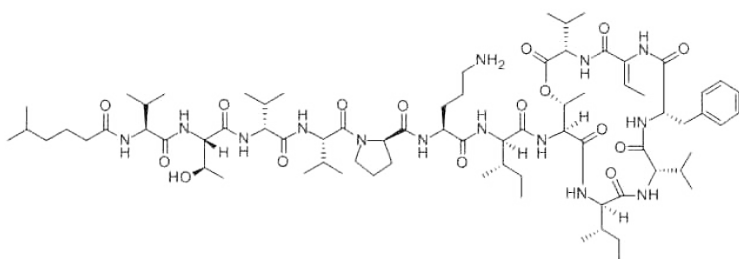


Figure 3.1: Kahalalide F

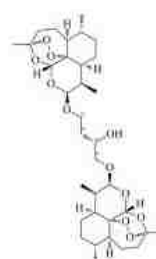


Figure 3.2: Dihydroartemisinin dimer prepared by Slade and colleagues.<sup>2</sup>

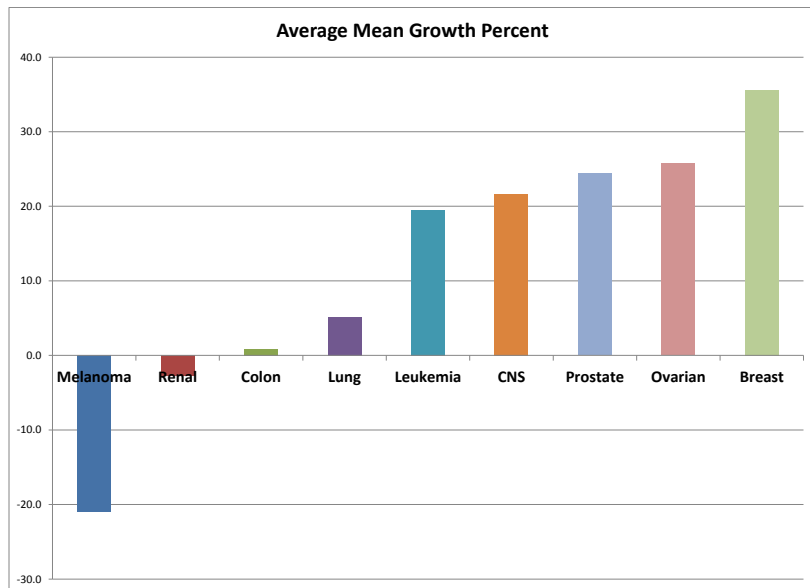
In addition to the examples discussed above, there are numerous other literature reports of compounds which possess both potent antiprotozoal and anticancer activity.<sup>151,152</sup>

For this reason, we sought the collaborative efforts of the National Cancer Institute (NCI) to test our compounds for anticancer activity. The NCI screened twenty-four of our compounds for biological activity against the cell lines in their NCI60 one-dose first-level screening process and numerous of these compounds were chosen by NCI



to move on to advanced levels of screening. As the NCI60 one-dose screen involves each compound being tested against approximately sixty cell lines at a 10  $\mu$ M concentration, this testing produced a large volume of data and showed that many of our compounds possess potent anti-neoplastic activity. The goal of this chapter is to highlight the conclusions gleaned from the testing done by the NCI.

Cancer Type	Average Mean Growth Percent
Melanoma	-21.0
Renal	-2.7
Colon	0.9
Lung	5.2
Leukemia	19.5
CNS	21.7
Prostate	24.4
Ovarian	25.7
Breast	35.6



**Figure 3.3**

The compounds tested exhibited a wide range of activity against the numerous cell lines screened. Figure 3.3 shows the average mean growth percents of the compounds against the different types of cancers screened. A lower mean growth percent correlates with increased anticancer activity. As can be seen in the figure, melanoma cell lines were most susceptible to our compounds with an average mean growth percent of -21.0. Against the renal cancer, colon cancer, and lung cancer cell lines tested, the compounds had average mean growth percents of around zero with values of -2.7, 0.9, and 5.2 respectively. Against the breast cancer, CNS cancer, leukemia, ovarian cancer,

and prostate cancer, the average mean growth percents ranged from 19.5 to 35.6. Figure 3.3 shows a superficial view of the anticancer activity as there is much information to be gleaned when looking deeper into the results at the individual cell lines tested in each cancer type category.

Compound ID	Mean Growth Percent
16	-55.3
12	-53.3
(3 <i>S</i> ,8 <i>R</i> )-1	-49.3
10	-47.5
15	-44.5
(3 <i>S</i> ,8 <i>S</i> )-1	-35.9
43	-27.9
41	-23.4
44	-19.9
42	-8.7
13	-8.3
47	-5.5
45	-1.7
14	5.1
46	14.6
38	20.8
37	41.5
11	49.0
39	61.8
40	74.4
(3 <i>R</i> ,8 <i>R</i> )-1	86.3
(3 <i>R</i> ,8 <i>S</i> )-1	91.6
48	96.2
9	104.9

Table 3.1: Mean growth percent values (listed in order of most active to least active) for each of our compounds against the cell lines screen in the NCI60 cancer cell panel.

### 3.2 Stereochemistry

Upon analyzing the growth percent values (Table 3.1) of each of our compounds screened at the NCI, the first obvious conclusion is that the stereochemistry of our lead

compound is extremely important and follows the same activity profile as seen in the antiLeishmanial activity profile. Compounds **(3S,8R)-1** and **(3S,8S)-1** showed significant anticancer activity whereas the **(3R,8R)-1** and **(3R,8S)-1** showed very little activity. In the NCI60 one-dose screen, **(3S,8R)-1** and **(3S,8S)-1** had mean growth percents of -49.26 and -35.88 respectively. In contrast, the mean growth percents of **(3R,8R)-1** and **(3R,8S)-1** were 86.25 and 91.59 respectively. When the results from individual cell lines are analyzed, the importance of the stereochemistry is even more striking. For example, in the lung cancer cell line HOP-62, the growth percents for **(3S,8R)-1** and **(3S,8S)-1** are -93.3 and -84.7 respectively whereas **(3R,8R)-1** and **(3R,8S)-1** had growth percents of 96.3 and 107.9 respectively.

Interestingly, there was one cell line in the panel where the stereochemistry appeared to be relatively unimportant. The MALME-3M melanoma line was similarly inhibited by all four stereoisomers of compound **1** with growth percent values ranging from -46.9 to -62.0 (Table 3.2). This was the only cell line tested in which **(3R,8R)-1** and **(3R,8S)-1** had negative growth percents. The unique activity against this cell line is highlighted by the narrow range of 15.1 between the highest and lowest growth percents across the four stereoisomers. The average range of growth percents for these stereoisomers against all other cell lines was 140.8. Following the range of 15.1 against the MALME-3M cell line, the next lowest range was 60.2 against the MCF7 breast cancer cell line (Table 3.2). The highest range of 213.2 was observed against the COLO205 colon cancer cell line (Table 3.2).

MALME-3M (Melanoma)		MCF7 (Breast Cancer)		COLO205 (Colon Cancer)	
Compound	Growth Percent	Compound	Growth Percent	Compound	Growth Percent
(3 <i>S</i> ,8 <i>S</i> )-1	-62.0	(3 <i>S</i> ,8 <i>R</i> )-1	19.8	(3 <i>S</i> ,8 <i>R</i> )-1	-92.5
(3 <i>S</i> ,8 <i>R</i> )-1	-59.8	(3 <i>S</i> ,8 <i>S</i> )-1	33.3	(3 <i>S</i> ,8 <i>S</i> )-1	-84.4
(3 <i>R</i> ,8 <i>R</i> )-1	-57.0	(3 <i>R</i> ,8 <i>R</i> )-1	49.7	(3 <i>R</i> ,8 <i>R</i> )-1	117.8
(3 <i>R</i> ,8 <i>S</i> )-1	-46.9	(3 <i>R</i> ,8 <i>S</i> )-1	80.0	(3 <i>R</i> ,8 <i>S</i> )-1	120.7
<b>Range</b>	<b>15.1</b>	<b>Range</b>	<b>60.2</b>	<b>Range</b>	<b>213.2</b>

Table 3.2

### 3.3 Lipophilicity

Compound	Carbon Chain Length	MALME-3M Growth Percent	COLO205 Growth Percent
<b>10</b>	16	-71.0	-97.2
(3 <i>S</i> ,8 <i>R</i> )-1	10	-59.8	-92.5
<b>9</b>	4	100.4	121.6
	<b>Range</b>	<b>171.4</b>	<b>218.8</b>

Table 3.3

Whereas the stereochemistry was unimportant for activity against the MALME-3M cell line, the lipophilicity was shown to be very important. Compounds (3*S*,8*R*)-1, **9**, and **10** have the same functional groups and stereochemistry but different length carbon chains with lengths of ten carbons, four carbons, and sixteen carbons respectively. The growth percents against MALME-3M for (3*S*,8*R*)-1, **9**, and **10** are -59.8, 100.4, and -71.0 respectively (Table 3.3).

In addition to the results from the MALME-3M cell line, the lipophilicity was shown to be extremely important for anticancer activity across the entire spectrum of the NCI60. Compounds (3*S*,8*R*)-1 and **10** have significant broad spectrum anticancer activity with mean growth percents of -49.3 and -47.5 respectively. The shorter carbon chain of Compound **9** causes nearly a complete loss of anticancer activity as its mean growth percent is 104.9. The importance of lipophilicity is further highlighted when looking at the results of colon cancer line COLO205 where Compound **10** has a growth

percent of -97.2 whereas Compound **9** has a growth percent of 121.6 meaning Compound **10** kills nearly all the cells and Compound **9** actually stimulates cell growth with its growth percent higher than 100.

### 3.4 Isothiocyanate

In addition to the aforementioned compounds with little anticancer activity ((**3R,8R**)-**1**, (**3R,8S**)-**1**, **9**), isothiocyanate compound **48** also had extremely low activity with a mean growth percent of 98.2. This highlights the importance of the functional group at the C-8 position as converting the C-8 group from an alcohol (Compound (**3S,8R**)-**1**) to an isothiocyanate (Compound **48**) significantly drops the anticancer activity as the mean growth percents for (**3S,8R**)-**1** and **48** are -49.3 and 98.2 respectively.

### 3.5 Analysis of different cell line categories

Cancer Type	Average Mean Growth Percent
Melanoma	-21.0
Renal	-2.7
Colon	0.9
Lung	5.2
Leukemia	19.5
CNS	21.7
Prostate	24.4
Ovarian	25.7
Breast	35.6

Figure Key	
Color	Growth Percent
Most Active	< -50
	-50 to 0
	0 to 50
Least Active	> 50

Table 3.4: Average mean growth percent values of compounds screened against each cancer cell line category.

**Chapter 4: Breast Cancer**

## Chapter 4: Breast Cancer

### 4.1 Overview

Our compounds were screened against six different breast cancer cell lines. The average mean growth percent across the six different breast cancer cell lines was 35.6. As shown in Table 4.1, the breast cancer cell lines had the highest average mean growth percent of the different cell types tested meaning that overall, our compounds were least active across the breast cancer cell lines. However, this relatively high average mean growth percent hides some of the potent activity some of our compounds exhibited against specific cell lines.

Cell Line	Average Mean Growth Percent	Molecular Classification	Clinically relevant protein expression <sup>153</sup>								Patient Age	Sex	Ethnicity
			ER	PGR	HER2	EGFR	CK5	CK8-18	CK19	CK14			
MDA-MB-231	-21.3	Normal-like/claudin-low	-	-	-	+	-	-	-	-	51	Female	Caucasian
BT-549	12.2	Normal-like/claudin-low	-	-	-	+	-	-	-	-	72	Female	Caucasian
HS 578T	47.8	Normal-like/claudin-low	-	-	-	+	-	-	-	-	74	Female	Caucasian
T-47D	51.4	Luminal	+	+	-	+	-	+	+	-	54	Female	N/A
MCF7	56.3	Luminal	+	+	-	-	-	+	ND	-	69	Female	Caucasian
MDA-MB-468	67.1	Basal-like	-	-	-	+	+	+	+	-	51	Female	Black
Average	35.6												

ER = estrogen receptor  
PGR = progesterone receptor  
HER2 = human epidermal growth factor receptor 2  
EGFR = epidermal growth factor receptor  
CK = cytokeratin  
+ = expression  
- = no expression  
ND = not determined  
N/A = data not available

"Clinically relevant protein expression" portion of table adapted from reference 153.  
Unless otherwise referenced above, cell line information was gathered from references 154-157.

Color	Growth Percent
Most Active	< -50
	-50 to 0
	0 to 50
Least Active	> 50

**Table 4.1**

Table 4.1 shows the average mean growth percent of our compounds against each of the six breast cell lines screened as well as their molecular classification, clinically relevant protein expression, and cell line source information. As shown in Table 4.1, the most activity was seen against the MDA-MB-231 cell line which is an adenomatous breast

cancer cell line derived from a 51 year-old Caucasian female. The least activity was seen against the MDA-MB-468 cell line which is also an adenomatous breast cancer cell line derived from a 51 year-old black female. Both the MDA-MB-231 line and the MDA-MB-468 line expressed receptors for epidermal growth factor (EGF) and transforming growth factor alpha (TGF- $\alpha$ ). As is shown in Table 4.1, MDA-MB-468 also expresses proteins CK5, CK8-18, and CK19 which are absent in the MDA-MB-231 cell line.

Table 4.2 shows the results for each compound against each breast cancer cell line. As discussed in section 3.3, the stereochemistry played a key role in the activity of the stereoisomers of Compound **1**. (**3S,8R**)-**1** and (**3S,8S**)-**1** had average growth percents of -25.8 and 11.9 respectively against the breast cancer cell lines screened. (**3R,8S**)-**1** and (**3R,8R**)-**1** were significantly less active with average growth percents of 91.4 and 83.3 respectively. Lipophilicity was also shown to be important as Compound **9** (4 carbon length chain), (**3S,8R**)-**1** (10 carbon length chain), and **10** (16 carbon length chain) had average growth percents of 99.4, -25.8, and -14.5 respectively.

Substituting an alcohol for the acetate at the C-3 position in (**3S,8R**)-**1** produced little change in the average growth percent as Compound **16** had an average growth percent of -21.8 as compared to -25.8 for (**3S,8R**)-**1**. Though the average growth percents were similar, Compound **16** was significantly more active against the BT-549 cell line with a growth percent of -90.9 compared to -47.2 for (**3S,8R**)-**1**. On the other hand, (**3S,8R**)-**1** was significantly more active against MDA-MB-231 with a growth percent of -93.2 as compared to -69.2 for compound **16**.



Compound ID	Breast Cancer Cell Lines						Average	Minimum	Maximum	Range
	MCF7	MDA-MB-231	HS 578T	BT-549	T-47D	MDA-MB-468				
(3 <i>R</i> ,8 <i>S</i> )-1	80.0	97.7	92.8	99.8	84.2	94.0	91.4	80.0	99.8	19.8
(3 <i>S</i> ,8 <i>R</i> )-1	19.8	-93.2	25.2	-47.2	-42.8	-16.5	-25.8	-93.2	25.2	118.4
(3 <i>R</i> ,8 <i>R</i> )-1	49.7	104.6	121.4	88.5	64.9	70.8	83.3	49.7	121.4	71.8
(3 <i>S</i> ,8 <i>S</i> )-1	33.3	-74.2	31.5	8.5	38.3	34.3	11.9	-74.2	38.3	112.4
9	105.8	109.7	95.9	98.6	94.7	91.5	99.4	91.5	109.7	18.1
10	24.9	-60.8	-2.1	-54.4	-32.4	37.7	-14.5	-60.8	37.7	98.6
11	75.8	-41.2	91.4	53.0	84.8	94.7	59.7	-41.2	94.7	135.9
12	14.4	-62.8	8.7	-56.5	-18.9	10.5	-17.4	-62.8	14.4	77.2
13	60.7	-56.5	48.5	-33.3	68.0	87.3	29.1	-56.5	87.3	143.8
14	27.1	-52.8	39.2	19.4	33.8	17.8	14.1	-52.8	39.2	92.0
15	25.2	-62.8	45.7	-39.2	-27.3	-11.3	-11.6	-62.8	45.7	108.6
16	16.2	-69.2	41.2	-90.9	-38.2	10.0	-21.8	-90.9	41.2	132.1
37	77.3	-25.6	NT	63.9	82.1	95.5	58.7	-25.6	95.5	121.1
38	71.6	-25.2	57.2	18.4	72.2	101.1	49.2	-25.2	101.1	126.4
39	75.8	15.0	NT	68.3	85.2	94.0	67.7	15.0	94.0	78.9
40	80.7	16.9	94.9	76.7	91.4	95.6	76.0	16.9	95.6	78.6
41	36.1	-32.1	21.0	-5.5	42.4	73.1	22.5	-32.1	73.1	105.1
42	76.2	-52.5	47.4	-18.8	89.2	93.2	39.1	-52.5	93.2	145.7
43	43.5	-72.5	12.6	-42.7	66.2	85.9	15.5	-72.5	85.9	158.4
44	59.2	-71.0	-4.1	-0.6	76.6	71.6	22.0	-71.0	76.6	147.6
45	76.9	-39.4	33.4	6.7	87.6	94.3	43.3	-39.4	94.3	133.7
46	74.5	-37.0	30.9	4.8	74.4	97.0	40.8	-37.0	97.0	134.0
47	61.5	-35.0	26.7	-29.1	66.2	97.7	31.3	-35.0	97.7	132.7
48	85.7	108.0	92.2	105.0	90.7	90.2	95.3	85.7	108.0	22.3
Average	56.3	-21.3	47.8	12.2	51.4	67.1				
Minimum	14.4	-93.2	-4.1	-90.9	-42.8	-16.5				
Maximum	105.8	109.7	121.4	105.0	94.7	101.1				
Range	91.4	202.9	125.5	195.9	137.6	117.6				

NT = Not Tested

Figure Key	
Color	Growth Percent
Most Active	< -50
	-50 to 0
	0 to 50
Least Active	> 50

Table 4.2

#### 4.2 Hansch Cluster Analysis on Breast Cancer Cell Lines Data

Compound ID	Cluster	Breast Cancer Cell Lines						Average	Minimum	Maximum	Range
		MCF7	MDA-MB-231	HS 578T	BT-549	T-47D	MDA-MB-468				
(3 <i>S</i> ,8 <i>R</i> )-1	5	19.8	-93.2	25.2	-47.2	-42.8	-16.5	-25.8	-93.2	25.2	118.4
11	5	75.8	-41.2	91.4	53.0	84.8	94.7	59.7	-41.2	94.7	135.9
12	4b	14.4	-62.8	8.7	-56.5	-18.9	10.5	-17.4	-62.8	14.4	77.2
13	8	60.7	-56.5	48.5	-33.3	68.0	87.3	29.1	-56.5	87.3	143.8
14	9	27.1	-52.8	39.2	19.4	33.8	17.8	14.1	-52.8	39.2	92.0
15	7	25.2	-62.8	45.7	-39.2	-27.3	-11.3	-11.6	-62.8	45.7	108.6
48	6	85.7	108.0	92.2	105.0	90.7	90.2	95.3	85.7	108.0	22.3
Average		44.1	-37.3	50.1	0.2	26.9	39.0				
Minimum		14.4	-93.2	8.7	-56.5	-42.8	-16.5				
Maximum		85.7	108.0	92.2	105.0	90.7	94.7				
Range		71.3	201.3	83.5	161.5	133.6	111.2				

Figure Key	
Color	Growth Percent
Most Active	< -50
	-50 to 0
	0 to 50
Least Active	> 50

Table 4.3

Table 4.3 shows the breast cancer testing results organized to assess the results per Hansch cluster analysis theory at the C-8 position. As shown in the table, the range of activity is wide over the six clusters tested. The alcohol compound (3*S*,8*R*)-1 from

cluster 5 was the most active compound against the MDA-MB-231, T-47D, and MDA-MB-468 cell lines while the mesyl amide compound **12** from cluster 4b was the most active against the remaining cell lines as shown in Table 4.4. Based on these results, it would make sense to synthesize more compounds with C-8 substituents from clusters 4b and 5 in an effort to seek even more active compounds. Across the whole set of breast cancer cell lines tested, compound (**3S,8R**)-**1** from cluster 5 was the most active with an average growth percent of -25.8. On the other end of the activity spectrum, the isothiocyanate compound **48** from cluster 6 was the least active compound against all of the cell lines except for the MDA-MB-468 cell line in which it was the second least active compound.

Cell Line	Most Active Cluster	C-8 Substituent	Growth Percent
MCF7	4b	-NHSO <sub>2</sub> Me	14.4
MDA-MB-231	5	-OH	-93.2
HS 578T	4b	-NHSO <sub>2</sub> Me	8.7
BT-549	4b	-NHSO <sub>2</sub> Me	-56.5
T-47D	5	-OH	-42.8
MDA-MB-468	5	-OH	-16.5

Figure Key	
Color	Growth Percent
Most Active	< -50
	-50 to 0
	0 to 50
Least Active	> 50

Table 4.4

### 4.3 Breast Cancer SAR Analysis of Amide Compounds

Eleven of the compounds we had tested by NCI have an acetate at the C-3 position and different amide functionalities with aromatic or heteroaromatic groups directly connected to the amide carbonyl group in the C-8 position as shown in Figure 4.1.

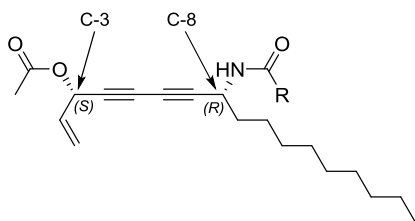


Figure 4.1 Generic structure of amides screened by NCI.

Compound ID	Breast Cancer Cell Lines						Average	Minimum	Maximum	Range
	MCF7	MDA-MB-231/ATCC	HS 578T	BT-549	T-47D	MDA-MB-468				
13	60.7	-56.5	48.5	-33.3	68.0	87.3	29.1	-56.5	87.3	143.8
37	77.3	-25.6	NT	63.9	82.1	95.5	58.7	-25.6	95.5	121.1
38	71.6	-25.2	57.2	18.4	72.2	101.1	49.2	-25.2	101.1	126.4
39	75.8	15.0	NT	68.3	85.2	94.0	67.7	15.0	94.0	78.9
40	80.7	16.9	94.9	76.7	91.4	95.6	76.0	16.9	95.6	78.6
41	36.1	-32.1	21.0	-5.5	42.4	73.1	22.5	-32.1	73.1	105.1
42	76.2	-52.5	47.4	-18.8	89.2	93.2	39.1	-52.5	93.2	145.7
43	43.5	-72.5	12.6	-42.7	66.2	85.9	15.5	-72.5	85.9	158.4
44	59.2	-71.0	-4.1	-0.6	76.6	71.6	22.0	-71.0	76.6	147.6
45	76.9	-39.4	33.4	6.7	87.6	94.3	43.3	-39.4	94.3	133.7
46	74.5	-37.0	30.9	4.8	74.4	97.0	40.8	-37.0	97.0	134.0
Average	66.6	-34.5	38.0	12.5	76.0	89.9				
Minimum	36.1	-72.5	-4.1	-42.7	42.4	71.6				
Maximum	80.7	16.9	94.9	76.7	91.4	101.1				
Range	44.6	89.4	98.9	119.3	49.0	29.5				
	NT= Not Tested									

Table 4.5

Some of the breast cancer cell lines were very sensitive to changes in the amide R group structure (Table 4.5). For example, the most active amide compound against BT-549 was Compound **43** which had a growth percent of -42.7 whereas the least active Compound **40** had a growth percent of 76.7. Of the breast cancer cell lines screened, our amide compounds had the widest range of activity against the BT-549 cell line with a range of 119.3 between the minimum and maximum growth percent.

Table 4.7 shows the R group of each compound and the corresponding BT-549 growth percent. As can be seen, incorporation of the pyrazinyl R group produced the most active compound with a growth percent of -42.7. The related 2-pyridyl compound showed a drop in activity down to a growth percent of -18.8. With a phenyl group in the R position, Compound **13** had a growth percent of -33.3. Placing groups in the 3-position of the phenyl group caused a marked reduction in activity with the 3-methyl, 3-bromo, 3-

trifluoromethyl, and 3,5-dichloro compounds having growth percents of 18.4, 63.9, 68.3, and 76.7 respectively.

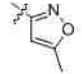
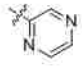
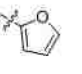
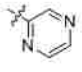

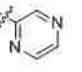
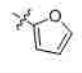
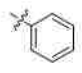
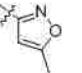

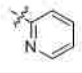
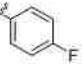
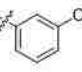
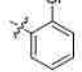
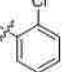
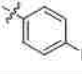
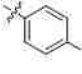
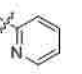
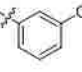
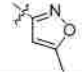
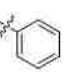
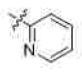
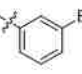
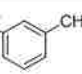
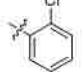
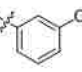
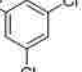
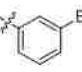
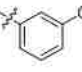
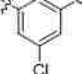

MCF7 Cell Line			MDA-MB-231 Cell Line			HS 578T Cell Line		
Compound ID	R group	MCF7 Growth Percent	Compound ID	R group	MDA-MB-231 Growth Percent	Compound ID	R group	HS 578T Growth Percent
41		36.1	43		-72.5	44		-4.1
43		43.5	44		-71.0	43		12.6
44		59.2	13		-66.5	41		21.0
13		60.7	42		-52.5	46		30.9
38		71.6	45		-39.4	45		33.4
46		74.5	46		-37.0	42		47.4
39		75.0	41		-32.1	13		48.5
42		76.2	37		-25.6	38		57.2
45		76.9	38		-25.2	40		94.9
37		77.3	39		15.0		Average	38.0
40		80.7	40		16.9		Minimum	-4.1
	Average	65.6		Average	-34.5		Maximum	94.9
	Minimum	36.1		Minimum	-72.5		Range	98.9
	Maximum	80.7		Maximum	16.9			
	Range	44.6		Range	89.4			

Table 4.6

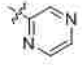
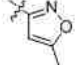

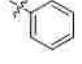
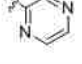

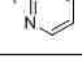
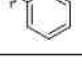
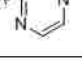


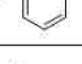

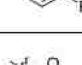
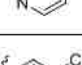
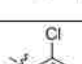
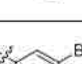
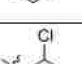
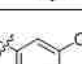
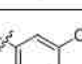
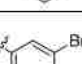
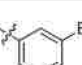
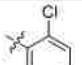
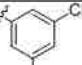
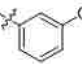
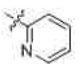

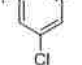
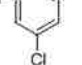
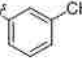
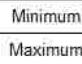
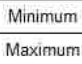
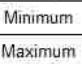
BT-549 Cell Line			T-47D Cell Line			MDA-MB-468 Cell Line		
Compound ID	R group	BT-549 Growth Percent	Compound ID	R group	T-47D Growth Percent	Compound ID	R group	MDA-MB-468 Growth Percent
43		-42.7	41		42.4	44		71.6
13		-33.3	43		66.2	41		73.1
42		-18.8	13		68.0	43		86.9
41		-5.5	38		72.2	13		87.3
44		-0.6	46		74.4	42		89.2
46		4.8	44		76.6	39		94.0
45		6.7	37		82.1	45		94.3
38		18.4	39		85.2	37		95.6
37		63.0	45		87.6	40		95.6
39		68.3	42		89.2	46		97.0
40		76.7	40		91.4	38		101.1
	Average	12.5		Average	76.0		Average	89.9
	Minimum	-42.7		Minimum	42.4		Minimum	71.6
	Maximum	76.7		Maximum	91.4		Maximum	101.1
	Range	119.3		Range	49.0		Range	29.5

Table 4.7

As shown in Table 4.6, against the MDA-MB-231 cell line, the pyrazinyl compound was once again the most active with a growth percent of -72.5. The 2-furyl compound was

nearly as active as the pyrazinyl compound with a growth percent of -71.0. Adding substituents into the 3-position of the phenyl compound once again markedly decreased activity with the phenyl, 3-bromo, 3-methyl, 3-trifluoromethyl, and 3,5-dichloro compounds having growth percents of -56.5, -25.6, -25.2, 15.0, and 16.9 respectively.

**Chapter 5: Prostate Cancer**

## Chapter 5: Prostate Cancer

### 5.1 Overview

Our compounds were screened two different prostate cancer cell lines. The average mean growth percent for all of the compounds against the two cell lines was 24.4. The two cell lines screen were DU-145 and PC-3 and their cell line characteristics and source information are shown in Table 5.1.<sup>154-162</sup> As can be seen in Table 5.1, both cell lines are androgen insensitive, possess p53 mutations, and do not express either prostate-specific antigen or 5 $\alpha$ -reductase. One difference is that the PC-3 line is more aggressive than the DU-145 line and thus the PC-3 line has higher metastatic potential. Overall, these cell lines appear relatively similar when looking at the commonly discussed characteristics shown in Table 5.1.

Cell Line	Average Mean Growth Percent	Androgen Sensitivity	PSA	5 $\alpha$ -Reductase	p53	Metastatic Potential	Isolation Site	Patient Age	Sex	Ethnicity
DU-145	13.6	AI	-	-	Deletion mutation of p53	Moderate	Brain	69	Male	Caucasian
PC-3	35.2	AI	-	-	Mutated p53	High	Bone	62	Male	Caucasian
<b>Average</b>	<b>24.4</b>									
AI = Androgen insensitive							<b>Figure Key</b>			
PSA = Prostate-specific antigen							<b>Color</b>	<b>Growth Percent</b>		
+ = expression							Most Active	< -50		
- = no expression								-50 to 0		
Cell line information was gathered from references 154-162.								0 to 50		
							Least Active	> 50		

**Table 5.1: Biological activity, characteristics, and source information for prostate cancer cell lines screened.**

However, the cell lines are clearly biologically unique as there are numerous published reports of their differing susceptibilities to different therapeutics. One example is their differing response to treatment with tumor necrosis factor related apoptosis inducing ligand (TRAIL). TRAIL (structure shown in Figure 5.1) is known as a “death ligand” that can induce apoptosis in cells regardless of the functionality of the tumor suppressor gene p53. As shown in Table 5.1, both DU-145 and PC-3 have mutated p53. TRAIL



exerts its effects via binding to TRAIL receptors which are also known as “death receptors”. This binding interaction triggers a signaling cascade resulting in apoptosis.<sup>163</sup> More importantly, TRAIL has been shown to selectively kill cancer cells while sparing normal cells though the mechanism of this selectivity is not well understood.<sup>163,164</sup> Figure 5.2 shows the differing expression levels of TRAIL receptors between DU-145 and PC-3. The arrow in Figure 5.2 highlights the absence of TR4 in the PC-3 cell line. Their differing susceptibilities to treatment with TRAIL are clearly exhibited in the fluorescent micrographs and bar graphs shown in Figure 5.3. PC-3 viability is dramatically reduced as compared to DU-145 viability as the multiplicity of infection (MOI) values increase.<sup>163</sup>

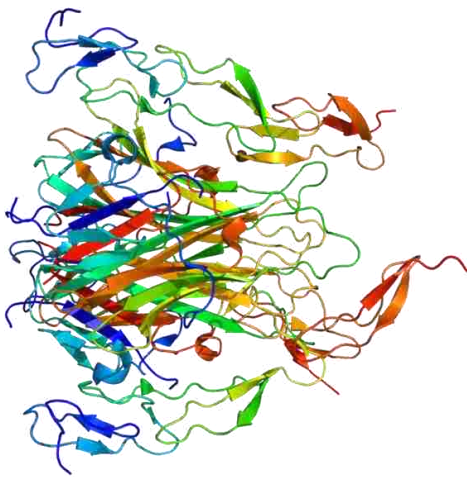


Figure 5.1: TRAIL structure<sup>165</sup>

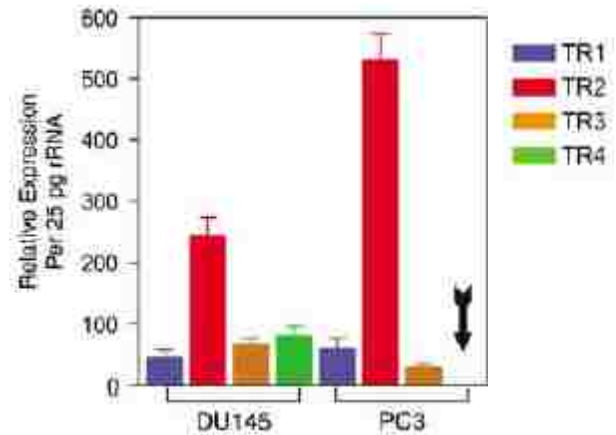


Figure 5.2: Trail Receptor (TR) expression<sup>163</sup>. Arrow indicates absence of TR4 expression in PC-3 cell line.

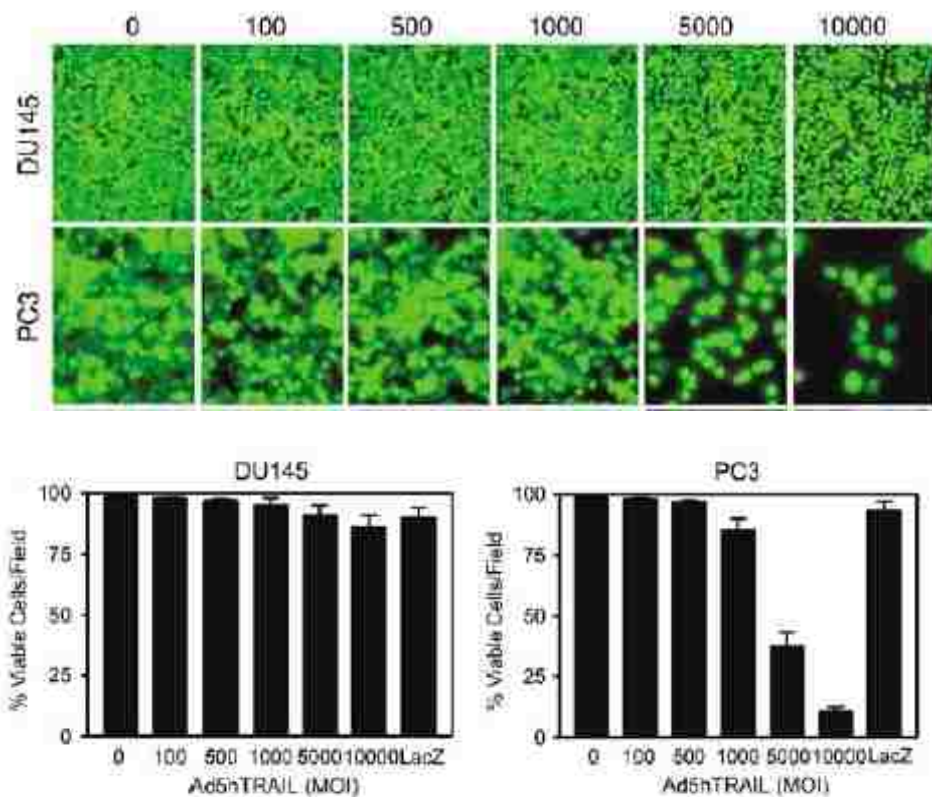


Figure 5.3: Fluorescent micrographs and bar graphs displaying the increased sensitivity of the PC-3 cell line to TRAIL treatment as compared to the DU-145 cell line. LacZ was delivered via AdCMV and was used as a control.<sup>163</sup> MOI = Multiplicity of Infection.

Table 5.2 shows the results for each compound against each prostate cancer cell line. Once again, the stereochemistry played a key role in the activity of the stereoisomers of Compound **1**. **(3S,8R)-1** and **(3S,8S)-1** had average growth percents of -65.9 and -51.7 respectively against the two prostate cancer cell lines screened. **(3R,8S)-1** and **(3R,8R)-1** were significantly less active with average growth percents of 92.4 and 82.8 respectively. Lipophilicity was also shown to be important as Compound **9** (4 carbon length chain), **(3S,8R)-1** (10 carbon length chain), and **10** (16 carbon length chain) had average growth percents of 106.3, -65.9, and -53.6 respectively.

Substituting an alcohol for the acetate at the C-3 position in **(3*S*,8*R*)-1** produced little change in the average growth percent as Compound **16** had an average growth percent of -65.3 as compared to -65.9 for **(3*S*,8*R*)-1**. When looking at the individual cell lines, Compound **16** and **(3*S*,8*R*)-1** had very similar growth percents against both the PC-3 and DU-145 cell lines. For PC-3, the growth percents for Compound **16** and **(3*S*,8*R*)-1** were -41.4 and -43.1 respectively while for DU-145, the growth percents were -89.3 and -88.8 respectively. This similarity is in contrast to cell lines of other cancer types where Compound **16** and **(3*S*,8*R*)-1** often showed significantly different toxicities to the same cell line.

Compound ID	Prostate Cancer Cell Line		Average	Minimum	Maximum	Range
	PC-3	DU-145				
(3R,8S)-1	75.4	109.4	92.4	75.4	109.4	34.0
(3S,8R)-1	-43.1	-88.8	-65.9	-88.8	-43.1	45.7
(3R,8R)-1	72.8	92.8	82.8	72.8	92.8	20.0
(3S,8S)-1	-17.9	-85.6	-51.7	-85.6	-17.9	67.6
9	107.1	105.5	106.3	105.5	107.1	1.6
10	-18.0	-89.1	-53.6	-89.1	-18.0	71.1
11	71.3	70.2	70.7	70.2	71.3	1.1
12	-23.3	-96.6	-59.9	-96.6	-23.3	73.2
13	35.3	18.1	26.7	18.1	35.3	17.2
14	16.2	4.9	10.6	4.9	16.2	11.3
15	-40.1	-95.9	-68.0	-95.9	-40.1	55.8
16	-41.4	-89.3	-65.3	-89.3	-41.4	47.9
37	54.0	81.5	67.8	54.0	81.5	27.5
38	57.3	57.2	57.2	57.2	57.3	0.1
39	71.1	96.9	84.0	71.1	96.9	25.9
40	98.5	101.9	100.2	98.5	101.9	3.3
41	20.0	-6.7	6.7	-6.7	20.0	26.7
42	48.6	15.0	31.8	15.0	48.6	33.6
43	13.2	-49.5	-18.2	-49.5	13.2	62.7
44	20.6	-60.8	-20.1	-60.8	20.6	81.4
45	50.2	25.0	37.6	25.0	50.2	25.2
46	58.7	61.5	60.1	58.7	61.5	2.8
47	59.0	47.0	53.0	47.0	59.0	12.0
48	99.5	102.2	100.8	99.5	102.2	2.7
Average	35.2	13.6				
Minimum	-43.1	-96.6				
Maximum	107.1	109.4				
Range	150.2	206.0				
Figure Key						
Color		Growth Percent				
Most Active		< -50				
		-50 to 0				
		0 to 50				
Least Active		> 50				

Table 5.2

## 5.2 Hansch Cluster Analysis on Prostate Cancer Cell Lines Data

Table 5.3 shows the prostate cancer testing results organized to assess the results per Hansch cluster analysis theory at the C-8 position. As shown in the table, the range of activity is wide over the six clusters tested. For the PC-3 cell line, the alcohol compound (3S,8R)-1 from cluster 5 is the most active whereas for the DU-145 cell line, the mesyl amide compound **12** from cluster 4b is the most active. Interesting, the amine compound **11** which is also in cluster 5 has dramatically different activity against both cell lines as compared to its cluster 5 mate (3S,8R)-1. For the DU-145 cell line, the growth percent of

compound **11** is 70.2 compared to a growth percent of -88.8 for **(3*S*,8*R*)-1**. Hansch cluster theory would not predict that two substituents from the same cluster would have such drastically different biological activities as changing the substituents within a cluster is theorized to “fine-tune” the activity. It would be interesting to evaluate more compounds from this cluster and several substituents from cluster 5 would be readily accessible synthetically as the methylamine, ethylamine, hydrazine, and methyl ether substituents would be relatively easy to substitute into the C-8 position.

Compound ID	Cluster	Prostate Cancer Cell Line		Average	Minimum	Maximum	Range
		PC-3	DU-145				
<b>(3<i>S</i>,8<i>R</i>)-1</b>	5	-43.1	-88.8	-65.9	-88.8	-43.1	45.7
<b>11</b>	5	71.3	70.2	70.7	70.2	71.3	1.1
<b>12</b>	4b	-23.3	-96.6	-59.9	-96.6	-23.3	73.2
<b>13</b>	8	35.3	18.1	26.7	18.1	35.3	17.2
<b>14</b>	9	16.2	4.9	10.6	4.9	16.2	11.3
<b>15</b>	7	-40.1	-95.9	-68.0	-95.9	-40.1	55.8
<b>48</b>	6	99.5	102.2	100.8	99.5	102.2	2.7
	<b>Average</b>	35.2	13.6				
	<b>Minimum</b>	-43.1	-96.6				
	<b>Maximum</b>	107.1	109.4				
	<b>Range</b>	150.2	206.0				
<b>Figure Key</b>							
		<b>Color</b>	<b>Growth Percent</b>				
		Most Active	< -50				
			-50 to 0				
			0 to 50				
		Least Active	> 50				

Table 5.3

Cell Line	Most Active Cluster	C-8 Substituent	Growth Percent
PC-3	5	-OH	-43.1
DU-145	4b	-NHSO <sub>2</sub> Me	-96.6

Table 5.4

### 5.3 Prostate Cancer SAR Analysis of Amide Compounds

Eleven of the compounds we had tested by NCI have an acetate at the C-3 position and different amide functionalities with aromatic or heteroaromatic groups directly connected to the amide carbonyl group in the C-8 position as shown in Figure 5.4.

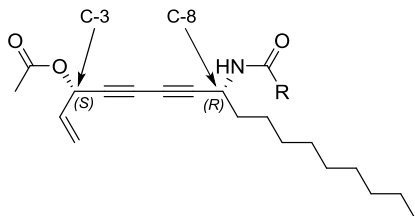


Figure 5.4 Generic structure of amides screened by NCI.


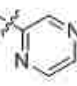
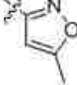
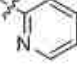
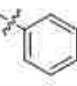
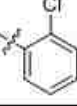
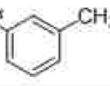
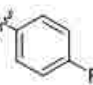
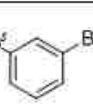
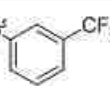
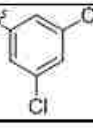
Compound ID	Prostate Cancer Cell Line		Average	Minimum	Maximum	Range
	PC-3	DU-145				
13	35.3	18.1	26.7	18.1	35.3	17.2
37	54.0	81.5	67.8	54.0	81.5	27.5
38	57.3	57.2	57.2	57.2	57.3	0.1
39	71.1	96.9	84.0	71.1	96.9	25.9
40	98.5	101.9	100.2	98.5	101.9	3.3
41	20.0	-6.7	6.7	-6.7	20.0	26.7
42	48.6	15.0	31.8	15.0	48.6	33.6
43	13.2	-49.5	-18.2	-49.5	13.2	62.7
44	20.6	-60.8	-20.1	-60.8	20.6	81.4
45	50.2	25.0	37.6	25.0	50.2	25.2
46	58.7	61.5	60.1	58.7	61.5	2.8
<b>Average</b>	48.0	30.9				
<b>Minimum</b>	13.2	-60.8				
<b>Maximum</b>	98.5	101.9				
<b>Range</b>	85.3	162.7				

Table 5.5

Across the set of amide compounds (Table 5.5), there was a wide range of activity against the DU-145 cell line. The most active compound was the 2-furyl compound **44** which had a growth percent of -60.8. The least active compound was the 3,5-dichloro compound **40** which exhibited virtually no activity with a growth percent of 101.9. Table 5.6 shows the growth percent of the DU-145 cell line and the associated R group for each

of the eleven amide compounds. Interestingly, the four most active compounds were the four compounds with heteroaromatic rings. Since the most active compound has the 2-furyl group, it would be interesting to evaluate the 3-furyl substituent as well as other 5-membered heteroaromatic rings such as thiophene and pyrrole. With the pyrazine compound also being very active, it would be intriguing to evaluate the effect of changing the spacing of the nitrogen atoms in the ring by substituting in pyrimidine and pyridazine rings. Triazine and tetrazine isomers could also easily be synthesized and evaluated. On the other side of the activity spectrum, four of the five least active compounds had substituents in the 3-position of the phenyl ring indicating that the steric bulk in the 3-position may have a negative impact on activity. Changing the phenyl group in compound **13** to the 3,5-dichlorophenyl group in compound **40** dropped the growth percent from 18.1 down to 101.9.

As shown in Table 5.5, the range of activity across the amide set was not as large against the PC-3 cell line. The most active compound was the pyrazyl compound **43** with a growth percent of 13.2. Once again, the 3,5-dichlorophenyl compound **40** had the least activity with a growth percent of 98.5. The activity of the 2-furyl compound dropped to 20.6 against the PC-3 cell line as compared to the growth percent of -60.8 against the DU-145 cell line.

DU-145 Cell Line		
Compound ID	R group	DU-145 Growth Percent
44		-60.8
43		-49.5
41		-6.7
42		15.0
13		18.1
45		25.0
38		57.2
46		61.5
37		85.5
39		96.9
40		101.9
	Average	30.9
	Minimum	-60.8
	Maximum	101.9
	Range	162.7

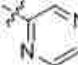
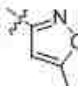

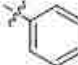
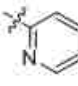
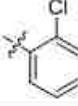
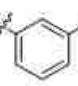
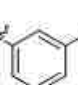
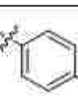
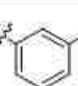
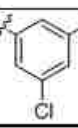
PC-3 Cell Line		
Compound ID	R group	PC-3 Growth Percent
43		13.2
41		20.0
44		20.6
13		35.3
42		48.6
45		50.2
37		54.0
38		57.3
46		58.7
39		71.1
40		98.5
	Average	48.0
	Minimum	13.2
	Maximum	98.5
	Range	85.3

Table 5.6



***Chapter 6: Renal Cancer***

## Chapter 6: Renal Cancer

### 6.1 Renal Cancer Overview

Our compounds were screened against eight different renal cancer cell lines. The average mean growth percent across the eight renal cancer cell lines was -2.7. As shown in Table 3.4, our compounds had the second most broad spectrum activity against renal cancer cell lines with only melanoma cell lines being more susceptible to our compounds. Table 6.1 shows the average mean growth percent of our compounds against each of the eight renal cancer cell lines screened. Table 6.1 also shows molecular characteristics and cell line source information for each of the eight cell lines.

Cell Line	Average Mean Growth Percent	Mutations/variants <sup>166</sup>	TP53 <sup>167</sup>	p53 Amino Acid Codon Change <sup>167</sup>	Patient Age	Sex	Ethnicity
SN12C	-29.1	TP53	336 GAG → TAG	E → STOP	43	Male	N/A
UO-31	-13.7	CDKN2A	wild-type	wild-type	N/A	Female	N/A
786-0	-11.2	CDKN2A, PTEN, TP53, VHL	278 CCT → GCT	P → A	58	Male	Caucasian
RXF 393	-8.1	CDKN2A, PTEN, TP53	275 CGC → CAC	R → H	54	Male	N/A
A498	-3.0	CDKN2A, VHL	wild-type	wild-type	52	Female	N/A
CAKI-1	9.9	CDKN2A	wild-type	wild-type	49	Male	Caucasian
TK-10	14.1	TP53	264 CTA → CGA	L → R	43	Male	N/A
ACHN	19.5	CDKN2A	wild-type	wild-type	22	Male	Caucasian
<b>Average</b>	<b>-2.7</b>						
					<b>Figure Key</b>		
N/A: Data not available					<b>Color</b>	<b>Growth Percent</b>	
CDKN2A: Cyclin-dependent kinase inhibitor 2A					Most Active	< -50	
PTEN: Phosphatase and tensin homologue						-50 to 0	
TP53: Tumor protein p53						0 to 50	
VHL: von Hippel-Lindau tumor suppressor					Least Active	> 50	
Unless otherwise referenced above, cell line information was gathered from references 154-157.							

Table 6.1

Table 6.2 shows the results for each compound against each renal cancer cell line. The stereochemistry played a key role in the activity of the stereoisomers of Compound **1**. **(3S,8R)-1** and **(3S,8S)-1** had average growth percents of -67.5 and -59.9 respectively against the eight renal cancer cell lines screened. **(3R,8S)-1** and **(3R,8R)-1** were significantly less active with average growth percents of 86.6 and 92.1 respectively. Lipophilicity was also shown to be important as Compound **9** (4 carbon length chain), **(3S,8R)-1** (10 carbon length chain), and **10** (16 carbon length chain) had average growth percents of 103.8, -67.5, and -73.8 respectively.

Substituting an alcohol for the acetate at the C-3 position in **(3S,8R)-1** produced little change in the average growth percent as Compound **16** had an average growth percent of -66.3 as compared to -67.5 for **(3S,8R)-1**. Even when looking at individual renal cancer cell lines, **(3S,8R)-1** and **16** had remarkably similar cytotoxicities with the largest difference in growth percent being seen in the SN12C cell line where the growth percents were -94.9 and -63.9 respectively.

Compound ID	Renal Cancer Cell Lines								Average	Minimum	Maximum	Range
	786-0	A498	ACHN	CAKI-1	RXF 393	SN12C	TK-10	UO-31				
(3R,8S)-1	96.0	96.8	96.6	95.4	NT	74.8	94.1	52.6	86.6	52.6	96.8	44.2
(3S,8R)-1	-39.9	-87.6	-40.0	-11.1	-79.9	-94.9	-93.4	-94.3	-67.5	-94.9	-11.1	83.9
(3R,8R)-1	90.2	108.2	98.1	100.0	NT	74.3	106.0	67.8	92.1	67.8	108.2	40.4
(3S,8S)-1	-44.6	-73.2	-37.8	-18.9	NT	-59.0	-91.3	-94.2	-59.9	-94.2	-18.9	75.3
9	98.8	94.9	104.7	103.9	99.7	100.5	119.5	108.2	103.8	94.9	119.5	24.6
10	-82.1	-78.6	-67.5	-34.6	-81.7	-65.2	-88.0	-93.0	-73.8	-93.0	-34.6	58.4
11	-50.1	101.6	81.3	98.0	NT	-49.0	114.4	63.4	51.4	-50.1	114.4	164.5
12	-62.2	-86.8	-43.1	-11.6	-85.2	-50.6	-95.7	-90.4	-65.7	-95.7	-11.6	84.2
13	-37.1	-69.2	14.9	8.9	6.8	-57.8	3.6	-23.1	-19.1	-69.2	14.9	84.1
14	-72.9	11.4	23.5	26.9	NT	-43.2	58.7	-90.7	-12.3	-90.7	58.7	149.4
15	-48.5	-62.9	-75.6	-41.7	-74.7	-53.5	-88.6	-85.6	-66.4	-88.6	-41.7	46.8
16	-59.3	-86.0	-47.8	-27.5	-71.1	-63.9	-92.6	-82.4	-66.3	-92.6	-27.5	65.2
37	23.6	69.8	28.2	61.9	72.1	-33.3	67.4	35.1	40.6	-33.3	72.1	105.4
38	19.7	14.5	23.4	-12.7	51.6	68.1	29.0	27.8	10.6	-68.1	51.6	119.7
39	28.7	68.3	46.8	66.9	80.4	10.8	139.7	43.4	60.6	10.8	139.7	128.9
40	47.2	97.0	67.0	70.9	83.7	27.3	101.6	51.5	68.3	27.3	101.6	74.3
41	-46.9	-73.2	13.5	-52.7	-68.3	-25.1	-38.2	-53.8	-43.1	-73.2	13.5	86.7
42	-70.5	-46.5	10.8	-48.8	-37.8	-75.9	4.0	-19.5	-35.5	-75.9	10.8	86.6
43	-90.6	-76.8	-0.1	-39.7	-63.1	-59.5	-25.2	-86.6	-55.2	-90.6	-0.1	90.6
44	-40.1	-75.4	12.6	-40.1	-44.5	-61.6	-13.2	-47.3	-38.7	-75.4	12.6	88.0
45	11.0	-73.2	19.6	-50.4	-14.5	-72.4	5.8	12.1	-20.2	-73.2	19.6	92.8
46	7.1	42.6	18.9	-43.3	15.1	-73.3	0.4	10.5	-2.7	-73.3	42.6	115.9
47	-46.0	6.9	15.5	-58.6	-27.7	-72.0	1.7	-11.6	-24.0	-72.0	15.5	87.5
48	97.6	104.8	104.5	97.5	84.9	91.8	118.9	70.6	96.3	70.6	118.9	48.3
Average	-11.2	-3.0	19.5	9.9	-8.1	-29.1	14.1	-13.7				
Minimum	-90.6	-87.6	-75.6	-58.6	-85.2	-94.9	-95.7	-94.3				
Maximum	98.8	108.2	104.7	103.9	99.7	100.5	139.7	108.2				
Range	189.4	195.8	180.3	162.6	185.0	195.5	235.4	202.5				
	NT = Not Tested											
	Figure Key											
	Color	Growth Percent										
	Most Active	< -50										
		-50 to 0										
		0 to 50										
	Least Active	> 50										

Table 6.2

## 6.2 Hansch Cluster Analysis on Renal Cancer Cell Lines Data

Table 6.3 shows the renal cancer testing results organized to assess the results per Hansch cluster analysis theory at the C-8 position. As shown in the table, the range of activity is wide over the six clusters tested. Isothiocyanate compound **48** clearly has the least activity across the board. Interestingly, the amino compound **11** mirrors the low activity of compound **48** against five of the seven common cell lines tested (compound **11** not screened against RXF 393). Yet for cell lines 786-0 and SN12C, compound **11** has potent activity with growth percents of -50.1 and -49.0 respectively whereas compound **48** maintains minimal activity against these same cell lines with growth percents of 97.6 and 91.8 respectively. Table 6.4 shows the most active cluster and substituent against each cell line.

Compound ID	Cluster	Renal Cancer Cell Lines								Average	Minimum	Maximum	Range
		786-0	A498	ACHN	CAKI-1	RXF 393	SN12C	TK-10	UO-31				
(3S,8R)-1	5	-38.9	-87.6	-40.0	-11.1	-79.9	-94.9	-93.4	-94.3	-67.5	-94.9	-11.1	83.9
11	5	-60.1	101.6	81.3	98.0	NT	-49.0	114.4	63.4	51.4	-50.1	114.4	164.5
12	4b	-62.2	-86.8	-43.1	-11.6	-85.2	-50.6	-95.7	-90.4	-65.7	-95.7	-11.6	84.2
13	8	-37.1	-69.2	14.9	8.9	6.8	-57.8	3.6	-23.1	-19.1	-69.2	14.9	84.1
14	9	-72.9	11.4	23.5	26.9	NT	-43.2	58.7	-90.7	-12.3	-90.7	58.7	149.4
15	7	-48.5	-62.9	-75.6	-41.7	-74.7	-53.5	-88.6	-85.6	-66.4	-88.6	-41.7	46.8
48	6	97.6	104.8	104.5	97.5	84.9	91.8	118.9	70.6	96.3	70.6	118.9	48.3
	Average	-30.3	-12.7	9.4	23.9	-29.6	-36.8	2.6	-35.7				
	Minimum	-72.9	-87.6	-75.6	-41.7	-85.2	-94.9	-95.7	-94.3				
	Maximum	97.6	104.8	104.5	98.0	84.9	91.8	118.9	70.6				
	Range	170.5	192.4	180.1	139.8	170.1	186.8	214.6	164.9				
		NT = Not Tested											
		Figure Key											
		Color	Growth Percent										
		Most Active	< -50										
			-50 to 0										
			0 to 50										
		Least Active	> 50										

Table 6.3

Cell Line	Most Active Cluster	C-8 Substituent	Growth Percent
786-0	9	-NHBU	-72.9
A498	5	-OH	-87.6
ACHN	7	-OSO <sub>2</sub> Me	-75.6
CAKI-1	7	-OSO <sub>2</sub> Me	-41.7
RXF 393	4b	-NHSO <sub>2</sub> Me	-85.2
SN12C	5	-OH	-94.9
TK-10	4b	-NHSO <sub>2</sub> Me	-95.7
UO-31	5	-OH	-94.3

Table 6.4

### 6.3 Renal Cancer SAR Analysis of Amide Compounds

Eleven of the compounds we had tested by NCI have an acetate at the C-3 position and different amide functionalities with aromatic or heteroaromatic groups directly connected to the amide carbonyl group in the C-8 position as shown in Figure 6.1.

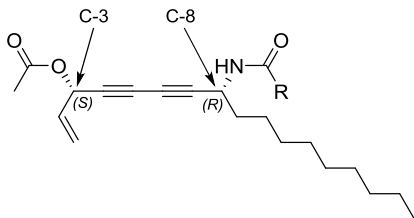


Figure 6.1 Generic structure of amides screened by NCI.

Table 6.5 shows the activity of our amide compounds against each of the different renal cell lines. The set of amide compounds showed a wide range of activity against the different cell lines indicating that changing the amide R group has a significant impact on activity. The ACHN cell line results stand out as our compounds had the narrowest range of activity against this cell line and only compound **43** had a growth percent below zero with a value of -0.1. One trend across all of the renal cell lines is that the five heterocycle R-groups are typically among the most active compounds. In seven of the eight cell lines, the five heterocycles compounds are amongst the top six most active compounds. It is only in the SN12C cell line where the isoxazole compound ranks below the top six most active compounds as it is the eighth most active. Another trend is that the phenyl R-groups with a substituent in the meta-position are most often the least active compounds. All of the meta-substituted compounds rank in the bottom five least active compounds against all cell lines except the SN12C cell line. Against the SN12C cell line, Compound **38** with a methyl group in the meta-position ranks fourth with a growth percent of -68.1. The fact that our compounds exhibit significantly different activity against the SN12C cell line is not surprising since it is a unique renal cell line in that it is the only one in the NCI60 panel that expresses neuronal system-specific enolases. In addition, the SN12C line does not express several renal specific miRNAs that are seen in the other cell lines.<sup>168,169</sup>

Compound ID	Renal Cancer Cell Lines								Average	Minimum	Maximum	Range
	786-0	A498	ACHN	CAKI-1	RXF 393	SN12C	TK-10	UO-31				
13	-37.1	-69.2	14.9	8.9	6.8	-57.8	3.6	-23.1	-19.1	-69.2	14.9	84.1
37	23.6	69.8	28.2	61.9	72.1	-33.3	67.4	35.1	40.6	-33.3	72.1	105.4
38	19.7	14.5	23.4	-12.7	51.6	-68.1	29.0	27.8	10.6	-68.1	51.6	119.7
39	28.7	68.3	46.8	66.9	80.4	10.8	139.7	43.4	60.6	10.8	139.7	128.9
40	47.2	97.0	67.0	70.9	83.7	27.3	101.6	51.5	68.3	27.3	101.6	74.3
41	-46.9	-73.2	13.5	-52.7	-68.3	-25.1	-38.2	-53.8	-43.1	-73.2	13.5	86.7
42	-70.5	-46.5	10.8	-48.8	-37.8	-75.9	4.0	-19.5	-35.5	-75.9	10.8	86.6
43	-90.6	-76.8	-0.1	-39.7	-63.1	-59.5	-25.2	-86.6	-55.2	-90.6	-0.1	90.6
44	-40.1	-75.4	12.6	-40.1	-44.5	-61.6	-13.2	-47.3	-38.7	-75.4	12.6	88.0
45	11.0	-73.2	19.6	-50.4	-14.5	-72.4	5.8	12.1	-20.2	-73.2	19.6	92.8
46	7.1	42.6	18.9	-43.3	15.1	-73.3	0.4	10.5	-2.7	-73.3	42.6	115.9
Average	-13.5	-11.1	23.2	-7.2	7.4	-44.4	25.0	-4.5				
Minimum	-90.6	-76.8	-0.1	-52.7	-68.3	-75.9	-38.2	-86.6				
Maximum	47.2	97.0	67.0	70.9	83.7	27.3	139.7	51.5				
Range	137.8	173.7	67.0	123.7	152.0	103.2	177.9	138.1				

Table 6.5

786-0 Cell Line			A498 Cell Line			ACHN Cell Line			CAKI-1 Cell Line		
Compound ID	R group	786-0 Growth Percent	Compound ID	R group	A498 Growth Percent	Compound ID	R group	ACHN Growth Percent	Compound ID	R group	CAKI-1 Growth Percent
43		-90.6	43		-76.8	43		-0.1	41		-52.7
42		-70.5	44		-75.4	42		10.8	45		-50.4
41		-46.9	41		-73.2	44		12.6	42		-48.8
44		-40.1	45		-73.2	41		13.5	46		-43.3
13		-37.1	13		-69.2	13		14.9	44		-40.1
46		7.1	42		-46.5	46		18.9	43		-39.7
45		11.0	38		14.5	45		19.6	38		-12.7
38		19.7	46		42.6	38		23.4	13		8.9
37		23.6	39		69.9	37		28.2	37		61.8
39		28.7	37		69.8	39		46.8	39		66.9
40		47.2	40		97.0	40		67.0	40		70.9
Average		-13.5	Average		-11.1	Average		23.2	Average		-7.2
Minimum		-90.6	Minimum		-76.8	Minimum		-0.1	Minimum		-52.7
Maximum		47.2	Maximum		97.0	Maximum		67.0	Maximum		70.9
Range		137.8	Range		173.7	Range		67.0	Range		123.7

Table 6.6

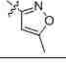
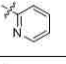
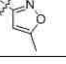
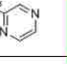
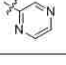
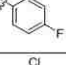
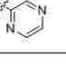
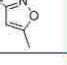
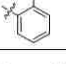
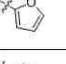
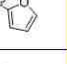
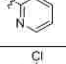
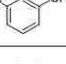
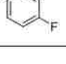
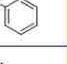
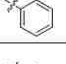
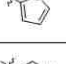
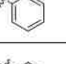
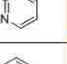
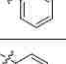
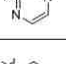
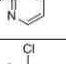
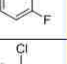
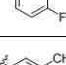
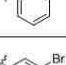
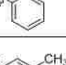
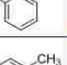
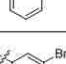
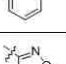
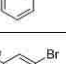
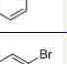
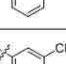
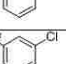
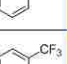
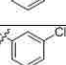
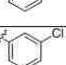
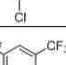

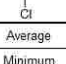

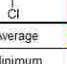
RXF 393 Cell Line			SN12C Cell Line			TK-10 Cell Line			UO-31 Cell Line		
Compound ID	R group	RXF 393 Growth Percent	Compound ID	R group	SN12C Growth Percent	Compound ID	R group	TK-10 Growth Percent	Compound ID	R group	UO-31 Growth Percent
41		-68.3	42		-75.9	41		-38.2	43		-86.6
43		-53.1	46		-73.3	43		-25.2	41		-53.8
44		-44.5	45		-72.4	44		-13.2	44		-47.3
42		-37.8	38		-68.1	46		0.4	13		-23.1
45		-14.5	44		-61.6	13		3.6	42		-19.5
13		6.8	43		-59.6	42		4.0	46		10.5
46		15.1	13		-57.8	45		5.8	45		12.1
38		51.6	37		-33.3	38		29.0	38		27.8
37		72.1	41		-25.1	37		67.4	37		35.1
39		80.4	39		10.6	40		101.6	39		43.4
40		83.7	40		27.3	39		139.7	40		51.5
	Average	7.4		Average	-44.4		Average	25.0		Average	-4.5
	Minimum	-68.3		Minimum	-75.9		Minimum	-38.2		Minimum	-86.6
	Maximum	83.7		Maximum	27.3		Maximum	139.7		Maximum	51.5
	Range	152.0		Range	103.2		Range	177.9		Range	138.1

Table 6.7



***Chapter 7: Ovarian Cancer***

## Chapter 7: Ovarian Cancer

### 7.1 Ovarian Cancer Overview

Our compounds were screened against seven different ovarian cancer cell lines. The average mean growth percent across the seven ovarian cancer cell lines was 25.7. As shown in Table 3.4, the activity of our compounds against ovarian cancer was less than all of the other types of cancer tested except for breast cancer. Table 7.1 shows the average growth percent of our compounds against each of the seven ovarian cancer cell lines screened. Table 7.1 also shows molecular characteristics and cell line source information for each of the seven cell lines. As shown in Table 7.1, there is disagreement amongst publications on the mutation status of TP53 in the IGROV1, OVCAR-4, and OVCAR-5 cell lines.<sup>166,167</sup>

Cell Line	Average Growth Percent	Endogenous Estrogen Level <sup>171</sup> (pg/10 <sup>6</sup> cells)	Mutations/variants <sup>166</sup>	TP53 <sup>167</sup>	p53 Amino Acid Codon Change <sup>167</sup>	Patient Age	Sex
IGROV1	0.6	37.9	TP53, BRCA1, SMAD4, PTEN	wild-type	wild-type	47	Female
OVCAR-8	17.7	50.7	TP53, ERBB2	deletion 126-132	deletion 126-132	64	Female
OVCAR-5	17.7	123.8	CDKN2A, KRAS	insertion 224	insertion 224	N/A	N/A
OVCAR-4	29.1	168.9	TP53	wild-type	wild-type	42	Female
NCI/ADR-RES	32.2	97.6	TP53, ERBB2	N/A	N/A	Derived from OVCAR-8 <sup>170</sup>	
OVCAR-3	36.0	43.0	TP53	248 CGG → CAG	R → Q	60	Female
SK-OV-3	46.8	152.4	TP53, CDKN2A, PIK3CA, APC	179 CAT → CGT	H → R	64	Female
Average	25.7						

N/A: Data not available  
 APC: Adenomatous polyposis coli  
 CDKN2A: Cyclin-dependent kinase inhibitor 2A  
 ERBB2: v-erb-b2 erythroblastic leukemia viral oncogene homologue 2  
 PTEN: Phosphatase and tensin homologue  
 TP53: Tumor protein p53  
 VHL: von Hippel-Lindau tumor suppressor  
 Unless otherwise referenced above, cell line information was gathered from references 154-157.

Figure Key	
Color	Growth Percent
Most Active	< -50
	-50 to 0
	0 to 50
Least Active	> 50

**Table 7.1**

Table 7.2 shows the results for each compound against each ovarian cancer cell line. The stereochemistry played a key role in the activity of the stereoisomers of Compound 1. (3*S*,8*R*)-1 and (3*S*,8*S*)-1 had average growth percents of -34.2 and -24.3 respectively against the seven ovarian cancer cell lines screened. (3*R*,8*S*)-1 and (3*R*,8*R*)-1 were

significantly less active with average growth percents of 97.6 and 103.3 respectively. Lipophilicity was also shown to be important as Compound **9** (4 carbon length chain), **(3S,8R)-1** (10 carbon length chain), and **10** (16 carbon length chain) had average growth percents of 107.7, -34.2, and -22.6 respectively.

Substituting an alcohol for the acetate at the C-3 position in **(3S,8R)-1** produced little change in the average growth percent as Compound **16** had an average growth percent of -37.8 as compared to -34.2 for **(3S,8R)-1**. Even when looking at individual ovarian cancer cell lines, **(3S,8R)-1** and **16** had remarkably similar cytotoxicities with the largest difference in growth percent being seen in the OVCAR-8 cell line where the growth percents were 8.8 and -27.6 respectively.

Compound ID	Ovarian Cancer Cell Lines							Average	Minimum	Maximum	Range
	IGROV1	OVCAR-3	OVCAR-4	OVCAR-5	OVCAR-8	NCI/ADR-RES	SK-OV-3				
(3R,8S)-1	76.5	108.4	99.6	95.4	104.8	94.0	104.4	97.6	76.5	108.4	31.8
(3S,8R)-1	-64.8	-83.3	0.4	-92.1	8.8	5.3	-13.5	-34.2	-92.1	8.8	101.0
(3R,8R)-1	103.4	109.6	106.5	109.6	79.1	103.3	111.5	103.3	79.1	111.5	32.5
(3S,8S)-1	-65.8	-40.9	-10.9	-76.5	7.4	13.7	3.2	-24.3	-76.5	13.7	90.3
9	120.7	123.4	100.1	101.0	104.4	94.4	109.8	107.7	94.4	123.4	29.0
10	-52.7	-31.4	-14.4	-60.3	2.3	9.6	-10.8	-22.6	-60.3	9.6	70.0
11	18.4	81.4	63.2	93.6	8.5	13.7	120.6	57.1	8.5	120.6	112.2
12	-56.1	-71.3	-24.8	-93.2	-5.0	4.6	-19.4	-37.9	-93.2	4.6	97.9
13	-3.9	57.2	9.2	1.3	-22.5	23.6	56.3	17.3	-22.5	57.2	79.7
14	20.6	11.0	-2.2	52.7	10.2	22.9	70.9	26.6	-2.2	70.9	73.1
15	-70.9	-82.7	4.6	-81.3	-4.9	13.2	15.4	-29.5	-82.7	15.4	98.1
16	-69.1	-92.2	-1.8	-88.7	-27.6	11.2	3.6	-37.8	-92.2	11.2	103.4
37	49.1	101.5	27.6	61.0	23.4	NT	61.2	54.0	23.4	101.5	78.1
38	14.8	82.0	44.3	46.0	-5.9	22.3	61.9	37.9	-5.9	82.0	87.8
39	75.8	97.8	55.2	91.9	33.3	NT	74.7	71.4	33.3	97.8	64.5
40	92.7	102.0	67.7	123.0	61.4	81.9	76.4	86.5	61.4	123.0	61.6
41	-64.8	19.0	3.0	9.0	-48.4	15.5	8.6	-8.3	-64.8	19.0	83.8
42	-49.9	47.5	2.5	2.9	3.0	14.1	37.7	8.3	-49.9	47.5	97.4
43	-67.3	12.3	0.2	-59.0	0.4	6.6	9.9	-13.8	-67.3	12.3	79.6
44	-53.8	13.5	19.8	-14.1	4.4	18.1	31.8	2.8	-53.8	31.8	85.6
45		49.6	15.6	32.4	-4.6	17.5	42.1	25.5	-4.6	49.6	54.2
46	3.8	78.4	32.1	41.9	-0.5	20.6	38.5	30.7	-0.5	78.4	78.9
47	-44.3	68.0	13.0	18.7	2.4	12.2	21.4	13.0	-44.3	68.0	112.3
48	101.7	103.4	87.9	110.9	90.4	90.4	107.5	98.9	87.9	110.9	23.0
Average	0.6	36.0	29.1	17.7	17.7	32.2	46.8				
Minimum	-70.9	-92.2	-24.8	-93.2	-48.4	4.6	-19.4				
Maximum	120.7	123.4	106.5	123.0	104.8	103.3	120.6				
Range	191.6	215.6	131.3	216.2	153.3	98.7	140.1				
	NT = Not Tested										
	Figure Key										
	Color	Growth Percent									
	Most Active	< -50									
		-50 to 0									
		0 to 50									
	Least Active	> 50									

Table 7.2

## 7.2 Hansch Cluster Analysis on Ovarian Cancer Cell Lines Data

Table 7.3 shows the ovarian cancer testing results organized to assess the results per Hansch cluster analysis theory at the C-8 position. As shown in the table, the range of activity is wide over the six clusters tested. Isothiocyanate compound **48** of cluster 6 clearly has the least activity across the board with an average growth percent of 98.9. Selectivity against certain cell lines is evident for many of the compounds. **(3S,8R)-1** and **11** both have similar growth percents against the OVCAR-8 line (8.8 and 8.5, respectively) and NCI/ADR-RES line (5.3 and 13.7, respectively). Yet the growth percents for **(3S,8R)-1** and **11** against OVCAR-3 (-83.3 and 81.4, respectively) and OVCAR-5 (-92.1 and 93.6, respectively) are strikingly different. Both **(3S,8R)-1** and **11** are cluster 5 compounds with **(3S,8R)-1** having a C-8 alcohol whereas **11** has a C-8 amino group. **(3S,8R)-1** (cluster 5), **12** (cluster 4b), and **15** (cluster 7) all had average growth percents below zero across the seven cell lines. Table 7.4 shows the most active cluster and substituent against each cell line.

Compound ID	Cluster	Ovarian Cancer Cell Lines							Average	Minimum	Maximum	Range
		IGROV1	OVCAR-3	OVCAR-4	OVCAR-5	OVCAR-8	NCI/ADR-RES	SK-OV-3				
(3S,8R)-1	5	-64.8	-83.3	0.4	-92.1	8.8	5.3	-13.5	-34.2	-92.1	8.8	101.0
11	5	18.4	81.4	63.2	93.6	8.5	13.7	120.6	57.1	8.5	120.6	112.2
12	4b	-56.1	-71.3	-24.8	-93.2	-5.0	4.6	-19.4	-37.9	-93.2	4.6	97.9
13	8	-3.9	57.2	9.2	1.3	-22.5	23.6	56.3	17.3	-22.5	57.2	79.7
14	9	20.6	11.0	-2.2	52.7	10.2	22.9	70.9	26.6	-2.2	70.9	73.1
15	7	-70.9	-82.7	4.6	-81.3	-4.9	13.2	15.4	-29.5	-82.7	15.4	98.1
48	6	101.7	103.4	87.9	110.9	90.4	90.4	107.5	98.9	87.9	110.9	23.0
Average		-7.9	2.2	19.8	-1.2	12.2	24.8	48.3				
Minimum		-70.9	-83.3	-24.8	-93.2	-22.5	4.6	-19.4				
Maximum		101.7	103.4	87.9	110.9	90.4	90.4	120.6				
Range		172.6	186.8	112.7	204.1	112.8	85.8	140.1				
		NT = Not Tested										
		Figure Key										
		Color	Growth Percent									
		Most Active	< -50									
			-50 to 0									
			0 to 50									
		Least Active	> 50									

Table 7.3

Cell Line	Most Active Cluster	C-8 Substituent	Growth Percent
IGROV1	7	-OSO <sub>2</sub> Me	-70.9
OVCAR-3	5	-OH	-83.3
OVCAR-4	4b	-NHSO <sub>2</sub> Me	-24.8
OVCAR-5	4b	-NHSO <sub>2</sub> Me	-93.2
OVCAR-8	8	-NHCOPh	-22.5
NCI/ADR-RES	4b	-NHSO <sub>2</sub> Me	4.6
SK-OV-3	4b	-NHSO <sub>2</sub> Me	-19.4

Table 7.4

### 7.3 SAR Analysis of Amide Compounds against Ovarian Cancer Cell Lines

Eleven of the compounds we had tested by NCI have an acetate at the C-3 position and different amide functionalities with aromatic or heteroaromatic groups directly connected to the amide carbonyl group in the C-8 position as shown in Figure 7.1.

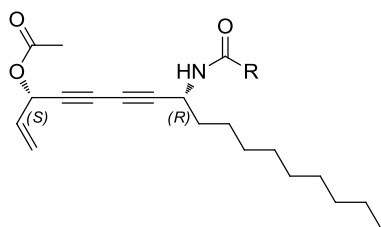


Figure 7.1 Generic structure of amides screened by NCI.

Table 7.5 shows the activity of our amide compounds against each of the different ovarian cancer cell lines. The set of amide compounds showed a wide range of activity against the different cell lines indicating that changing the amide R group has a significant impact on activity.

Ovarian Cancer Cell Lines											
Compound ID	IGROV1	OVCAR-3	OVCAR-4	OVCAR-5	OVCAR-8	NCI/ADR-RES	SK-OV-3	Average	Minimum	Maximum	Range
13	-3.9	57.2	9.2	1.3	-22.5	23.6	56.3	17.3	-22.5	57.2	79.7
37	49.1	101.5	27.6	61.0	23.4	NT	61.2	54.0	23.4	101.5	78.1
38	14.8	82.0	44.3	46.0	-5.9	22.3	61.9	37.9	-5.9	82.0	87.8
39	75.8	97.8	55.2	91.9	33.3	NT	74.7	71.4	33.3	97.8	64.5
40	92.7	102.0	67.7	123.0	61.4	81.9	76.4	86.5	61.4	123.0	61.6
41	-64.8	19.0	3.0	9.0	-48.4	15.5	8.6	-8.3	-64.8	19.0	83.8
42	-49.9	47.5	2.5	2.9	3.0	14.1	37.7	8.3	-49.9	47.5	97.4
43	-67.3	12.3	0.2	-59.0	0.4	6.6	9.9	-13.8	-67.3	12.3	79.6
44	-53.8	13.5	19.8	-14.1	4.4	18.1	31.8	2.8	-53.8	31.8	85.6
45	NT	49.6	15.6	32.4	-4.6	17.5	42.1	25.5	-4.6	49.6	54.2
46	3.8	78.4	32.1	41.9	-0.5	20.6	38.5	30.7	-0.5	78.4	78.9
<b>Average</b>	-0.3	60.1	25.2	30.6	4.0	24.5	45.4				
<b>Minimum</b>	-67.3	12.3	0.2	-59.0	-48.4	6.6	8.6				
<b>Maximum</b>	92.7	102.0	67.7	123.0	61.4	81.9	76.4				
<b>Range</b>	160.1	89.7	67.5	181.9	109.9	75.3	67.8				
	NT = Not Tested										
	<b>Figure Key</b>										
	<b>Color</b>	<b>Growth Percent</b>									
	Most Active	< -50									
		-50 to 0									
		0 to 50									
	Least Active	> 50									

Table 7.5

As a set, the amides were most active against the IGROV1 cell line in which the average growth percent was -0.3. The four heterocyclic compounds were most active against IGROV1 and all had growth percents of -49.9 or less. The unique activity against the IGROV1 cell line may be explained by its own uniqueness as a “hypermutated” cell line. There is evidence that the IGROV1 cell line may not be a good model cell line for ovarian cancer as most tumor cells from patients do not exhibit the high rate of mutation seen in IGROV1. Figure 7.2 plots cell lines and tumor cells based on mutation rates and fraction of genome altered and it is very evident that the IGROV1 line is an outlier.<sup>172</sup> The fraction of genome altered is a measure of copy number alterations (CNAs) where chromosomes acquire or lose extra copies of the same gene. As can be seen in Figure 7.2, many of the ovarian cancer cell lines (red dots) used in research fall well outside of the grouping of blue dots representing actual tumor cells. This had led many people to question the validity of the cell line models commonly used in ovarian cancer research.<sup>172,173</sup>

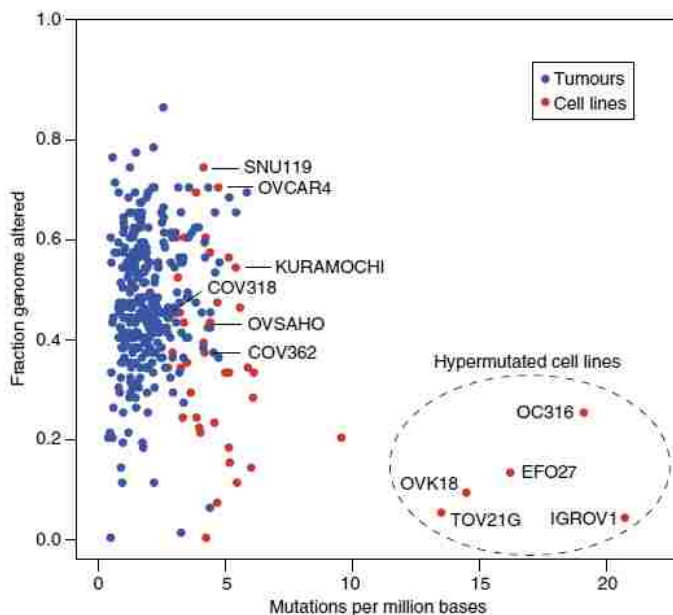


Figure 7.2: Mutation rates and fraction of genome alteration rates for different ovarian cancer cell lines.<sup>172</sup>

The activity of the amides against the OVCAR-5 line is also interesting. Pyrazine compound **43** (growth percent = -59.0) is much more active than pyridine compound **42** (growth percent = 2.9) indicating the importance of the second nitrogen atom in the pyrazine ring. Across all of the other ovarian cancer cell lines, the activities of **42** and **43** fall much closer together. Future research against the OVCAR-5 cell line could involve increasing the number of nitrogen atoms in the ring as well as changing their location.

The OVCAR-3 cell line results are remarkable for the inactivity of our amide compounds which had an average growth percent of 60.1. Though the amides were relatively inactive, there were compounds outside of the amide set that were quite active such as sulfonamide compound **12** which had a growth percent of -71.3. It would be interesting to synthesize and evaluate the methyl amide analogue to determine the importance of the sulfonyl group versus the carbonyl group.

IGROV1 Cell Line			OVCAR-3 Cell Line			OVCAR-4 Cell Line		
Compound ID	R group	IGROV1 Growth Percent	Compound ID	R group	OVCAR-3 Growth Percent	Compound ID	R group	OVCAR-4 Growth Percent
43		-67.3	43		12.3	43		0.2
41		-64.8	44		13.5	42		2.5
44		-53.8	41		19.0	41		3.0
42		-49.9	42		47.5	13		9.2
13		-3.9	45		49.6	45		15.6
46		3.8	13		57.2	44		19.8
38		14.8	46		78.4	37		27.6
37		49.1	38		82.0	46		32.1
39		75.8	39		97.8	38		44.3
40		92.7	37		101.5	39		55.2
	Average	-0.3	40		102.0	40		67.7
	Minimum	-67.3		Average	60.1		Average	25.2
	Maximum	92.7		Minimum	12.3		Minimum	0.2
	Range	160.1		Maximum	102.0		Maximum	67.7
				Range	89.7		Range	67.5

Table 7.6



OVCAR-5 Cell Line			OVCAR-8 Cell Line			NCI/ADR-RES Cell Line		
Compound ID	R group	OVCAR-5 Growth Percent	Compound ID	R group	OVCAR-8 Growth Percent	Compound ID	R group	NCI/ADR-RES Growth Percent
43		-59.0	41		-48.4	43		6.6
44		-14.1	13		-22.5	42		14.1
13		1.3	38		-5.9	41		15.5
42		2.9	45		-4.6	45		17.5
41		9.0	46		-0.5	44		18.1
45		32.4	43		0.4	46		20.6
46		41.9	42		3.0	38		22.3
38		46.0	44		4.4	13		23.6
37		61.0	37		23.4	40		81.9
39		91.9	39		33.3		Average	24.5
40		123.0	40		63.4		Minimum	6.6
	Average	30.6		Average	4.0		Maximum	81.9
	Minimum	-59.0		Minimum	-48.4		Range	75.3
	Maximum	123.0		Maximum	61.4			
	Range	181.9		Range	109.9			

Table 7.7

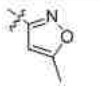
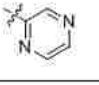
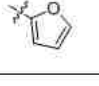
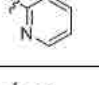
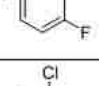
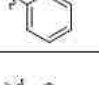
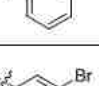
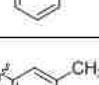
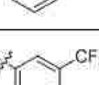
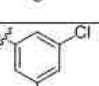
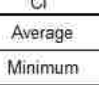
SK-OV-3 Cell Line		
Compound ID	R group	SK-OV-3 Growth Percent
41		8.6
43		9.9
44		31.8
42		37.7
46		38.5
45		42.1
13		56.3
37		61.2
38		61.9
39		74.7
40		76.4
	Average	45.4
	Minimum	8.6
	Maximum	76.4
	Range	67.8

Table 7.8

**Chapter 8: CNS Cancer**

## Chapter 8: CNS Cancer

### 8.1 CNS Cancer Overview

Our compounds were screened against six different central nervous system (CNS) cancer cell lines. The average mean growth percent across the six CNS cancer cell lines was 21.7. Table 8.1 shows the average growth percent of our compounds against each of the six CNS cancer cell lines screened. Table 8.1 also shows molecular characteristics and cell line source information for each of the six cell lines. Five of the six cell lines had relatively similar average mean growth percents ranging from 0.7 to 28.1. The outlier was the SNB-19 glioblastoma cell line which had a growth percent of 72.4.

Cell Line	Average Mean Growth Percent	Cancer Type	Mutations/variants <sup>166</sup>	TP53 <sup>167</sup>	p53 Amino Acid Codon Change <sup>167</sup>	MDR Rating <sup>174</sup>	Patient Age	Sex
SF-539	0.7	Gliosarcoma	TP53, PTEN, RB1	wild-type	wild-type	6.6	34	Female
U251	7.7	Glioblastoma	TP53, CDKN2A, PTEN	273 CGT → CAT	R → H	-12.3	75	Male
SF-295	8.3	Glioblastoma	TP53, CDKN2A, PTEN	248 CGG → CAG	R → Q	4.8	67	Female
SF-268	12.8	Highly anaplastic astrocytoma	TP53, CDKN2A	273 CGT → CAT	R → H	16.9	24	Female
SNB-75	28.1	Glioblastoma	TP53	258 GAA → AAA	E → K	1.8	78	Female
SNB-19	72.4	Glioblastoma	TP53, CDKN2A, PTEN	273 CGT → CAT	R → H	-10.8	47	Male
Average	21.7							

N/A: Data not available  
CDKN2A: Cyclin-dependent kinase inhibitor 2A  
PTEN: Phosphatase and tensin homologue  
RB1: Retinoblastoma 1  
TP53: Tumor protein p53  
Unless otherwise referenced above, cell line information was gathered from references 154-157.

Figure Key	
Color	Growth Percent
Most Active	< -50
	-50 to 0
	0 to 50
Least Active	> 50

**Table 8.1**

Table 8.2 shows the results for each compound against each CNS cancer cell line. The stereochemistry played a key role in the activity of the stereoisomers of Compound **1**. **(3S,8R)-1** and **(3S,8S)-1** had average growth percents of -37.5 and -29.5 respectively against the six CNS cancer cell lines screened. **(3R,8S)-1** and **(3R,8R)-1** were significantly less active with average growth percents of 89.1 and 88.6 respectively. Lipophilicity was also shown to be important as Compound **9** (4 carbon length chain),

(**3S,8R**)-1 (10 carbon length chain), and **10** (16 carbon length chain) had average growth percents of 107.3, -37.5, and -44.3 respectively.

Substituting an alcohol for the acetate at the C-3 position in (**3S,8R**)-1 produced a significant change in the average growth percent as Compound **16** had an average growth percent of -64.6 as compared to -37.5 for (**3S,8R**)-1. Compound **16** was remarkably active against the U251 cell line exhibiting a growth percent of -100.0.

Compound ID	CNS Cancer Cell Lines						Average	Minimum	Maximum	Range
	SF-268	SF-295	SF-539	SNB-19	SNB-75	U251				
( <b>3R,8S</b> )-1	87.3	103.7	102.3	71.5	74.1	95.5	89.1	71.5	103.7	32.2
( <b>3S,8R</b> )-1	-23.4	-22.9	-90.6	12.8	-47.9	-53.2	-37.5	-90.6	12.8	103.3
( <b>3R,8R</b> )-1	87.8	101.4	104.0	82.2	77.2	79.0	88.6	77.2	104.0	26.8
( <b>3S,8S</b> )-1	-11.7	-45.9	-76.6	58.1	-25.8	-74.9	-29.5	-76.6	58.1	134.7
<b>9</b>	116.7	105.2	100.9	119.8	95.0	105.8	107.3	95.0	119.8	24.8
<b>10</b>	-67.4	NT	-86.5	54.7	-49.3	-73.1	-44.3	-86.5	54.7	141.2
<b>11</b>	56.3	NT	98.7	94.9	74.6	89.3	82.7	56.3	98.7	42.4
<b>12</b>	-64.3	-75.6	-95.6	-26.3	-37.5	-92.0	-65.2	-95.6	-26.3	69.4
<b>13</b>	18.5	31.4	21.4	95.4	30.3	51.9	41.5	18.5	95.4	76.9
<b>14</b>	-0.3	NT	-7.8	85.8	14.8	21.9	22.9	-7.8	85.8	93.6
<b>15</b>	-49.7	-20.6	-56.6	6.0	-15.2	-96.2	-38.7	-96.2	6.0	102.3
<b>16</b>	-80.8	-57.9	-84.8	-1.2	-62.6	-100.0	-64.6	-100.0	-1.2	98.8
<b>37</b>	56.5	NT	68.7	88.8	79.3	74.9	73.6	56.5	88.8	32.3
<b>38</b>	38.7	48.1	45.8	93.0	86.5	NT	62.4	38.7	93.0	54.3
<b>39</b>	74.9	NT	89.9	87.6	73.8	78.6	81.0	73.8	89.9	16.0
<b>40</b>	73.4	NT	97.4	97.8	79.9	NT	87.1	73.4	97.8	24.4
<b>41</b>	-50.4	NT	-92.4	78.9	-20.4	NT	-21.1	-92.4	78.9	171.3
<b>42</b>	3.5	NT	23.1	96.6	34.4	NT	39.4	3.5	96.6	93.0
<b>43</b>	-32.6	NT	-96.2	80.0	-22.8	NT	-17.9	-96.2	80.0	176.2
<b>44</b>	-16.8	-72.5	-73.4	83.5	0.0	NT	-15.8	-73.4	83.5	156.9
<b>45</b>	10.2	-4.0	-12.6	99.8	24.5	NT	23.6	-12.6	99.8	112.4
<b>46</b>	11.6	17.3	-1.8	89.5	69.7	NT	37.3	-1.8	89.5	91.3
<b>47</b>	-21.6	NT	-63.2	92.5	52.5	NT	15.0	-63.2	92.5	155.7
<b>48</b>	89.7	NT	101.9	95.8	89.7	NT	94.3	89.7	101.9	12.2
<b>Average</b>	12.8	8.3	0.7	72.4	28.1	7.7				
<b>Minimum</b>	-80.8	-75.6	-96.2	-26.3	-62.6	-100.0				
<b>Maximum</b>	116.7	105.2	104.0	119.8	95.0	105.8				
<b>Range</b>	197.6	180.8	200.2	146.1	157.6	205.8				

Table 8.2

## 8.2 Hansch Cluster Analysis on CNS Cancer Cell Lines Data

Table 8.3 shows the CNS cancer testing results organized to assess the results per Hansch cluster analysis theory at the C-8 position. As shown in the table, the range of activity is wide over the six clusters tested. Isothiocyanate compound **48** of cluster 6 clearly has the least activity across the board with an average growth percent of 94.3. Selectivity against certain cell lines is evident for many of the compounds. The C-8 mesyl amide compound

**12** from cluster 4b was the most active compound against four of the six CNS cell lines (SF-268, SF-295, SF-539, and SNB-19) and was also the most active overall with an average growth percent of -65.2 across the six cell lines. The C-8 alcohol compound **(3S,8R)-1** from cluster 5 was most active against the SNB-75 cell line and the C-8 mesylate ester compound **15** from cluster 7 was the most active against the U251 cell line. Table 8.4 shows the growth percents for the compounds from the most active cluster against each cell line.

		CNS Cancer Cell Lines									
Compound ID	Cluster	SF-268	SF-295	SF-539	SNB-19	SNB-75	U251	Average	Minimum	Maximum	Range
<b>(3S,8R)-1</b>	5	-23.4	-22.9	-90.6	12.8	-47.9	-53.2	-37.5	-90.6	12.8	103.3
11	5	56.3	NT	98.7	94.9	74.6	89.3	82.7	56.3	98.7	42.4
12	4b	-64.3	-75.6	-95.6	-26.3	-37.5	-92.0	-65.2	-95.6	-26.3	69.4
13	8	18.5	31.4	21.4	95.4	30.3	51.9	41.5	18.5	95.4	76.9
14	9	-0.3	NT	-7.8	85.8	14.8	21.9	22.9	-7.8	85.8	93.6
15	7	-49.7	-20.6	-56.6	6.0	-15.2	-96.2	-38.7	-96.2	6.0	102.3
48	6	89.7	NT	101.9	95.8	89.7	NT	94.3	89.7	101.9	12.2
	Average	3.8	-21.9	-4.1	52.1	15.5	-13.1				
	Minimum	-64.3	-75.6	-95.6	-26.3	-47.9	-96.2				
	Maximum	89.7	31.4	101.9	95.8	89.7	89.3				
	Range	154.0	107.0	197.5	122.1	137.6	185.5				

Table 8.3

Cell Line	Most Active Cluster	C-8 Substituent	Compound ID	Growth Percent
SF-268	4b	-NHSO <sub>2</sub> Me	12	-64.3
SF-295	4b	-NHSO <sub>2</sub> Me	12	-75.6
SF-539	4b	-NHSO <sub>2</sub> Me	12	-95.6
SNB-19	4b	-NHSO <sub>2</sub> Me	12	-26.3
SNB-75	5	-OH	<b>(3S,8R)-1</b>	-47.9
U251	7	-OSO <sub>2</sub> Me	15	-96.2

Table 8.4

### 3.6.2.3. SAR Analysis of Amide Compounds against CNS Cancer Cell Lines

Across the set of amide compounds, there was considerable variability in activity against the different CNS cancer cell lines (Table 8.5). Very little activity was seen against the SNB-19 and U251 cell lines with the lowest growth percent against each cell line being 78.9 and 51.9 respectively. The effect of changing the amide group on the activity against the U251 cell line is less conclusive as only four of the amide compounds were screened against the U251 cell line.

The SF-539 cell line was very sensitive to the nature of the amide group as the growth percents ranged from -96.2 for compound **43** all the way up to 97.4 for compound **40**. Of particular interest for this cell line is the difference in growth percents between pyrazyl compound **43** (GP = -96.2) and 2-pyridine compound **42** (GP = 23.1). This seems to indicate that the second aromatic nitrogen atom in the pyrazyl compound is extremely important for activity. Isoxazole compound **41** (GP = -50.4) and 2-furyl compound **44** (GP = -72.5) were the most active compounds against the SF-268 and SF-295 cell lines respectively.

Compound ID	CNS Cancer Cell Lines						Average	Minimum	Maximum	Range
	SF-268	SF-295	SF-539	SNB-19	SNB-75	U251				
13	18.5	31.4	21.4	95.4	30.3	51.9	41.5	18.5	95.4	76.9
37	56.5	NT	68.7	88.8	79.3	74.9	73.6	56.5	88.8	32.3
38	38.7	48.1	45.8	93.0	86.5	NT	62.4	38.7	93.0	54.3
39	74.9	NT	89.9	87.6	73.8	78.6	81.0	73.8	89.9	16.0
40	73.4	NT	97.4	97.8	79.9	NT	87.1	73.4	97.8	24.4
41	-50.4	NT	-92.4	78.9	-20.4	NT	-21.1	-92.4	78.9	171.3
42	3.5	NT	23.1	96.6	34.4	NT	39.4	3.5	96.6	93.0
43	-32.6	NT	-96.2	80.0	-22.8	NT	-17.9	-96.2	80.0	176.2
44	-16.8	-72.5	-73.4	83.5	0.0	NT	-15.8	-73.4	83.5	156.9
45	10.2	-4.0	-12.6	99.8	24.5	NT	23.6	-12.6	99.8	112.4
46	11.6	17.3	-1.8	89.5	69.7	NT	37.3	-1.8	89.5	91.3
Average	17.1	4.1	6.4	90.1	39.6	68.4				
Minimum	-50.4	-72.5	-96.2	78.9	-22.8	51.9				
Maximum	74.9	48.1	97.4	99.8	86.5	78.6				
Range	125.3	120.7	193.6	20.8	109.3	26.7				

Table 8.5

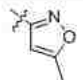
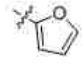
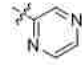
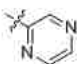
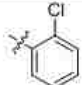
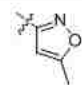
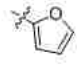
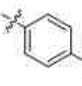

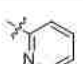

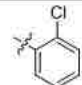
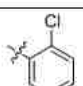
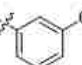
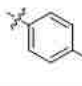
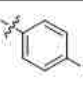
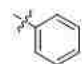
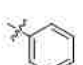
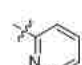
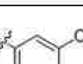
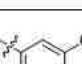
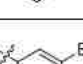

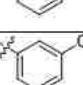
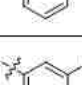
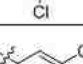
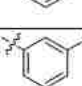
SF-268 Cell Line			SF-295 Cell Line			SF-539 Cell Line		
Compound ID	R group	SF-268 Growth Percent	Compound ID	R group	SF-295 Growth Percent	Compound ID	R group	SF-539 Growth Percent
41		-50.4	44		-72.5	43		-96.2
43		-32.6	45		-4.0	41		-92.4
44		-16.8	46		17.3	44		-73.4
42		3.5	13		31.4	45		-12.6
45		10.2	38		48.1	46		-1.8
46		11.6		Average	4.1	13		21.4
13		18.5		Minimum	-72.5	42		23.1
38		38.7		Maximum	48.1	38		45.8
37		56.5		Range	120.7	37		88.7
40		73.4				39		89.9
39		74.9				40		97.4
	Average	17.1					Average	6.4
	Minimum	-50.4					Minimum	-96.2
	Maximum	74.9					Maximum	97.4
	Range	125.3					Range	193.6

Table 8.6



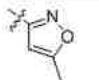
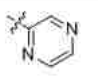
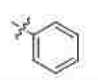
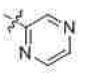
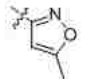
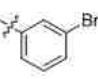
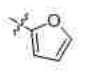

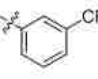
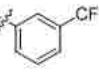
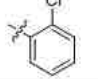
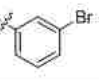
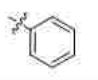
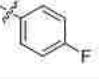
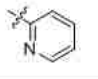
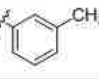
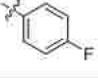
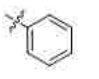
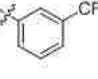
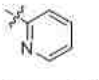
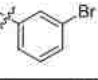
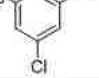
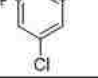
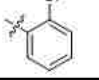
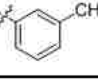
SNB-19 Cell Line			SNB-75 Cell Line			U251 Cell Line		
Compound ID	R group	SNB-19 Growth Percent	Compound ID	R group	SNB-75 Growth Percent	Compound ID	R group	U251 Growth Percent
41		78.9	43		-22.8	13		51.9
43		80.0	41		-20.4	37		74.9
44		83.5	44		0.0	39		78.6
39		87.5	45		24.5		Average	68.4
37		88.8	13		30.3		Minimum	51.9
46		89.5	42		34.4		Maximum	78.6
38		93.0	46		69.7		Range	26.7
13		95.4	39		73.0			
42		96.8	37		78.3			
40		97.8	40		79.9			
45		99.8	38		86.5			
	Average	90.1		Average	39.6			
	Minimum	78.9		Minimum	-22.8			
	Maximum	99.8		Maximum	86.5			
	Range	20.8		Range	109.3			

Table 8.7

***Chapter 9: Melanoma***

## Chapter 9: Melanoma

### 9.1 Melanoma Overview

Our compounds were screened against nine different melanoma cell lines. The average mean growth percent across the nine melanoma cell lines was -21.0. As shown in Table 3.4, our compounds had the most broad spectrum activity against melanoma as compared to the eight other classes of cancers cell lines. Table 9.1 shows the average mean growth percent of our compounds against each of the nine melanoma cell lines screened. Table 9.1 also shows molecular characteristics and cell line source information for each of the nine cell lines. The range of biological activity against the different cell lines was broad as the average mean growth percent was -58.2 against the LOX IMVI cell line as compared to 10.9 against the SK-MEL-28 cell line.

Cell Line	Average Mean Growth Percent	Mutations/variants <sup>166</sup>	TP53 <sup>167</sup>	p53 Amino Acid Codon Change <sup>167</sup>	Antigen Expression	Patient Age	Sex	Ethnicity
LOX IMVI	-58.2	BRAF, CDKN2A	wild-type	wild-type	N/A	58	Male	N/A
SK-MEL-5	-40.3	BRAF, CDKN2A	wild-type	wild-type	Blood Type O, Rh+, HLA A2, A11, B40, Bw16	24	Female	Caucasian
MALME-3M	-30.4	BRAF, CDKN2A	wild-type	wild-type	HLA A2, Aw30, B13, B40(+/-), DRw7	43	Male	Caucasian
SK-MEL-2	-24.3	TP53, NRAS	245 GGC → AGC	G → S	Blood Type A, Rh+	60	Male	Caucasian
UACC-257	-19.5	BRAF	wild-type	wild-type	N/A	N/A	N/A	N/A
MDA-MB-435	-15.5	TP53, BRAF, CDKN2A	N/A	N/A	N/A	N/A	N/A	N/A
M14	-6.6	TP53, BRAF, CDKN2A	266 GGA → GAA	G → E	N/A	N/A	N/A	N/A
UACC-62	-5.3	BRAF, CDKN2A, PTEN	wild-type	wild-type	N/A	N/A	N/A	N/A
SK-MEL-28	10.9	TP53, BRAF, EGFR	145 TGT → GTT	C → V	Blood Type A, Rh+, HLA A11, A26, B40, DRw4	51	Male	N/A
Average	-21.0							

Figure Key	
Color	Growth Percent
Most Active	< -50
	-50 to 0
	0 to 50
Least Active	> 50

N/A: Data not available  
 BRAF: v-raf murine sarcoma viral oncogene homologue B1  
 CDKN2A: Cyclin-dependent kinase inhibitor 2A  
 EGFR: Epidermal growth factor receptor  
 NRAS: Neuroblastoma RAS viral (v-ras) oncogene homologue  
 PTEN: Phosphatase and tensin homologue  
 TP53: Tumor protein p53  
 Unless otherwise referenced above, cell line information was gathered from references 154-157.

**Table 9.1**

Table 9.2 shows the results for each compound against each melanoma cell line.

As discussed in section 3.3, the stereochemistry played a key role in the activity of the stereoisomers of Compound 1. (3*S*,8*R*)-1 and (3*S*,8*S*)-1 had average growth percents of -

68.4 and -58.4 respectively against the melanoma cell lines screened. **(3R,8S)-1** and **(3R,8R)-1** were significantly less active with average growth percents of 71.0 and 66.8 respectively. Lipophilicity was also shown to be important as Compound **9** (4 carbon length chain), **(3S,8R)-1** (10 carbon length chain), and **10** (16 carbon length chain) had average growth percents of 107.7, -68.4, and -80.3 respectively. Substituting an alcohol for the acetate at the C-3 position in **(3S,8R)-1** produced a slightly more active compound as Compound **16** had an average growth percent of -74.2 as compared to -68.4 for **(3S,8R)-1**.

Compound ID	Melanoma Cell Lines									Average	Minimum	Maximum	Range
	LOX IMVI	MALME-3M	M14	MDA-MB-435	SK-MEL-2	SK-MEL-28	SK-MEL-5	UACC-257	UACC-62				
(3R,8S)-1	NT	-46.9	104.4	99.6	NT	100.9	NT	NT	97.1	71.0	-46.9	104.4	151.2
(3S,8R)-1	-94.3	-59.8	-76.4	-53.0	-57.4	-75.8	-95.2	-3.6	-99.7	-68.4	-99.7	-3.6	96.0
(3R,8R)-1	NT	-57.0	100.7	88.3	NT	97.8	NT	85.9	85.1	66.8	-57.0	100.7	157.7
(3S,8S)-1	NT	-62.0	-26.3	-75.8	NT	-58.9	NT	-47.0	-80.3	-58.4	-80.3	-26.3	54.0
9	92.3	100.4	101.7	105.0	135.8	113.9	97.6	117.9	104.4	107.7	92.3	135.8	43.5
10	-91.9	-71.0	-83.8	-74.2	-86.7	-85.4	-97.8	-64.2	-67.6	-80.3	-97.8	-64.2	33.5
11	-93.3	7.3	8.1	-44.1	84.4	96.9	13.2	NT	64.9	17.2	-93.3	96.9	190.2
12	-93.5	-56.3	-78.3	-62.3	-73.6	-66.3	-98.9	-67.3	-68.7	-73.9	-98.9	-56.3	42.6
13	-90.5	-62.5	-87.3	-37.2	-33.6	-37.9	-87.0	-83.0	-51.2	-63.3	-90.5	-33.6	57.0
14	-82.1	-30.9	6.8	-25.3	-25.6	27.0	-65.9	NT	-14.4	-26.3	-82.1	27.0	109.1
15	-89.4	-53.7	-83.6	-30.7	-58.8	-27.9	-99.8	-76.1	-72.0	-65.8	-99.8	-27.9	72.0
16	-91.9	-45.2	-93.3	-51.4	-69.0	-58.1	-99.9	-92.7	-66.2	-74.2	-99.9	-45.2	54.6
37	-66.7	-3.6	27.6	16.3	-35.0	69.1	14.1	41.3	44.9	12.0	-66.7	69.1	135.8
38	-68.6	-42.0	1.8	-30.0	-56.2	58.7	NT	-48.2	-3.2	-23.5	-68.6	58.7	127.2
39	-32.8	18.0	27.3	40.8	NT	91.1	76.4	76.5	80.1	47.2	-32.8	91.1	123.9
40	11.1	89.4	39.7	62.9	49.5	102.1	NT	91.0	97.6	67.9	11.1	102.1	91.0
41	-69.8	-65.5	-37.0	-65.5	-79.7	-64.1	NT	-89.7	-37.9	-63.6	-89.7	-37.0	52.7
42	-71.3	-69.5	-24.6	-57.7	-55.3	-30.3	NT	-62.3	-19.7	-48.8	-71.3	-19.7	51.6
43	-77.0	-68.2	-47.0	-56.8	-52.3	-65.9	NT	-77.7	-40.7	-60.7	-77.7	-40.7	37.0
44	-81.7	-68.7	-19.6	-56.3	-49.7	-42.2	NT	-77.6	-22.0	-52.2	-81.7	-19.6	62.1
45	-67.7	-60.0	0.2	-51.1	-44.2	-41.0	NT	-56.2	-40.5	-45.1	-67.7	0.2	68.0
46	-75.8	-50.7	6.3	-49.0	-51.2	54.1	NT	-32.8	-47.4	-30.8	-75.8	54.1	129.8
47	-69.3	-65.4	-21.5	-57.4	-46.1	1.6	NT	-43.4	-69.7	-46.4	-69.7	1.6	71.3
48	81.8	93.4	95.4	94.0	117.7	103.4	NT	99.8	99.9	98.2	81.8	117.7	35.9
Average	-58.2	-30.4	-6.6	-15.5	-24.3	10.9	-40.3	-19.5	-5.3				
Minimum	-94.3	-71.0	-93.3	-75.8	-86.7	-85.4	-99.9	-92.7	-99.7				
Maximum	92.3	100.4	104.4	105.0	135.8	113.9	97.6	117.9	104.4				
Range	186.6	171.4	197.7	180.8	222.5	199.3	197.5	210.7	204.1				
NT = Not Tested													
Figure Key													
Color Growth Percent													
Most Active < -50													
-50 to 0													
0 to 50													
Least Active > 50													

Table 9.2

## 9.2 Hansch Cluster Analysis on Lung Cancer Cell Lines Data

Table 9.3 shows the melanoma testing results organized to assess the results per Hansch cluster analysis theory at the C-8 position. As shown in the table, the range of activity is wide over the six clusters tested. The alcohol compound **(3S,8R)-1** from cluster 5 was the most active compound against the LOX IMVI, SK-MEL-28, and UACC-62 cell lines.

The phenyl amide compound **13** from cluster 8 was the most active against the MALME-3M, M14 and UACC-257 cell lines. The mesyl amide compound **12** from cluster 4b was the most active against the MDA-MB-435 and SK-MEL-2 cell lines. The mesyl ester compound **15** from cluster 7 was the most active against the SK-MEL-5 cell line. Across the whole set of melanoma cell lines tested, compound **12** from cluster 4b was the most active with an average growth percent of -73.9. On the other end of the activity spectrum, the isothiocyanate compound **48** from cluster 6 was the least active compound against all of the melanoma cell lines which it was screened against.

Compound ID	Cluster	Melanoma Cell Lines									Average	Minimum	Maximum	Range
		LOX IMVI	MALME-3M	M14	MDA-MB-435	SK-MEL-2	SK-MEL-28	SK-MEL-5	UACC-257	UACC-62				
(3S,8R)-1	5	-94.3	-59.9	-76.4	-33.9	-57.1	-75.8	-95.2	-3.6	-99.7	-84.4	-99.7	-3.6	96.0
11	5	-93.3	7.3	8.1	-44.1	84.4	95.9	13.2	NT	84.9	17.2	-93.3	96.9	190.2
12	4b	-93.5	-56.3	-78.3	-62.3	-73.6	-66.3	-98.9	-67.3	-67.3	-73.9	-98.9	-56.3	42.6
13	8	-90.5	-62.5	-87.3	-37.2	-33.6	-37.9	-87.0	NT	-51.2	-63.3	-90.5	-33.6	57.0
14	9	-82.1	-30.9	6.8	-25.3	-25.6	27.0	-65.9	NT	-14.4	-26.3	-82.1	27.0	109.1
15	7	-89.4	-53.7	-83.6	-30.7	-58.8	-27.9	-99.8	-76.1	-72.0	-65.8	-99.8	-27.9	72.0
48	6	81.8	93.4	95.4	94.0	117.7	103.4	NT	99.8	99.9	98.2	81.8	117.7	35.9
Average		-65.9	-23.2	-30.7	-22.7	-6.7	2.8	-72.3	-26.0	-20.2				
Minimum		-94.3	-62.5	-87.3	-62.3	-73.6	-75.8	-99.8	-83.0	-99.7				
Maximum		81.8	93.4	95.4	94.0	117.7	103.4	13.2	99.8	99.9				
Range		176.1	155.9	182.7	156.3	191.3	179.2	113.0	182.7	199.6				

NT = Not Tested

Table 9.3

Cell Line	Most Active Cluster	C-8 Substituent	Compound ID	Growth Percent
LOX IMVI	5	-OH	(3S,8R)-1	-94.3
MALME-3M	8	-NHCOPh	13	-62.5
M14	8	-NHCOPh	13	-87.3
MDA-MB-435	4b	-NH <sub>2</sub> SO <sub>2</sub> Me	12	-62.3
SK-MEL-2	4b	-NH <sub>2</sub> SO <sub>2</sub> Me	12	-73.6
SK-MEL-28	5	-OH	(3S,8R)-1	-75.8
SK-MEL-5	7	-OSO <sub>2</sub> Me	15	-99.8
UACC-257	8	-NHCOPh	13	-83.0
UACC-62	5	-OH	(3S,8R)-1	-99.7

Table 9.4

### 9.3 SAR Analysis of Amide Compounds against Melanoma Cell Lines

Eleven of the compounds we had tested by NCI have an acetate at the C-3 position and different amide functionalities with aromatic or heteroaromatic groups directly connected to the amide carbonyl group in the C-8 position as shown in Figure 9.1.

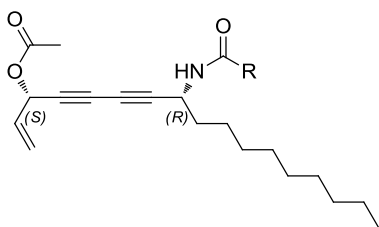


Figure 9.1 Generic structure of amides screened by NCI.

Table 9.5 shows the activity of our amide compounds against each of the different melanoma cell lines. The set of amide compounds showed a wide range of activity against the different cell lines indicating that changing the amide R group has a significant impact on activity. The widest range of activity was seen against the UACC-257 cell line in which compound **13** (R = phenyl) had a growth percent of -83.0 whereas compound **40** (R = 3,5 dichlorophenyl) had a growth percent of 91.0.

Compound ID	Melanoma Cell Lines									Average	Minimum	Maximum	Range
	LOX IMVI	MALME-3M	M14	MDA-MB-435	SK-MEL-2	SK-MEL-28	SK-MEL-5	UACC-257	UACC-62				
13	-90.5	-62.5	-87.3	-37.2	-33.6	-37.9	-87.0	-83.0	-51.2	-63.3	-90.5	-33.6	57.0
37	-66.7	-3.6	27.6	16.3	-35.0	69.1	14.1	41.3	44.9	12.0	-66.7	69.1	135.8
38	-68.6	-42.0	1.8	-30.0	-56.2	58.7	NT	-48.2	-3.2	-23.5	-68.6	58.7	127.2
39	-32.8	18.0	27.3	40.8	NT	91.1	76.4	76.5	80.1	47.2	-32.8	91.1	123.9
40	11.1	89.4	39.7	62.9	49.5	102.1	NT	91.0	97.6	67.9	11.1	102.1	91.0
41	-69.8	-65.5	-37.0	-65.5	-79.7	-64.1	NT	-89.7	-37.9	-63.6	-89.7	-37.0	52.7
42	-71.3	-69.5	-24.6	-57.7	-55.3	-30.3	NT	-62.3	-19.7	-48.8	-71.3	-19.7	51.6
43	-77.0	-68.2	-47.0	-56.8	-52.3	-65.9	NT	-77.7	-40.7	-60.7	-77.7	-40.7	37.0
44	-81.7	-68.7	-19.6	-56.3	-49.7	-42.2	NT	-77.6	-22.0	-52.2	-81.7	-19.6	62.1
45	-67.7	-60.0	0.2	-51.1	-44.2	-41.0	NT	-56.2	-40.5	-45.1	-67.7	0.2	68.0
46	-75.8	-50.7	6.3	-49.0	-51.2	54.1	NT	-32.8	-47.4	-30.8	-75.8	54.1	129.8
Average	-62.8	-34.8	-10.2	-25.8	-40.8	8.5	1.2	-29.0	-3.6				
Minimum	-90.5	-69.5	-87.3	-65.5	-79.7	-65.9	-87.0	-89.7	-51.2				
Maximum	11.1	89.4	39.7	62.9	49.5	102.1	76.4	91.0	97.6				
Range	101.6	158.9	127.0	128.4	129.2	168.0	163.3	180.6	148.8				
	NT = Not Tested												
	Figure Key												
	Color	Growth Percent											
	Most Active	< -50											
		-50 to 0											
		0 to 50											
	Least Active	> 50											

Table 9.5

LOX IMVI Cell Line		
Compound ID	R group	LOX IMVI Growth Percent
13		-90.5
44		-81.7
43		-77.0
46		-75.8
42		-71.3
41		-69.8
38		-68.6
45		-67.7
37		-66.7
39		-32.8
40		11.1
	Average	-62.8
	Minimum	-90.5
	Maximum	11.1
	Range	101.6

MALME-3M Cell Line		
Compound ID	R group	MALME-3M Growth Percent
42		-69.5
44		-68.7
43		-68.2
41		-65.5
13		-62.5
45		-60.0
46		-50.7
38		-42.0
37		-3.6
39		18.0
40		89.4
	Average	-34.8
	Minimum	-69.5
	Maximum	89.4
	Range	158.9

M14 Cell Line		
Compound ID	R group	M14 Growth Percent
13		-87.3
43		-47.0
41		-37.0
42		-24.6
44		-19.6
45		0.2
38		1.8
46		6.3
39		27.3
37		27.6
40		39.7
	Average	-10.2
	Minimum	-87.3
	Maximum	39.7
	Range	127.0

Table 9.6

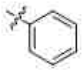
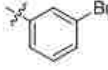
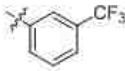
MDA-MB-435 Cell Line		
Compound ID	R group	MDA-MB-435 Growth Percent
41		-65.5
42		-57.7
43		-56.8
44		-56.3
45		-61.1
46		-49.0
13		-37.2
38		-30.0
37		16.3
39		40.8
40		62.9
	Average	-25.8
	Minimum	-65.5
	Maximum	62.9
	Range	128.4

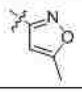
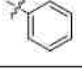
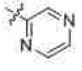

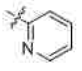
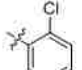
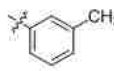
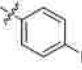
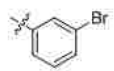
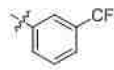
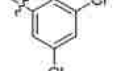
SK-MEL-2 Cell Line		
Compound ID	R group	SK-MEL-2 Growth Percent
41		-79.7
38		-66.2
42		-55.3
43		-52.3
46		-51.2
44		-49.7
45		-44.2
37		-35.0
13		-33.6
40		49.5
	Average	-40.8
	Minimum	-79.7
	Maximum	49.5
	Range	129.2

SK-MEL-28 Cell Line		
Compound ID	R group	SK-MEL-28 Growth Percent
43		-65.9
41		-64.1
44		-42.2
45		-41.0
13		-37.9
42		-30.3
46		54.1
38		58.7
37		69.1
39		91.1
40		102.1
	Average	8.5
	Minimum	-65.9
	Maximum	102.1
	Range	168.0

Table 9.7



SK-MEL-5 Cell Line		
Compound ID	R group	SK-MEL-5 Growth Percent
13		-87.0
37		14.1
39		76.4
	Average	1.2
	Minimum	-87.0
	Maximum	76.4
	Range	163.3

UACC-257 Cell Line		
Compound ID	R group	UACC-257 Growth Percent
41		-89.7
13		-83.0
43		-77.7
44		-77.6
42		-62.3
45		-56.2
38		-48.2
46		-32.8
37		41.3
39		76.5
40		91.0
	Average	-29.0
	Minimum	-89.7
	Maximum	91.0
	Range	180.6

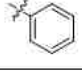
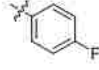
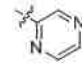
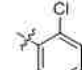
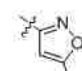

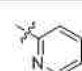
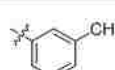
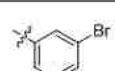
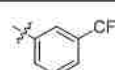
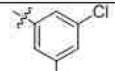
UACC-62 Cell Line		
Compound ID	R group	UACC-62 Growth Percent
13		-51.2
46		-47.4
43		-40.7
45		-40.5
41		-37.9
44		-22.0
42		-19.7
38		-3.2
37		44.9
39		80.1
40		97.6
	Average	-3.6
	Minimum	-51.2
	Maximum	97.6
	Range	148.8

Table 9.8

**Chapter 10: Lung Cancer**

## Chapter 10: Lung Cancer

### 10.1 Lung Cancer Overview

Our compounds were screened against eight different lung cancer cell lines. The average mean growth percent across the eight lung cancer cell lines was 5.2. Table 10.1 shows the average mean growth percent of our compounds against each of the eight lung cancer cell lines screened. Figure 3.X also shows molecular characteristics and cell line source information for each of the eight cell lines. The range of biological activity against the different cell lines was broad as the average mean growth percent was -50.7 against the NCI-H522 cell line as compared to 79.9 against the NCI-H322M cell line.

Cell Line	Average Mean Growth Percent	Cancer Type	Mutations/Variants <sup>166</sup>	p53 sequence codon change <sup>167</sup>	p53 sequence amino acid change <sup>167</sup>	Patient Age	Sex	Ethnicity
NCI-H522	-50.7	Adenocarcinoma (Stage 2)	TP53	deletion 191 G	deletion 191 G	58	Male	N/A
HOP-92	-44.2	Large cell, undifferentiated	TP53, CDKN2A	175 CGC → CTC	175 R → L	62	Male	N/A
NCI-H226	-8.9	Squamous cell carcinoma, mesothelioma	CDKN2A	309 CCC → GCC	309 P → A	N/A	Male	N/A
HOP-62	-2.2	Adenocarcinoma	TP53, CDKN2A, KRAS	insertion 212-225	insertion 212-225	60	Female	N/A
NCI-H23	-1.9	Adenocarcinoma	TP53, STK11, KRAS	246 ATG → ATC	246 M → I	51	Male	Black
NCI-H460	22.3	Large cell, carcinoma	CDKN2A, KRAS, PIK3CA, STK11	wild-type	wild-type	N/A	Male	N/A
A549/ATCC	47.1	Adenocarcinoma	CDKN2A, KRAS, STK11	wild-type	wild-type	58	Male	Caucasian
NCI-H322M	79.9	Small cell bronchoalveolar carcinoma	TP53	248 CGG → CTG	248 R → L	52	Male	Caucasian
Average	5.2							

N/A: Data not available  
 CDKN2A: Cyclin-dependent kinase inhibitor 2A  
 KRAS: v-Ki-ras2 Kirsten rat sarcoma viral oncogene homologue  
 PIK3CA: Phosphoinositide-3-kinase, catalytic,  $\alpha$  polypeptide  
 STK11: Serine/threonine kinase 11/LKB1 (Peutz-Jehgers syndrome)  
 TP53: Tumor protein p53  
 Unless otherwise referenced above, cell line information was gathered from references 154-157.

Figure Key	
Color	Growth Percent
Most Active	< -50
	-50 to 0
	0 to 50
Least Active	> 50

**Table 10.1**

Table 10.2 shows the results for each compound against each lung cancer cell line. As discussed in section 3.3, the stereochemistry played a key role in the activity of the stereoisomers of Compound **1**. (**3S,8R**)-**1** and (**3S,8S**)-**1** had average growth percents of -54.5 and -43.0 respectively against the breast cancer cell lines screened. (**3R,8S**)-**1** and (**3R,8R**)-**1** were significantly less active with average growth percents of 96.2 and 89.5 respectively. Lipophilicity was also shown to be important as Compound **9** (4 carbon length chain), (**3S,8R**)-**1** (10 carbon length chain), and **10** (16 carbon length chain) had average growth percents of 100.6, -54.5, and -34.3 respectively. Substituting an

alcohol for the acetate at the C-3 position in **(3*S*,8*R*)-1** produced little change in the average growth percent as Compound **16** had an average growth percent of -54.7 as compared to -54.5 for **(3*S*,8*R*)-1**.

Compound ID	Lung Cancer Cell Line								Average	Minimum	Maximum	Range
	A549/ATCC	HOP-62	HOP-92	NCI-H226	NCI-H23	NCI-H322M	NCI-H460	NCI-H522				
(3 <i>R</i> ,8 <i>S</i> )-1	110.9	107.9	NT	82.6	103.7	87.6	101.6	78.7	96.2	78.7	110.9	32.2
(3 <i>S</i> ,8 <i>R</i> )-1	-15.5	-93.3	-72.6	-60.5	-81.8	38.7	-54.9	-96.4	-54.5	-96.4	38.7	135.1
(3 <i>R</i> ,8 <i>R</i> )-1	89.9	96.3	NT	75.6	105.7	96.9	101.2	60.8	89.5	60.8	105.7	44.9
(3 <i>S</i> ,8 <i>S</i> )-1	6.9	-84.7	NT	-67.5	-63.8	33.9	-35.8	-90.1	-43.0	-90.1	33.9	124.1
9	108.6	118.1	52.7	92.9	94.3	116.3	103.2	119.1	100.6	52.7	119.1	66.4
10	0.5	-88.5	-71.2	-66.6	-43.9	98.5	-18.6	-84.7	-34.3	-88.5	98.5	187.0
11	103.2	44.9	NT	NT	13.1	107.0	96.3	NT	72.9	13.1	107.0	93.8
12	-37.7	-32.8	-66.2	-50.9	-71.8	6.2	-49.4	-97.2	-50.0	-97.2	6.2	103.5
13	43.3	-19.7	-61.4	-38.2	-35.7	99.6	-14.9	-79.5	-13.3	-79.5	99.6	179.1
14	50.2	-60.4	NT	NT	-7.1	96.4	22.9	NT	20.2	-60.4	96.4	155.8
15	-19.9	-15.5	-75.6	-42.3	-47.1	-36.5	-35.8	-87.5	-45.0	-87.5	-15.5	71.9
16	-44.6	-72.9	-71.5	-26.3	-68.0	-5.3	-35.9	-94.9	-54.7	-94.9	-5.3	89.6
37	92.6	99.8	-29.5	-12.1	9.6	112.2	51.4	-78.0	25.7	-78.0	112.2	190.1
38	71.7	5.1	-54.2	NT	-2.9	93.6	31.1	-94.3	7.2	-94.3	93.6	187.9
39	80.5	105.6	45.7	6.9	39.3	103.6	70.1	-24.4	52.3	-24.4	105.6	130.0
40	101.9	107.4	86.2	NT	44.9	194.4	98.9	-34.0	78.8	-34.0	107.4	141.5
41	25.5	77.2	NT	NT	-16.9	84.8	2.2	-95.7	-12.9	-95.7	84.8	180.5
42	38.0	-40.5	-78.3	NT	-18.2	94.1	7.4	-75.3	-10.1	-78.3	94.1	172.3
43	10.5	-43.0	-78.0	NT	-27.1	82.1	-14.6	-90.1	-22.9	-90.1	82.1	172.1
44	18.3	-47.3	-79.4	NT	-0.6	87.2	-25.9	-84.9	-18.9	-84.9	87.2	172.0
45	40.0	-54.5	-75.2	NT	-26.3	97.0	5.1	-93.2	-15.3	-93.2	97.0	190.2
46	82.0	11.0	NT	NT	-18.8	97.8	27.1	-96.8	17.4	-96.8	97.8	194.6
47	72.1	-80.9	-78.3	NT	-18.7	109.6	22.0	-74.3	-6.9	-80.9	109.6	190.5
48	102.4	103.1	NT	NT	95.5	112.4	99.5	98.2	101.8	95.5	112.4	17.0
Average	47.1	-2.2	-44.2	-8.9	-1.9	79.9	22.3	-50.7				
Minimum	-44.6	-93.3	-79.4	-67.5	-81.8	-36.5	-55.9	-97.2				
Maximum	110.9	118.1	86.2	105.7	116.3	116.3	103.2	119.1				
Range	155.5	211.4	165.5	160.4	187.5	152.8	159.1	216.3				

NT = Not Tested

Figure Key	
Color	Growth Percent
Most Active	< -50
	-50 to 0
	0 to 50
Least Active	> 50

Table 10.2

## 10.2 Hansch Cluster Analysis on Lung Cancer Cell Lines Data

Table 10.3 shows the lung cancer testing results organized to assess the results per Hansch cluster analysis theory at the C-8 position. As shown in the table, the range of activity is wide over the six clusters tested. The alcohol compound **(3*S*,8*R*)-1** from cluster 5 was the most active compound against the HOP-62, NCI-H226, NCI-H23, and NCI-H460 cell lines. The mesyl amide compound **12** from cluster 4b was the most active against the A549/ATCC and NCI-H522 cell lines. The mesyl ester compound **15** from cluster 7 was the most active against the HOP-92 and NCI-H322M cell lines. Across the whole set of lung cancer cell lines tested, compound **(3*S*,8*R*)-1** from cluster 5 was the most active with an average growth percent of -54.5. On the other end of the activity

spectrum, the isothiocyanate compound **48** from cluster 6 was the least active compound against all of the lung cancer cell lines which it was screened against.

Compound ID (3S,8R)-1	Cluster	Lung Cancer Cell Line								Average	Minimum	Maximum	Range
		A549/ATCC	HOP-62	HOP-92	NCI-H226	NCI-H23	NCI-H322M	NCI-H460	NCI-H522				
11	5	-15.5	-93.3	-72.8	-54.5	-81.8	-37.7	-54.3	-54.4	-96.4	38.7	135.1	
12	4b	-37.7	-32.8	-66.2	-50.9	-71.8	6.2	-49.4	-97.2	-50.0	-97.2	6.2	
13	8	43.3	-19.7	-61.4	-38.2	-35.7	99.6	-14.9	-79.5	-13.3	-79.5	99.6	
14	9	50.2	-60.4	NT	NT	-7.1	95.4	22.9	NT	20.2	-60.4	95.4	
15	7	-19.9	-15.5	-75.6	-42.3	-47.1	-36.5	-35.8	-87.5	-45.0	-87.5	-15.5	
48	6	102.4	103.1	NT	NT	95.5	112.4	99.5	98.2	101.8	95.5	112.4	
	Average	32.3	-10.5	-69.0	-48.0	-19.3	60.4	9.1	-52.5				
	Minimum	-37.7	-93.3	-75.6	-60.5	-81.8	-36.5	-54.9	-97.2				
	Maximum	103.2	103.1	-61.4	-38.2	95.5	112.4	99.5	98.2				
	Range	141.0	196.4	14.2	22.3	177.2	148.9	154.4	195.4				

Table 10.3

Cell Line	Most Active Cluster	C-8 Substituent	Compound ID	Growth Percent
A549/ATCC	4b	-NH <sub>2</sub> SO <sub>2</sub> Me	12	-37.7
HOP-62	5	-OH	(3S,8R)-1	-93.3
HOP-92	7	-OSO <sub>2</sub> Me	15	-75.6
NCI-H226	5	-OH	(3S,8R)-1	-60.5
NCI-H23	5	-OH	(3S,8R)-1	-81.8
NCI-H322M	7	-OSO <sub>2</sub> Me	15	-36.5
NCI-H460	5	-OH	(3S,8R)-1	-54.9
NCI-H522	4b	-NH <sub>2</sub> SO <sub>2</sub> Me	12	-97.2

Table 10.4

### 10.3 SAR Analysis of Amide Compounds against Lung Cancer Cell Lines

Eleven of the compounds we had tested by NCI have an acetate at the C-3 position and different amide functionalities with aromatic or heteroaromatic groups directly connected to the amide carbonyl group in the C-8 position as shown in Figure 10.1.

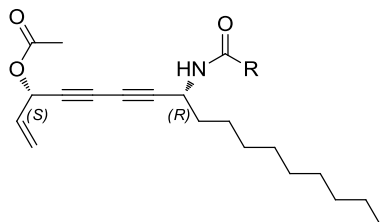




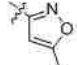
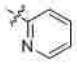
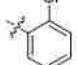
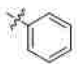
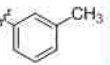
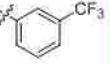
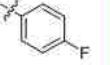
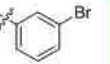
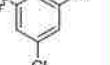
Figure 10.1 Generic structure of amides screened by NCI.

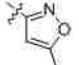
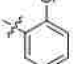

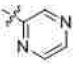
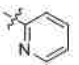
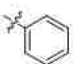
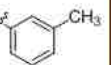
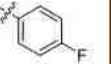
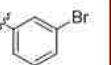
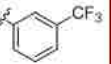
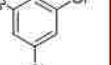
Table 10.5 shows the activity of our amide compounds against each of the different lung cancer cell lines. The set of amide compounds showed a wide range of activity against the different cell lines indicating that changing the amide R group has a significant impact on activity. The only cell line in which the R group appeared to have

little effect on activity was the NCI-H322M cell line against which there was negligible activity across all of the amide compounds with an average mean growth percent of 96.0. On the other end of the activity spectrum, the average mean growth percent was -76.9 against the NCI-H522 cell line. It would be interesting to evaluate the cellular differences between the NCI-H322 and NCI-H522 cell lines as it could help elucidate a possible mechanism of action for this class of compounds. The widest range of activity was seen against the HOP-92 cell line in which furan compound **44** had a growth percent of -79.4 whereas *m*-bromo compound **40** had a growth percent of 86.2.

Compound ID	Lung Cancer Cell Lines								Average	Minimum	Maximum	Range
	A549/ATCC	HOP-62	HOP-92	NCI-H226	NCI-H23	NCI-H322M	NCI-H460	NCI-H522				
13	43.3	-19.7	-61.4	-38.2	-35.7	89.6	-14.9	-79.5	-13.3	-79.5	99.6	179.1
37	92.6	59.8	-29.5	-12.1	9.6	112.2	51.4	-78.0	25.7	-78.0	112.2	190.1
38	71.7	5.1	-54.2	NT	-2.9	93.6	31.1	-94.3	7.2	-94.3	93.6	187.9
39	80.5	105.6	45.7	6.9	30.3	103.6	70.1	-24.4	52.3	-24.4	105.6	130.0
40	101.6	107.4	86.2	NT	44.9	104.4	98.9	-34.0	72.8	-34.0	107.4	141.5
41	25.5	-77.2	NT	NT	-16.9	84.8	2.2	-95.7	-12.9	-95.7	84.8	180.5
42	38.0	-40.5	-78.3	NT	-16.2	94.1	7.4	-75.3	-10.1	-78.3	94.1	172.3
43	10.5	-43.0	-78.0	NT	-27.1	82.1	-14.6	-80.1	-22.9	-80.1	82.1	172.1
44	18.3	-47.3	-79.4	NT	-0.6	87.2	-25.9	-84.9	-18.9	-84.9	87.2	172.0
45	40.0	-54.5	-75.2	NT	-26.3	87.0	5.1	-93.2	-15.3	-93.2	97.0	190.2
46	82.0	11.0	NT	NT	-16.8	87.8	27.1	-96.8	17.4	-96.8	97.8	194.6
Average	54.9	0.6	-36.0	-14.5	-5.2	96.0	21.6	-76.9				
Minimum	10.5	-77.2	-79.4	-38.2	-35.7	82.1	-25.9	-96.8				
Maximum	101.6	107.4	86.2	6.9	44.9	112.2	98.9	-24.4				
Range	91.0	184.7	165.5	45.1	80.7	30.1	124.8	72.5				

Table 10.5

A549 Cell Line		
Compound ID	R group	A549 Growth Percent
43		10.5
44		18.3
41		25.5
42		38.0
45		40.0
13		43.3
38		71.7
39		80.6
46		82.0
37		92.6
40		101.6
	Average	54.3
	Minimum	10.5
	Maximum	101.6
	Range	91.0

HOP-62 Cell Line		
Compound ID	R group	HOP-62 Growth Percent
41		-77.2
45		-64.5
44		-47.3
43		-43.0
42		-40.5
13		-19.7
38		5.1
46		11.0
37		38.8
39		105.6
40		107.4
	Average	0.6
	Minimum	-77.2
	Maximum	107.4
	Range	184.7


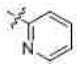
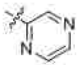
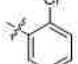
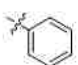
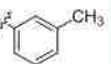
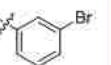
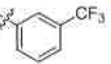
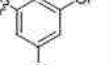
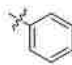
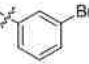
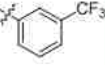
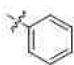
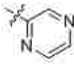
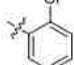
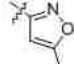
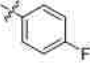
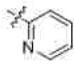
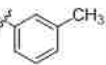

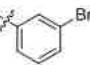
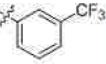
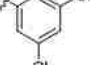
HOP-92 Cell Line		
Compound ID	R group	HOP-92 Growth Percent
44		-79.4
42		-78.3
43		-78.0
45		-75.2
13		-61.4
38		-64.2
37		-29.5
39		45.7
40		86.2
	Average	-36.0
	Minimum	-79.4
	Maximum	86.2
	Range	165.5

Table 10.6

NCI-H226 Cell Line		
Compound ID	R group	NCI-H226 Growth Percent
13		-38.2
37		-12.1
39		6.9
	Average	-14.5
	Minimum	-38.2
	Maximum	6.9
	Range	45.1

NCI-H23 Cell Line		
Compound ID	R group	NCI-H23 Growth Percent
13		-35.7
43		-27.1
45		-26.3
41		-16.9
46		-16.8
42		-16.2
38		-2.9
44		-0.6
37		9.6
39		30.3
40		44.9
	Average	-5.2
	Minimum	-35.7
	Maximum	44.9
	Range	80.7

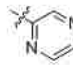
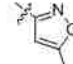

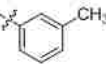
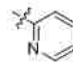
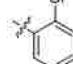
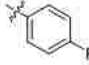
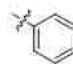
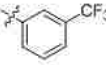
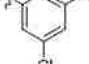
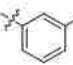

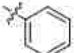
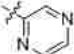
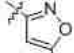
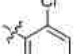
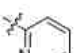
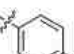
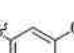
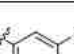
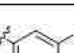

NCI-H322M Cell Line		
Compound ID	R group	NCI-H322M Growth Percent
43		82.1
41		84.8
44		87.2
38		93.6
42		94.1
45		97.0
46		97.8
13		99.8
39		103.6
40		104.4
37		112.2
	Average	96.0
	Minimum	82.1
	Maximum	112.2
	Range	30.1

Table 10.7



NCI-H460 Cell Line		
Compound ID	R group	NCI-H460 Growth Percent
44		-25.9
13		-14.9
43		-14.6
41		2.2
45		5.1
42		7.4
46		27.1
38		31.1
37		51.4
39		70.1
40		98.9
	Average	21.6
	Minimum	-25.9
	Maximum	98.9
	Range	124.8

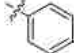

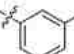

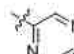
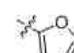
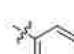
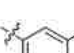
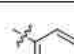
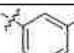
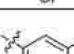
NCI-H522 Cell Line		
Compound ID	R group	NCI-H522 Growth Percent
46		-96.8
41		-95.7
38		-94.3
45		-93.2
43		-90.1
44		-84.9
13		-79.5
37		-78.0
42		-75.3
40		-34.0
39		-24.4
	Average	-76.9
	Minimum	-96.8
	Maximum	-24.4
	Range	72.5

Table 10.8

**Chapter 11: Leukemia**

## Chapter 11: Leukemia

### 11.1 Leukemia Overview

Our compounds were screened against six different leukemia cell lines. The average mean growth percent across the six leukemia cell lines was 20.4. Table 11.1 shows the average mean growth percent of our compounds against each of the leukemia cell lines screened. Figure 3.X also shows molecular characteristics and cell line source information for each cell line. Compared to the other cancer types, our compounds on average had a very narrow range of activity against the different leukemia cell lines with the most active average mean growth percent of 14.7 and the least active average mean growth percent of 25.3 against the MOLT-4 and K-562 cell lines respectively.

Cell Line	Average Mean Growth Percent	Cancer Type	Mutations/Variants <sup>166</sup>	p53 sequence codon change <sup>167</sup>	p53 sequence amino acid change <sup>167</sup>	Patient Age	Sex	Ethnicity
MOLT-4	14.7	Acute Lymphoblastic Leukemia (ALL)	TP53, CDKN2A, NRAS, PTEN, STK11	wild-type	wild-type	19	Male	N/A
RPMI-8226	17.3	Plasmacytoma; myeloma	TP53, KRAS, EGFR	285 GAG → AAG	285 E → L	61	Male	N/A
CCRF-CEM	18.7	Acute Lymphoblastic Leukemia (ALL)	TP53, CDKN2A, KRAS, PTEN, FLT3	248 CGG → CAG	248 R → Q	4	Female	Caucasian
HL-60(TB)	21.2	Acute Promyelocytic Leukemia	TP53, CDKN2A, NRAS	248 CGG → CTG	248 R → L	36	Female	Caucasian
SR	25.3	Large Cell Immunoblastic Lymphoma	CDKN2A	wild-type	wild-type	11	Male	Caucasian
K-562	25.3	Chronic Myelogenous Leukemia (CML)	TP53, CDKN2A, PDGFRA	N/A	N/A	53	Female	N/A
Average	20.4							

N/A: Data not available  
 CDKN2A: Cyclin-dependent kinase inhibitor 2A  
 EGFR: Epidermal growth factor receptor  
 FLT3: fms-related tyrosine kinase 3  
 KRAS: v-Ki-ras2 Kirsten rat sarcoma viral oncogene homologue  
 NRAS: Neuroblastoma RAS viral (v-ras) oncogene homologue  
 PDGFRA: Platelet-derived growth factor receptor,  $\alpha$  polypeptide  
 PTEN: Phosphatase and tensin homologue  
 STK11: Serine/threonine kinase 11/LKB1 (Peutz-Jehgers syndrome)  
 TP53: Tumor protein p53

Unless otherwise referenced above, cell line information was gathered from references 154-157.

Figure Key	
Color	Growth Percent
Most Active	< -50
	-50 to 0
	0 to 50
Least Active	> 50

**Table 11.1**

Table 11.2 shows the results for each compound against each leukemia cell line. As discussed in section 3.3, the stereochemistry played a key role in the activity of the stereoisomers of Compound **1**. (**3S,8R**)-**1** and (**3S,8S**)-**1** had average growth percents of -7.5 and -12.5 respectively against the colon cancer cell lines screened. (**3R,8S**)-**1** and (**3R,8R**)-**1** were significantly less active with average growth percents of 89.1 and 69.1 respectively. Lipophilicity was also shown to be important as Compound **9** (4 carbon length chain), (**3S,8R**)-**1** (10 carbon length chain), and **10** (16 carbon length chain) had

average growth percents of 108.2, -7.5, and -10.4 respectively. Substituting an alcohol for the acetate at the C-3 position in **(3*S*,8*R*)-1** produced a significant change in the average growth percent as Compound **16** had an average growth percent of -29.2 as compared to -7.5 for **(3*S*,8*R*)-1**.

Compound ID	Leukemia Cell Line						Average	Minimum	Maximum	Range
	CCRF-CEM	HL-60(TB)	K-562	MOLT-4	RPMI-8226	SR				
<b>(3<i>R</i>,8<i>S</i>)-1</b>	95.1	84.0	98.3	82.9	87.0	87.1	89.1	82.9	98.3	15.4
<b>(3<i>S</i>,8<i>R</i>)-1</b>	1.4	-13.8	7.7	-3.4	-25.4	-11.6	-7.5	-25.4	7.7	33.1
<b>(3<i>R</i>,8<i>R</i>)-1</b>	63.1	82.8	76.8	57.8	71.2	62.9	69.1	57.8	82.8	25.0
<b>(3<i>S</i>,8<i>S</i>)-1</b>	-9.7	-26.5	1.4	-11.4	-14.9	-14.0	-12.5	-26.5	1.4	27.9
<b>9</b>	111.8	108.6	103.5	103.1	111.0	111.3	108.2	103.1	111.8	8.7
<b>10</b>	3.3	-32.8	3.9	-3.3	1.1	-34.9	-10.4	-34.9	3.9	38.8
<b>11</b>	8.6	68.7	9.9	12.8	5.7	22.3	21.3	5.7	68.7	63.0
<b>12</b>	-20.4	-12.1	2.0	-19.6	-19.2	-26.9	-16.0	-26.9	2.0	28.9
<b>13</b>	4.5	-31.7	10.0	-0.4	-12.6	NT	-6.0	-31.7	10.0	41.7
<b>14</b>	10.4	19.7	15.2	17.8	3.9	20.1	14.5	3.9	20.1	16.2
<b>15</b>	1.5	-7.3	5.1	5.8	-14.9	NT	-2.0	-14.9	5.8	20.8
<b>16</b>	-27.5	-65.3	-7.9	-11.8	-33.6	NT	-29.2	-65.3	-7.9	57.4
<b>37</b>	NT	44.1	34.4	9.6	34.2	40.9	32.6	9.6	44.1	34.5
<b>38</b>	14.2	17.5	19.2	7.4	NT	22.0	16.0	7.4	22.0	14.6
<b>39</b>	NT	78.9	45.5	10.9	49.3	63.9	49.7	10.9	78.9	68.1
<b>40</b>	24.9	81.0	57.7	9.9	NT	57.6	46.2	9.9	81.0	71.1
<b>41</b>	2.8	-4.5	2.9	4.3	NT	7.8	2.7	-4.5	7.8	12.3
<b>42</b>	NT	1.7	3.8	3.6	NT	5.1	3.6	1.7	5.1	3.4
<b>43</b>	5.7	-1.2	1.8	-0.3	NT	7.7	2.7	-1.2	7.7	9.0
<b>44</b>	5.8	-5.7	4.9	3.9	NT	13.0	4.4	-5.7	13.0	18.6
<b>45</b>	8.5	4.0	9.7	5.8	NT	19.4	9.5	4.0	19.4	15.4
<b>46</b>	7.7	34.2	10.5	3.7	NT	10.1	13.2	3.7	34.2	30.4
<b>47</b>	NT	1.5	1.3	0.3	NT	1.2	1.1	0.3	1.5	1.3
<b>48</b>	62.8	82.9	90.4	64.0	NT	65.9	73.2	62.8	90.4	27.6
<b>Average</b>	18.7	21.2	25.3	14.7	17.3	25.3				
<b>Minimum</b>	-27.5	-65.3	-7.9	-19.6	-33.6	-34.9				
<b>Maximum</b>	111.8	108.6	103.5	103.1	111.0	111.3				
<b>Range</b>	139.3	173.9	111.3	122.7	144.7	146.1				
NT = Not Tested										
<b>Figure Key</b>										
<b>Color</b>		<b>Growth Percent</b>								
Most Active		< -50								
		-50 to 0								
		0 to 50								
Least Active		> 50								

Table 11.2

## 11.2 Hansch Cluster Analysis on Leukemia Cell Lines Data

Table 11.3 shows the leukemia testing results organized to assess the results per Hansch cluster analysis theory at the C-8 position. As shown in the table, the range of activity is wide over the six clusters tested. The mesyl amide compound **12** from cluster 4b was the most active compound against CCRF-CEM, K-562, MOLT-4, and SR cell lines. The phenyl amide compound **13** from cluster 8 was the most active against the HL-60(TB) cell line. The alcohol compound **(3*S*,8*R*)-1** from cluster 5 was the most active against the

RPMI-8226 cell line. Across the whole set of leukemia cell lines tested, compound **12** from cluster 4b was the most active with an average growth percent of -16.0. On the other end of the activity spectrum, the isothiocyanate compound **48** from cluster 6 was the least active compound against all of the leukemia cell lines which it was screened against.

Compound ID	Cluster	Leukemia Cell Line						Average	Minimum	Maximum	Range
		CCRF-CEM	HL-60(TB)	K-562	MOLT-4	RPMI-8226	SR				
(3 <i>S</i> ,8 <i>R</i> )-1	5	1.4	-13.8	7.7	-3.4	-25.4	-11.6	-7.5	-25.4	7.7	33.1
11	5	8.6	68.7	9.9	12.8	5.7	22.3	21.3	5.7	68.7	63.0
12	4b	-20.4	-12.1	2.0	-19.6	-26.9	-16.0	-16.0	-26.9	2.0	28.9
13	8	4.5	-31.7	10.0	-0.4	-12.6	NT	-6.0	-31.7	10.0	41.7
14	9	10.4	19.7	15.2	17.8	3.9	20.1	14.5	3.9	20.1	16.2
15	7	1.5	-7.3	5.1	5.8	-14.9	NT	-2.0	-14.9	5.8	20.8
48	6	62.8	82.9	90.4	64.0	NT	65.9	73.2	62.8	90.4	27.6
	Average	9.8	15.2	20.0	11.0	-10.4	14.0				
	Minimum	-20.4	-31.7	2.0	-19.6	-25.4	-26.9				
	Maximum	62.8	82.9	90.4	64.0	5.7	65.9				
	Range	83.2	114.6	88.4	83.5	31.1	92.8				

Table 11.3

Cell Line	Most Active Cluster	C-8 Substituent	Compound ID	Growth Percent
CCRF-CEM	4b	-NHSO <sub>2</sub> Me	12	-20.4
HL-60(TB)	8	-NHCOPh	13	-31.7
K-562	4b	-NHSO <sub>2</sub> Me	12	2.0
MOLT-4	4b	-NHSO <sub>2</sub> Me	12	-19.6
RPMI-8226	5	-OH	(3 <i>S</i> ,8 <i>R</i> )-1	-25.4
SR	4b	-NHSO <sub>2</sub> Me	12	-26.9

Table 11.4

### 11.3 SAR Analysis of Amide Compounds against Leukemia Cell Lines

Eleven of the compounds we had tested by NCI have an acetate at the C-3 position and different amide functionalities with aromatic or heteroaromatic groups directly connected to the amide carbonyl group in the C-8 position as shown in Figure 11.1.

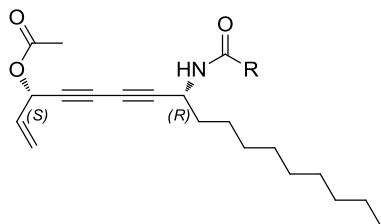


Figure 11.1 Generic structure of amides screened by NCI.

Table 11.5 shows the activity of our amide compounds against each of the different leukemia cell lines. The widest range of activity was seen against the HL-60(TB) cell line in which compound **13** (R = phenyl) had a growth percent of -31.7 whereas compound **40** (R = 3,5 dichlorophenyl) had a growth percent of 81.0. On the other hand, the R group appeared to have little influence on the anticancer activity against the CCRF-CEM and MOLT-4 cell lines. The range of activity against the CCRF-CEM and MOLT-4 cell lines was very narrow with range values of 22.1 and 11.2 respectively.

Compound ID	Leukemia Cell Lines						Average	Minimum	Maximum	Range
	CCRF-CEM	HL-60(TB)	K-562	MOLT-4	RPMI-8226	SR				
13	4.5	-31.7	10.0	-0.4	-12.6	NT	-6.0	-31.7	10.0	41.7
37	NT	44.1	34.4	9.6	34.2	40.9	32.6	9.6	44.1	34.5
38	14.2	17.5	19.2	7.4	NT	22.0	16.0	7.4	22.0	14.6
39	NT	78.9	45.5	10.9	49.3	63.9	49.7	10.9	78.9	68.1
40	24.9	81.0	57.7	9.9	NT	57.6	46.2	9.9	81.0	71.1
41	2.8	-4.5	2.9	4.3	NT	7.8	2.7	-4.5	7.8	12.3
42	NT	1.7	3.8	3.6	NT	5.1	3.6	1.7	5.1	3.4
43	5.7	-1.2	1.8	-0.3	NT	7.7	2.7	-1.2	7.7	9.0
44	5.8	-5.7	4.9	3.9	NT	13.0	4.4	-5.7	13.0	18.6
45	8.5	4.0	9.7	5.8	NT	19.4	9.5	4.0	19.4	15.4
46	7.7	34.2	10.5	3.7	NT	10.1	13.2	3.7	34.2	30.4
Average	9.3	19.8	18.2	5.3	23.6	24.8				
Minimum	2.8	-31.7	1.8	-0.4	-12.6	5.1				
Maximum	24.9	81.0	57.7	10.9	49.3	63.9				
Range	22.1	112.7	55.9	11.2	62.0	58.8				
NT = Not Tested										
Figure Key										
Color		Growth Percent								
Most Active		< -50								
		-50 to 0								
		0 to 50								
Least Active		> 50								

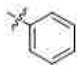
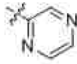
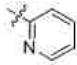
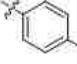

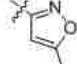
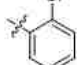
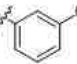
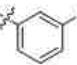
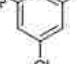
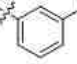
Table 11.5

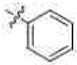
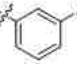
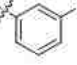
CCRF-CEM Cell Line		
Compound ID	R group	CCRF-CEM Growth Percent
41		2.8
13		4.5
43		5.7
44		5.8
46		7.7
45		8.5
38		14.2
40		24.9
	Average	9.3
	Minimum	2.8
	Maximum	24.9
	Range	22.1

HL-60(TB) Cell Line		
Compound ID	R group	HL-60(TB) Growth Percent
13		-31.7
44		-5.7
41		-4.5
43		-1.2
42		1.7
45		4.0
38		17.5
46		34.2
37		44.1
39		78.9
40		81.0
	Average	19.8
	Minimum	-31.7
	Maximum	81.0
	Range	112.7

K-562 Cell Line		
Compound ID	R group	K-562 Growth Percent
43		1.8
41		2.9
42		3.8
44		4.9
45		9.7
13		10.0
46		10.5
38		19.2
37		34.4
39		45.5
40		57.7
	Average	18.2
	Minimum	1.8
	Maximum	57.7
	Range	55.9

Table 11.6

MOLT-4 Cell Line		
Compound ID	R group	MOLT-4 Growth Percent
13		-0.4
43		-0.3
42		3.6
46		3.7
44		3.9
41		4.3
45		5.8
38		7.4
37		9.6
40		9.9
39		10.9
	Average	5.3
	Minimum	-0.4
	Maximum	10.9
	Range	11.2

RPMI-8226 Cell Line		
Compound ID	R group	RPMI-8226 Growth Percent
13		-12.6
37		34.2
39		49.3
	Average	23.6
	Minimum	-12.6
	Maximum	49.3
	Range	62.0

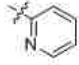
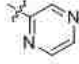
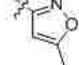
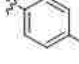

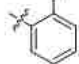
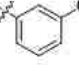
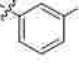
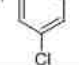
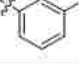
SR Cell Line		
Compound ID	R group	SR Growth Percent
42		5.1
43		7.7
41		7.8
46		10.1
44		13.0
45		19.4
38		22.0
37		40.9
40		57.6
39		63.9
	Average	24.8
	Minimum	5.1
	Maximum	63.9
	Range	58.8

Table 11.7



***Chapter 12: Colon Cancer***

## Chapter 12: Colon Cancer

### 12.1 Colon Cancer Overview

Our compounds were screened against seven different colon cancer cell lines. The average mean growth percent across the seven colon cancer cell lines was 0.9. Table 12.1 shows the average mean growth percent of our compounds against each of the seven colon cancer cell lines screened. Table 12.1 also shows molecular characteristics and cell line source information for each of the seven cell lines.

Cell Line	Average Mean Growth Percent	Cancer Type	Mutations/Variants <sup>166</sup>	p53 sequence codon change <sup>167</sup>	p53 sequence amino acid change <sup>167</sup>	Patient Age	Sex	Ethnicity
HCC-2998	-20.7	Adenocarcinoma	TP53, APC, RB1	213 CGA → TGA	175 R → STOP	N/A	N/A	N/A
HCT-116	-19.1	Colorectal carcinoma	CDKN2A, CTNNB1, KRAS, PIK3CA, BRCA2	wild-type	wild-type	N/A	Male	N/A
COLO 205	-11.9	Dukes' type D, colorectal adenocarcinoma	TP53, APC, BRAF, SMAD4	286 GGA → GAA	175 G → E	70	Male	Caucasian
SW-620	-7.6	Dukes' type C, colorectal adenocarcinoma	TP53, APC, KRAS	273 CGT → CAT	273 R → H	51	Male	Caucasian
HCT-15	9.2	Dukes' type C, colorectal adenocarcinoma	TP53, APC, KRAS, PIK3CA, BRCA2	wild-type or 153 CCC → GCC	wild-type or 153 P → A	N/A	Male	N/A
KM12	17.2	Adenocarcinoma, Grade III	TP53, APC, PTEN, BRCA2	179 CAT → CGT	179 H → R	N/A	N/A	N/A
HT29	38.9	Colorectal adenocarcinoma	TP53, APC, BRAF, PIK3CA, SMAD4	273 CGT → CAT	273 R → H	44	Female	Caucasian
<b>Average</b>	<b>0.9</b>							

N/A: Data not available  
 APC: Adenomatous polyposis coli  
 BRAF: v-raf murine sarcoma viral oncogene homologue B1  
 BRCA2: Familial breast/ovarian cancer gene 2  
 CDKN2A: Cyclin-dependent kinase inhibitor 2A  
 CTNNB1: Catenin (cadherin associated protein) β1  
 KRAS: v-Ki-ras2 Kirsten rat sarcoma viral oncogene homologue  
 PIK3CA: Phosphoinositide-3-kinase, catalytic, α polypeptide  
 PTEN: Phosphatase and tensin homologue  
 RB1: Retinoblastoma 1  
 SMAD4: SMAD, mothers against DPP homologue 4 (MADH4)  
 TP53: Tumor protein p53  
 Unless otherwise referenced above, cell line information was gathered from references 154-157.

Figure Key	
Color	Growth Percent
Most Active	< -50
	-50 to 0
	0 to 50
Least Active	> 50

**Table 12.1**

Table 12.2 shows the results for each compound against each colon cancer cell line. As discussed in section 3.3, the stereochemistry played a key role in the activity of the stereoisomers of Compound **1**. (**3S,8R**)-**1** and (**3S,8S**)-**1** had average growth percents of -74.1 and -59.1 respectively against the colon cancer cell lines screened. (**3R,8S**)-**1** and (**3R,8R**)-**1** were significantly less active with average growth percents of 104.9 and 92.9 respectively. Lipophilicity was also shown to be important as Compound **9** (4 carbon length chain), (**3S,8R**)-**1** (10 carbon length chain), and **10** (16 carbon length chain) had average growth percents of 104.2, -74.1, and -75.4 respectively. Substituting an alcohol for the acetate at the C-3 position in (**3S,8R**)-**1** produced little change in the

average growth percent as Compound **16** had an average growth percent of -72.7 as compared to -74.1 for **(3S,8R)-1**.

Compound ID	Colon Cancer Cell Lines							Average	Minimum	Maximum	Range
	COLO 205	HCC-2998	HCT-116	HCT-15	HT29	KM12	SW-620				
<b>(3R,8S)-1</b>	120.7	106.8	97.5	86.3	101.3	110.4	111.1	104.9	86.3	120.7	34.4
<b>(3S,8R)-1</b>	-92.5	-90.7	-82.5	-71.5	-27.7	-79.4	-74.1	-74.1	-92.5	-27.7	64.8
<b>(3R,8R)-1</b>	117.8	102.6	69.6	78.2	89.7	99.1	93.4	92.9	69.6	117.8	48.2
<b>(3S,8S)-1</b>	-84.4	-87.2	-73.7	-29.4	-25.3	-62.9	-50.4	-59.1	-87.2	-25.3	61.9
<b>9</b>	121.6	93.5	92.1	107.2	109.5	104.9	100.8	104.2	92.1	121.6	29.5
<b>10</b>	-97.2	-91.4	-95.3	-70.8	-27.0	-80.0	-66.0	-75.4	-97.2	-27.0	70.3
<b>11</b>	76.5	110.5	-19.7	6.7	85.8	30.1	4.3	42.0	-19.7	110.5	130.2
<b>12</b>	-86.9	-96.4	-97.2	-80.2	-56.9	-82.3	-76.7	-82.4	-97.2	-56.9	40.3
<b>13</b>	-31.0	-89.3	-100.0	-25.0	47.0	15.0	-35.6	-31.3	-100.0	47.0	147.0
<b>14</b>	-74.4	-8.6	0.8	10.5	35.5	4.3	4.2	-3.9	-74.4	35.5	109.9
<b>15</b>	-63.9	-92.4	-100.0	-58.2	-13.1	-47.5	-68.9	-63.4	-100.0	-13.1	86.9
<b>16</b>	-57.6	-91.1	-100.0	-70.5	-20.0	-86.1	-83.6	-72.7	-100.0	-20.0	80.0
<b>37</b>	95.4	29.5	8.8	25.2	90.3	90.0	19.2	51.2	8.8	95.4	86.6
<b>38</b>	-16.3	-43.8	8.1	25.6	93.3	57.2	3.4	18.2	-43.8	93.3	137.1
<b>39</b>	110.7	45.8	21.1	48.0	102.7	101.5	36.8	66.7	21.1	110.7	89.6
<b>40</b>	89.9	93.3	40.4	92.3	105.7	105.8	49.0	82.3	40.4	105.8	65.4
<b>41</b>	-87.3	-86.0	-36.1	0.1	-31.8	-28.5	-57.9	-46.8	-87.3	0.1	87.3
<b>42</b>	-79.1	-85.4	-73.4	1.4	22.3	1.0	-28.2	-34.5	-85.4	22.3	107.6
<b>43</b>	-88.4	-62.6	-53.5	-0.7	-27.1	-29.3	-58.9	-45.8	-88.4	-0.7	87.8
<b>44</b>	-83.7	-85.3	-37.8	1.6	2.5	-21.5	-63.1	-41.0	-85.3	2.5	87.8
<b>45</b>	-80.7	-84.0	4.6	15.0	27.6	24.6	-20.8	-16.3	-84.0	27.6	111.6
<b>46</b>	-17.1	-32.0	8.4	21.5	85.3	66.6	-13.6	17.0	-32.0	85.3	117.3
<b>47</b>	-78.4	-65.9	-37.2	10.7	56.2	NT	-11.3	-21.0	-78.4	56.2	134.7
<b>48</b>	99.8	113.1	96.8	97.9	108.5	101.6	105.0	103.2	96.8	113.1	16.3
<b>Average</b>	-11.9	-20.7	-19.1	9.2	38.9	17.2	-7.6				
<b>Minimum</b>	-97.2	-96.4	-100.0	-80.2	-56.9	-86.1	-83.6				
<b>Maximum</b>	121.6	113.1	97.5	107.2	109.5	110.4	111.1				
<b>Range</b>	218.8	209.6	197.5	187.5	166.4	196.5	194.7				
	NT = Not Tested										

Table 12.2

## 12.2 Hansch Cluster Analysis on Colon Cancer Cell Lines Data

Table 12.3 shows the colon cancer testing results organized to assess the results per Hansch cluster analysis theory at the C-8 position. As shown in the table, the range of activity is wide over the six clusters tested. The mesyl amide compound **12** from cluster 4b was the most active compound against five (HCC-2998, HCT-15, HT29, KM12, and SW-620) of the seven cell lines tested. The alcohol compound **(3S,8R)-1** from cluster 5 was the most active against the COLO 205 cell line and the phenyl amide compound **13** was the most active against the HCT-116 cell line. Across the whole set of colon cancer cell lines tested, compound **12** from cluster 4b was the most active with an average growth percent of -82.4. On the other end of the activity spectrum, the isothiocyanate compound **48** from cluster 6 was the least active compound against all of the colon cancer cell screened.

Compound ID	Cluster	Colon Cancer Cell Lines							Average	Minimum	Maximum	Range
		COLO 205	HCC-2998	HCT-116	HCT-15	HT29	KM12	SW-620				
(3 <i>S</i> ,8 <i>R</i> )-1	5	-92.5	-90.7	-82.5	-71.5	-27.7	-79.4	-74.1	-92.5	-27.7	64.8	
11	5	76.5	110.5	-19.7	6.7	85.8	30.1	42.0	-19.7	110.5	130.2	
12	4b	-86.9	-96.4	-97.2	-80.2	-56.9	-82.3	-76.7	-82.4	-97.2	-56.9	
13	8	-31.0	-89.3	-100.0	-25.0	47.0	15.0	-35.6	-31.3	-100.0	47.0	
14	9	-74.4	-8.6	0.8	10.5	35.5	4.3	4.2	-3.9	-74.4	35.5	
15	7	-63.9	-92.4	-100.0	-56.2	-13.1	-47.5	-68.9	-63.4	-100.0	-13.1	
48	6	99.8	113.1	96.8	97.9	108.5	101.6	105.0	103.2	96.8	113.1	
	Average	-24.6	-22.0	-43.1	-17.1	25.6	-8.3	-20.2				
	Minimum	-92.5	-96.4	-100.0	-80.2	-56.9	-82.3	-76.7				
	Maximum	99.8	113.1	96.8	97.9	108.5	101.6	105.0				
	Range	192.2	209.6	196.8	178.1	165.4	183.9	181.6				
	NT = Not Tested											
	Figure Key											
	Color	Growth Percent										
	Most Active	< -50										
		-50 to 0										
		0 to 50										
	Least Active	> 50										

Table 12.3

Cell Line	Most Active Cluster	C-8 Substituent	Compound ID	Growth Percent
COLO 205	5	-OH	(3 <i>S</i> ,8 <i>R</i> )-1	-92.5
HCC-2998	4b	-NHSO <sub>2</sub> Me	12	-96.4
HCT-116	8	-NHCOPh	13	-100.0
HCT-15	4b	-NHSO <sub>2</sub> Me	12	-80.2
HT29	4b	-NHSO <sub>2</sub> Me	12	-56.9
KM12	4b	-NHSO <sub>2</sub> Me	12	-82.3
SW-620	4b	-NHSO <sub>2</sub> Me	12	-76.7

Table 12.4

### 12.3 SAR Analysis of Amide Compounds against Colon Cancer Cell Lines

Eleven of the compounds we had tested by NCI have an acetate at the C-3 position and different amide functionalities with aromatic or heteroaromatic groups directly connected to the amide carbonyl group in the C-8 position as shown in Figure 12.1.

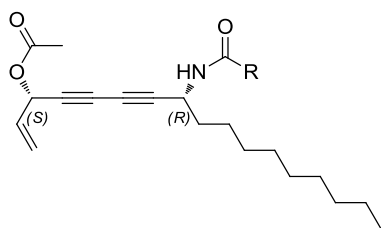


Figure 12.1 Generic structure of amides screened by NCI.

Table 12.5 shows the activity of our amide compounds against each of the different colon cancer cell lines. The set of amide compounds showed a wide range of activity against the different cell lines indicating that changing the amide R group has a significant impact on activity. The widest range of activity was seen against the COLO

205 cell line in which pyrazine compound **43** had a growth percent of -88.4 whereas *m*-trifluoromethyl compound **39** had a growth percent of 110.7.

Compound ID	Colon Cancer Cell Lines							Average	Minimum	Maximum	Range
	COLO 205	HCC-2998	HCT-116	HCT-15	HT29	KM12	SW-620				
13	-31.0	-89.3	-100.0	-25.0	47.0	15.0	-35.6	-31.3	-100.0	47.0	147.0
37	95.4	29.5	8.8	25.2	90.3	90.0	19.2	51.2	8.8	95.4	86.6
38	-16.3	-43.8	8.1	25.6	93.3	57.2	3.4	18.2	-43.8	93.3	137.1
39	110.7	45.8	21.1	48.0	102.7	101.5	36.8	66.7	21.1	110.7	89.6
40	89.9	93.3	40.4	92.3	105.7	105.8	49.0	82.3	40.4	105.8	65.4
41	-87.3	-86.0	-36.1	0.1	-31.8	-28.5	-57.9	-46.8	-87.3	0.1	87.3
42	-79.1	-85.4	-73.4	1.4	22.3	1.0	-28.2	-34.5	-85.4	22.3	107.6
43	-88.4	-62.6	-53.5	-0.7	-27.1	-29.3	-58.9	-45.8	-88.4	-0.7	87.8
44	-83.7	-85.3	-37.8	1.6	2.5	-21.5	-63.1	-41.0	-85.3	2.5	87.8
45	-80.7	-84.0	4.6	15.0	27.6	24.6	-20.8	-16.3	-84.0	27.6	111.6
46	-17.1	-32.0	8.4	21.5	85.3	66.6	-13.6	17.0	-32.0	85.3	117.3
Average	-17.0	-36.3	-19.0	18.6	47.1	34.8	-15.4				
Minimum	-88.4	-89.3	-100.0	-25.0	-31.8	-29.3	-63.1				
Maximum	110.7	93.3	40.4	92.3	105.7	105.8	49.0				
Range	199.2	182.7	140.4	117.3	137.5	135.1	112.1				

Figure Key

Color	Growth Percent
Most Active	< -50
	-50 to 0
	0 to 50
Least Active	> 50

Table 12.5

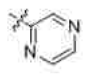
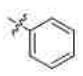
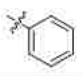
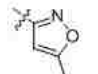
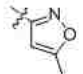

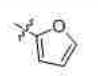
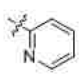
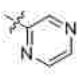
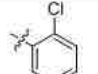


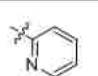
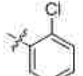
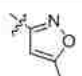
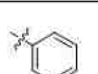
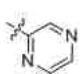
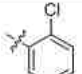
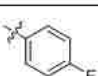
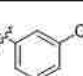
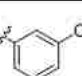
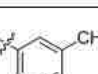
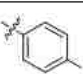
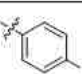
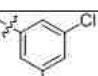
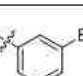
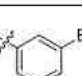
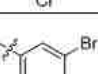
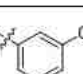
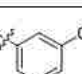
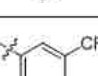
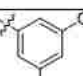
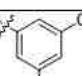
COLO 205 Cell Line			HCC-2998 Cell Line			HCT-116 Cell Line		
Compound ID	R group	COLO 205 Growth Percent	Compound ID	R group	HCC-2998 Growth Percent	Compound ID	R group	HCT-116 Growth Percent
43		-88.4	13		-89.3	13		-100.0
41		-87.3	41		-86.0	42		-73.4
44		-83.7	42		-85.4	43		-53.5
45		-80.7	44		-85.3	44		-37.8
42		-79.1	45		-84.0	41		-36.1
13		-31.0	43		-62.6	45		4.6
46		-17.1	38		-43.8	38		8.1
38		-16.3	46		-32.0	46		8.4
40		89.8	37		29.5	37		8.8
37		95.4	39		45.8	39		21.1
39		110.7	40		93.3	40		40.4
	Average	-17.0		Average	-36.3		Average	-19.0
	Minimum	-88.4		Minimum	-89.3		Minimum	-100.0
	Maximum	110.7		Maximum	93.3		Maximum	40.4
	Range	199.2		Range	182.7		Range	140.4

Table 12.6

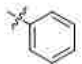
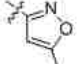
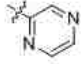
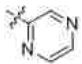
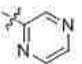
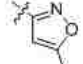
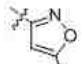
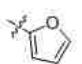

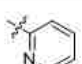
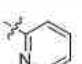
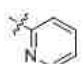

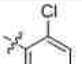
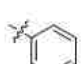
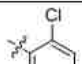
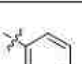
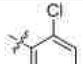

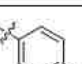
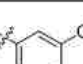
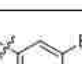
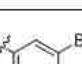
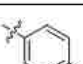
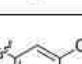
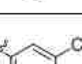
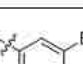
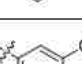
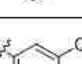
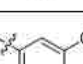
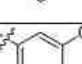
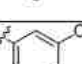
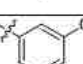
HCT-15 Cell Line			HT29 Cell Line			KM12 Cell Line		
Compound ID	R group	HCT-15 Growth Percent	Compound ID	R group	HT29 Growth Percent	Compound ID	R group	KM12 Growth Percent
13		-25.0	41		-31.8	43		-29.3
43		-0.7	43		-27.1	41		-28.5
41		0.1	44		2.5	44		-21.5
42		1.4	42		22.3	42		1.0
44		1.6	45		27.6	13		15.0
45		15.0	13		47.0	45		24.6
46		21.5	46		85.3	38		57.2
37		25.2	37		90.3	46		66.6
38		25.6	38		93.3	37		90.0
39		48.0	39		102.7	39		101.5
40		92.3	40		105.7	40		105.8
	Average	16.6		Average	47.1		Average	34.8
	Minimum	-25.0		Minimum	-31.8		Minimum	-29.3
	Maximum	92.3		Maximum	105.7		Maximum	105.8
	Range	117.3		Range	137.5		Range	135.1

Table 12.7


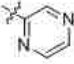
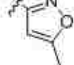
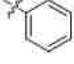
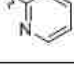
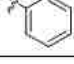
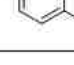


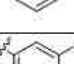
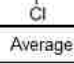
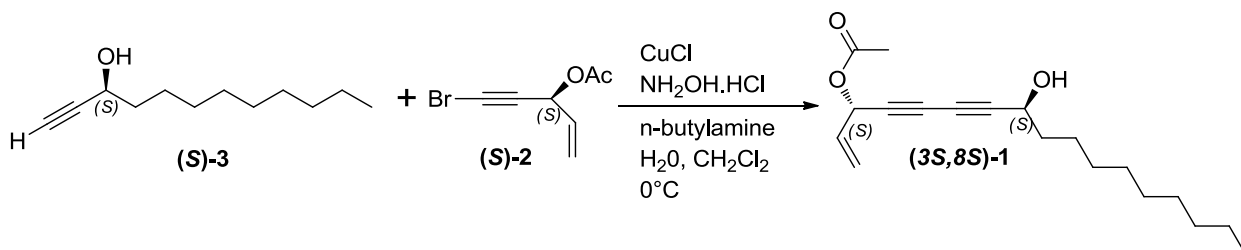
SW-620 Cell Line		
Compound ID	R group	SW-620 Growth Percent
44		-63.1
43		-68.9
41		-57.9
13		-35.6
42		-28.2
45		-20.8
46		-13.6
38		3.4
37		19.2
39		36.8
40		49.0
	Average	-15.4
	Minimum	-63.1
	Maximum	49.0
	Range	112.1

Table 12.8



***Chapter 13: Experimentals***

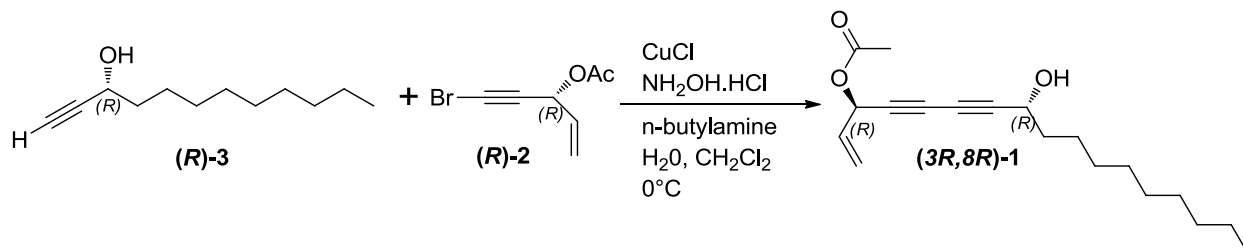
## Chapter 13: Experimentals



### (3S,8S)-8-hydroxyheptadeca-1-en-4,6-diyn-3-yl acetate (3S,8S)-1

Copper (I) chloride (0.008 g, 0.08 mmol) was added to a stirred 30 % solution (1.65 mL) of n-butylamine in distilled water at 0 °C which resulted in a deep blue solution. A few crystals of NH<sub>2</sub>OH.HCl were added until solution was colorless. A solution of (S)-3 (0.101 g, 0.55 mmol) in CH<sub>2</sub>Cl<sub>2</sub> (0.82 mL) was added under argon atmosphere which resulted in yellow reaction mixture. After 10 minutes, a solution of (S)-2 (0.153 g, 0.75 mmol) in CH<sub>2</sub>Cl<sub>2</sub> (1.0 mL) was added dropwise over 5 minutes. A few crystals of NH<sub>2</sub>OH.HCl were added as necessary whenever solution turned blue or green. After 1 hour, reaction was quenched with water, extracted 3 times with CH<sub>2</sub>Cl<sub>2</sub>, dried over Na<sub>2</sub>SO<sub>4</sub>, and concentrated under reduced pressure. Immediate purification by flash chromatography on silica gel (hexanes – 15% EtOAc/hexanes) afforded (3S,8S)-1 (0.135 g, 80.2%, yellow oil). TLC  $R_f$  = 0.414 (25% EtOAc/hexanes);  $[\alpha]_D^{17} = -29.1^\circ$  ( $c = 0.6$ , CHCl<sub>3</sub>/0.75% ethanol); <sup>1</sup>H NMR (500 MHz, CHLOROFORM-d)  $\delta$  5.83 - 5.95 (m, 2H), 5.52 - 5.59 (dd,  $J = 1.22, 16.63$  Hz, 1H), 5.33 - 5.39 (dd,  $J = 1.10, 10.03$  Hz, 1H), 4.43 (m, 1H), 2.11 (s, 3H), 1.91 (d,  $J = 4.40$  Hz, 1H), 1.66 - 1.77 (m, 2H), 1.44 (quint,  $J = 7.58$  Hz, 2H), 1.22 - 1.35 (m, 12H), 0.85 - 0.91 (t,  $J = 6.97$  Hz, 3H); <sup>13</sup>C NMR (125 MHz, CHLOROFORM-d)  $\delta$  169.5, 131.9, 119.7, 81.3, 74.3, 70.8, 68.6, 64.4, 62.8, 37.4, 31.8, 29.5, 29.4, 29.3, 29.2, 25.0, 22.7, 20.9, 14.1; IR (ATR) 3413, 2925, 2855, 2258, 2157,

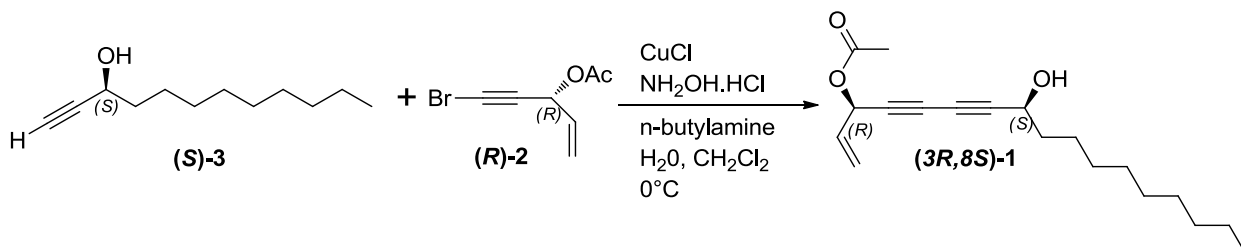
1748, 1371, 1220, 1015  $\text{cm}^{-1}$ ; HRMS (ESI-TOF)  $[\text{M} + \text{H}]^+$  calcd. for  $\text{C}_{19}\text{H}_{29}\text{O}_3$  305.2117, found 305.2138.



**(3*R*,8*R*)-8-hydroxyheptadeca-1-en-4,6-diyn-3-yl acetate (3*R*,8*R*)-1**

Copper (I) chloride (0.008 g, 0.08 mmol) was added to a stirred 30 % solution (1.65 mL) of n-butylamine in distilled water at 0 °C which resulted in a deep blue solution. A few crystals of  $\text{NH}_2\text{OH}\cdot\text{HCl}$  were added until solution was colorless. A solution of (**R**)-**3** (0.098 g, 0.54 mmol) in  $\text{CH}_2\text{Cl}_2$  (0.82 mL) was added under argon atmosphere which resulted in yellow reaction mixture. After 10 minutes, a solution of (**R**)-**2** (0.230 g, 1.1 mmol) in  $\text{CH}_2\text{Cl}_2$  (1.0 mL) was added dropwise over 3.5 minutes. A few crystals of  $\text{NH}_2\text{OH}\cdot\text{HCl}$  were added as necessary whenever solution turned blue or green. After 1 hour, reaction was quenched with water, extracted 3 times with  $\text{CH}_2\text{Cl}_2$ , dried over  $\text{Na}_2\text{SO}_4$ , and concentrated under reduced pressure. Immediate purification by flash chromatography on silica gel (hexanes – 15% EtOAc/hexanes) afforded (**3*R*,8*R*)-1** (0.088 g, 53.9%, yellow oil).  $[\alpha]_{\text{D}}^{18} = +31.7^\circ$  ( $c = 0.9$ ,  $\text{CHCl}_3/0.75\%$  ethanol);  $^1\text{H}$  NMR (500 MHz,  $\text{CHLOROFORM-d}$ )  $\delta$  5.83 - 5.94 (m, 2H), 5.52 - 5.59 (m, 1H), 5.33 - 5.38 (m, 1H), 4.43 (m, 1H), 2.10 - 2.13 (d,  $J = 0.49$  Hz, 3H), 1.92 (d,  $J = 4.16$  Hz, 1H), 1.65 - 1.78 (m, 2H), 1.40 - 1.48 (m, 2H), 1.22 - 1.35 (m, 12H), 0.88 (t,  $J = 6.97$  Hz, 3H);  $^{13}\text{C}$  NMR (125 MHz,  $\text{CHLOROFORM-d}$ )  $\delta$  169.5, 131.9, 119.7, 81.3, 74.3, 70.8, 68.5, 64.4, 62.8,

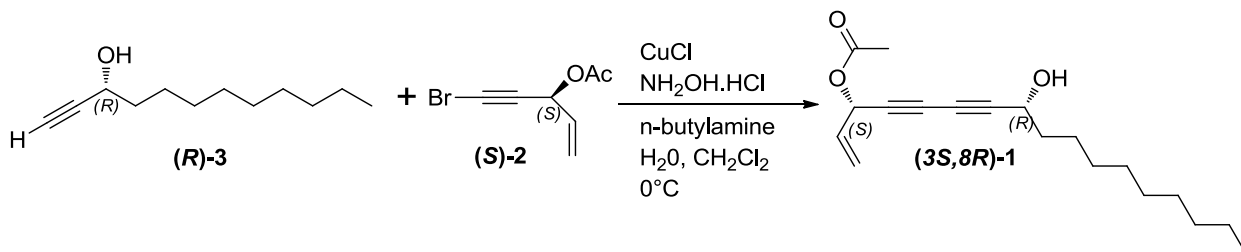
37.4, 31.9, 29.5, 29.5, 29.3, 29.2, 25.0, 22.7, 20.9, 14.1; IR (ATR) 3440, 2924, 2855, 2256, 2157, 1748, 1371, 1219, 1015  $\text{cm}^{-1}$ ; HRMS (ESI-TOF)  $[\text{M} + \text{H}]^+$  calcd. for  $\text{C}_{19}\text{H}_{29}\text{O}_3$  305.2117, found 305.2132.



**(3R,8S)-8-hydroxyheptadeca-1-en-4,6-diyn-3-yl acetate (3R,8S)-1**

Copper (I) chloride (0.007 g, 0.07 mmol) was added to a stirred 30 % solution (1.65 mL) of n-butylamine in distilled water at 0 °C which resulted in a deep blue solution. A few crystals of NH<sub>2</sub>OH.HCl were added until solution was colorless. A solution of (S)-3 (0.107 g, 0.59 mmol) in CH<sub>2</sub>Cl<sub>2</sub> (0.82 mL) was added under argon atmosphere which resulted in yellow reaction mixture. After 10 minutes, a solution of (R)-2 (0.147 g, 0.72 mmol) in CH<sub>2</sub>Cl<sub>2</sub> (1.0 mL) was added dropwise over 5 minutes. A few crystals of NH<sub>2</sub>OH.HCl were added as necessary whenever solution turned blue or green. After 1 hour, reaction was quenched with water, extracted 3 times with CH<sub>2</sub>Cl<sub>2</sub>, dried over Na<sub>2</sub>SO<sub>4</sub>, and concentrated under reduced pressure. Immediate purification by flash chromatography on silica gel (hexanes – 15% EtOAc/hexanes) afforded (3R,8S)-1 (0.128 g, 71.5%, yellow oil). TLC  $R_f$  = 0.414 (25% EtOAc/hexanes);  $[\alpha]_D^{17} = +44.6^\circ$  ( $c = 1.2$ , CHCl<sub>3</sub>/0.75% ethanol); <sup>1</sup>H NMR (500 MHz, CHLOROFORM-d)  $\delta$  5.83 - 5.95 (m, 2H), 5.55 (d,  $J = 16.63$  Hz, 1H), 5.36 (d,  $J = 9.78$  Hz, 1H), 4.43 (m, 1H), 2.08 - 2.15 (s, 3H), 1.93 (d,  $J = 4.65$  Hz, 1H), 1.65 - 1.78 (m, 2H), 1.39 - 1.48 (m, 2H), 1.19 - 1.36 (m, 12H),

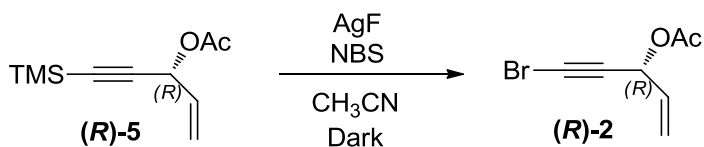
0.88 (t,  $J = 6.85$  Hz, 3H);  $^{13}\text{C}$  NMR (125 MHz, CHLOROFORM- $d$ )  $\delta$  169.5, 131.9, 119.7, 81.3, 74.3, 70.8, 68.5, 64.4, 62.8, 37.4, 31.8, 29.5, 29.4, 29.3, 29.2, 25.0, 22.7, 20.9, 14.1; IR (ATR) 3432, 2924, 2855, 2257, 2157, 1748, 1371, 1219, 1015  $\text{cm}^{-1}$ ; HRMS (ESI-TOF)  $[\text{M} + \text{H}]^+$  calcd. for  $\text{C}_{19}\text{H}_{29}\text{O}_3$  305.2117, found 305.2167.



**(3*S*,8*R*)-8-hydroxyheptadeca-1-en-4,6-diyn-3-yl acetate (3*S*,8*R*)-1**

Copper (I) chloride (0.015 g, 0.15 mmol) was added to a stirred 30 % solution (3.3 mL) of n-butylamine in distilled water at 0 °C which resulted in a deep blue solution. A few crystals of NH<sub>2</sub>OH.HCl were added until solution was colorless. A solution of (R)-3 (0.202 g, 1.10 mmol) in CH<sub>2</sub>Cl<sub>2</sub> (1.7 mL) was added under argon atmosphere which resulted in yellow reaction mixture. After 10 minutes, a solution of (S)-2 (0.277 g, 1.36 mmol) in CH<sub>2</sub>Cl<sub>2</sub> (2.0 mL) was added dropwise over 5 minutes. A few crystals of NH<sub>2</sub>OH.HCl were added as necessary whenever solution turned blue or green. After 45 minutes, reaction was quenched with water, extracted 3 times with CH<sub>2</sub>Cl<sub>2</sub>, dried over Na<sub>2</sub>SO<sub>4</sub>, and concentrated under reduced pressure. Immediate purification by flash chromatography on silica gel (hexanes – 15% EtOAc/hexanes) afforded (3*S*,8*R*)-1 (0.225 g, 66.7%, yellow oil). TLC  $R_f = 0.429$  (25% EtOAc/hexanes);  $[\alpha]_D^{17} = -46.0^\circ$  ( $c = 0.7$ , CHCl<sub>3</sub>/0.75% ethanol);  $^1\text{H}$  NMR (500 MHz, CHLOROFORM- $d$ )  $\delta$  5.81 - 5.97 (m, 2H), 5.51 - 5.61 (m, 1H), 5.31 - 5.41 (m, 1H), 4.43 (t,  $J = 6.60$  Hz, 1H), 2.08 - 2.19 (s, 3H),

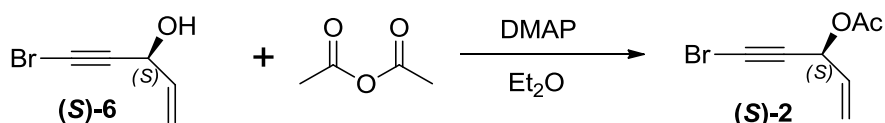
1.80 – 1.96 (br. s., 1H), 1.72 (m, 2H), 1.39 - 1.53 (m, 2H), 1.18 - 1.37 (m, 12H), 0.84 - 0.97 (t,  $J = 6.90$  Hz, 3H);  $^{13}\text{C}$  NMR (125 MHz, CHLOROFORM- $d$ )  $\delta$  169.5, 131.9, 119.7, 81.3, 74.3, 70.8, 68.6, 64.4, 62.8, 37.4, 31.9, 29.5, 29.5, 29.3, 29.2, 25.0, 22.7, 20.9, 14.1; IR (ATR) 3413, 2926, 2855, 2257, 2158, 1749, 1371, 1219, 1014  $\text{cm}^{-1}$ ; HRMS (ESI-TOF)  $[\text{M} + \text{H}]^+$  calcd. for  $\text{C}_{19}\text{H}_{29}\text{O}_3$  305.2117, found 305.2106.



#### **(R)-5-bromopent-1-en-4-yn-3-yl acetate (R)-2**

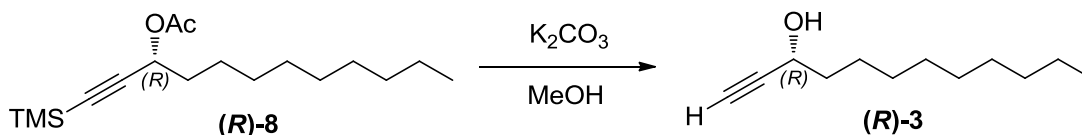
To a solution of **(R)-5** (6.4 g, 32.4 mmol) in acetonitrile (135 mL) was added N-bromosuccinimide (7.0 g, 39.5 mmol) followed by AgF (5.3 g, 42.0 mmol). The reaction flask was then wrapped in aluminum foil to block out light. After 48 hours, reaction mixture was filtered through fine-fritted funnel and rinsed through with  $\text{Et}_2\text{O}$ . Filtrate was diluted with  $\text{Et}_2\text{O}$ , washed with  $\text{H}_2\text{O}$ , dried over  $\text{Na}_2\text{SO}_4$ , and concentrated under reduced pressure. Purification by flash chromatography on silica gel (Hexanes – 10%  $\text{EtOAc}$ /Hexanes) afforded **(R)-2** (3.6 g, 54.1%, yellow oil).

$R_f = 0.462$  (15%  $\text{EtOAc}$ /hexanes);  $[\alpha]_{\text{D}}^{21} = +30.5^\circ$  ( $c = 1.6$ ,  $\text{CHCl}_3$ );  $^1\text{H}$  NMR (500 MHz, CHLOROFORM- $d$ )  $\delta$  5.84 - 5.94 (m, 2H), 5.51 - 5.58 (m, 1H), 5.35 (d,  $J = 9.05$  Hz, 1H), 2.12 (s, 3H);  $^{13}\text{C}$  NMR (125 MHz, CHLOROFORM- $d$ )  $\delta$  169.5, 132.3, 119.4, 75.4, 64.8, 47.9, 20.9; IR (ATR) 2217, 1742, 1371, 1220  $\text{cm}^{-1}$ ; MS (EI)  $[\text{M}]^+ 202$



**(S)-5-bromopent-1-en-4-yn-3-yl acetate (S)-2**

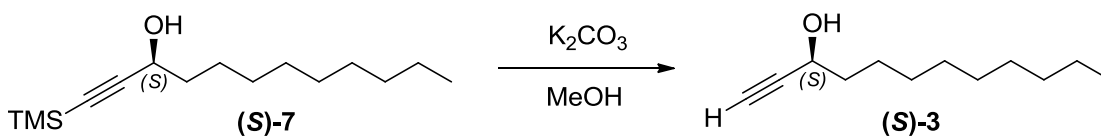
To a solution of (S)-6 (4.7 g, 29.2 mmol) in Et<sub>2</sub>O (360 mL) was added DMAP (0.37 g, 3.0 mmol) followed by acetic anhydride (4.4 mL, 46.6 mmol). After stirring for 2 hours at ambient temperature, reaction was quenched with water, extracted with Et<sub>2</sub>O, washed with water and brine, and dried over Na<sub>2</sub>SO<sub>4</sub>. Purification by flash chromatography on silica gel (Hexanes – 10% EtOAc/Hexanes) afforded (S)-2 (3.6 g, 81.5%, light yellow oil).  $R_f = 0.462$  (15% EtOAc/hexanes);  $[\alpha]_D^{21} = -28.2^\circ$  ( $c = 1.8$ , CHCl<sub>3</sub>); <sup>1</sup>H NMR (500 MHz, CHLOROFORM-d)  $\delta$  5.82 - 5.92 (m, 2H), 5.50 - 5.57 (m, 1H), 5.34 (d,  $J = 8.80$  Hz, 1H), 2.09 - 2.12 (s, 3H); <sup>13</sup>C NMR (125 MHz, CHLOROFORM-d)  $\delta$  169.5, 132.2, 119.3, 75.4, 64.8, 47.8, 20.9; IR (ATR) 2217, 1742, 1371, 1220 cm<sup>-1</sup>; MS (EI) [M]<sup>+</sup>202



**(R)-dodec-1-yn-3-ol (R)-3**

To a solution of (R)-8 (3.3 g, 11.1 mmol) in methanol (225 mL) was added K<sub>2</sub>CO<sub>3</sub> (3.1 g, 22.3 mmol). Solution was stirred at ambient temperature under argon atmosphere. After 22 hours, reaction was quenched with saturated NH<sub>4</sub>Cl, extracted three times with CH<sub>2</sub>Cl<sub>2</sub>, dried over Na<sub>2</sub>SO<sub>4</sub>, and concentrated under reduced pressure. Concentrate was purified by loading on to a 2-inch pad of silica gel and eluting with 25% EtOAc/Hexanes which afforded (R)-3 (2.0 g, 100%, clear oil).  $R_f = 0.259$  (15% EtOAc/hexanes);  $[\alpha]_D^{23} =$

+2.9° ( $c = 10.4$ ,  $\text{CHCl}_3$ );  $^1\text{H NMR}$  (500 MHz,  $\text{CHLOROFORM-d}$ )  $\delta$  4.35 (m., 1H), 2.43 - 2.47 (d,  $J = 2.20$  Hz, 1H), 2.34 - 2.40 (br. s., 1H), 1.64 - 1.76 (m, 2H), 1.39 - 1.49 (m, 2H), 1.20 - 1.35 (m, 12H), 0.83 - 0.90 (t,  $J = 6.97$  Hz, 3H);  $^{13}\text{C NMR}$  (125 MHz,  $\text{CHLOROFORM-d}$ )  $\delta$  85.1, 72.7, 62.2, 37.6, 31.8, 29.5, 29.3, 29.2, 25.0, 22.6, 14.1; IR (ATR) 3382, 3311, 2923, 2854, 1466  $\text{cm}^{-1}$ ; MS (EI)  $[\text{M} - 1]^+$  181.

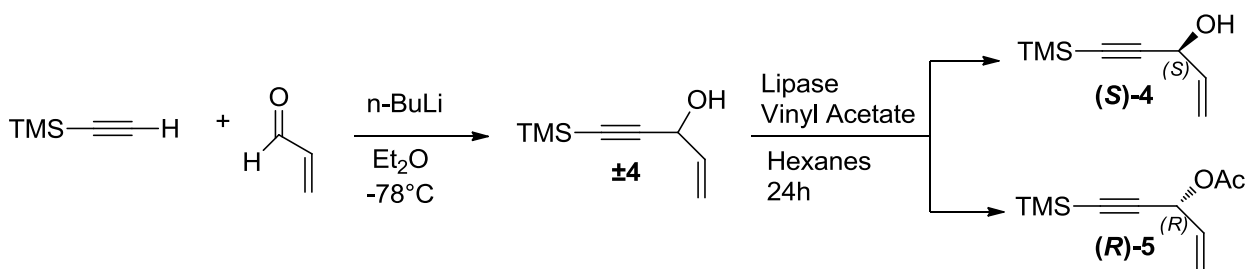


### **(S)-dodec-1-yn-3-ol (S)-3**

To a solution of **(S)-7** (2.0 g, 7.9 mmol) in methanol (160 mL) was added  $\text{K}_2\text{CO}_3$  (4.4 g, 31.7 mmol). Solution was stirred at ambient temperature under argon atmosphere. After 3 hours and 25 minutes, reaction was quenched with saturated  $\text{NH}_4\text{Cl}$ , extracted three times with  $\text{CH}_2\text{Cl}_2$ , dried over  $\text{Na}_2\text{SO}_4$ , and concentrated under reduced pressure.

Purification by flash chromatography on silica gel (Hexanes – 15% EtOAc/Hexanes) afforded **(S)-3** (1.3 g, 91.8%, clear oil).  $R_f = 0.190$  (15% EtOAc/hexanes);  $[\alpha]_D^{21} = -3.4^\circ$  ( $c = 11.9$ ,  $\text{CHCl}_3$ );  $^1\text{H NMR}$  (500 MHz,  $\text{CHLOROFORM-d}$ )  $\delta$  4.33 - 4.41 (m, 1H), 2.46 (d,  $J = 1.96$  Hz, 1H), 2.09 (d,  $J = 5.38$  Hz, 1H), 1.65 - 1.78 (m, 2H), 1.40 - 1.51 (m, 2H), 1.20 - 1.36 (m, 12H), 0.88 (t,  $J = 6.85$  Hz, 3H);  $^{13}\text{C NMR}$  (125 MHz,  $\text{CHLOROFORM-d}$ )  $\delta$  85.0, 72.8, 62.3, 37.6, 31.9, 29.5, 29.3, 29.2, 25.0, 22.6, 14.1; IR (ATR) 3382, 3311, 2924, 2854, 1466  $\text{cm}^{-1}$ ; MS(EI)  $[\text{M} - 1]^+$  181.





**(S)-5-(trimethylsilyl)pent-1-en-4-yn-3-ol (S)-4; (R)-5-(trimethylsilyl)pent-1-en-4-yn-3-yl acetate (R)-5**

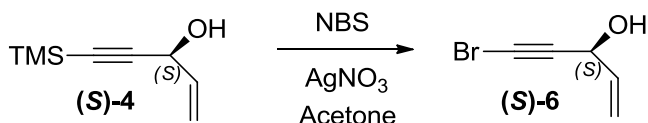
To a solution of (trimethylsilyl)acetylene (7.81 g, 11.0 mL, 79.5 mmol) in dry Et<sub>2</sub>O (95 mL) at -78 °C was added dropwise a solution of n-butyllithium (2.25 M in hexanes, 31 mL, 69.8 mmol) over 30 minutes under an Ar atmosphere. The reaction mixture was then stirred for 30 minutes before a solution of acrolein (3.7 g, 4.4 mL, 65.9 mmol) in Et<sub>2</sub>O (5 mL) was added dropwise over 10 minutes. The resulting mixture was allowed to gradually warm to ambient temperature. After stirring for 20 hours, the mixture was quenched by slow addition of saturated NH<sub>4</sub>Cl. The mixture was extracted with Et<sub>2</sub>O, washed with H<sub>2</sub>O and brine, dried over Na<sub>2</sub>SO<sub>4</sub>, and concentrated to near dryness. The resultant yellow oil (±4) was used directly in the next reaction without further purification.

The yellow oil (±4) was dissolved in dry hexanes (302 mL) followed by the addition of ground, activated 4-Å molecular sieves (3.11 g) and lipase (*Pseudomonas fluorescens*, Amano Lipase AK, 1.89 g). To the well-stirred suspension was added vinyl acetate (29.0 mL, 314.6 mmol) over 10 minutes. The suspension was stirred under an Ar atmosphere for 24 hours and then filtered through a pad of Celite and concentrated. The resulting yellow oil was purified by silica gel chromatography (3-25% EtOAc/hexanes) to give (S)-4 (5.0 g, 48.7%, clear oil, ee 96.8) and (R)-5 (5.8 g, 45.2%, clear oil, ee 96.0).

Data for **±4**:  $R_f = 0.167$  (15% EtOAc/hexanes);  **$^1\text{H}$  NMR** (500 MHz, CHLOROFORM-d)  $\delta$  5.93 - 6.02 (m, 1H), 5.44 - 5.51 (d,  $J = 16.87$  Hz, 1H), 5.21 - 5.26 (d,  $J = 10.27$  Hz, 1H), 4.88 (m, 1H), 1.99 (d,  $J = 5.62$  Hz, 1H), 0.15 - 0.22 (m, 9H);  **$^{13}\text{C}$  NMR** (125 MHz, CHLOROFORM-d)  $\delta$  136.6, 116.6, 103.9, 91.2, 63.6, -0.2; IR (ATR) 3354, 2961, 2175, 1250, 839  $\text{cm}^{-1}$ ; HRMS (ESI-TOF)  $[\text{M} + \text{H}]^+$  calcd. for  $\text{C}_8\text{H}_{15}\text{OSi}$  155.0892, found 155.0878.

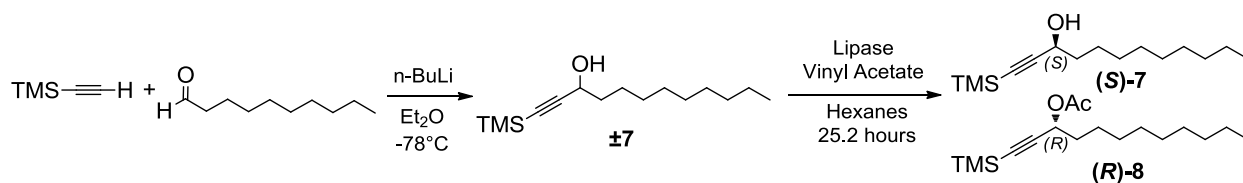
Data for **(S)-4**:  $R_f = 0.167$  (15% EtOAc/hexanes);  $[\alpha]_{\text{D}}^{22} = +29.4^\circ$  ( $c = 1.4$ ,  $\text{CHCl}_3$ );  **$^1\text{H}$  NMR** (500 MHz, CHLOROFORM-d)  $\delta$  5.97 (ddd,  $J = 5.38, 10.15, 17.00$  Hz, 1H), 5.48 (dt,  $J = 1.28, 17.00$  Hz, 1H), 5.24 (dt,  $J = 1.25, 10.21$  Hz, 1H), 4.88 (m, 1H), 1.96 (br. s., 1H), 0.18 - 0.20 (s, 9H);  **$^{13}\text{C}$  NMR** (125 MHz, CHLOROFORM-d)  $\delta$  136.6, 116.6, 103.9, 91.2, 63.6, -0.2; IR (ATR) 3359, 2961, 2175, 1250, 839  $\text{cm}^{-1}$ ; HRMS (ESI-TOF)  $[\text{M} + \text{H}]^+$  calcd. for  $\text{C}_8\text{H}_{15}\text{OSi}$  155.0892, found 155.0874.

Data for **(R)-5**:  $R_f = 0.449$  (15% EtOAc/hexanes);  $[\alpha]_{\text{D}}^{22} = +27.4^\circ$  ( $c = 7.7$ ,  $\text{CHCl}_3$ );  **$^1\text{H}$  NMR** (500 MHz, CHLOROFORM-d)  $\delta$  5.82 - 5.90 (m, 2H), 5.51 - 5.56 (m, 1H), 5.28 - 5.32 (m, 1H), 2.09 (s, 3H), 0.16 - 0.19 (s, 9H);  **$^{13}\text{C}$  NMR** (125 MHz, CHLOROFORM-d)  $\delta$  169.4, 132.7, 118.9, 100.0, 92.2, 64.5, 21.0, -0.3; IR (ATR) 2962, 2182, 1745, 1223, 840  $\text{cm}^{-1}$ ; HRMS (ESI-TOF)  $[\text{M} + \text{H}]^+$  calcd. for  $\text{C}_{10}\text{H}_{17}\text{O}_2\text{Si}$  191.0998, found 191.0988.



**(S)-5-bromopent-1-en-4-yn-3-ol (S)-6**

To a solution of (S)-4 (1.9 g, 12.2 mmol) in acetone (42 mL) was added N-bromosuccinimide (3.4 g, 19.4 mmol) and AgNO<sub>3</sub> (0.43 g, 2.5 mmol). Reaction mixture was stirred for 4 hours under Ar atmosphere at ambient temperature. Reaction mixture was then chilled to 0°C, quenched with H<sub>2</sub>O, extracted with Et<sub>2</sub>O, washed with H<sub>2</sub>O and brine, dried over Na<sub>2</sub>SO<sub>4</sub>, and concentrated under reduced pressure. Purification by flash chromatography on silica gel (Hexanes – 10% EtOAc/Hexanes) afforded (S)-6 (1.95 g, 99.7%, yellow oil).  $R_f = 0.207$  (15% EtOAc/hexanes);  $[\alpha]_D^{23} = +22.8^\circ$  ( $c = 10.5$ , CHCl<sub>3</sub>); <sup>1</sup>H NMR (500 MHz, CHLOROFORM-d)  $\delta$  5.89 - 6.03 (m, 1H), 5.43 - 5.54 (m, 1H), 5.21 - 5.32 (m, 1H), 4.86 - 4.97 (m, 1H), 2.02 (br. s., 1H); C13 NMR; IR (ATR) 3376, 2213, 2181, 1709, 1651, 1404, 1254, 983 cm<sup>-1</sup>; HRMS (ESI-TOF) [M]<sup>+</sup> calcd. for C<sub>5</sub>H<sub>5</sub>BrO 159.9524, found 159.9558.



**(S)-1-(trimethylsilyl)dodec-1-yn-3-ol (S)-7; (R)-1-(trimethylsilyl)dodec-1-yn-3-yl acetate (R)-8**

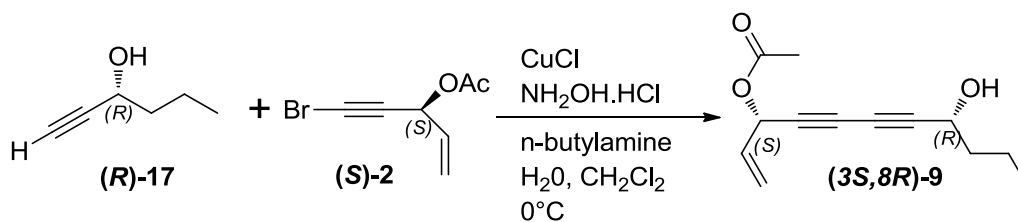
To a solution of (trimethylsilyl)acetylene (15.62 g, 22.0 mL, 155.6 mmol) in dry Et<sub>2</sub>O (185 mL) at -78 °C was added dropwise a solution of n-butyllithium (2.3 M in hexanes, 61 mL, 140.3 mmol) over 1 hour via syringe pump under an Ar atmosphere. The reaction mixture was then stirred for 10 minutes before a solution of decanal (20.75 g, 25.0 mL, 127.5 mmol) in Et<sub>2</sub>O (15 mL) was added dropwise over 40 minutes via syringe pump. The resulting mixture was allowed to gradually warm to ambient temperature. After stirring for 17 hours, the mixture was quenched by slow addition of saturated NH<sub>4</sub>Cl (36 mL) followed by H<sub>2</sub>O (18 mL). The mixture was extracted with Et<sub>2</sub>O, washed with H<sub>2</sub>O and brine, dried over Na<sub>2</sub>SO<sub>4</sub>, and concentrated to near dryness. The resultant yellow oil (±7) was used directly in the next reaction without further purification.

The yellow oil (±7) was dissolved in dry hexanes (500 ml) followed by the addition of ground, activated 4-Å molecular sieves (8.31 g) and lipase (*Pseudomonas fluorescens*, Amano Lipase AK, 4.89 g). To the well-stirred suspension was added vinyl acetate (48.0 mL, 520.8 mmol) over 10 minutes. The suspension was stirred under an Ar atmosphere for 25 hours and 10 minutes and then filtered through a pad of Celite and concentrated. The resulting yellow oil was purified by silica gel chromatography (2-15% EtOAc/hexanes) to give (S)-7 (11.1 g, 34.3%, yellow oil, *ee* 94.2) and (R)-8 (16.9 g, 44.7%, yellow oil, *ee* 100.0).

Data for **±7**:  $R_f = 0.365$  (15% EtOAc/hexanes);  $^1\text{H NMR}$  (500 MHz, CHLOROFORM-d)  $\delta$  4.35 (t,  $J = 6.60$  Hz, 1H), 1.62 - 1.75 (m, 2H), 1.40 - 1.50 (m, 2H), 1.23 - 1.37 (m, 12H), 0.85 - 0.92 (t,  $J = 6.85$  Hz, 3H), 0.14 - 0.21 (s, 9H);  $^{13}\text{C NMR}$  (125 MHz, CHLOROFORM-d)  $\delta$  106.9, 89.3, 62.9, 37.7, 31.9, 29.5, 29.3, 29.2, 25.1, 22.7, 14.1, -0.1; **IR** (ATR): 3328, 2957, 2924, 2854, 2172, 1467, 1250, 841, 760  $\text{cm}^{-1}$ ; MS(EI)  $[\text{M} - 1]^+$  253

Data for (**S**)-**7**:  $R_f = 0.365$  (15% EtOAc/hexanes);  $[\alpha]_{\text{D}}^{18} = +0.4^\circ$  ( $c = 5.1$ ,  $\text{CHCl}_3$ );  $^1\text{H NMR}$  (500 MHz, CHLOROFORM-d)  $\delta$  4.35 (q,  $J = 6.19$  Hz, 1H), 1.82 (d,  $J = 5.38$  Hz, 1H), 1.63 - 1.75 (m, 2H), 1.40 - 1.50 (m, 2H), 1.23 - 1.36 (m, 12H), 0.85 - 0.93 (t,  $J = 6.72$  Hz, 3H), 0.13 - 0.23 (s, 9H);  $^{13}\text{C NMR}$  (125 MHz, CHLOROFORM-d)  $\delta$  106.9, 89.3, 62.9, 37.7, 31.9, 29.5, 29.3, 29.2, 25.1, 22.7, 14.1, -0.1; **IR** (ATR): 3330, 2957, 2924, 2855, 2173, 1467, 1250, 840, 760  $\text{cm}^{-1}$ ; MS(EI)  $[\text{M} - 1]^+$  253

Data for (**R**)-**8**:  $R_f = 0.538$  (15% EtOAc/hexanes);  $[\alpha]_{\text{D}}^{22} = +32.1^\circ$  ( $c = 1.7$ ,  $\text{CHCl}_3$ );  $^1\text{H NMR}$  (500 MHz, CHLOROFORM-d)  $\delta$  5.38 (t,  $J = 6.72$  Hz, 1H), 2.08 (d,  $J = 0.73$  Hz, 3H), 1.68 - 1.80 (m, 2H), 1.37 - 1.46 (m, 2H), 1.21 - 1.36 (m, 12H), 0.84 - 0.93 (t,  $J = 6.85$  Hz, 3H), 0.10 - 0.26 (d,  $J = 0.73$  Hz, 9H);  $^{13}\text{C NMR}$  (125 MHz, CHLOROFORM-d)  $\delta$  169.9, 102.8, 90.2, 64.4, 34.8, 31.9, 29.4, 29.4, 29.3, 29.0, 24.9, 22.7, 21.1, 14.1, -0.2; **IR** (ATR): 2956, 2926, 2855, 2180, 1746, 1467, 1371, 1250, 1230, 1089, 842, 760  $\text{cm}^{-1}$ ; HRMS (ESI-TOF)  $[\text{M} + \text{H}]^+$  calcd. for  $\text{C}_{17}\text{H}_{33}\text{O}_2\text{Si}$  297.2250, found 297.2244.

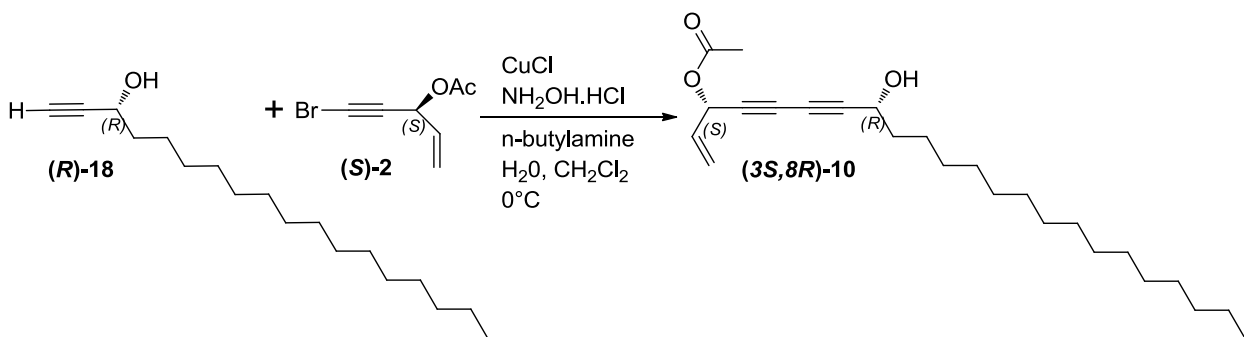


**JH-4-198, TJL-2-064**

**(3*S*,8*R*)-8-hydroxyundeca-1-en-4,6-diyne-3-yl acetate (3*S*,8*R*)-9**

Copper (I) chloride (0.015 g, 0.15 mmol) was added to a stirred 30 % solution (2.5 mL) of n-butylamine in distilled water at 0 °C which resulted in a deep blue solution. A few crystals of NH<sub>2</sub>OH.HCl were added until solution was colorless. A solution of (**R**)-17 (0.081 g, 0.82 mmol) in CH<sub>2</sub>Cl<sub>2</sub> (1.4 mL) was added under argon atmosphere which resulted in yellow reaction mixture. After 10 minutes, a solution of (**S**)-2 (0.247 g, 1.21 mmol) in CH<sub>2</sub>Cl<sub>2</sub> (2.0 mL) was added dropwise over 5 minutes. A few crystals of NH<sub>2</sub>OH.HCl were added as necessary whenever solution turned blue or green. After 1 hour and 40 minutes, reaction was quenched with water, extracted 3 times with CH<sub>2</sub>Cl<sub>2</sub>, dried over Na<sub>2</sub>SO<sub>4</sub>, and concentrated under reduced pressure. Immediate purification by flash chromatography on silica gel (hexanes – 15% EtOAc/hexanes) afforded (**3*S*,8*R*)-9** (0.083 g, 45.9%, yellow oil). TLC  $R_f = 0.292$  (25% EtOAc/hexanes);  $[\alpha]_D^{21} = -55.2^\circ$  (CHCl<sub>3</sub>); <sup>1</sup>H NMR (500 MHz, CHLOROFORM-*d*)  $\delta$  5.83 - 5.94 (m, 2H), 5.52 - 5.59 (m, 1H), 5.33 - 5.39 (m, 1H), 4.45 (q,  $J = 6.25$  Hz, 1H), 2.11 (s, 3H), 1.94 (d,  $J = 5.26$  Hz, 1H), 1.71 (m, 2H), 1.44 - 1.53 (m, 2H), 0.95 (t,  $J = 7.40$  Hz, 3H); <sup>13</sup>C NMR (125 MHz, CHLOROFORM-*d*)  $\delta$  169.5, 131.9, 119.7, 81.3, 74.3, 70.8, 68.6, 64.4, 62.6, 39.4, 20.9,

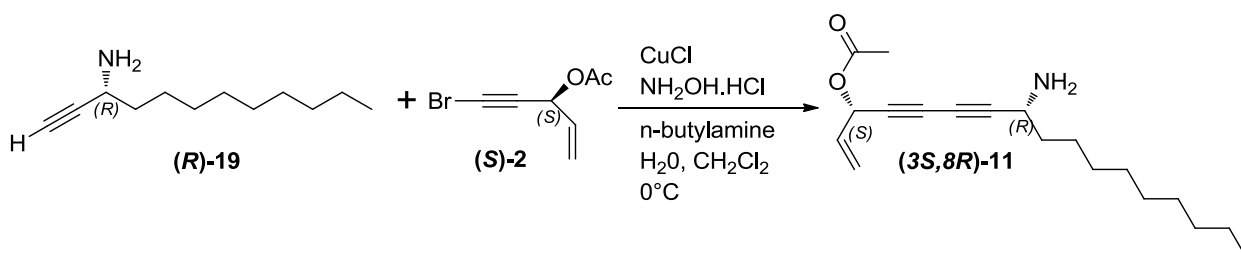
18.3, 13.6; IR (ATR) 3420, 2961, 2935, 2875, 2256, 2158, 1746, 1371, 1219, 1016, 974  $\text{cm}^{-1}$ ; MS(EI)  $[\text{M} - 1]^+$  219.



**(3*S*,8*R*)-8-hydroxytricos-1-en-4,6-diyn-3-yl acetate (3*S*,8*R*)-10**

Copper (I) chloride (0.004 g, 0.04 mmol) was added to a stirred 30 % solution (0.9 mL) of n-butylamine in distilled water at 0 °C which resulted in a deep blue solution. A few crystals of  $\text{NH}_2\text{OH}\cdot\text{HCl}$  were added until solution was colorless. A solution of **(*R*)-18** (0.074 g, 0.28 mmol) in  $\text{CH}_2\text{Cl}_2$  (0.45 mL) was added under argon atmosphere which resulted in yellow reaction mixture. After 10 minutes, a solution of **(*S*)-2** (0.069 g, 0.34 mmol) in  $\text{CH}_2\text{Cl}_2$  (0.54 mL) was added dropwise over 5 minutes. A few crystals of  $\text{NH}_2\text{OH}\cdot\text{HCl}$  were added as necessary whenever solution turned blue or green. After 25 minutes, reaction was quenched with water, extracted 3 times with  $\text{CH}_2\text{Cl}_2$ , dried over  $\text{Na}_2\text{SO}_4$ , and concentrated under reduced pressure. Immediate purification by flash chromatography on silica gel afforded **(3*S*,8*R*)-10** (0.058 g, 53.9%, light orange solid). TLC  $R_f = 0.353$  (25% EtOAc/hexanes);  $[\alpha]_D^{22} = -39.7^\circ$  ( $c = 1.3$ ,  $\text{CHCl}_3$ );  $^1\text{H}$  NMR (500 MHz,  $\text{CHLOROFORM-d}$ )  $\delta$  5.82 - 5.95 (m, 2H), 5.52 - 5.58 (m, 1H), 5.33 - 5.38 (m, 1H), 4.42 (t,  $J = 6.72$  Hz, 1H), 2.10 - 2.13 (s, 3H), 1.95 - 2.05 (br.s., 1H), 1.66 - 1.77 (m, 2H), 1.43 (m, 2H), 1.21 - 1.35 (m, 24H), 0.86 - 0.90 (t,  $J = 6.97$  Hz, 3H);  $^{13}\text{C}$  NMR (125

MHz, CHLOROFORM-*d*)  $\delta$  169.5, 131.9, 119.7, 81.3, 74.3, 70.8, 68.5, 64.4, 62.8, 37.4, 31.9, 29.7, 29.7, 29.6, 29.6, 29.5, 29.5, 29.3, 29.2, 25.0, 22.7, 20.9, 14.1; IR (ATR) 3355, 2915, 2849, 2258, 2158, 1746, 1223, 1017  $\text{cm}^{-1}$ ; MS(EI)  $[\text{M} - 1]^+$  387.

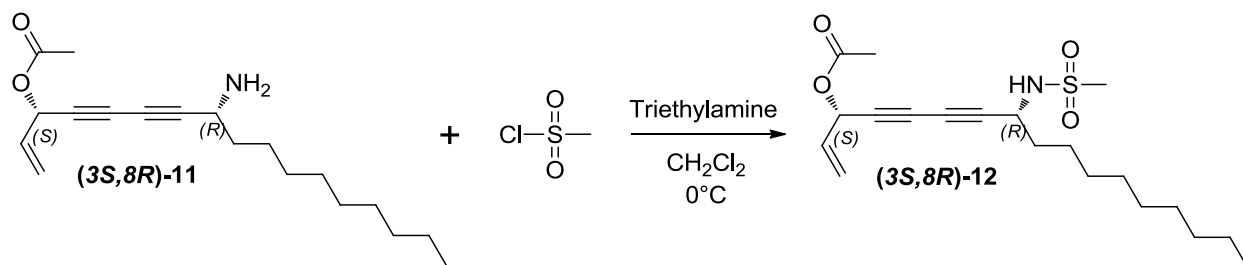


**(3S,8R)-8-aminoheptadeca-1-en-4,6-diyn-3-yl acetate (3S,8R)-11**

Copper (I) chloride (0.075 g, 0.75 mmol) was added to a stirred 30 % solution (14.5 mL) of n-butylamine in distilled water at 0 °C which resulted in a deep blue solution. A few crystals of  $\text{NH}_2\text{OH}\cdot\text{HCl}$  were added until solution was colorless. A solution of **(R)-19** (0.877 g, 4.83 mmol) in  $\text{CH}_2\text{Cl}_2$  (7.3 mL) was added under argon atmosphere which resulted in yellow reaction mixture. After 10 minutes, a solution of **(S)-2** (1.330 g, 6.55 mmol) in  $\text{CH}_2\text{Cl}_2$  (9.5 mL) was added dropwise over 12 minutes. A few crystals of  $\text{NH}_2\text{OH}\cdot\text{HCl}$  were added as necessary whenever solution turned blue or green. After 20 minutes, GC/MS showed that there still remained some **(R)-19**. After 1 hour of stirring, added a second solution of **(S)-2** (0.160 g, 0.79 mmol) in  $\text{CH}_2\text{Cl}_2$  (2.0 mL). Fifteen minutes after the second solution of was **(S)-2** added, reaction was quenched with water, extracted 3 times with  $\text{CH}_2\text{Cl}_2$ , dried over  $\text{Na}_2\text{SO}_4$ , and concentrated under reduced pressure. Immediate purification by flash chromatography on silica gel (hexanes – 50% EtOAc/hexanes) afforded **(3S,8R)-11** (0.976 g, 66.5%, red, orange oil). TLC  $R_f = 0.286$  (60% EtOAc/hexanes);  $[\alpha]_D^{18} = +22.5^\circ$  ( $c = 0.18$ ,  $\text{CHCl}_3$ );  $^1\text{H}$  NMR (500 MHz,



CHLOROFORM-*d*)  $\delta$  5.84 - 5.94 (m, 2H), 5.55 (d,  $J = 16.14$  Hz, 1H), 5.35 (d,  $J = 9.54$  Hz, 1H), 3.60 (t,  $J = 6.85$  Hz, 1H), 2.11 (s, 3H), 1.38 - 1.67 (m, 6H), 1.22 - 1.34 (m, 12H), 0.89 (t,  $J = 6.72$  Hz, 3H);  $^{13}\text{C}$  NMR (125 MHz, CHLOROFORM-*d*)  $\delta$  169.5, 132.1, 119.6, 84.5, 73.0, 71.3, 66.3, 64.5, 44.0, 37.4, 31.8, 29.5, 29.4, 29.3, 29.2, 25.9, 22.6, 20.9, 14.1; IR (ATR) 3297, 2924, 2854, 2254, 1746, 1220  $\text{cm}^{-1}$ ; HRMS (ESI-TOF)  $[\text{M} + \text{H}]^+$  calcd. for  $\text{C}_{19}\text{H}_{30}\text{NO}_2$  304.2277, found 304.2265.

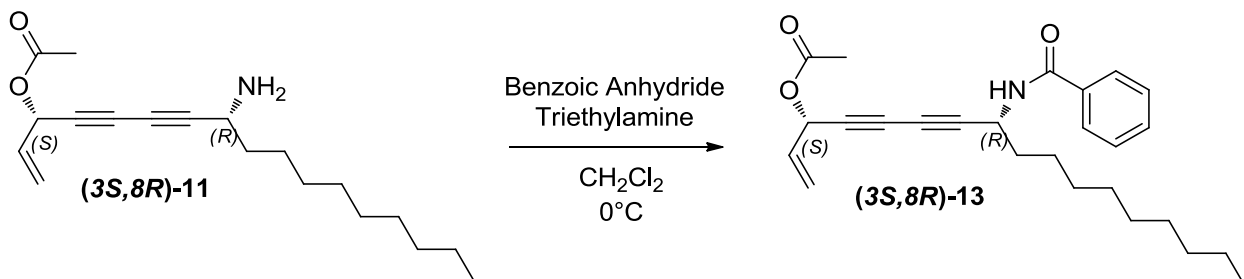


#### 4-087

##### (3*S*,8*R*)-8-(methanesulfonamido)heptadeca-1-en-4,6-diyn-3-yl acetate (3*S*,8*R*)-12

To a solution of (3*S*,8*R*)-11 (0.056 g, 0.19 mmol) in  $\text{CH}_2\text{Cl}_2$  (1.4 mL) at  $0^\circ\text{C}$  under Ar atmosphere was added triethylamine (0.06 mL, 0.43 mmol) followed by methanesulfonyl chloride (0.02 mL, 0.26 mmol). After 1 hour and 50 minutes, reaction was quenched with water, extracted three times with  $\text{CH}_2\text{Cl}_2$ , dried over  $\text{Na}_2\text{SO}_4$ , and concentrated under reduced pressure. Purification by flash chromatography on silica gel (hexanes – 25% EtOAc/hexanes) afforded (3*S*,8*R*)-12 (0.047 g, 66.7%) as a light brown oil. TLC  $R_f = 0.413$  (40% EtOAc/hexanes);  $[\alpha]_D^{23} = +29.6^\circ$  ( $c = 2.37$ ,  $\text{CHCl}_3$ );  $^1\text{H}$  NMR (500 MHz, CHLOROFORM-*d*)  $\delta$  5.80 - 5.94 (m, 2H), 5.50 - 5.59 (m, 1H), 5.32 - 5.41 (m, 1H), 4.67 (d,  $J = 9.11$  Hz, 1H), 4.25 (m, 1H), 3.03 - 3.13 (s, 3H), 2.06 - 2.16 (s, 3H), 1.71 - 1.77 (m, 2H), 1.42 - 1.50 (m, 2H), 1.24 - 1.33 (m, 12H), 0.86 - 0.91 (t,  $J = 7.02$  Hz, 3H);  $^{13}\text{C}$  NMR

(125 MHz, CHLOROFORM-d)  $\delta$  169.4, 131.7, 119.8, 78.9, 74.6, 70.3, 68.5, 64.3, 46.0, 41.6, 36.2, 31.8, 29.4, 29.3, 29.2, 28.8, 25.4, 22.6, 20.8, 14.1; IR (ATR) 3286, 2927, 2856, 2258, 1747, 1326, 1220, 1155  $\text{cm}^{-1}$ ; HRMS (ESI-TOF)  $[\text{M} + \text{H}]^+$  calcd. for  $\text{C}_{20}\text{H}_{32}\text{NO}_4\text{S}$  382.2052, found 383.2072.

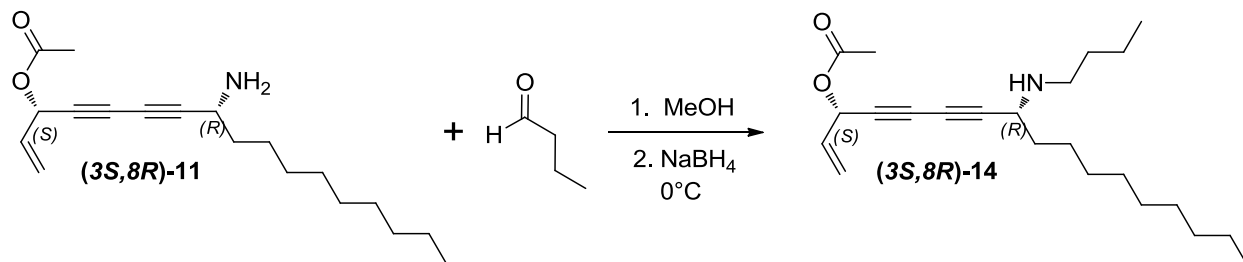


#### 4-053, 4-037

#### (3*S*,8*R*)-8-benzamidoheptadeca-1-en-4,6-diyn-3-yl acetate (3*S*,8*R*)-13

To a solution of (3*S*,8*R*)-11 (0.046 g, 0.15 mmol) in  $\text{CH}_2\text{Cl}_2$  (1.6 mL) at  $0^\circ\text{C}$  under Ar was added benzoic anhydride (0.047 g, 0.21 mmol) followed by triethylamine (0.03 mL, 0.22 mmol). Reaction mixture was stirred for 15 minutes at  $0^\circ\text{C}$  and then allowed to warm to ambient temperature. After 1 hour and 15 minutes, reaction mixture was quenched with water, extracted three times with  $\text{CH}_2\text{Cl}_2$ , dried over  $\text{Na}_2\text{SO}_4$ , and concentrated under reduced pressure. Purification by flash chromatography on silica gel (hexanes – 15% EtOAc/hexanes) afforded (3*S*,8*R*)-13 (0.031 g, 51.2%) as a beige oil. TLC  $R_f$  = 0.340 (25% EtOAc/hexanes);  $[\alpha]_D^{17} = -2.9^\circ$  ( $c = 0.66$ ,  $\text{CHCl}_3$ );  $^1\text{H}$  NMR (500 MHz, CHLOROFORM-d)  $\delta$  7.76 - 7.80 (m, 2H), 7.51 - 7.55 (m, 1H), 7.43 - 7.47 (m, 2H), 6.30 (d,  $J = 8.56$  Hz, 1H), 5.82 - 5.93 (m, 2H), 5.52 - 5.58 (m, 1H), 5.33 - 5.38 (m, 1H), 5.01 - 5.09 (q,  $J = 7.42$  Hz, 1H), 2.10 - 2.13 (s, 3H), 1.73 - 1.83 (m, 2H), 1.44 - 1.52 (m, 2H), 1.23 - 1.37 (m, 12H), 0.86 - 0.91 (t,  $J = 6.97$  Hz, 3H);  $^{13}\text{C}$  NMR (125 MHz,

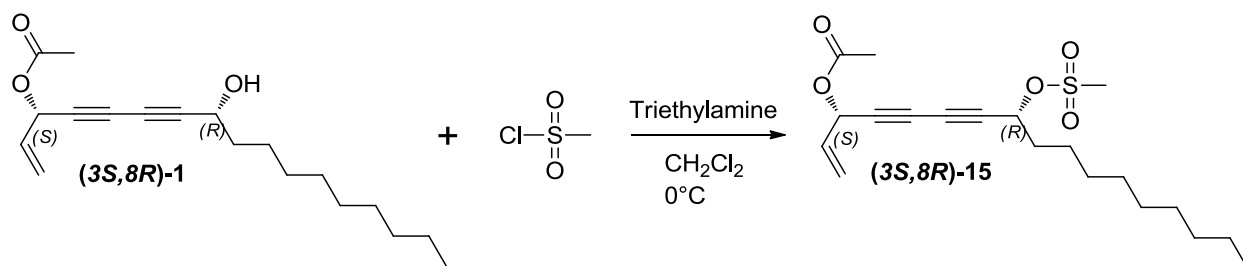
CHLOROFORM-*d*)  $\delta$  169.5, 166.3, 133.7, 131.9, 131.8, 128.6, 127.0, 119.7, 79.9, 73.4, 71.0, 67.0, 64.4, 42.3, 35.7, 31.8, 29.5, 29.4, 29.2, 29.1, 25.6, 22.7, 20.9, 14.1; IR (ATR) 3307, 2925, 2855, 2258, 1747, 1638, 1527, 1219  $\text{cm}^{-1}$ ; HRMS (ESI-TOF)  $[\text{M} + \text{H}]^+$  calcd. for  $\text{C}_{26}\text{H}_{34}\text{NO}_3$  408.2539, found 408.2538.



**(3*S*,8*R*)-8-(butylamino)heptadeca-1-en-4,6-diyn-3-yl acetate (3*S*,8*R*)-14**

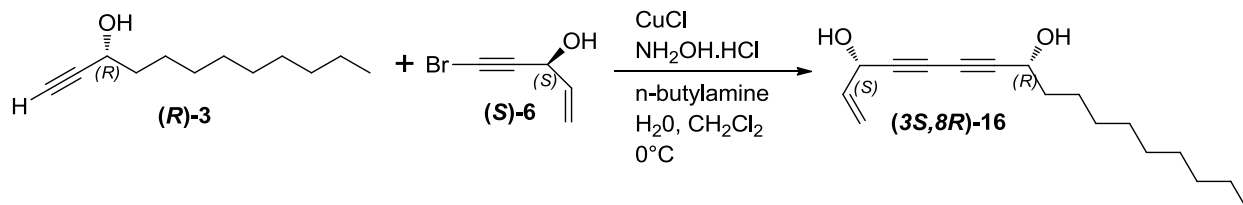
To a solution of **(3*S*,8*R*)-11** (0.239 g, 0.79 mmol) in methanol (4.1 mL) under argon atmosphere was added butyraldehyde (0.11 mL, 1.2 mmol). Reaction mixture was stirred at ambient temperature for 20 minutes and then chilled to 0°C at which time  $\text{NaBH}_4$  was added (0.028 g, 0.73 mmol). Reaction mixture was stirred for 1 hour and 20 minutes and then diluted with EtOAc, washed with saturated  $\text{NaHCO}_3$ , dried over  $\text{Na}_2\text{SO}_4$ , and concentrated under reduced pressure. Purification by flash chromatography on silica gel (hexanes – 10% EtOAc/hexanes) afforded **(3*S*,8*R*)-14** (0.151 g, 53.4%) as a yellow oil. TLC  $R_f$  = 0.350 (25% EtOAc/hexanes);  $^1\text{H}$  NMR (500 MHz, CHLOROFORM-*d*)  $\delta$  5.85 - 5.95 (m, 2H), 5.53 - 5.58 (m, 1H), 5.33 - 5.37 (m, 1H), 3.41 (dd,  $J$  = 5.75, 8.19 Hz, 1H), 2.84 (ddd,  $J$  = 5.99, 8.38, 11.07 Hz, 1H), 2.56 (ddd,  $J$  = 5.87, 8.31, 11.00 Hz, 1H), 2.11 - 2.12 (s, 3H), 1.54 - 1.69 (m, 2H), 1.20 - 1.52 (m, 19H), 0.93 (t,  $J$  = 7.21 Hz, 3H), 0.86 - 0.90 (t,  $J$  = 6.97, 3H);  $^{13}\text{C}$  NMR (125 MHz, CHLOROFORM-*d*)  $\delta$  169.5, 132.1, 119.6,

83.5, 72.3, 71.4, 67.0, 64.6, 50.8, 47.3, 35.8, 32.2, 31.9, 29.5, 29.5, 29.3, 29.3, 26.0, 22.7, 20.9, 20.5, 14.1, 14.0; IR (ATR) 2925, 2855, 2252, 1748, 1218  $\text{cm}^{-1}$ ; HRMS (ESI-TOF)  $[\text{M} + \text{H}]^+$  calcd. for  $\text{C}_{23}\text{H}_{38}\text{NO}_2$  360.2903, found 360.2878.



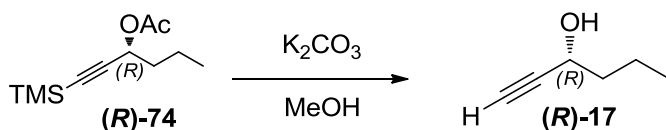
**(3*S*,8*R*)-8-((methylsulfonyl)oxy)heptadeca-1-en-4,6-diyne-3-yl acetate (3*S*,8*R*)-15**

To a solution of **(3*S*,8*R*)-1** (0.027 g, 0.09 mmol) in  $\text{CH}_2\text{Cl}_2$  (0.3 mL) at  $0^\circ\text{C}$  under Ar atmosphere was added triethylamine (0.02 mL, 0.14 mmol) followed by methanesulfonyl chloride (0.01 mL, 0.13 mmol). After 1 hour, reaction was quenched with water, extracted three times with  $\text{CH}_2\text{Cl}_2$ , dried over  $\text{Na}_2\text{SO}_4$ , and concentrated under reduced pressure. Purification by flash chromatography on silica gel afforded **(3*S*,8*R*)-15** (0.021 mg, 62.4%) as a beige oil. TLC  $R_f$  = 0.355 (25% EtOAc/hexanes);  $[\alpha]_{\text{D}}^{21} = +35.6^\circ$  ( $c = 2.0$ ,  $\text{CHCl}_3$ );  $^1\text{H}$  NMR (500 MHz,  $\text{CHLOROFORM-d}$ )  $\delta$  5.84 - 5.93 (m, 2H), 5.52 - 5.57 (m, 1H), 5.36 - 5.40 (m, 1H), 5.22 (t,  $J = 6.60$  Hz, 1H), 3.10 - 3.13 (s, 3H), 2.11 - 2.13 (s, 3H), 1.84 - 1.96 (m, 2H), 1.48 (m, 2H), 1.23 - 1.36 (m, 12H), 0.86 - 0.91 (t,  $J = 6.97$  Hz, 3H);  $^{13}\text{C}$  NMR (125 MHz,  $\text{CHLOROFORM-d}$ )  $\delta$  169.4, 131.5, 120.0, 76.5, 75.1, 72.0, 71.5, 69.8, 64.2, 39.2, 35.5, 31.8, 29.4, 29.3, 29.2, 28.8, 24.6, 22.6, 20.8, 14.1; HRMS (ESI-TOF)  $[\text{M} + \text{Na}]^+$  calcd. for  $\text{C}_{20}\text{H}_{30}\text{NaO}_5\text{S}$  405.1712, found 405.1708.



**(3*S*,8*R*)-heptadeca-1-en-4,6-diyne-3,8-diol (3*S*,8*R*)-16**

Copper (I) chloride (0.011 g, 0.11 mmol) was added to a stirred 30 % solution (1.6 mL) of n-butylamine in distilled water at 0 °C which resulted in a deep blue solution. A few crystals of NH<sub>2</sub>OH.HCl were added until solution was colorless. A solution of (***R***)-**3** (0.105 g, 0.58 mmol) in CH<sub>2</sub>Cl<sub>2</sub> (0.9 mL) was added under argon atmosphere which resulted in yellow reaction mixture. After 10 minutes, a solution of (***S***)-**6** (0.155 g, 0.96 mmol) in CH<sub>2</sub>Cl<sub>2</sub> (1.4 mL) was added dropwise over 5 minutes. A few crystals of NH<sub>2</sub>OH.HCl were added as necessary whenever solution turned blue or green. After 55 minutes, reaction was quenched with water, extracted three times with CH<sub>2</sub>Cl<sub>2</sub>, dried over Na<sub>2</sub>SO<sub>4</sub>, and concentrated under reduced pressure. Immediate purification by flash chromatography on silica gel (15% EtOAc/hexanes) afforded (***3S***,***8R***)-**16** (0.046 g, 30.4%) as a reddish-brown oil. TLC  $R_f$  = 0.429 (40% EtOAc/hexanes);  $[\alpha]_D^{22} = +22.3^\circ$  ( $c = 1.3$ , CHCl<sub>3</sub>); <sup>1</sup>H NMR (500 MHz, CHLOROFORM-*d*)  $\delta$  5.95 (ddd,  $J = 5.38, 10.15, 17.00$  Hz, 1H), 5.44 - 5.53 (d,  $J = 17.12$  Hz, 1H), 5.23 - 5.30 (d,  $J = 10.03$  Hz, 1H), 4.95 (d,  $J = 4.65$  Hz, 1H), 4.44 (t,  $J = 6.48$  Hz, 1H), 2.21 (br. s., 1H), 2.05 (br. s., 1H), 1.66 - 1.79 (m, 2H), 1.40 - 1.50 (m, 2H), 1.21 - 1.37 (m, 12H), 0.89 (t,  $J = 6.97$  Hz, 3H); <sup>13</sup>C NMR (125 MHz, CHLOROFORM-*d*)  $\delta$  135.8, 117.3, 81.1, 77.8, 70.3, 68.7, 63.5, 62.8, 37.4, 31.9, 29.5, 29.5, 29.3, 29.2, 25.0, 22.7, 14.1; IR (ATR) 3350, 2916, 2850, 1020 cm<sup>-1</sup>; HRMS (ESI-TOF)  $[M + H]^+$  calcd. for C<sub>17</sub>H<sub>27</sub>NO<sub>2</sub> 263.2011, found 263.2044.

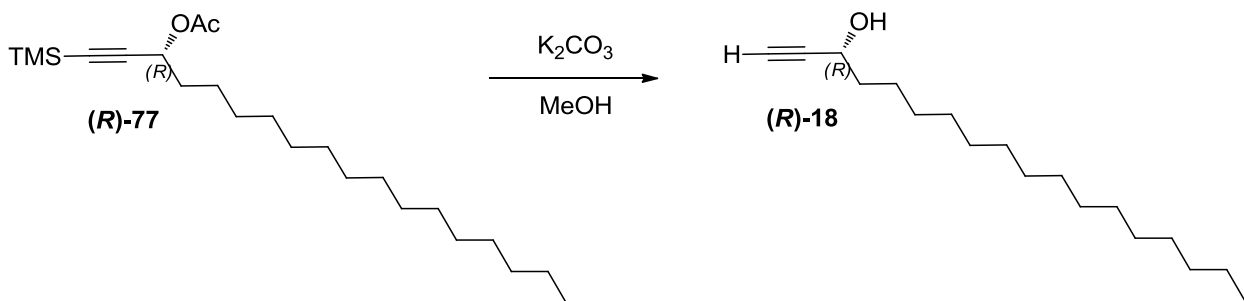


**(R)-hex-1-yn-3-ol (R)-17**

To a solution of **(R)-74** (0.34 g, 1.6 mmol) in methanol (40 mL) was added  $\text{K}_2\text{CO}_3$  (0.53 g, 3.8 mmol). Solution was stirred at ambient temperature under argon atmosphere.

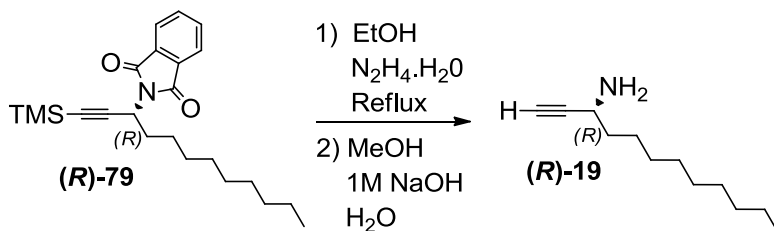
After 22.75 hours, reaction was quenched with saturated  $\text{NH}_4\text{Cl}$ , extracted three times with  $\text{CH}_2\text{Cl}_2$ , dried over  $\text{Na}_2\text{SO}_4$ , and concentrated under reduced pressure which afforded **(R)-17** (0.13 g, 84.9%, light yellow oil, *ee* 100.0). **(R)-17** was in the synthesis of **(3S,8R)-19** without further purification.

$[\alpha]_{\text{D}}^{18} = +5.5^\circ$  ( $c = 0.2$ ,  $\text{CHCl}_3$ );  $^1\text{H}$  NMR (500 MHz,  $\text{CHLOROFORM-d}$ )  $\delta$  4.39 (t,  $J = 5.87$  Hz, 1H), 2.47 (d,  $J = 2.20$  Hz, 1H), 1.91 (br. s., 1H), 1.65 - 1.77 (m, 2H), 1.45 - 1.55 (m, 2H), 0.93 - 0.99 (t,  $J = 7.34$  Hz, 3H);  $^{13}\text{C}$  NMR (125 MHz,  $\text{CHLOROFORM-d}$ )  $\delta$  85.0, 72.8, 62.1, 39.7, 18.3, 13.7; IR (ATR) 3313, 2959, 2928, 1466  $\text{cm}^{-1}$ ; MS(EI)  $[\text{M} - 1]^+ 97$ .



**(R)-octadec-1-yn-3-ol (R)-18**

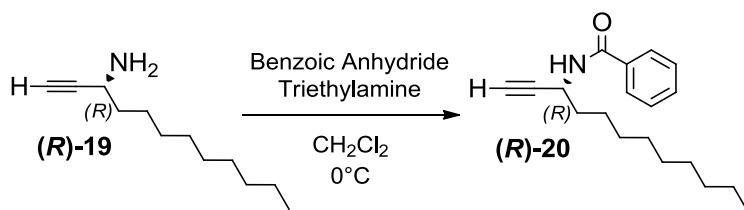
To a solution of **(R)-77** (0.147 g, 0.39 mmol) in methanol (8.0 mL) was added  $\text{K}_2\text{CO}_3$  (0.108 g, 0.78 mmol). Solution was stirred at ambient temperature under argon atmosphere. After 15 hours and 50 minutes, reaction was quenched with saturated  $\text{NH}_4\text{Cl}$ , extracted three times with  $\text{CH}_2\text{Cl}_2$ , dried over  $\text{Na}_2\text{SO}_4$ , and concentrated under reduced pressure which afforded **(R)-18** (quantitative yield, yellow solid, *ee* 100.0). **(R)-18** was in the synthesis of **(3S,8R)-10** without further purification.  $[\alpha]_{\text{D}}^{17} = +1.5^\circ$  ( $c = 1.4$ ,  $\text{CHCl}_3$ );  $^1\text{H}$  NMR (500 MHz,  $\text{CHLOROFORM-d}$ )  $\delta$  4.38 (m, 1H), 2.47 (d,  $J = 2.20$  Hz, 1H), 1.82 (br. s., 1H), 1.66 - 1.77 (m, 2H), 1.42 - 1.52 (m, 2H), 1.20-1.39 (m, 24H), 0.89 (t,  $J = 6.97$  Hz, 3H);  $^{13}\text{C}$  NMR (125 MHz,  $\text{CHLOROFORM-d}$ )  $\delta$  85.0, 72.8, 62.3, 37.6, 31.9, 29.7, 29.7, 29.7, 29.6, 29.5, 29.5, 29.4, 29.2, 25.0, 22.7, 14.1; IR (ATR) 3292, 3279, 2914, 2848, 2117, 1470  $\text{cm}^{-1}$



### **(R)-dodec-1-yn-3-amine (R)-19**

To a solution of **(R)-79** (4.1 g, 10.7 mmol) in 200 proof ethanol (107 mL) was added 85% hydrazine monohydrate in H<sub>2</sub>O (0.66 mL). Solution was heated to reflux under Ar atmosphere. After 3 hours and 25 minutes, added more 85% hydrazine monohydrate in H<sub>2</sub>O (0.2 mL) as GC/MS showed that starting material remained at 2 hours and 55 minutes. Thirty minutes later, reaction was cooled to ambient temperature. Reaction pH was adjusted to pH~3 with 3M HCl. It was then filtered through a Celite pad and rinsed through with methanol. Filtrate pH was adjusted to pH~13 with 1M NaOH, diluted with H<sub>2</sub>O, and stirred for 1 hour at ambient temperature. Reaction mixture was then extracted with Et<sub>2</sub>O, washed with saturated NaHCO<sub>3</sub>, and dried over Na<sub>2</sub>SO<sub>4</sub>. Extract was concentrated under reduced pressure at 0°C followed by purification by silica gel chromatography (Hexanes – 60% EtOAc/Hexanes) to give **(R)-19** (1.8 g, 88.9%, light yellow oil). TLC  $R_f = 0.174$  (60% EtOAc/hexanes);  $[\alpha]_D^{21} = -5.9^\circ$  ( $c = 11.0$ , CHCl<sub>3</sub>); <sup>1</sup>H NMR (500 MHz, CHLOROFORM-d)  $\delta$  3.55 (t,  $J = 6.36$  Hz, 1H), 2.24 - 2.32 (m, 1H), 2.17 (br. s., 2H), 1.52 - 1.67 (m, 2H), 1.44 (m, 2H), 1.18 - 1.36 (m, 12H), 0.87 (t,  $J = 6.85$  Hz, 3H); <sup>13</sup>C NMR (125 MHz, CHLOROFORM-d)  $\delta$  87.5, 70.4, 43.3, 37.8, 31.9, 29.5, 29.3, 29.3, 29.3, 25.9, 22.6, 14.1; IR (ATR) 3311, 2923, 2854 cm<sup>-1</sup>; HRMS (ESI-TOF)  $[M + H]^+$  calcd. for C<sub>11</sub>H<sub>24</sub>N 182.1909, found 182.1903.

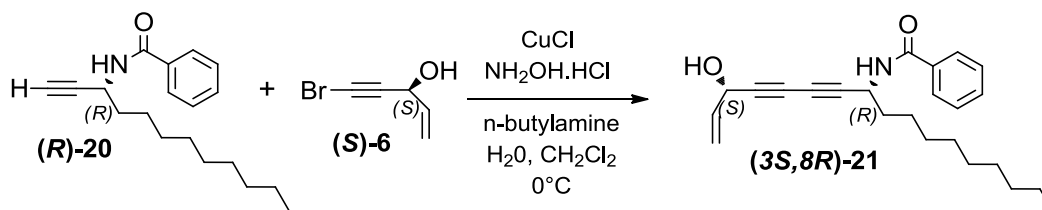




**(R)-N-(dodec-1-yn-3-yl)benzamide (R)-20**

To a solution of **(R)-19** (0.134 g, 0.74 mmol) in CH<sub>2</sub>Cl<sub>2</sub> (6.9 mL) at 0°C under Ar was added benzoic anhydride (0.209 g, 0.92 mmol) followed by triethylamine (0.15 mL, 1.1 mmol). Reaction mixture was stirred for 15 minutes at 0°C and then allowed to warm to ambient temperature. After 1 hour and 10 minutes, reaction mixture was quenched with water, extracted three times with CH<sub>2</sub>Cl<sub>2</sub>, washed two times with saturated NaHCO<sub>3</sub>, dried over Na<sub>2</sub>SO<sub>4</sub>, and concentrated under reduced pressure. Purification by flash chromatography on silica gel (hexanes – 10% EtOAc/hexanes) afforded **(R)-20** (0.116 g, 55.1%) as a white solid.

TLC  $R_f$  = 0.420 (25% EtOAc/hexanes);  $[\alpha]_D^{21} = +21.7^\circ$  ( $c = 1.4$ , CHCl<sub>3</sub>); <sup>1</sup>H NMR (500 MHz, CHLOROFORM-d)  $\delta$  7.77 - 7.81 (m, 2H), 7.49 - 7.54 (m, 1H), 7.41 - 7.46 (m, 2H), 6.35 (d,  $J = 8.07$  Hz, 1H), 4.96 (ddt,  $J = 2.45, 6.17, 8.04$  Hz, 1H), 2.30 - 2.32 (d,  $J = 2.45$  Hz, 1H), 1.72 - 1.84 (m, 2H), 1.45 - 1.54 (m, 2H), 1.22 - 1.38 (m, 12H), 0.85 - 0.91 (t,  $J = 6.97$  Hz, 3H); <sup>13</sup>C NMR (125 MHz, CHLOROFORM-d)  $\delta$  166.3, 134.0, 131.7, 128.6, 127.0, 83.3, 71.3, 41.8, 35.8, 31.8, 29.5, 29.5, 29.2, 29.1, 25.6, 22.6, 14.1; IR (ATR) 3311, 3282, 2917, 2849, 2361, 1641, 1528 cm<sup>-1</sup>.

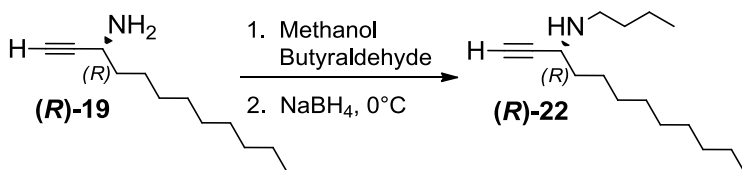


***N*-((3*S*,8*R*)-3-hydroxyheptadeca-1-en-4,6-diyn-8-yl)benzamide (3*S*,8*R*)-21**

Copper (I) chloride (0.004 g, 0.038 mmol) was added to a stirred 30 % solution (0.9 mL) of n-butylamine in distilled water at 0 °C which resulted in a deep blue solution. A few crystals of NH<sub>2</sub>OH.HCl were added until solution was colorless. A solution of (**R**)-20 (0.086 g, 0.30 mmol) in CH<sub>2</sub>Cl<sub>2</sub> (0.5 mL) was added under argon atmosphere which resulted in yellow reaction mixture. After 10 minutes, a solution of (**S**)-6 (0.081 g, 0.50 mmol) in CH<sub>2</sub>Cl<sub>2</sub> (0.7 mL) was added dropwise over 5 minutes. A few crystals of NH<sub>2</sub>OH.HCl were added as necessary whenever solution turned blue or green. After 45 minutes, analysis of the reaction mixture by GC/MS showed that there was still some R-XX present. At 1 hour and 15 minutes, added additional (**S**)-6 (0.036 g, 0.22 mmol) in CH<sub>2</sub>Cl<sub>2</sub> (0.5 mL). Reaction was stirred an additional 15 minutes and then quenched with water, extracted 3 times with CH<sub>2</sub>Cl<sub>2</sub>, dried over Na<sub>2</sub>SO<sub>4</sub>, and concentrated under reduced pressure. Immediate purification by flash chromatography on silica gel (Hexanes - 25% EtOAc/hexanes) afforded (**3S,8R**)-21 (0.105 g, 95.3%) as a beige oil.

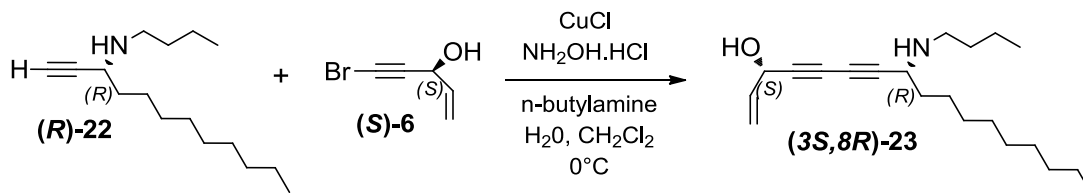
TLC  $R_f$  = 0.192 (25% EtOAc/hexanes);  $[\alpha]_D^{18} = +50.9^\circ$  ( $c = 1.0$ , CHCl<sub>3</sub>); <sup>1</sup>H NMR (500 MHz, CHLOROFORM-*d*)  $\delta$  7.76 - 7.80 (m, 2H), 7.49 - 7.54 (m, 1H), 7.41 - 7.46 (t,  $J = 7.76$  Hz, 2H), 6.43 (d,  $J = 8.39$  Hz, 1H), 5.94 (ddd,  $J = 5.34, 10.17, 17.04$  Hz, 1H), 5.44 - 5.50 (m, 1H), 5.25 (dd,  $J = 0.76, 10.17$  Hz, 1H), 5.05 (q,  $J = 7.38$  Hz, 1H), 4.92 - 4.96 (m, 1H), 2.55 (br. s., 1H), 1.73 - 1.84 (m, 2H), 1.43 - 1.51 (m, 2H), 1.22 - 1.37 (m, 12H), 0.88

(t,  $J = 6.99$  Hz, 3H);  $^{13}\text{C}$  NMR (125 MHz, CHLOROFORM- $d$ )  $\delta$  166.4, 135.8, 133.7, 131.8, 128.6, 127.0, 117.2, 79.6, 77.0, 70.3, 67.2, 63.4, 42.4, 35.7, 31.8, 29.5, 29.4, 29.2, 29.1, 25.7, 22.6, 14.1; IR (ATR) 3275, 2922, 2854, 1633, 1524  $\text{cm}^{-1}$ ; HRMS (ESI-TOF)  $[\text{M} + \text{H}]^+$  calcd. for  $\text{C}_{24}\text{H}_{32}\text{NO}_2$  366.2433, found 366.2436.



**(R)-N-butylundec-1-yn-3-amine (R)-22**

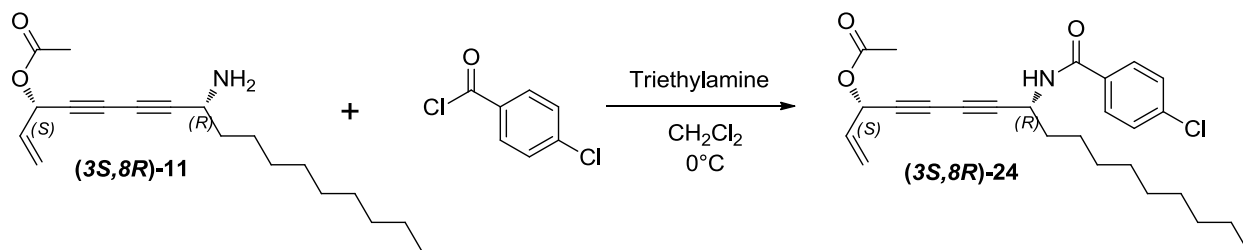
To a solution of (R)-19 (0.162 g, 0.89 mmol) in methanol (4.1 mL) under argon atmosphere was added butyraldehyde (0.11 mL, 1.2 mmol). Reaction mixture was stirred at ambient temperature for 20 minutes and then chilled to 0°C at which time NaBH<sub>4</sub> was added (0.035 g, 0.91 mmol). Reaction mixture was stirred for 1 hour and then diluted with EtOAc, washed with saturated NaHCO<sub>3</sub>, dried over Na<sub>2</sub>SO<sub>4</sub>, and concentrated under reduced pressure to yield (R)-22 (0.188 g, 88.9%) as a clear oil. TLC  $R_f = 0.566$  (40% EtOAc/hexanes);  $[\alpha]_D^{18} = +15.1^\circ$  ( $c = 1.7$ , CHCl<sub>3</sub>);  $^1\text{H}$  NMR (500 MHz, CHLOROFORM- $d$ )  $\delta$  3.36 (t,  $J = 6.86$  Hz, 1H), 2.82 - 2.91 (m, 1H), 2.54 - 2.63 (m, 1H), 2.27 (s, 1H), 1.20 - 1.68 (m, 21H), 0.85 - 0.98 (m, 6H);  $^{13}\text{C}$  NMR (125 MHz, CHLOROFORM- $d$ )  $\delta$  85.8, 71.1, 50.1, 47.2, 35.9, 32.1, 31.9, 29.5, 29.5, 29.4, 29.3, 26.0, 22.7, 20.5, 14.1, 14.0; IR (ATR) 3659, 3248, 2925, 1686, 1525, 1253  $\text{cm}^{-1}$ .



**(3S,8R)-8-(butylamino)heptadeca-1-en-4,6-diyn-3-ol (3S,8R)-23**

Copper (I) chloride (0.006 g, 0.06 mmol) was added to a stirred 30 % solution (1.1 mL) of n-butylamine in distilled water at 0 °C which resulted in a deep blue solution. A few crystals of NH<sub>2</sub>OH.HCl were added until solution was colorless. A solution of (R)-22 (0.087 g, 0.37 mmol) in CH<sub>2</sub>Cl<sub>2</sub> (0.55 mL) was added under argon atmosphere which resulted in yellow reaction mixture. After 10 minutes, a solution of (S)-6 (0.118 g, 0.73 mmol) in CH<sub>2</sub>Cl<sub>2</sub> (1.1 mL) was added dropwise over 5 minutes. A few crystals of NH<sub>2</sub>OH.HCl were added as necessary whenever solution turned blue or green. After 45 minutes, reaction was quenched with water, extracted 3 times with CH<sub>2</sub>Cl<sub>2</sub>, dried over Na<sub>2</sub>SO<sub>4</sub>, and concentrated under reduced pressure. Immediate purification by flash chromatography on silica gel (hexanes – 15% EtOAc/hexanes) afforded (3S,8R)-23 (0.063 g, 53.9%, tan solid). TLC  $R_f$  = 0.473 (40% EtOAc/hexanes);  $[\alpha]_D^{21} = +59.7^\circ$  ( $c = 1.0$ , CHCl<sub>3</sub>); <sup>1</sup>H NMR (500 MHz, CHLOROFORM-d)  $\delta$  5.95 (ddd,  $J = 5.38, 10.15, 17.00$  Hz, 1H), 5.46 (td,  $J = 1.01, 17.30$  Hz, 1H), 5.22 - 5.27 (td,  $J = 1.10, 10.03$  Hz, 1H), 4.92 (d,  $J = 5.38$  Hz, 1H), 3.42 (dd,  $J = 5.62, 8.31$  Hz, 1H), 2.83 (ddd,  $J = 6.24, 8.62, 11.07$  Hz, 1H), 2.56 (ddd,  $J = 5.62, 8.50, 11.07$  Hz, 1H), 1.74 – 2.20 (br. s., 1H), 1.20 - 1.69 (m, 21H), 0.90 – 0.94 (t,  $J=7.21$  Hz, 3 H), 0.85 – 0.89 (t,  $J=6.97$  Hz, 3 H); <sup>13</sup>C NMR (125 MHz, CHLOROFORM-d)  $\delta$  136.2, 117.0, 82.9, 76.1, 70.7, 67.3, 63.4, 50.8, 47.2, 35.7, 32.0, 31.9, 29.5, 29.5, 29.3, 29.3, 26.0, 22.7, 20.5, 14.1, 14.0; IR (ATR) 3676, 3249,

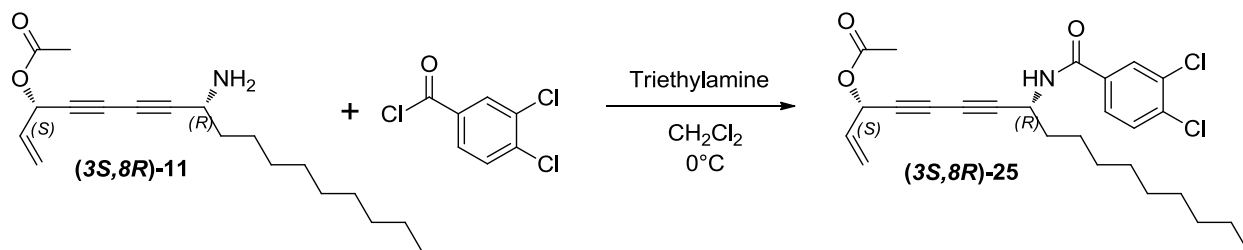
2922, 2853, 2682, 1028  $\text{cm}^{-1}$ ; HRMS (ESI-TOF)  $[\text{M} + \text{H}]^+$  calcd. for  $\text{C}_{21}\text{H}_{36}\text{NO}$   
318.2797, found 318.2787.



**(3S,8R)-8-(4-chlorobenzamido)heptadeca-1-en-4,6-diyne-3-yl acetate (3S,8R)-24**

To a solution of (3S,8R)-11 (0.056 g, 0.19 mmol) in  $\text{CH}_2\text{Cl}_2$  (1.8 mL) at  $0^\circ\text{C}$  under Ar atmosphere was added triethylamine (0.04 mL, 0.29 mmol) followed by a solution of 4-chlorobenzoyl chloride (0.05 g, 0.29 mmol) in  $\text{CH}_2\text{Cl}_2$  (1 mL). Reaction mixture was stirred at  $0^\circ\text{C}$  for 3 hours and 15 minutes. Reaction was then quenched with water, extracted three times with  $\text{CH}_2\text{Cl}_2$ , washed with saturated  $\text{NaHCO}_3$ , dried over  $\text{Na}_2\text{SO}_4$ , and concentrated under reduced pressure. Purification by flash chromatography on silica gel (hexanes – 15% EtOAc/hexanes) afforded (3S,8R)-24 (0.028 g, 34.4%) as a yellow oil. TLC  $R_f = 0.260$  (15% EtOAc/hexanes);  $[\alpha]_{\text{D}}^{18} = -19.9^\circ$  ( $c = 0.9$ ,  $\text{CHCl}_3$ );  $^1\text{H}$  NMR (500 MHz,  $\text{CHLOROFORM-d}$ )  $\delta$  7.70 - 7.75 (m, 2H), 7.39 - 7.44 (m, 2H), 6.39 (d,  $J = 8.56$  Hz, 1H), 5.81 - 5.92 (m, 2H), 5.50 - 5.58 (m, 1H), 5.31 - 5.39 (m, 1H), 5.01 (q,  $J = 7.50$  Hz, 1H), 2.09 - 2.12 (s, 3H), 1.72 - 1.82 (m, 2H), 1.41 - 1.51 (m, 2H), 1.22 - 1.36 (m, 12H), 0.85 - 0.91 (t,  $J = 6.97$  Hz, 3H);  $^{13}\text{C}$  NMR (125 MHz,  $\text{CHLOROFORM-d}$ )  $\delta$  169.5, 165.3, 138.1, 132.1, 131.8, 128.9, 128.5, 119.8, 79.7, 73.5, 70.9, 67.1, 64.4, 42.5, 35.6, 31.8, 29.5, 29.4, 29.2, 29.1, 25.7, 22.6, 20.9, 14.1; IR (ATR) 3301, 2925, 2855,

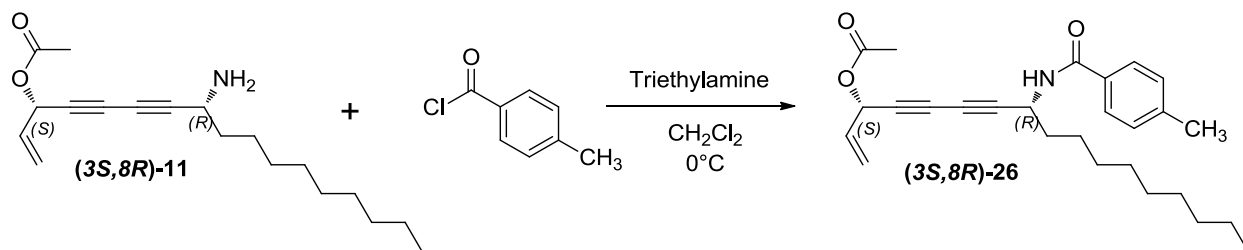
2259, 1748, 1638, 1532, 1486, 1220  $\text{cm}^{-1}$ ; HRMS (ESI-TOF)  $[\text{M} + \text{H}]^+$  calcd. for  $\text{C}_{26}\text{H}_{33}\text{ClNO}_3$  442.2149, found 442.2096.



**(3S,8R)-8-(3,4-dichlorobenzamido)heptadeca-1-en-4,6-diyne-3-yl acetate (3S,8R)-25**

To a solution of (3S,8R)-11 (0.060 g, 0.20 mmol) in  $\text{CH}_2\text{Cl}_2$  (2.0 mL) at  $0^\circ\text{C}$  under Ar atmosphere was added triethylamine (0.03 mL, 0.24 mmol) followed by a solution of 3,4-dichlorobenzoyl chloride (0.051 g, 0.25 mmol) in  $\text{CH}_2\text{Cl}_2$  (1 mL). Reaction mixture was stirred at  $0^\circ\text{C}$  for 1.5 hours. Reaction was then quenched with water, extracted three times with  $\text{CH}_2\text{Cl}_2$ , washed with saturated  $\text{NaHCO}_3$ , dried over  $\text{Na}_2\text{SO}_4$ , and concentrated under reduced pressure. Purification by flash chromatography on silica gel (hexanes – 15% EtOAc/hexanes) afforded (3S,8R)-25 (0.039 g, 41.1%) as a yellow oil. TLC  $R_f$  = 0.231 (15% EtOAc/hexanes);  $[\alpha]_D^{22} = -19.9^\circ$  ( $c = 1.0$ ,  $\text{CHCl}_3$ );  $^1\text{H}$  NMR (500 MHz,  $\text{CHLOROFORM-d}$ )  $\delta$  7.90 (d,  $J = 2.20$  Hz, 1H), 7.63 (dd,  $J = 2.08, 8.44$  Hz, 1H), 7.51 (d,  $J = 8.56$  Hz, 1H), 6.60 (d,  $J = 8.31$  Hz, 1H), 5.82 - 5.91 (m, 2H), 5.50 - 5.57 (m, 1H), 5.32 - 5.37 (m, 1H), 4.99 (t,  $J = 7.50$  Hz, 1H), 2.10 - 2.13 (s, 3H), 1.72 - 1.82 (m, 2H), 1.40 - 1.50 (m, 2H), 1.23 - 1.34 (m, 12H), 0.85 - 0.90 (t,  $J = 6.97$  Hz, 3H);  $^{13}\text{C}$  NMR (125 MHz,  $\text{CHLOROFORM-d}$ )  $\delta$  169.6, 164.2, 136.2, 133.5, 133.1, 131.8, 130.6, 129.3, 126.3, 119.8, 79.4, 73.6, 70.9, 67.2, 64.5, 42.6, 35.5, 31.8, 29.5, 29.4, 29.2, 29.0, 25.7,

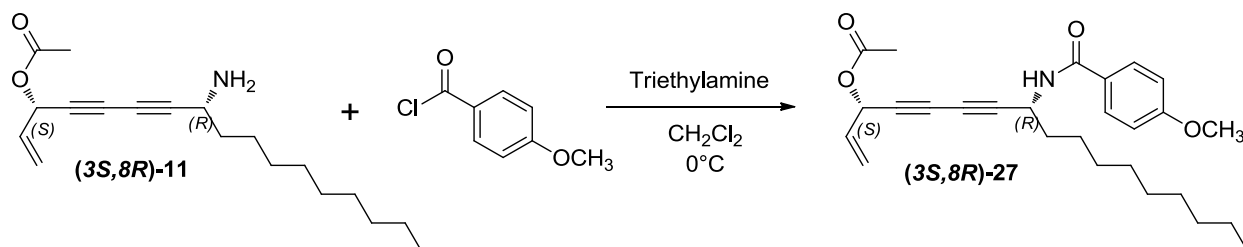
22.6, 20.9, 14.1; IR (ATR) 3253, 2923, 2855, 1744, 1636, 1535, 1226 cm<sup>-1</sup>; HRMS (ESI-TOF) [M + H]<sup>+</sup> calcd. for C<sub>26</sub>H<sub>32</sub>Cl<sub>2</sub>NO<sub>3</sub> 476.1759, found 476.1770.



**(3S,8R)-8-(4-methylbenzamido)heptadeca-1-en-4,6-diyn-3-yl acetate (3S,8R)-26**

To a solution of (3S,8R)-11 (0.032 g, 0.10 mmol) in CH<sub>2</sub>Cl<sub>2</sub> (1.0 mL) at 0°C under Ar atmosphere was added triethylamine (0.06 mL, 0.43 mmol) followed by a solution of *p*-toluoyl chloride (0.02 mL, 0.15 mmol) in CH<sub>2</sub>Cl<sub>2</sub> (1.0 mL). Reaction mixture was stirred at 0°C for 45 minutes. Reaction was then quenched with water, extracted three times with CH<sub>2</sub>Cl<sub>2</sub>, dried over Na<sub>2</sub>SO<sub>4</sub>, and concentrated under reduced pressure. Purification by flash chromatography on silica gel (hexanes – 15% EtOAc/hexanes) afforded (3S,8R)-26 but it was contaminated with *p*-toluic acid per GC/MS analysis. Diluted product with ether, washed four times with saturated NaHCO<sub>3</sub>, washed once with brine, dried over Na<sub>2</sub>SO<sub>4</sub>, and concentrated under reduced pressure which afforded purified (3S,8R)-26 (0.030 g, 67.7%, yellow oil). TLC *R*<sub>f</sub> = 0.538 (25% EtOAc/hexanes); [α]<sub>D</sub><sup>21</sup> = -12.5° (*c* = 0.8, CHCl<sub>3</sub>); <sup>1</sup>H NMR (500 MHz, CHLOROFORM-*d*) δ 7.67 (d, *J* = 8.31 Hz, 2H), 7.22 - 7.26 (m, 2H), 6.27 (d, *J* = 8.31 Hz, 1H), 5.83 - 5.93 (m, 2H), 5.52 - 5.58 (m, 1H), 5.33 - 5.38 (m, 1H), 5.01 - 5.08 (q, *J* = 7.50 Hz, 1H), 2.40 (s, 3H), 2.10 - 2.14 (s, 3H), 1.72 - 1.82 (m, 2H), 1.43 - 1.52 (m, 2H), 1.22 - 1.36 (m, 12H), 0.88 (t, *J* = 6.97 Hz, 3H); <sup>13</sup>C NMR (125 MHz, CHLOROFORM-*d*) δ 169.5, 166.2, 142.3, 131.9, 130.9, 129.2, 127.0,

119.7, 80.1, 73.3, 71.0, 66.9, 64.4, 42.3, 35.7, 31.8, 29.5, 29.4, 29.2, 29.1, 25.6, 22.6, 21.5, 20.9, 14.1; IR (ATR) 3670, 3268, 2920, 2853, 2259, 1744, 1632, 1530, 1504, 1219  $\text{cm}^{-1}$ ; HRMS (ESI-TOF)  $[M + H]^+$  calcd. for  $\text{C}_{27}\text{H}_{36}\text{NO}_3$  422.2695, found 422.2672.

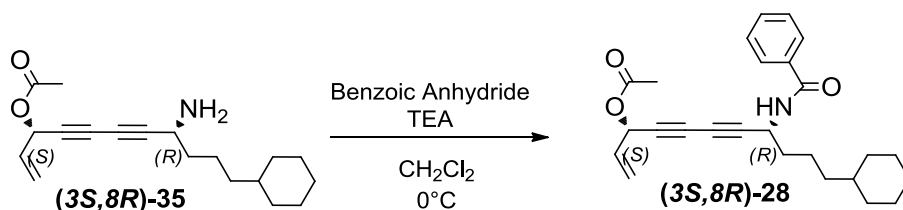


**(3S,8R)-8-(4-methoxybenzamido)heptadeca-1-en-4,6-diyn-3-yl acetate (3S,8R)-27**

To a solution of **(3S,8R)-11** (0.045 g, 0.15 mmol) in  $\text{CH}_2\text{Cl}_2$  (2.0 mL) at  $0^\circ\text{C}$  under Ar atmosphere was added triethylamine (0.06 mL, 0.43 mmol) followed by a solution of 4-methoxybenzoyl chloride (0.043 g, 0.25 mmol) in  $\text{CH}_2\text{Cl}_2$  (1 mL). Reaction mixture was stirred at  $0^\circ\text{C}$  for 1 hour and 50 minutes. Reaction was then quenched with water, extracted three times with  $\text{CH}_2\text{Cl}_2$ , washed with saturated  $\text{NaHCO}_3$ , dried over  $\text{Na}_2\text{SO}_4$ , and concentrated under reduced pressure. Purification by flash chromatography on silica gel (hexanes – 15% EtOAc/hexanes) afforded **(3S,8R)-27** (0.014 g, 21.8%) as a yellow oil.  $[\alpha]_{\text{D}}^{18} = -19.7^\circ$  ( $c = 0.3$ ,  $\text{CHCl}_3$ );  $^1\text{H NMR}$  (500 MHz,  $\text{CHLOROFORM-d}$ )  $\delta$  7.70 - 7.77 (m, 2H), 6.90 - 6.97 (m, 2H), 6.18 (d,  $J = 8.48$  Hz, 1H), 5.83 - 5.93 (m, 2H), 5.52 - 5.58 (m, 1H), 5.33 - 5.38 (m, 1H), 5.04 (q,  $J = 7.40$  Hz, 1H), 3.86 (s, 3H), 2.10 - 2.13 (s, 3H), 1.71 - 1.83 (m, 2H), 1.42 - 1.52 (m, 2H), 1.19 - 1.38 (m, 12H), 0.85 - 0.92 (t,  $J = 6.98$  Hz, 3H);  $^{13}\text{C NMR}$  (125 MHz,  $\text{CHLOROFORM-d}$ )  $\delta$  169.4, 165.8, 162.4, 132.0, 128.8, 126.1, 119.7, 113.8, 80.2, 73.4, 71.0, 66.9, 64.4, 55.4, 42.3, 35.8, 31.8, 29.5, 29.4,



29.2, 29.1, 25.7, 22.6, 20.9, 14.1; IR (ATR) 3277, 2924, 2854, 2263, 1733, 1628, 1506, 1242  $\text{cm}^{-1}$ ; HRMS (ESI-TOF)  $[M + H]^+$  calcd. for  $\text{C}_{27}\text{H}_{36}\text{NO}_4$  438.2644, found 438.2611.

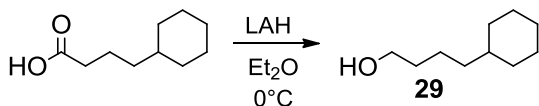


**(3*S*,8*R*)-8-benzamido-11-cyclohexylundeca-1-en-4,6-diyne-3-yl acetate (3*S*,8*R*)-28**

To a solution (3*S*,8*R*)-35 (0.047 g, 0.15 mmol) in  $\text{CH}_2\text{Cl}_2$  (1.7 mL) at  $0^\circ\text{C}$  under Ar was added benzoic anhydride (0.045 g, 0.20 mmol) followed by triethylamine (0.03 mL, 0.22 mmol). Reaction mixture was stirred for 15 minutes at  $0^\circ\text{C}$  and then allowed to warm to ambient temperature. After 1 hour and 30 minutes, reaction mixture was quenched with water, extracted three times with  $\text{CH}_2\text{Cl}_2$ , washed with saturated  $\text{NaHCO}_3$ , dried over  $\text{Na}_2\text{SO}_4$ , and concentrated under reduced pressure. Purification by flash chromatography on silica gel (hexanes – 15% EtOAc/hexanes) afforded (3*S*,8*R*)-28 (0.050 g, 79.6%) as a yellow oil

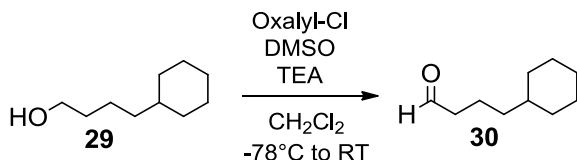
$R_f = 0.400$  (25% EtOAc/hexanes);  $[\alpha]_D^{18} = -4.3^\circ$  ( $c = 0.6$ ,  $\text{CHCl}_3$ );  $^1\text{H NMR}$  (500 MHz,  $\text{CHLOROFORM-d}$ )  $\delta$  7.78 (d,  $J = 7.34$  Hz, 2H), 7.52 (t,  $J = 7.34$  Hz, 1H), 7.44 (t,  $J = 7.46$  Hz, 2H), 6.41 (d,  $J = 8.31$  Hz, 1H), 5.82 - 5.93 (m, 2H), 5.51 - 5.59 (d,  $J = 16.14$  Hz, 1H), 5.35 (d,  $J = 9.29$  Hz, 1H), 5.04 (q,  $J = 7.42$  Hz, 1H), 2.11 (s, 3H), 1.60 - 1.82 (m, 7H), 1.43 - 1.53 (m, 2H), 1.09 - 1.27 (m, 6H), 0.80 - 0.93 (m, 2H)  $^{13}\text{C NMR}$  (125 MHz,  $\text{CHLOROFORM-d}$ )  $\delta$  169.5, 166.3, 133.7, 131.8, 131.8, 128.6, 127.0, 119.7, 80.0, 73.3, 71.0, 66.9, 64.4, 42.3, 37.4, 36.8, 35.9, 33.3, 33.2, 26.6, 26.3, 23.0, 20.9; IR (ATR) 3300,

2922, 2851, 2257, 1747, 1639, 1527, 1219  $\text{cm}^{-1}$ ; HRMS (ESI-TOF)  $[\text{M} + \text{H}]^+$  calcd. for  $\text{C}_{26}\text{H}_{32}\text{NO}_3$  406.2382, found 406.2365.



#### 4-cyclohexylbutan-1-ol **29**

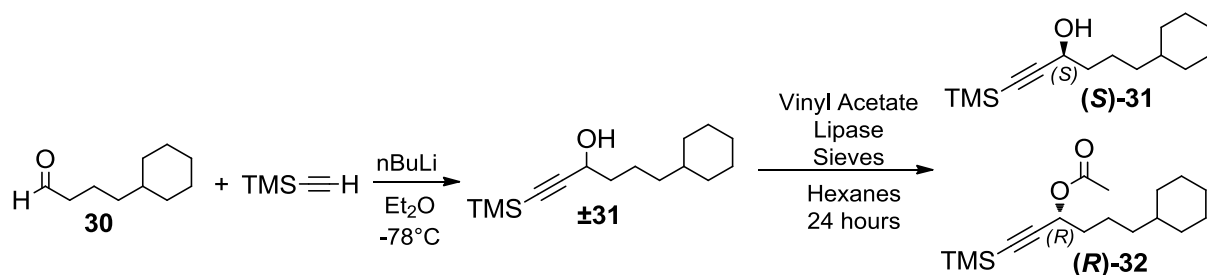
To a solution of cyclohexanebutyric acid (2.508 g, 14.7 mmol) in Et<sub>2</sub>O (58 mL) at 0°C under Ar was added lithium aluminum hydride (1.250 g, 32.9 mmol) in two portions. Reaction mixture was stirred for two hours at 0°C and then quenched with H<sub>2</sub>O (1.3 mL). After stirring 20 minutes, added 4M NaOH (1.3 mL). After stirring 30 minutes, added H<sub>2</sub>O (5.2 mL). After stirring 1 hour, filtered through Celite, dried over Na<sub>2</sub>SO<sub>4</sub>, and concentrated under reduced pressure which afforded **29** (1.391 g, 60.4%) as a light yellow oil. **29** used without further purification in the synthesis of **30**. TLC  $R_f$  = 0.259 (25% EtOAc/hexanes); <sup>1</sup>H NMR (500 MHz, CHLOROFORM-*d*)  $\delta$  3.60 - 3.65 (t,  $J$  = 7.34 Hz, 2H), 1.59 - 1.73 (m, 6H), 1.49 - 1.57 (m, 2H), 1.30 - 1.38 (m, 2H), 1.11 - 1.26 (m, 6H), 0.80 - 0.92 (m, 2H); <sup>13</sup>C NMR (125 MHz, CHLOROFORM-*d*)  $\delta$  63.0, 37.6, 37.2, 33.3, 33.0, 26.7, 26.4, 23.0; IR(ATR) 3340, 2920, 2850, 1448  $\text{cm}^{-1}$ .



#### 4-cyclohexylbutanal **30**

A solution of oxalyl chloride (0.88 mL, 10.3 mmol) in  $\text{CH}_2\text{Cl}_2$  (72 mL) was chilled to  $-78^\circ\text{C}$ . Added solution of DMSO (1.3 mL) in  $\text{CH}_2\text{Cl}_2$  (7.2 mL) was added over three minutes and stirred for two more minutes. Next, a solution of **29** (1.34 g, 8.6 mmol) in  $\text{CH}_2\text{Cl}_2$  (7.2 mL) was added over three minutes. Reaction mixture stirred for 40 minutes at  $-78^\circ\text{C}$ . Added triethylamine (6.0 mL) over three minutes and allowed reaction to warm to RT. After 2 hours and 40 minutes, quenched with  $\text{H}_2\text{O}$  and adjusted to pH  $\sim 4$  with 1M HCl. Extracted with  $\text{CH}_2\text{Cl}_2$ , washed with  $\text{H}_2\text{O}$ , washed with brine, dried over  $\text{Na}_2\text{SO}_4$ , and concentrated under reduced pressure. Ran resultant yellow oil through thin pad of silica gel with 25% EtOAc/hexanes which afforded **30** (1.26 g, 95.0%) as a clear oil.

TLC  $R_f = 0.593$  (25% EtOAc/hexanes);  $^1\text{H}$  NMR (500 MHz, CHLOROFORM- $d$ )  $\delta$  9.74 - 9.76 (t,  $J = 1.88$  Hz, 1H), 2.37 - 2.42 (dt,  $J = 1.95, 7.50$  Hz, 2H), 1.59 - 1.73 (m, 7H), 1.14 - 1.26 (m, 6H), 0.80 - 0.92 (m, 2H);  $^{13}\text{C}$  NMR (125 MHz, CHLOROFORM- $d$ )  $\delta$  202.9, 44.1, 37.4, 36.9, 33.1, 26.6, 26.3, 19.4; IR (ATR) 2920, 2850, 1728, 1711, 1448  $\text{cm}^{-1}$ .



**(S)-6-cyclohexyl-1-(trimethylsilyl)hex-1-yn-3-ol (S)-31; (R)-6-cyclohexyl-1-(trimethylsilyl)hex-1-yn-3-yl acetate (R)-32**

To a solution of (trimethylsilyl)acetylene (1.5 mL, 10.8 mmol) in dry Et<sub>2</sub>O (13 mL) at -78 °C was added dropwise a solution of n-butyllithium (2.25 M in hexanes, 4.2 mL, 9.4 mmol) over five minutes under an Ar atmosphere. The reaction mixture was then stirred for 50 minutes before a solution of **30** (1.26 g, 8.1 mmol) in Et<sub>2</sub>O (8 mL) was added dropwise over five minutes. Stirred at -78 °C for 10 minutes and then allowed to warm to ambient temperature. After stirring for 2 hours, the mixture was quenched by slow addition of saturated NH<sub>4</sub>Cl. The mixture was extracted with Et<sub>2</sub>O, washed with H<sub>2</sub>O and brine, dried over Na<sub>2</sub>SO<sub>4</sub>, and concentrated under reduced pressure which afforded **±31** (2.04 g, 99.5%) as a yellow oil. The resultant yellow oil (**±31**) was used directly in the next reaction without further purification.

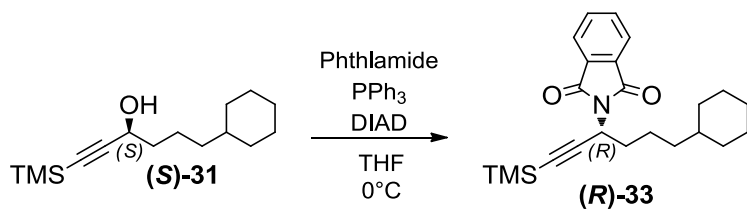
**±31** (2.00 g, 7.9 mmol) was dissolved in dry hexanes (31 ml) followed by the addition of ground, activated 4-Å molecular sieves (0.52 g) and lipase (*Pseudomonas fluorescens*, Amano Lipase AK, 0.30 g). To the well-stirred suspension was added vinyl acetate (3.0 mL, 32.5 mmol) over 3 minutes. The suspension was stirred under an Ar atmosphere for 24 hours and then filtered through a pad of Celite and concentrated under reduced

pressure. The resulting yellow oil was purified by silica gel chromatography (hexanes-15% EtOAc/hexanes) to give (**S**)-**31** (0.66 g, 33.3%, yellow oil) and (**R**)-**32** (0.78 g, 33.3%, yellow oil).

Data for  $\pm$ **31** racemic: TLC  $R_f$  = 0.371 (15% EtOAc/hexanes);  $^1\text{H}$  NMR (500 MHz, CHLOROFORM-*d*)  $\delta$  4.35 (t,  $J$  = 6.60 Hz, 1H), 1.82 (br. s., 1H), 1.61 - 1.75 (m, 7H), 1.39 - 1.50 (m, 2H), 1.16 - 1.28 (m, 6H), 0.82 - 0.93 (m, 2H), 0.18 (s, 9H);  $^{13}\text{C}$  NMR (125 MHz, CHLOROFORM-*d*)  $\delta$  106.9, 89.3, 62.9, 37.9, 37.4, 36.9, 33.3, 33.3, 26.7, 26.4, 22.3, -0.1; IR (ATR) 3684, 3361, 2922, 2852, 2174, 1250, 840  $\text{cm}^{-1}$ .

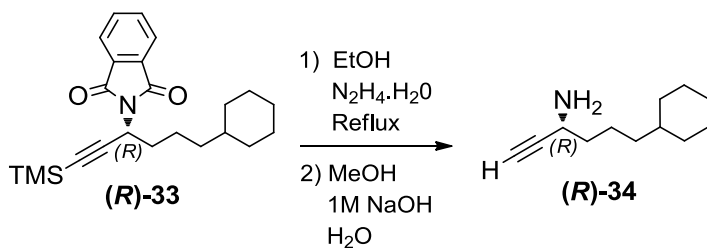
Data for (**S**)-**31**: TLC  $R_f$  = 0.371 (15% EtOAc/hexanes);  $[\alpha]_{\text{D}}^{18} = +3.6^\circ$  ( $c$  = 1.1,  $\text{CHCl}_3$ ); IR (ATR) 3676, 3314, 2921, 2852, 2171, 1249, 840  $\text{cm}^{-1}$ ; HRMS (ESI-TOF)  $[\text{M} + \text{H}]^+$  calcd. for  $\text{C}_{15}\text{H}_{29}\text{OSi}$  253.1988, found 253.1983.

Data for (**R**)-**32**: TLC  $R_f$  = 0.567 (15% EtOAc/hexanes);  $[\alpha]_{\text{D}}^{21} = +69.7^\circ$  ( $c$  = 1.4,  $\text{CHCl}_3$ ); IR (ATR) 2922, 2852, 2182, 1747, 1230, 841  $\text{cm}^{-1}$ .



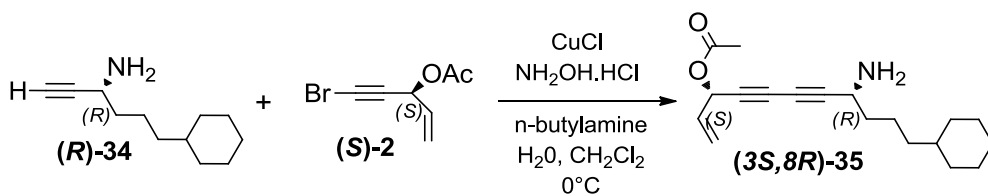
**(R)-2-(6-cyclohexyl-1-(trimethylsilyl)hex-1-yn-3-yl)isoindoline-1,3-dione (R)-33**

To a solution of (*S*)-**31** (0.447 g, 1.8 mmol) in THF (14 mL) was added phthalimide (0.374 g, 2.5 mmol) followed by triphenylphosphine (0.665 g, 2.5 mmol). The reaction mixture was then chilled to 0°C followed by the dropwise addition of DIAD (0.67 mL, 3.2 mmol) and stirred at 0°C under Ar atmosphere. After 3 hours, reaction mixture was concentrated under reduced pressure, diluted with Et<sub>2</sub>O, and chilled to 0°C. Slowly added hexanes until precipitate formed. Precipitate was filtered off through Celite and the filtrate was concentrated under reduced pressure. The resultant yellow oil was purified by silica gel chromatography (Hexanes – 5% EtOAc/Hexanes) to afford (*R*)-**33** (0.643 g, 95,3%, yellow crystals). TLC  $R_f$  = 0.415 (15% EtOAc/hexanes);  $[\alpha]_D^{18}$  = -2.4° ( $c$  = 1.0, CHCl<sub>3</sub>); IR (ATR) 2920, 2855, 2173, 1709, 1385 cm<sup>-1</sup>; HRMS (ESI-TOF) [M + H]<sup>+</sup> calcd. for C<sub>23</sub>H<sub>32</sub>NO<sub>2</sub>Si 382.2202, found 382.2209.



### **(R)-6-cyclohexylhex-1-yn-3-amine (R)-34**

To a solution of **(R)-33** (0.620 g, 1.6 mmol) in 200 proof ethanol (18 mL) was added 85% hydrazine monohydrate in H<sub>2</sub>O (0.10 mL). Solution was heated to reflux under Ar atmosphere. After four hours, reaction was cooled to ambient temperature. Reaction pH was adjusted to pH~3 with 1M HCl. It was then filtered through a Celite pad and rinsed through with methanol. Filtrate pH was adjusted to pH~13 with 1M NaOH and stirred for 50 minutes at ambient temperature. Reaction mixture was then diluted with H<sub>2</sub>O, extracted with Et<sub>2</sub>O, washed with saturated NaHCO<sub>3</sub>, and dried over Na<sub>2</sub>SO<sub>4</sub>. Extract was concentrated under reduced pressure at 0°C. After concentration, it was observed that there was still H<sub>2</sub>O in the concentrate. Diluted concentrate with Et<sub>2</sub>O, washed with brine, dried over Na<sub>2</sub>SO<sub>4</sub>, and concentrated under reduced pressure at 0°C. The resultant yellow oil was purified by flash chromatography on silica gel (Hexanes – 60% EtOAc/Hexanes) to give **(R)-34** (0.174 g, 59.7%, light yellow oil). TLC  $R_f = 0.189$  (60% EtOAc/hexanes);  $[\alpha]_D^{18} = -4.9^\circ$  ( $c = 0.5$ , CHCl<sub>3</sub>); IR (ATR) 3309, 2921, 2851 cm<sup>-1</sup>; HRMS (ESI-TOF)  $[M + H]^+$  calcd. for C<sub>12</sub>H<sub>22</sub>N 180.1752, found 180.1749.

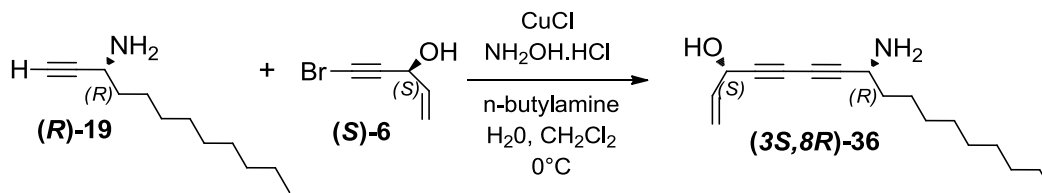


**(3S,8R)-8-amino-11-cyclohexylundeca-1-en-4,6-diyne-3-yl acetate (3S,8R)-35**

Copper (I) chloride (0.0099 g, 0.10 mmol) was added to a stirred 30 % solution (1.7 mL) of n-butylamine in distilled water at 0 °C which resulted in a deep blue solution. A few crystals of NH<sub>2</sub>OH.HCl were added until solution was colorless. A solution of **(R)-34** (0.0918 g, 0.51 mmol) in CH<sub>2</sub>Cl<sub>2</sub> (1.0 mL) was added under argon atmosphere which resulted in yellow reaction mixture. After 10 minutes, a solution of **(S)-2** (0.20 g, 0.99 mmol) in CH<sub>2</sub>Cl<sub>2</sub> (1.0 mL) was added dropwise over 5 minutes. A few crystals of NH<sub>2</sub>OH.HCl were added as necessary whenever solution turned blue or green. After 20 minutes, reaction was quenched with water, extracted 3 times with CH<sub>2</sub>Cl<sub>2</sub>, dried over Na<sub>2</sub>SO<sub>4</sub>, and concentrated under reduced pressure. Immediate purification by flash chromatography on silica gel (hexanes – 50% EtOAc/hexanes) afforded **(3S,8R)-35** (0.109 g, 70.6%, red-orange oil).

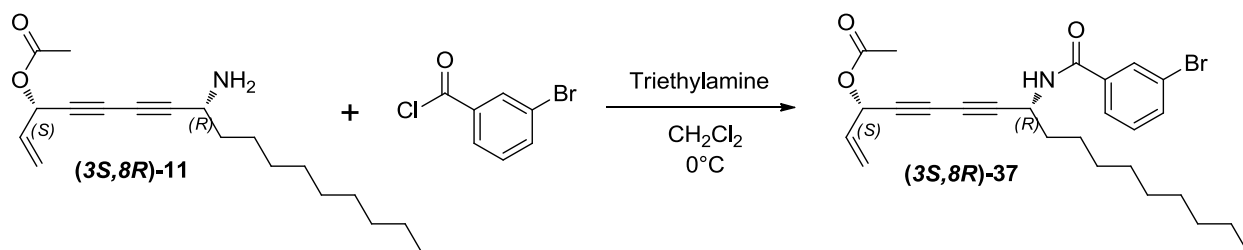
$[\alpha]_{\text{D}}^{18} = +6.2^\circ$  ( $c = 1.3$ , CHCl<sub>3</sub>); <sup>1</sup>H NMR (500 MHz, CHLOROFORM-d)  $\delta$  5.83 - 5.94 (m, 2H), 5.50 - 5.58 (dd,  $J = 1.50, 16.46$  Hz, 1H), 5.31 - 5.37 (dd,  $J = 1.38, 9.60$  Hz, 1H), 3.55 - 3.62 (t,  $J = 6.73$  Hz, 1H), 2.09 - 2.11 (s, 3H), 1.50 - 1.74 (m, 9H), 1.35 - 1.49 (m, 2H), 1.07 - 1.27 (m, 6H), 0.80 - 0.92 (m, 2H); <sup>13</sup>C NMR (125 MHz, CHLOROFORM-d)  $\delta$  169.5, 132.1, 119.5, 84.6, 73.0, 71.3, 66.2, 64.5, 44.0, 37.7, 37.4, 37.0, 33.3, 33.3, 26.6, 26.3, 23.1, 20.9; IR (ATR) 2921, 2851, 2254, 1746, 1219 cm<sup>-1</sup>.





**(3S,8R)-8-aminoheptadeca-1-en-4,6-diyn-3-ol (3S,8R)-36**

Copper (I) chloride (0.008 g, 0.08 mmol) was added to a stirred 30 % solution (1.65 mL) of n-butylamine in distilled water at 0 °C which resulted in a deep blue solution. A few crystals of NH<sub>2</sub>OH.HCl were added until solution was colorless. A solution of (**R**)-**19** (0.106 g, 0.58 mmol) in CH<sub>2</sub>Cl<sub>2</sub> (0.8 mL) was added under argon atmosphere which resulted in yellow reaction mixture. After 10 minutes, a solution of (**S**)-**6** (0.180 g, 1.11 mmol) in CH<sub>2</sub>Cl<sub>2</sub> (1.7 mL) was added dropwise over 5 minutes. A few crystals of NH<sub>2</sub>OH.HCl were added as necessary whenever solution turned blue or green. After 45 minutes, reaction was quenched with water, extracted 3 times with CH<sub>2</sub>Cl<sub>2</sub>, dried over Na<sub>2</sub>SO<sub>4</sub>, and concentrated under reduced pressure. Immediate purification by flash chromatography on silica gel (hexanes – 50% EtOAc/hexanes) afforded (**3S,8R**)-**36** (0.068 g, 44.6%, brown oil). TLC  $R_f = 0.097$  (60% EtOAc/hexanes);  $[\alpha]_D^{21} = +37.0^\circ$  ( $c = 1.4$ , CHCl<sub>3</sub>); IR (ATR) 3675, 3345, 2988, 2901, 1066.

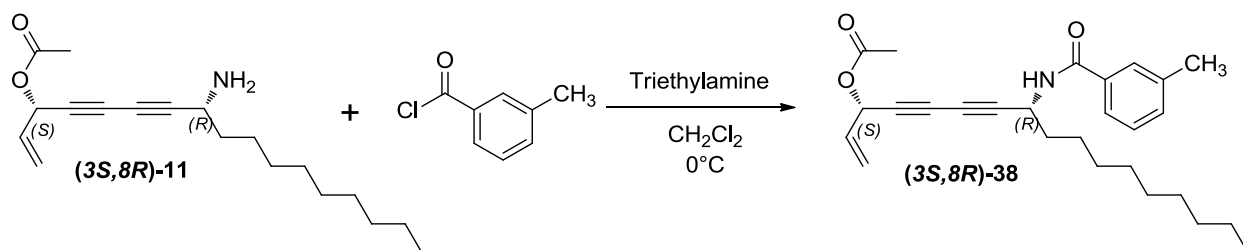


**(3*S*,8*R*)-8-(3-bromobenzamido)heptadeca-1-en-4,6-diyn-3-yl acetate (3*S*,8*R*)-37**

To a solution of (3*S*,8*R*)-11 (0.060 g, 0.20 mmol) in CH<sub>2</sub>Cl<sub>2</sub> (1.0 mL) at 0°C under Ar atmosphere was added triethylamine (0.04 mL, 0.29 mmol) followed by a solution of 3-bromobenzoyl chloride (0.03 mL, 0.23 mmol) in CH<sub>2</sub>Cl<sub>2</sub> (1 mL). Reaction mixture was stirred at 0°C for 1 hour and 10 minutes. Reaction was then quenched with saturated NH<sub>4</sub>Cl, diluted with Et<sub>2</sub>O, extracted three times with Et<sub>2</sub>O, washed with water, saturated NaHCO<sub>3</sub>, and brine, dried over Na<sub>2</sub>SO<sub>4</sub>, and concentrated under reduced pressure.

Purification by flash chromatography on silica gel (hexanes – 15% EtOAc/hexanes) afforded (3*S*,8*R*)-37 (0.051 g, 53.2%) as a yellow-orange oil.

TLC  $R_f$  = 0.491 (25% EtOAc/hexanes);  $[\alpha]_D^{18}$  = -11.6° ( $c$  = 2.3, CHCl<sub>3</sub>); <sup>1</sup>H NMR (500 MHz, CHLOROFORM-*d*) δ 7.93 (s, 1H), 7.71 (d,  $J$  = 7.58 Hz, 1H), 7.62 - 7.66 (m, 1H), 7.31 (t,  $J$  = 7.83 Hz, 1H), 6.51 (d,  $J$  = 8.31 Hz, 1H), 5.83 - 5.92 (m, 2H), 5.51 - 5.58 (m, 1H), 5.32 - 5.38 (m, 1H), 5.01 (q,  $J$  = 7.34 Hz, 1H), 2.11 (s, 3H), 1.73 - 1.82 (m, 2H), 1.42 - 1.51 (m, 2H), 1.22 - 1.35 (m, 12H), 0.88 (t,  $J$  = 6.85 Hz, 3H) <sup>13</sup>C NMR (125 MHz, CHLOROFORM-*d*) δ 169.6, 165.0, 135.7, 134.7, 131.8, 130.2, 130.2, 125.7, 122.7, 119.8, 79.6, 73.5, 70.9, 67.2, 64.5, 42.5, 35.6, 31.8, 29.5, 29.4, 29.2, 29.0, 25.6, 22.6, 20.9, 14.1; IR (ATR) 3246, 2920, 2852, 1745, 1634, 1530, 1218 cm<sup>-1</sup>; HRMS (ESI-TOF)  $[M + H]^+$  calcd. for C<sub>26</sub>H<sub>33</sub>BrNO<sub>3</sub> 486.1644, found 486.1675.

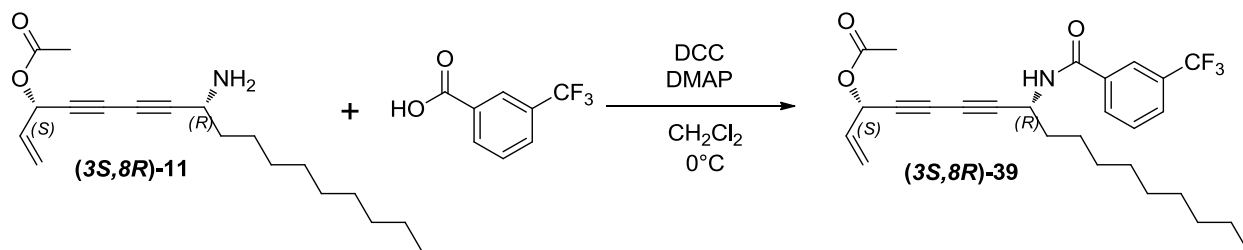


**(3*S*,8*R*)-8-(3-methylbenzamido)heptadeca-1-en-4,6-diyne-3-yl acetate (3*S*,8*R*)-38**

To a solution of (3*S*,8*R*)-11 (0.059 g, 0.20 mmol) in CH<sub>2</sub>Cl<sub>2</sub> (1.0 mL) at 0°C under Ar atmosphere was added triethylamine (0.04 mL, 0.29 mmol) followed by a solution of m-toluyloylbenzoyl chloride (0.03 mL, 0.23 mmol) in CH<sub>2</sub>Cl<sub>2</sub> (1 mL). Reaction mixture was stirred at 0°C for 1 hour and 40 minutes. Reaction was then quenched with saturated NH<sub>4</sub>Cl, diluted with Et<sub>2</sub>O, extracted three times with Et<sub>2</sub>O, washed with water, saturated NaHCO<sub>3</sub>, and brine, dried over Na<sub>2</sub>SO<sub>4</sub>, and concentrated under reduced pressure.

Purification by flash chromatography on silica gel (hexanes – 15% EtOAc/hexanes) afforded (3*S*,8*R*)-38 but was contaminated with m-toluyloylcarboxylic acid. Product was diluted with Et<sub>2</sub>O, washed ten times with saturated NaHCO<sub>3</sub>, washed twice with brine, dried over Na<sub>2</sub>SO<sub>4</sub>, and concentrated under reduced pressure to afford (3*S*,8*R*)-38 (0.035 g, 42.7%) as a yellow solid. TLC *R<sub>f</sub>* = 0.358 (25% EtOAc/hexanes); [α]<sub>D</sub><sup>18</sup> = -6.8° (*c* = 1.9, CHCl<sub>3</sub>); <sup>1</sup>H NMR (500 MHz, CHLOROFORM-*d*) δ 7.59 (s, 1H), 7.55 (t, *J* = 3.30 Hz, 1H), 7.32 (d, *J* = 5.14 Hz, 2H), 6.33 (d, *J* = 8.31 Hz, 1H), 5.83 - 5.92 (m, 2H), 5.52 - 5.59 (d, *J* = 15.65 Hz, 1H), 5.33 - 5.38 (d, *J* = 9.05 Hz, 1H), 5.04 (q, *J* = 7.34 Hz, 1H), 2.40 (s, 3H), 2.11 (s, 3H), 1.73 - 1.82 (m, 2H), 1.43 - 1.52 (m, 2H), 1.22 - 1.36 (m, 12H), 0.88 (t, *J* = 6.97 Hz, 3H); <sup>13</sup>C NMR (125 MHz, CHLOROFORM-*d*) δ 169.5, 166.5, 138.5, 133.7, 132.5, 131.9, 128.5, 127.7, 124.0, 119.7, 80.0, 73.3, 71.0, 66.9, 64.4, 42.3, 35.7, 31.8, 29.5, 29.4, 29.2, 29.1, 25.6, 22.6, 21.3, 20.9, 14.1; IR (ATR) 3258, 2920,

2852, 1742, 1637, 1529, 1218  $\text{cm}^{-1}$ ; HRMS (ESI-TOF)  $[\text{M} + \text{H}]^+$  calcd. for  $\text{C}_{27}\text{H}_{36}\text{NO}_3$   
422.2695, found 422.2714.



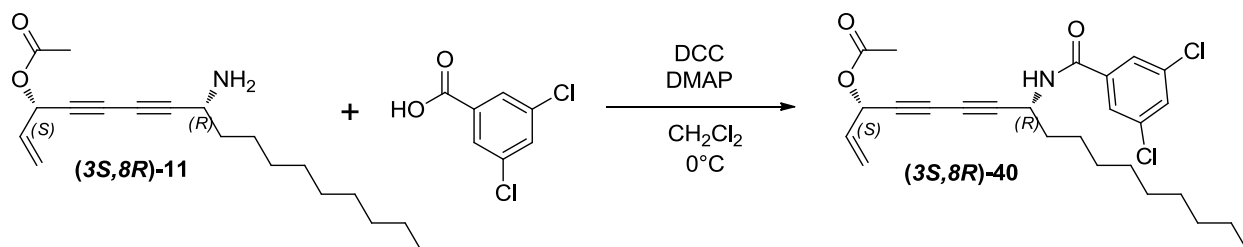
**(3S,8R)-8-(3-(trifluoromethyl)benzamido)heptadeca-1-en-4,6-diyn-3-yl acetate**

**(3S,8R)-39**

To a suspension of 3-(trifluoromethyl)benzoic acid (0.045 g, 0.24 mmol) in  $\text{CH}_2\text{Cl}_2$  (1.0 mL) at  $0^\circ\text{C}$  under Ar was added DCC (0.051 g, 0.25 mmol). Then a solution of (3S,8R)-11 (0.060 g, 0.20 mmol) in  $\text{CH}_2\text{Cl}_2$  (1.0 mL) was added followed by addition of DMAP (5.8 mg, 0.047 mmol). After 1 hour and 20 minutes, reaction was quenched with saturated  $\text{NH}_4\text{Cl}$ , diluted with  $\text{Et}_2\text{O}$ , extracted three times with  $\text{Et}_2\text{O}$ , washed with water, saturated  $\text{NaHCO}_3$ , and brine, dried over  $\text{Na}_2\text{SO}_4$ , and concentrated under reduced pressure. Purification by flash chromatography on silica gel (hexanes – 20%  $\text{EtOAc}$ /hexanes) afforded (3S,8R)-39 (0.058 g, 62.2%) as a yellow oil.

TLC  $R_f$  = 0.481 (20%  $\text{EtOAc}$ /hexanes);  $[\alpha]_D^{18}$  =  $-8.2^\circ$  ( $c$  = 0.5,  $\text{CHCl}_3$ );  $^1\text{H}$  NMR (500 MHz,  $\text{CHLOROFORM-d}$ )  $\delta$  8.06 (s, 1H), 7.99 (d,  $J$  = 7.83 Hz, 1H), 7.77 (d,  $J$  = 7.58 Hz, 1H), 7.54 - 7.61 (t,  $J$  = 7.83 Hz, 1H), 6.69 (d,  $J$  = 8.31 Hz, 1H), 5.81 - 5.92 (m, 2H), 5.49 - 5.59 (m, 1H), 5.31 - 5.39 (m, 1H), 5.03 (q,  $J$  = 7.34 Hz, 1H), 2.11 (s, 3H), 1.74 - 1.85 (m, 2H), 1.42 - 1.53 (m, 2H), 1.20 - 1.37 (m, 12H), 0.88 (t,  $J$  = 6.85 Hz, 3H);  $^{13}\text{C}$  NMR (125 MHz,  $\text{CHLOROFORM-d}$ )  $\delta$  169.6, 165.0, 134.5, 131.8, 130.4, 129.2, 128.4, 128.3,

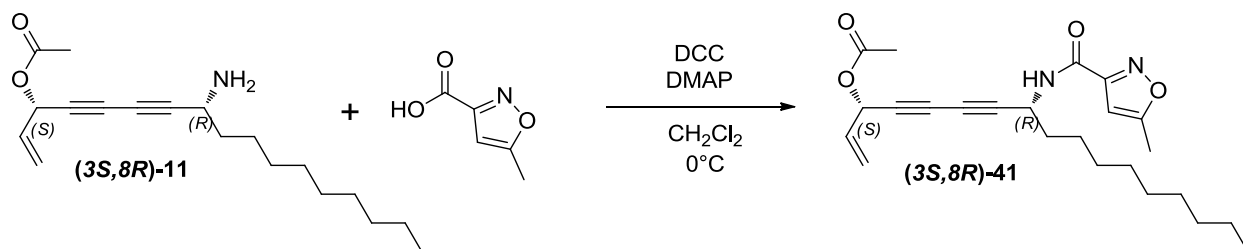
124.1, 124.1, 119.8, 79.5, 73.5, 70.9, 67.2, 64.5, 42.6, 35.6, 31.8, 29.5, 29.4, 29.2, 29.0, 25.7, 22.6, 20.9, 14.1; IR (ATR) 3245, 2921, 2853, 1749, 1640, 1534, 1124  $\text{cm}^{-1}$ ; HRMS (ESI-TOF)  $[\text{M} + \text{H}]^+$  calcd. for  $\text{C}_{27}\text{H}_{33}\text{F}_3\text{NO}_3$  476.2413, found 476.2429.



**(3S,8R)-8-(3,5-dichlorobenzamido)heptadeca-1-en-4,6-diyne-3-yl acetate (3S,8R)-40**

To a suspension of 3,5-dichlorobenzoic acid (0.044 g, 0.23 mmol) in  $\text{CH}_2\text{Cl}_2$  (1.0 mL) at  $0^\circ\text{C}$  under Ar was added DCC (0.048 g, 0.23 mmol). Then a solution of (3S,8R)-11 (0.061 g, 0.20 mmol) in  $\text{CH}_2\text{Cl}_2$  (1.0 mL) was added followed by addition of DMAP (3.7 mg, 0.030 mmol). After 2 hours and 40 minutes, reaction was quenched with saturated  $\text{NH}_4\text{Cl}$ , diluted with  $\text{Et}_2\text{O}$ , extracted three times with  $\text{Et}_2\text{O}$ , washed two times with water, washed 5 times with 1M NaOH, washed 2 times with brine, dried over  $\text{Na}_2\text{SO}_4$ , and concentrated under reduced pressure. Purification by flash chromatography on silica gel (hexanes – 10% EtOAc/hexanes) afforded (3S,8R)-40 (0.037 g, 39.1%) as a yellow oil. TLC  $R_f$  = 0.448 (15% EtOAc/hexanes);  $[\alpha]_D^{18}$  =  $-14.9^\circ$  ( $c$  = 0.9,  $\text{CHCl}_3$ );  $^1\text{H}$  NMR (500 MHz, CHLOROFORM- $d$ )  $\delta$  7.67 (d,  $J$  = 1.71 Hz, 2H), 7.49 - 7.51 (m, 1H), 6.53 (d,  $J$  = 8.31 Hz, 1H), 5.83 - 5.92 (m, 2H), 5.52 - 5.58 (m, 1H), 5.33 - 5.38 (m, 1H), 4.99 (q,  $J$  = 7.50 Hz, 1H), 2.12 (s, 3H), 1.72 - 1.82 (m, 2H), 1.42 - 1.52 (m, 2H), 1.22 - 1.36 (m, 12H), 0.88 (t,  $J$  = 6.97 Hz, 3H);  $^{13}\text{C}$  NMR (125 MHz, CHLOROFORM- $d$ )  $\delta$  169.6, 163.9, 136.6, 135.5, 131.7, 131.6, 125.7, 119.8, 79.3, 73.6, 70.9, 67.4, 64.5, 42.7, 35.5, 31.8,

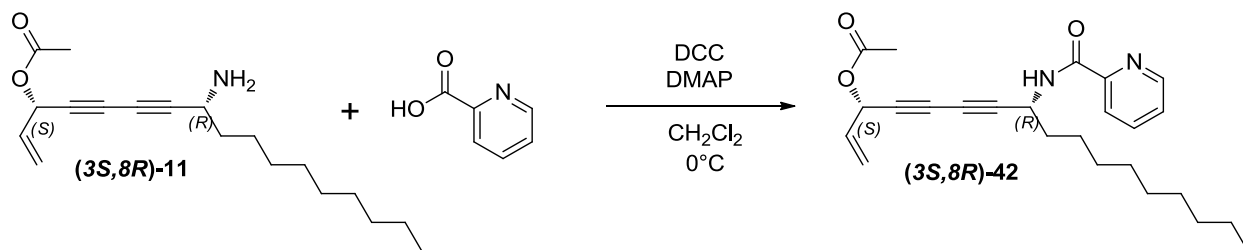
29.5, 29.4, 29.2, 29.0, 25.6, 22.6, 20.9, 14.1; IR (ATR) 3255, 2924, 2855, 1746, 1637, 1567, 1531, 1220  $\text{cm}^{-1}$ ; HRMS (ESI-TOF)  $[\text{M} + \text{H}]^+$  calcd. for  $\text{C}_{26}\text{H}_{32}\text{Cl}_2\text{NO}_3$  476.1759, found 476.1803.



**(3S,8R)-8-(5-methylisoxazole-3-carboxamido)heptadeca-1-en-4,6-diyne-3-yl acetate**  
**(3S,8R)-41**

To a suspension of 5-methylisoxazole-3-carboxylic acid (0.052 g, 0.41 mmol) in  $\text{CH}_2\text{Cl}_2$  (1.6 mL) at  $0^\circ\text{C}$  under Ar was added DCC (0.062 g, 0.30 mmol). Then a solution of **(3S,8R)-11** (0.080 g, 0.26 mmol) in  $\text{CH}_2\text{Cl}_2$  (1.0 mL) was added followed by addition of DMAP (5.5 mg, 0.045 mmol). After 17 hours, reaction was quenched with saturated  $\text{NH}_4\text{Cl}$ , extracted with  $\text{CH}_2\text{Cl}_2$ , washed with water and brine, dried over  $\text{Na}_2\text{SO}_4$ , and concentrated under reduced pressure. . Purification by flash chromatography on silica gel (hexanes – 15% EtOAc/hexanes) afforded **(3S,8R)-41** (23.1 mg, 21.2%) as a yellow oil. TLC  $R_f = 0.295$  (25% EtOAc/hexanes);  $[\alpha]_D^{18} = +31.8^\circ$  ( $c = 0.25$ ,  $\text{CHCl}_3$ );  $^1\text{H}$  NMR (500 MHz,  $\text{CHLOROFORM-d}$ )  $\delta$  6.93 (d,  $J = 8.56$  Hz, 1H), 6.44 (d,  $J = 0.98$  Hz, 1H), 5.82 - 5.92 (m, 2H), 5.51 - 5.58 (m, 1H), 5.32 - 5.38 (m, 1H), 4.96 (q,  $J = 7.58$  Hz, 1H), 2.47 - 2.51 (d,  $J = 0.73$  Hz, 3H), 2.09 - 2.13 (s, 3H), 1.73 - 1.80 (q,  $J = 7.58$  Hz, 2H), 1.42 - 1.50 (m, 2H), 1.22 - 1.35 (m, 12H), 0.85 - 0.90 (t,  $J = 7.09$  Hz, 3H);  $^{13}\text{C}$  NMR (125 MHz,  $\text{CHLOROFORM-D}$ )  $\delta$  171.4, 169.4, 158.2, 158.0, 131.9, 119.7, 101.4, 79.1, 73.5, 70.9, 67.2, 64.4, 41.8, 35.4, 31.8, 29.4, 29.4, 29.2, 29.0, 25.5, 22.6, 20.9, 14.1, 12.3; IR

(ATR) 3315, 2921, 2853, 1746, 1657, 1535, 1218  $\text{cm}^{-1}$ ; HRMS (ESI-TOF)  $[\text{M} + \text{H}]^+$   
calcd. for  $\text{C}_{24}\text{H}_{33}\text{N}_2\text{O}_4$  413.2440, found 413.2477.



#### 4-118

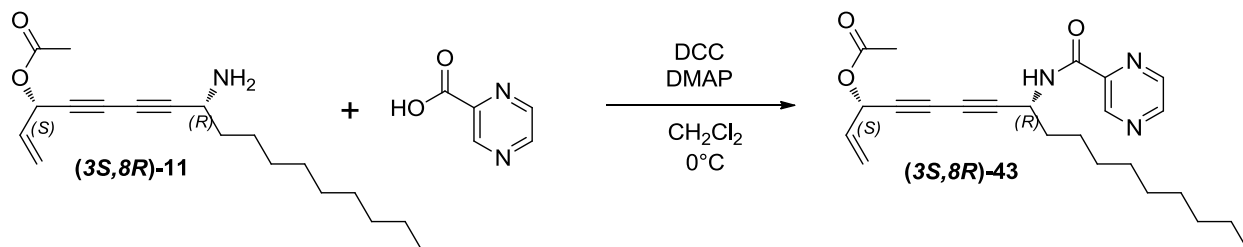
##### **(3S,8R)-8-(picolinamido)heptadeca-1-en-4,6-diyne-3-yl acetate (3S,8R)-42**

To a suspension of pyridine-2-carboxylic acid (0.031 g, 0.25 mmol) in  $\text{CH}_2\text{Cl}_2$  (1.0 mL) at  $0^\circ\text{C}$  under Ar was added DCC (0.054 g, 0.26 mmol). Then a solution of **(3S,8R)-11** (0.060 g, 0.20 mmol) in  $\text{CH}_2\text{Cl}_2$  (1.0 mL) was added followed by addition of DMAP (3.9 mg, 0.032 mmol). After 2 hours and 10 minutes, reaction was quenched with saturated  $\text{NH}_4\text{Cl}$ , diluted with  $\text{Et}_2\text{O}$ , extracted three times with  $\text{Et}_2\text{O}$ , washed with water, saturated  $\text{NaHCO}_3$ , and brine, dried over  $\text{Na}_2\text{SO}_4$ , and concentrated under reduced pressure.

Purification by flash chromatography on silica gel (hexanes – 20%  $\text{EtOAc}$ /hexanes) afforded **(3S,8R)-42** (0.061 g, 75.5%) as a yellow oil.

TLC  $R_f = 0.357$  (25%  $\text{EtOAc}$ /hexanes);  $[\alpha]_D^{18} = +1.9^\circ$  ( $c = 0.8$ ,  $\text{CHCl}_3$ );  $^1\text{H}$  NMR (500 MHz,  $\text{CHLOROFORM-d}$ )  $\delta$  8.56 (d,  $J = 4.65$  Hz, 1H), 8.15 - 8.23 (t,  $J = 8.32$  Hz, 2H), 7.81 - 7.89 (apparent dt,  $J = 1.47, 7.75$  Hz, 1H), 7.41 - 7.48 (m, 1H), 5.81 - 5.94 (m, 2H), 5.53 (d,  $J = 16.14$  Hz, 1H), 5.33 (d,  $J = 9.29$  Hz, 1H), 4.96 - 5.05 (q,  $J = 7.50$  Hz, 1H), 2.09 (s, 3H), 1.76 - 1.85 (q,  $J = 7.50$  Hz, 2H), 1.44 - 1.53 (m, 2H), 1.20 - 1.37 (m, 12H), 0.87 (t,  $J = 6.85$  Hz, 3H);  $^{13}\text{C}$  NMR (125 MHz,  $\text{CHLOROFORM-d}$ )  $\delta$  169.4, 163.2,

149.2, 148.1, 137.3, 131.9, 126.4, 122.4, 119.7, 79.9, 73.1, 71.1, 66.7, 64.4, 41.8, 35.6, 31.8, 29.4, 29.4, 29.2, 29.0, 25.6, 22.6, 20.8, 14.1; IR (ATR) 3381, 2924, 2856, 2261, 1747, 1678, 1508, 1220  $\text{cm}^{-1}$ ; HRMS (ESI-TOF)  $[\text{M} + \text{H}]^+$  calcd. for  $\text{C}_{25}\text{H}_{33}\text{N}_2\text{O}_3$  409.2491, found 409.2517.



**(3S,8R)-8-(pyrazine-2-carboxamido)heptadeca-1-en-4,6-diyn-3-yl acetate (3S,8R)-43**

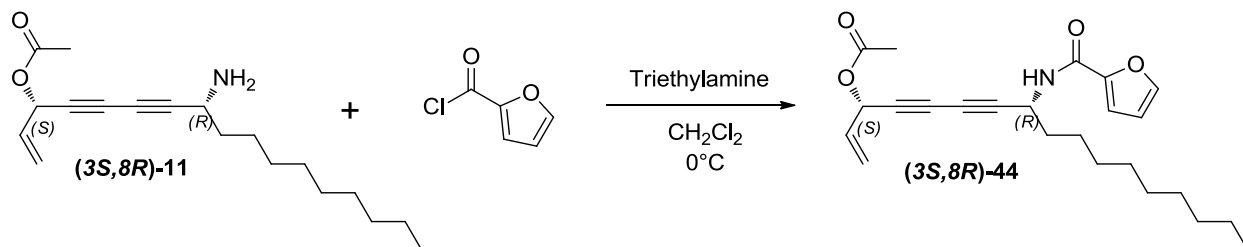
To a suspension of pyrazinecarboxylic acid (0.033 g, 0.27 mmol) in  $\text{CH}_2\text{Cl}_2$  (1.0 mL) at  $0^\circ\text{C}$  under Ar was added DCC (0.053 g, 0.26 mmol). Then a solution of **(3S,8R)-11** (0.062 g, 0.20 mmol) in  $\text{CH}_2\text{Cl}_2$  (1.0 mL) was added followed by addition of DMAP (5.2 mg, 0.043 mmol). After 1 hour and 30 minutes, reaction was quenched with saturated  $\text{NH}_4\text{Cl}$ , diluted with  $\text{Et}_2\text{O}$ , extracted three times with  $\text{Et}_2\text{O}$ , washed with water, saturated  $\text{NaHCO}_3$ , and brine, dried over  $\text{Na}_2\text{SO}_4$ , and concentrated under reduced pressure.

Purification by flash chromatography on silica gel (hexanes – 25%  $\text{EtOAc}$ /hexanes) afforded **(3S,8R)-43** (0.057 g, 68.1%) as a yellow oil. TLC  $R_f = 0.226$  (25%

$\text{EtOAc}$ /hexanes);  $[\alpha]_D^{18} = 0.0^\circ$  ( $c = 1.1$ ,  $\text{CHCl}_3$ );  $^1\text{H}$  NMR (500 MHz,  $\text{CHLOROFORM-d}$ )  $\delta$  9.39 (s, 1H), 8.75 - 8.79 (s, 1H), 8.54 (s, 1H), 7.94 (d,  $J = 8.56$  Hz, 1H), 5.81 - 5.92 (m, 2H), 5.53 (d,  $J = 15.65$  Hz, 1H), 5.33 (d,  $J = 9.05$  Hz, 1H), 4.97 - 5.06 (q,  $J = 7.50$  Hz, 1H), 2.09 (s, 3H), 1.76 - 1.85 (q,  $J = 7.58$  Hz, 2H), 1.42 - 1.52 (m, 2H), 1.19 - 1.36 (m, 12H), 0.86 (t,  $J = 6.72$  Hz, 3H);  $^{13}\text{C}$  NMR (125 MHz,  $\text{CHLOROFORM-d}$ )  $\delta$  169.4,



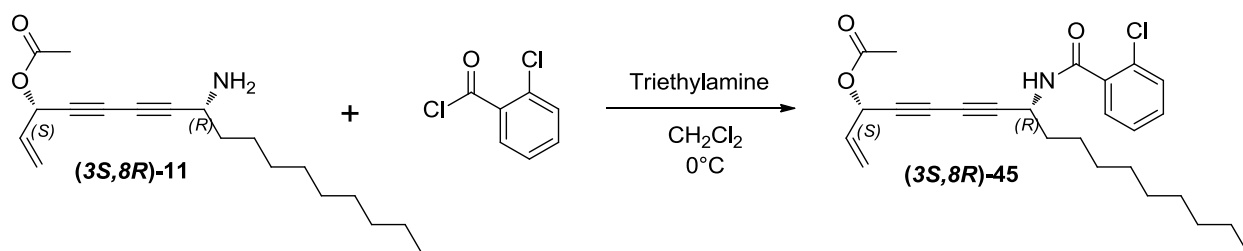
161.9, 147.5, 144.5, 143.8, 142.5, 131.8, 119.7, 79.3, 73.4, 70.8, 67.0, 64.3, 41.8, 35.5, 31.8, 29.4, 29.3, 29.2, 29.0, 25.6, 22.6, 20.8, 14.1; IR (ATR) 3325, 2924, 2856, 2260, 1746, 1675, 1513, 1220, 1012  $\text{cm}^{-1}$ ; HRMS (ESI-TOF)  $[\text{M} + \text{H}]^+$  calcd. for  $\text{C}_{24}\text{H}_{32}\text{N}_3\text{O}_3$  410.2444, found 410.2467.



**(3*S*,8*R*)-8-(furan-2-carboxamido)heptadeca-1-en-4,6-diyne-3-yl acetate (3*S*,8*R*)-44**

To a solution of **(3*S*,8*R*)-11** (0.060 g, 0.20 mmol) in  $\text{CH}_2\text{Cl}_2$  (1.0 mL) at  $0^\circ\text{C}$  under Ar atmosphere was added triethylamine (0.04 mL, 0.29 mmol) followed by a solution of 2-furoyl chloride (0.02 mL, 0.21 mmol) in  $\text{CH}_2\text{Cl}_2$  (1 mL). Reaction mixture was stirred at  $0^\circ\text{C}$  for 1 hour and 5 minutes. Reaction was then quenched with saturated  $\text{NH}_4\text{Cl}$ , diluted with  $\text{Et}_2\text{O}$ , extracted three times with  $\text{Et}_2\text{O}$ , washed with water, saturated  $\text{NaHCO}_3$ , and brine, dried over  $\text{Na}_2\text{SO}_4$ , and concentrated under reduced pressure. Purification by flash chromatography on silica gel (hexanes – 15%  $\text{EtOAc}$ /hexanes) afforded **(3*S*,8*R*)-44** but it was contaminated with furan-2-carboxylic anhydride. Product was diluted with  $\text{Et}_2\text{O}$  and washed 10 times with saturated  $\text{NaHCO}_3$ . However, it was still contaminated with furan-2-carboxylic anhydride. It was again diluted in  $\text{Et}_2\text{O}$  and stirred rapidly with 6M  $\text{NaOH}$  (aq.). It was then extracted three times with  $\text{Et}_2\text{O}$ , washed with water, saturated  $\text{NaHCO}_3$ , and brine, dried over  $\text{Na}_2\text{SO}_4$ , and concentrated under reduced pressure to afford **(3*S*,8*R*)-44** (0.042 g, 53.5%) as a yellow oil. TLC  $R_f = 0.224$  (25%  $\text{EtOAc}$ /hexanes);  $[\alpha]_{\text{D}}^{18} = -14.0^\circ$  ( $c = 0.5$ ,  $\text{CHCl}_3$ );  $^1\text{H NMR}$  (500 MHz,  $\text{CHLOROFORM-}d_3$ )

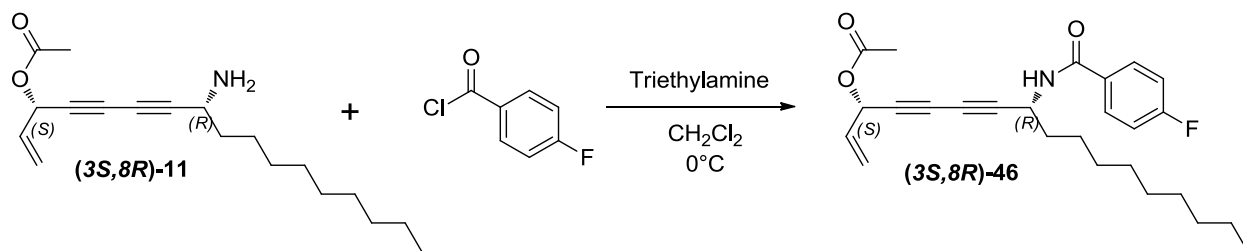
d)  $\delta$  7.43 - 7.47 (m, 1H), 7.14 (d,  $J = 3.42$  Hz, 1H), 6.47 - 6.54 (m, 2H), 5.82 - 5.93 (m, 2H), 5.51 - 5.58 (d,  $J = 15.65$  Hz, 1H), 5.35 (d,  $J = 9.05$  Hz, 1H), 4.95 - 5.03 (q,  $J = 7.50$  Hz, 1H), 2.10 (s, 3H), 1.76 (q,  $J = 7.58$  Hz, 2H), 1.42 - 1.51 (m, 2H), 1.21 - 1.35 (m, 12H), 0.88 (t,  $J = 6.85$  Hz, 3H);  $^{13}\text{C}$  NMR (125 MHz, CHLOROFORM- $d$ )  $\delta$  169.5, 157.1, 147.3, 144.1, 131.9, 119.7, 114.9, 112.3, 79.7, 73.4, 70.9, 67.0, 64.4, 41.5, 35.6, 31.8, 29.5, 29.4, 29.2, 29.0, 25.6, 22.6, 20.9, 14.1; IR (ATR) 3305, 2925, 2855, 1748, 1652, 1521, 1221  $\text{cm}^{-1}$ ; HRMS (ESI-TOF)  $[\text{M} + \text{H}]^+$  calcd. for  $\text{C}_{24}\text{H}_{32}\text{NO}_4$  398.2331, found 398.2358.



**(3*S*,8*R*)-8-(2-chlorobenzamido)heptadeca-1-en-4,6-diyne-3-yl acetate (3*S*,8*R*)-45**

To a solution of **(3*S*,8*R*)-11** (0.060 g, 0.20 mmol) in  $\text{CH}_2\text{Cl}_2$  (2.0 mL) at  $0^\circ\text{C}$  under Ar atmosphere was added triethylamine (0.04 mL, 0.29 mmol) followed by a solution of 2-chlorobenzoyl chloride (0.03 mL, 0.24 mmol) in  $\text{CH}_2\text{Cl}_2$  (1 mL). Reaction mixture was stirred at  $0^\circ\text{C}$  for 4 hours and 30 minutes. Reaction was then quenched with saturated  $\text{NH}_4\text{Cl}$ , diluted with  $\text{Et}_2\text{O}$ , extracted three times with  $\text{Et}_2\text{O}$ , washed with water, saturated  $\text{NaHCO}_3$ , and brine, dried over  $\text{Na}_2\text{SO}_4$ , and concentrated under reduced pressure. Purification by flash chromatography on silica gel (hexanes – 15%  $\text{EtOAc}$ /hexanes) afforded **(3*S*,8*R*)-45** but was contaminated per NMR. Product was diluted in  $\text{Et}_2\text{O}$ , washed ten times with saturated  $\text{NaHCO}_3$ , washed two times with brine, dried over

Na<sub>2</sub>SO<sub>4</sub> and concentrated under reduced pressure to afford **(3*S*,8*R*)-45** (0.043 g, 49.5%) as a yellow oil. TLC *R<sub>f</sub>* = 0.327 (25% EtOAc/hexanes); [α]<sub>D</sub><sup>18</sup> = -7.3° (*c* = 0.5, CHCl<sub>3</sub>); <sup>1</sup>H NMR (500 MHz, CHLOROFORM-*d*) δ 7.66 (dd, *J* = 1.34, 7.46 Hz, 1H), 7.31 - 7.42 (m, 3H), 6.44 (d, *J* = 8.31 Hz, 1H), 5.83 - 5.92 (m, 2H), 5.51 - 5.58 (d, *J* = 15.65 Hz, 1H), 5.35 (d, *J* = 8.80 Hz, 1H), 5.01 - 5.07 (q, *J* = 7.42 Hz, 1H), 2.10 (s, 3H), 1.76 - 1.84 (m, 2H), 1.49 (quin, *J* = 7.40 Hz, 2H), 1.22 - 1.38 (m, 12H), 0.88 (t, *J* = 6.97 Hz, 3H); <sup>13</sup>C NMR (125 MHz, CHLOROFORM-*d*) δ 169.4, 165.2, 134.2, 131.9, 131.6, 130.6, 130.3, 130.2, 127.1, 119.7, 79.5, 73.4, 70.9, 67.1, 64.4, 42.4, 35.5, 31.8, 29.4, 29.4, 29.2, 29.0, 25.6, 22.6, 20.9, 14.1; IR (ATR) 3256, 2924, 2854, 1742, 1644, 1525, 1222 cm<sup>-1</sup>; HRMS (ESI-TOF) [M + H]<sup>+</sup> calcd. for C<sub>26</sub>H<sub>33</sub>ClNO<sub>3</sub> 442.2149, found 442.2179.

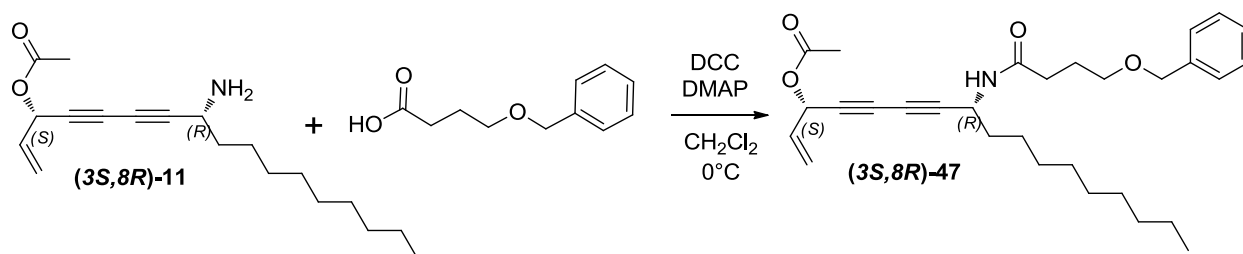


**(3*S*,8*R*)-8-(4-fluorobenzamido)heptadeca-1-en-4,6-diyn-3-yl acetate (3*S*,8*R*)-46**

To a solution of **(3*S*,8*R*)-11** (0.059 g, 0.20 mmol) in CH<sub>2</sub>Cl<sub>2</sub> (2.0 mL) at 0°C under Ar atmosphere was added triethylamine (0.04 mL, 0.29 mmol) followed by a solution of 4-fluorobenzoyl chloride (0.03 mL, 0.25 mmol) in CH<sub>2</sub>Cl<sub>2</sub> (1 mL). Reaction mixture was stirred at 0°C for 1 hour and 40 minutes. Reaction mixture was then quenched with water, extracted three times with CH<sub>2</sub>Cl<sub>2</sub>, washed with water and saturated NaHCO<sub>3</sub>, dried over Na<sub>2</sub>SO<sub>4</sub>, and concentrated under reduced pressure. Purification by flash chromatography on silica gel (hexanes – 10% EtOAc/hexanes) afforded **(3*S*,8*R*)-46** but was contaminated

with 4-fluorobenzoic acid. Product was diluted with Et<sub>2</sub>O, washed five times with saturated NaHCO<sub>3</sub>, dried over Na<sub>2</sub>SO<sub>4</sub>, and concentrated under reduced pressure to afford **(3*S*,8*R*)-46** (0.057 g, 68.6%, light yellow oil).

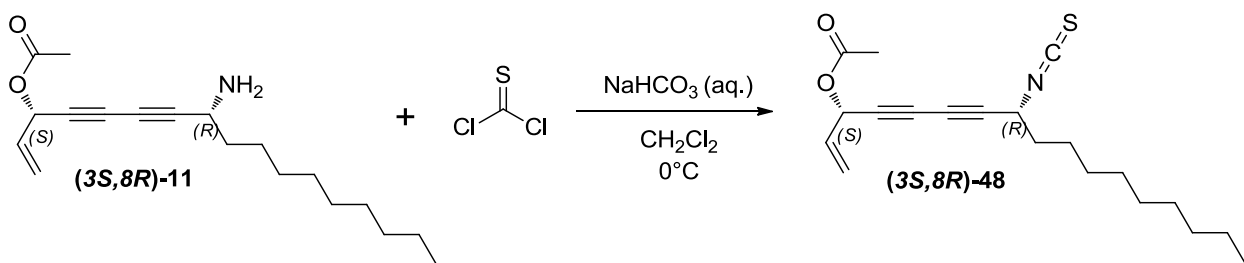
TLC  $R_f$  = 0.194 (15% EtOAc/hexanes);  $[\alpha]_D^{18}$  = -4.4° ( $c$  = 1.3, CHCl<sub>3</sub>); <sup>1</sup>H NMR (500 MHz, CHLOROFORM-*d*)  $\delta$  7.81 (dd,  $J$  = 5.26, 8.68 Hz, 2H), 7.11 (t,  $J$  = 8.56 Hz, 2H), 6.48 (d,  $J$  = 8.31 Hz, 1H), 5.82 - 5.92 (m, 2H), 5.50 - 5.58 (m, 1H), 5.32 - 5.38 (m, 1H), 5.01 (q,  $J$  = 7.50 Hz, 1H), 2.11 (s, 3H), 1.70 - 1.82 (m, 2H), 1.41 - 1.51 (m, 2H), 1.21 - 1.35 (m, 12H), 0.88 (t,  $J$  = 6.97 Hz, 3H); <sup>13</sup>C NMR (125 MHz, CHLOROFORM-*d*)  $\delta$  169.5, 165.8, 165.3, 163.8, 131.8, 129.9, 129.9, 129.5, 129.4, 119.7, 115.7, 115.5, 79.8, 73.4, 70.9, 67.0, 64.4, 42.4, 35.6, 31.8, 29.5, 29.4, 29.2, 29.0, 25.7, 22.6, 20.9, 14.1; IR (ATR) 3290, 2926, 2855, 2259, 1748, 1639, 1501, 1221 cm<sup>-1</sup>; HRMS (ESI-TOF)  $[M + H]^+$  calcd. for C<sub>26</sub>H<sub>33</sub>FNO<sub>3</sub> 426.2444, found 426.2455.



**(3*S*,8*R*)-8-(4-(benzyloxy)butanamido)heptadeca-1-en-4,6-diyne-3-yl acetate (3*S*,8*R*)-47**

To a suspension of 4-benzyloxybutyric acid (0.069 g, 0.36 mmol) in CH<sub>2</sub>Cl<sub>2</sub> (1.0 mL) at 0°C under Ar was added DCC (0.052 g, 0.25 mmol). Then a solution of **(3*S*,8*R*)-11** (0.060 g, 0.20 mmol) in CH<sub>2</sub>Cl<sub>2</sub> (1.0 mL) was added followed by addition of DMAP (4.3 mg, 0.035 mmol). After 3 hours, reaction was quenched with saturated NH<sub>4</sub>Cl, diluted

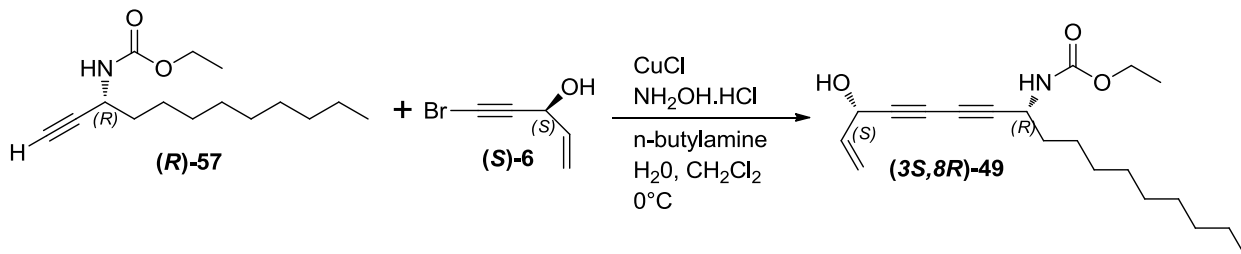
with Et<sub>2</sub>O, extracted three times with Et<sub>2</sub>O, washed two times with water, washed 5 times with saturated NaHCO<sub>3</sub>, washed 2 times with brine, dried over Na<sub>2</sub>SO<sub>4</sub>, and concentrated under reduced pressure. Purification by flash chromatography on silica gel (hexanes – 25% EtOAc/hexanes) afforded **(3*S*,8*R*)-47** (0.067 g, 70.9%) as a yellow oil. TLC *R<sub>f</sub>* = 0.164 (25% EtOAc/hexanes);  $[\alpha]_D^{18} = +20.0^\circ$  (*c* = 1.8, CHCl<sub>3</sub>); <sup>1</sup>H NMR (500 MHz, CHLOROFORM-*d*)  $\delta$  7.28 - 7.39 (m, 5H), 6.06 (d, *J* = 8.56 Hz, 1H), 5.82 - 5.93 (m, 2H), 5.51 - 5.59 (d, *J* = 15.65 Hz, 1H), 5.35 (d, *J* = 9.05 Hz, 1H), 4.79 (q, *J* = 7.34 Hz, 1H), 4.47 - 4.55 (m, 2H), 3.53 (t, *J* = 5.87 Hz, 2H), 2.31 (t, *J* = 7.09 Hz, 2H), 2.10 (s, 3H), 1.94 (quin, *J* = 6.48 Hz, 2H), 1.52 - 1.60 (m, 2H), 1.36 (br. s., 2H), 1.22 - 1.34 (m, 12H), 0.88 (t, *J* = 6.97 Hz, 3H); <sup>13</sup>C NMR (125 MHz, CHLOROFORM-*d*)  $\delta$  171.7, 169.4, 138.1, 131.9, 128.4, 127.7, 127.7, 119.7, 80.3, 73.1, 73.0, 71.0, 69.3, 66.5, 64.4, 41.5, 35.4, 33.4, 31.8, 29.4, 29.4, 29.2, 29.0, 25.5, 25.5, 22.6, 20.8, 14.1; IR (ATR) 3286, 2924, 2855, 2258, 1748, 1646, 1533, 1219 cm<sup>-1</sup>; HRMS (ESI-TOF)  $[M + H]^+$  calcd. for C<sub>30</sub>H<sub>42</sub>NO<sub>4</sub> 480.3114, found 480.3120.



**(3*S*,8*R*)-8-isothiocyanatoheptadeca-1-en-4,6-diyne-3-yl acetate (3*S*,8*R*)-48**

To a solution of **(3*S*,8*R*)-11** (0.072 g, 0.24 mmol) in CH<sub>2</sub>Cl<sub>2</sub> (0.9 mL) was added saturated aqueous NaHCO<sub>3</sub> (0.9 mL). Reaction was then cooled to 0°C under Ar atmosphere and thiophosgene 0.035 mL, 0.46 mmol) was added. Reaction mixture was stirred at 0°C for 1 hour and 20 minutes. Reaction was then diluted with CH<sub>2</sub>Cl<sub>2</sub> and

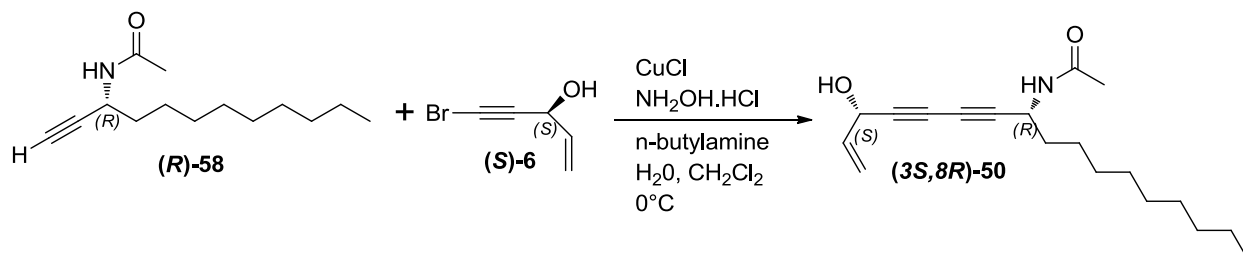
saturated aqueous NaHCO<sub>3</sub>, extracted three times with CH<sub>2</sub>Cl<sub>2</sub>, washed with brine, dried over Na<sub>2</sub>SO<sub>4</sub>, and concentrated under reduced pressure. Purification by flash chromatography on silica gel (hexanes – 5% EtOAc/hexanes) afforded **(3*S*,8*R*)-48** (0.029 g, 35.3%) as a light brown oil. TLC *R<sub>f</sub>* = 0.304 (10% EtOAc/hexanes); [ $\alpha$ ]<sub>D</sub><sup>18</sup> = -17.0° (*c* = 0.31, CHCl<sub>3</sub>); <sup>1</sup>H NMR (500 MHz, CHLOROFORM-*d*)  $\delta$  5.84 - 5.94 (m, 2H), 5.56 (d, *J* = 16.14 Hz, 1H), 5.38 (d, *J* = 9.29 Hz, 1H), 4.48 (t, *J* = 6.60 Hz, 1H), 2.12 (s, 3H), 1.82 - 1.90 (m, 2H), 1.44 - 1.54 (m, 2H), 1.23 - 1.36 (m, 12H), 0.89 (t, *J* = 6.97 Hz, 3H); <sup>13</sup>C NMR (125 MHz, CHLOROFORM-*d*)  $\delta$  169.4, 137.8, 131.6, 119.9, 75.5, 75.1, 70.3, 68.6, 64.3, 49.4, 36.7, 31.8, 29.4, 29.3, 29.2, 28.7, 25.4, 22.6, 20.8, 14.1; IR (ATR) 2926, 2855, 2039, 1748, 1218 cm<sup>-1</sup>; HRMS (ESI-TOF) [*M* + *H*]<sup>+</sup> calcd. for C<sub>20</sub>H<sub>28</sub>NO<sub>2</sub>S 346.1841, found 346.1871.



**ethyl ((3*S*,8*R*)-3-hydroxyheptadeca-1-en-4,6-diyn-8-yl)carbamate (3*S*,8*R*)-49**

Copper (I) chloride (0.007 g, 0.07 mmol) was added to a stirred 30 % solution (1.0 mL) of n-butylamine in distilled water at 0 °C which resulted in a deep blue solution. A few crystals of NH<sub>2</sub>OH.HCl were added until solution was colorless. A solution of **(*R*)-57** (0.084 g, 0.33 mmol) in CH<sub>2</sub>Cl<sub>2</sub> (0.5 mL) was added under argon atmosphere which resulted in yellow reaction mixture. After 10 minutes, a solution of **(*S*)-6** (0.067 g, 0.42 mmol) in CH<sub>2</sub>Cl<sub>2</sub> (0.6 mL) was added dropwise over 5 minutes. A few crystals of

NH<sub>2</sub>OH.HCl were added as necessary whenever solution turned blue or green. After 16 minutes, analysis of the reaction mixture by GC/MS showed that there was still some (**R**)-**57** present. At 50 minutes, added additional (**S**)-**6** (0.043 g, 0.27 mmol) in CH<sub>2</sub>Cl<sub>2</sub> (0.5 mL). Reaction was stirred an additional 1 hour and then quenched with water, extracted 3 times with CH<sub>2</sub>Cl<sub>2</sub>, dried over Na<sub>2</sub>SO<sub>4</sub>, and concentrated under reduced pressure.. Immediate purification by flash chromatography on silica gel (hexanes – 10% EtOAc/hexanes) afforded (**3S,8R**)-**49** (0.065 g, 58.4%, brown-orange solid). TLC  $R_f$  = 0.192 (25% EtOAc/hexanes);  $[\alpha]_D^{21} = +67.3^\circ$  ( $c = 1.0$ , CHCl<sub>3</sub>); <sup>1</sup>H NMR (500 MHz, CHLOROFORM-d)  $\delta$  5.95 (ddd,  $J = 5.38, 10.27, 17.12$  Hz, 1H), 5.48 (dt,  $J = 1.10, 17.12$  Hz, 1H), 5.26 (dt,  $J = 1.01, 10.21$  Hz, 1H), 4.94 (t,  $J = 5.75$  Hz, 1H), 4.83 (d,  $J = 7.83$  Hz, 1H), 4.54 (d,  $J = 7.34$  Hz, 1H), 4.13 (m, 2H), 2.16 (d,  $J = 5.62$  Hz, 1H), 1.63 - 1.70 (m, 2H), 1.38 - 1.46 (m, 2H), 1.22 - 1.34 (m, 15H), 0.85 - 0.92 (t,  $J = 6.97$  Hz, 3H); <sup>13</sup>C NMR (125 MHz, CHLOROFORM-d)  $\delta$  155.5, 135.8, 117.2, 79.9, 76.8, 70.4, 66.9, 63.4, 61.3, 43.7, 35.8, 31.8, 29.5, 29.4, 29.2, 29.0, 25.5, 22.7, 14.5, 14.1; IR (ATR) 3299, 2923, 2854, 1686, 1530, 1255 cm<sup>-1</sup>; HRMS (ESI-TOF)  $[M + H]^+$  calcd. for C<sub>20</sub>H<sub>32</sub>NO<sub>3</sub> 334.2382, found 334.2372.

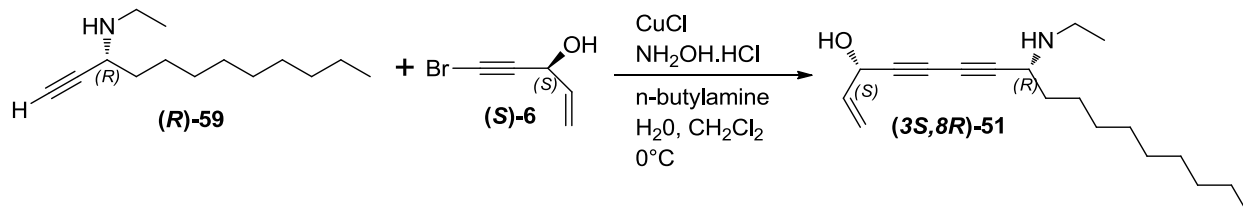


***N*-((3*S*,8*R*)-3-hydroxyheptadeca-1-en-4,6-diyn-8-yl)acetamide (3*S*,8*R*)-50**

Copper (I) chloride (0.007 g, 0.07 mmol) was added to a stirred 30 % solution (1.0 mL) of n-butylamine in distilled water at 0 °C which resulted in a deep blue solution. A few crystals of NH<sub>2</sub>OH.HCl were added until solution was colorless. A solution of (**R**)-58 (0.074 g, 0.33 mmol) in CH<sub>2</sub>Cl<sub>2</sub> (0.5 mL) was added under argon atmosphere which resulted in yellow reaction mixture. After 10 minutes, a solution of (**S**)-6 (0.109 g, 0.68 mmol) in CH<sub>2</sub>Cl<sub>2</sub> (1.0 mL) was added dropwise over 5 minutes. A few crystals of NH<sub>2</sub>OH.HCl were added as necessary whenever solution turned blue or green. After 45 minutes, reaction was quenched with water, extracted 3 times with CH<sub>2</sub>Cl<sub>2</sub>, dried over Na<sub>2</sub>SO<sub>4</sub>, and concentrated under reduced pressure. Immediate purification by flash chromatography on silica gel (hexanes – 40% EtOAc/hexanes) afforded (**3S,8R**)-50 (0.093 g, 92.5%, brown oil). TLC  $R_f$  = 0.118 (40% EtOAc/hexanes);  $[\alpha]_D^{21} = +133.7^\circ$  ( $c = 0.9$ , CHCl<sub>3</sub>); <sup>1</sup>H NMR (500 MHz, CHLOROFORM-*d*)  $\delta$  5.94 (ddd,  $J = 5.38, 10.15, 17.00$  Hz, 1H), 5.78 (d,  $J = 8.31$  Hz, 1H), 5.44 - 5.51 (d,  $J = 16.87$  Hz, 1H), 5.26 (d,  $J = 10.27$  Hz, 1H), 4.93 (d,  $J = 4.89$  Hz, 1H), 4.82 (q,  $J = 7.50$  Hz, 1H), 2.44 (br. s., 1H), 2.00 (s, 3H), 1.62 - 1.70 (m, 2H), 1.37 - 1.45 (m, 2H), 1.22 - 1.35 (m, 12H), 0.86 - 0.91 (t,  $J = 6.85$  Hz, 3H); <sup>13</sup>C NMR (125 MHz, CHLOROFORM-*d*)  $\delta$  169.1, 135.9, 117.2, 79.7, 76.9, 70.3, 66.9, 63.4, 41.9, 35.6, 31.8, 29.5, 29.4, 29.3, 29.1, 25.6, 23.2, 22.7, 14.1; IR



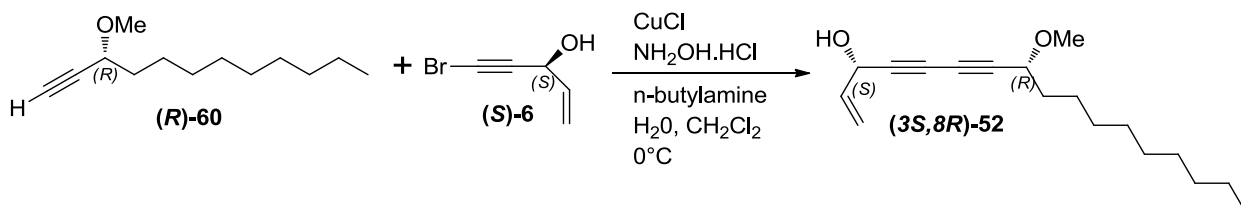
(ATR) 3255, 2917, 2851, 1650, 1542  $\text{cm}^{-1}$ ; HRMS (ESI-TOF)  $[\text{M} + \text{H}]^+$  calcd. for  $\text{C}_{19}\text{H}_{30}\text{NO}_2$  304.2277, found 304.2281.



**(3S,8R)-8-(ethylamino)heptadeca-1-en-4,6-diyne-3-ol (3S,8R)-51**

Copper (I) chloride (0.007 g, 0.07 mmol) was added to a stirred 30 % solution (1.2 mL) of n-butylamine in distilled water at 0 °C which resulted in a deep blue solution. A few crystals of  $\text{NH}_2\text{OH.HCl}$  were added until solution was colorless. A solution of (R)-59 (0.077 g, 0.37 mmol) in  $\text{CH}_2\text{Cl}_2$  (0.6 mL) was added under argon atmosphere which resulted in yellow reaction mixture. After 10 minutes, a solution of (S)-6 (0.110 g, 0.68 mmol) in  $\text{CH}_2\text{Cl}_2$  (1.0 mL) was added dropwise over 5 minutes. A few crystals of  $\text{NH}_2\text{OH.HCl}$  were added as necessary whenever solution turned blue or green. After 55 minutes, reaction was quenched with water, extracted 3 times with  $\text{CH}_2\text{Cl}_2$ , dried over  $\text{Na}_2\text{SO}_4$ , and concentrated under reduced pressure. Immediate purification by flash chromatography on silica gel (hexanes – 40% EtOAc/hexanes) afforded (3S,8R)-51 (0.032 g, 30.0%, brown solid). TLC  $R_f$  = 0.300 (60% EtOAc/hexanes);  $[\alpha]_D^{20} = +55.0^\circ$  ( $c = 0.5$ ,  $\text{CHCl}_3$ );  $^1\text{H}$  NMR (500 MHz,  $\text{CHLOROFORM-d}$ )  $\delta$  5.96 (ddd,  $J = 5.50, 10.11, 17.03$  Hz, 1H), 5.48 (td,  $J = 1.24, 17.03$  Hz, 1H), 5.26 (td,  $J = 1.06, 10.29$  Hz, 1H), 4.92 - 4.97 (m, 1H), 3.44 (dd,  $J = 5.50, 8.34$  Hz, 1H), 2.92 (qd,  $J = 7.20, 11.05$  Hz, 1H), 2.62 (qd,  $J = 7.20, 11.05$  Hz, 1H), 1.54 - 1.78 (m, 3H), 1.37 - 1.52 (m, 2H), 1.21 - 1.35 (m, 12H), 1.12 (t,  $J = 7.27$  Hz, 3H), 0.89 (t,  $J = 6.92$  Hz, 3H);  $^{13}\text{C}$  NMR (125 MHz,

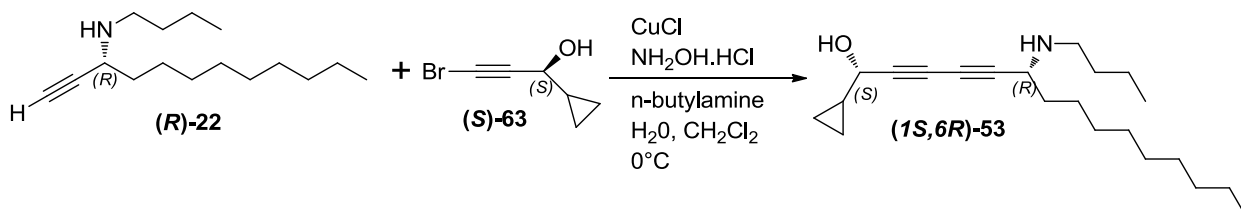
CHLOROFORM-d)  $\delta$  136.1, 117.1, 83.0, 76.0, 70.8, 67.3, 63.5, 50.6, 41.8, 35.7, 31.9, 29.5, 29.5, 29.3, 29.3, 26.0, 22.7, 15.1, 14.1; IR (ATR) 3675, 3251, 2924, 2855, 2678, 1029  $\text{cm}^{-1}$ ; HRMS (ESI-TOF)  $[M + H]^+$  calcd. for  $\text{C}_{19}\text{H}_{32}\text{NO}$  290.2484, found 290.2460.



**(3S,8R)-8-methoxyheptadeca-1-en-4,6-diyne-3-ol (3S,8R)-52**

Copper (I) chloride (0.006 g, 0.06 mmol) was added to a stirred 30 % solution (1.5 mL) of n-butylamine in distilled water at 0 °C which resulted in a deep blue solution. A few crystals of NH<sub>2</sub>OH.HCl were added until solution was colorless. A solution of (R)-60 (0.102 g, 0.52 mmol) in CH<sub>2</sub>Cl<sub>2</sub> (0.75 mL) was added under argon atmosphere which resulted in yellow reaction mixture. After 10 minutes, a solution of (S)-6 (0.114 g, 0.71 mmol) in CH<sub>2</sub>Cl<sub>2</sub> (1.1 mL) was added dropwise over 5 minutes. A few crystals of NH<sub>2</sub>OH.HCl were added as necessary whenever solution turned blue or green. After 20 minutes, analysis of the reaction mixture by GC/MS showed that there was still some (R)-60 present. At 50 minutes, added additional (S)-6 (0.075 g, 0.47 mmol) in CH<sub>2</sub>Cl<sub>2</sub> (0.5 mL). Reaction was stirred an additional 1 hour and then quenched with water, extracted 3 times with CH<sub>2</sub>Cl<sub>2</sub>, dried over Na<sub>2</sub>SO<sub>4</sub>, and concentrated under reduced pressure.. Immediate purification by flash chromatography on silica gel (hexanes – 10% EtOAc/hexanes) afforded (3S,8R)-52 (0.089 g, 62.1%, brown oil). TLC  $R_f$  = 0.396 (25% EtOAc/hexanes);  $[\alpha]_D^{22} = +73.2^\circ$  ( $c = 0.5$ , CHCl<sub>3</sub>); <sup>1</sup>H NMR (500 MHz, EtOAc/hexanes);

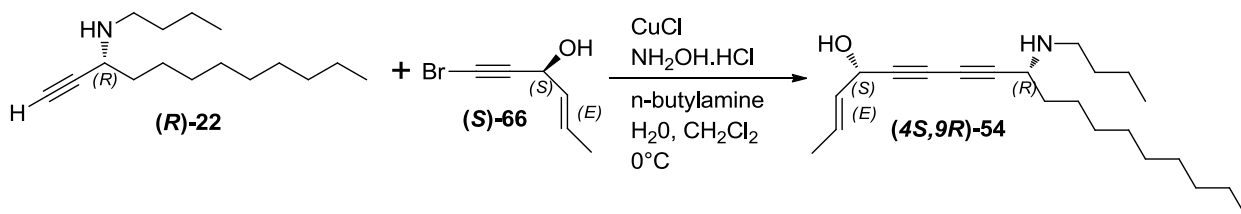
CHLOROFORM-*d*)  $\delta$  5.96 (ddd,  $J = 5.38, 10.27, 17.12$  Hz, 1H), 5.49 (ddd,  $J = 0.98, 1.47, 17.12$  Hz, 1H), 5.25 - 5.29 (ddd,  $J = 0.98, 1.47, 10.27$  Hz, 1H), 4.95 (t,  $J = 5.75$  Hz, 1H), 4.00 (t,  $J = 6.48$  Hz, 1H), 3.39 - 3.42 (s, 3H), 2.10 (d,  $J = 6.60$  Hz, 1H), 1.66 - 1.78 (m, 2H), 1.38 - 1.47 (m, 2H), 1.22 - 1.34 (m, 12H), 0.86 - 0.91 (t,  $J = 6.97$  Hz, 3H);  $^{13}\text{C}$  NMR (125 MHz, CHLOROFORM-*d*)  $\delta$  135.8, 117.3, 79.6, 77.1, 71.7, 70.4, 69.5, 63.5, 56.7, 35.3, 31.9, 29.5, 29.5, 29.3, 29.2, 25.1, 22.7, 14.1; IR (ATR) 3666, 3404, 2927, 2856, 1099  $\text{cm}^{-1}$ ; MS(EI)  $[\text{M} - 1]^+$  275.



**(1*S*,6*R*)-6-(butylamino)-1-cyclopropylpentadeca-2,4-diyne-1-ol (1*S*,6*R*)-53**

Copper (I) chloride (0.007 g, 0.07 mmol) was added to a stirred 30 % solution (1.25 mL) of n-butylamine in distilled water at 0 °C which resulted in a deep blue solution. A few crystals of NH<sub>2</sub>OH.HCl were added until solution was colorless. A solution of (R)-22 (0.104 g, 0.44 mmol) in CH<sub>2</sub>Cl<sub>2</sub> (0.63 mL) was added under argon atmosphere which resulted in yellow reaction mixture. After 10 minutes, a solution of (S)-63 (0.135 g, 0.77 mmol) in CH<sub>2</sub>Cl<sub>2</sub> (1.1 mL) was added dropwise over 5 minutes. A few crystals of NH<sub>2</sub>OH.HCl were added as necessary whenever solution turned blue or green. After 1 hour and 10 minutes, reaction was quenched with water, extracted 3 times with CH<sub>2</sub>Cl<sub>2</sub>, dried over Na<sub>2</sub>SO<sub>4</sub>, and concentrated under reduced pressure. Immediate purification by flash chromatography on silica gel (hexanes – 20% EtOAc/hexanes) afforded (1*S*,6*R*)-53 (0.058 g, 39.9%, yellow solid). TLC  $R_f = 0.345$  (40% EtOAc/hexanes);  $[\alpha]_D^{21} = +61.2^\circ$  (*c*

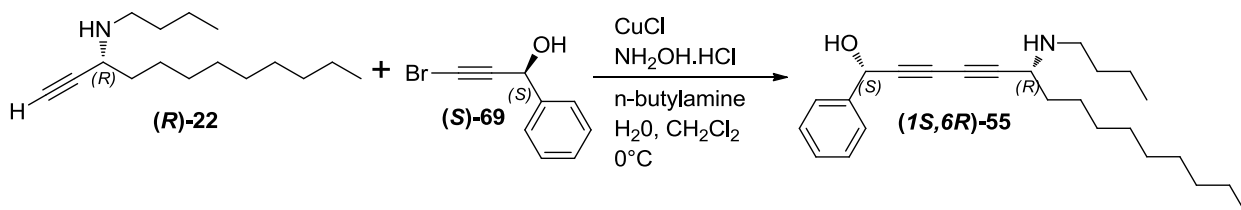
= 2.1, CHCl<sub>3</sub>); <sup>1</sup>H NMR (500 MHz, CHLOROFORM-d) δ 4.17 (d, *J* = 6.85 Hz, 1H), 3.41 (dd, *J* = 5.62, 8.31 Hz, 1H), 2.83 (ddd, *J* = 6.24, 8.62, 11.07 Hz, 1H), 2.56 (ddd, *J* = 5.62, 8.50, 11.07 Hz, 1H), 1.74 – 2.19 (br.s., 1H), 1.54 - 1.71 (m, 2H), 1.20 - 1.52 (m, 20H), 0.84 - 0.96 (m, 6H), 0.57 (m, 2H), 0.41 - 0.51 (m, 2H); <sup>13</sup>C NMR (125 MHz, CHLOROFORM-d) δ 82.3, 76.7, 69.3, 67.4, 66.0, 50.8, 47.2, 35.7, 32.0, 31.9, 29.5, 29.5, 29.3, 29.3, 26.0, 22.7, 20.5, 17.2, 14.1, 14.0, 3.3, 1.8; IR (ATR) 3259, 2924, 2854, 2714, 1040 cm<sup>-1</sup>; HRMS (ESI-TOF) [M + H]<sup>+</sup> calcd. for C<sub>22</sub>H<sub>38</sub>NO 332.2953, found 332.2935.



**(4*S*,9*R*,*E*)-9-(butylamino)octadeca-2-en-5,7-diyn-4-ol (4*S*,9*R*)-54**

Copper (I) chloride (0.010 g, 0.10 mmol) was added to a stirred 30 % solution (1.25 mL) of n-butylamine in distilled water at 0 °C which resulted in a deep blue solution. A few crystals of NH<sub>2</sub>OH.HCl were added until solution was colorless. A solution of (R)-22 (0.100 g, 0.42 mmol) in CH<sub>2</sub>Cl<sub>2</sub> (0.63 mL) was added under argon atmosphere which resulted in yellow reaction mixture. After 10 minutes, a solution of (S)-66 (0.133 g, 0.76 mmol) in CH<sub>2</sub>Cl<sub>2</sub> (1.1 mL) was added dropwise over 5 minutes. A few crystals of NH<sub>2</sub>OH.HCl were added as necessary whenever solution turned blue or green. After 3 hours, reaction was quenched with water, extracted 3 times with CH<sub>2</sub>Cl<sub>2</sub>, dried over Na<sub>2</sub>SO<sub>4</sub>, and concentrated under reduced pressure. Immediate purification by flash chromatography on silica gel (hexanes – 20% EtOAc/hexanes) afforded (4*S*,9*R*)-54 (0.049 g, 35.6%, tan solid). TLC *R<sub>f</sub>* = 0.400 (40% EtOAc/hexanes); [α]<sub>D</sub><sup>21</sup> = +70.4° (*c* =

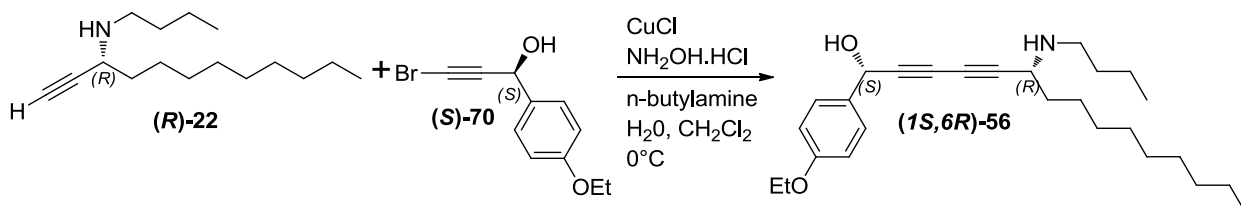
2.0, CHCl<sub>3</sub>); <sup>1</sup>H NMR (500 MHz, CHLOROFORM-d) δ 5.85 - 5.95 (m, 1H), 5.56 - 5.64 (m, 1H), 4.86 (d, *J* = 6.36 Hz, 1H), 3.42 (dd, *J* = 5.62, 8.31 Hz, 1H), 2.83 (ddd, *J* = 6.11, 8.68, 11.13 Hz, 1H), 2.56 (ddd, *J* = 5.62, 8.74, 11.07 Hz, 1H), 1.71 - 1.76 (m, 3H), 1.21 - 1.70 (m, 22H), 0.85 - 0.96 (m, 6H); <sup>13</sup>C NMR (126 MHz, CHLOROFORM-d) δ 129.5, 129.3, 82.6, 77.0, 70.2, 67.5, 63.0, 50.8, 47.2, 35.7, 32.0, 31.9, 29.5, 29.5, 29.3, 29.3, 26.0, 22.6, 20.5, 17.5, 14.1, 14.0; IR (ATR) 3254, 2923, 2853, 2682, 1467 cm<sup>-1</sup>; HRMS (ESI-TOF) [M + H]<sup>+</sup> calcd. for C<sub>22</sub>H<sub>38</sub>NO 332.2953, found 332.2950.



**(1*S*,6*R*)-6-(butylamino)-1-phenylpentadeca-2,4-diyne-1-ol (1*S*,6*R*)-**55****

Copper (I) chloride (0.008 g, 0.08 mmol) was added to a stirred 30 % solution (1.25 mL) of n-butylamine in distilled water at 0 °C which resulted in a deep blue solution. A few crystals of NH<sub>2</sub>OH.HCl were added until solution was colorless. A solution of (R)-**22** (0.101 g, 0.43 mmol) in CH<sub>2</sub>Cl<sub>2</sub> (0.63 mL) was added under argon atmosphere which resulted in yellow reaction mixture. After 10 minutes, a solution of (S)-**69** (0.159 g, 0.75 mmol) in CH<sub>2</sub>Cl<sub>2</sub> (1.1 mL) was added dropwise over 5 minutes. A few crystals of NH<sub>2</sub>OH.HCl were added as necessary whenever solution turned blue or green. After 50 minutes, reaction was quenched with water, extracted 3 times with CH<sub>2</sub>Cl<sub>2</sub>, dried over Na<sub>2</sub>SO<sub>4</sub>, and concentrated under reduced pressure. Immediate purification by flash chromatography on silica gel (hexanes – 20% EtOAc/hexanes) afforded (1*S*,6*R*)-**55** (0.056 g, 35.7%, brownish yellow solid). TLC *R<sub>f</sub>* = 0.388 (40% EtOAc/hexanes); [α]<sub>D</sub><sup>21</sup> =

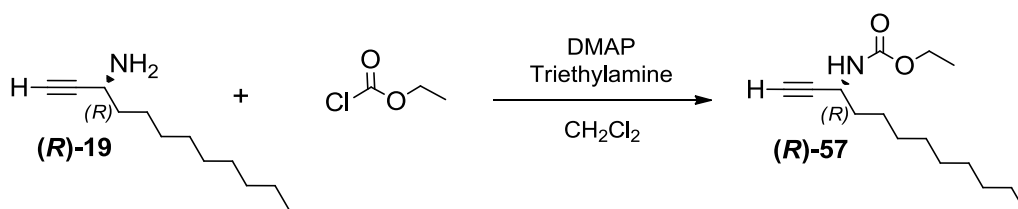
+22.3° ( $c = 2.2$ ,  $\text{CHCl}_3$ );  $^1\text{H NMR}$  (500 MHz,  $\text{CHLOROFORM-d}$ )  $\delta$  7.51 - 7.55 (m, 2H), 7.37 - 7.41 (m, 2H), 7.32 - 7.36 (m, 1H), 5.51 (s, 1H), 3.41 (dd,  $J = 5.50, 8.44$  Hz, 1H), 2.82 (ddd,  $J = 6.24, 8.74, 11.19$  Hz, 1H), 2.55 (ddd,  $J = 5.62, 8.74, 11.07$  Hz, 1H), 1.22 - 1.70 (m, 22H), 0.86 - 0.96 (m, 6H);  $^{13}\text{C NMR}$  (125 MHz,  $\text{CHLOROFORM-d}$ )  $\delta$  140.0, 128.6, 128.5, 126.6, 82.9, 77.2, 70.9, 67.5, 64.7, 50.8, 47.2, 35.6, 31.9, 31.9, 29.5, 29.5, 29.3, 29.3, 26.0, 22.7, 20.4, 14.1, 14.0; IR (ATR) 3666, 3274, 2923, 2854, 2685  $\text{cm}^{-1}$ ; HRMS (ESI-TOF)  $[\text{M} + \text{H}]^+$  calcd. for  $\text{C}_{25}\text{H}_{38}\text{NO}$  368.2953, found 368.2932.



**(1S,6R)-6-(butylamino)-1-(4-ethoxyphenyl)pentadeca-2,4-diyne-1-ol (1S,6R)-56**

Copper (I) chloride (0.011 g, 0.11 mmol) was added to a stirred 30 % solution (1.25 mL) of n-butylamine in distilled water at 0 °C which resulted in a deep blue solution. A few crystals of  $\text{NH}_2\text{OH.HCl}$  were added until solution was colorless. A solution of (R)-22 (0.105 g, 0.44 mmol) in  $\text{CH}_2\text{Cl}_2$  (0.63 mL) was added under argon atmosphere which resulted in yellow reaction mixture. After 10 minutes, a solution of (S)-70 (0.194 g, 0.76 mmol) in  $\text{CH}_2\text{Cl}_2$  (1.1 mL) was added dropwise over 5 minutes. A few crystals of  $\text{NH}_2\text{OH.HCl}$  were added as necessary whenever solution turned blue or green. After 2 hours and 20 minutes, reaction was quenched with water, extracted 3 times with  $\text{CH}_2\text{Cl}_2$ , dried over  $\text{Na}_2\text{SO}_4$ , and concentrated under reduced pressure. Immediate purification by flash chromatography on silica gel (hexanes – 20% EtOAc/hexanes) afforded (1S,6R)-56 (0.068 g, 37.3%, brownish yellow solid). TLC  $R_f = 0.424$  (40% EtOAc/hexanes);  $[\alpha]_D^{21} =$

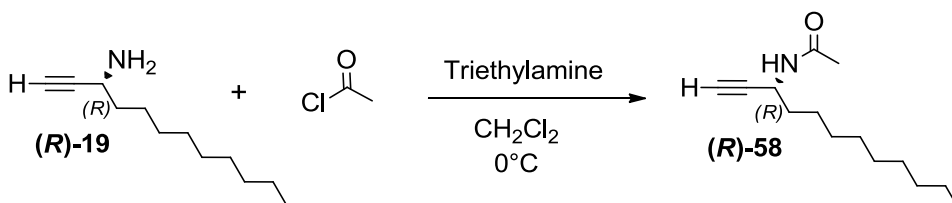
+17.2° ( $c = 2.9$ , CHCl<sub>3</sub>); <sup>1</sup>H NMR (500 MHz, CHLOROFORM-d) δ 7.42 - 7.48 (m, 2H), 6.88 - 6.94 (m, 2H), 5.48 (s, 1H), 4.05 (q,  $J = 7.09$  Hz, 2H), 3.42 (dd,  $J = 5.75, 8.19$  Hz, 1H), 2.85 (ddd,  $J = 6.36, 8.31, 11.25$  Hz, 1H), 2.56 (ddd,  $J = 5.75, 8.38, 11.07$  Hz, 1H), 1.22 - 1.70 (m, 25H), 0.86 - 0.96 (m, 6H); <sup>13</sup>C NMR (125 MHz, CHLOROFORM-d) δ 159.0, 132.2, 128.0, 114.5, 82.7, 77.5, 70.6, 67.6, 64.3, 63.4, 50.8, 47.2, 35.6, 31.9, 31.9, 29.5, 29.5, 29.3, 29.3, 26.0, 22.6, 20.4, 14.7, 14.1, 14.0; IR (ATR) 3245, 2923, 2853, 2675, 1511, 1245 cm<sup>-1</sup>; HRMS (ESI-TOF) [M + H]<sup>+</sup> calcd. for C<sub>27</sub>H<sub>42</sub>NO<sub>2</sub> 412.3216, found 412.3232.



### **(R)-ethyl dodec-1-yn-3-ylcarbamate (R)-57**

To a solution of (**R**)-**19** (0.119 g, 0.66 mmol) in CH<sub>2</sub>Cl<sub>2</sub> (3.4 mL) at ambient temperature under Ar was added DMAP (0.008 g, 0.07 mmol), triethylamine (0.10 mL, 0.72 mmol), and ethyl chloroformate (0.07 mL, 0.74 mmol). After 19 hours, reaction mixture was quenched with water, extracted three times with CH<sub>2</sub>Cl<sub>2</sub>, dried over Na<sub>2</sub>SO<sub>4</sub>, and concentrated under reduced pressure. Purification by flash chromatography on silica gel (hexanes – 5% EtOAc/hexanes) afforded (**R**)-**57** (0.110 g, 66.3%) as a white solid. TLC  $R_f = 0.367$  (15% EtOAc/hexanes);  $[\alpha]_D^{21} = +31.5^\circ$  ( $c = 1.3$ , CHCl<sub>3</sub>); <sup>1</sup>H NMR (500 MHz, CHLOROFORM-d) δ 4.75 - 4.86 (d,  $J = 6.36$  Hz, 1H), 4.40 - 4.50 (d,  $J = 6.36$  Hz, 1H), 4.10 - 4.19 (q,  $J = 7.50$  Hz, 2H), 2.28 (d,  $J = 2.45$  Hz, 1H), 1.63 - 1.71 (m, 2H), 1.43 (quin,  $J = 7.46$  Hz, 2H), 1.21 - 1.36 (m, 15H), 0.85 - 0.92 (t,  $J = 6.97$  Hz, 3H); <sup>13</sup>C NMR

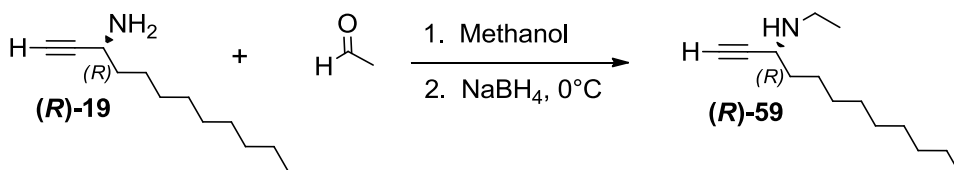
(125 MHz, CHLOROFORM-*d*)  $\delta$  155.6, 83.4, 71.0, 61.1, 43.1, 36.0, 31.9, 29.5, 29.5, 29.3, 29.1, 25.5, 22.7, 14.6, 14.1; IR (ATR) 3315, 2919, 2851, 1680, 1530, 1254  $\text{cm}^{-1}$ ; MS(EI)  $[M - 29 (\text{CH}_2\text{CH}_3)]^+ 224$ .



**(R)-N-(dodec-1-yn-3-yl)acetamide (R)-58**

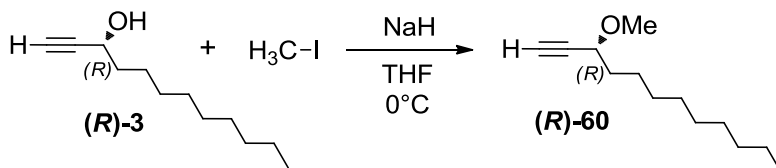
To a solution of (R)-19 (0.128 g, 0.70 mmol) in CH<sub>2</sub>Cl<sub>2</sub> (3.0 mL) at 0 °C under Ar was added triethylamine (0.23 mL, 1.65 mmol) followed by a solution of acetyl chloride (0.10 mL, 1.4 mmol) in CH<sub>2</sub>Cl<sub>2</sub> (0.8 mL). After 40 minutes, reaction mixture was quenched with water, extracted three times with CH<sub>2</sub>Cl<sub>2</sub>, washed with brine, dried over Na<sub>2</sub>SO<sub>4</sub>, and concentrated under reduced pressure. Purification by flash chromatography on silica gel (hexanes – 40% EtOAc/hexanes) afforded (R)-58 (0.097 g, 61.4%) as a white solid. TLC  $R_f = 0.196$  (40% EtOAc/hexanes);  $[\alpha]_D^{21} = +38.1^\circ$  ( $c = 1.1$ , CHCl<sub>3</sub>); <sup>1</sup>H NMR (500 MHz, CHLOROFORM-*d*)  $\delta$  5.73 (d,  $J = 7.83$  Hz, 1H), 4.69 - 4.76 (m, 1H), 2.24 - 2.28 (m, 1H), 1.98 - 2.01 (s, 3H), 1.60 - 1.71 (m, 2H), 1.38 - 1.47 (m, 2H), 1.22 - 1.33 (m, 12H), 0.88 (t,  $J = 6.85$  Hz, 3H); <sup>13</sup>C NMR (125 MHz, CHLOROFORM-*d*)  $\delta$  168.9, 83.3, 71.0, 41.3, 35.7, 31.8, 29.5, 29.4, 29.3, 29.1, 25.5, 23.2, 22.6, 14.1; IR (ATR) 3294, 3271, 2917, 2850, 1737, 1647, 1547, 1372  $\text{cm}^{-1}$ .





**(R)-N-ethyldodec-1-yn-3-amine (R)-59**

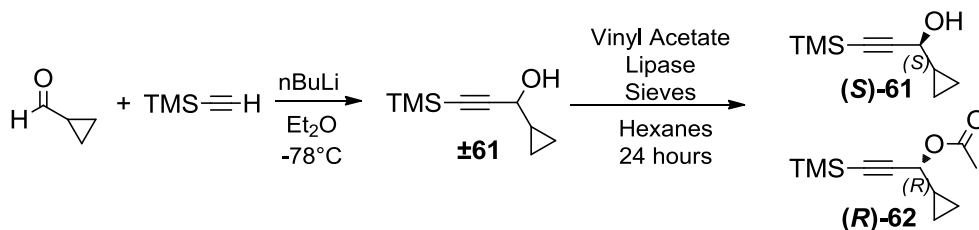
To a solution of **(R)-19** (0.205 g, 1.13 mmol) in methanol (5.5 mL) under argon atmosphere was added acetaldehyde (0.10 mL, 1.8 mmol). Reaction mixture was stirred at ambient temperature for 20 minutes and then chilled to 0°C at which time NaBH<sub>4</sub> was added (0.038 g, 0.99 mmol). Reaction mixture was stirred for 55 minutes and then diluted with EtOAc, washed with saturated NaHCO<sub>3</sub>, dried over Na<sub>2</sub>SO<sub>4</sub>, and concentrated under reduced pressure to yield **(R)-59** (0.206 g, 87.1%) as a clear oil. TLC  $R_f = 0.379$  (40% EtOAc/hexanes);  $[\alpha]_D^{20} = +19.2^\circ$  ( $c = 1.0$ , CHCl<sub>3</sub>); <sup>1</sup>H NMR (500 MHz, CHLOROFORM-*d*)  $\delta$  3.39 (ddd,  $J = 2.18, 5.77, 8.12$  Hz, 1H), 2.94 (m, 1H), 2.65 (m, 1H), 2.27 (d,  $J = 2.01$  Hz, 1H), 1.54 - 1.71 (m, 2H), 1.40 - 1.53 (m, 2H), 1.21 - 1.36 (m, 13H), 1.09 - 1.17 (t,  $J = 7.20$  Hz, 3H), 0.88 (t,  $J = 7.03$  Hz, 3H); <sup>13</sup>C NMR (125 MHz, CHLOROFORM-*d*)  $\delta$  71.3, 49.9, 41.5, 35.8, 31.9, 29.5, 29.5, 29.4, 29.3, 25.9, 22.7, 15.0, 14.1; IR (ATR) 3675 3311 2923, 2855 cm<sup>-1</sup>; MS(EI)  $[M - 1]^+$  208.



**(R)-3-methoxydodec-1-yne (R)-60**

To a suspension of NaH (60% in mineral oil, 0.088 g, 2.2 mmol) in THF at 0°C under Ar atmosphere was added a solution of **(R)-3** (0.302 g, 1.66 mmol) in THF (1.8 mL). After stirring for 45 minutes, methyl iodide (0.38 mL, 6.1 mmol) was added. After 3 hours,

reaction was quenched by slow addition of saturated  $\text{NH}_4\text{Cl}$ , extracted with  $\text{Et}_2\text{O}$ , washed with water, washed with brine, dried over  $\text{Na}_2\text{SO}_4$ , and concentrated under reduced pressure at  $0^\circ\text{C}$ . Purification by flash chromatography on silica gel (hexanes – 5%  $\text{EtOAc}$ /hexanes) afforded **(R)-60** (0.291 g, 89.3%, clear oil). TLC  $R_f = 0.185$  (5%  $\text{EtOAc}$ /hexanes);  $[\alpha]_D^{21} = +31.7^\circ$  ( $c = 1.3$ ,  $\text{CHCl}_3$ );  $^1\text{H}$  NMR (500 MHz,  $\text{CHLOROFORM-d}$ )  $\delta$  3.93 (dt,  $J = 2.08, 6.54$  Hz, 1H), 3.39 - 3.44 (s, 3H), 2.44 (d,  $J = 2.20$  Hz, 1H), 1.64 - 1.78 (m, 2H), 1.41 - 1.49 (m, 2H), 1.22 - 1.35 (m, 12H), 0.85 - 0.92 (t,  $J = 6.97$  Hz, 3H);  $^{13}\text{C}$  NMR (125 MHz,  $\text{CHLOROFORM-d}$ )  $\delta$  82.8, 73.6, 71.1, 56.4, 35.5, 31.9, 29.5, 29.3, 29.3, 25.1, 22.7, 14.1; IR (ATR) 3311, 2925, 2854, 1102  $\text{cm}^{-1}$ ; MS(EI)  $[\text{M} - 1]^+$  195.



**(S)-1-cyclopropyl-3-(trimethylsilyl)prop-2-yn-1-ol (S)-61; (R)-1-cyclopropyl-3-(trimethylsilyl)prop-2-yn-1-yl acetate (R)-62**

To a solution of (trimethylsilyl)acetylene (1.5 mL, 10.7 mmol) in dry  $\text{Et}_2\text{O}$  (12 mL) at  $-78^\circ\text{C}$  was added dropwise a solution of n-butyllithium (2.3 M in hexanes, 4.2 mL, 9.7 mmol) over 10 minutes under an Ar atmosphere. The reaction mixture was then stirred for 30 minutes before a solution of cyclopropanecarboxaldehyde (0.68 mL, 9.0 mmol) in  $\text{Et}_2\text{O}$  (2 mL) was added dropwise over 10 minutes. The resulting mixture was allowed to gradually warm to ambient temperature. After stirring for 24 hours, the mixture was quenched by slow addition of saturated  $\text{NH}_4\text{Cl}$  followed by  $\text{H}_2\text{O}$ . The mixture was

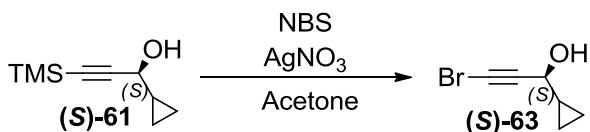
extracted with Et<sub>2</sub>O, washed with H<sub>2</sub>O and brine, dried over Na<sub>2</sub>SO<sub>4</sub>, and concentrated to near dryness. The resultant light orange-yellow oil (**±61**) was used directly in the next reaction without further purification.

**±61** was dissolved in dry hexanes (36 ml) followed by the addition of ground, activated 4-Å molecular sieves (0.40 g) and lipase (*Pseudomonas fluorescens*, Amano Lipase AK, 0.23 g). To the well-stirred suspension was added vinyl acetate (3.4 mL, 36.9 mmol) over 3 minutes. The suspension was stirred under an Ar atmosphere for 24 hours and then filtered through a pad of Celite and concentrated. The resulting yellow oil was purified by silica gel flash chromatography (Hexanes – 25% EtOAc/hexanes) to give (**S**)-**61** (0.62 g, 40.7%, light yellow oil) and (**R**)-**62** (0.74 g, 38.9%, faint pink oil).

Data for **±61**:  $R_f = 0.211$  (15% EtOAc/hexanes); <sup>1</sup>H NMR (500 MHz, CHLOROFORM-d)  $\delta$  4.23 (t,  $J = 5.75$  Hz, 1H), 2.15 (d,  $J = 5.14$  Hz, 1H), 1.18 - 1.27 (m, 1H), 0.39 - 0.58 (m, 4H), 0.12 - 0.19 (s, 9H); <sup>13</sup>C NMR (125 MHz, CHLOROFORM-d)  $\delta$  104.1, 89.6, 65.9, 16.7, 3.1, 1.4, -0.2; IR (ATR) 3335, 2961, 2900, 2175, 1250, 840 cm<sup>-1</sup>.

Data for (**S**)-**61**:  $R_f = 0.211$  (15% EtOAc/hexanes);  $[\alpha]_D^{17} = +42.8^\circ$  ( $c = 1.8$ , CHCl<sub>3</sub>); <sup>1</sup>H NMR (500 MHz, CHLOROFORM-d)  $\delta$  4.24 (t,  $J = 6.11$  Hz, 1H), 2.02 (d,  $J = 6.11$  Hz, 1H), 1.18 - 1.28 (m, 1H), 0.38 - 0.60 (m, 4H), 0.11 - 0.24 (s, 9H); <sup>13</sup>C NMR (125 MHz, CHLOROFORM-d)  $\delta$  104.1, 89.6, 65.9, 16.7, 3.2, 1.4, -0.2; IR (ATR) 3344, 2962, 2900, 2174, 1250, 839 cm<sup>-1</sup>.

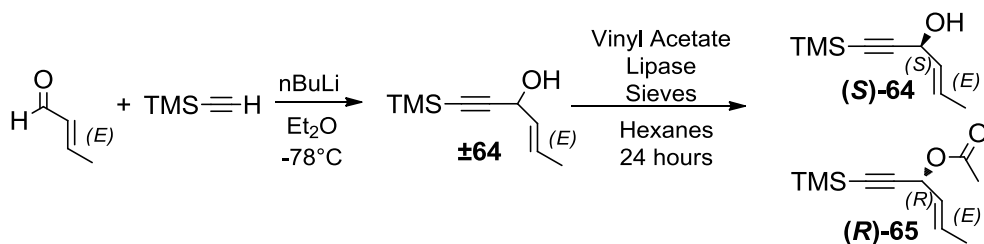
Data for **(R)**-**62**:  $R_f = 0.476$  (15% EtOAc/hexanes);  $[\alpha]_D^{17} = +42.4^\circ$  ( $c = 2.4$ ,  $\text{CHCl}_3$ );  $^1\text{H}$  NMR (500 MHz, CHLOROFORM- $d$ )  $\delta$  5.31 (d,  $J = 6.60$  Hz, 1H), 2.08 - 2.13 (s, 3H), 1.20 - 1.29 (m, 1H), 0.43 - 0.60 (m, 4H), 0.14 - 0.19 (s, 9H);  $^{13}\text{C}$  NMR (125 MHz, CHLOROFORM- $d$ )  $\delta$  170.0, 100.2, 90.5, 67.6, 21.2, 14.1, 3.4, 2.0, -0.3; IR (ATR) 2964, 2182, 1742, 1231, 842  $\text{cm}^{-1}$ .



4-166

**(S)-3-bromo-1-cyclopropylprop-2-yn-1-ol (S)-63**

To a solution of **(S)**-**61** (0.57 g, 3.4 mmol) in acetone (10 mL) was added N-bromosuccinimide (0.92 g, 5.1 mmol) followed by  $\text{AgNO}_3$  (0.12 g, 0.70 mmol). The reaction was stirred for 5 hours and 20 minutes at ambient temperature under Ar atmosphere. Reaction was then chilled to  $0^\circ\text{C}$ , quenched with  $\text{H}_2\text{O}$ , extracted with  $\text{Et}_2\text{O}$ , washed with water and brine, and concentrated under reduced pressure at  $0^\circ\text{C}$ . The resulting yellow oil was purified by silica gel flash chromatography (Hexanes-10% EtOAc/hexanes) to give **(S)**-**63** (0.51 g, 85.4%, light yellow oil);  $R_f = 0.213$  (15% EtOAc/hexanes);  $[\alpha]_D^{22} = +46.2^\circ$  ( $c = 2.4$ ,  $\text{CHCl}_3$ );  $^1\text{H}$  NMR (500 MHz, CHLOROFORM- $d$ )  $\delta$  4.19 (d,  $J = 6.60$  Hz, 1H), 2.03 - 2.14 (br. s., 1H), 1.21 - 1.30 (m, 1H), 0.52 - 0.63 (m, 2H), 0.40 - 0.52 (m, 2H);  $^{13}\text{C}$  NMR (125 MHz, CHLOROFORM- $d$ )  $\delta$  79.0, 66.7, 45.2, 17.2, 3.3, 1.6; IR (ATR) 3345, 3005, 2901, 2212, 1025  $\text{cm}^{-1}$ .



**(S,E)-1-(trimethylsilyl)hex-4-en-1-yn-3-ol (S)-64; (R,E)-1-(trimethylsilyl)hex-4-en-1-yn-3-yl acetate (R)-65**

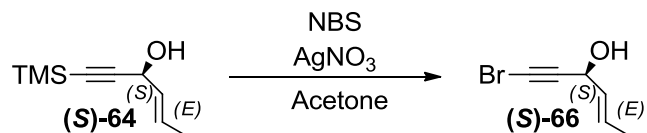
To a solution of (trimethylsilyl)acetylene (1.5 mL, 10.7 mmol) in dry Et<sub>2</sub>O (12 mL) at -78 °C was added dropwise a solution of n-butyllithium (2.3 M in hexanes, 4.2 mL, 9.7 mmol) over 10 minutes under an Ar atmosphere. The reaction mixture was then stirred for 30 minutes before a solution of crotonaldehyde (0.75 mL, 8.9 mmol) in Et<sub>2</sub>O (2 mL) was added dropwise over 10 minutes. The resulting mixture was allowed to gradually warm to ambient temperature. After stirring for 22 hours, the mixture was quenched by slow addition of saturated NH<sub>4</sub>Cl followed by H<sub>2</sub>O. The mixture was extracted with Et<sub>2</sub>O, washed with H<sub>2</sub>O and brine, dried over Na<sub>2</sub>SO<sub>4</sub>, and concentrated to near dryness. The resultant yellow oil (**±64**) was used directly in the next reaction without further purification.

**±64** was dissolved in dry hexanes (35 ml) followed by the addition of ground, activated 4-Å molecular sieves (0.38 g) and lipase (*Pseudomonas fluorescens*, Amano Lipase AK, 0.24 g). To the well-stirred suspension was added vinyl acetate (3.4 mL, 36.2 mmol) over 3 minutes. The suspension was stirred under an Ar atmosphere for 24 hours and then filtered through a pad of Celite and concentrated. The resulting yellow oil was purified by silica gel flash chromatography (Hexanes – 25% EtOAc/hexanes) to give (S)-**64** (0.67 g, 44.1%, yellow oil) and (R)-**65** (0.79 g, 41.6%, yellow oil).

Data for **±64**:  $R_f = 0.235$  (15% EtOAc/hexanes);  $^1\text{H}$  NMR (500 MHz, CHLOROFORM-d)  $\delta$  5.88 (m, 1H), 5.57 - 5.64 (m, 1H), 4.80 (d,  $J = 6.11$  Hz, 1H), 2.11 (br. s., 1H), 1.73 (m, 3H), 0.15 - 0.21 (s, 9H);  $^{13}\text{C}$  NMR (125 MHz, CHLOROFORM-d)  $\delta$  129.9, 128.9, 104.8, 90.5, 63.2, 17.5, -0.2; IR (ATR) 3341, 2962, 2173, 1250, 842  $\text{cm}^{-1}$ .

Data for (**S**)-**64**:  $R_f = 0.235$  (15% EtOAc/hexanes);  $[\alpha]_{\text{D}}^{17} = +56.6^\circ$  ( $c = 2.1$ ,  $\text{CHCl}_3$ );  $^1\text{H}$  NMR (500 MHz, CHLOROFORM-d)  $\delta$  5.85 - 5.94 (m, 1H), 5.61 (ddd,  $J = 1.59, 6.24, 15.16$  Hz, 1H), 4.81 (d,  $J = 6.11$  Hz, 1H), 1.98 (br. s., 1H), 1.74 (d,  $J = 6.60$  Hz, 3H), 0.16 - 0.22 (s, 9H);  $^{13}\text{C}$  NMR (125 MHz, CHLOROFORM-d)  $\delta$  129.9, 129.0, 104.8, 90.5, 63.3, 17.5, -0.2; IR (ATR) 3662, 3346, 2965, 2901, 2173, 1250, 839  $\text{cm}^{-1}$ .

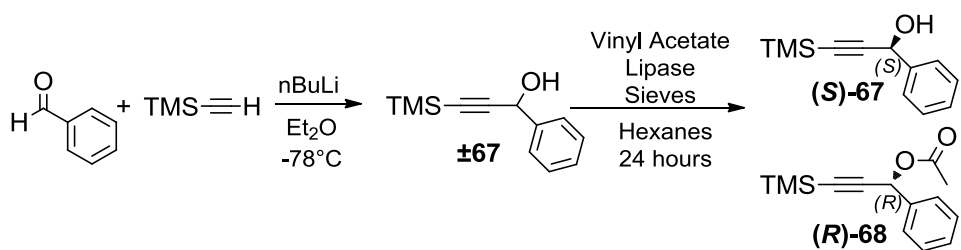
Data for (**R**)-**65**:  $R_f = 0.510$  (15% EtOAc/hexanes);  $[\alpha]_{\text{D}}^{17} = -9.0^\circ$  ( $c = 2.0$ ,  $\text{CHCl}_3$ );  $^1\text{H}$  NMR (500 MHz, CHLOROFORM-d)  $\delta$  5.95 - 6.04 (m, 1H), 5.84 (d,  $J = 6.60$  Hz, 1H), 5.50 - 5.58 (m, 1H), 2.08 (s, 3H), 1.74 (d,  $J = 6.60$  Hz, 3H), 0.16 - 0.21 (s, 9H);  $^{13}\text{C}$  NMR (125 MHz, CHLOROFORM-d)  $\delta$  169.6, 131.7, 126.0, 100.8, 91.6, 64.5, 21.2, 17.6, -0.3; IR (ATR) 3661, 2966, 2180, 1746, 1224, 841  $\text{cm}^{-1}$ .



#### 4-153

#### **(S,E)-1-bromohex-4-en-1-yn-3-ol (S)-66**

To a solution of (S)-64 (0.60 g, 3.5 mmol) in acetone (11 mL) was added N-bromosuccinimide (0.97 g, 5.5 mmol) followed by AgNO<sub>3</sub> (0.14 g, 0.80 mmol). The reaction was stirred for 3 hours at ambient temperature under Ar atmosphere. Reaction was then chilled to 0°C, quenched with H<sub>2</sub>O, extracted with Et<sub>2</sub>O, washed with water and brine, and concentrated under reduced pressure at 0°C. The resulting yellow oil was purified by silica gel flash chromatography (Hexanes-15% EtOAc/hexanes) to give (S)-66 (0.59 g, 95.6%, light yellow oil). TLC  $R_f$  = 0.212 (15% EtOAc/hexanes);  $[\alpha]_D^{17} = +54.5^\circ$  ( $c = 1.4$ , CHCl<sub>3</sub>); <sup>1</sup>H NMR (500 MHz, CHLOROFORM-d)  $\delta$  5.86 - 5.96 (m, 1H), 5.61 (qdd,  $J = 1.66, 6.22, 15.21$  Hz, 1H), 4.84 (d,  $J = 6.11$  Hz, 1H), 2.01 (br.s., 1H), 1.75 (qd,  $J = 0.82, 6.60$  Hz, 3H); <sup>13</sup>C NMR (125 MHz, CHLOROFORM-d)  $\delta$  129.5, 129.5, 79.4, 63.8, 46.4, 17.5; IR (ATR) 3292, 2972, 2212, 1444, 951 cm<sup>-1</sup>.



**(S)-1-phenyl-3-(trimethylsilyl)prop-2-yn-1-ol (S)-67; (R)-1-phenyl-3-(trimethylsilyl)prop-2-yn-1-yl acetate (R)-68**

To a solution of (trimethylsilyl)acetylene (1.5 mL, 10.7 mmol) in dry Et<sub>2</sub>O (12 mL) at -78 °C was added dropwise a solution of n-butyllithium (2.3 M in hexanes, 4.2 mL, 9.7 mmol) over 10 minutes under an Ar atmosphere. The reaction mixture was then stirred for 30 minutes before a solution of benzaldehyde (0.91 mL, 9.0 mmol) in Et<sub>2</sub>O (2 mL) was added dropwise over 10 minutes. The resulting mixture was allowed to gradually warm to ambient temperature. After stirring for 22.5 hours, the mixture was quenched by slow addition of saturated NH<sub>4</sub>Cl followed by H<sub>2</sub>O. The mixture was extracted with Et<sub>2</sub>O, washed with H<sub>2</sub>O and brine, dried over Na<sub>2</sub>SO<sub>4</sub>, and concentrated to near dryness. The resultant yellow oil (**±67**) was used directly in the next reaction without further purification.

**±67** was dissolved in dry hexanes (35 ml) followed by the addition of ground, activated 4-Å molecular sieves (0.46 g) and lipase (*Pseudomonas fluorescens*, Amano Lipase AK, 0.28 g). To the well-stirred suspension was added vinyl acetate (3.3 mL, 35.8 mmol) over 3 minutes. The suspension was stirred under an Ar atmosphere for 24 hours and then filtered through a pad of Celite and concentrated. The resulting yellow oil was

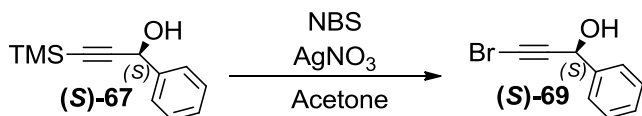


purified by silica gel flash chromatography (Hexanes – 25% EtOAc/hexanes) to give (**S**)-**67** (0.89 g, 48.8%, clear oil) and (**R**)-**68** (0.98 g, 44.6%, clear oil).

Data for  $\pm$ **67**:  $R_f = 0.295$  (15% EtOAc/hexanes);  $^1\text{H}$  NMR (500 MHz, CHLOROFORM-d)  $\delta$  7.54 - 7.59 (m, 2H), 7.38 - 7.43 (m, 2H), 7.33 - 7.37 (m, 1H), 5.47 (d,  $J = 4.65$  Hz, 1H), 2.27 (d,  $J = 5.62$  Hz, 1H), 0.22 (s, 9H);  $^{13}\text{C}$  NMR (125 MHz, CHLOROFORM-d)  $\delta$  140.2, 128.6, 128.4, 126.7, 104.8, 91.6, 65.0, -0.2; IR (ATR) 3377, 2962, 2174, 1251, 1040, 843  $\text{cm}^{-1}$ .

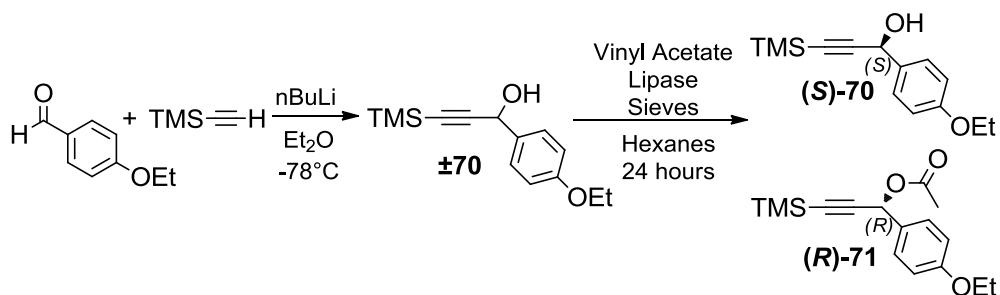
Data for (**S**)-**67**:  $R_f = 0.295$  (15% EtOAc/hexanes);  $[\alpha]_{\text{D}}^{22} = -19.4^\circ$  ( $c = 2.6$ ,  $\text{CHCl}_3$ );  $^1\text{H}$  NMR (500 MHz, CHLOROFORM-d)  $\delta$  7.54 - 7.58 (m, 2H), 7.38 - 7.43 (m, 2H), 7.32 - 7.37 (m, 1H), 5.47 (s, 1H), 2.34 (br. s., 1H), 0.22 (s, 9H);  $^{13}\text{C}$  NMR (125 MHz, CHLOROFORM-d)  $\delta$  140.2, 128.6, 128.4, 126.7, 104.9, 91.6, 65.0, -0.2; IR (ATR) 3394, 2963, 2174, 1250, 1041, 840  $\text{cm}^{-1}$ .

Data for (**R**)-**68**:  $R_f = 0.429$  (15% EtOAc/hexanes);  $[\alpha]_{\text{D}}^{21} = +32.7^\circ$  ( $c = 2.8$ ,  $\text{CHCl}_3$ );  $^1\text{H}$  NMR (500 MHz, CHLOROFORM-d)  $\delta$  7.54 (dd,  $J = 1.47, 7.83$  Hz, 2H), 7.34 - 7.43 (m, 3H), 6.51 (s, 1H), 2.11 (s, 3H), 0.21 (s, 9H);  $^{13}\text{C}$  NMR (125 MHz, CHLOROFORM-d)  $\delta$  169.7, 136.9, 128.9, 128.6, 127.8, 101.2, 92.4, 65.8, 21.1, -0.3; IR (ATR) 3666, 2963, 2182, 1742, 1222, 841  $\text{cm}^{-1}$ .



**(S)-3-bromo-1-phenylprop-2-yn-1-ol (S)-69**

To a solution of (S)-67 (0.83 g, 4.1 mmol) in acetone (12 mL) was added N-bromosuccinimide (1.13 g, 6.4 mmol) followed by AgNO<sub>3</sub> (0.14 g, 0.80 mmol). The reaction was stirred for 3 hours at ambient temperature under Ar atmosphere. Reaction was then chilled to 0°C, quenched with H<sub>2</sub>O, extracted with Et<sub>2</sub>O, washed with water and brine, and concentrated under reduced pressure at 0°C. The resulting yellow oil was purified by silica gel flash chromatography (Hexanes-10% EtOAc/hexanes) to give (S)-69 (0.64 g, 73.7%, light yellow oil); *R<sub>f</sub>* = 0.143 (15% EtOAc/hexanes); [α]<sub>D</sub><sup>17</sup> = -5.6° (*c* = 1.0, CHCl<sub>3</sub>); <sup>1</sup>H NMR (500 MHz, CHLOROFORM-*d*) δ 7.53 (m, 2H), 7.33 - 7.44 (m, 3H), 5.50 (s, 1H), 2.28 (br. s., 1H); <sup>13</sup>C NMR (125 MHz, CHLOROFORM-*d*) δ 139.8, 128.7, 128.6, 126.6, 79.7, 65.5, 47.4; IR (ATR) 3395, 2974, 2901, 2212, 2181, 1029 cm<sup>-1</sup>.



**(S)-1-(4-ethoxyphenyl)-3-(trimethylsilyl)prop-2-yn-1-ol (S)-70; (R)-1-(4-ethoxyphenyl)-3-(trimethylsilyl)prop-2-yn-1-yl acetate (R)-71**

To a solution of (trimethylsilyl)acetylene (1.5 mL, 10.7 mmol) in dry Et<sub>2</sub>O (12 mL) at -78°C was added dropwise a solution of n-butyllithium (2.3 M in hexanes, 4.2 mL, 9.7 mmol) over 10 minutes under an Ar atmosphere. The reaction mixture was then stirred

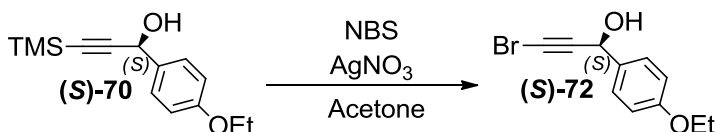
for 30 minutes before a solution of 4-ethoxybenzaldehyde (1.24 mL, 8.9 mmol) in Et<sub>2</sub>O (2 mL) was added dropwise over 10 minutes. The resulting mixture was allowed to gradually warm to ambient temperature. After stirring for 24 hours, the mixture was quenched by slow addition of saturated NH<sub>4</sub>Cl followed by H<sub>2</sub>O. The mixture was extracted with Et<sub>2</sub>O, washed with H<sub>2</sub>O and brine, dried over Na<sub>2</sub>SO<sub>4</sub>, and concentrated to near dryness. The resultant yellow oil (**±70**) was used directly in the next reaction without further purification.

**±70** was dissolved in dry hexanes (35 ml) followed by the addition of ground, activated 4-Å molecular sieves (0.57 g) and lipase (*Pseudomonas fluorescens*, Amano Lipase AK, 0.33 g). To the well-stirred suspension was added vinyl acetate (3.3 mL, 35.8 mmol) over 3 minutes. The suspension was stirred under an Ar atmosphere for 24 hours and then filtered through a pad of Celite and concentrated. The resulting yellow oil was purified by silica gel flash chromatography (Hexanes – 25% EtOAc/hexanes) to give (**S**)-**70** (0.99 g, 44.8%, light yellow oil) and (**R**)-**71** (0.93 g, 35.9%, clear oil).

Data for **±70**: TLC  $R_f$  = 0. (15% EtOAc/hexanes); <sup>1</sup>H NMR (500 MHz, CHLOROFORM-d)  $\delta$  7.44 - 7.48 (m, 2H), 6.88 - 6.92 (m, 2H), 5.40 (s, 1H), 4.04 (q,  $J$  = 7.09 Hz, 2H), 2.31 (br. s., 1H), 1.42 (t,  $J$  = 7.09 Hz, 3H), 0.18 - 0.25 (s, 9H); <sup>13</sup>C NMR (125 MHz, CHLOROFORM-d)  $\delta$  159.0, 132.4, 128.1, 114.4, 105.2, 91.2, 64.5, 63.4, 14.8, -0.2; IR (ATR) 3410, 2961, 2173, 1511, 1248, 840 cm<sup>-1</sup>.

Data for (*S*)-**70**: TLC  $R_f = 0.185$  (15% EtOAc/hexanes);  $[\alpha]_D^{17} = -18.0^\circ$  ( $c = 2.5$ ,  $\text{CHCl}_3$ );  $^1\text{H}$  NMR (500 MHz,  $\text{CHLOROFORM-d}$ )  $\delta$  7.43 - 7.49 (m, 2H), 6.87 - 6.93 (m, 2H), 5.41 (s, 1H), 4.05 (q,  $J = 6.93$  Hz, 2H), 2.22 (br. s., 1H), 1.42 (t,  $J = 6.97$  Hz, 3H), 0.18 - 0.25 (s, 9H);  $^{13}\text{C}$  NMR (125 MHz,  $\text{CHLOROFORM-d}$ )  $\delta$  159.0, 132.4, 128.1, 114.4, 105.1, 91.2, 64.6, 63.4, 14.8, -0.2; IR (ATR) 3463, 2980, 2174, 1511, 1249, 841  $\text{cm}^{-1}$ .

Data for (*R*)-**71**: TLC  $R_f = 0.377$  (15% EtOAc/hexanes);  $[\alpha]_D^{17} = +5.6^\circ$  ( $c = 1.8$ ,  $\text{CHCl}_3$ );  $^1\text{H}$  NMR (500 MHz,  $\text{CHLOROFORM-d}$ )  $\delta$  7.43 - 7.49 (m, 2H), 6.87 - 6.92 (m, 2H), 6.45 (s, 1H), 4.05 (q,  $J = 6.93$  Hz, 2H), 2.09 (s, 3H), 1.42 (t,  $J = 6.97$  Hz, 3H), 0.17 - 0.27 (s, 9H);  $^{13}\text{C}$  NMR (126 MHz,  $\text{CHLOROFORM-d}$ )  $\delta$  169.8, 159.4, 129.4, 129.0, 114.4, 101.6, 92.0, 65.6, 63.5, 21.2, 14.8, -0.3; IR (ATR) 2963, 2181, 1743, 1513, 1223, 842  $\text{cm}^{-1}$ .

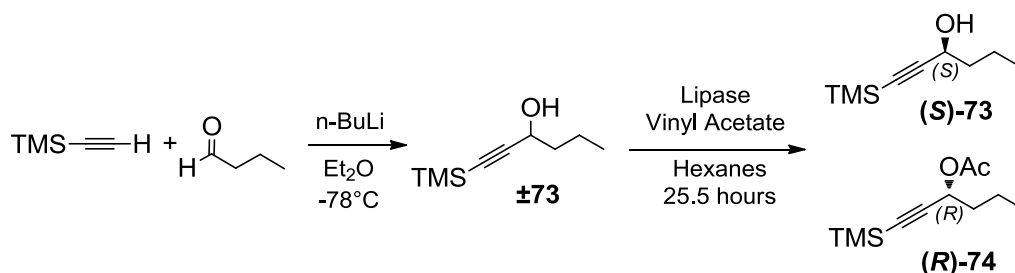


4-168

### (*S*)-3-bromo-1-(4-ethoxyphenyl)prop-2-yn-1-ol (*S*)-**72**

To a solution of (*S*)-**70** (0.93 g, 3.8 mmol) in acetone (11 mL) was added N-bromosuccinimide (1.02 g, 5.6 mmol) followed by  $\text{AgNO}_3$  (0.13 g, 0.75 mmol). The reaction was stirred for 2.5 hours at ambient temperature under Ar atmosphere. Reaction was then chilled to  $0^\circ\text{C}$ , quenched with  $\text{H}_2\text{O}$ , extracted with  $\text{Et}_2\text{O}$ , washed with water and brine, and concentrated under reduced pressure. The resulting yellow oil was purified by silica gel flash chromatography (Hexanes-15% EtOAc/hexanes) to give (*S*)-**72** (0.68 g,

70.9%, yellow oil);  $R_f = 0.186$  (15% EtOAc/hexanes);  $[\alpha]_D^{22} = -9.4^\circ$  ( $c = 3.2$ ,  $\text{CHCl}_3$ );  $^1\text{H}$  NMR (500 MHz, CHLOROFORM- $d$ )  $\delta$  7.40 - 7.45 (d,  $J = 8.56$  Hz, 2H), 6.88 - 6.92 (d,  $J = 8.56$  Hz, 2H), 5.42 (s, 1H), 4.04 (q,  $J = 7.01$  Hz, 2H), 2.41 (br. s., 1H), 1.43 (t,  $J = 6.97$  Hz, 3H);  $^{13}\text{C}$  NMR (125 MHz, CHLOROFORM- $d$ )  $\delta$  159.1, 132.0, 128.0, 114.5, 79.9, 65.0, 63.5, 47.0, 14.7; IR (ATR) 3374, 2980, 2212, 1611, 1510, 1241  $\text{cm}^{-1}$ .



**(S)-1-(trimethylsilyl)hex-1-yn-3-ol (S)-73; (R)-1-(trimethylsilyl)hex-1-yn-3-yl acetate (R)-74**

To a solution of (trimethylsilyl)acetylene (0.78 g, 1.1 mL, 8.0 mmol) in dry Et<sub>2</sub>O (8 mL) at -78 °C was added dropwise a solution of n-butyllithium (2.25 M in hexanes, 3.3 mL, 7.3 mmol) over five minutes under an Ar atmosphere. The reaction mixture was then stirred for 30 minutes before a solution of butyraldehyde (0.48 g, 0.6 mL, 6.7 mmol) in Et<sub>2</sub>O (2.5 mL) was added dropwise over five minutes. The resulting mixture was allowed to gradually warm to ambient temperature. After stirring for 1.5 hours, the mixture was quenched by slow addition of saturated NH<sub>4</sub>Cl. The mixture was extracted with Et<sub>2</sub>O, washed with H<sub>2</sub>O and brine, dried over Na<sub>2</sub>SO<sub>4</sub>, and concentrated to near dryness. The

resultant yellow oil (**±73**) was used directly in the next reaction without further purification.

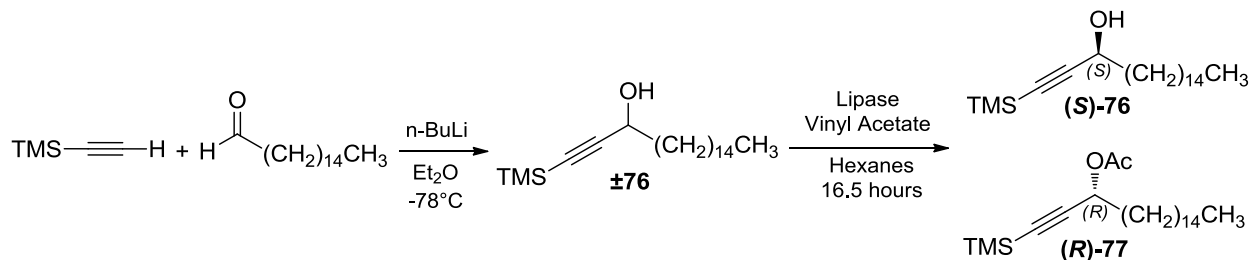
The yellow oil (**±73**) was dissolved in dry hexanes (26 ml) followed by the addition of ground, activated 4-Å molecular sieves (0.28 g) and lipase (*Pseudomonas fluorescens*, Amano Lipase AK, 0.17 g). To the well-stirred suspension was added vinyl acetate (2.5 mL, 27.1 mmol) over 3 minutes. The suspension was stirred under an Ar atmosphere for 25.5 hours and then filtered through a pad of Celite and concentrated. The resulting yellow oil was purified by silica gel chromatography (hexanes-15% EtOAc/hexanes) to give (**S**)-**73** (0.52 g, 45.6%, light yellow oil) and (**R**)-**74** (0.70 g, 49.7%, clear oil).

Data for **±73** racemic: TLC  $R_f = 0.370$  (15% EtOAc/hexanes);  $^1\text{H}$  NMR (500 MHz, CHLOROFORM- $d$ )  $\delta$  4.36 (t,  $J = 6.60$  Hz, 1H), 2.03 (br. s., 1H), 1.60 - 1.73 (m, 2H), 1.41 - 1.52 (m, 2H), 0.92 - 0.98 (t,  $J = 7.34$  Hz, 3H), 0.14 - 0.20 (s, 9H);  $^{13}\text{C}$  NMR (125 MHz, CHLOROFORM- $d$ )  $\delta$  106.9, 89.2, 62.6, 39.7, 18.4, 13.7, -0.1; IR (ATR) 3330, 2961, 2874, 2174, 1250, 839  $\text{cm}^{-1}$ ; HRMS (ESI-TOF)  $[\text{M} + \text{H}]^+$  calcd. for  $\text{C}_9\text{H}_{19}\text{OSi}$  171.1205, found 171.1195.

Data for (**S**)-**73**: TLC  $R_f = 0.370$  (15% EtOAc/hexanes);  $[\alpha]_D^{18} = -7.1^\circ$  ( $c = 2.4$ ,  $\text{CHCl}_3$ );  $^1\text{H}$  NMR (500 MHz, CHLOROFORM- $d$ )  $\delta$  4.33 - 4.40 (q,  $J = 6.03$  Hz, 1H), 1.97 (d,  $J = 5.14$  Hz, 1H), 1.61 - 1.74 (m, 2H), 1.41 - 1.52 (m, 2H), 0.95 (t,  $J = 7.34$  Hz, 3H), 0.14 - 0.19 (s, 9H);  $^{13}\text{C}$  NMR (125 MHz, CHLOROFORM- $d$ )  $\delta$  106.9, 89.2, 62.6, 39.7, 18.4,

13.7, -0.1; IR (ATR) 3340, 2960, 2875, 2172, 1250, 839  $\text{cm}^{-1}$ ; HRMS (ESI-TOF)  $[\text{M} + \text{H}]^+$  calcd. for  $\text{C}_9\text{H}_{19}\text{OSi}$  171.1205, found 171.1196.

Data for **(R)-74**: TLC  $R_f = 0.556$  (15% EtOAc/hexanes);  $[\alpha]_D^{22} = +105.7^\circ$  ( $c = 3.5$ ,  $\text{CHCl}_3$ );  $^1\text{H}$  NMR (500 MHz,  $\text{CHLOROFORM-d}$ )  $\delta$  5.38 (t,  $J = 6.72$  Hz, 1H), 2.04 - 2.12 (s, 3H), 1.64 - 1.78 (m, 2H), 1.38 - 1.50 (m, 2H), 0.93 (t,  $J = 7.34$  Hz, 3H), 0.10 - 0.20 (s, 9H);  $^{13}\text{C}$  NMR (125 MHz,  $\text{CHLOROFORM-d}$ )  $\delta$  169.8, 102.7, 90.1, 64.1, 36.8, 21.1, 18.3, 13.6, -0.2; IR (ATR) 2962, 2876, 2179, 1747, 1229, 842  $\text{cm}^{-1}$ .



**(S)-1-(trimethylsilyloxy)octadec-1-yn-3-ol (S)-76; (R)-1-(trimethylsilyloxy)octadec-1-yn-3-yl acetate (R)-77**

To a solution of (trimethylsilyloxy)acetylene (0.36 mL, 2.6 mmol) in dry  $\text{Et}_2\text{O}$  (3.3 mL) at  $-4^\circ\text{C}$  (brine/ice bath) was added dropwise a solution of  $n$ -butyllithium (2.25 M in hexanes, 1 mL, 2.25 mmol) over 30 minutes under an Ar atmosphere. The reaction mixture was then stirred for 30 minutes before a solution of palmitaldehyde (0.51 g, 2.1 mmol)  $\text{Et}_2\text{O}$  (1 mL) was added dropwise over five minutes. After stirring for 1 hour 5 minutes, the

mixture was quenched by slow addition saturated  $\text{NH}_4\text{Cl}$ . The mixture was extracted with  $\text{Et}_2\text{O}$ , washed with  $\text{H}_2\text{O}$  and brine, dried over  $\text{Na}_2\text{SO}_4$ , and concentrated under reduced pressure to afford  $\pm\mathbf{76}$  (0.79 g, 98.4%, yellow oil). The resultant yellow oil ( $\pm\mathbf{76}$ ) was used directly in the next reaction without further purification.

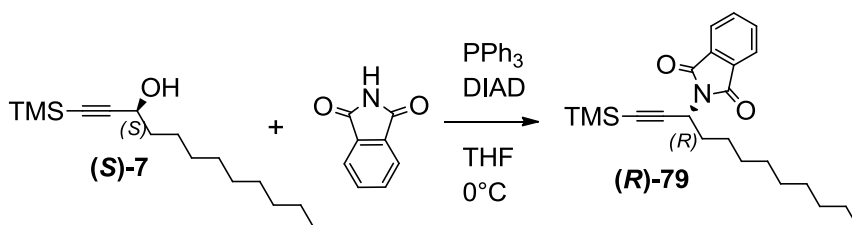
The yellow oil  $\pm\mathbf{76}$  (0.64 g, 1.9 mmol) was dissolved in dry hexanes (7.4 ml) followed by the addition of ground, activated 4-Å molecular sieves (0.16 g) and lipase (*Pseudomonas fluorescens*, Amano Lipase AK, 0.10 g). To the well-stirred suspension was added vinyl acetate (0.7 mL, 7.6 mmol) over two minutes. The suspension was stirred under an Ar atmosphere for 16.5 hours and then filtered through a pad of Celite and concentrated. The resulting yellow oil was purified by silica gel chromatography (Hexanes-2% EtOAc/hexanes) to give (*S*)-**76** (0.27 g, 43.1%, clear oil) and (*R*)-**77** (0.18 g, 25.3%, yellow oil).

Data for  $\pm\mathbf{76}$ :  $R_f = 0.407$  (15% EtOAc/hexanes)

Data for (*S*)-**76**: TLC  $R_f = 0.407$  (15% EtOAc/hexanes);  $[\alpha]_D^{17} = +0.4^\circ$  ( $c = 1.2$ ,  $\text{CHCl}_3$ );  $^1\text{H}$  NMR (500 MHz,  $\text{CHLOROFORM-d}$ )  $\delta$  4.35 (t,  $J = 6.48$  Hz, 1H), 1.88 (br. s., 1H), 1.63-1.75 (m, 2H), 1.39 - 1.50 (m, 2H), 1.22 - 1.36 (m, 24H), 0.85 - 0.92 (t,  $J = 6.97$  Hz, 3H), 0.15 - 0.20 (s, 9H);  $^{13}\text{C}$  NMR (125 MHz,  $\text{CHLOROFORM-d}$ )  $\delta$  106.9, 89.2, 62.9, 37.7, 31.9, 29.7, 29.7, 29.5, 29.5, 29.4, 29.2, 25.1, 22.7, 14.1, -0.1; IR (ATR) 3457, 2923, 2853, 2175, 1250, 841  $\text{cm}^{-1}$ .



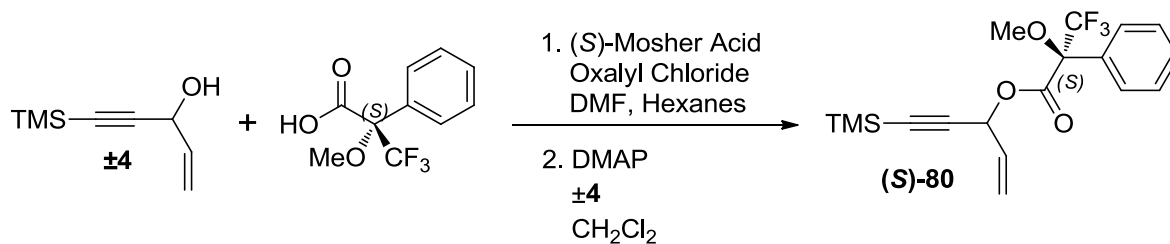
Data for **(R)-77**: TLC  $R_f = 0.625$  (15% EtOAc/hexanes);  $[\alpha]_D^{23} = +51.7^\circ$  ( $c = 1.2$ ,  $\text{CHCl}_3$ );  $^1\text{H}$  NMR (500 MHz,  $\text{CHLOROFORM-d}$ )  $\delta$  5.38 (t,  $J = 6.72$  Hz, 1H), 2.09 (s, 3H), 1.70 - 1.78 (m, 2H), 1.42 (m, 2H), 1.24 - 1.33 (m, 24H), 0.86 - 0.91 (t,  $J = 6.97$  Hz, 3H), 0.16 - 0.19 (s, 9H);  $^{13}\text{C}$  NMR (125 MHz,  $\text{CHLOROFORM-d}$ )  $\delta$  169.9, 102.8, 90.2, 64.4, 34.8, 31.9, 29.7, 29.7, 29.7, 29.7, 29.6, 29.5, 29.4, 29.4, 29.0, 24.9, 22.7, 21.1, 14.1, -0.2; IR (ATR) 2923, 2853, 2180, 1747, 1230, 842  $\text{cm}^{-1}$ .



**(R)-2-(1-(trimethylsilyl)dodec-1-yn-3-yl)isoindoline-1,3-dione (R)-79**

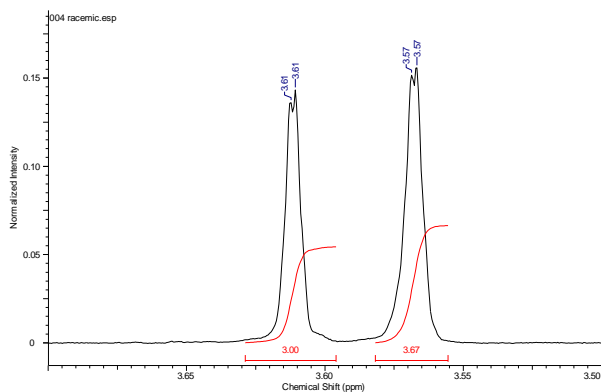
To a solution of **(S)-7** (3.5 g, 13.8 mmol) in THF (105 mL) was added phthalimide (3.0 g, 20.2 mmol) followed by triphenylphosphine (5.3 g, 20.1 mmol). The reaction mixture was then chilled to  $0^\circ\text{C}$  followed by the dropwise addition of DIAD (5.2 mL, 24.8 mmol) and stirred at  $0^\circ\text{C}$  under Ar atmosphere. After 1.5 hours, reaction mixture was concentrated under reduced pressure, diluted with  $\text{Et}_2\text{O}$ , and chilled to  $0^\circ\text{C}$ . Precipitate was filtered off through Celite and the filtrate was concentrated under reduced pressure. The resultant yellow oil was purified by silica gel chromatography (Hexanes – 5% EtOAc/Hexanes) to afford **(R)-79** (5.3 g, 100.0%, yellow solid). TLC  $R_f = 0.278$  (10% EtOAc/hexanes);  $[\alpha]_D^{23} = -3.7^\circ$  ( $c = 5.4$ ,  $\text{CHCl}_3$ );  $^1\text{H}$  NMR (500 MHz,  $\text{CHLOROFORM-d}$ )  $\delta$  7.84 - 7.88 (m, 2H), 7.70 - 7.75 (m, 2H), 5.02 (t,  $J = 8.07$  Hz 1H), 1.98-2.14 (m, 2H), 1.44 (m, 2H), 1.20 - 1.36 (m, 12H), 0.84 - 0.90 (t, 6.97 Hz, 3H), 0.12 - 0.18 (s, 9H);  $^{13}\text{C}$

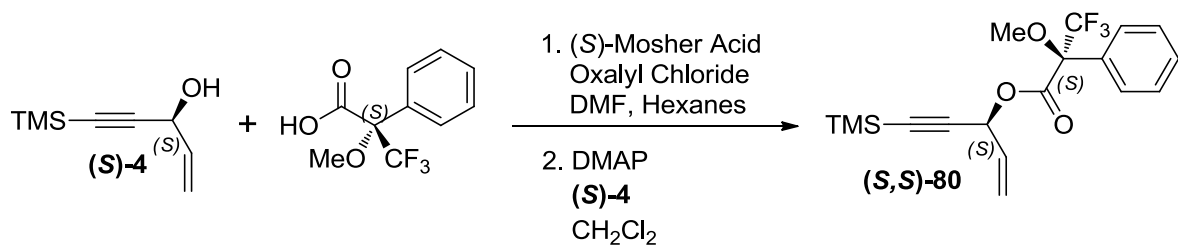
NMR (125 MHz, CHLOROFORM-d)  $\delta$  167.0, 134.0, 131.9, 123.4, 101.9, 88.2, 42.4, 33.4, 31.8, 29.4, 29.4, 29.2, 28.8, 26.3, 22.6, 14.1, -0.1; IR (ATR) 3473, 2922, 2851, 2173, 1776, 1709, 1385, 1249  $\text{cm}^{-1}$ ; HRMS (ESI-TOF)  $[\text{M} + \text{H}]^+$  calcd. for  $\text{C}_{23}\text{H}_{34}\text{NO}_2\text{Si}$  384.2359, found 384.2349.



### (S)-80 Mosher Ester of $\pm 4$

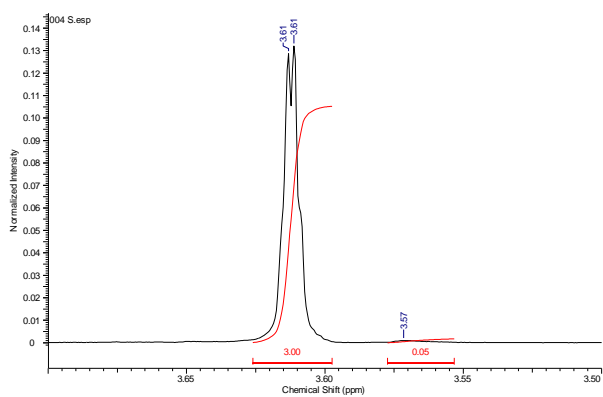
Methoxy protons ratio 3.00:3.67

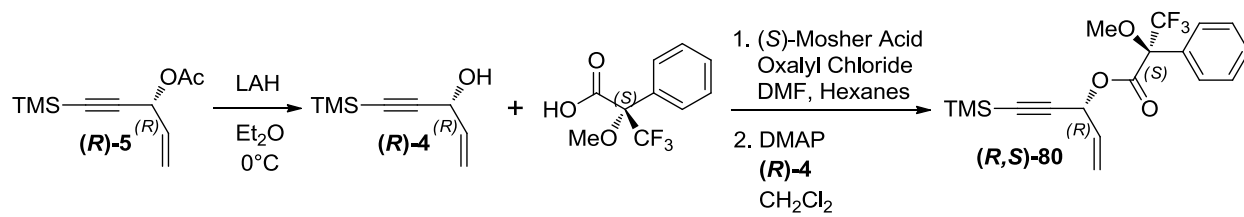




**(S,S)-80 Mosher Ester of (S)-4**

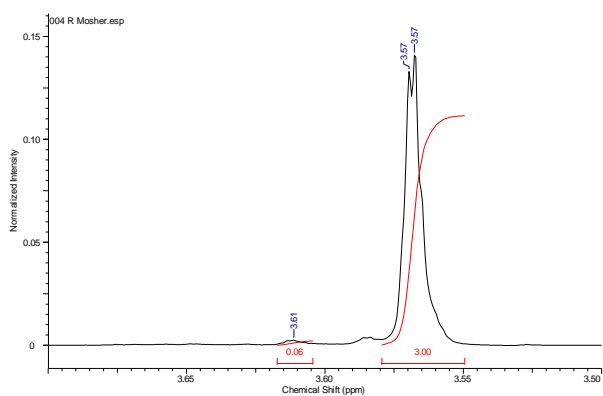
Methoxy protons ratio 3.00:0.05; (S)-4 *ee* = 96.8

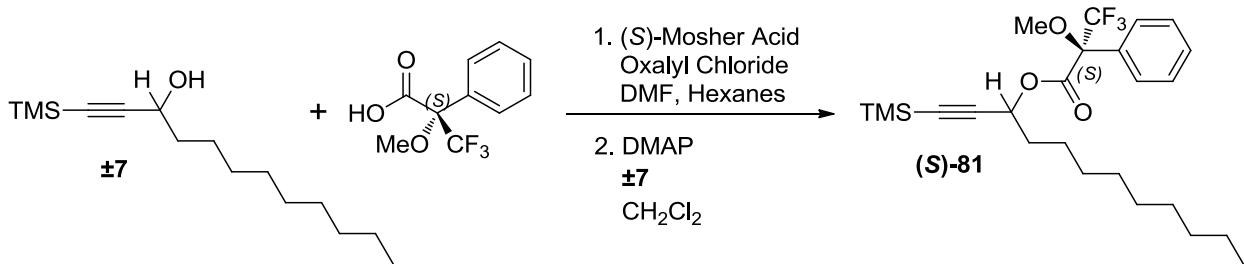




**(R,S)**-**80** Mosher Ester of **(R)**-**4** to determine ee of **(R)**-**5**

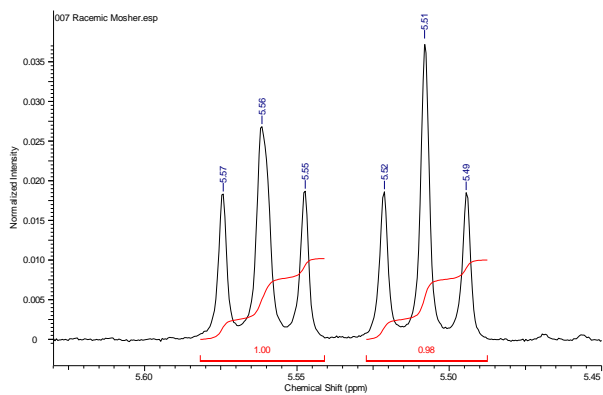
Methoxy protons ratio 0.06:3.00; **(R)**-**5** ee = 96.0

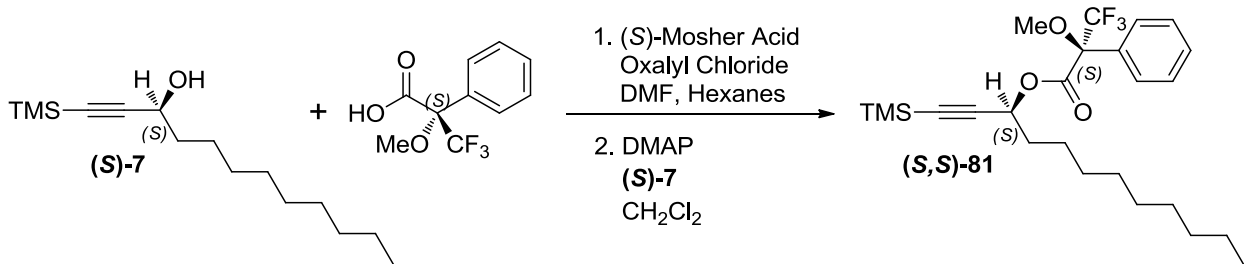




**(S)-81 Mosher Ester of  $\pm 7$**

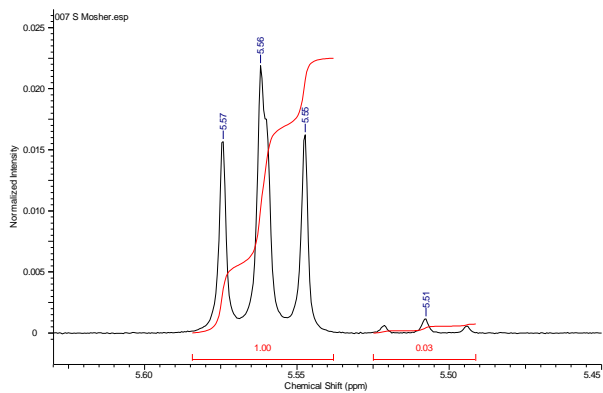
Methine proton ratio 1.00:0.98

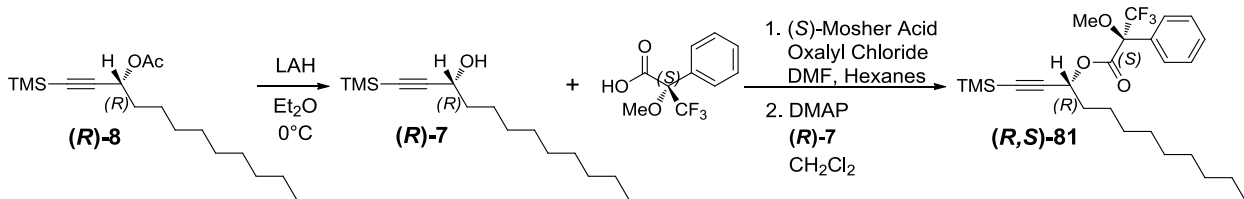




**(S,S)-81 Mosher Ester of (S)-7**

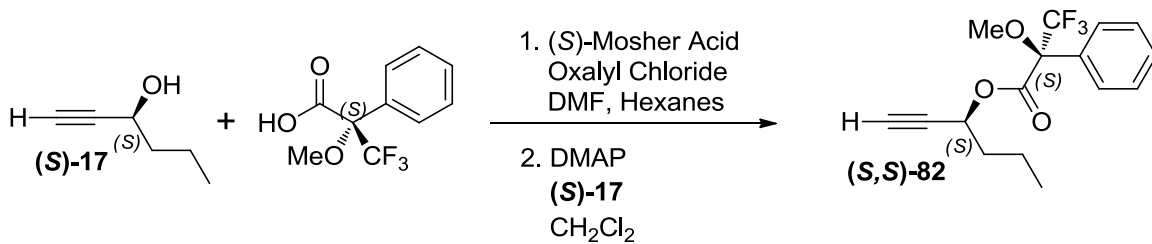
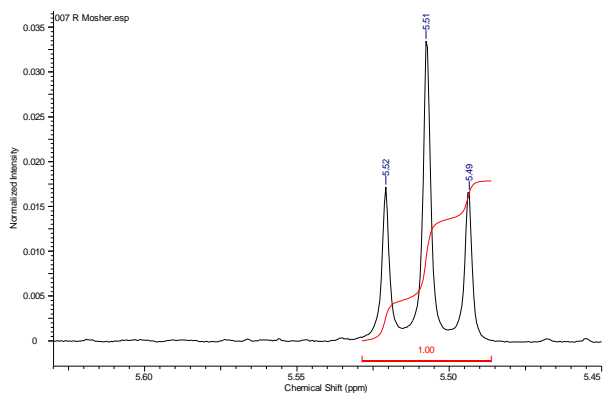
Methine proton ratio 1.00:0.03; (S)-7 *ee* = 94.2





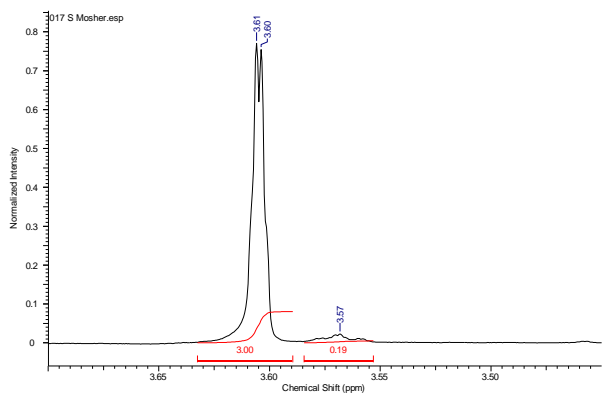
**(R,S)-81 Mosher Ester of (R)-7 to determine *ee* of (R)-8**

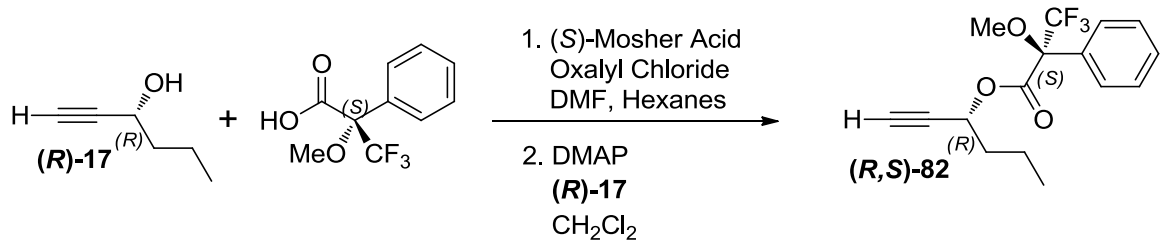
Methine proton ratio 0.00:1.00; **(R)-8** *ee* = 100.0



**(S,S)-82 Mosher Ester of (S)-17**

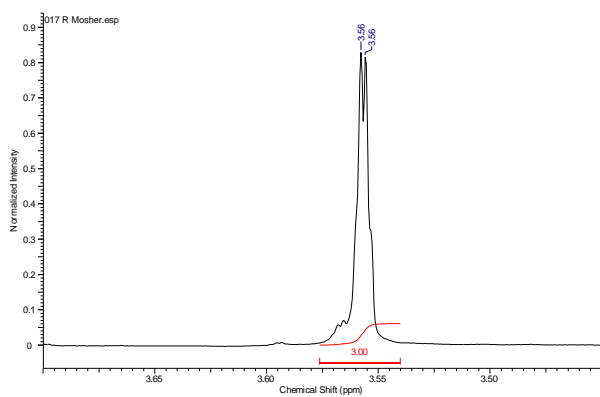
Methoxy protons ratio 3.00:0.19 ; **(S)-17** *ee* = 88.0



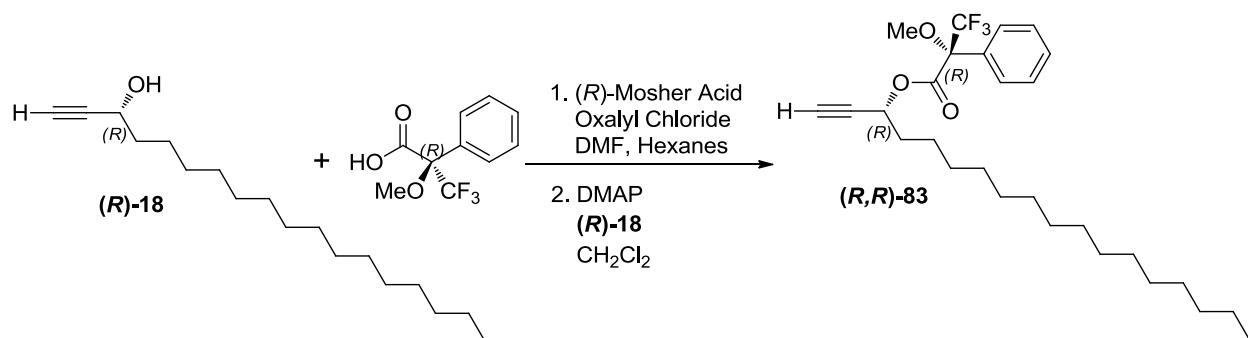


**(R,S)-82 Mosher Ester of (R)-17**

Methoxy protons ratio 0.00:3.00 ; **(R)-17** *ee* = 100.0

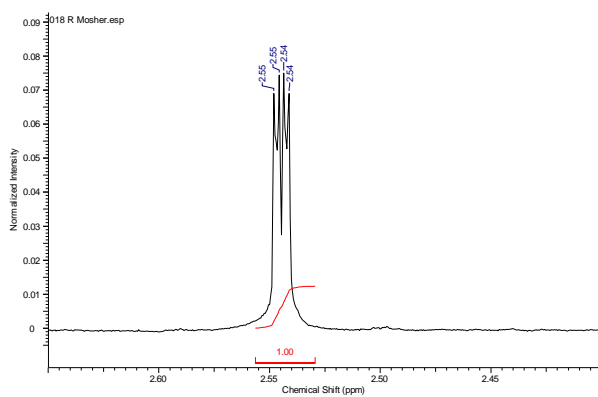


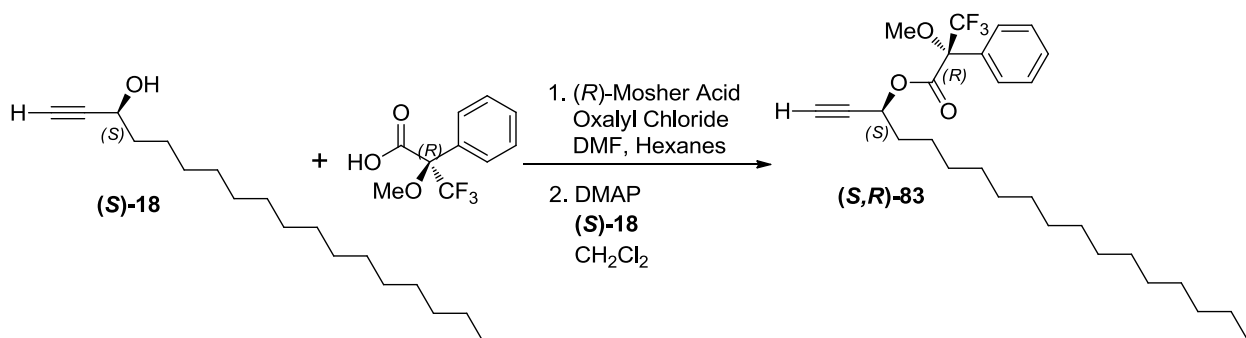




***(R,R)*-83 Mosher Ester of *(R)*-18**

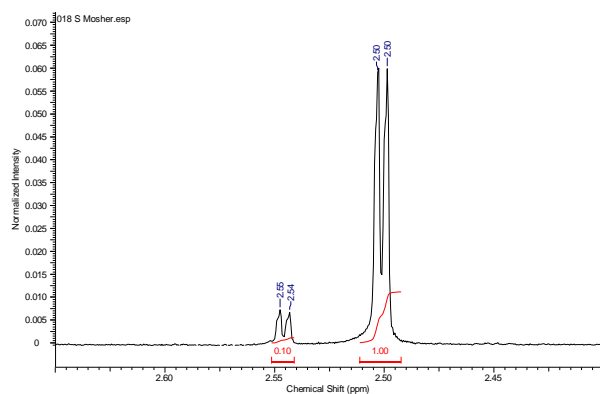
Terminal alkyne proton ratio 1.00:0.00; *(R)*-18 *ee* = 100.0



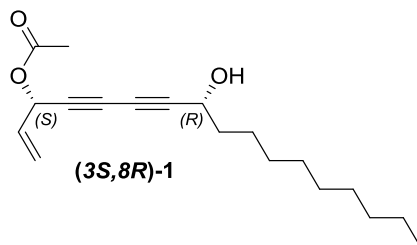


**(*S,R*)-83 Mosher Ester of (*S*)-18**

Terminal alkyne proton ratio 0.10:1.00; (*S*)-18 *ee* = 81.8

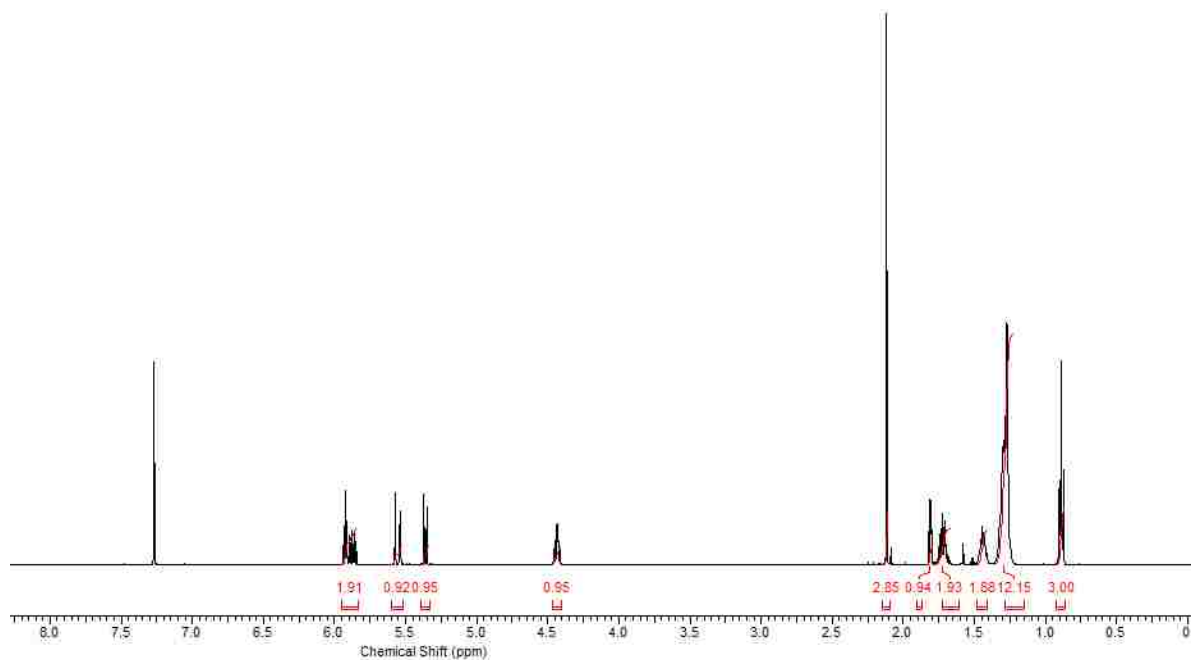


***Appendix A: Selected NMR spectra from synthesized compounds***

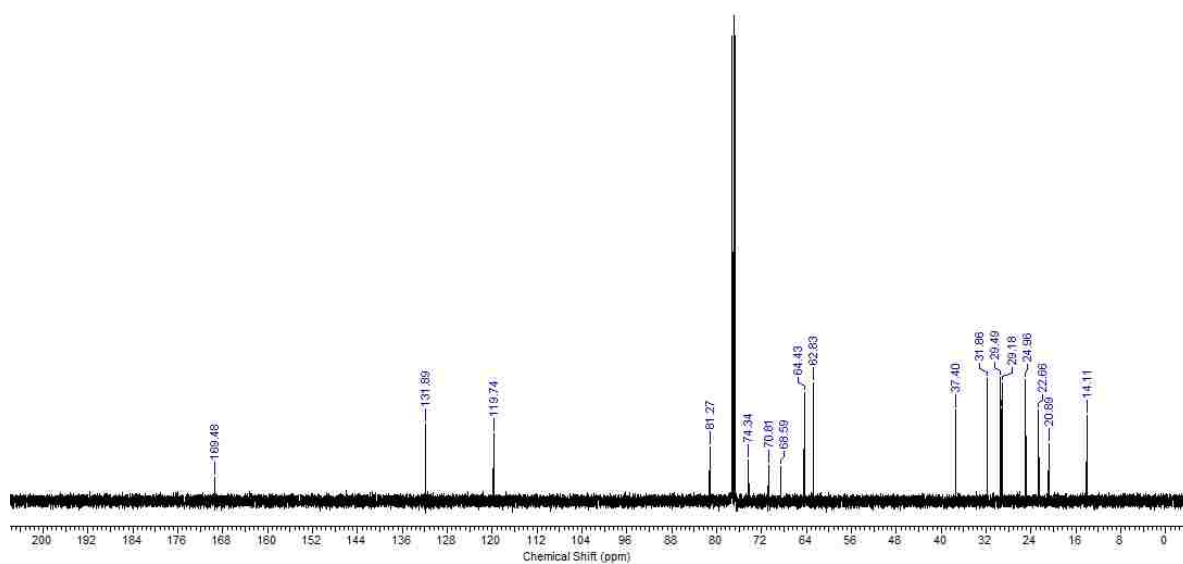


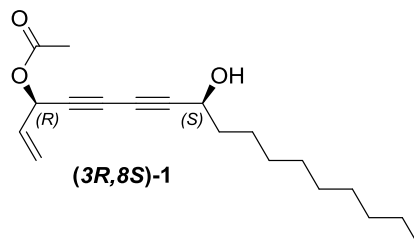
**(3*S*,8*R*)-8-hydroxyheptadeca-1-en-4,6-diyne-3-yl acetate**

**<sup>1</sup>H NMR:**



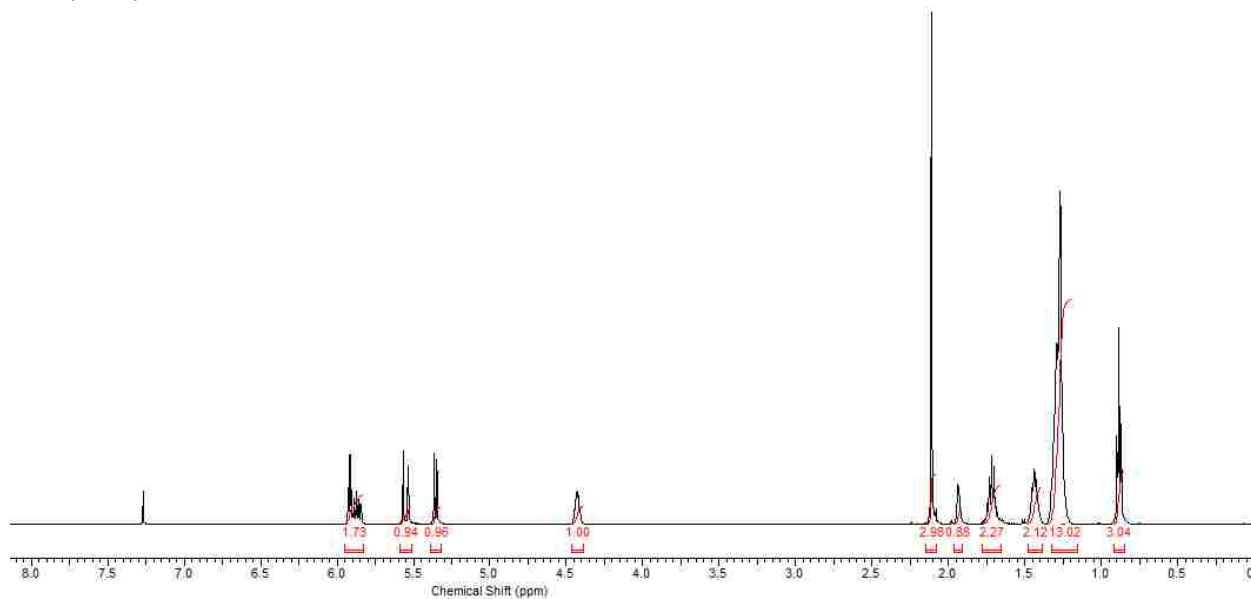
**<sup>13</sup>C NMR:**



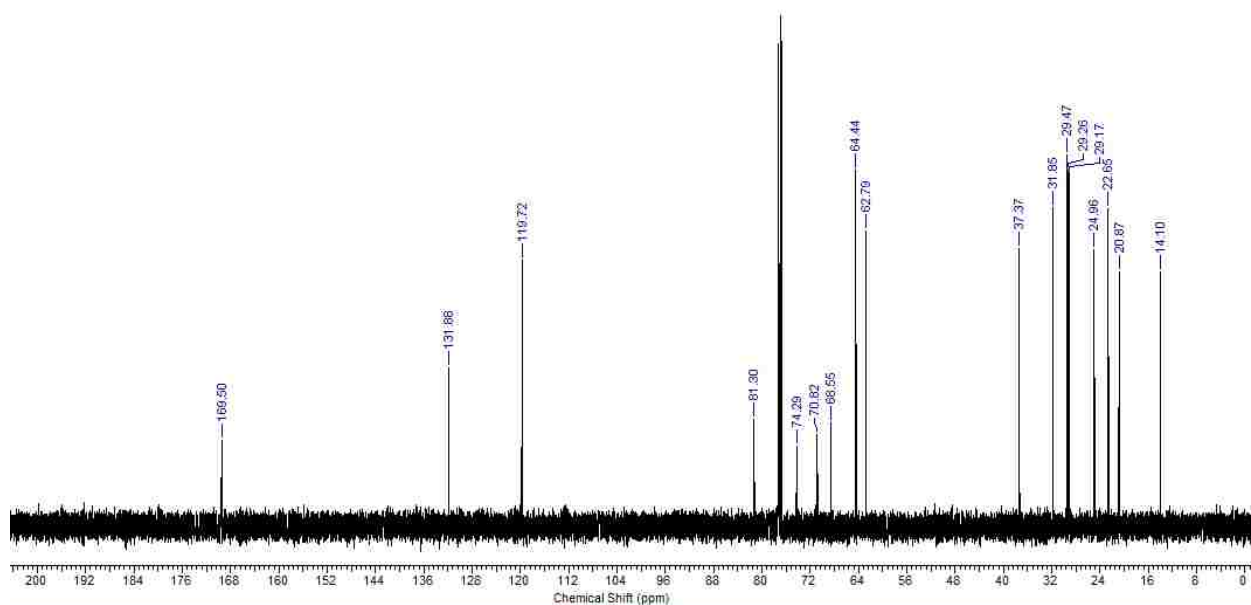


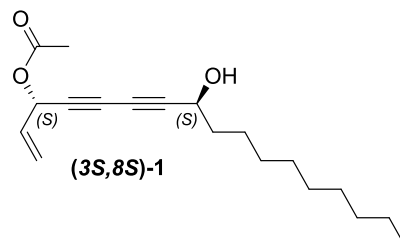
(3R,8S)-8-hydroxyheptadeca-1-en-4,6-diyne-3-yl acetate

<sup>1</sup>H NMR:



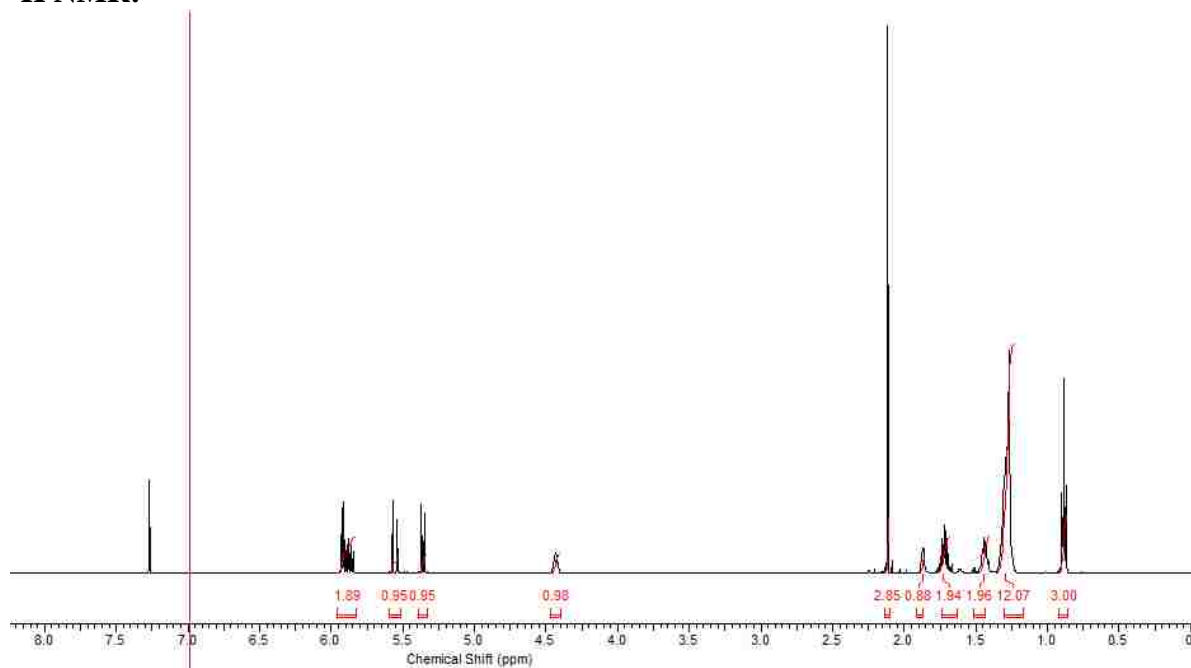
<sup>13</sup>C NMR:



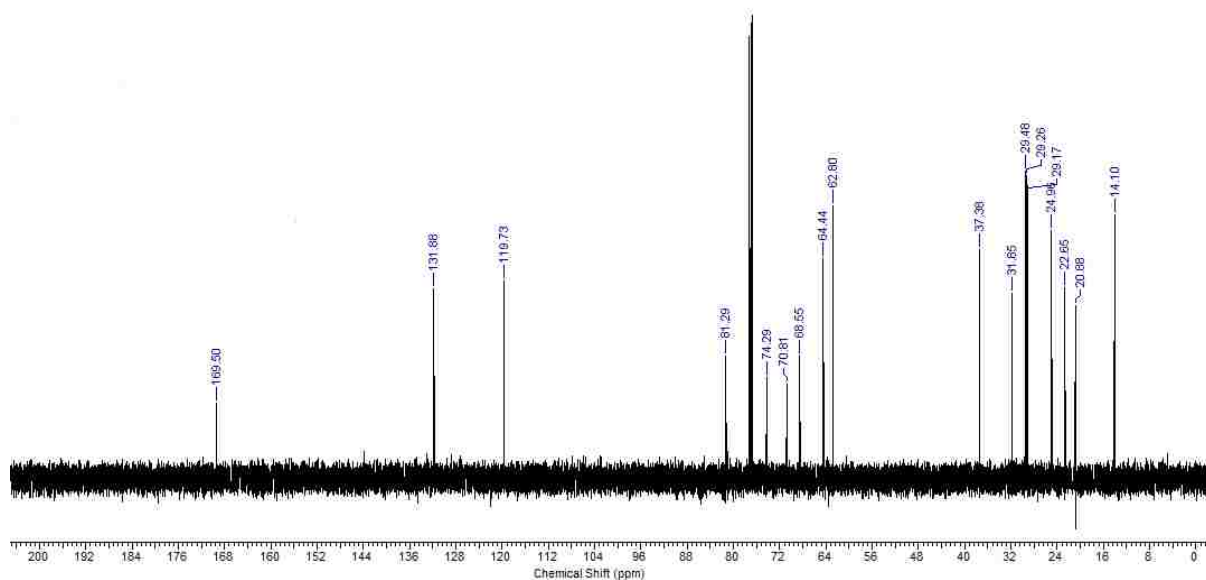


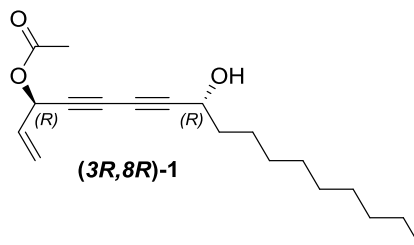
(3S,8S)-8-hydroxyheptadeca-1-en-4,6-diyne-3-yl acetate

<sup>1</sup>H NMR:



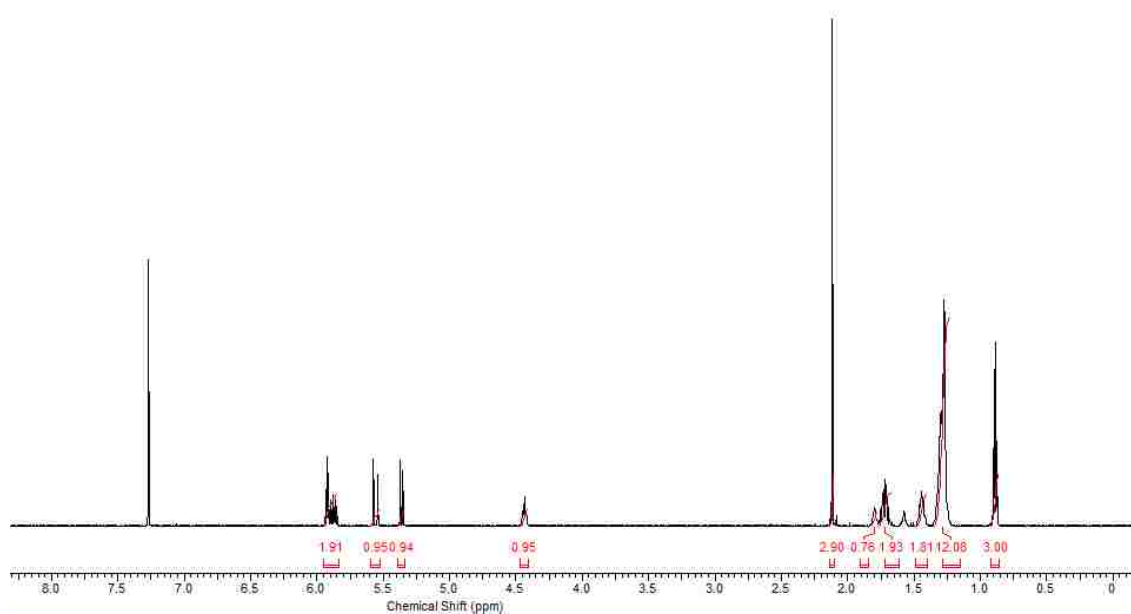
<sup>13</sup>C NMR:



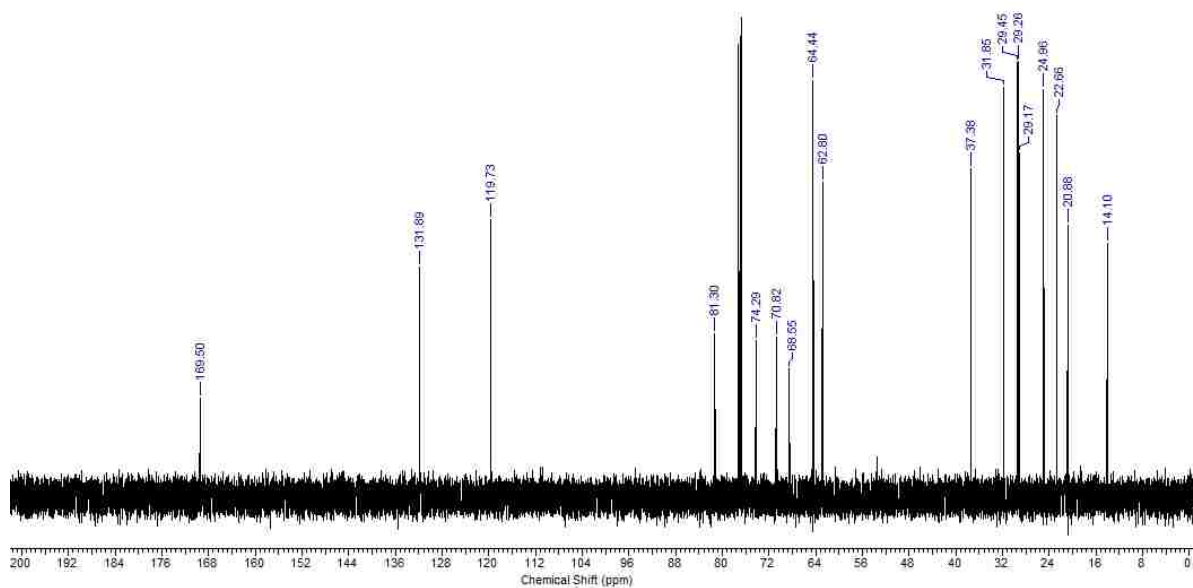


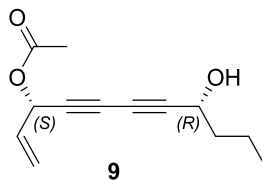
**(3R,8R)-8-hydroxyheptadeca-1-en-4,6-diyne-3-yl acetate**

**<sup>1</sup>H NMR:**



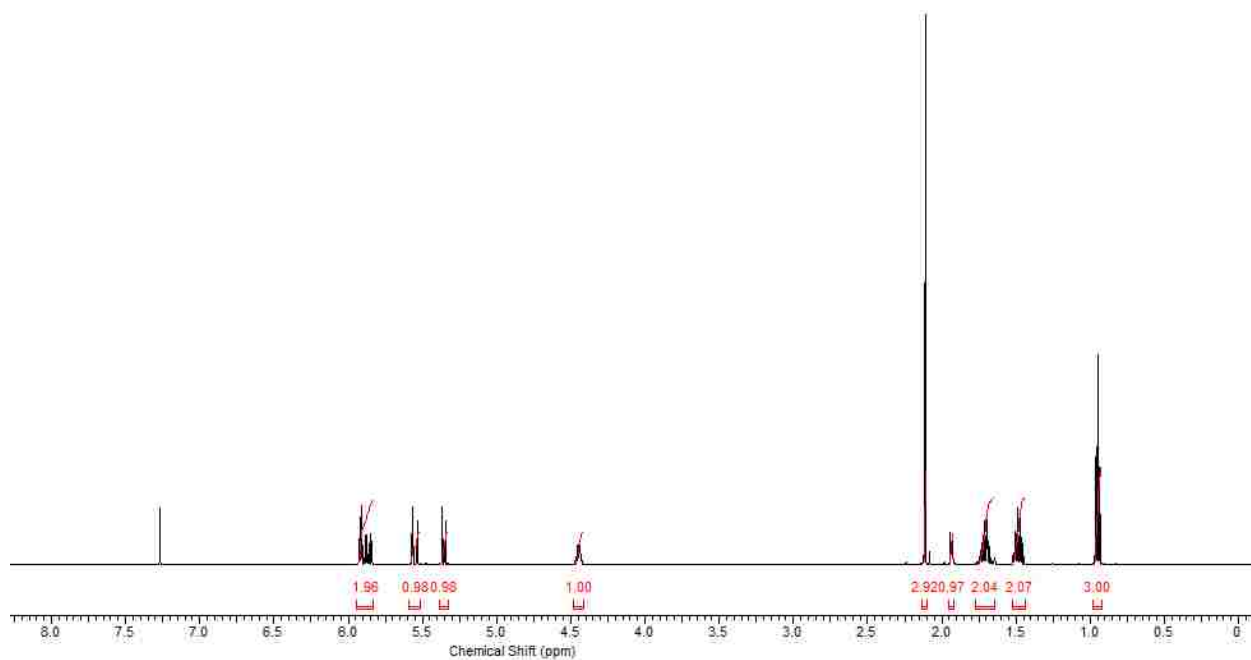
**<sup>13</sup>C NMR:**



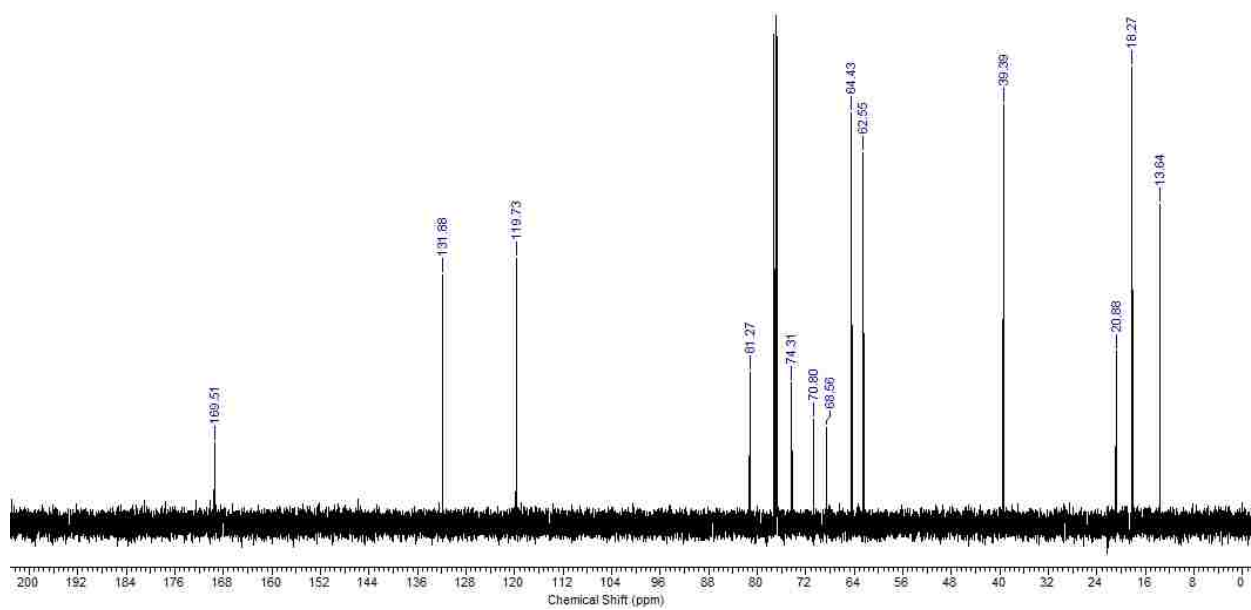


**(3*S*,8*R*)-8-hydroxyundeca-1-en-4,6-diyne-3-yl acetate**

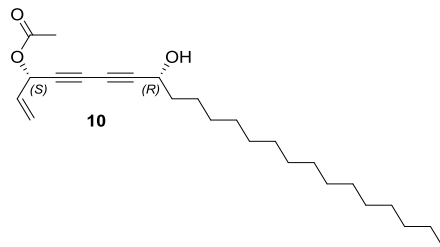
**<sup>1</sup>H NMR:**



**<sup>13</sup>C NMR:**

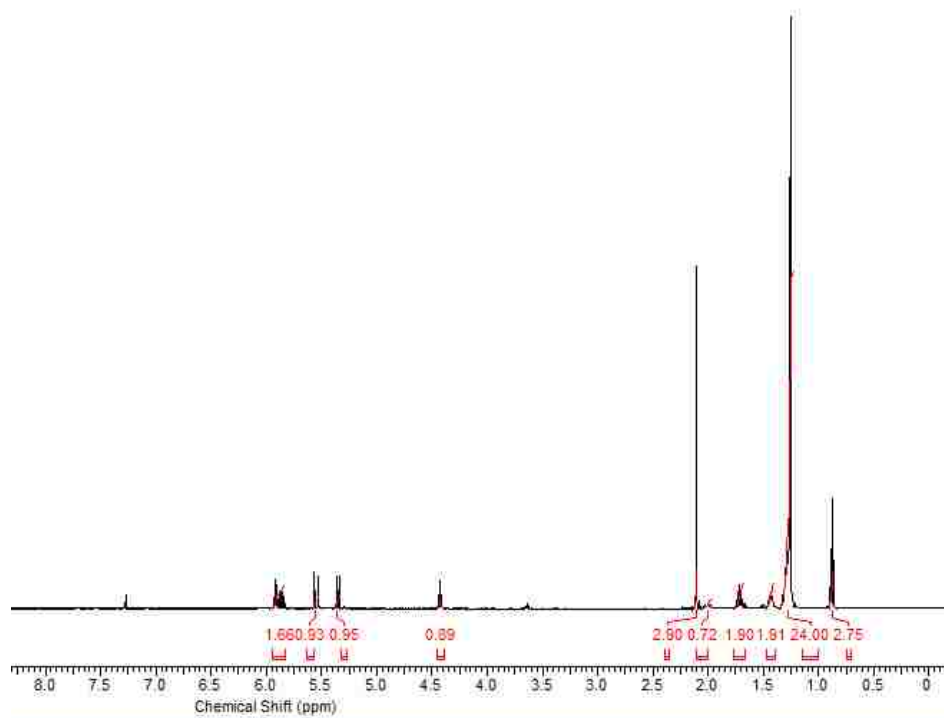




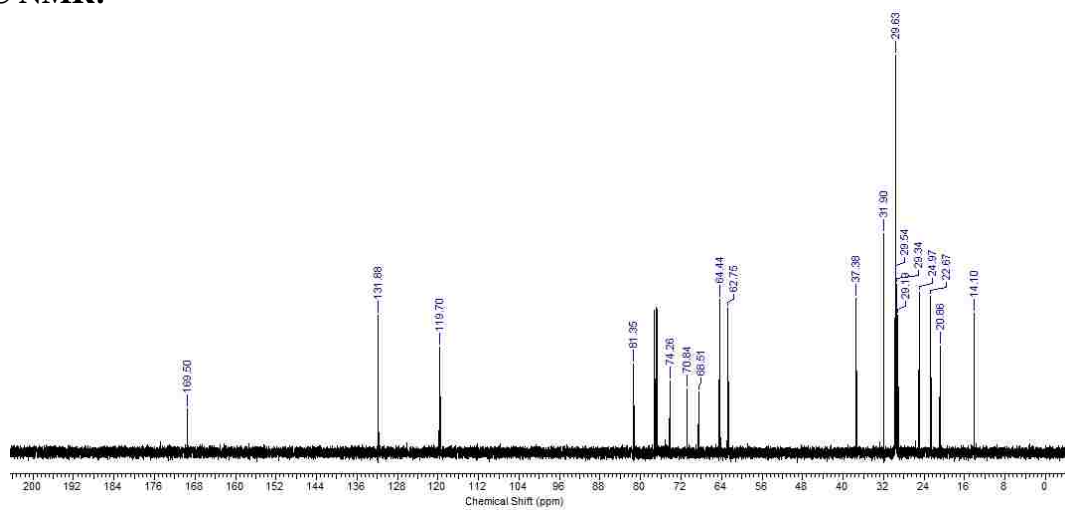


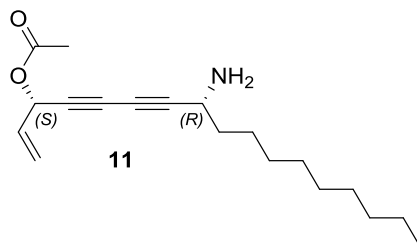
**(3*S*,8*R*)-8-hydroxytricos-1-en-4,6-diyne-3-yl acetate**

**<sup>1</sup>H NMR:**



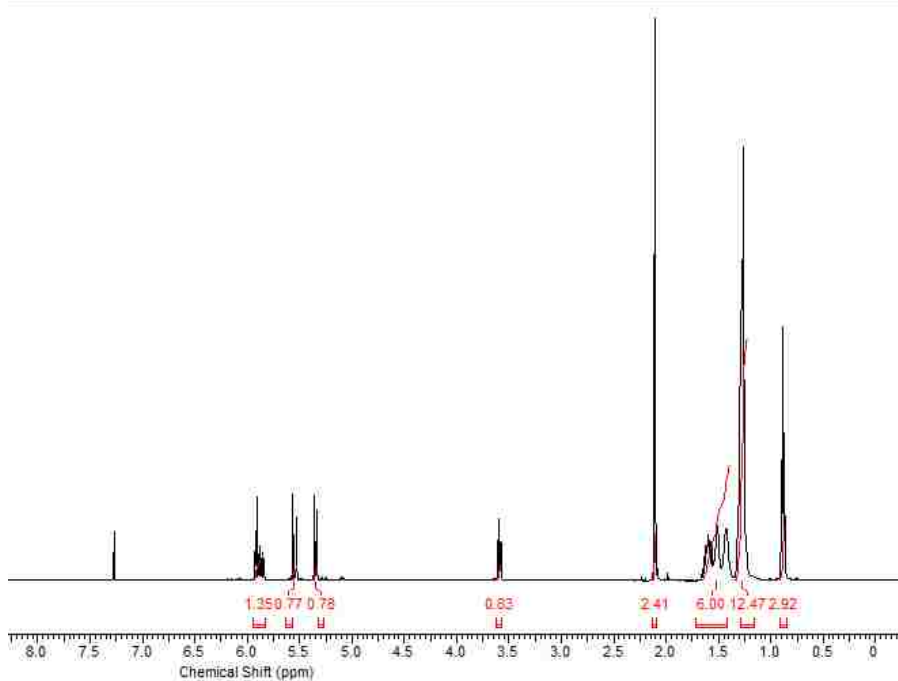
**<sup>13</sup>C NMR:**



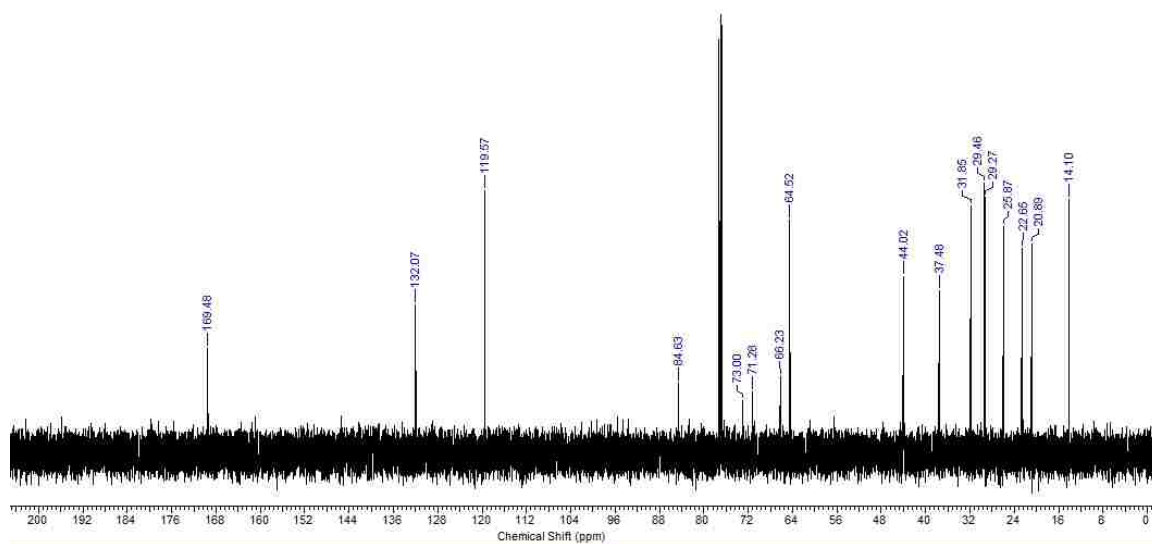


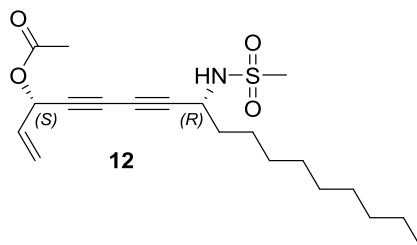
**(3*S*,8*R*)-8-aminoheptadeca-1-en-4,6-diyne-3-yl acetate**

**<sup>1</sup>H NMR:**



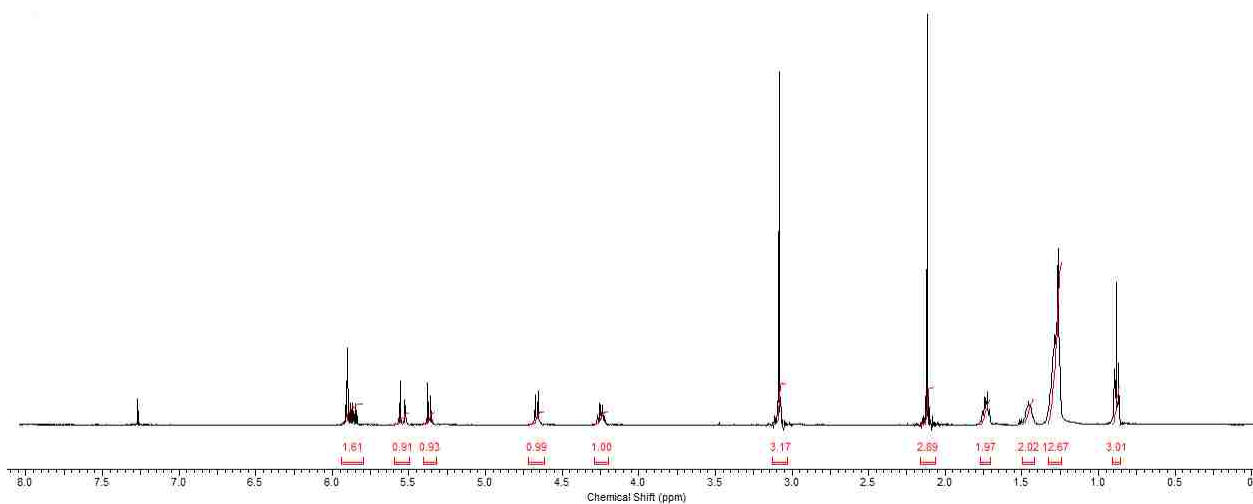
**<sup>13</sup>C NMR:**



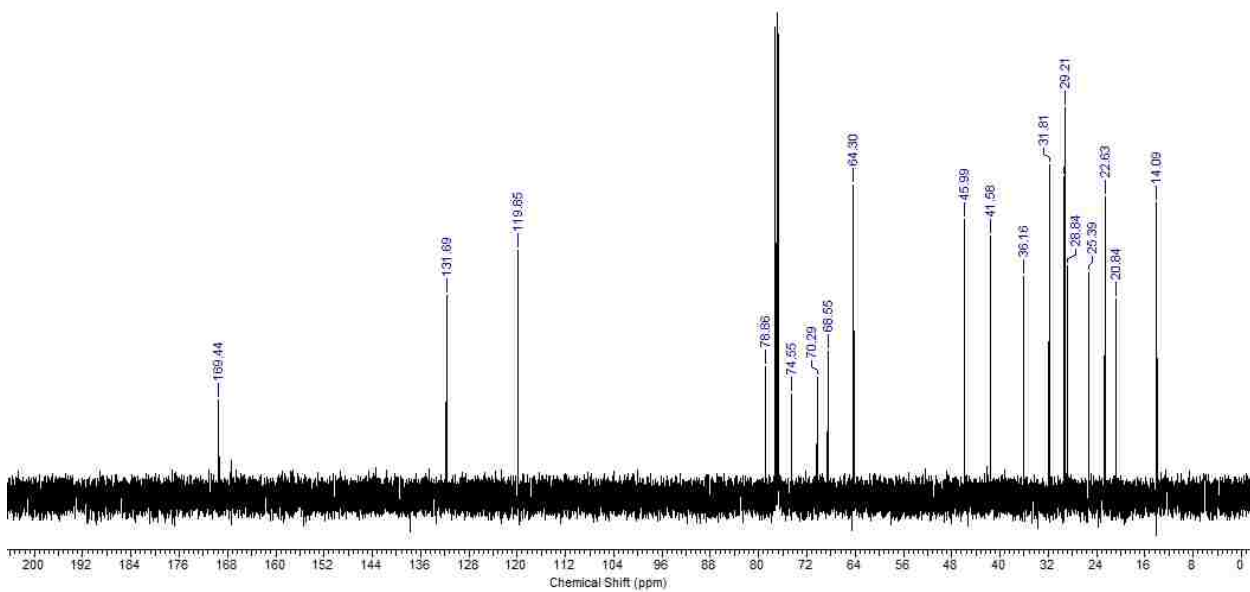


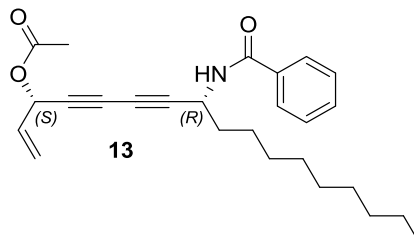
**(3*S*,8*R*)-8-(methylsulfonamido)heptadeca-1-en-4,6-diyn-3-yl acetate**

**<sup>1</sup>H NMR:**



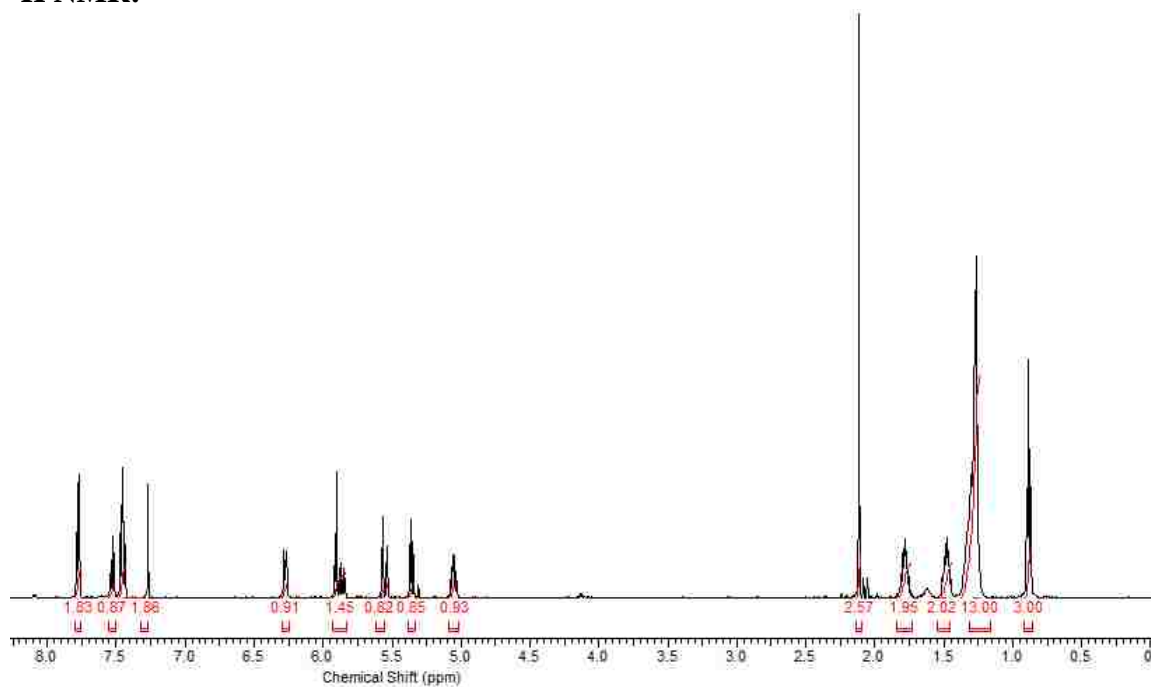
**<sup>13</sup>C NMR:**



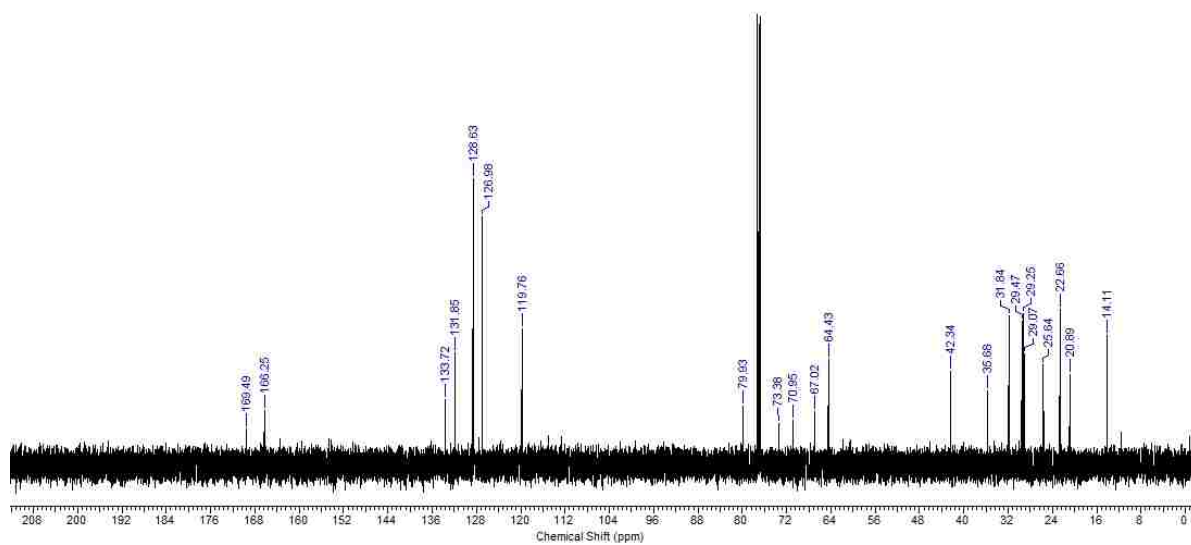


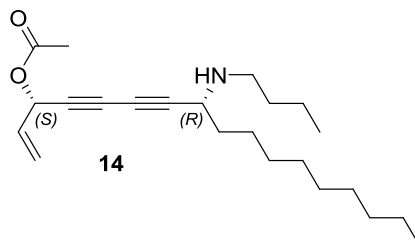
**(3*S*,8*R*)-8-benzamidoheptadeca-1-en-4,6-diyne-3-yl acetate**

**<sup>1</sup>H NMR:**



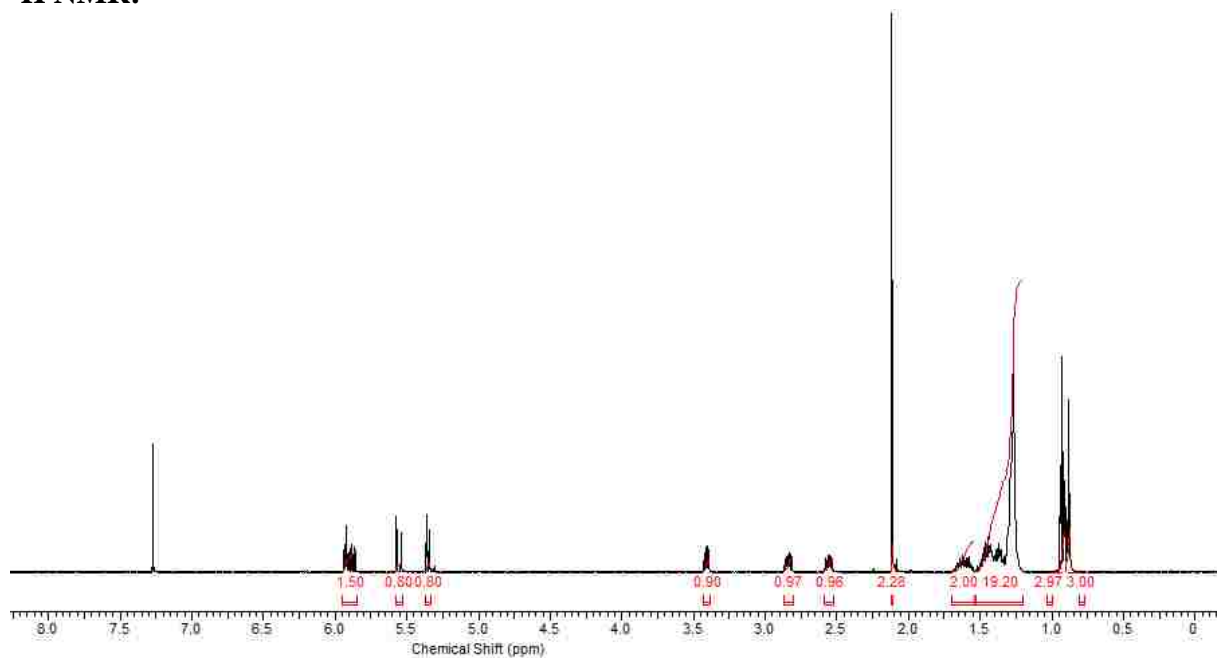
**<sup>13</sup>C NMR:**



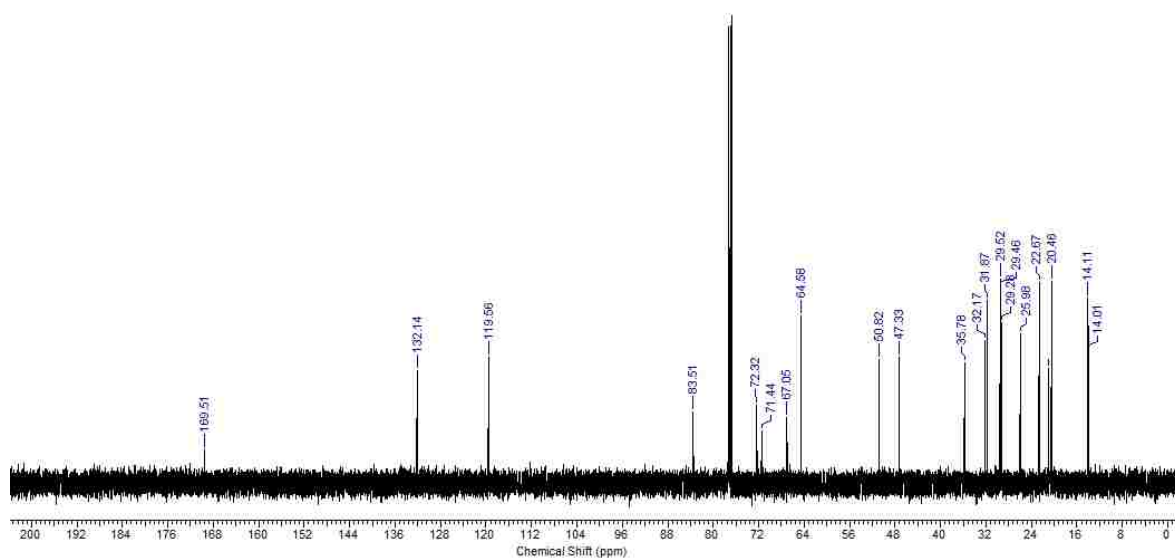


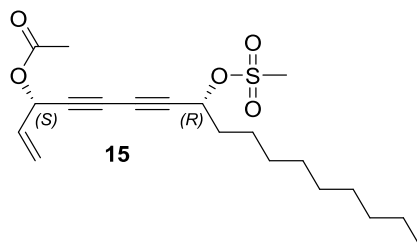
**(3*S*,8*R*)-8-(butylamino)heptadeca-1-en-4,6-diyne-3-yl acetate**

**<sup>1</sup>H NMR:**



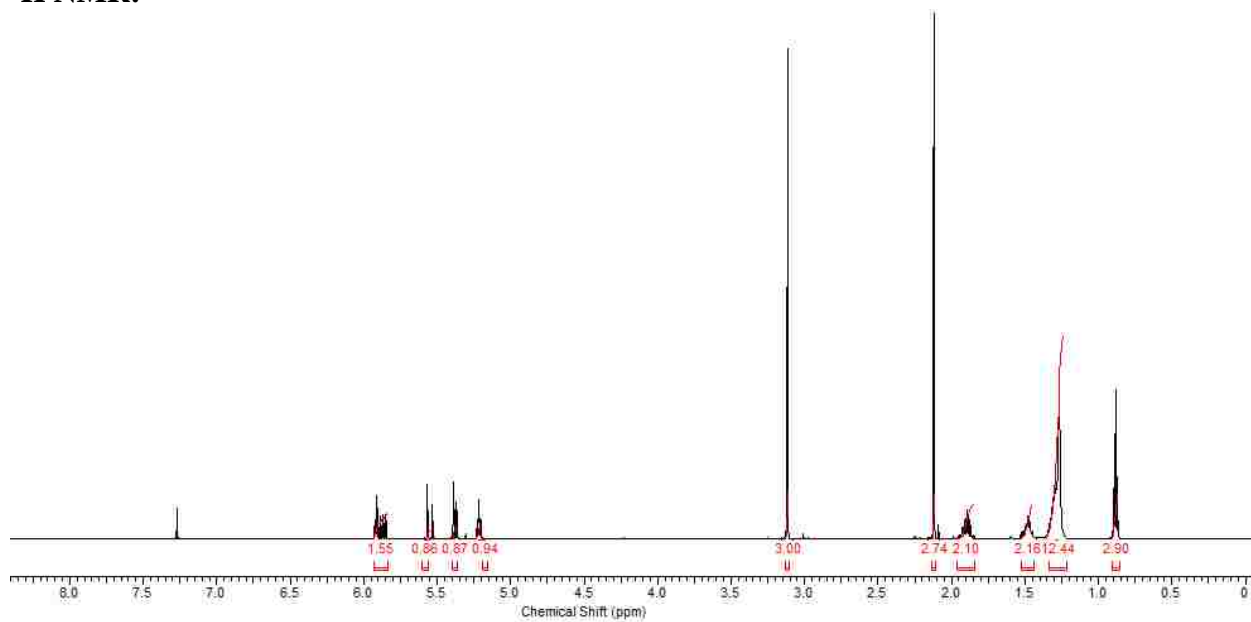
**<sup>13</sup>C NMR:**



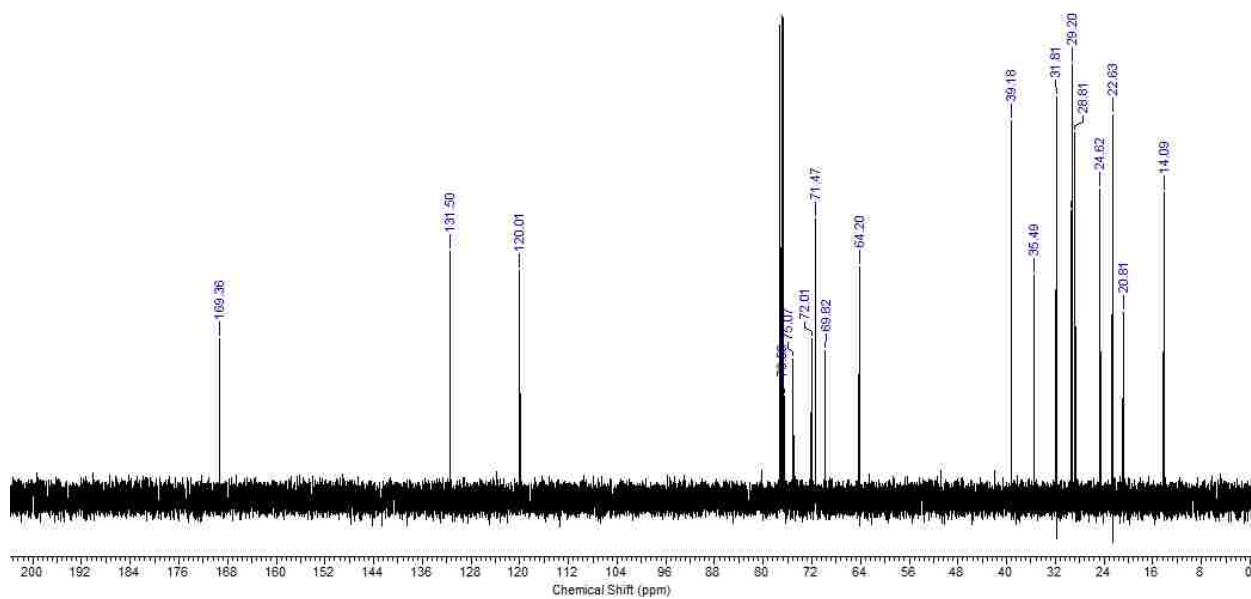


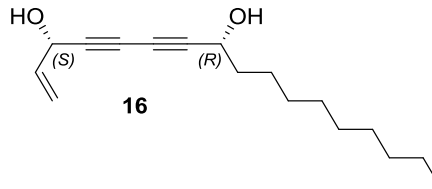
**(3*S*,8*R*)-8-((methylsulfonyl)oxy)heptadeca-1-en-4,6-diyne-3-yl acetate**

**<sup>1</sup>H NMR:**



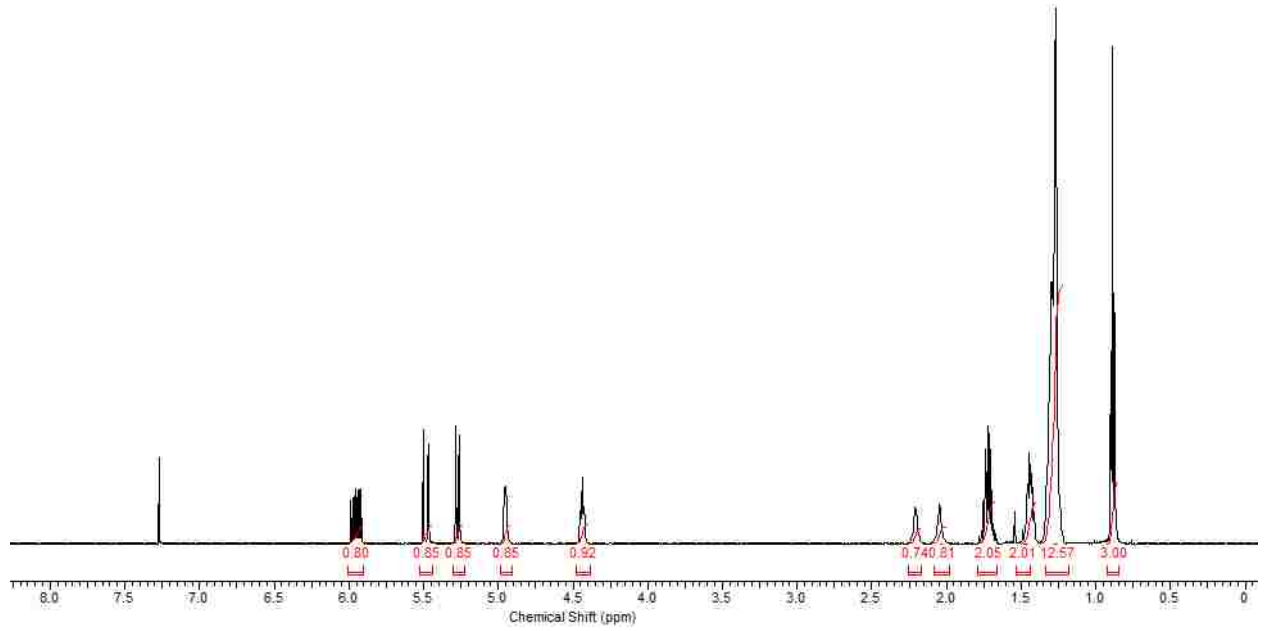
**<sup>13</sup>C NMR:**



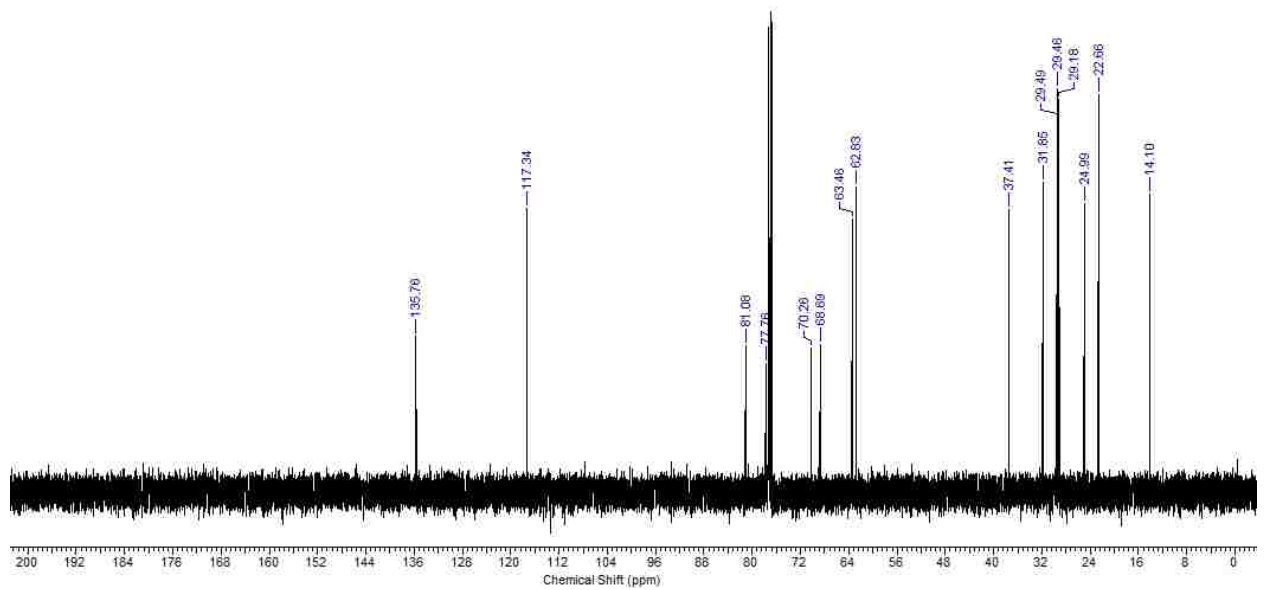


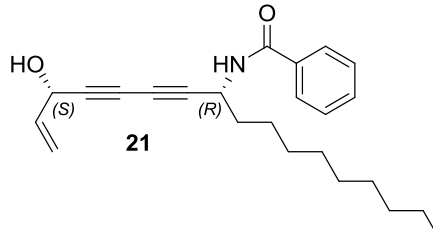
**(3*S*,8*R*)-heptadeca-1-en-4,6-diyne-3,8-diol**

**<sup>1</sup>H NMR:**



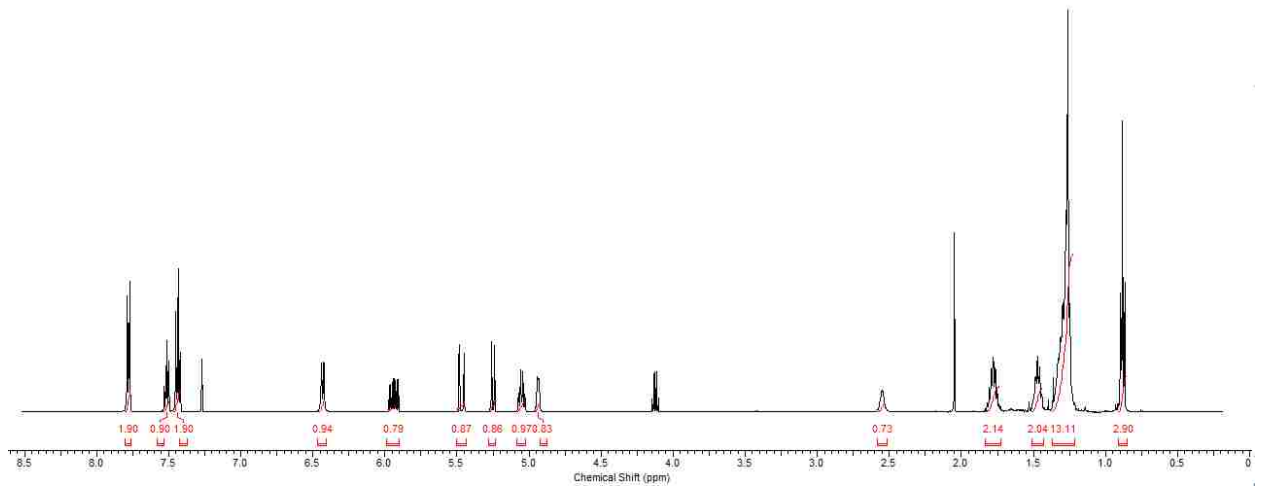
**<sup>13</sup>C NMR:**



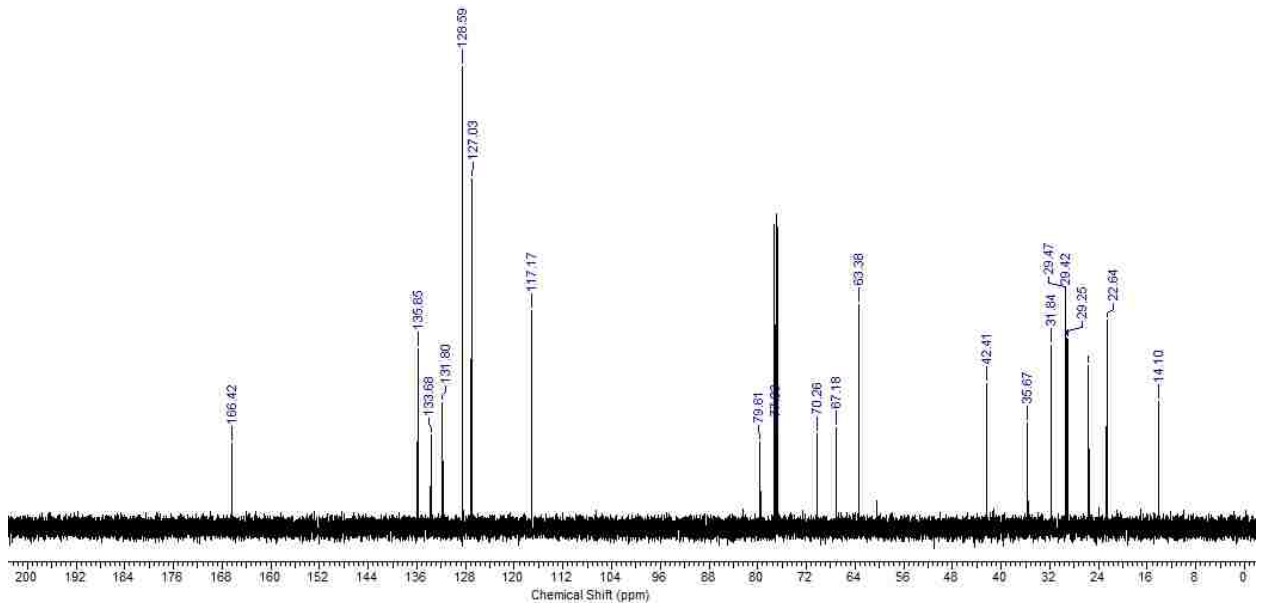


*N*-((3*S*,8*R*)-3-hydroxyheptadeca-1-en-4,6-diyn-8-yl)benzamide

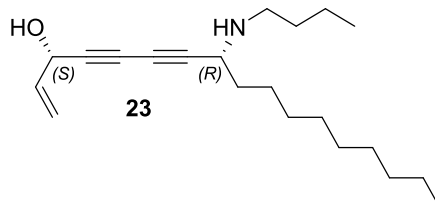
**<sup>1</sup>H NMR:**



**<sup>13</sup>C NMR:**

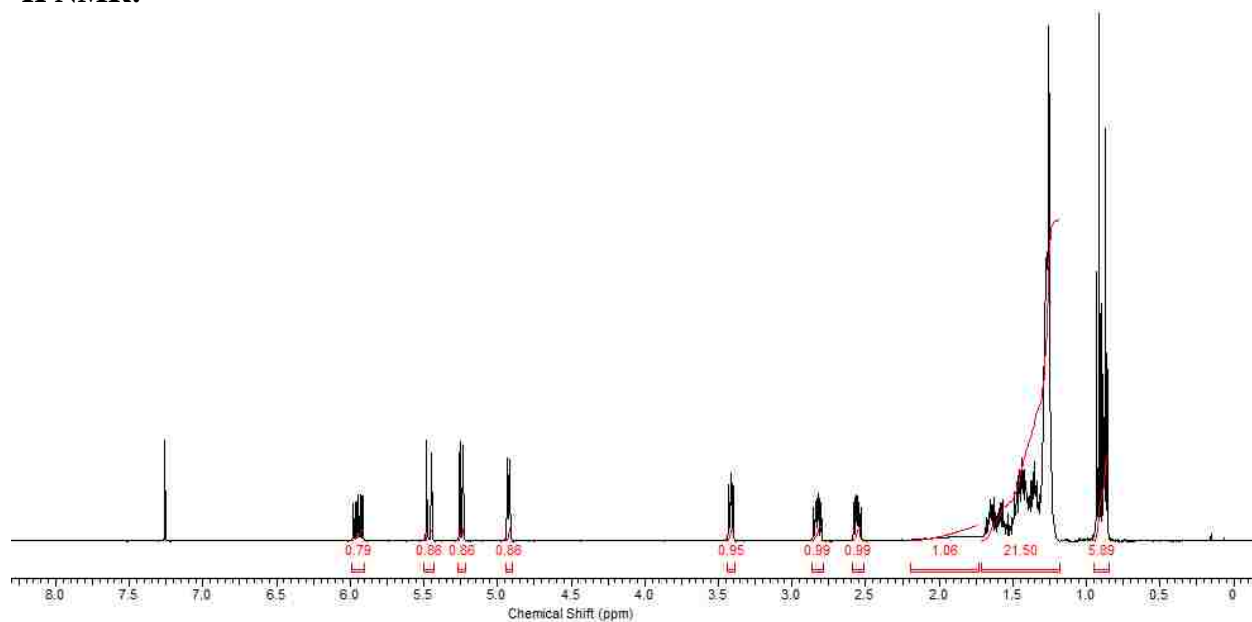




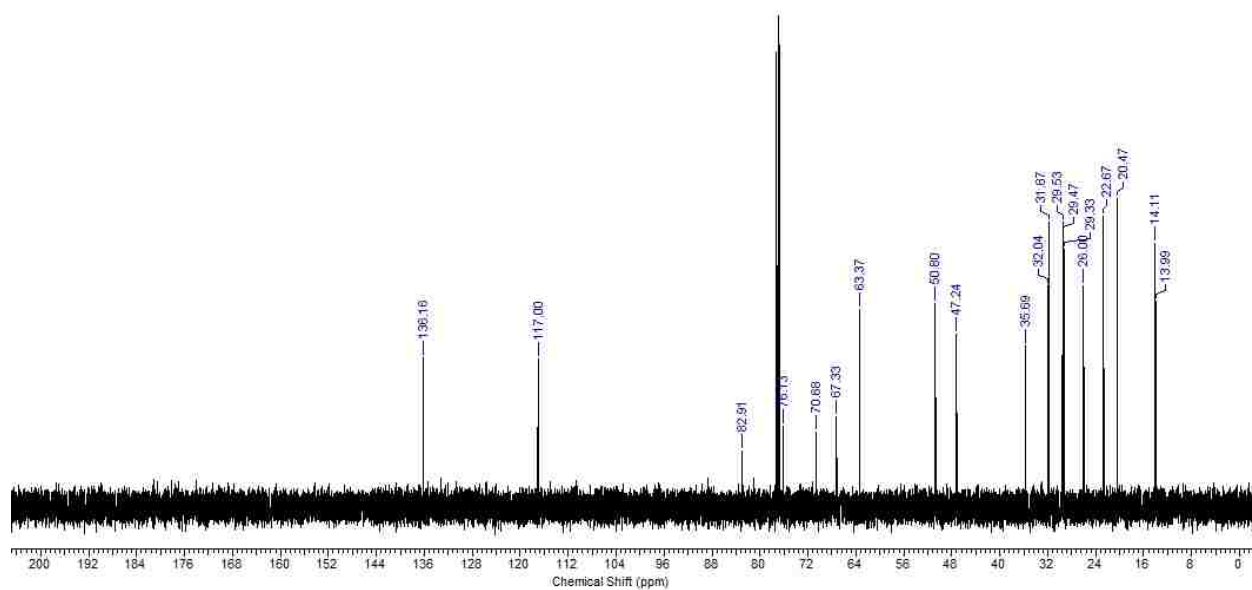


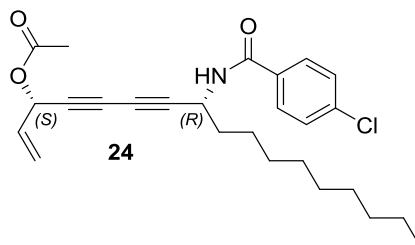
**(3*S*,8*R*)-8-(butylamino)heptadeca-1-en-4,6-diyn-3-ol**

**<sup>1</sup>H NMR:**



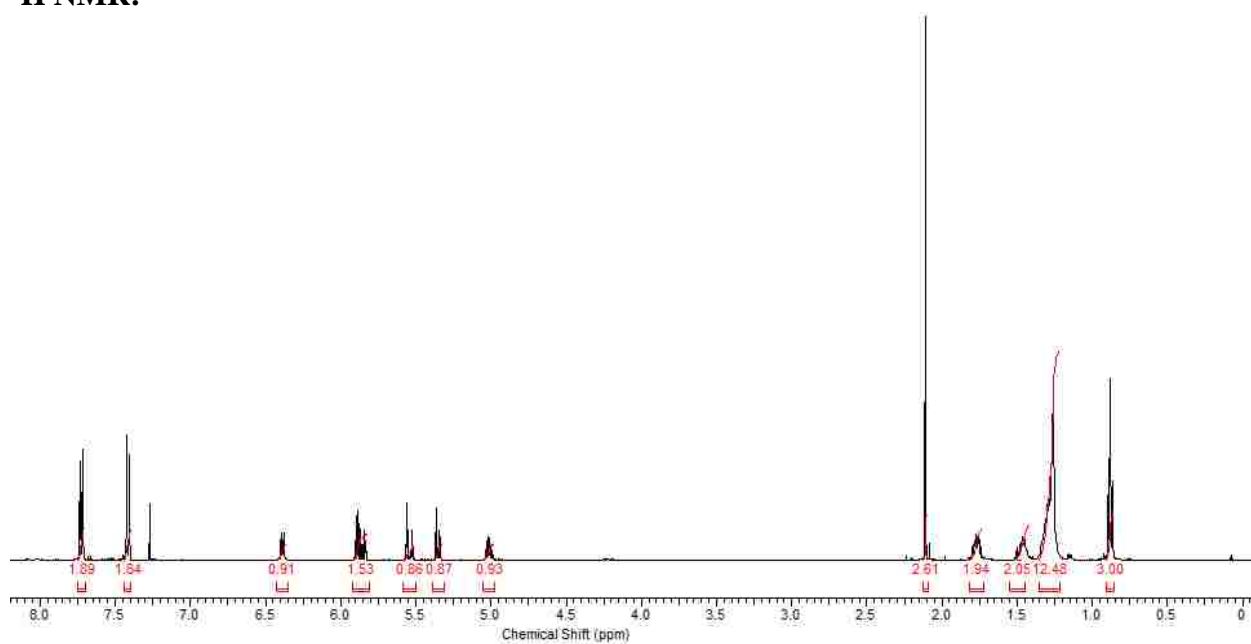
**<sup>13</sup>C NMR:**



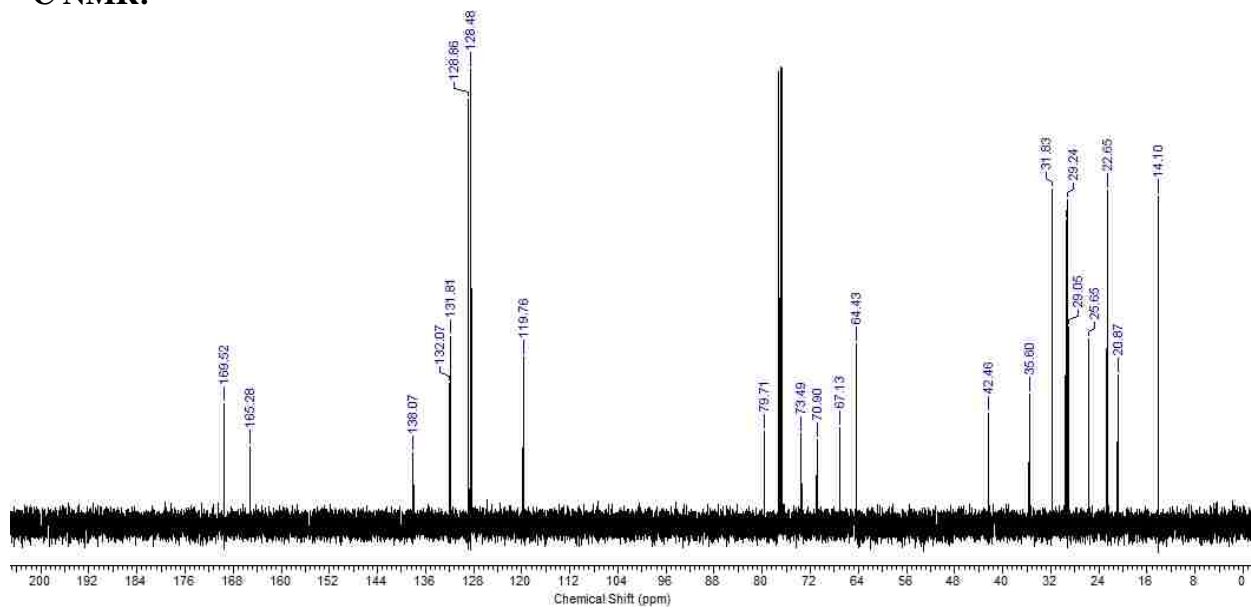


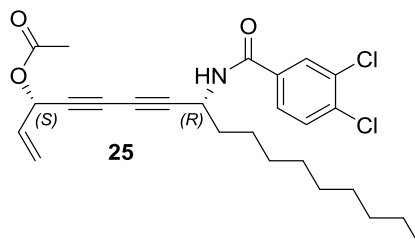
**(3*S*,8*R*)-8-(4-chlorobenzamido)heptadeca-1-en-4,6-diyn-3-yl acetate**

**<sup>1</sup>H NMR:**



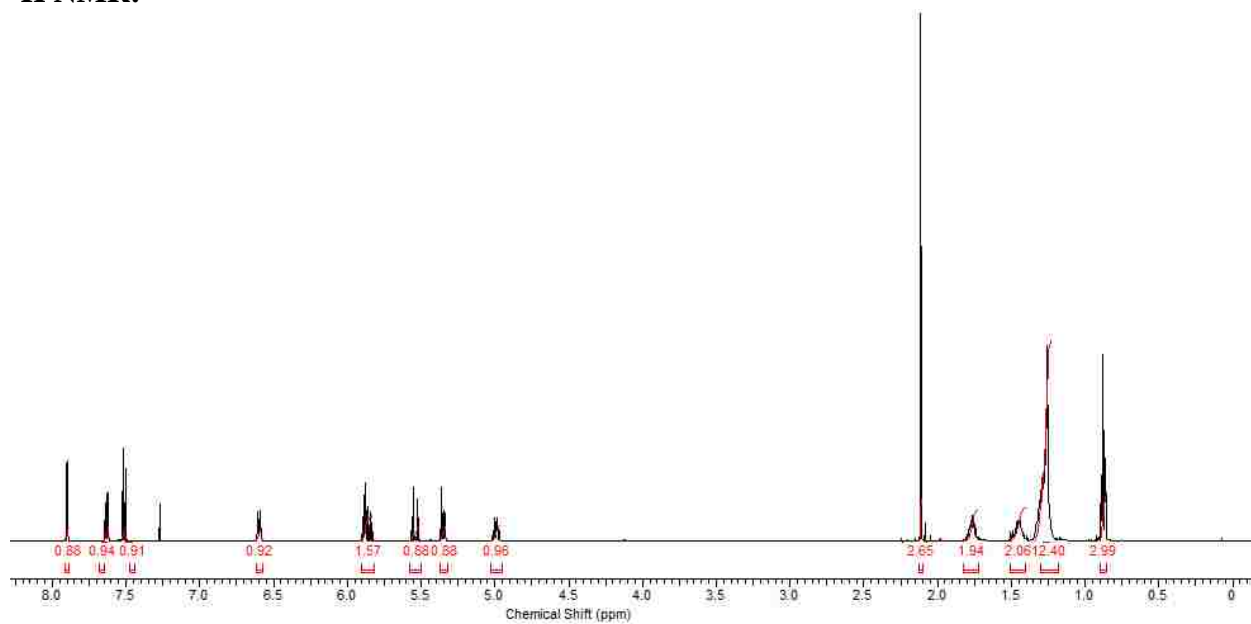
**<sup>13</sup>C NMR:**



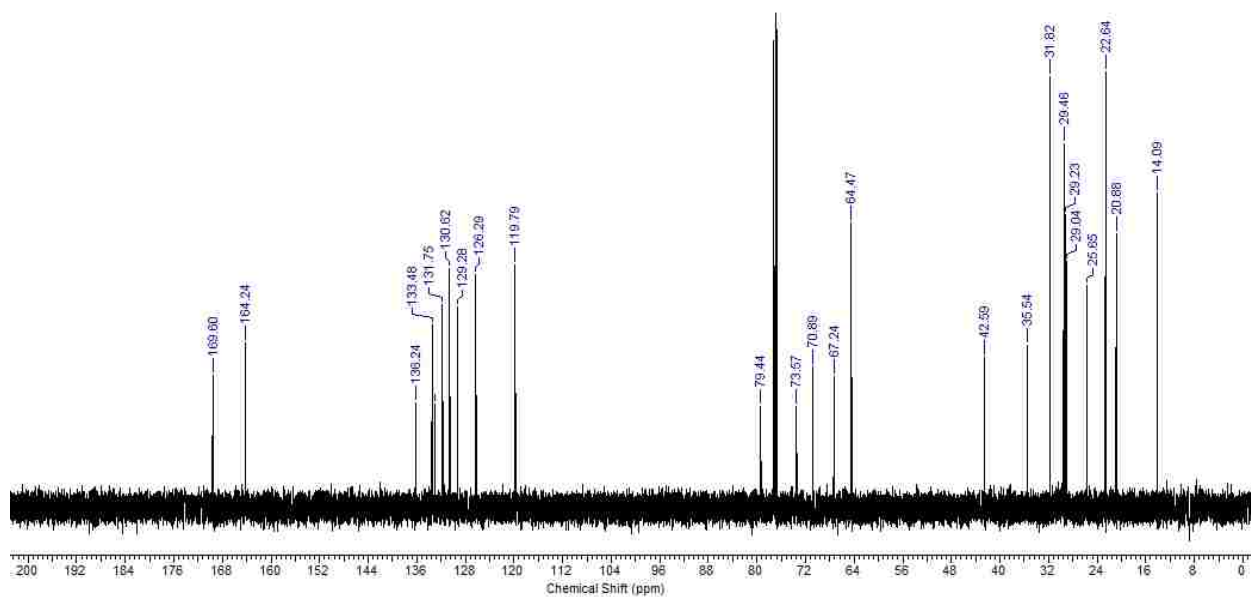


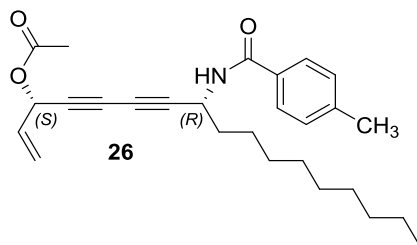
**(3*S*,8*R*)-8-(3,4-dichlorobenzamido)heptadeca-1-en-4,6-diyne-3-yl acetate**

**<sup>1</sup>H NMR:**



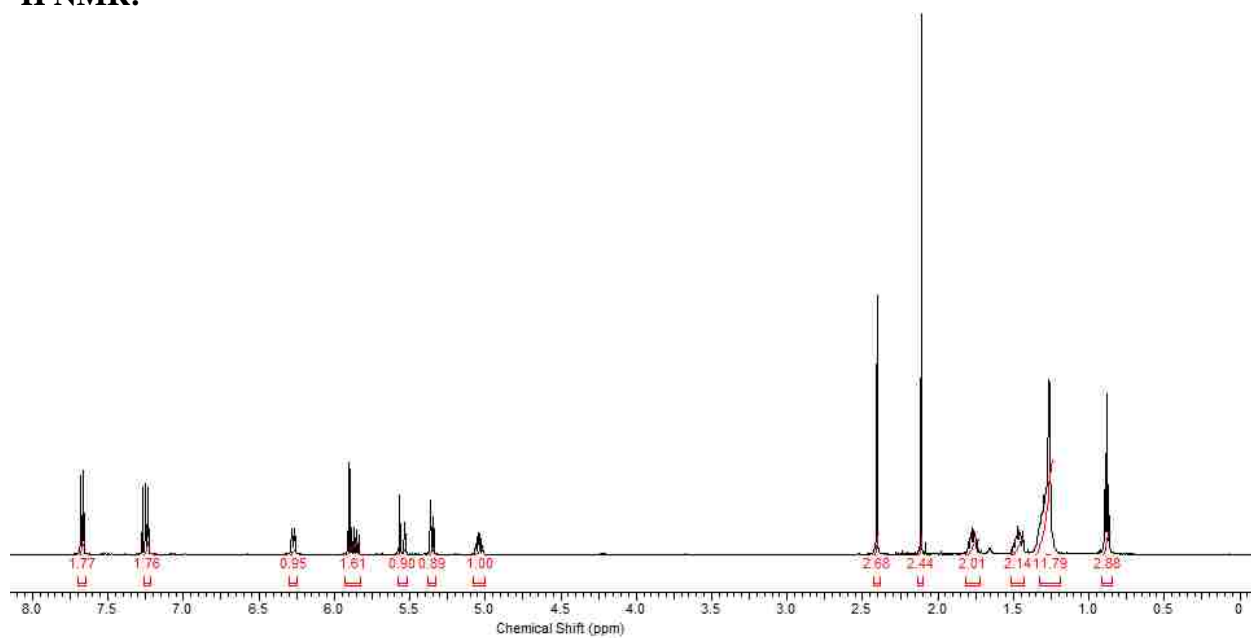
**<sup>13</sup>C NMR:**



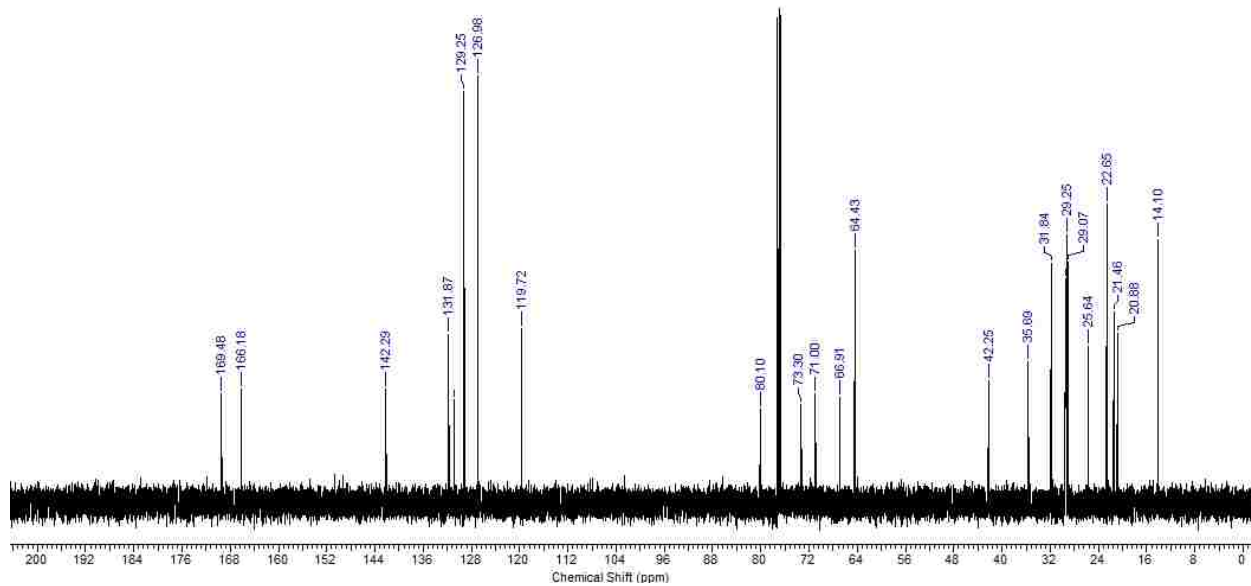


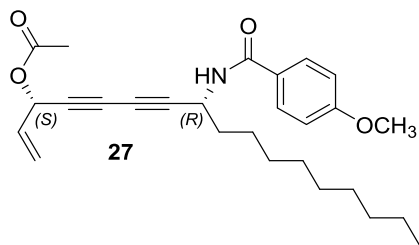
**(3*S*,8*R*)-8-(4-methylbenzamido)heptadeca-1-en-4,6-diyn-3-yl acetate**

**<sup>1</sup>H NMR:**



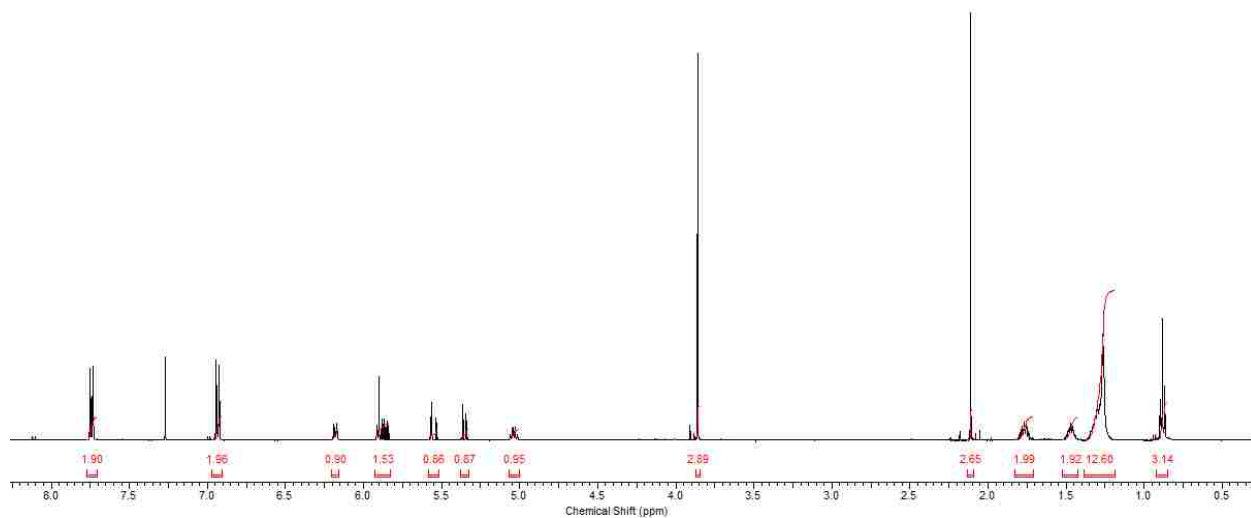
**<sup>13</sup>C NMR:**



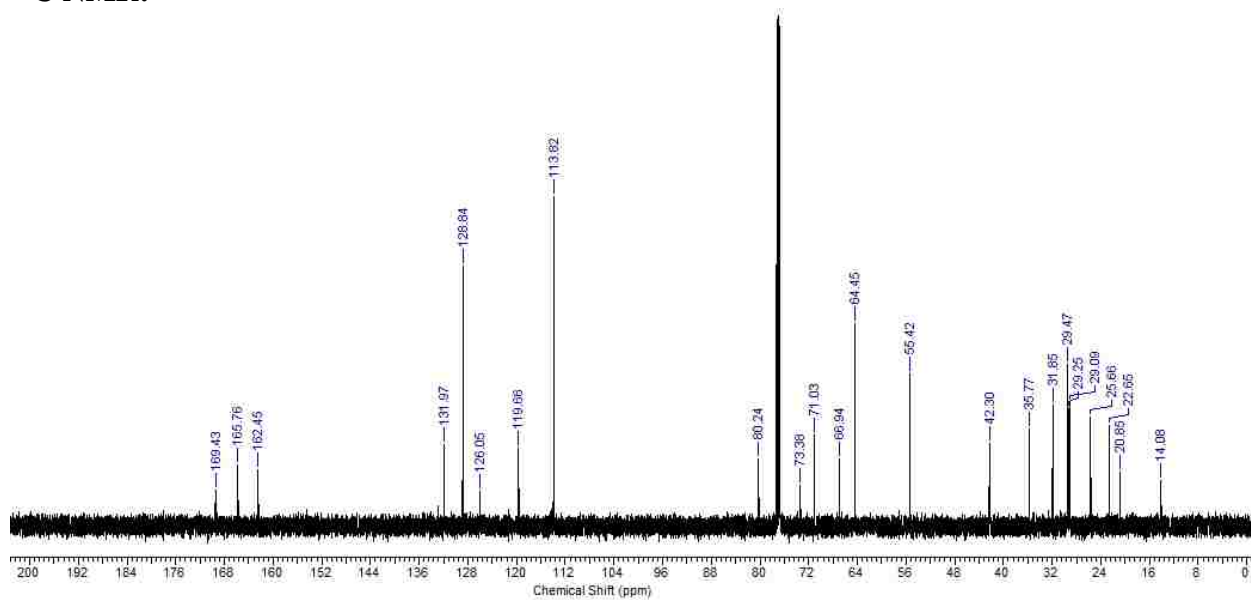


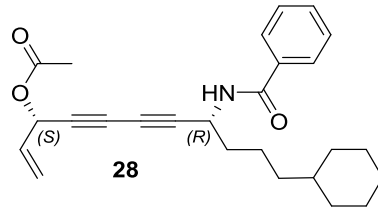
**(3*S*,8*R*)-8-(4-methoxybenzamido)heptadeca-1-en-4,6-diyne-3-yl acetate**

**<sup>1</sup>H NMR:**



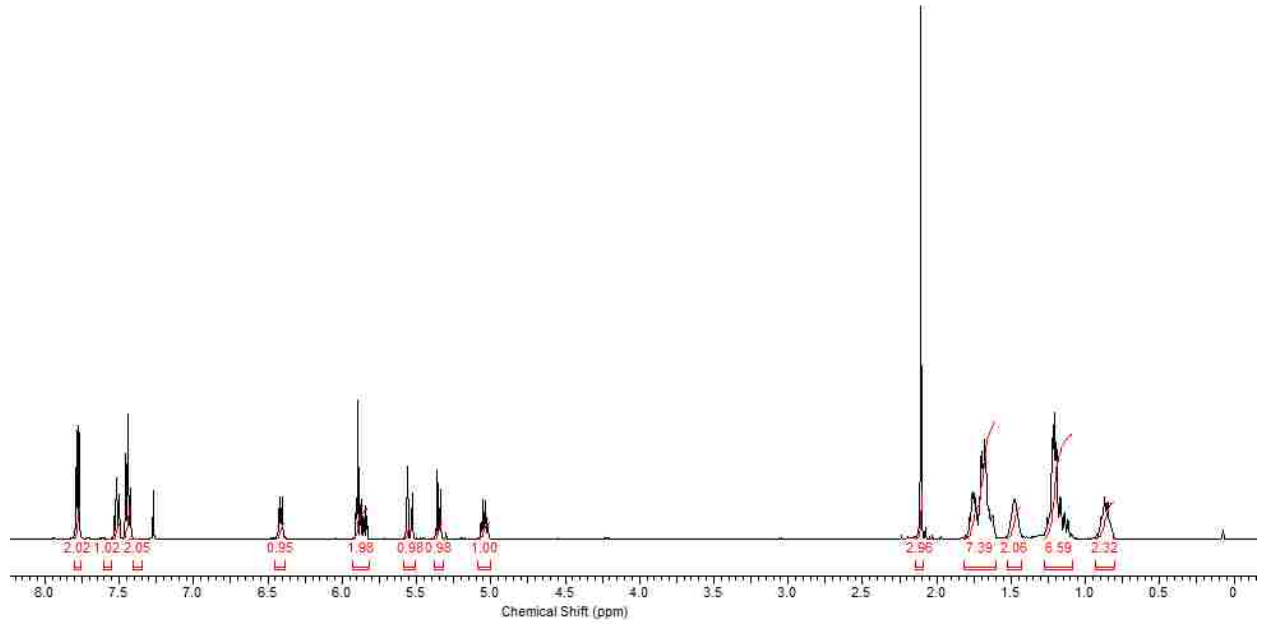
**<sup>13</sup>C NMR:**



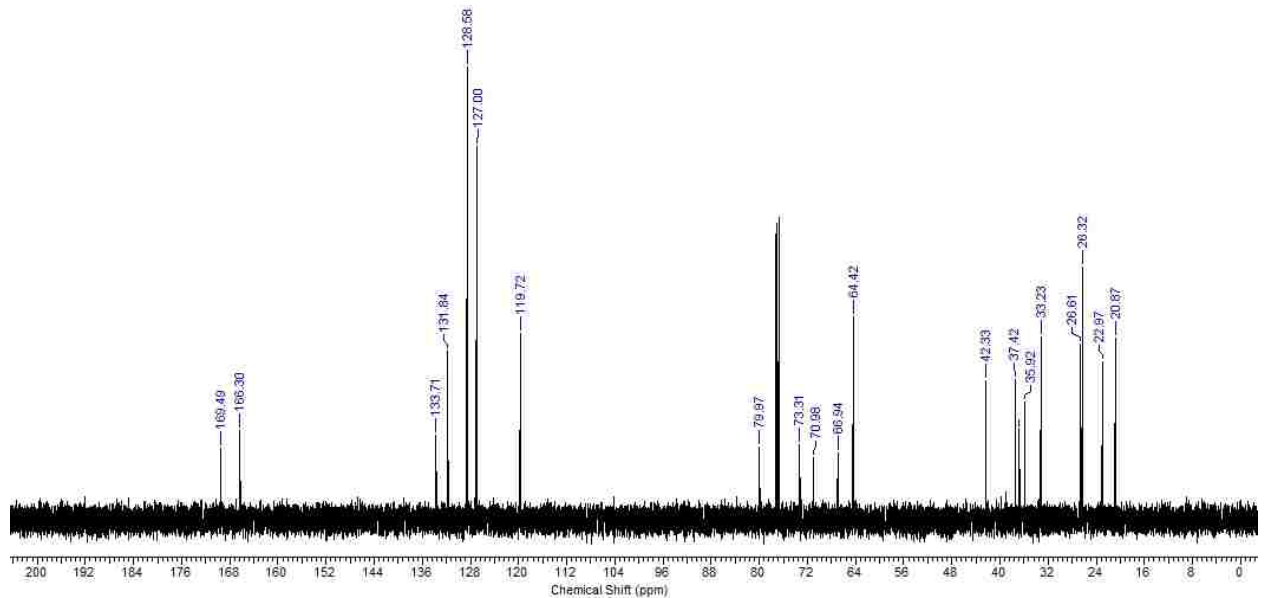


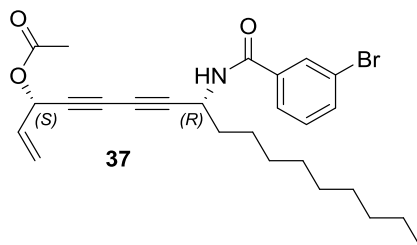
**(3*S*,8*R*)-8-benzamido-11-cyclohexylundeca-1-en-4,6-diyn-3-yl acetate**

**<sup>1</sup>H NMR:**



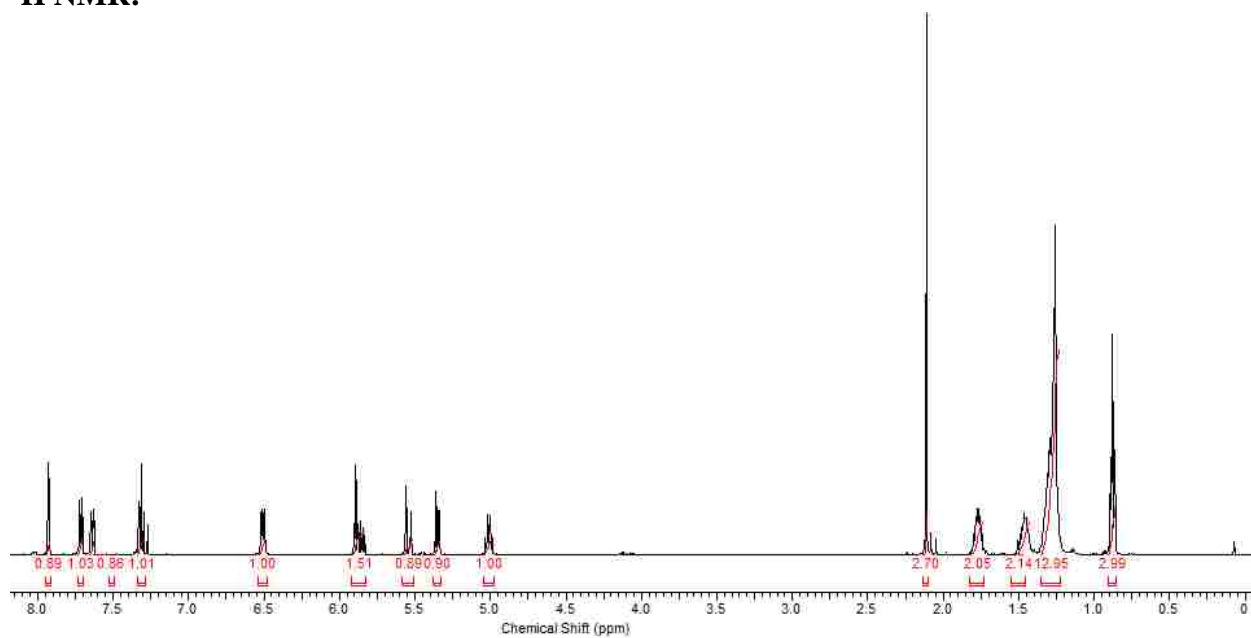
**<sup>13</sup>C NMR:**



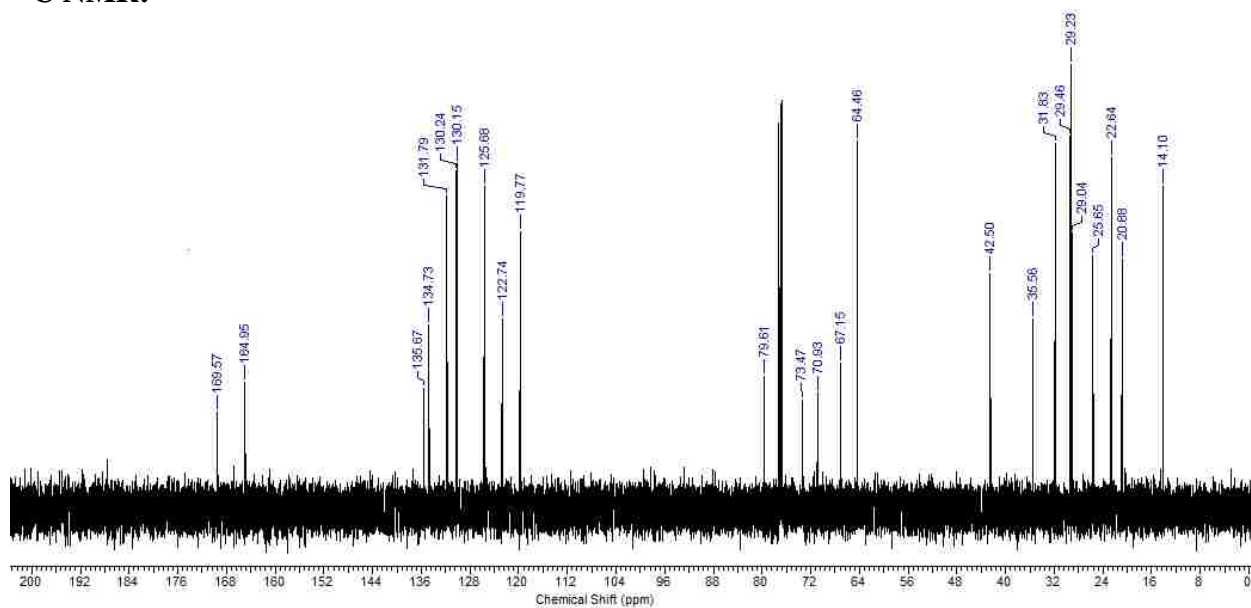


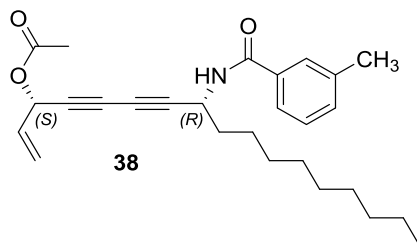
**(3*S*,8*R*)-8-(3-bromobenzamido)heptadeca-1-en-4,6-diyn-3-yl acetate**

**<sup>1</sup>H NMR:**



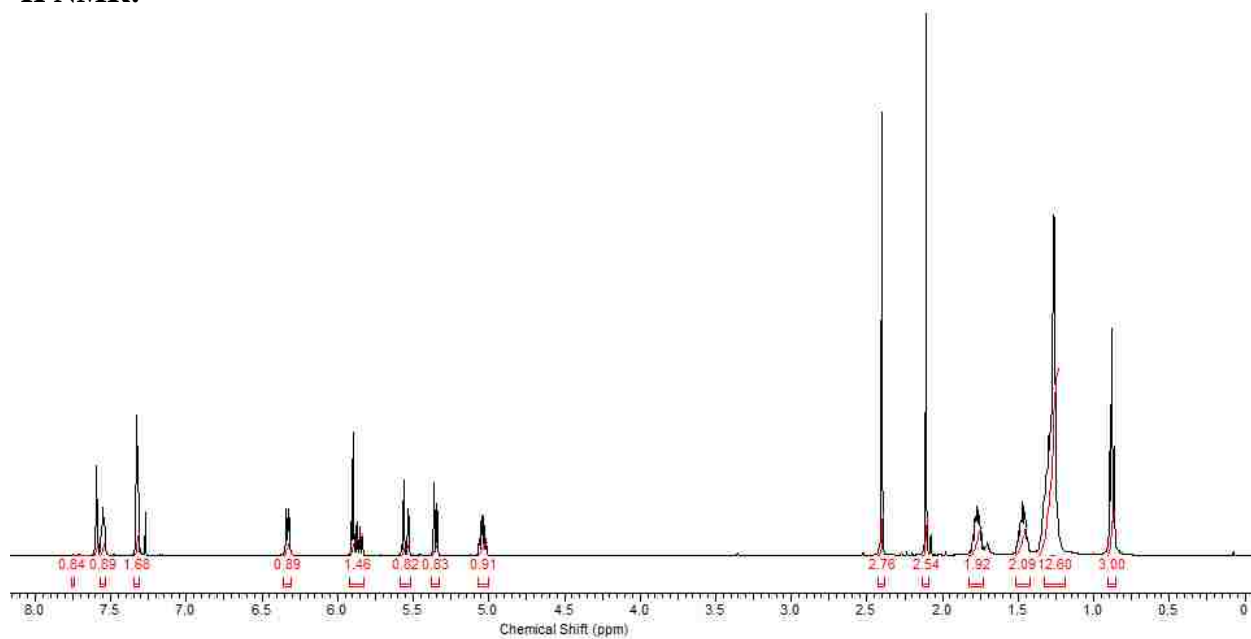
**<sup>13</sup>C NMR:**



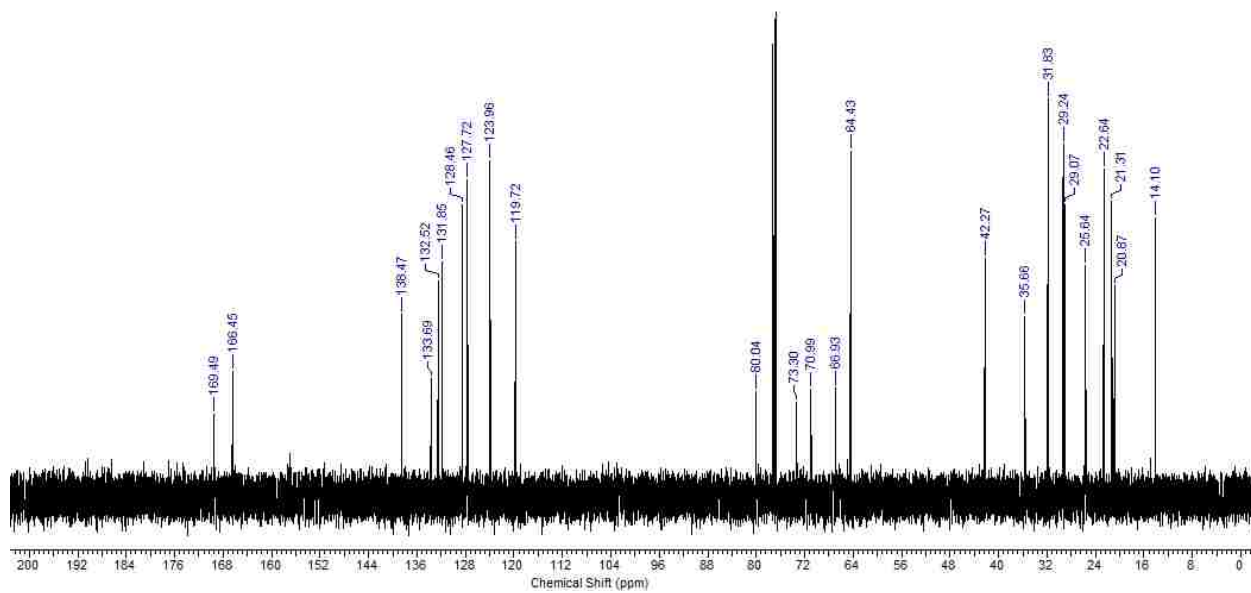


**(3*S*,8*R*)-8-(3-methylbenzamido)heptadeca-1-en-4,6-diyn-3-yl acetate**

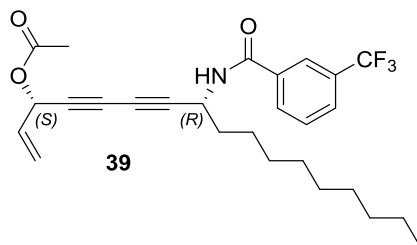
**<sup>1</sup>H NMR:**



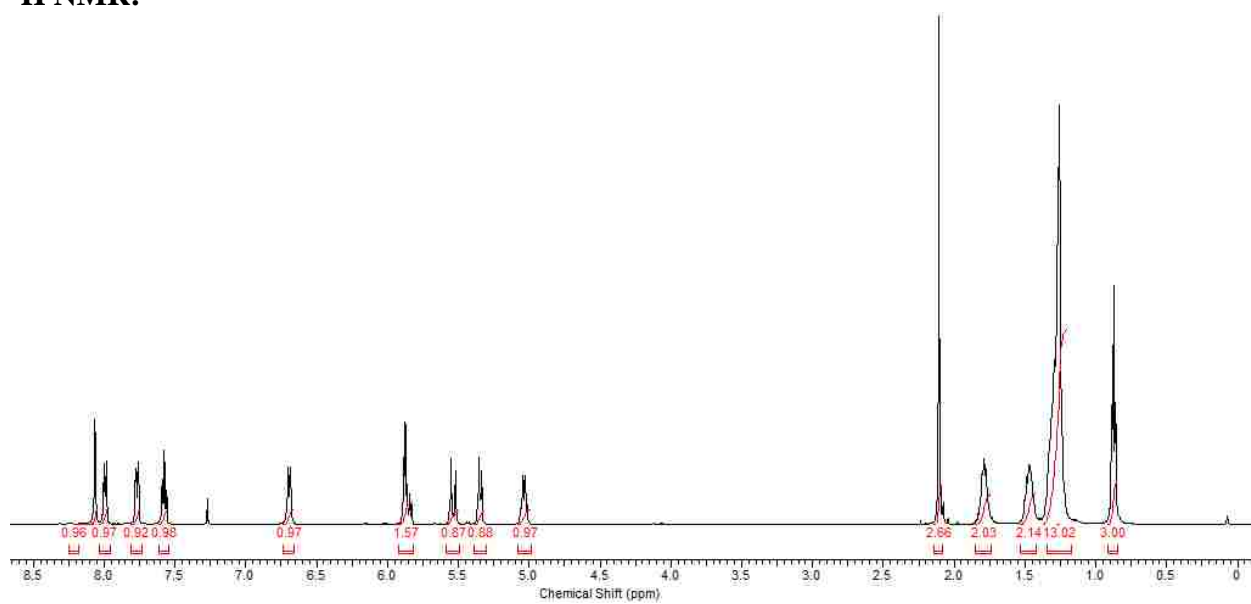
**<sup>13</sup>C NMR:**

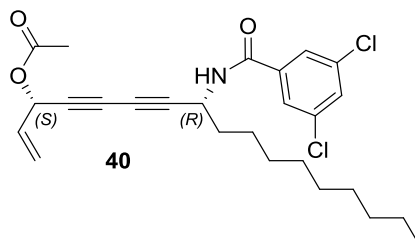






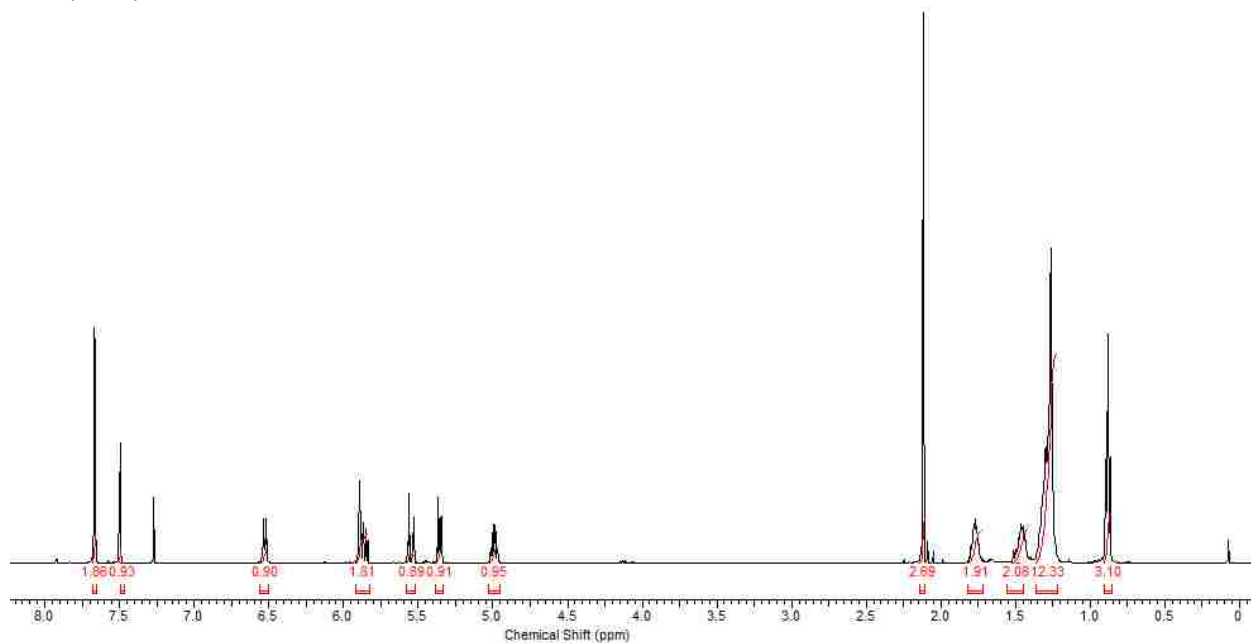
**(3*S*,8*R*)-8-(3-(trifluoromethyl)benzamido)heptadeca-1-en-4,6-diyne-3-yl acetate**  
**<sup>1</sup>H NMR:**



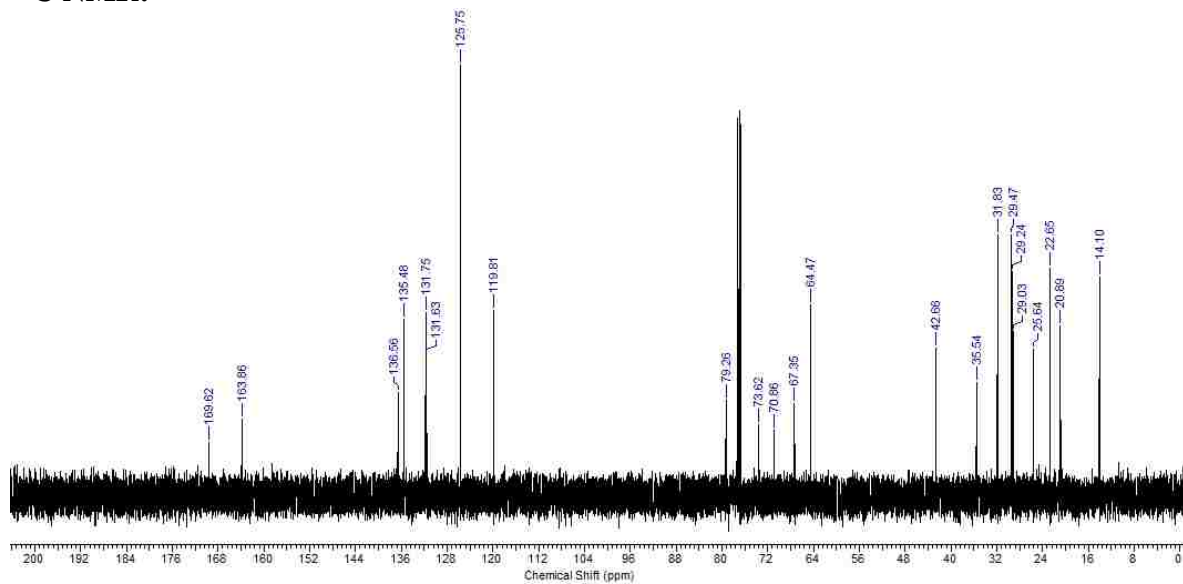


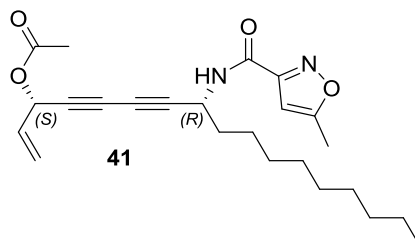
**(3*S*,8*R*)-8-(3,5-dichlorobenzamido)heptadeca-1-en-4,6-diyne-3-yl acetate**

**<sup>1</sup>H NMR:**

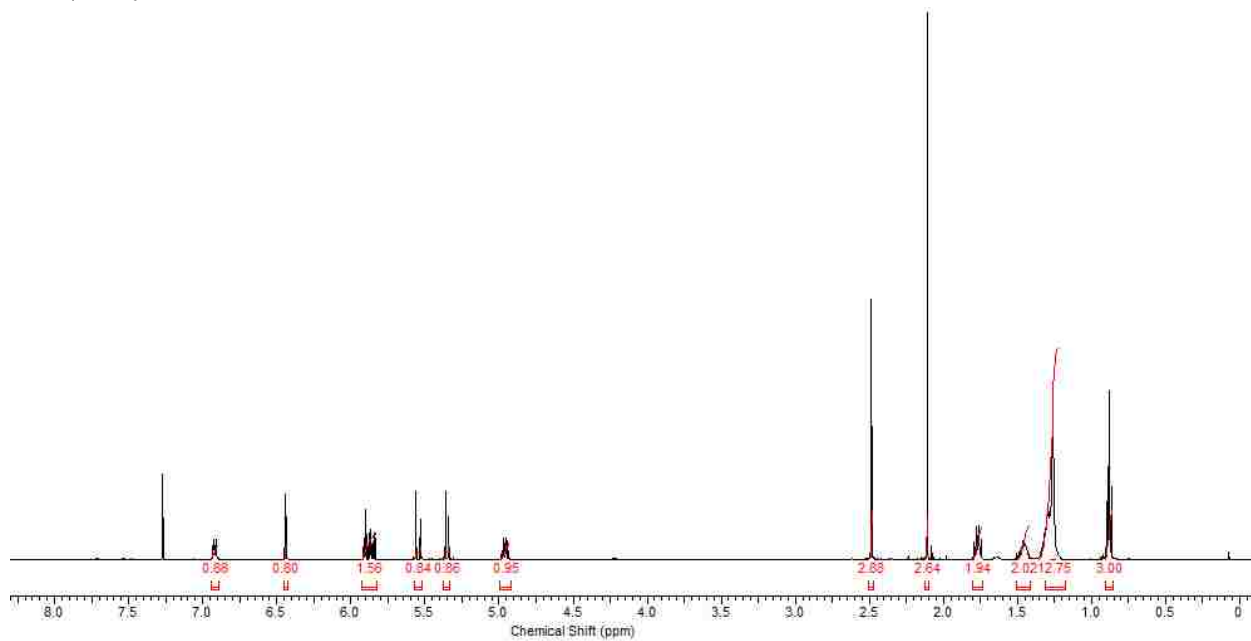


**<sup>13</sup>C NMR:**

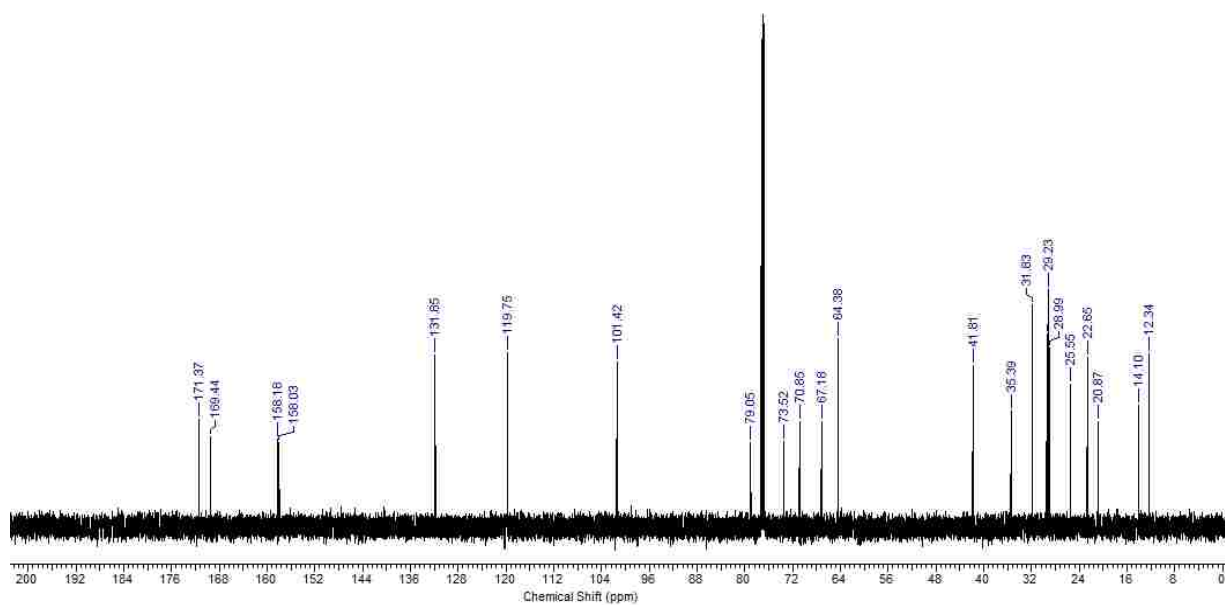


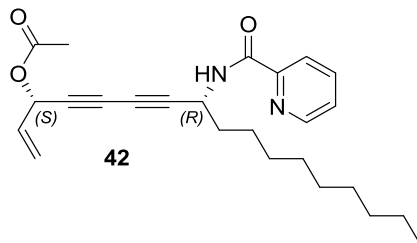


**(3*S*,8*R*)-8-(5-methylisoxazole-3-carboxamido)heptadeca-1-en-4,6-diyn-3-yl acetate**  
<sup>1</sup>H NMR:



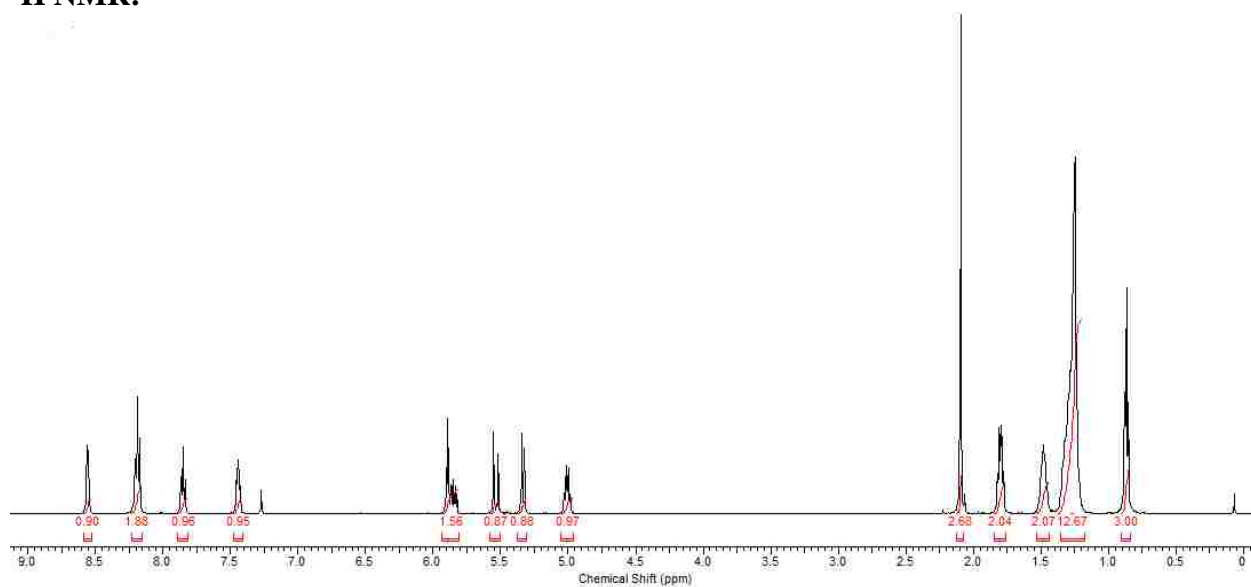
<sup>13</sup>C NMR:



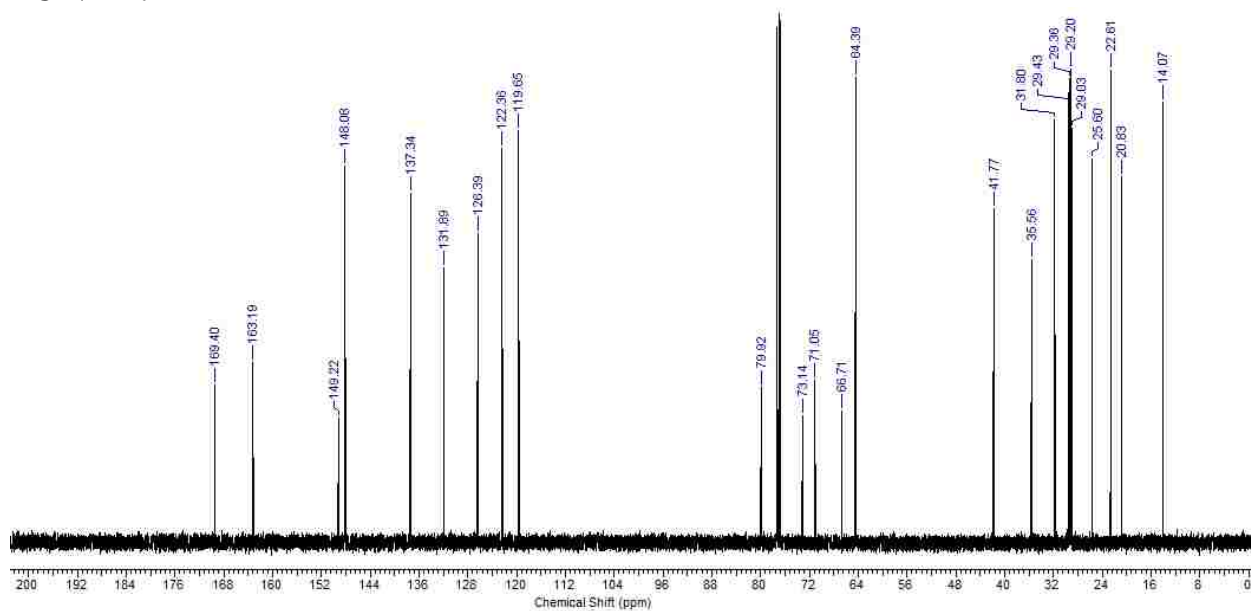


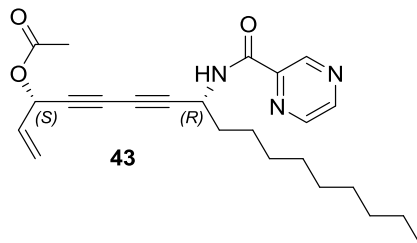
**(3*S*,8*R*)-8-(picolinamido)heptadeca-1-en-4,6-diyn-3-yl acetate**

**<sup>1</sup>H NMR:**



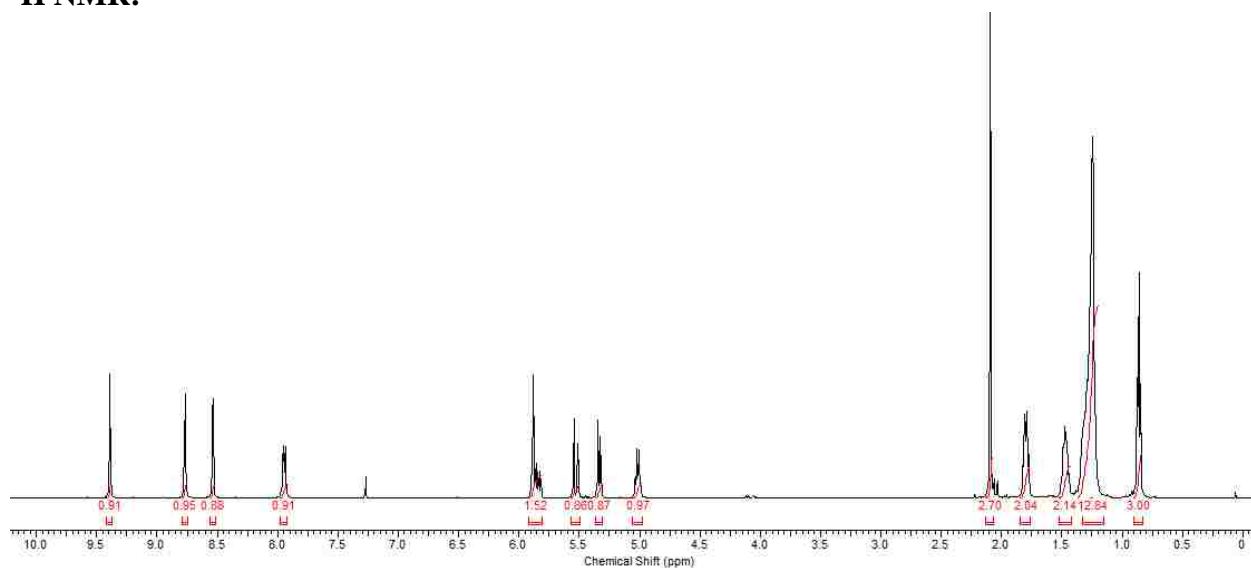
**<sup>13</sup>C NMR:**



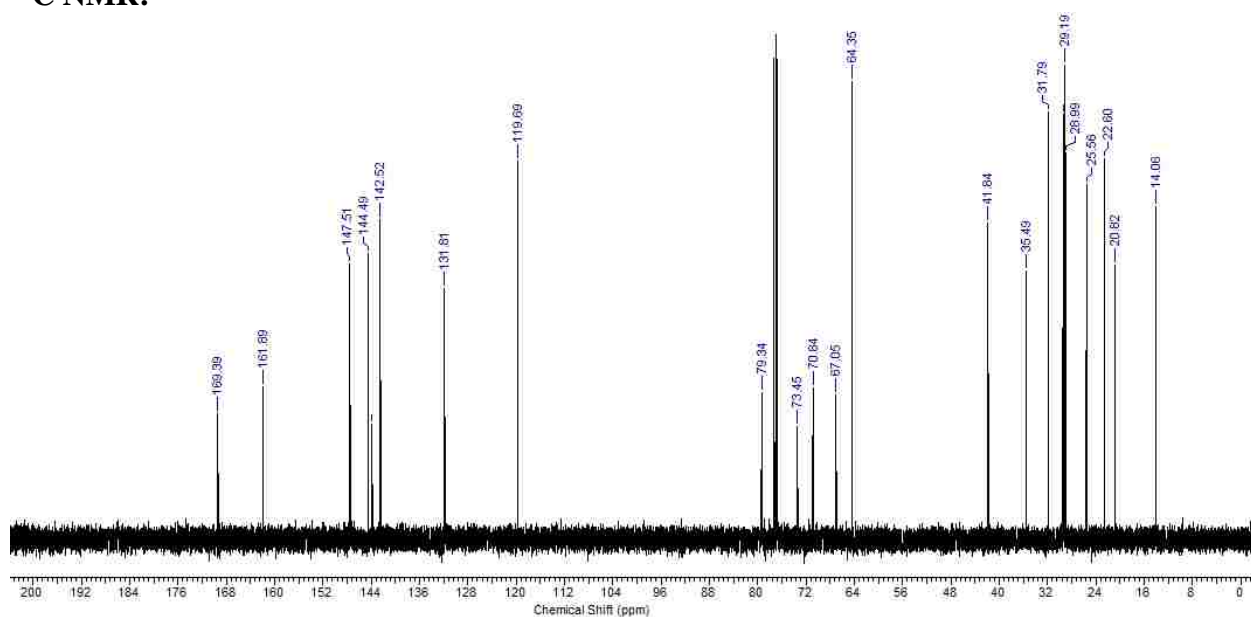


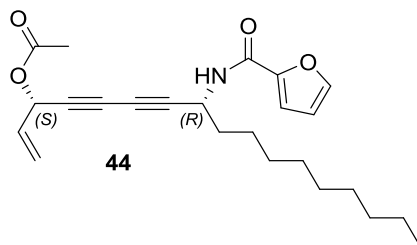
**(3*S*,8*R*)-8-(pyrazine-2-carboxamido)heptadeca-1-en-4,6-diyne-3-yl acetate**

**<sup>1</sup>H NMR:**



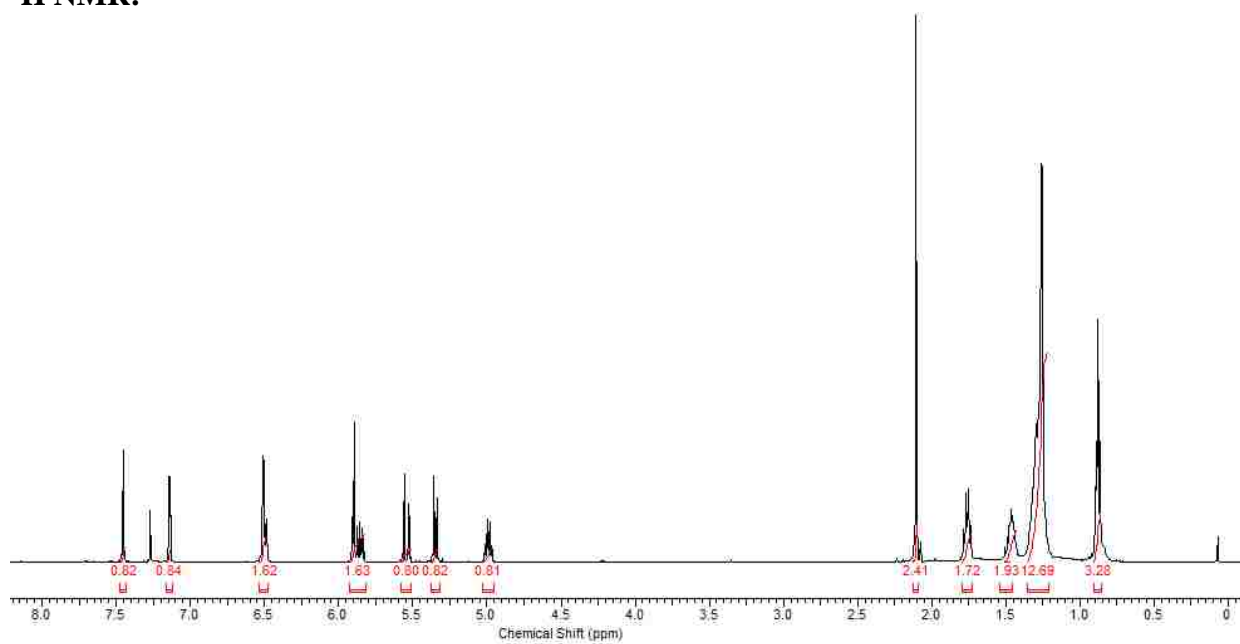
**<sup>13</sup>C NMR:**



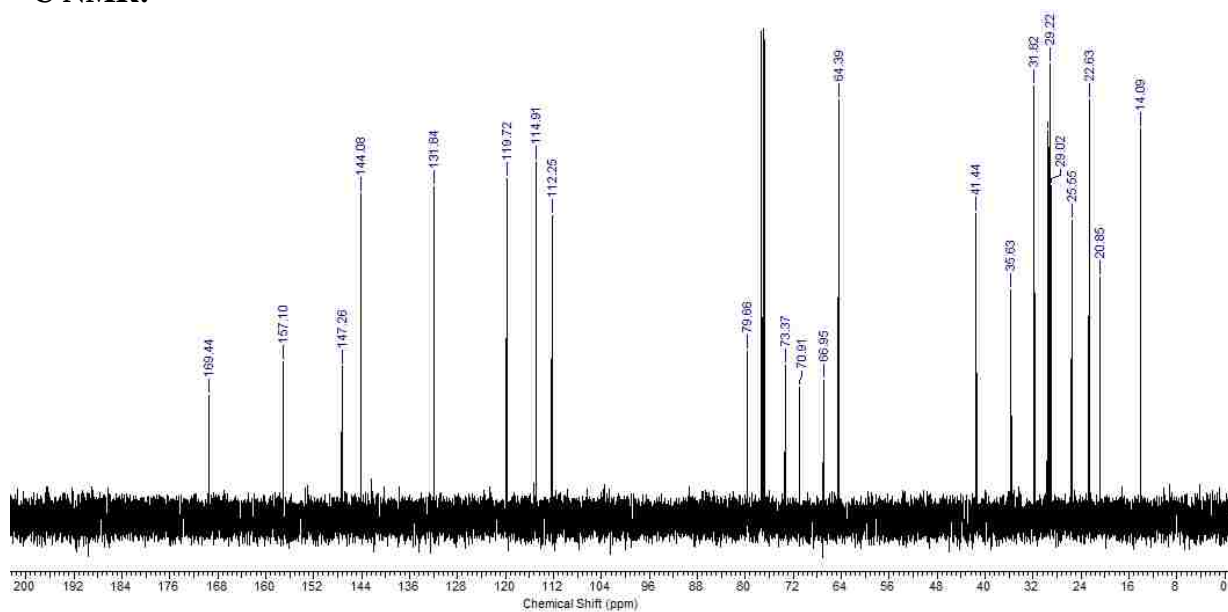


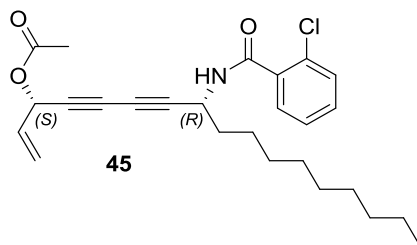
**(3*S*,8*R*)-8-(furan-2-carboxamido)heptadeca-1-en-4,6-diyne-3-yl acetate**

**<sup>1</sup>H NMR:**



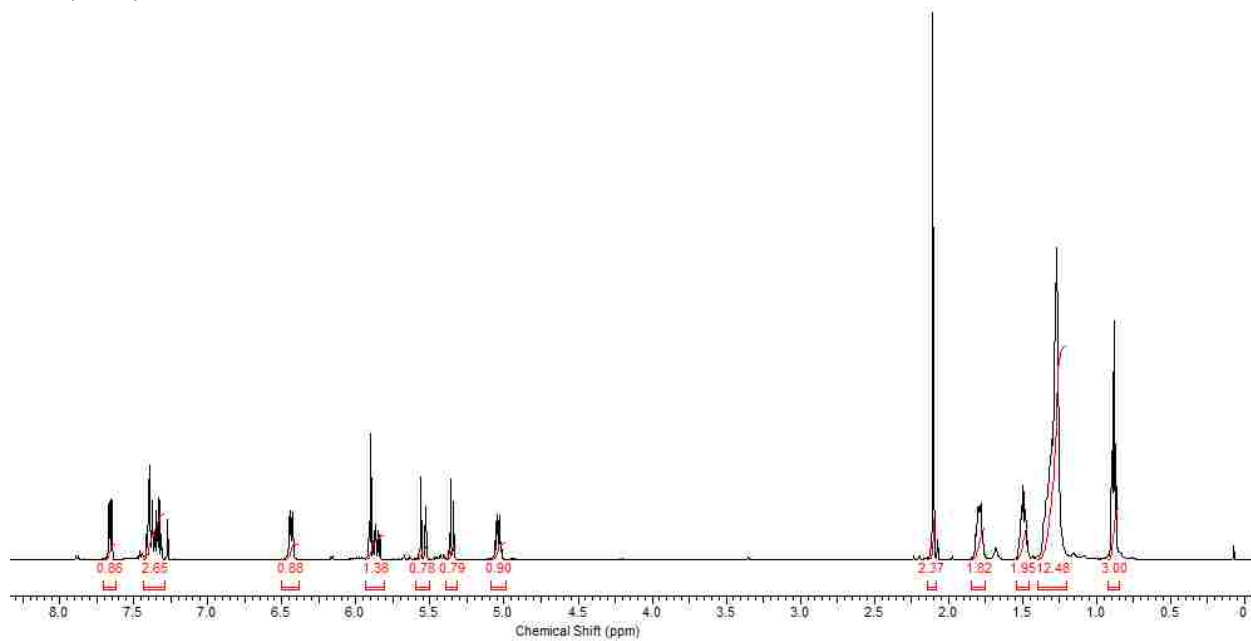
**<sup>13</sup>C NMR:**



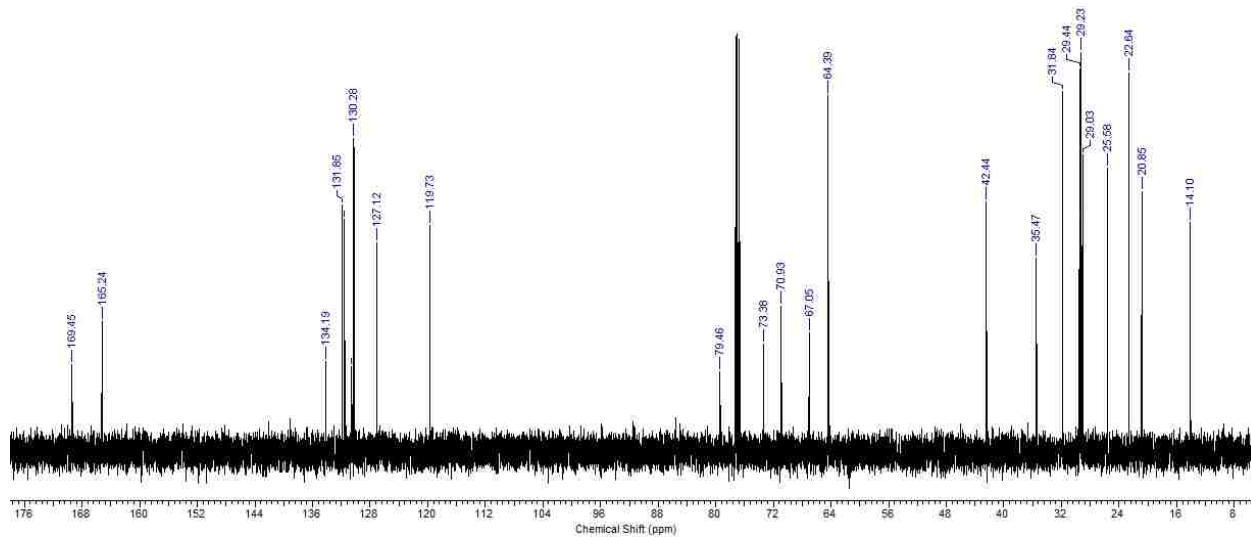


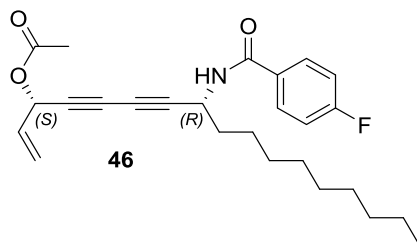
**(3*S*,8*R*)-8-(2-chlorobenzamido)heptadeca-1-en-4,6-diyn-3-yl acetate**

**<sup>1</sup>H NMR:**



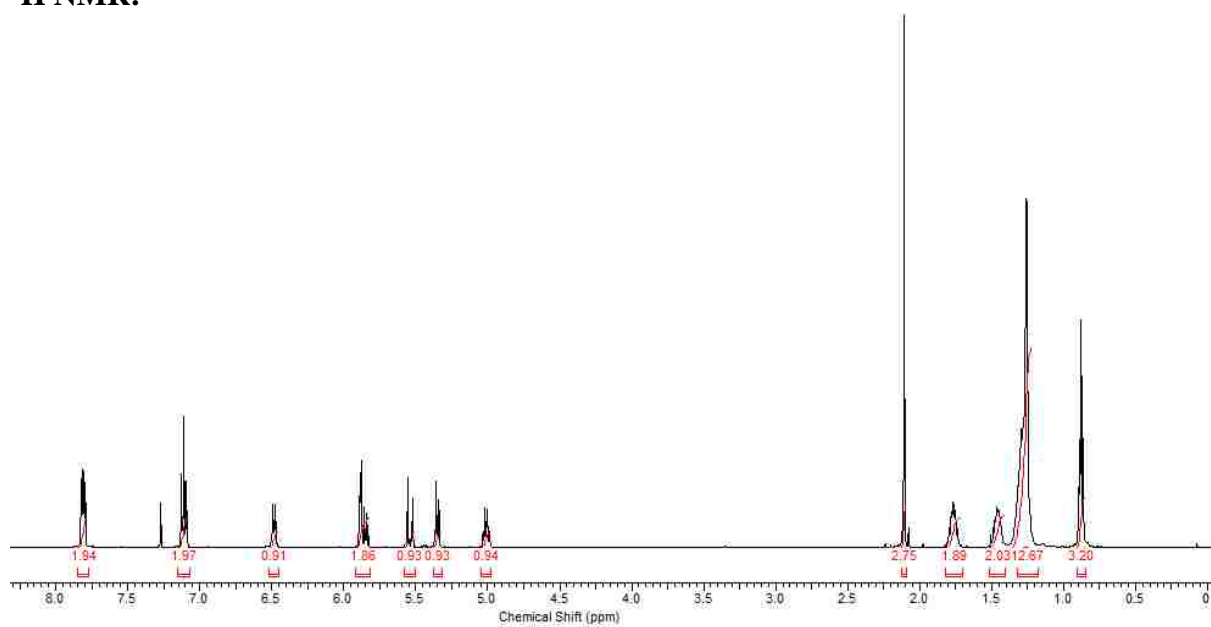
**<sup>13</sup>C NMR:**



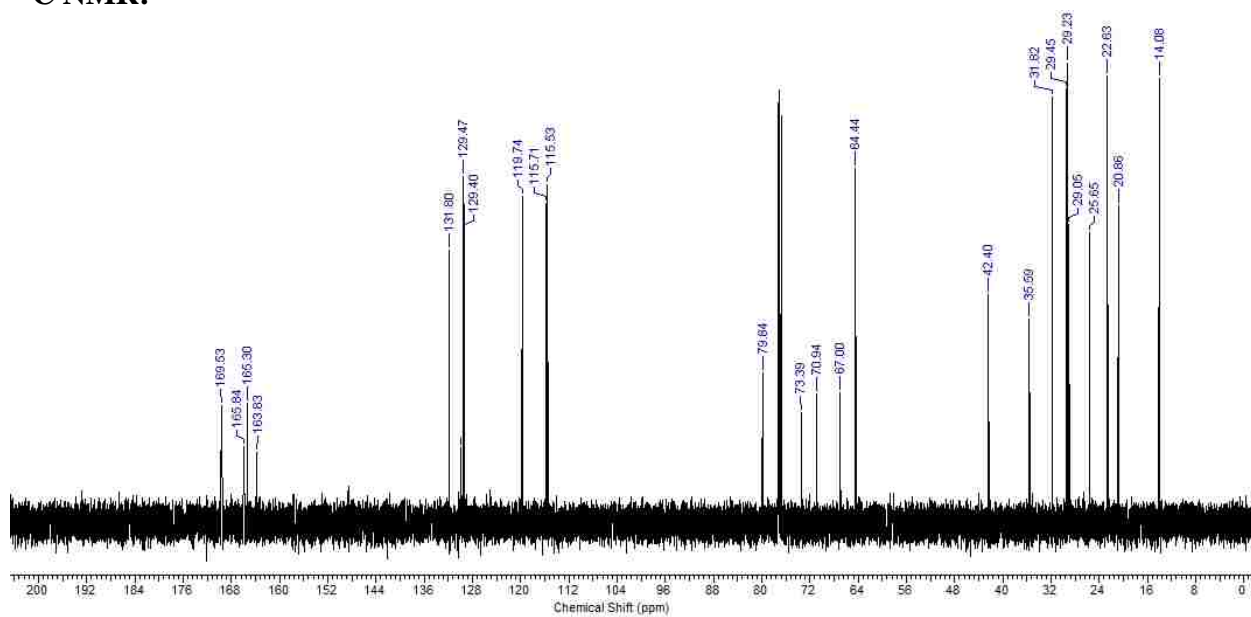


**(3*S*,8*R*)-8-(4-fluorobenzamido)heptadeca-1-en-4,6-diyn-3-yl acetate**

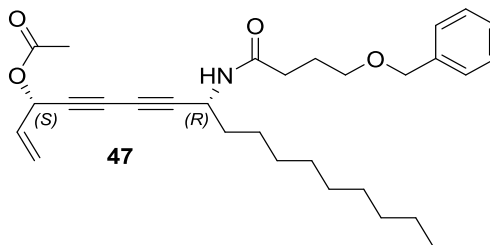
**<sup>1</sup>H NMR:**



**<sup>13</sup>C NMR:**

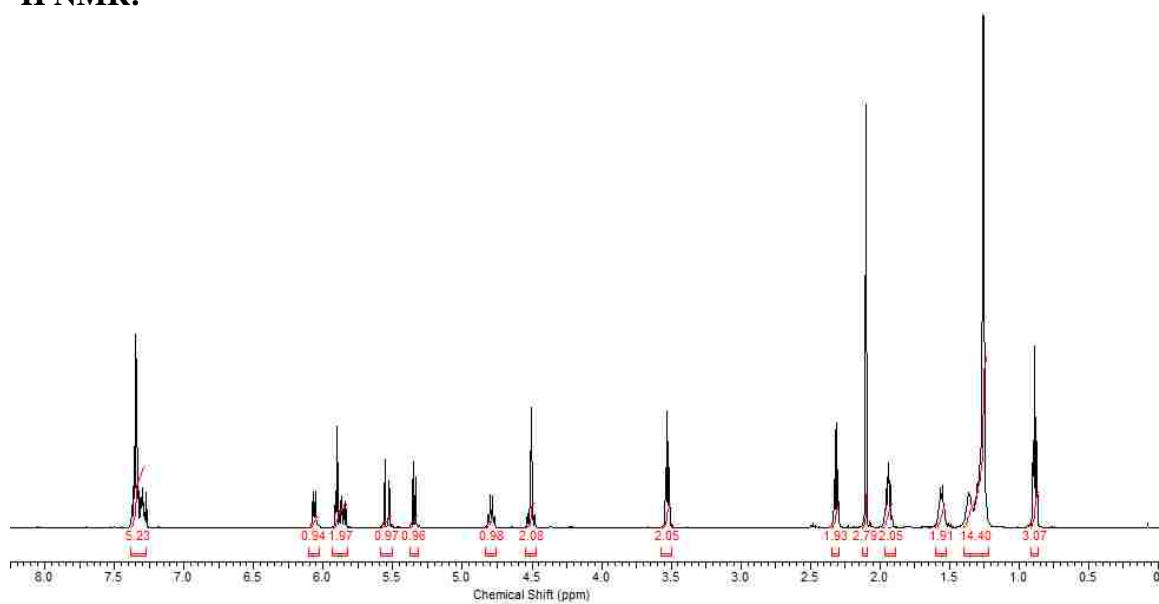




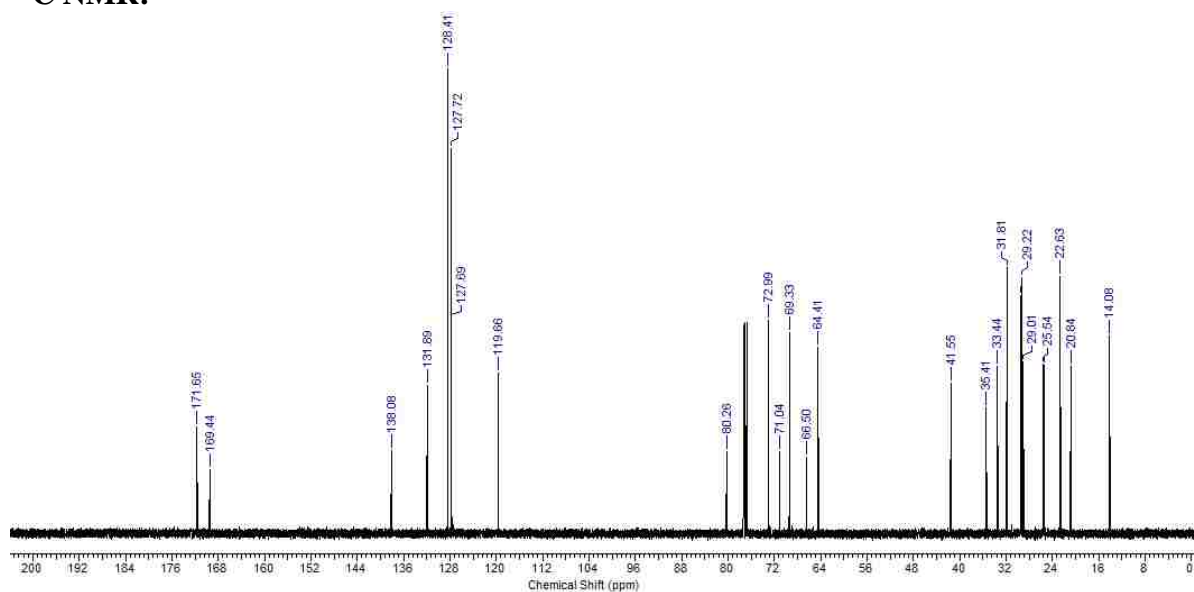


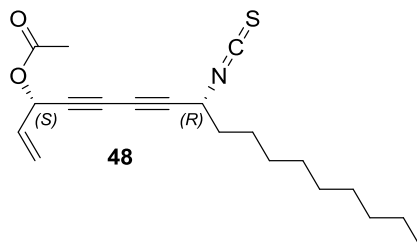
**(3*S*,8*R*)-8-(4-(benzyloxy)butanamido)heptadeca-1-en-4,6-diyn-3-yl acetate**

**<sup>1</sup>H NMR:**



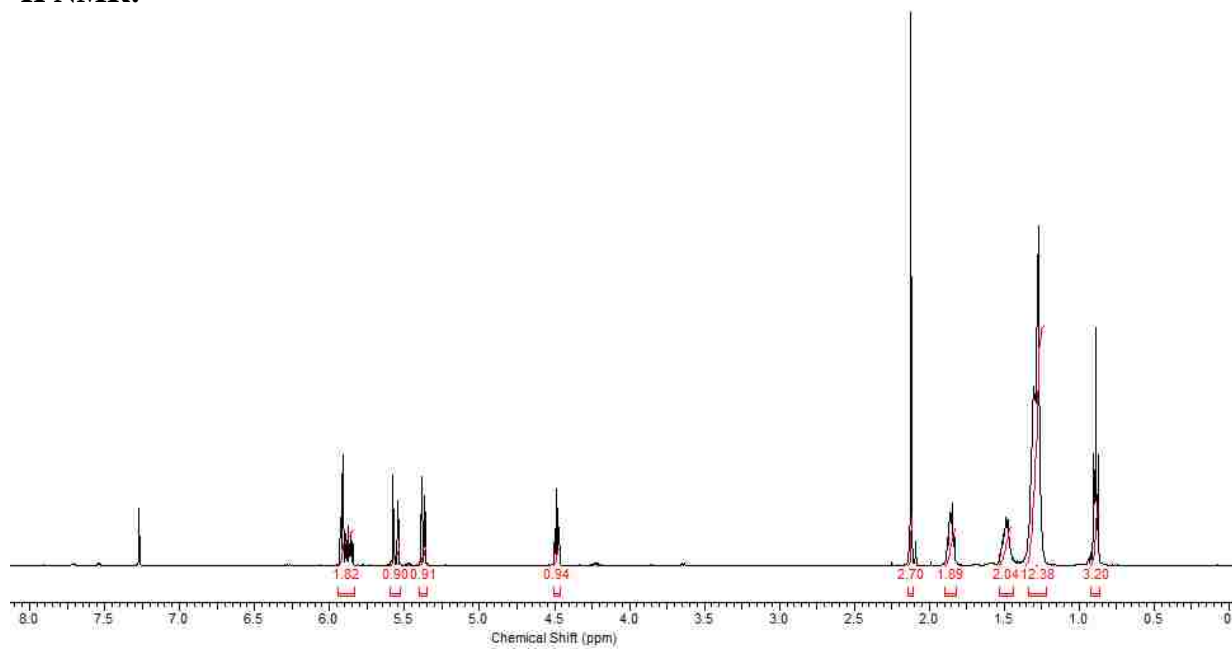
**<sup>13</sup>C NMR:**



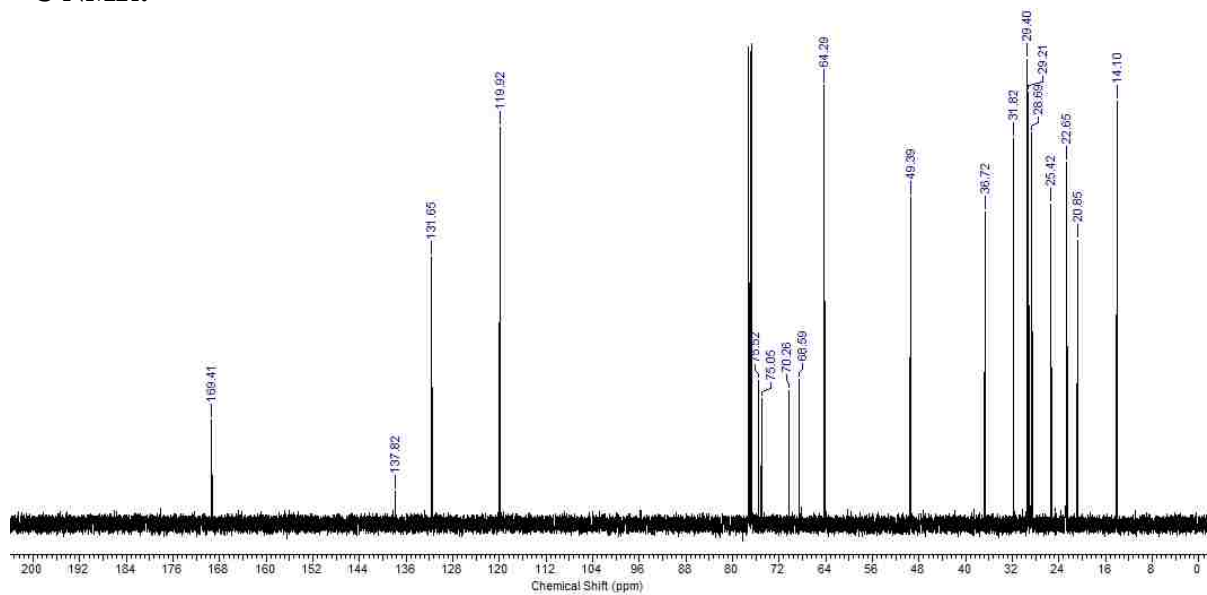


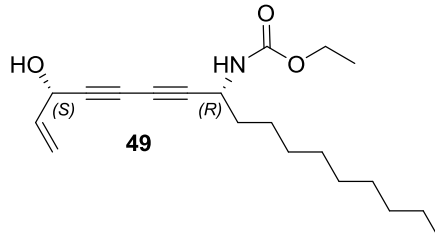
**(3*S*,8*R*)-8-isothiocyanatoheptadeca-1-en-4,6-diyne-3-yl acetate**

**<sup>1</sup>H NMR:**



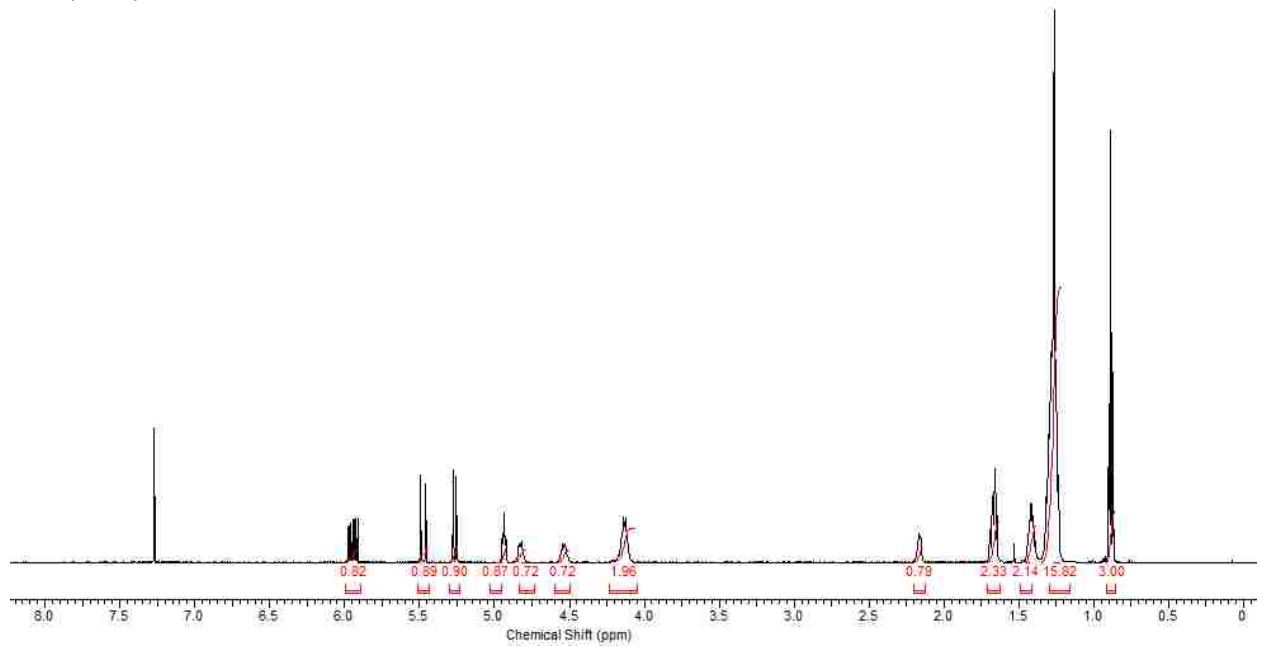
**<sup>13</sup>C NMR:**



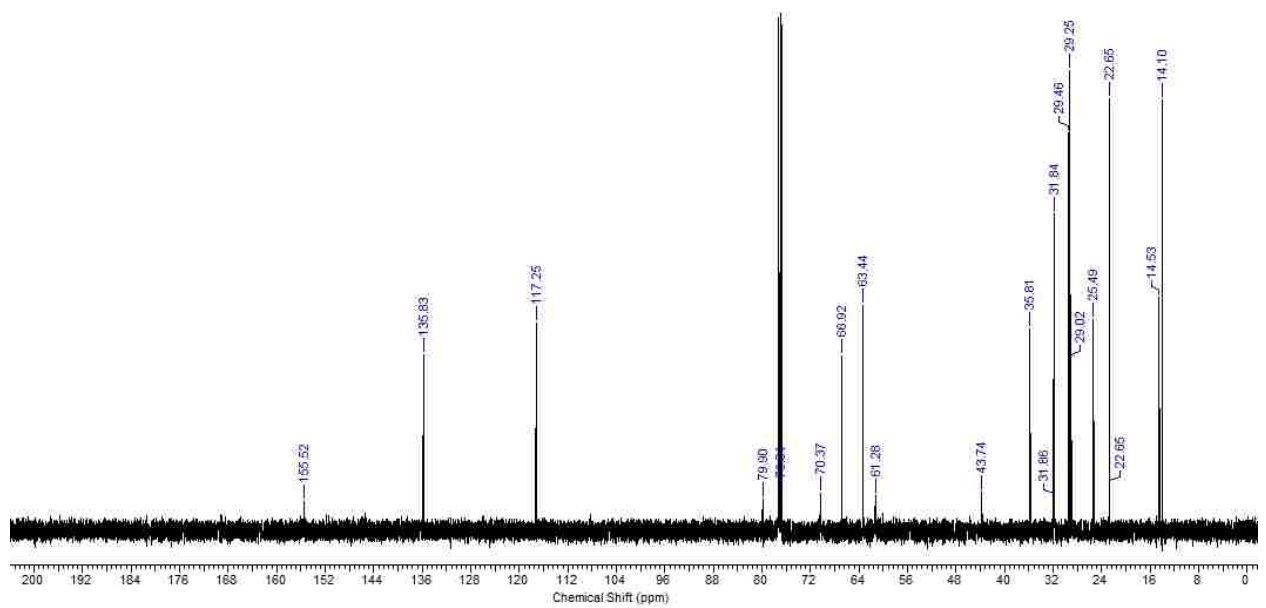


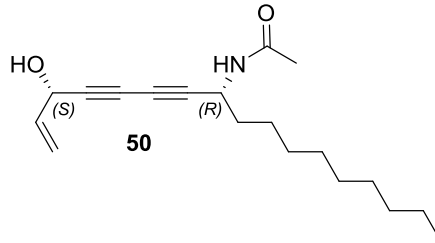
**ethyl ((3*S*,8*R*)-3-hydroxyheptadeca-1-en-4,6-diyn-8-yl)carbamate**

**<sup>1</sup>H NMR:**



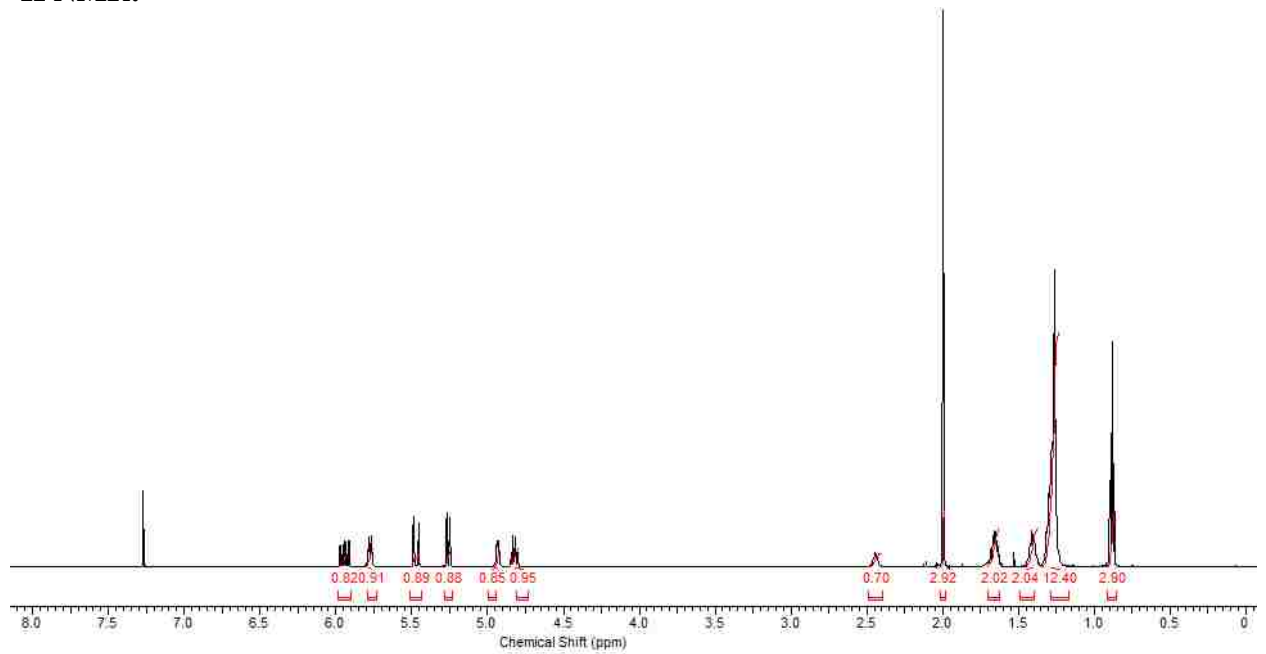
**<sup>13</sup>C NMR:**



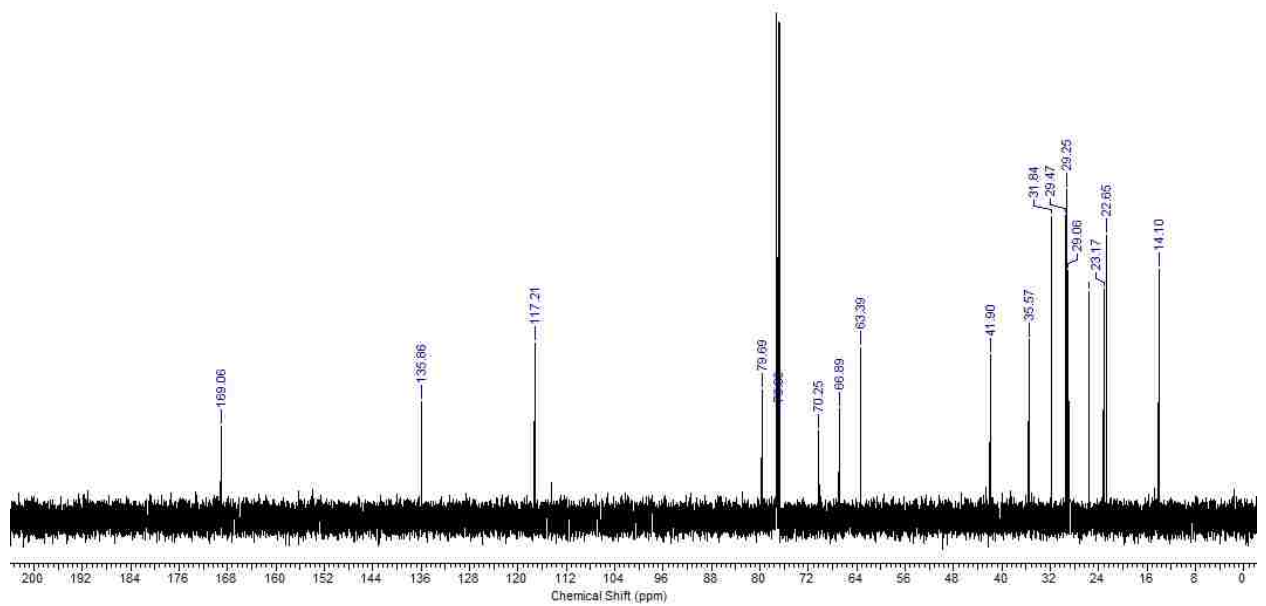


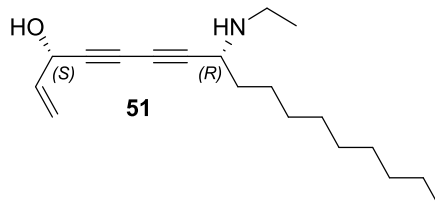
***N*-((3*S*,8*R*)-3-hydroxyheptadeca-1-en-4,6-diyne-8-yl)acetamide**

**<sup>1</sup>H NMR:**



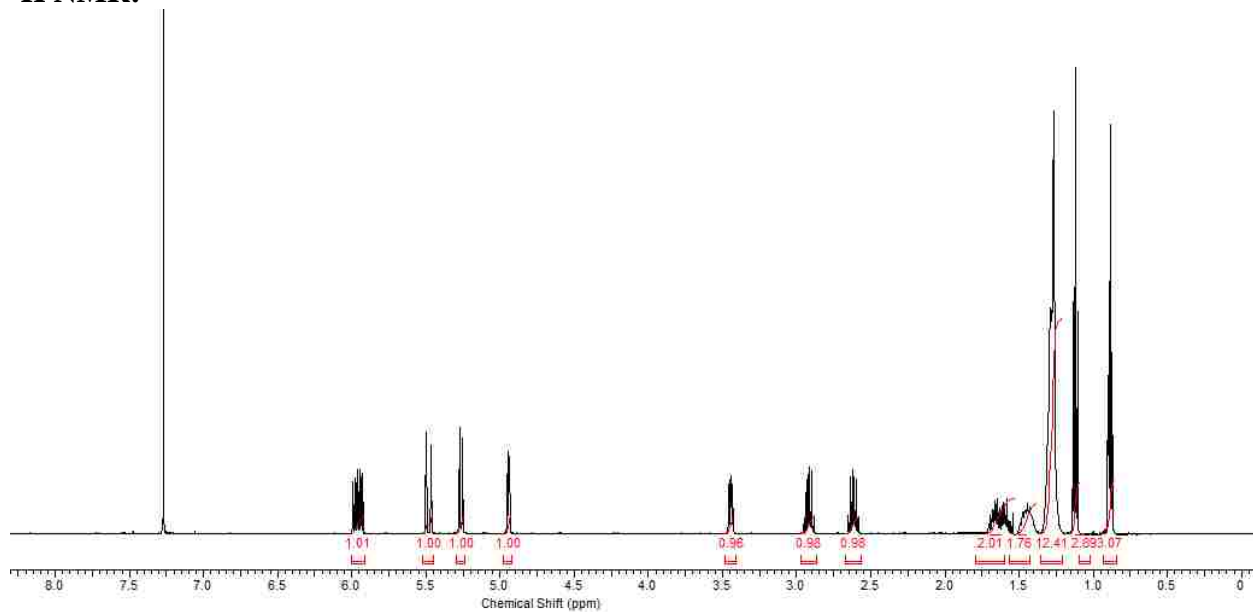
**<sup>13</sup>C NMR:**



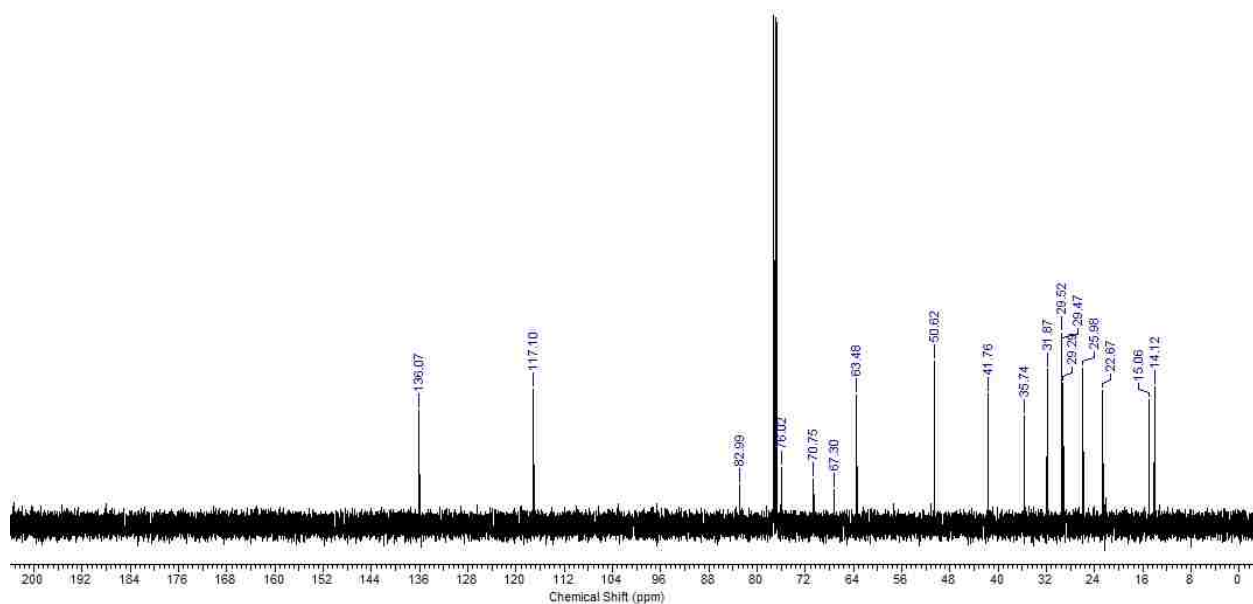


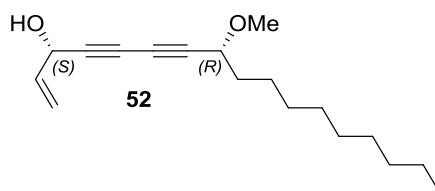
**(3*S*,8*R*)-8-(ethylamino)heptadeca-1-en-4,6-diyn-3-ol**

**<sup>1</sup>H NMR:**



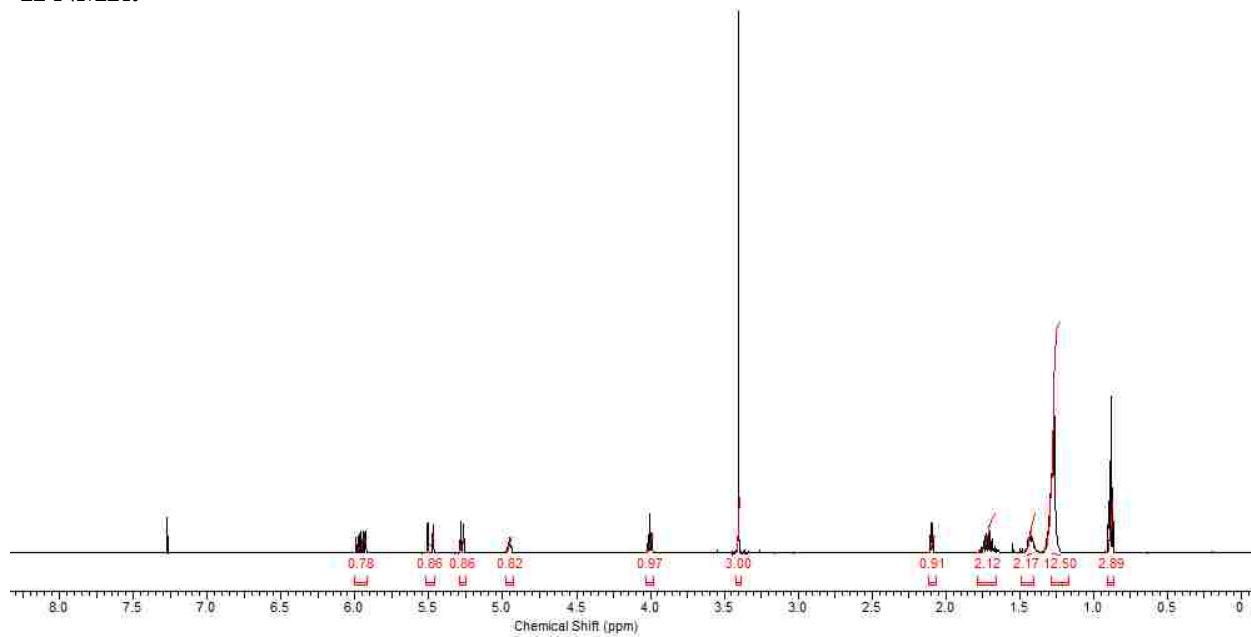
**<sup>13</sup>C NMR:**



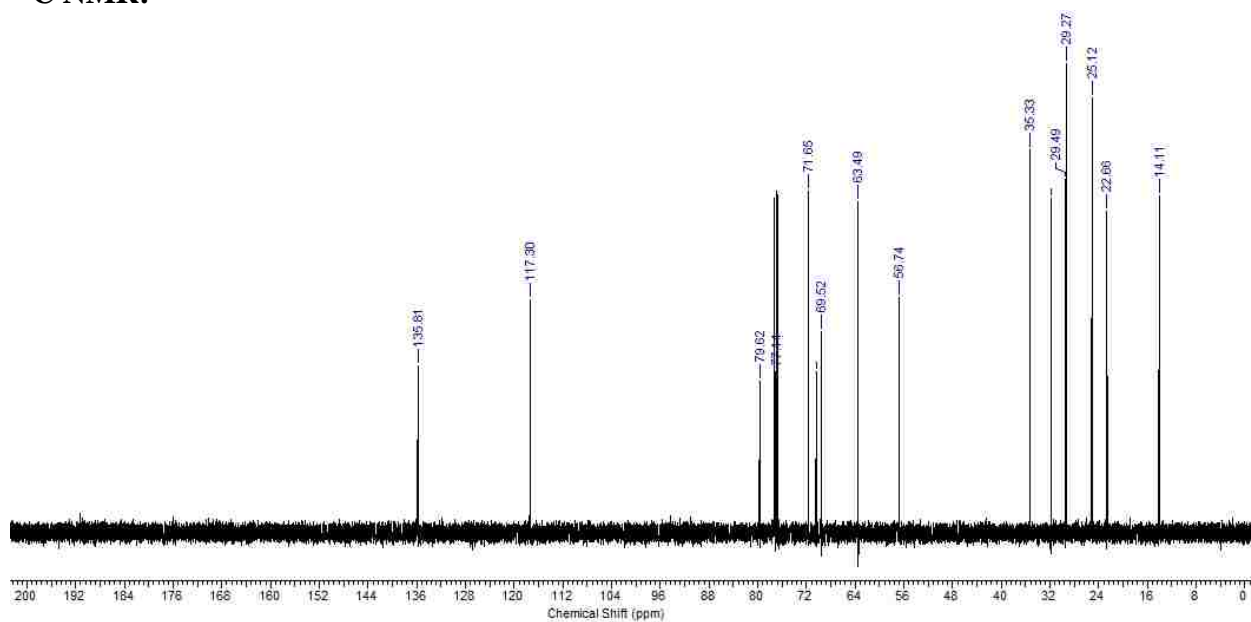


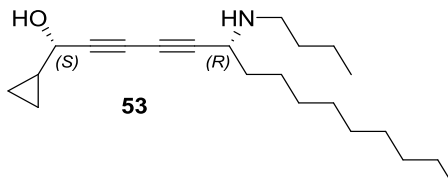
**(3*S*,8*R*)-8-methoxyheptadeca-1-en-4,6-diyne-3-ol**

**<sup>1</sup>H NMR:**



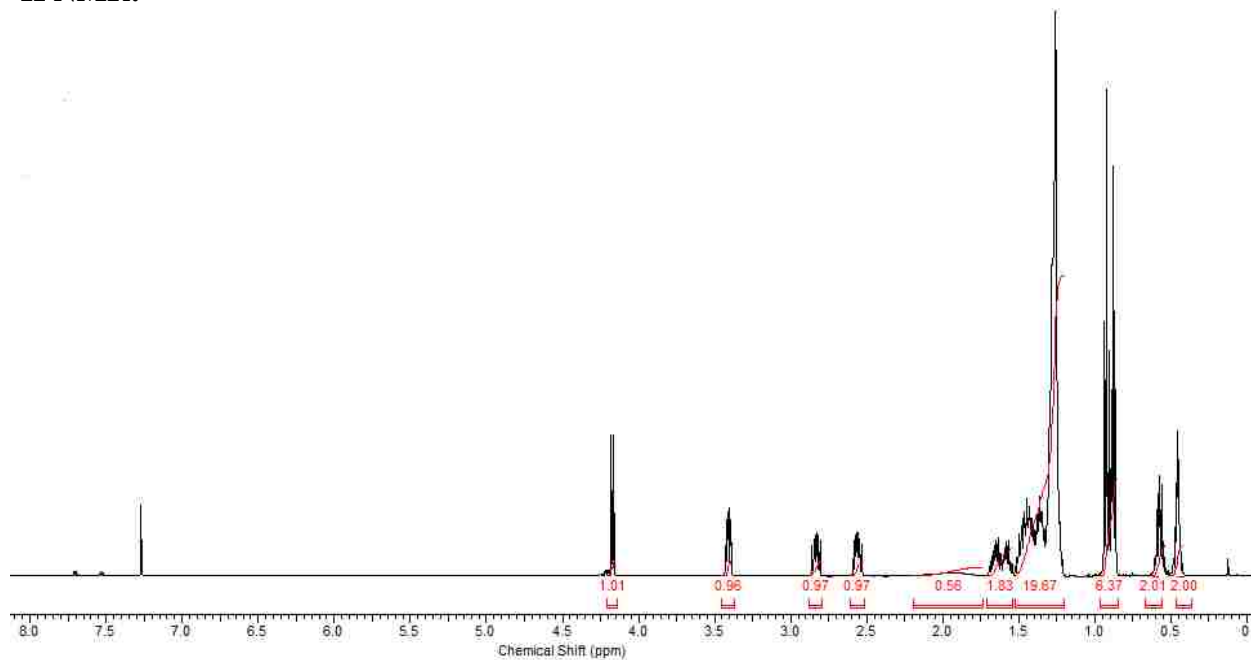
**<sup>13</sup>C NMR:**



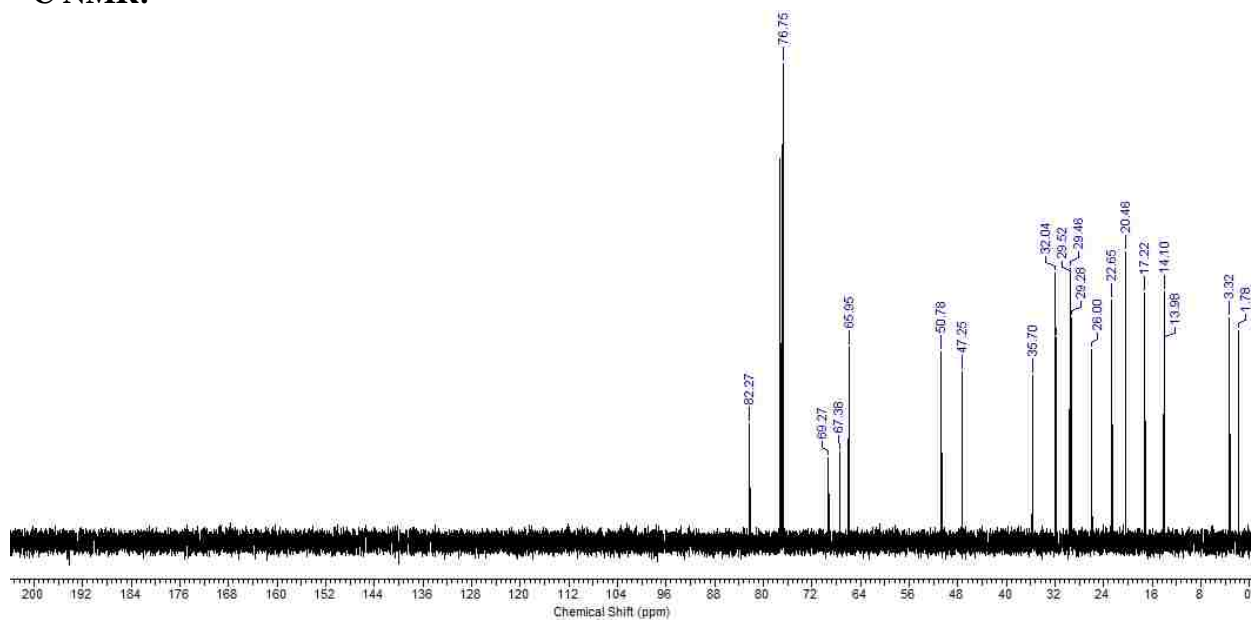


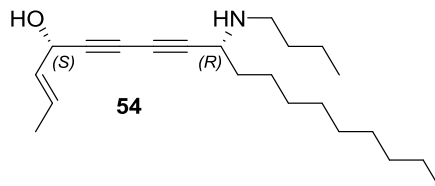
**(1*S*,6*R*)-6-(butylamino)-1-cyclopropylpentadeca-2,4-diyne-1-ol**

**<sup>1</sup>H NMR:**



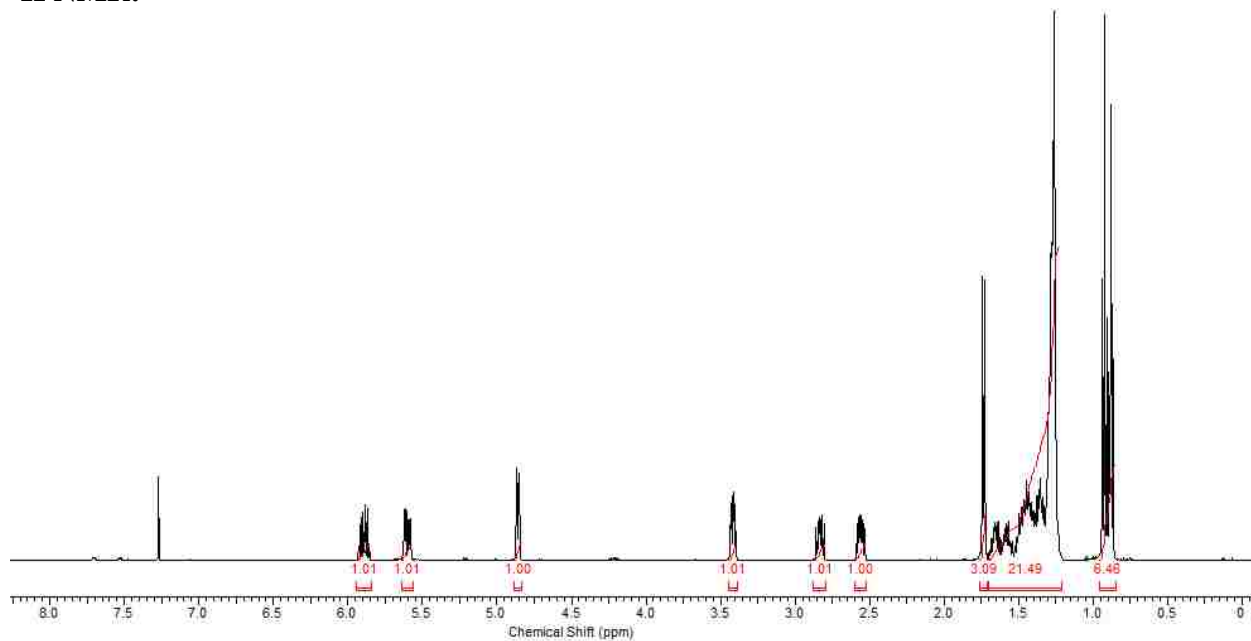
**<sup>13</sup>C NMR:**



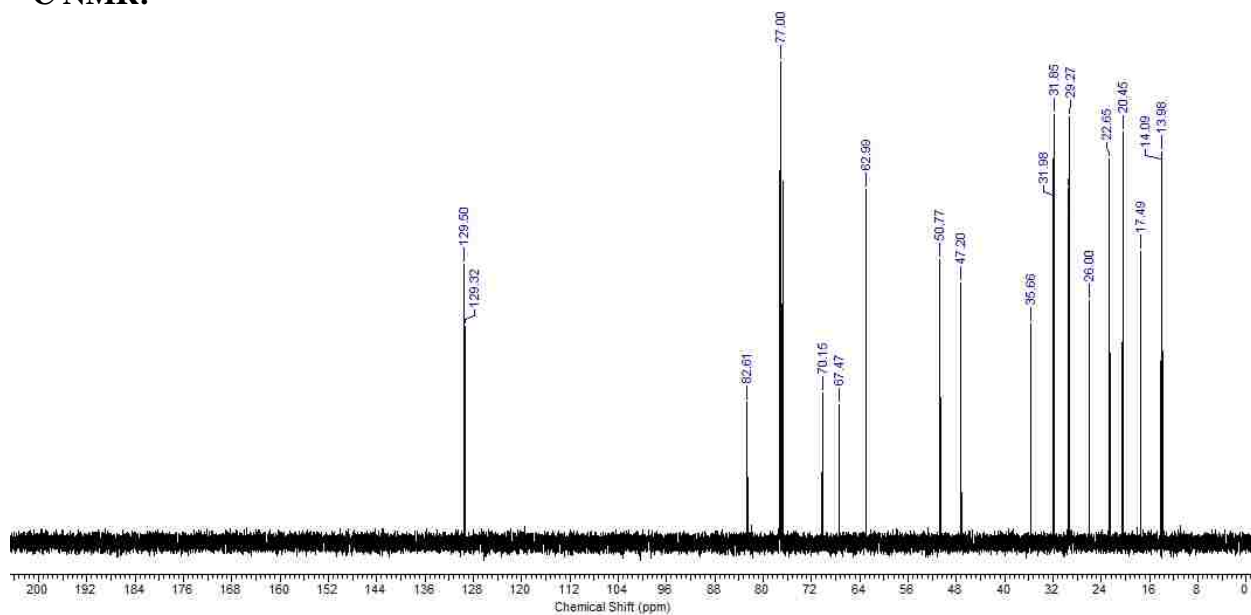


**(4*S*,9*R*,*E*)-9-(butylamino)octadeca-2-en-5,7-diyn-4-ol**

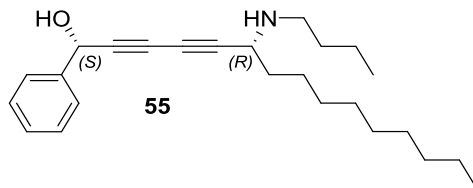
**<sup>1</sup>H NMR:**



**<sup>13</sup>C NMR:**

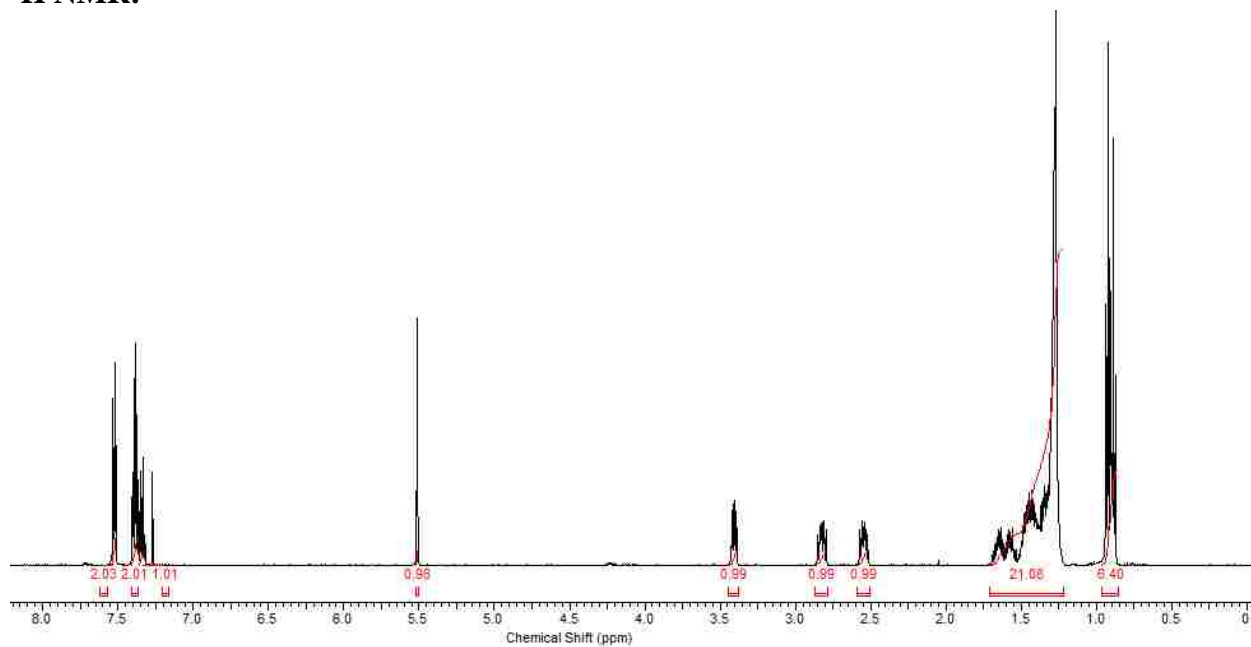




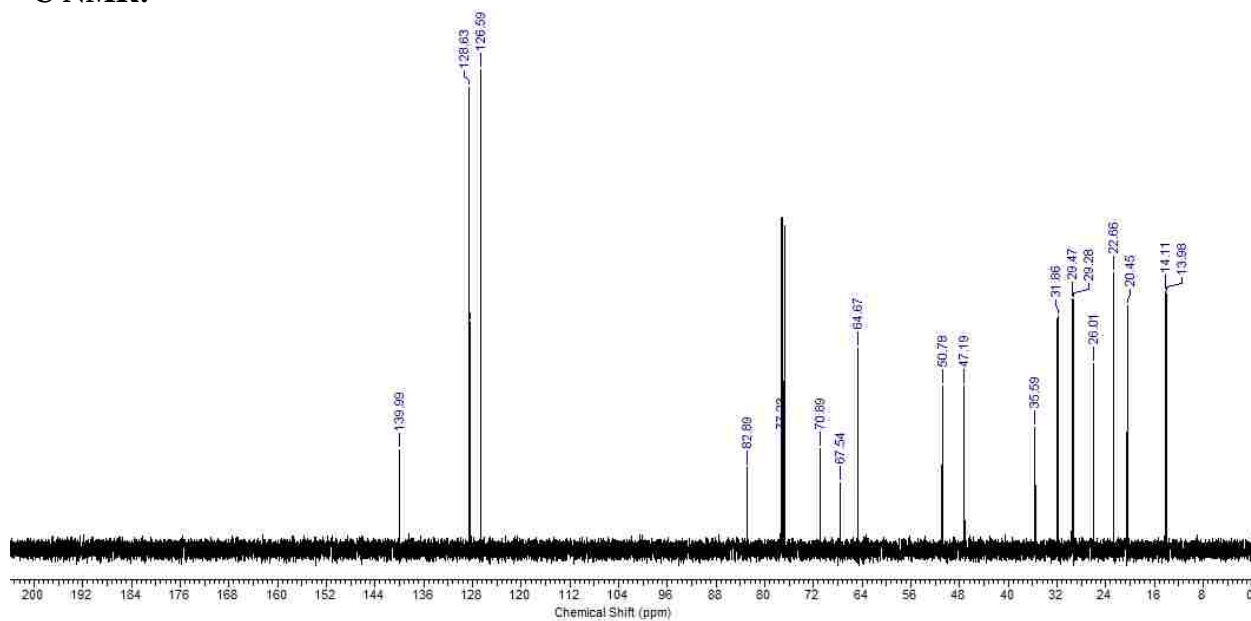


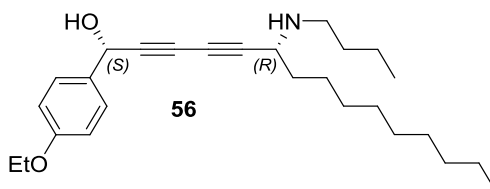
**(1*S*,6*R*)-6-(butylamino)-1-phenylpentadeca-2,4-diyne-1-ol**

**<sup>1</sup>H NMR:**



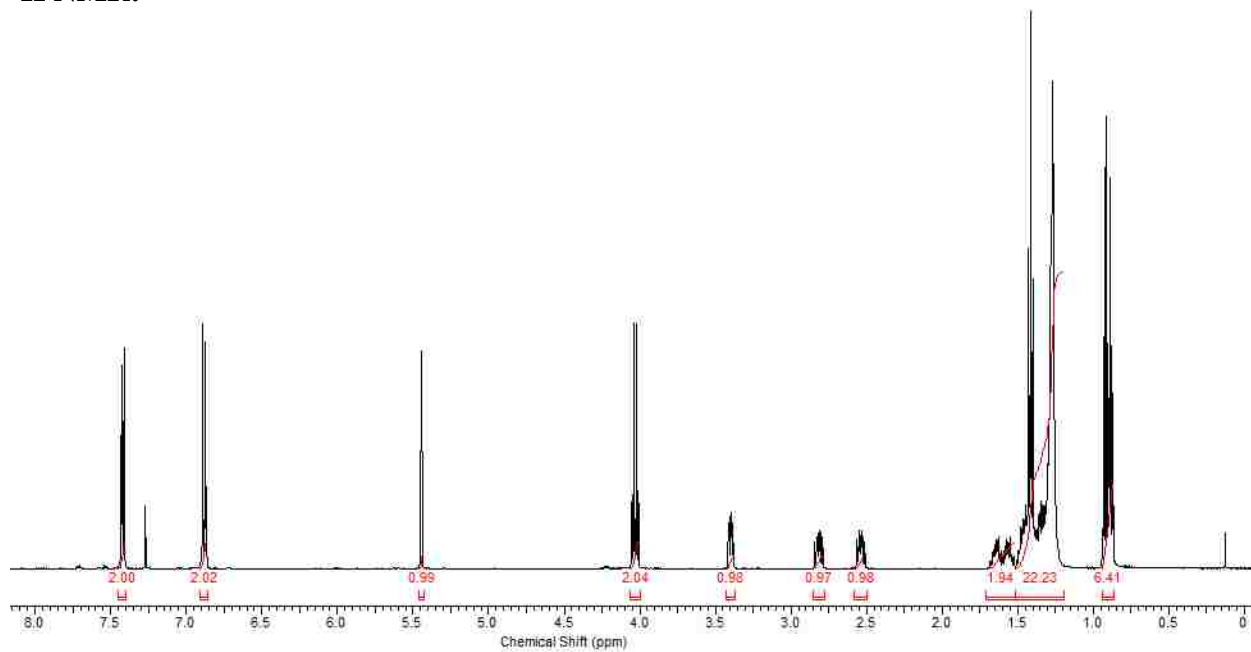
**<sup>13</sup>C NMR:**



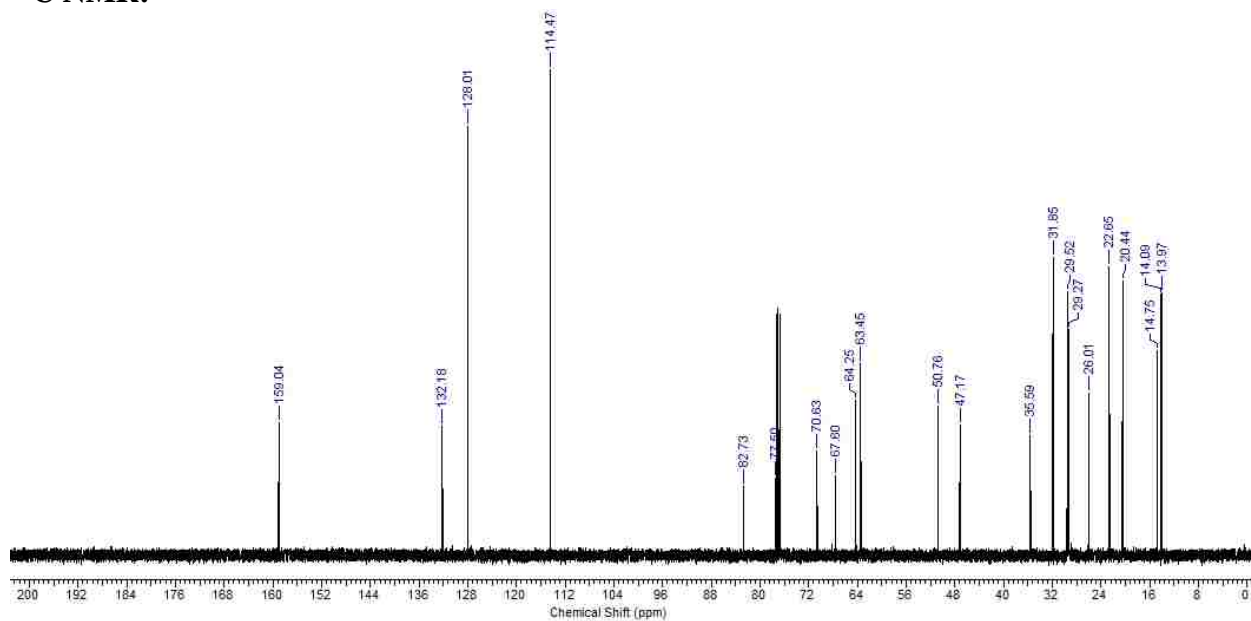


**(1*S*,6*R*)-6-(butylamino)-1-(4-ethoxyphenyl)pentadeca-2,4-diyne-1-ol**

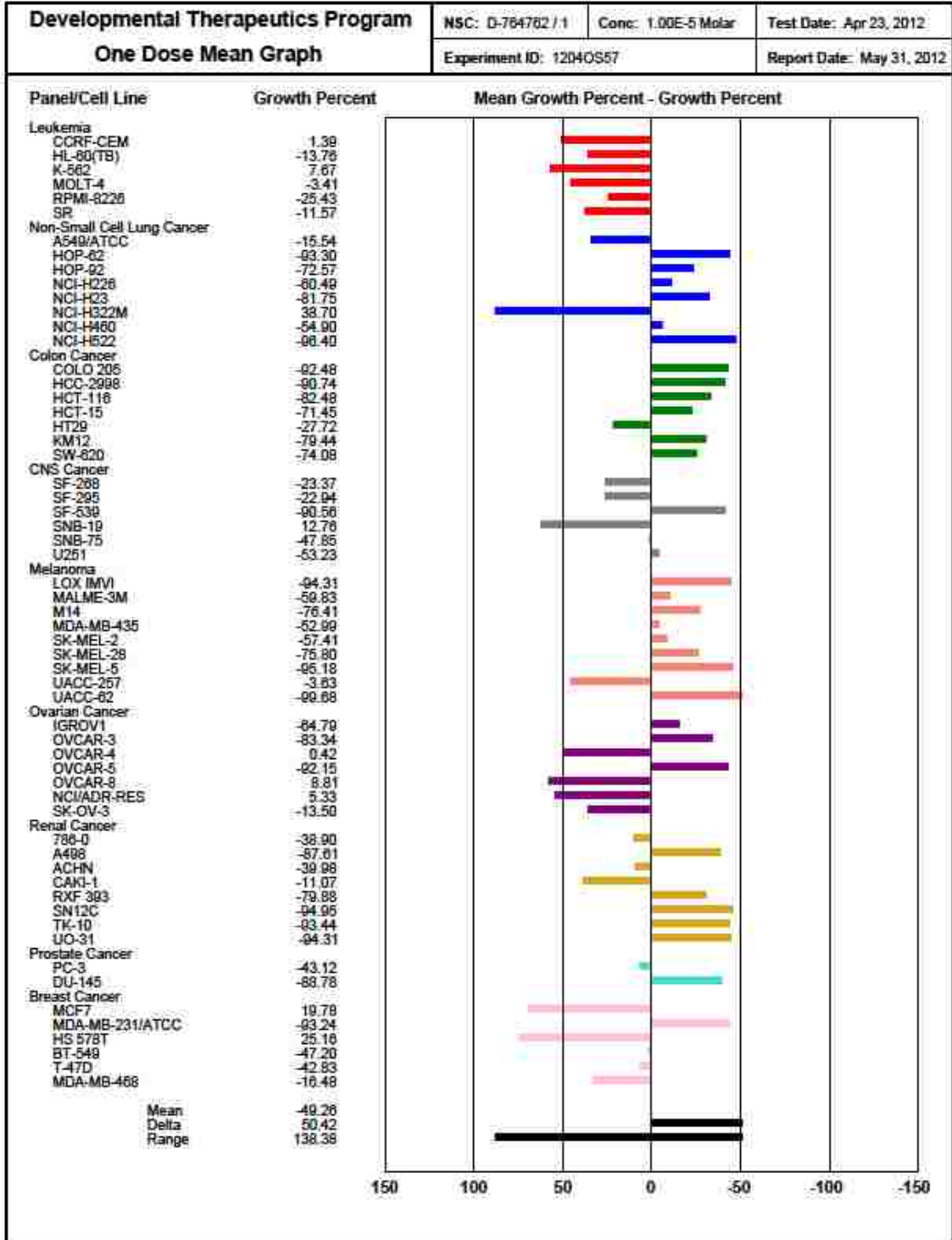
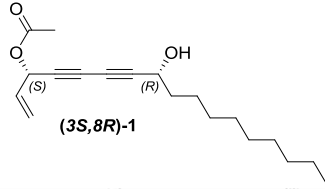
**<sup>1</sup>H NMR:**

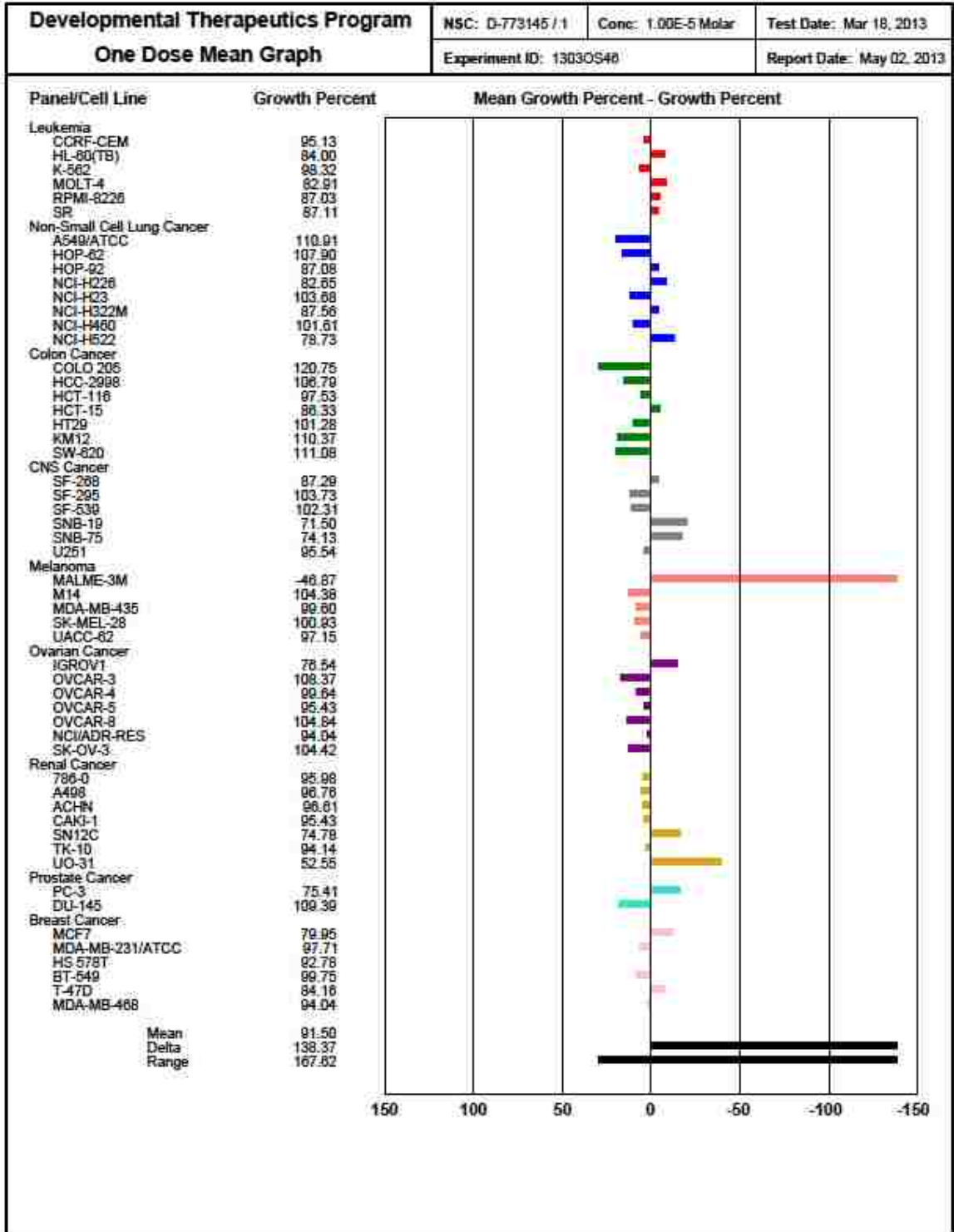
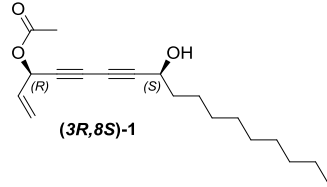


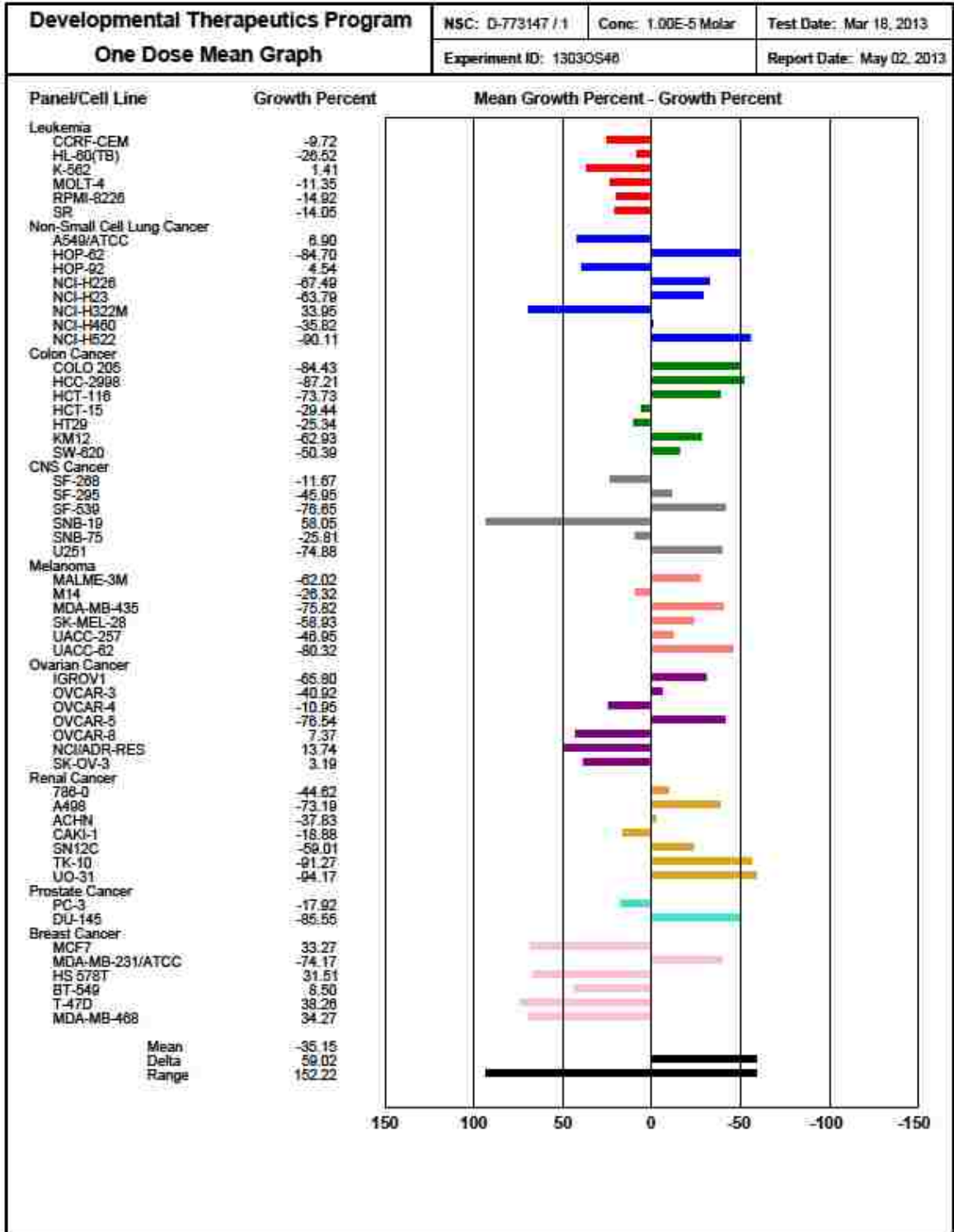
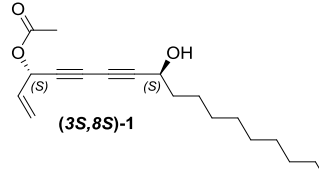
**<sup>13</sup>C NMR:**

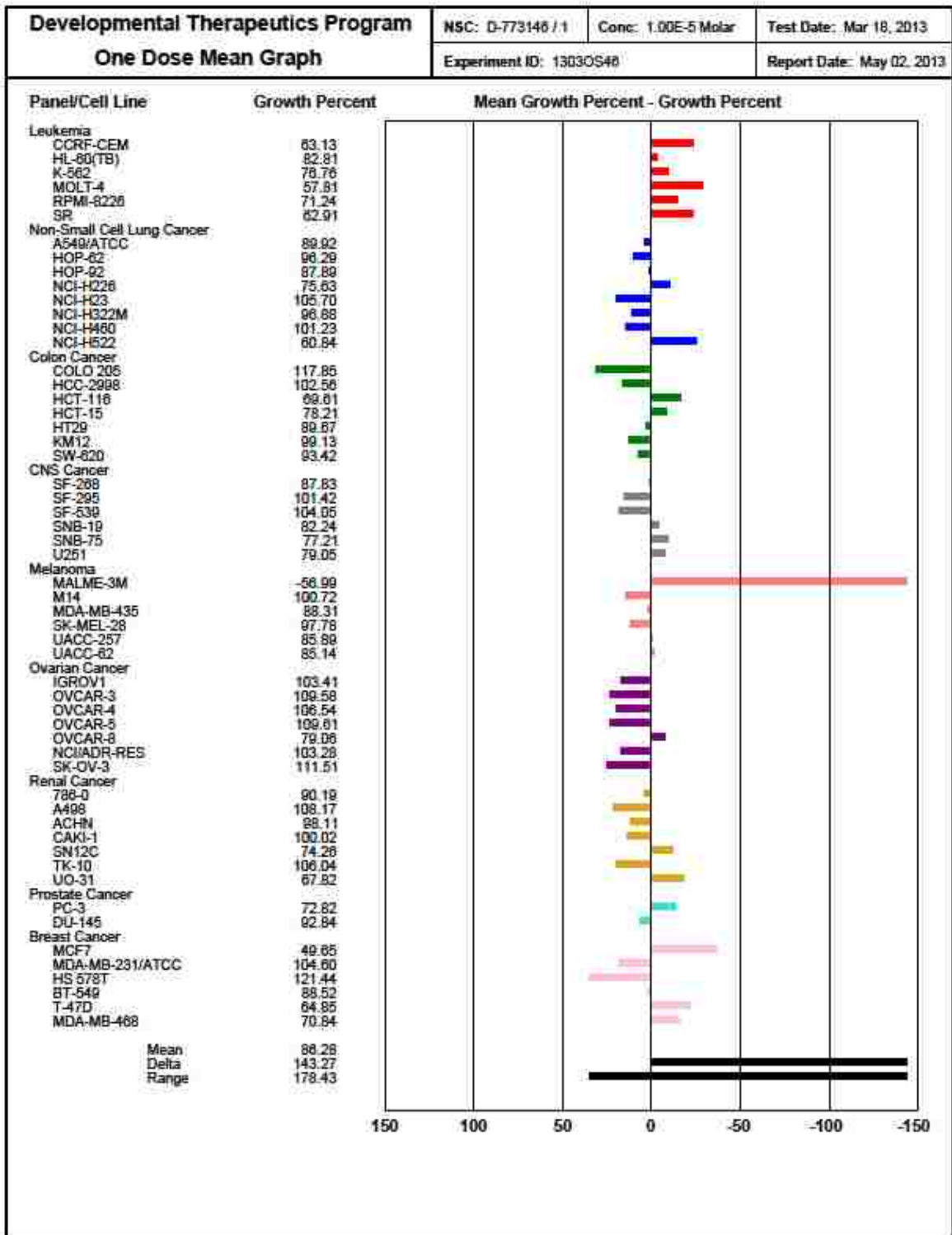
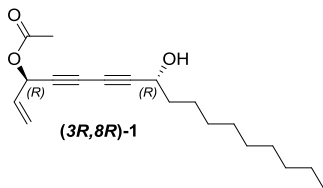


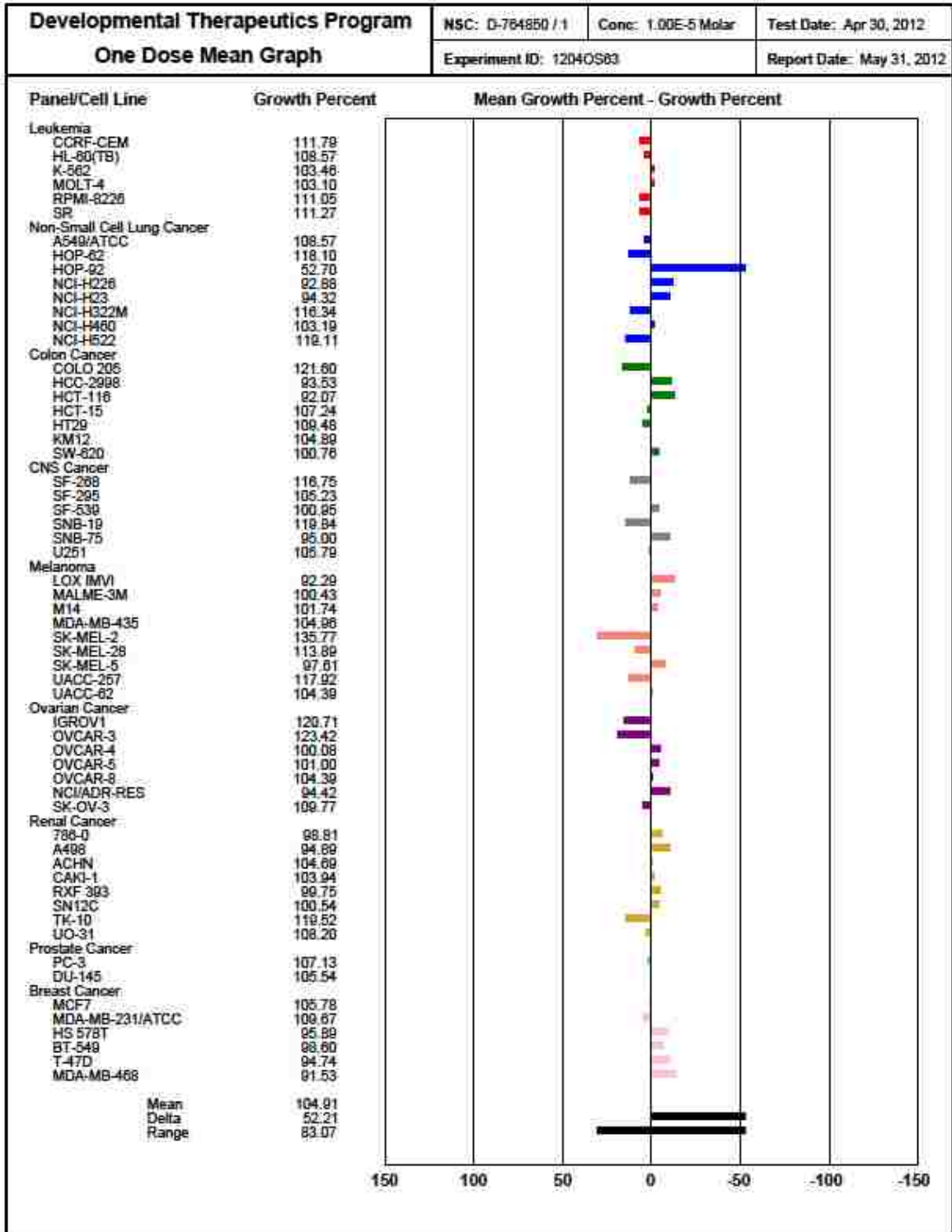
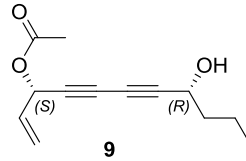
***Appendix B: National Cancer Institute One Dose Screening Results***



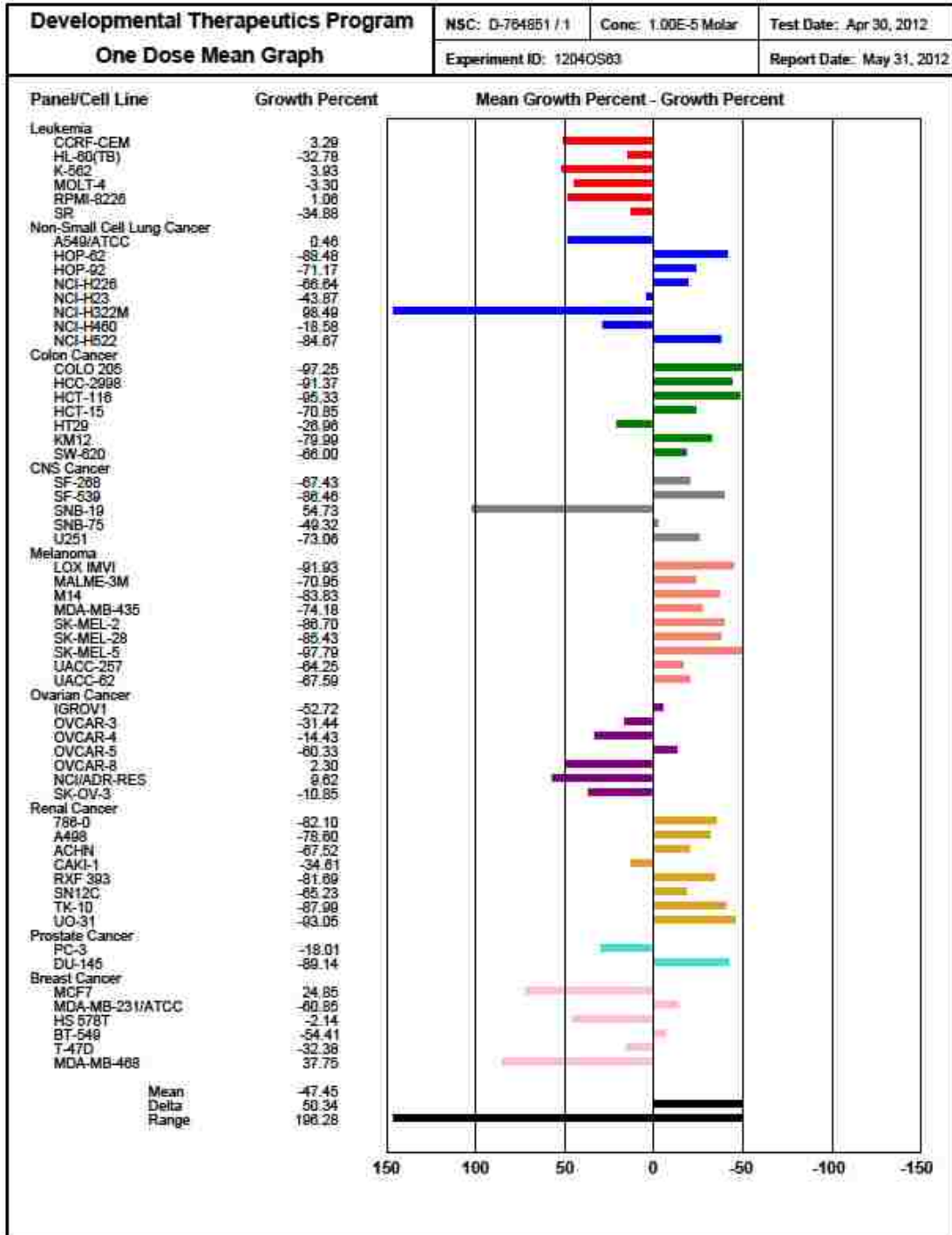
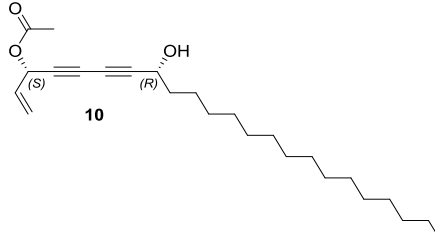


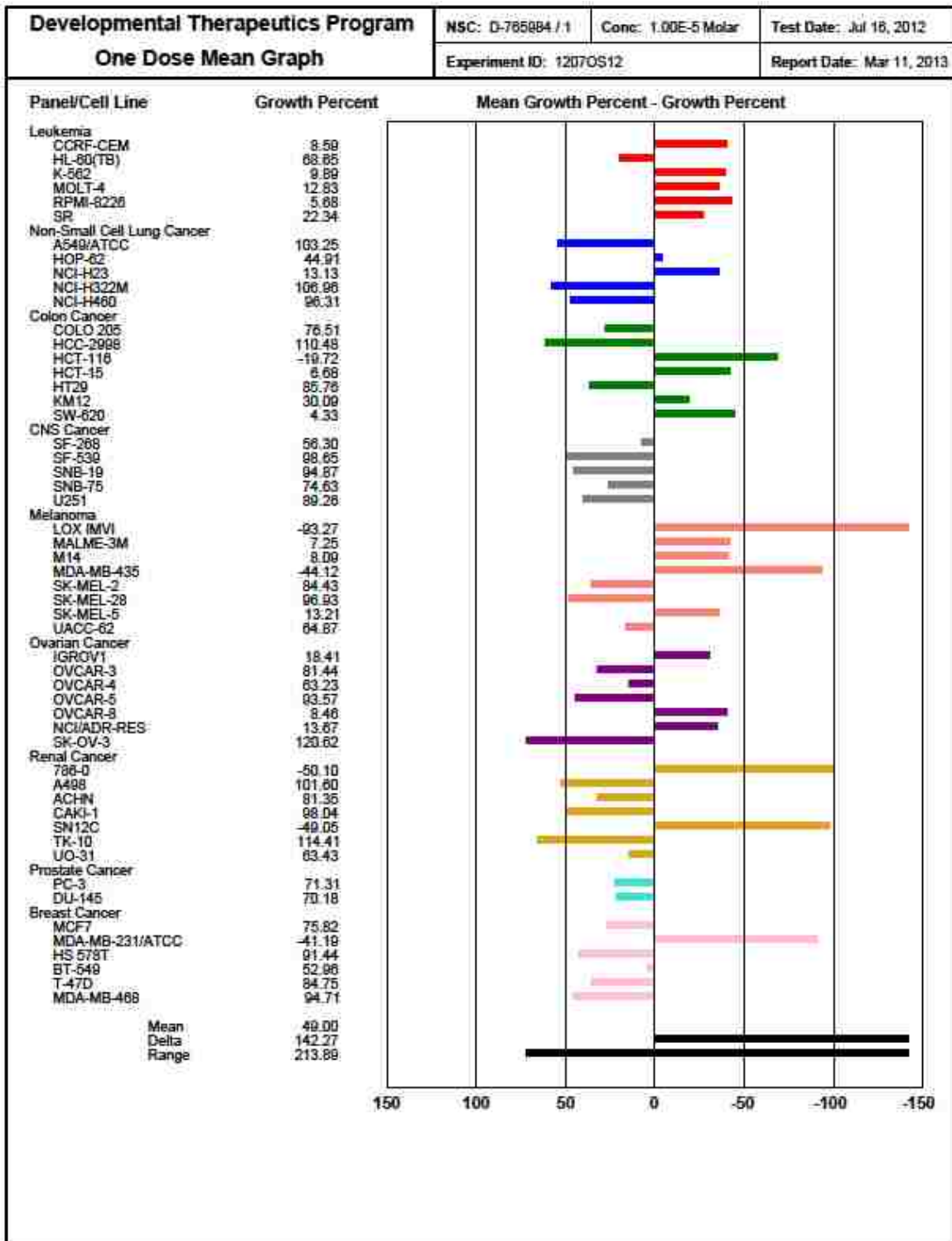
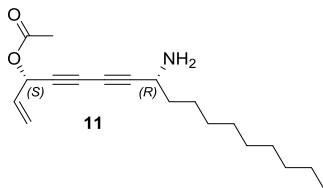


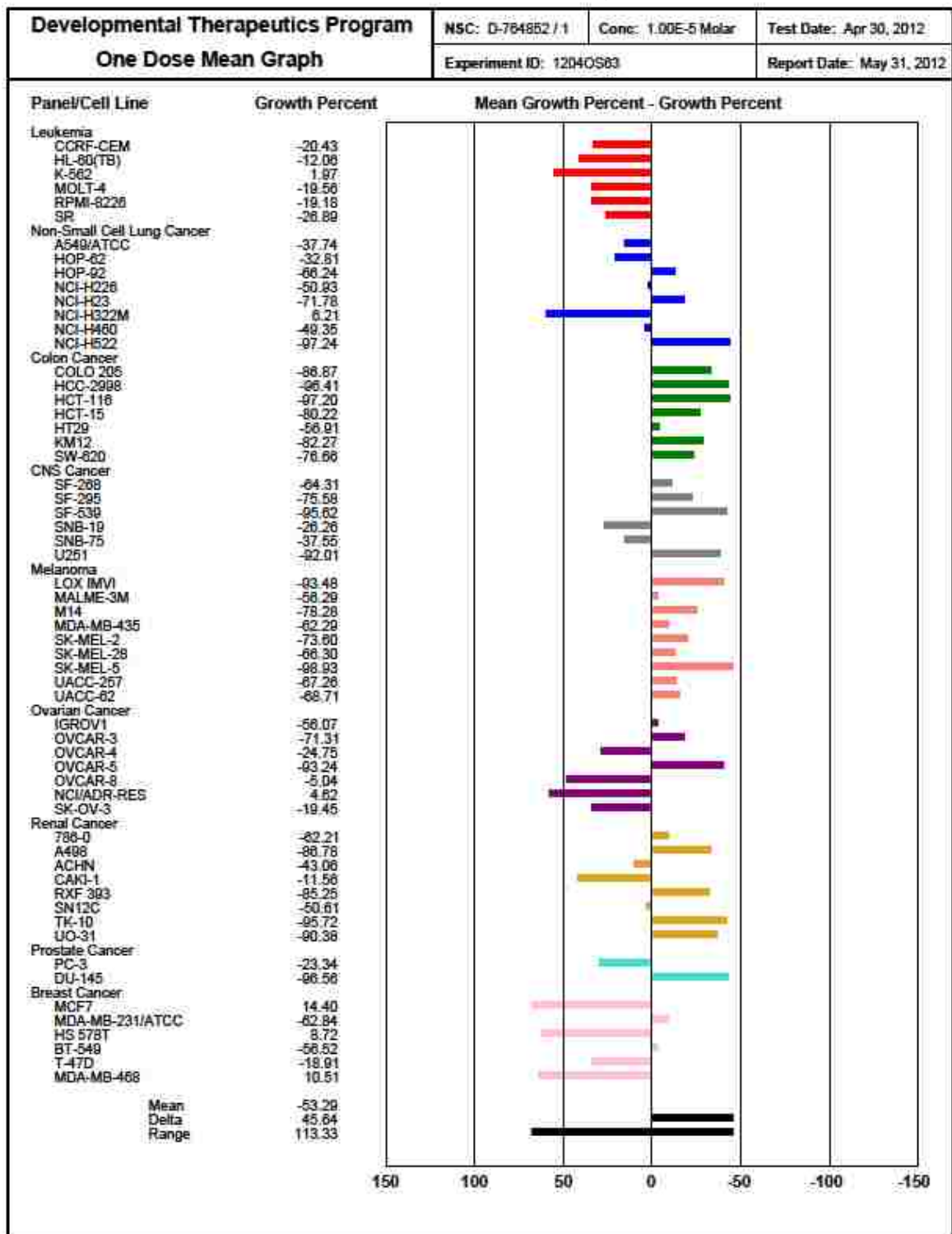
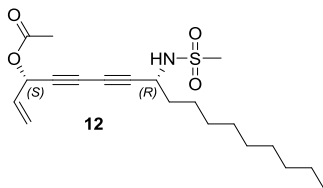


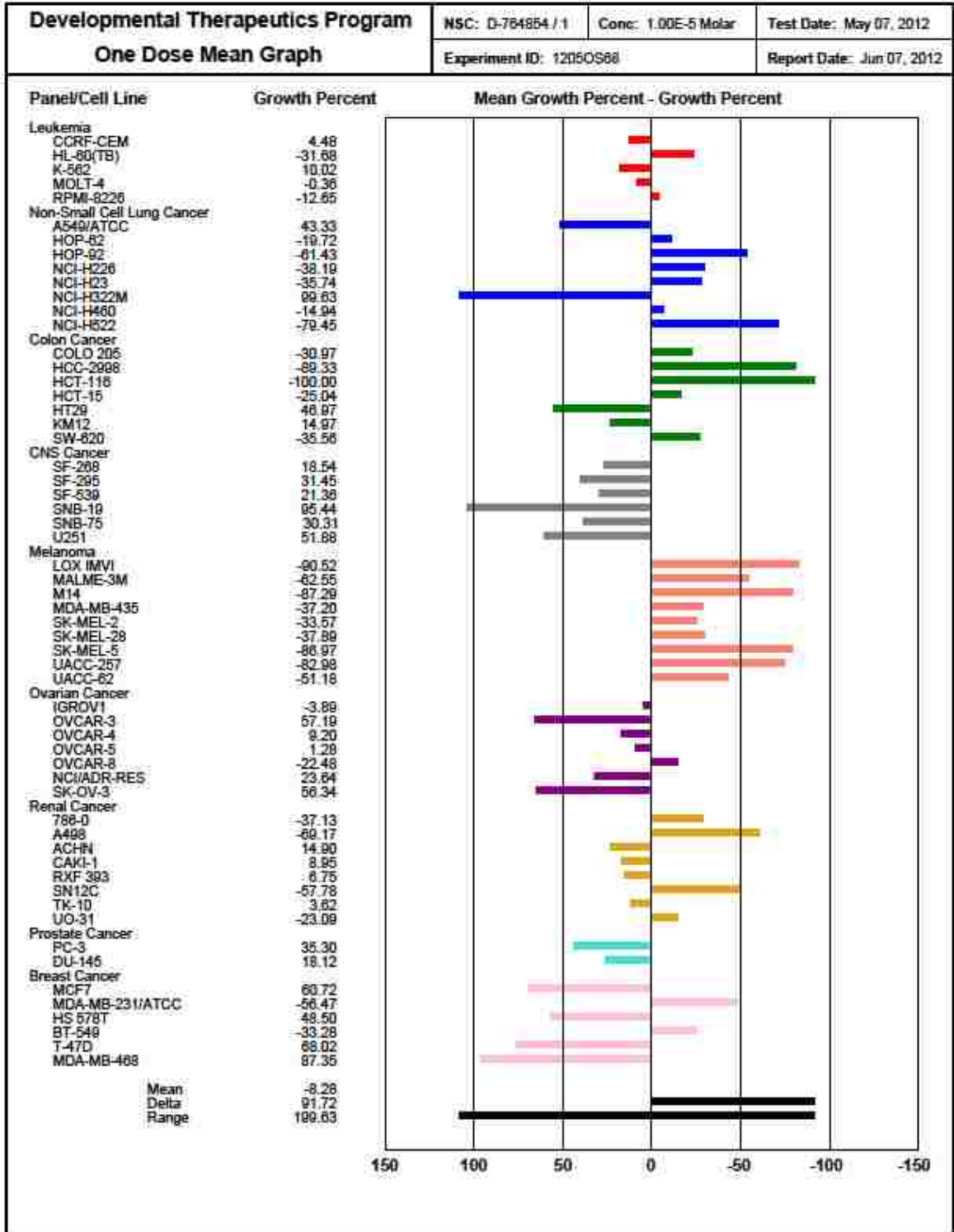
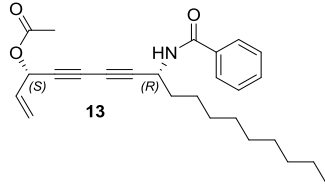


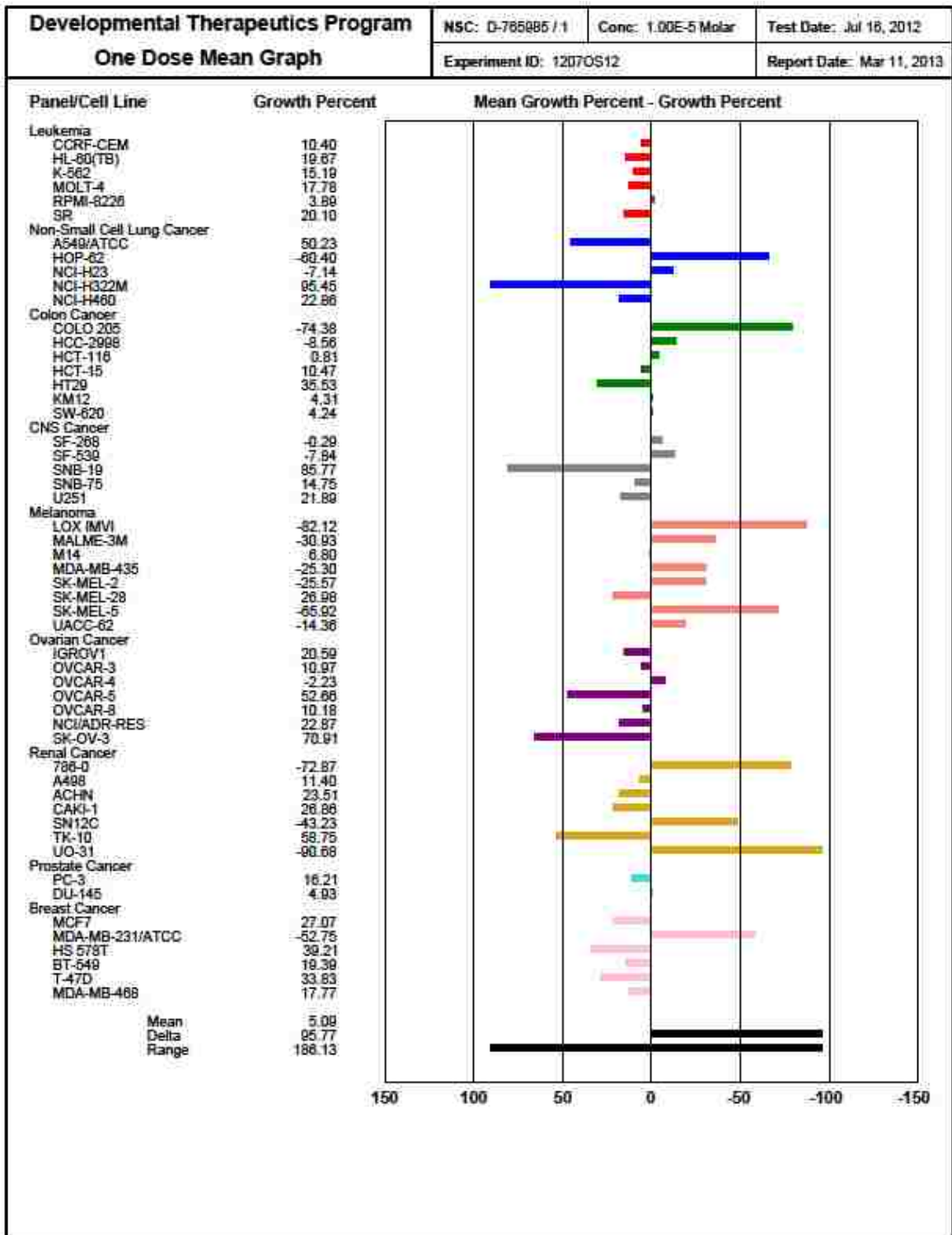
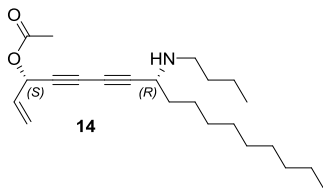


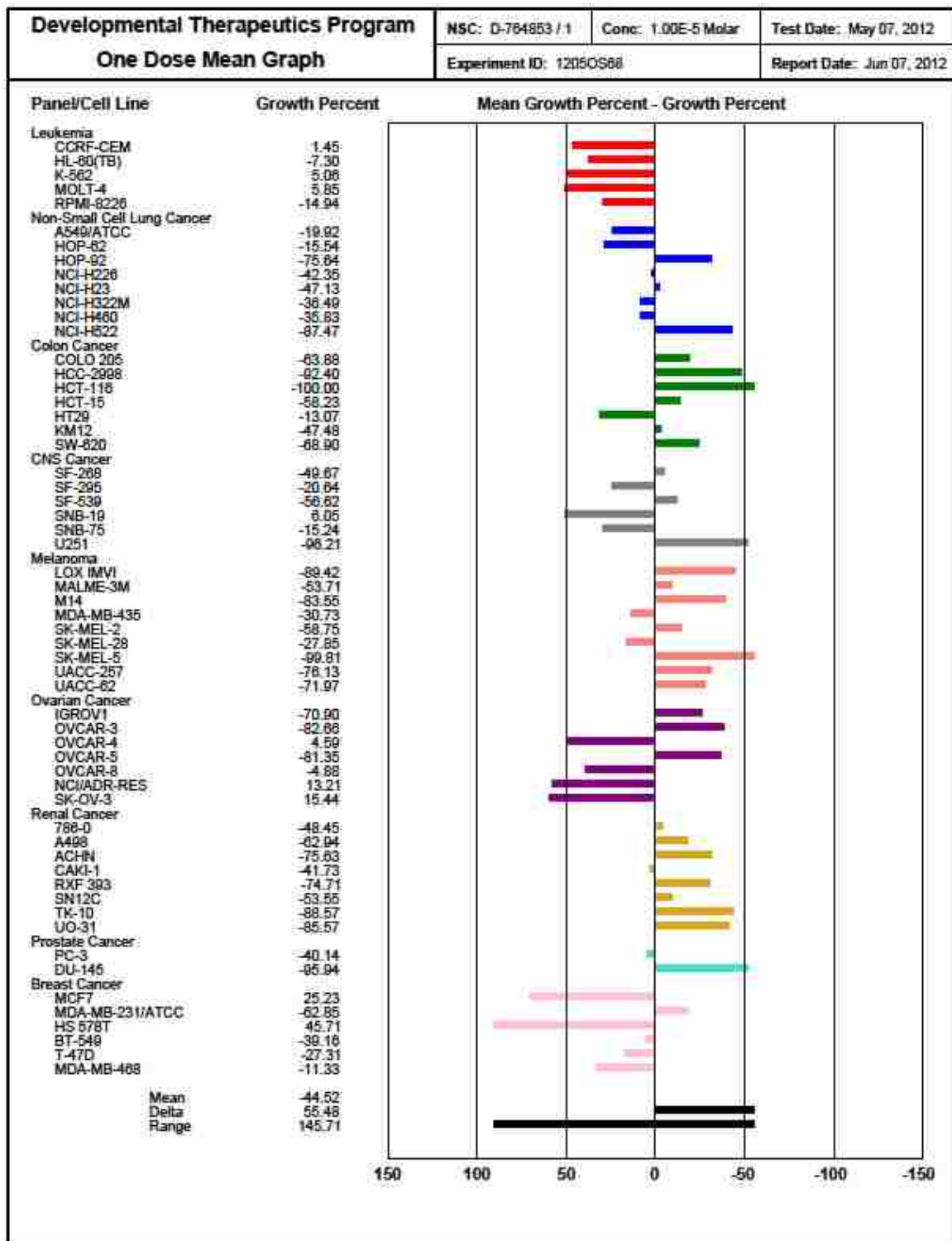
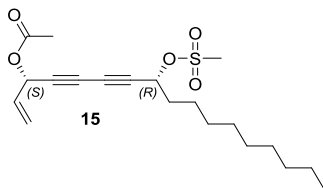


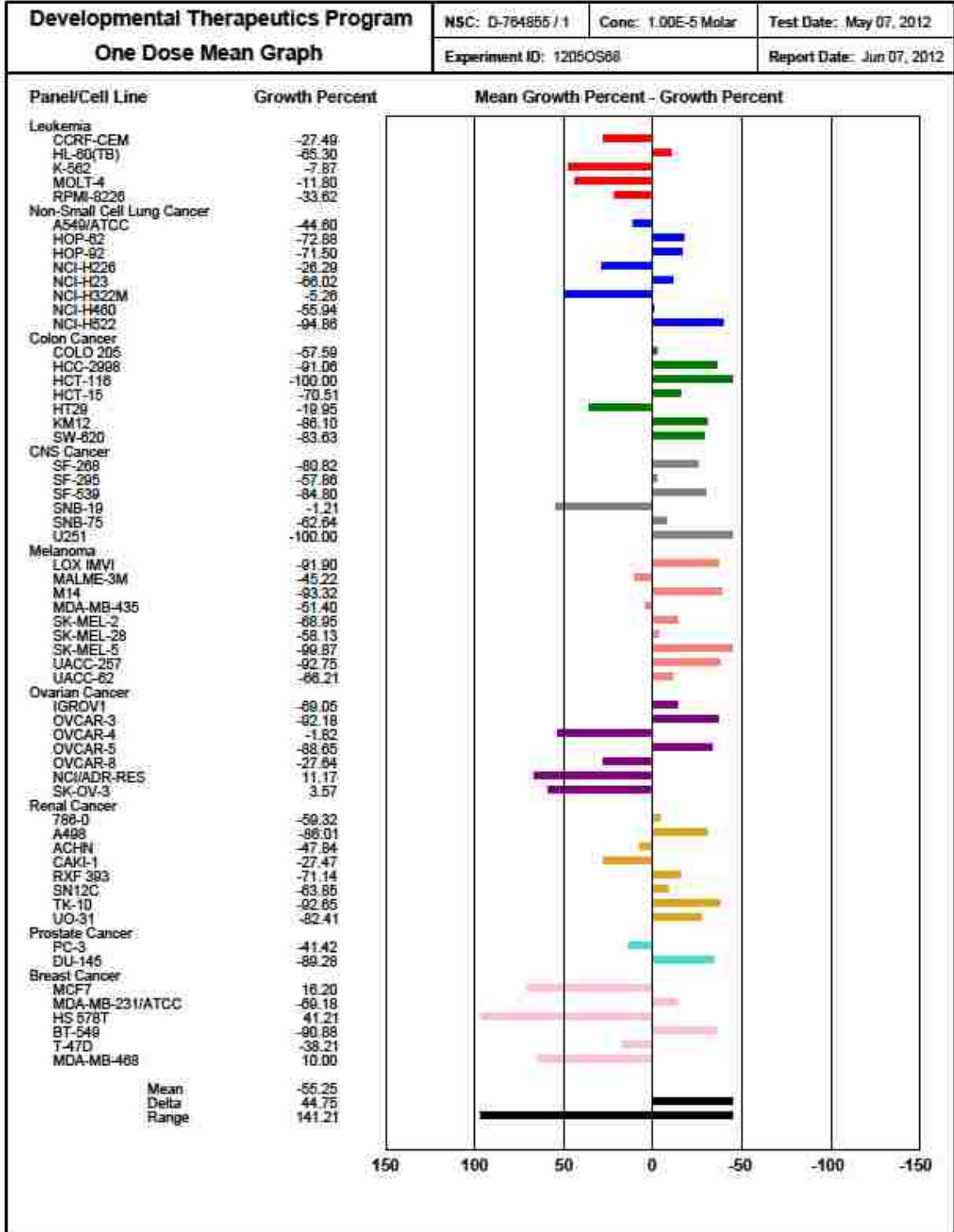
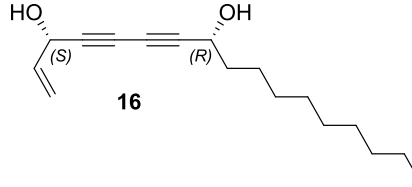


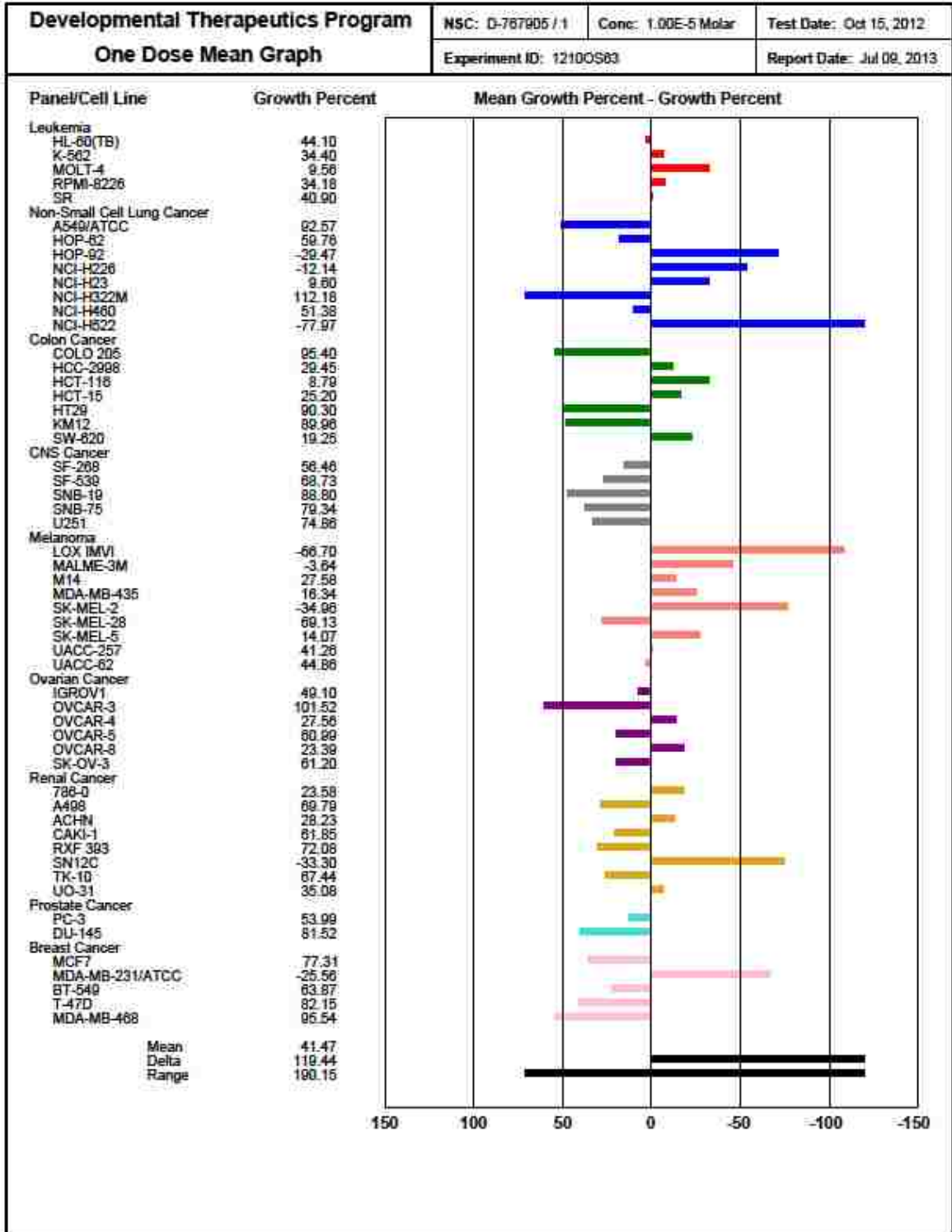
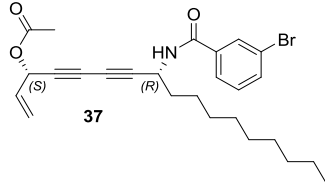




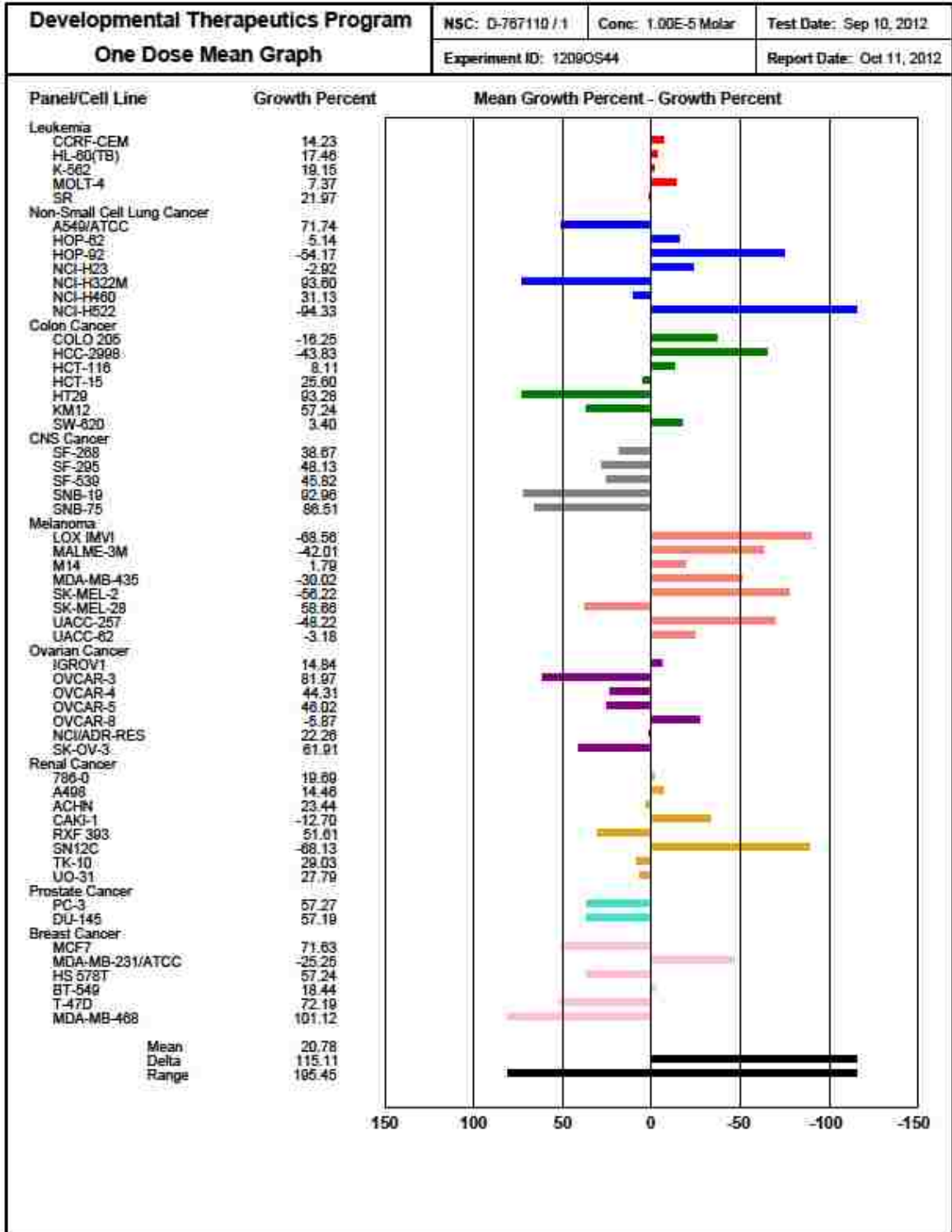
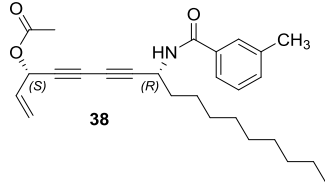


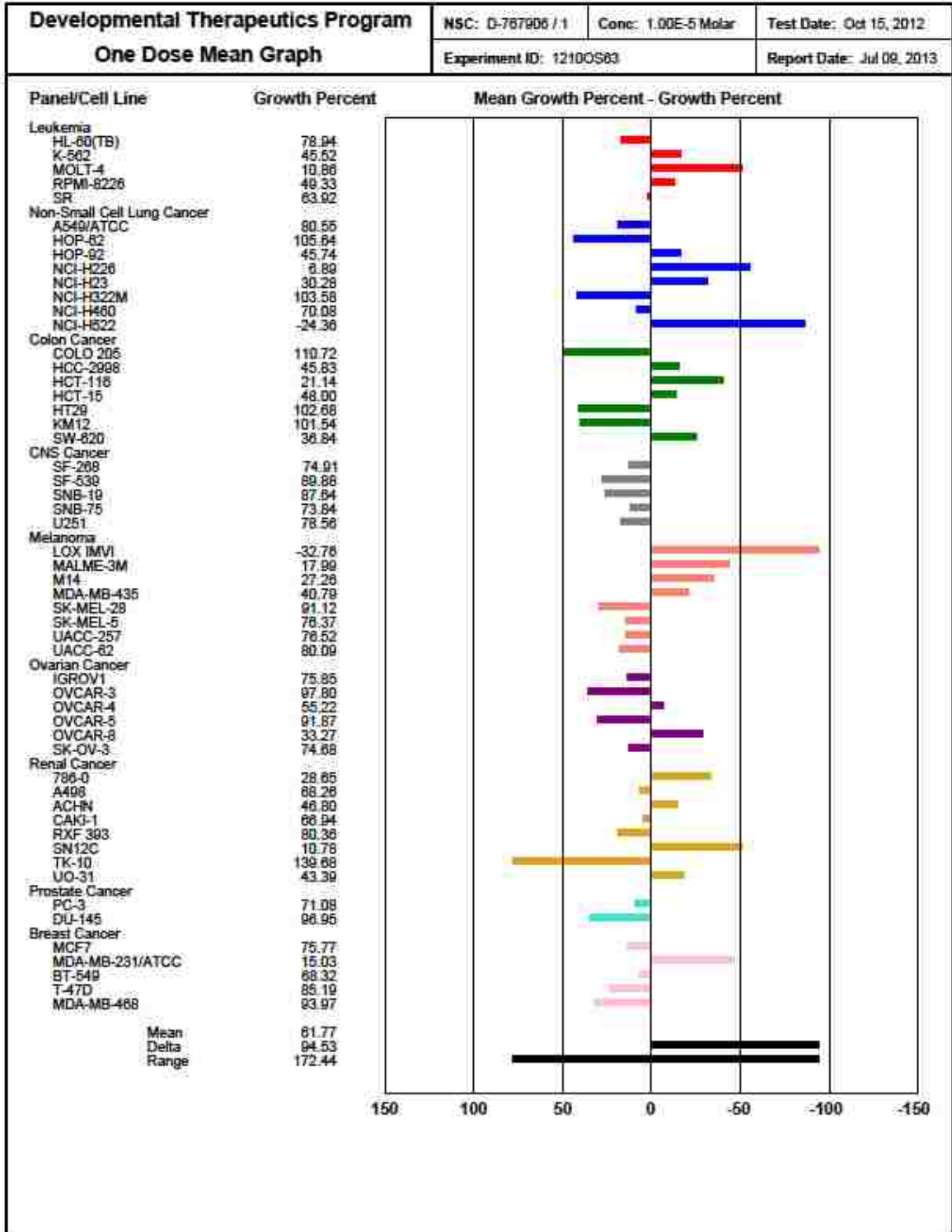
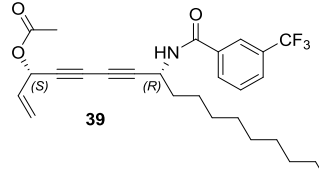


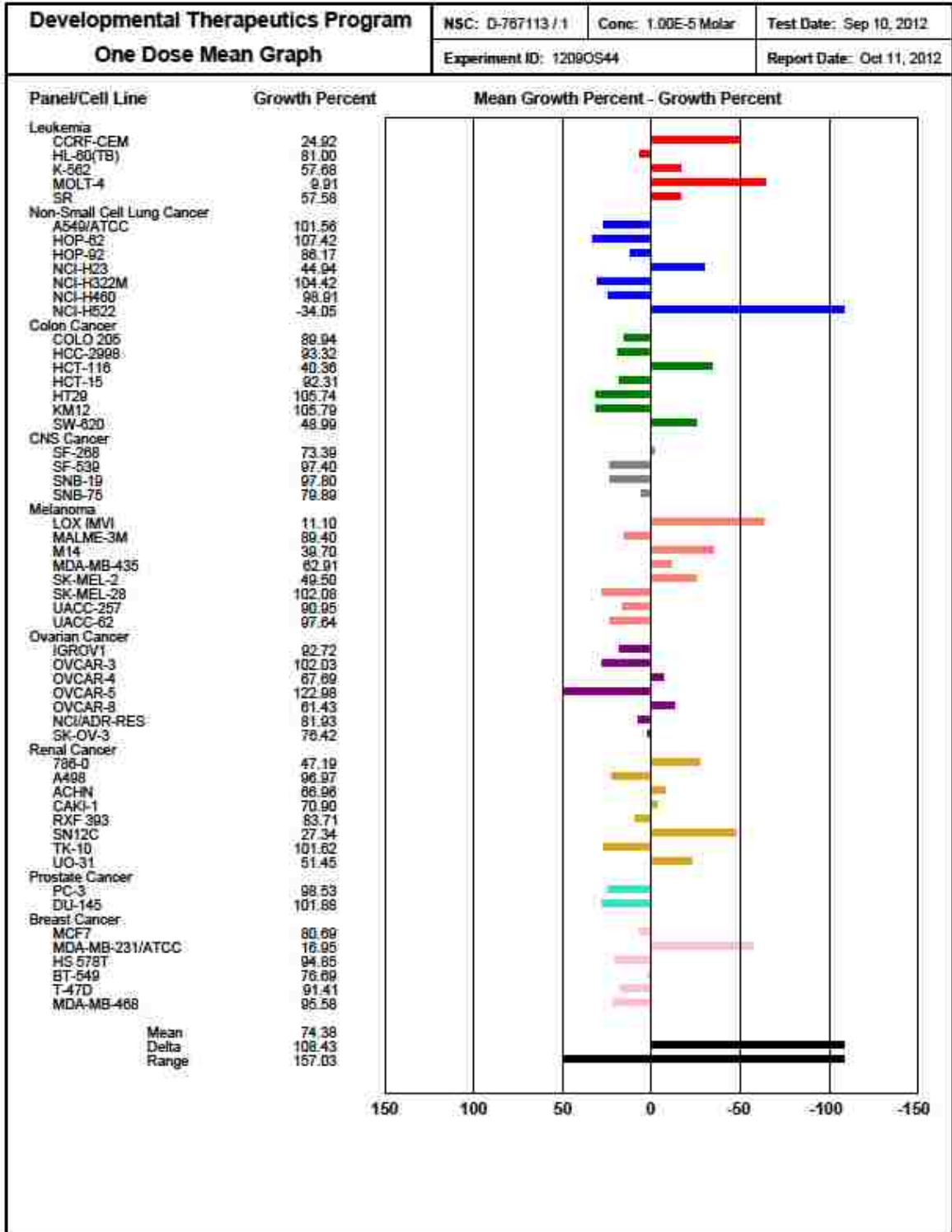
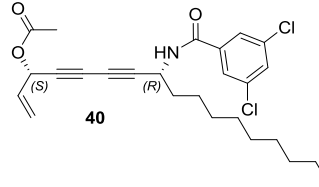


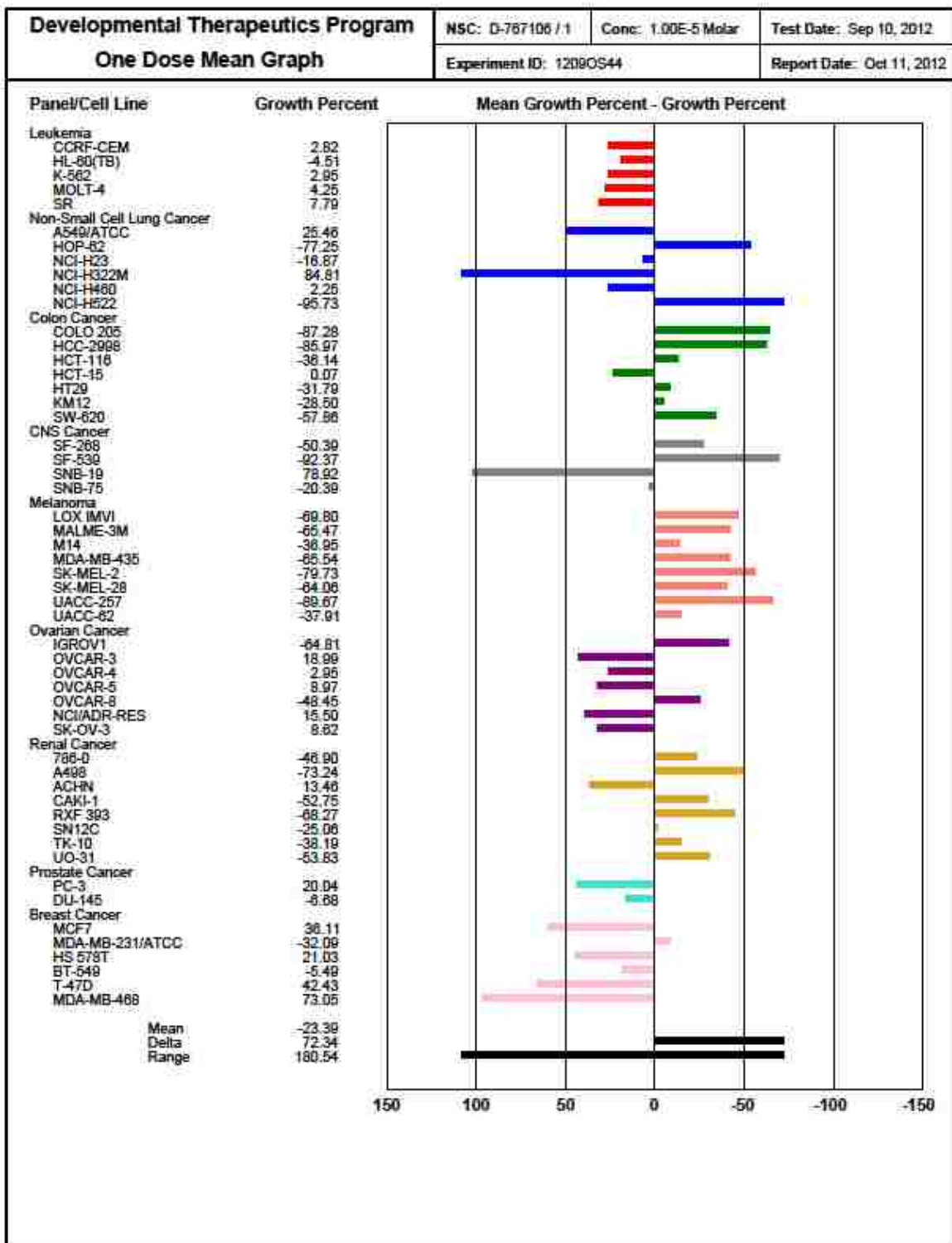
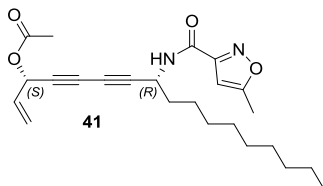


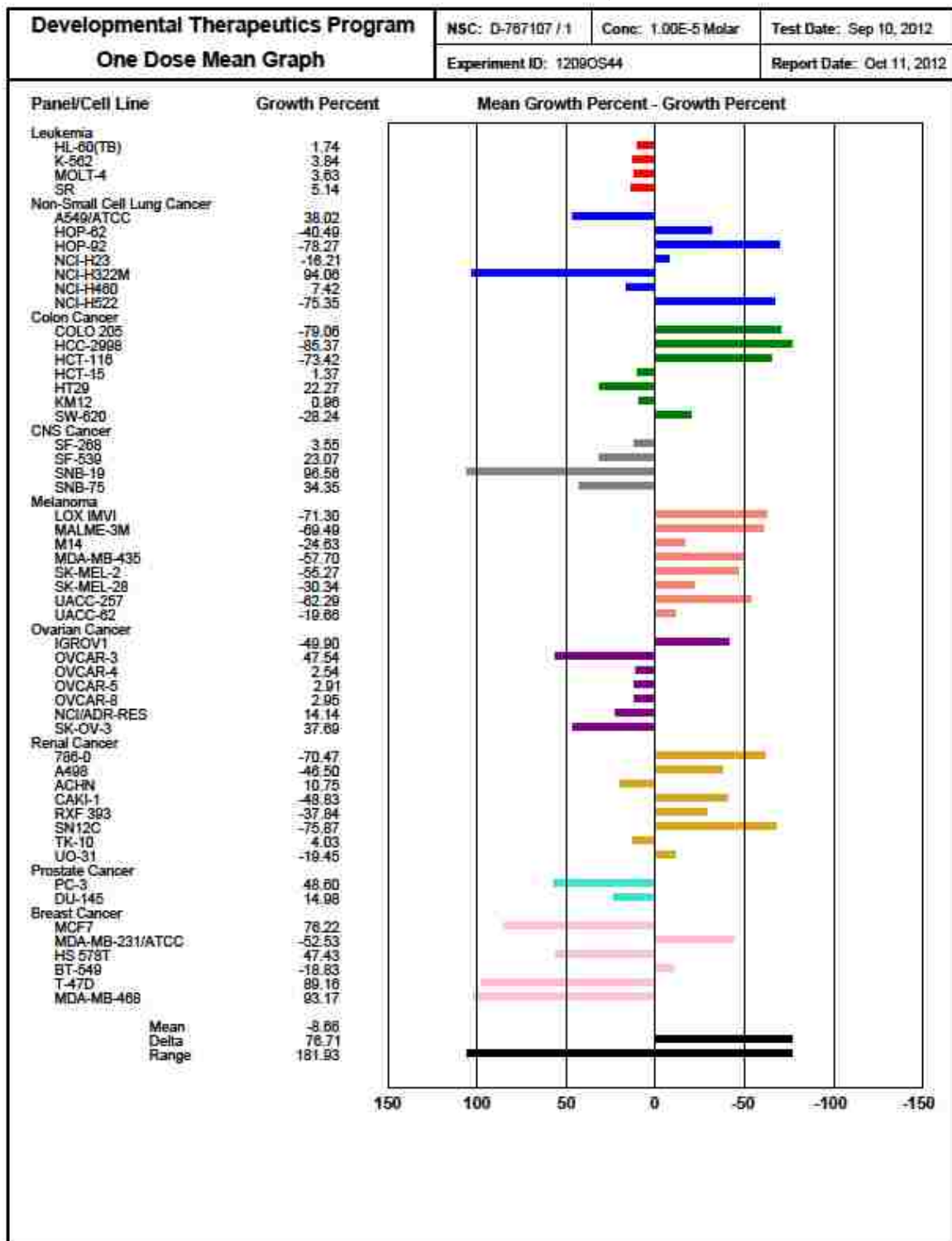
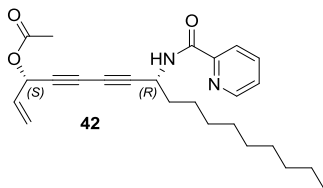


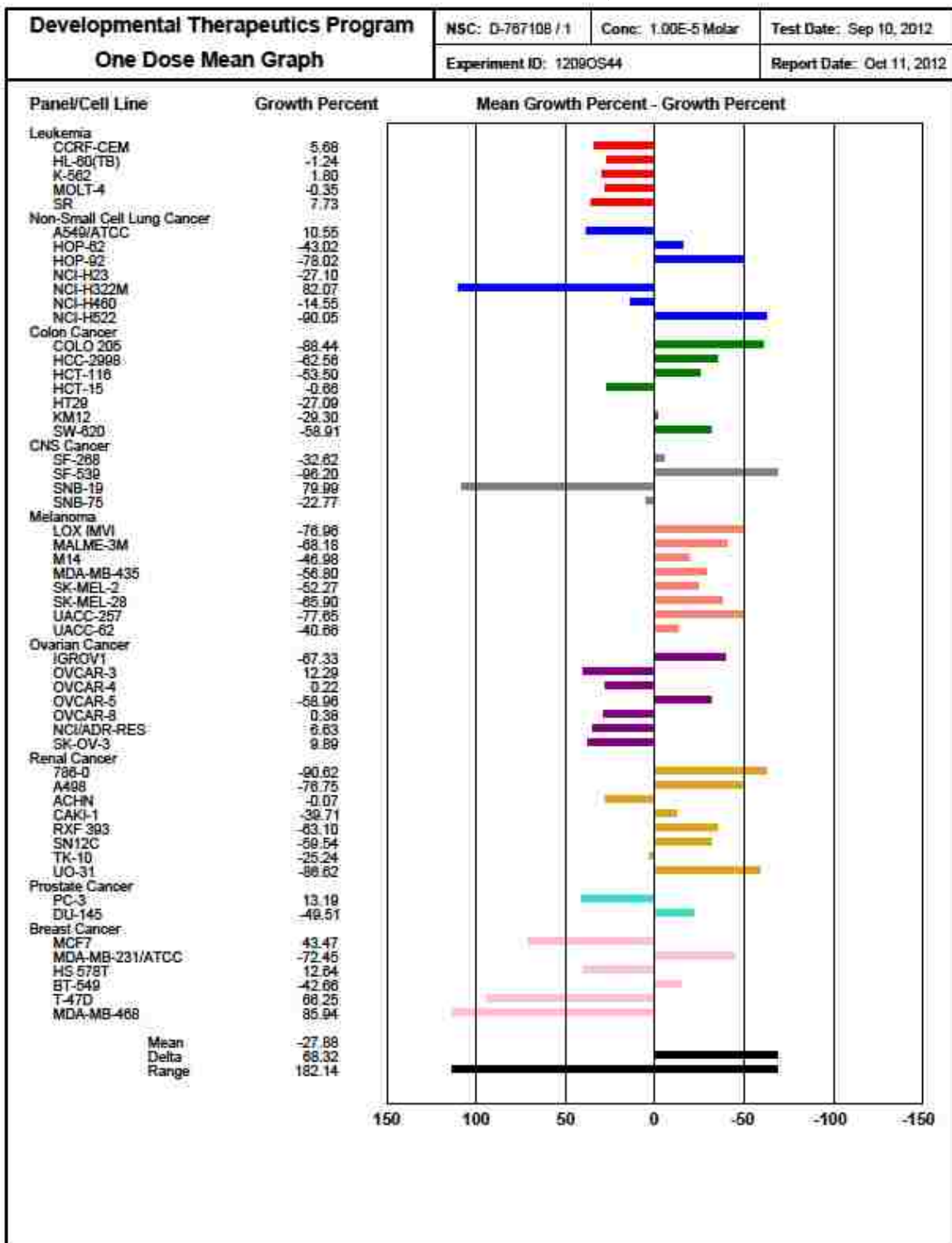
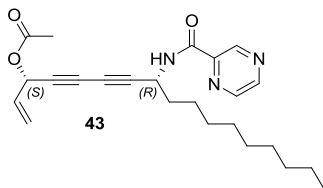


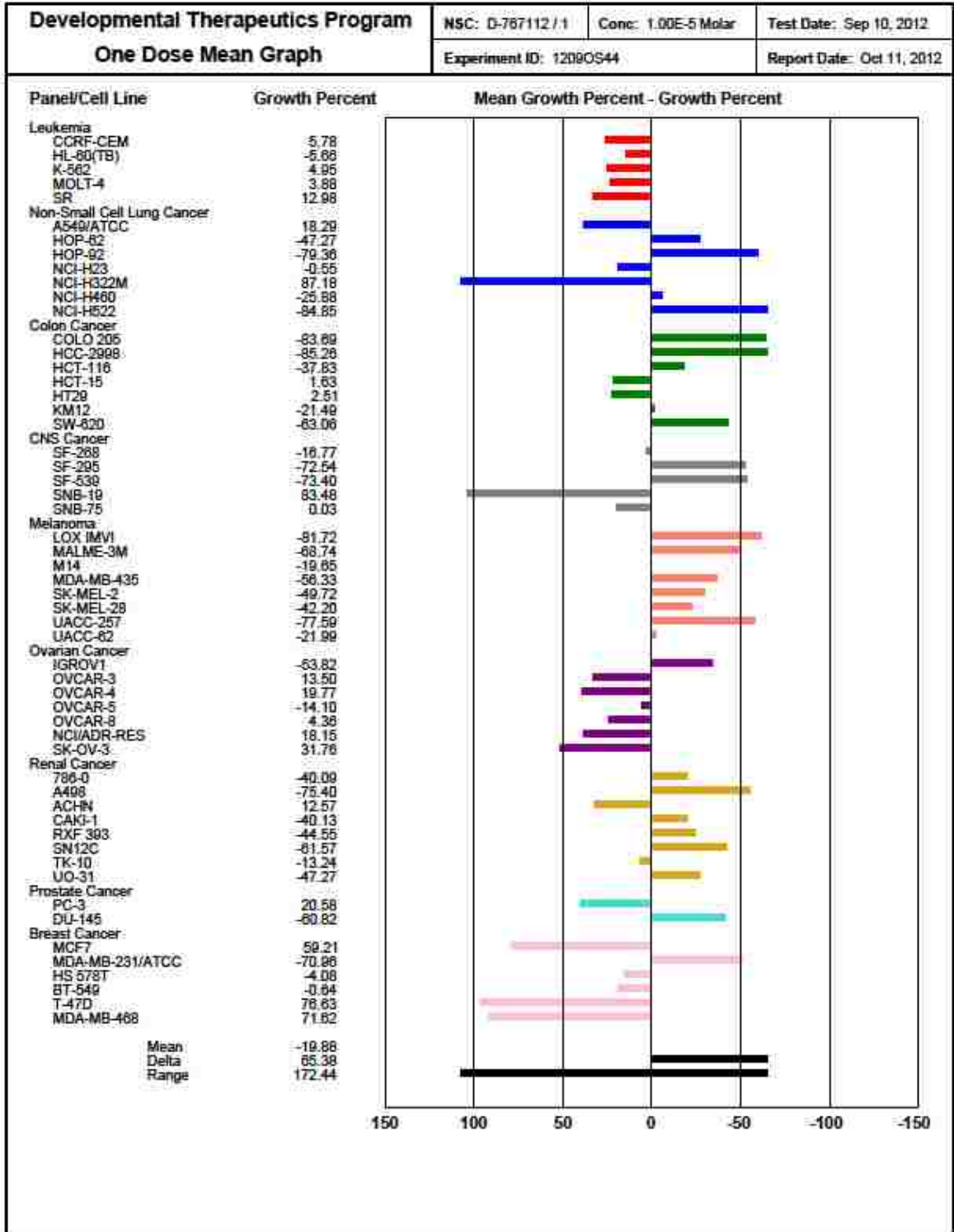
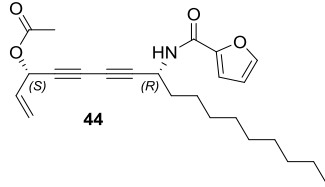


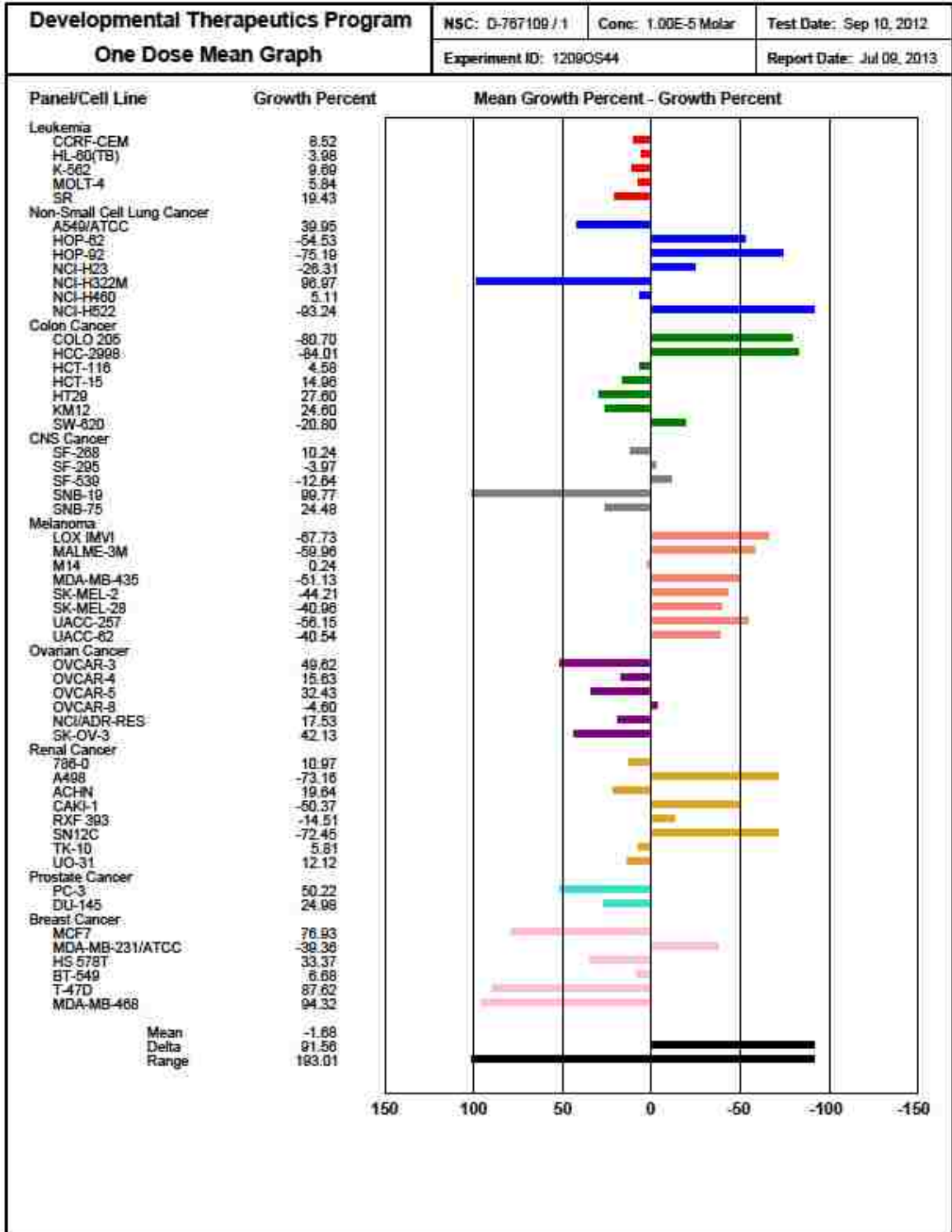
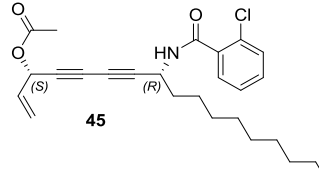




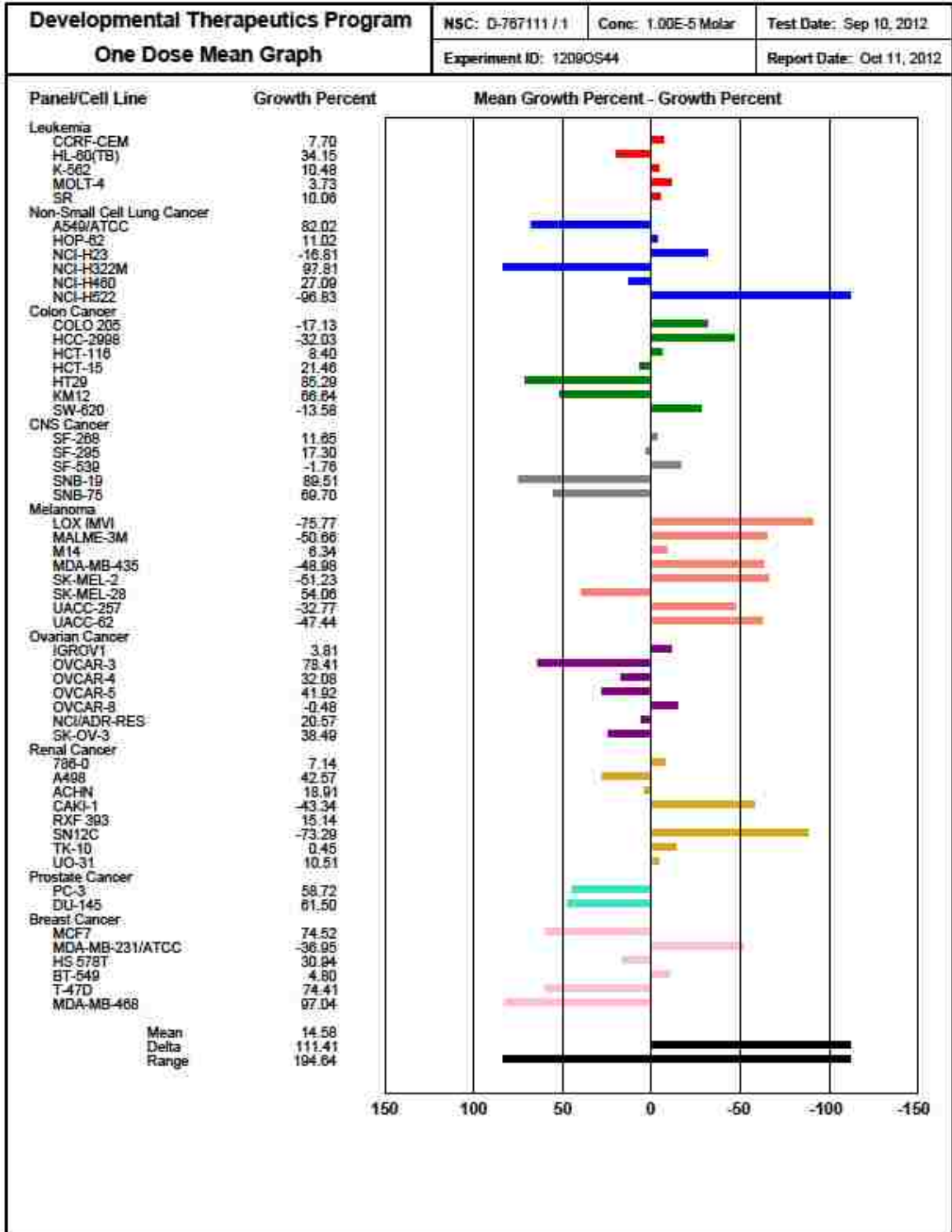
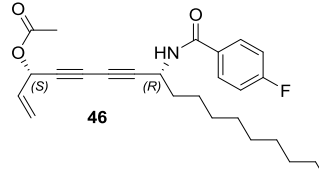


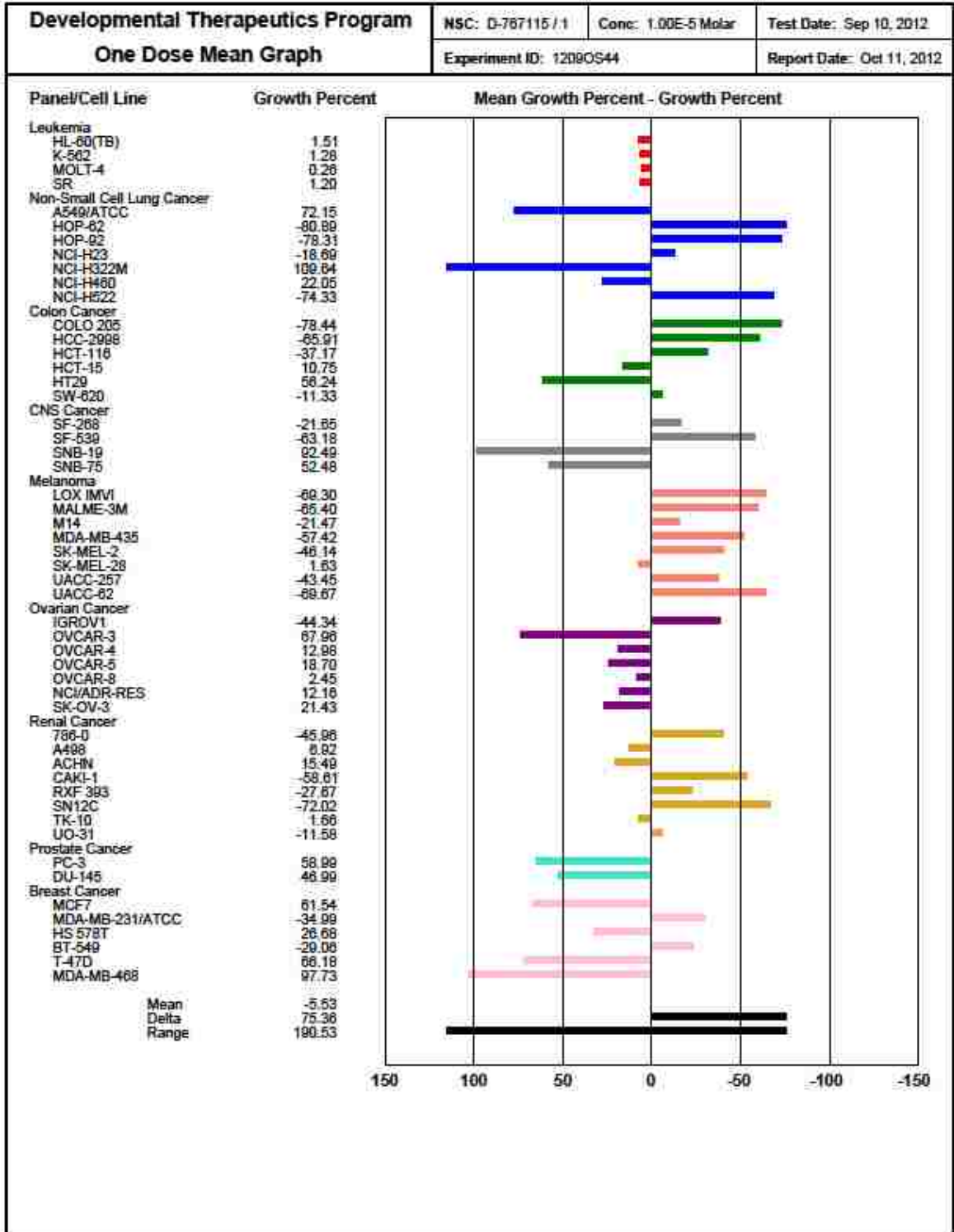
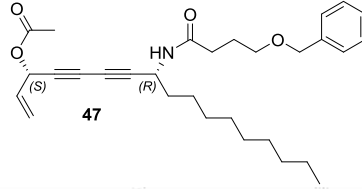


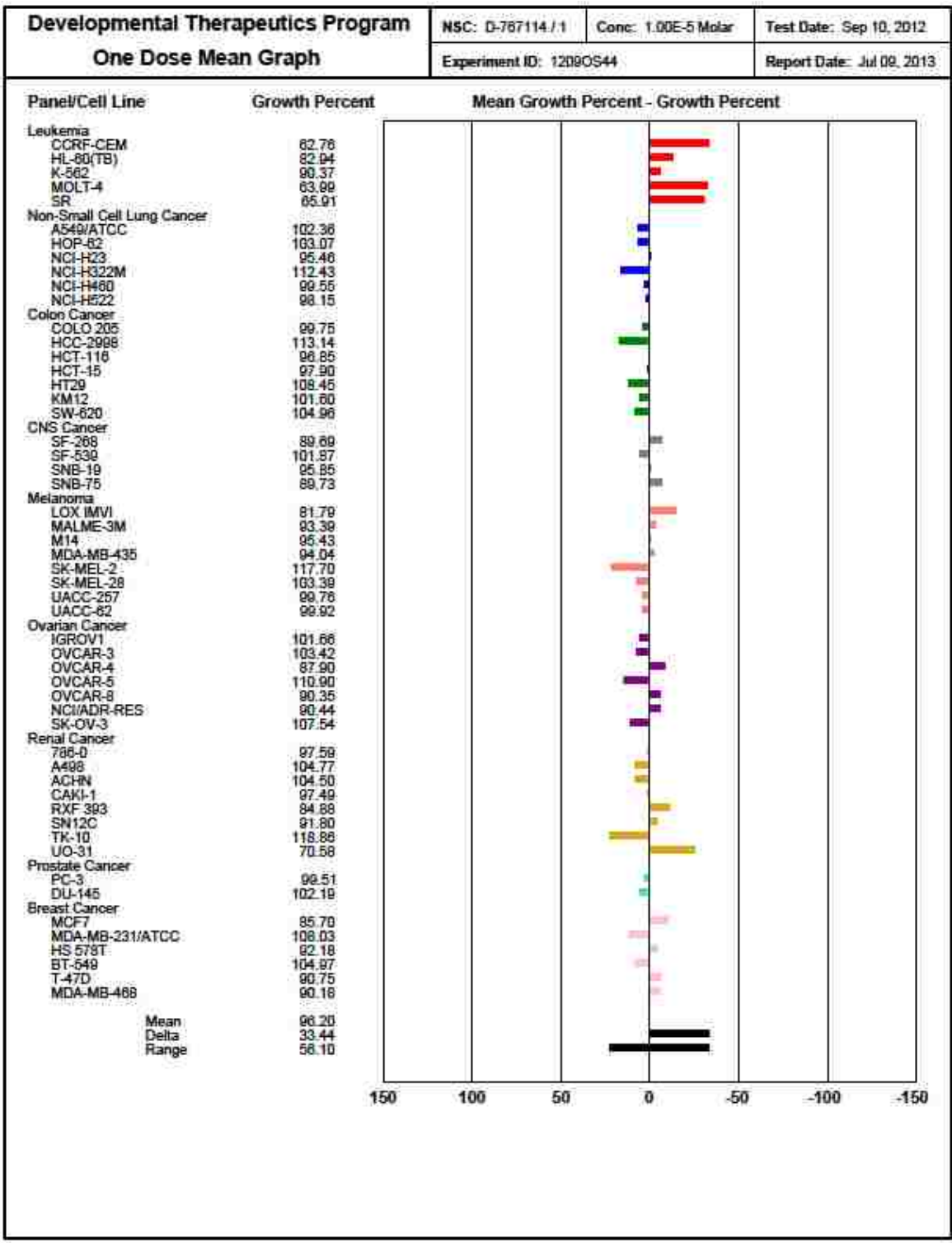
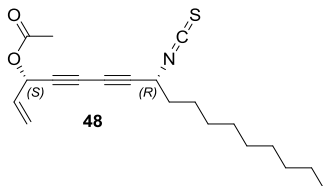












## References

- 1) <http://www.who.int/mediacentre/factsheets/fs094/en/>
- 2) [http://www.who.int/vaccine\\_research/diseases/soa\\_parasitic/en/index3.html](http://www.who.int/vaccine_research/diseases/soa_parasitic/en/index3.html)
- 3) Desjeux, P. Leishmaniasis: Current Situation and New Perspectives. *Comp. Immun. Microbiol. Infect. Dis.* **2004**, *27*, 305-318.
- 4) <http://www.stanford.edu/class/humbio153/ImmuneEvasion/Analysis.html>
- 5) Hailu, A.; Musa, A.M.; Royce, C.; Wasunna, M. Visceral Leishmaniasis: New Health Tools are Needed. *PLoS Medicine* **2005**, *2*(7), 590-594.
- 6) Schmidt, G.D.; Roberts, L.S. *Foundations of Parasitology*, 7<sup>th</sup> ed.; McGraw Hill, New York, **2005**, 61-88.
- 7) Herwaldt, B.L. Leishmaniasis. *Lancet* **1999**, *354*, 1191-1199.
- 8) Jhingran, A.; Chatterjee, M.; Madhubala, R. *Leishmania: Epidemiological Trends and Diagnosis. Leishmania: After the Genome*, Caister Academic Press, Norfolk, UK, **2008**, 1-13.
- 9) <http://www.dpd.cdc.gov/dpdx/Html/Leishmaniasis.htm>
- 10) Grevelink, S.A.; Lerner, E.A. Leishmaniasis. *J. Amer. Acad. Derm.* **1996**, *34*(2), 257-272.
- 11) Guerin, P.J.; Olliaro, P.; Sundar, S.; Boelaert, M.; Croft, S.L.; Desjeux, P.; Wasunna, M.K.; Bryceson, A.D.M. Visceral Leishmaniasis: Current Status of Control, Diagnosis, and Treatment, and a Proposed Research and Development Agenda. *Lancet Infect. Dis.* **2002**, *2*, 494-501.
- 12) Sundar, S. Drug Resistance in Indian Visceral Leishmaniasis. *Trop. Med. Int. Health.* **2001**, *6*, 849-854.
- 13) Lira, R.; Sundar, S.; Makharia, A.; Kenney, R.; Gam, A.; Saraiva, E.; Sacks, D. Evidence that the High Incidence of Treatment Failures in Indian Kala-azar is Due to the Emergence of Antimony-resistant Strains of *Leishmania donovani*. *J. Infect. Dis.*, **1999**, 564-567.
- 14) Laniado-Laborin, R.; Cabrales-Vargas, M.N. Amphotericin B: Side Effects and Toxicity. *Rev. Iberoam. Micol.* **2009**, *26*(4), 223-227.
- 15) Di Giorgio, C.; Faraut-Gambarelli, F.; Imbert, A.; Minodier, P.; Gasquet, M.; Dumon, H. Flow Cytometric Assessment of Amphotericin B Susceptibility in *Leishmania infantum* Isolates from Patients with Visceral Leishmaniasis. *J. Antimicrob. Chemother.* **1999**, *44*, 71-76.
- 16) Croft, S.L.; Sundar, S.; Fairlamb, A.H. Drug Resistance in Leishmaniasis. *Clin. Microbiol. Rev.* **2006**, *19*, 111-126.
- 17) Jha, T. K. Evaluation of Diamidine Compound (pentamidine isethionate) in the Treatment Resistant Cases of Kala-azar Occurring in North Bihar, India. *Trans. R. Soc. Trop. Med. Hyg.* **1983**, *77*, 167-170.
- 18) Jha, S.N.; Singh, N.K.; Jha, T.K. Changing Response to Diamidine Compounds in Cases of Kala-azar Unresponsive to Antimonial. *J. Assoc. Physicians India* **1991**, *39*, 314-316.
- 19) Thakur, C.P.; Kumar, M.; Pandey, A.K. Comparison of Regimes of Treatment of Antimony-Resistant Kala-azar Patients: A Randomized Study. *Am. J. Trop. Med. Hyg.* **1991**, *45*(4), 435-441.
- 20) Saugar, J.M.; Delgado, J.; Hornillos, V.; Luque-Ortega, J.R.; Amat-Guerri, F.; Acuna, A.U.; Rivas, L. Synthesis and Biological Evaluation of Fluorescent

- Leishmanicidal Analogues of Hexadecylphosphocholine (Miltefosine) as Probes of Antiparasite Mechanisms. *J. Med. Chem.* **2007**, *50*, 5994-6003.
- 21) Sundar, S.; Olliaro, P.L. Miltefosine in the Treatment of Leishmaniasis: Clinical Evidence for Informed Clinical Risk Management. *Therap. Clin. Risk Manage.* **2007**, *3(5)*, 733-740.
  - 22) Croft, S.L.; Neal, R.A.; Pendergast, W.; Chan, J.H. The Activity of Alkylphosphocholines and Related Derivatives Against *Leishmania donovani*. *Biochem. Pharmacol.* **1987**, *36*, 2633-2636.
  - 23) Perez-Victoria, F.J.; Sanchez-Canete, M.P.; Seifert, K.; Croft, S.L.; Sundar, S.; Castanys, S.; Gamarro, F. Mechanisms of Experimental Resistance of *Leishmania* to Miltefosine: Implications for Clinical Use. *Drug Resistance Updates* **2006**, *9*, 26-39.
  - 24) Sundar, S.; Jha, T.K.; Thakur, C.P.; Sinha, P.K.; Bhattacharya, S.K. Injectable Paromomycin for Visceral Leishmaniasis in India. *New Eng. J. Med.* **2007**, *356(25)*, 2571-2581.
  - 25) Teklemariam, S.; Hiwot, A.G.; Frommel, D.; Miko, T.L.; Ganlov, G.; Bryceson, A. Aminosalicylic Acid and its Combination with Sodium Stibogluconate in the Treatment of Diffuse Cutaneous Leishmaniasis Caused by *Leishmania aethiopica*. *Trans. R. Soc. Trop. Med. Hyg.* **1994**, *88*, 334-339.
  - 26) Gad, G.F.; Mohamed, H.A.; Ashour, H.M. Aminoglycoside Resistance Rates, Phenotypes, and Mechanisms of Gram-Negative Bacteria from Infected Patients in Upper Egypt. *Plos One* **2011**, *6(2)* e17224, 1-7.
  - 27) Jha, T.K.; Sundar, S.; Thakur, C.P.; Felton, J.M.; Sabin, A.J.; Horton, J. A Phase II Dose-Ranging Study of Sitamaquine for the Treatment of Visceral Leishmaniasis in India. *Am. J. Trop. Med. Hyg.* **2005**, *73(6)*, 1005-1011.
  - 28) Bories, C.; Cojean, S.; Huteau, F.; Loiseau, P.M. Selection and Phenotype Characterisation of Sitamaquine-Resistant Promastigotes of *Leishmania donovani*. *Biomed. Pharm.* **2008**, *62(3)*, 164-167.
  - 29) Tarbet, E.B.; Larson, D.; Anderson, B.J.; Bailey, K.W.; Wong, M.H.; Smees, D.F. Evaluation of Imiquimod for Topical Treatment of Vaccinia Virus Cutaneous Infections in Immunosuppressed Hairless Mice. *Antiviral Res.* **2011**, *90*, 126-133.
  - 30) Arevalo, I.; Ward, B.; Miller, R.; Meng, T.C.; Najjar, E.; Alvarez, E.; Matlashewski, G.; Llanos-Cuentas, A. Successful Treatment of Drug-Resistant Cutaneous Leishmaniasis in Humans by Use of Imiquimod, an Immunomodulator. *Clin. Infect. Dis.* **2001**, *33*, 1847-1851.
  - 31) Haldar, A.K.; Sen, P.; Roy, S. Use of Antimony in the Treatment of Leishmaniasis: Current Status and Future Directions. *Molec. Bio. Inter.* **2011**, *article ID 571242*, 1-23.
  - 32) Shaked-Mishan, P.; Ulrich, N.; Ephros, M.; Zilberstein, D. Novel Intracellular Sb<sup>V</sup> Reducing Activity Correlates with Antimony Susceptibility in *Leishmania donovani*. *J. Bio. Chem.* **2001**, *276(6)*, 3971-3976.
  - 33) Sereno, D.; Cavaleyra, M.; Zemzoumi, K.; Maquaire, S.; Ouaisi, A.; Lemesre, J.L. Axenically Grown Amastigotes of *Leishmania infantum* Used as an *in vitro* Model to Investigate the Pentavalent Antimony Mode of Action. *Antimicrob. Agents Chemother.* **1998**, *42*, 3097-3102.

- 34) Wyllie, S.; Fairlamb, A.H. Differential Toxicity of Antimonial Compounds and their Effects on Glutathione Homeostasis in a Human Leukaemia Monocyte Cell Line. *Biochem. Pharmacol.* **2006**, *71*, 257-267.
- 35) Baiocco, P.; Colotti, G.; Franceschini, S.; Ilari, A. Molecular Basis of Antimony Treatment in Leishmaniasis. *J. Med. Chem.* **2009**, *52*, 2603-2612.
- 36) Khan, M.O.F. Trypanothione Reductase: A Viable Chemotherapeutic Target for Antitrypanosomal and AntiLeishmanial Drug Design. *Drug Target Insights* **2007**, *2*, 129-146.
- 37) Wisner, M.F. *Protozoa and Human Disease*. 1<sup>st</sup> ed.; Garland Science, New York, **2011**, 1-218.
- 38) Demicheli, C.; Frezard, F.; Mangrum, J.B.; Farrell, N.P. Interaction of Trivalent Antimony with a CCHC Zinc Finger Domain: Potential Relevance to the Mechanism of Antimonial Drugs. *Chem. Commun.* **2008**, 4828-4830
- 39) Webb, J.R.; McMaster, W.R. Molecular Cloning and Expression of a *Leishmania* major Gene Encoding a Single-stranded DNA-binding Protein Containing Nine "CCHC" Zinc Finger Motifs. *J. Biol. Chem.* **1993**, *268*(19), 13994-14002.
- 40) Frezard, F.; Demicheli, C.; Ribeiro, R.R. Pentavalent Antimonials: New Perspectives for Old Drugs. *Molecules* **2009**, *14*, 2317-2336.
- 41) Chakraborty, A.K.; Majumder, H.K. Mode of Action of Pentavalent Antimonials: Specific Inhibition of Type I DNA Topoisomerase of *Leishmania donovani*. *Biochem. Biophys. Res. Commun.* **1988**, *152*(2), 605-611.
- 42) Vasudevan, G.; Carter, N.S.; Drew, M.E.; Beverley, S.M.; Sanchez, M.A.; Seyfang, A.; Ullman, B.; Landfear, S.M. Cloning of *Leishmania* Nucleoside Transporter Genes by Rescue of a Transport-deficient Mutant. *Proc. Natl. Acad. Sci. USA* **1998**, *95*, 9873-9878.
- 43) Kouni, M.H. Potential Chemotherapeutic Targets in the Purine Metabolism of Parasites. *Pharmacol. Therap.* **2003**, *99*, 283-309.
- 44) Boitz, J.M.; Ullman, B.; Jardim, A.; Carter, N.S. Purine Salvage in *Leishmania*: Complex or Simple by Design? *Trends in Parasitology* **2012**, *28*(8), 345-352.
- 45) Demicheli, C.; Frezard, F.; Lecouvey, M.; Garneir-Suillerot, A. Antimony (V) Complex Formation with Adenine Nucleosides in Aqueous Solution. *Biochimica et Biophysica Acta* **2002**, *1570*, 192-198.
- 46) Chai, Y.; Yan, S.; Wong, I.L.K.; Chow, L.M.C.; Sun, H. Complexation of Antimony (SbV) with Guanosine 5'-monophosphate and Guanosine 5'-diphospho-D-mannose: Formation of Both Mono- and Bis-adducts. *J. Inorg. Bio.* **2005**, *99*, 2257-2263.
- 47) Roberts, W.L.; McMurray, W.J.; Rainey, P.M. Characterization of the Antimonial AntiLeishmanial Agent Meglumine Antimonate (Glucantime). *Antimicrob. Agents Chemother.* **1998**, *42*(5), 1076-1082.
- 48) Dos Santos Ferreira, C.; de Castro Pimenta, A.M.; Demicheli, C.; Frezard, F. Characterization of Reactions of Antimoniate and Meglumine Antimoniate with a Guanine Ribonucleoside at Different pH. *BioMetals* **2006**, *19*, 573-581.
- 49) Alexander, J.; Russel, D.G. The Interaction of *Leishmania* Species with Macrophages. *Adv. Parasitol.* **1992**, *31*, 175-254.
- 50) Carter, N.S.; Drew, M.E.; Sanchez, M.; Vasudevan, G.; Landfear, S.M.; Ullman, B. Cloning of a Novel Inosine-Guanosine Transporter Gene from *Leishmania*

- donovani* by Functional Rescue of a Transport-deficient Mutant. *J. Biol. Chem.* **2000**, 275(27), 20935-20941.
- 51) Monzote, L. Current Treatment in Leishmaniasis: A Review. *Open Antimicrob. Agents J.* **2009**, 1, 9-19.
  - 52) Brajtburg, J.; Powderly, W.G.; Kobayashi, G.S.; Medoff, G. Amphotericin B: Current Understanding of Mechanisms of Action. *Antimicrob. Agents Chemother.* **1990**, 34(2), 183-188.
  - 53) Ramos, H.; Valdivieso, E.; Gamargo, M.; Dagger, F.; Cohen, B.E. Amphotericin B Kills Unicellular *Leishmanias* by Forming Aqueous Pores Permeable to Small Cations and Anions. *J. Membrane Biol.* **1996**, 152, 65-75.
  - 54) Pucadyil, T.J.; Tewary, P.; Madhubala, R.; Chattopadhyay, A. Cholesterol is Required for *Leishmania donovani* Infection: Implications in Leishmaniasis. *Molec. Biochem. Parasitol.* **2004**, 133, 145-152.
  - 55) Paila, Y.D.; Saha, B.; Chattopadhyay, A. Amphotericin B Inhibits Entry of *Leishmania donovani* into Primary Macrophages. *Biochem. Biophys. Res. Comm.* **2010**, 399, 429-433.
  - 56) Vercesi, A.E.; Docampo, R. Ca<sup>2+</sup> Transport by Digitonin-permeabilized *Leishmania donovani*. *Biochem. J.* **1992**, 284, 463-467.
  - 57) Basselin, M.; Denise, H.; Coombs, G.H.; Barrett, M.P. Resistance to Pentamidine in *Leishmania mexicana* Involves Exclusion of the Drug from the Mitochondrion. *Antimicrob. Agents Chemother.* **2002**, 46(12), 3731-3738.
  - 58) Paris, C.; Loiseau, P.M.; Bories, C.; Breard, J. Miltefosine Induces Apoptosis-Like Death in *Leishmania donovani* Promastigotes. *Antimicrob. Agents Chemother.* **2004**, 48(3), 852-859.
  - 59) Verma, N.K.; Dey, C.S. Possible Mechanism of Miltefosine-Mediated Death of *Leishmania donovani*. *Antimicrob. Agents Chemother.* **2004**, 48(8), 3010-3015.
  - 60) Moreira, M.E.C.; Del Portillo, H.A.; Milder, R.V.; Balanco, J.M.F.; Barcinski, M.A. Heat Shock Induction of Apoptosis in Promastigotes of the Unicellular Organism *Leishmania (Leishmania) amazonensis*. *J. Cell. Physiol.* **1996**, 167, 305-313.
  - 61) Elmore, S. Apoptosis: A Review of Programmed Cell Death. *Toxicol. Path.* **2007**, 35, 495-516.
  - 62) Wassef, M.K.; Fioretti, T.B.; Dwyer, D.M. Lipid Analyses of Isolated Surface Membranes of *Leishmania donovani* Promastigotes. *Lipids* **1985**, 20(2), 108-115.
  - 63) Rakotomanga, M.; Blanc, S.; Gaudin, K.; Chaminade, P.; Loiseau, P.M. Miltefosine Affects Lipid Metabolism in *Leishmania donovani* Promastigotes. *Antimicrob. Agents Chemother.* **2007**, 51(4), 1425-1430.
  - 64) <http://www.bioinfo.org.cn/book/biochemistry/chapt20/bio5.htm>
  - 65) Jimenez-Lopez, J.M.; Carrasco, M.P.; Segovia, J.L.; Marco, C. Hexadecylphosphocholine Inhibits Phosphatidylcholine Biosynthesis and the Proliferation of HepG2 Cells. *Eur. J. Biochem.* **2002**, 269, 4649-4655.
  - 66) Croft, S.L.; Seifert, K.; Duchene, M. Antiprotozoal Activities of Phospholipid Analogues. *Molec. Biochem. Parasitol.* **2003**, 126, 165-172.
  - 67) Furtado, V.C.S.; Takiya, C.M.; Braulio, V.B. Phosphatidylethanolamine N-Methyltransferase Activity is Increased in Rat Intestinal Brush-Border Membrane by Chronic Ethanol Ingestion. *Alcohol & Alcoholism* **2002**, 37(6), 561-565.

- 68) Myler, P.J.; Fasel, Nicholas. *Leishmania: After the Genome*; Caister Academic Press: Norfolk, U.K., 2008.
- 69) Wieder, T.; Orfanos, C.E.; Geilen, C.C. Induction of Ceramide-mediated Apoptosis by the Anticancer Phospholipid Analog, Hexadecylphosphocholine. *J. Biol. Chem.* **1998**, *273(18)*, 11025-11031.
- 70) Smith, T.K.; Sharma, D.K.; Crossman, A.; Dix, A.; Brimacombe, J.S.; Ferguson, M.A.J. Parasite and Mammalian GPI Biosynthetic Pathways Can Be Distinguished Using Synthetic Substrate Analogues. *EMBO J.* **1997**, *16(22)*, 6667-6675.
- 71) Dorlo, T.P.C.; Balasegaram, M.; Beijnen, J.H.; de Vries, P.J. Miltefosine: A Review of its Pharmacology and Therapeutic Efficacy in the Treatment of Leishmaniasis. *J. Antimicrob. Chemother.* **2012**, 1-22.
- 72) Ferguson, M.A.J. The Structure, Biosynthesis and Functions of Glycosylphosphatidylinositol Anchors, and the Contributions of Trypanosome Research. *J. Cell Sci.* **1999**, *112*, 2799-2809.
- 73) Rang, H.P.; Dale, M.M.; Ritter, J.M.; Flower, R.J. *Rang and Dale's Pharmacology*, 6<sup>th</sup> ed.; Churchill Livingstone Elsevier, Philadelphia, PA, **2007**, 1-829.
- 74) Fernandez, M.M.; Malchiodi, E.L.; Algranati, I.D. Differential Effects of Paromomycin on Ribosomes of *Leishmania Mexicana* and Mammalian Cells. *Antimicrob. Agents Chemother.* **2011**, *55(1)*, 86-93.
- 75) Carvalho, L.; Luque-Ortega, J.R.; Lopez-Martin, C.; Castanys, S.; Rivas, L.; Gamarro, F. The 8-Aminoquinoline Analogue Sitamaquine Causes Oxidative Stress in *Leishmania donovani* Promastigotes by Targeting Succinate Dehydrogenase. *Antimicrob. Agents Chemother.* **2011**, *55(9)*, 4204-4210.
- 76) Oyedotun, K.S.; Lemire, B.D. The Quaternary Structure of the *Saccharomyces cerevisiae* Succinate Dehydrogenase. *J. Biol. Chem.* **2004**, *279(10)*, 9424-9431.
- 77) Dong, L.F.; Jameson, V.J.A.; Tilly, D.; Cerny, J.; Mahdavian, E.; Marin-Hernandez, A.; Hernandez-Esquivel, L.; Rodriguez-Enriquez, S.; Stursa, J.; Witting, P.K.; Stantic, B.; Rohlena, J.; Truksa, J.; Kluckova, K.; Dyason, J.C.; Ledvina, M.; Salvatore, B.A.; Moreno-Sanchez, R.; Coster, M.J.; Ralph, S.J.; Smith, R.A.J.; Neuzil, J. Mitochondrial Targeting of Vitamin E Succinate Enhances its Pro-apoptotic and Anti-cancer Activity via Mitochondrial Complex II. *J. Biol. Chem.* **2011**, *286(5)*, 3717-3728.
- 78) Carvalho, L.; Luque-Ortega, J.R.; Manzano, J.I.; Castanys, S.; Rivas, L.; Gamarro, F. Tafenoquine, an Antiplasmodial 8-Aminoquinoline, Targets *Leishmania* Respiratory Complex III and Induces Apoptosis. *Antimicrob. Agents Chemother.* **2010**, *54(12)*, 5344-5351.
- 79) Davies, C.R.; Kaye, P.; Croft, S.L.; Sundar, S. Leishmaniasis: New Approaches to Disease Control. *BMJ* **2003**, *326*, 377-382.
- 80) Kedzierski, L. Leishmaniasis Vaccine: Where Are We Today? *J. Glob. Infect. Dis.* **2010**, *2(2)*, 177-185.
- 81) Hailu, A.; Musa, A.M.; Royce, C.; Wasunna, M. Visceral Leishmaniasis: New Health Tools Are Needed. *PLoS Med.* **2005**, *2(7)*, 590-594.
- 82) Tabbara, K.S.; Peters, N.C.; Afrin, F.; Mendez, S.; Bertholet, S.; Belkaid, Y.; Sacks, D.L. Conditions Influencing the Efficacy of Vaccination with Live



- Organisms Against *Leishmania* major Infection. *Infect. Immun.* **2005**, 73(8), 4714-4722.
- 83) Nagill, R.; Kaur, S. Vaccine Candidates for Leishmaniasis: A Review *Internat. Immunopharm.* **2011**, 11, 1464-1488.
  - 84) Titus, R.G.; Gueiros-Filho, F.J.; de Freitas, L.A.R.; Beverley, S.M. Development of a Safe Live *Leishmania* Vaccine Line by Gene Replacement. *Proc. Natl. Acad. Sci. USA* **1995**, 92, 10267-10271.
  - 85) Amaral, V.F.; Teva, A.; Oliveira-Neto, M.P.; Silva, A.J.; Pereira, M.S.; Cupolillo, E.; Porrozzi, R.; Coutinho, S.G.; Pirmez, C.; Beverley, S.M.; Grimaldi Jr, G. Study of the Safety, Immunogenicity and Efficacy of Attenuated and Killed *Leishmania (Leishmania) major* Vaccines in a Rhesus Monkey (*Mucaca mulatta*) Model of the Human Disease. *Mem. Inst. Oswaldo Cruz*, **2002**, 97(7), 1041-1048.
  - 86) Aebischer, T.; Moody, S.F.; Handman, E. Persistence of Virulent *Leishmania* major in Murine Cutaneous Leishmaniasis: a Possible Hazard for the Host. *Infect. Immun.* **1993**, 61(1), 220-226.
  - 87) Uzonna, J.E.; Wei, G.; Yurkowski, D.; Bretscher, P. Immune Elimination of *Leishmania* major in Mice: Implications for Immune Memory, Vaccination, and Reactivation Disease. *J. Immunol.* **2001**, 167, 6967-6974.
  - 88) Stenger, S.; Donhauser, N.; Thuring, H.; Rollinghoff, M.; Bogdan, C. Reactivation of Latent Leishmaniasis by Inhibition of Inducible Nitric Oxide Synthase. *J. Exp. Med.* **1996**, 183, 1501-1514.
  - 89) Kubar, J.; Marty, P.; Lelievre, A.; Quaranta, J.F.; Staccini, P.; Caroli-Bosc, C.; Le Fichoux, Y. Visceral Leishmaniasis in HIV-positive Patients: Primary Infection, Reactivation and Latent Infection. Impact of the CD4+ T-lymphocyte Counts. *AIDS* **1998**, 12, 2147-2153.
  - 90) Silvestre, R.; Cordeiro-da-Silva, A.; Ouaiissi, A. Live Attenuated *Leishmania* Vaccines: A Potential Strategic Alternative. *Arch. Immunol. Ther. Exp.* **2008**, 56, 123-126.
  - 91) Misra, A.; Dube, A.; Srivastava, B.; Sharma, P.; Srivastava, J.K.; Katiyar, J.C.; Naik, S. Successful Vaccination Against *Leishmania donovani* Infection in Indian Langur Using Alum-precipitated Autoclaved *Leishmania major* with BCG. *Vaccine* **2001**, 19, 3485-3492.
  - 92) Mohebbi, M.; Khamesipour, A.; Mobedi, I.; Zarei, Z.; Hashemi-Fesharki, R. Double-blind Randomized Efficacy Field Trial of Alum Precipitated Autoclaved *Leishmania* major Vaccine Mixed with BCG Against Canine Visceral Leishmaniasis in Meshkin-Shahr District, I.R. Iran. *Vaccine* **2004**, 22, 4097-4100.
  - 93) Noazin, S.; Modabber, F.; Khamesipour, A.; Smith, P.G.; Moulton, L.H.; Nasser, K.; Sharifi, I.; Khalil, E.A.G.; Bernal, I.D.V.; Antunes, C.M.F.; Kieny, M.P.; Tanner, M. First Generation Leishmaniasis Vaccines: A Review of Field Efficacy Trials. *Vaccine* **2008**, 26, 6759-6767.
  - 94) Coler, R.N.; Reed S.G. Second-generation Vaccines Against Leishmaniasis. *TRENDS in Parasitol.* **2005**, 21(5), 244-249.
  - 95) Yang, D.M.; Fairweather, N.; Button, L.L.; McMaster, W.R.; Kahl, L.P.; Liew, F.Y. Oral *Salmonella typhimurium* (AroA<sup>-</sup>) Vaccine Expressing a Major Leishmanial Surface Protein (gp63) Preferentially Induces T Helper 1 Cells and

- Protective Immunity Against Leishmaniasis. *J. Immunol.* **1990**, *145*(7), 2281-2285.
- 96) Rivier, D.; Bovay, P.; Shah, R.; Didisheim, S.; Mael, J. Vaccination Against *Leishmania* major in a CBA Mouse Model of Infection: Role of Adjuvants and Mechanism of Protection. *Parasite Immunol.* **1999**, *21*, 461-473.
- 97) Bhowmick, S.; Ravindran, R.; Ali, N. gp63 in Stable Cationic Liposomes Confers Sustained Vaccine Immunity to Susceptible BALB/c Mice Infected with *Leishmania donovani*. *Infect. Immun.* **2008**, *76*(3), 1003-1015.
- 98) Da Silva, V.O.; Borja-Cabrera, G.P.; Pontes, N.N.C.; de Souza, E.P.; Luz, K.G.; Palatnik, M.; de Sousa, C.B.P. A Phase III Trial of Efficacy of the FML-vaccine Against Canine Kala-azar in an Endemic Area of Brazil (Sao Goncalo do Amaranto, RN). *Vaccine* **2001**, *19*, 1082-1092.
- 99) Borja-Cabrera, G.P.; Correia Pontes, N.N.; da Silva, V.O.; de Souza, E.P.; Santos, W.R.; Gomes, E.M.; Luz, K.G.; Palatnik, M.; Palatnik de Sousa, C.B. Long Lasting Protection Against Canine Kala-azar Using the FML-QuilA Saponin Vaccine in an Endemic Area of Brazil (Sao Goncalo do Amarante, RN). *Vaccine* **2002**, *20*, 3277-3284.
- 100) Lemesre, J.L.; Holzmuller, P.; Goncalves, R.B.; Bourdoiseau, G.; Hugnet, C.; Cavaleyra, M.; Papierok, G. Long-lasting Protection Against Canine Visceral Leishmaniasis Using the LiESAp-MDP Vaccine in Endemic Areas of France: Double-blind Randomised Efficacy Field Trial. *Vaccine* **2007**, *25*, 4223-4234.
- 101) Skeiky, Y.A.W.; Kennedy, M.; Kaufman, D.; Borges, M.M.; Guderian, J.A.; Scholler, J.K.; Ovendale, P.J.; Picha, K.S.; Morrissey, P.J.; Grabstein, K.H.; Campos-Neto, A.; Reed, S.G. LeIF: A Recombinant *Leishmania* Protein That Induces an IL-12-Mediated Th1 Cytokine Profile. *J. Immunol.* **1998**, *161*, 6171-6179.
- 102) Webb, J.R.; Campos-Neto, A.; Ovendale, P.J.; Martin, T.I.; Stromberg, E.J.; Badaro, R.; Reed, S.G. Human and Murine Immune Responses to a Novel *Leishmania* major Recombinant Protein Encoded by Members of a Multicopy Gene Family. *Infect. Immun.* **1998**, *66*(7), 3279-3289.
- 103) Webb, J.R.; Kaufmann, D.; Campos-Neto, A.; Reed, S.G. Molecular Cloning of a Novel Protein Antigen of *Leishmania* major that Elicits a Potent Immune Response in Experimental Murine Leishmaniasis. *J. Immunol.* **1996**, *157*, 5034-5041.
- 104) Skeiky, Y.A.W.; Coler, R.N.; Brannon, M.; Stromberg, E.; Greeson, K.; Crane, R.T.; Campos-Neto, A.; Reed, S.G. Protective Efficacy of a Tandemly Linked, Multi-subunit Recombinant Leishmanial Vaccine (Leish-111f) Formulated in MPL Adjuvant. *Vaccine* **2002**, *20*, 3292-3303.
- 105) Gradoni, L.; Manzillo, V.F.; Pagano, A.; Piantedosi, D.; De Luna, R.; Gramiccia, M.; Scalone, A.; Di Muccio, T.; Oliva, G. Failure of a Multi-subunit Recombinant Leishmanial Vaccine (MML) to Protect Dogs from *Leishmania infantum* Infection and to Prevent Disease Progression in Infected Animals. *Vaccine* **2005**, *23*, 5245-5251.
- 106) Bertholet, S.; Goto, Y.; Carter, L.; Bhatia, A.; Howard, R.F.; Carter, D.; Coler, R.N.; Vedvick, T.S.; Reed, S.G. Optimized Subunit Vaccine Protects Against Experimental Leishmaniasis. *Vaccine* **2009**, *27*, 7036-7045.

- 107) Miret, J.; Nascimento, E.; Sampaio, W.; Franca, J.C.; Fujiwara, R.T.; Vale, A.; Dias, E.S.; Vieira, E.; da Costa, R.T.; Mayrink, W.; Campos-Neto, A.; Reed, S. Evaluation of an Immunochemotherapeutic Protocol Constituted of N-methyl Meglumine Antimoniate (Glucantime) and the Recombinant Leish-110f + MPL-SE Vaccine to Treat Canine Visceral Leishmaniasis. *Vaccine* **2008**, *26*, 1585-1594.
- 108) Ghalib, H.; Modabber, F. Consultation Meeting on the Development of Therapeutic Vaccines for Post Kala Azar Dermal Leishmaniasis. *Kinetoplastid Biology and Disease* **2007**, *6:7*, 1-14.
- 109) Liu, M.A.; Wahren, B.; Karlsson Hedestam, G.B. DNA Vaccines: Recent Developments and Future Possibilities. *Human Gene Ther.* **2006**, *17*, 1051-1061.
- 110) Xu, D.; Liew, F.Y. Protection Against Leishmaniasis by Injection of DNA Encoding a Major Surface Glycoprotein, gp63, of *L. major*. *Immunology* **1995**, *84*, 173-176.
- 111) Sukumaran, B.; Tewary, P.; Saxena, S.; Madhubala, R. Vaccination with DNA Encoding ORFF Antigen Confers Protective Immunity in Mice Infected with *Leishmania donovani*. *Vaccine* **2003**, *21*, 1292-1299.
- 112) Ramiro, M.J.; Zarate, J.J.; Hanke, T.; Rodriguez, D.; Rodriguez, J.R.; Esteban, M.; Lucientes, J.; Castillo, J.A.; Larraga, V. Protection in Dogs Against Visceral Leishmaniasis caused by *Leishmania infantum* is Achieved by Immunization with a Heterologous Prime-Boost Regime using DNA and Vaccinia Recombinant Vectors Expressing LACK. *Vaccine* **2003**, *21*, 2474-2484.
- 113) De Oliveira Gomes, D.C.; Pinto, E.F.; de Melo, L.D.B.; Lima, W.P.; Larraga, V.; Lopes, U.G.; Rossi-Bergmann, B. Intranasal Delivery of Naked DNA Encoding the LACK Antigen Leads to Protective Immunity Against Visceral Leishmaniasis in Mice. *Vaccine* **2007**, *25*, 2168-2172.
- 114) Tapia, E.; Perez-Jimenez, E.; Lopez-Fuertes, L.; Gonzalo, R.; Gherardi, M.M.; Esteban, M. The Combination of DNA Vectors Expressing IL-12 + IL-18 Elicits High Protective Immune Response Against Cutaneous Leishmaniasis After Priming with DNA-p36/LACK and the Cytokines, Followed by a Booster with a Vaccinia Virus Recombinant Expressing p36/LACK. *Microbes and Infection* **2003**, *5*, 73-84.
- 115) Rafati, S.; Zahedifard, F.; Nazgouee, F. Prime-boost Vaccination Using Cysteine Proteinases Type I and II of *Leishmania infantum* Confers Protective Immunity in Murine Visceral Leishmaniasis. *Vaccine* **2006**, *24*, 2169-2175.
- 116) Claborn, D.M. The Biology and Control of Leishmaniasis Vectors. *J. Glob. Infect. Dis.* **2010**, *2(2)*, 127-134.
- 117) Coleman, R.E.; Burkett, D.A.; Sherwood, V.; Caci, J.; Hockberg, L.; Weina, P.A. Prevention and Control of Leishmaniasis During Operation Iraqi Freedom. *Wing Beats* **2004**, *Winter*, 10-16.
- 118) Ritmeijer, K.; Davies, C.; van Zorge, R.; Wang, S.; Schorscher, J.; Dongu'du S.I.; Davidson, R.N. Evaluation of a Mass Distribution Programme for Fine-Mesh Impregnated Bednets Against Visceral Leishmaniasis in Eastern Sudan. *Trop. Med. Internat. Health* **2007**, *12(3)*, 404-414.
- 119) Ashford, R.W. Leishmaniasis Reservoirs and Their Significance in Control. *Clinics in Dermatology* **1996**, *14*, 523-532.

- 120) Diniz, S.A.; Silva, F.L.; Neta, A.V.C.; Bueno, R.; Guerra, R.M.S.N.C.; Abreu-Silva, A.L.; Santos, R.L. Animal Reservoirs for Visceral Leishmaniasis in Densely Populated Urban Areas. *J. Infect. Developing Countries* **2008**, *2*(1), 24-33.
- 121) Ashford, D.A.; David, J.R.; Freire, M.; David, R.; Sherlock, I.; Da Conceicao Eulalio, M.; Sampaio, D.P.; Badaro, R. Studies on Control of Visceral Leishmaniasis: Impact of Dog Control on Canine and Human Visceral Leishmaniasis in Jacobina, Bahia, Brazil. *Am. J. Trop. Med. Hyg.* **1998**, *59*(1), 53-57.
- 122) Reithinger, R.; Coleman, P.G.; Alexander, B.; Vieira, E.P.; Assis, G.; Davies, C.R. Are Insecticide-Impregnated Dog Collars a Feasible Alternative to Dog Culling as a Strategy for Controlling Canine Visceral Leishmaniasis in Brazil? *Internat. J. Parasitol.* **2004**, *34*, 55-62.
- 123) <https://www.msu.edu/course/zol/316/lspscope.htm>
- 124) Senn, M.; Gunzenhauser, S.; Brun, R.; Sequin, U. Antiprotozoal Polyacetylenes from the Tanzanian Medicinal Plant *Cussonia zimmermannii*. *J. Nat. Prod.* **2007**, *70* (10), 1565-1569.
- 125) Chodkiewicz, W. *W. Ann. Chim.* **1957**, *2*, 819-869.
- 126) Burgess, K.; Jennings, L. D. Enantioselective Esterifications of Unsaturated Alcohols Mediated by a Lipase Prepared from *Pseudomonas* sp. *J. Am. Chem. Soc.* **1991**, *113* (16), 6129-6139.
- 127) Ratnayake, A. S.; Hemscheidt, T. *J. Am. Chem. Soc.* **2002**, *4* (26), 4667-4669.
- 128) Dale, J. A.; Dull, D. L.; Mosher, H. S. *J. Org. Chem.* **1969**, *34* (9), 2543-2549.
- 129) Malkov, A. V.; Gordon, M. R.; Stoncius, S.; Hussain, J.; Kocovsky, P. *Org. Lett.* **2009**, *11* (23), 5390-5393.
- 130) Yun, H.; Danishefsky, S. J. *J. Org. Chem.* **2003**, *68* (11), 4519-4522.
- 131) Kim, S.; Lee, Y. M.; Kang, H. R.; Cho, J.; Lee, T.; Kim, D. *Org. Lett.* **2007**, *9* (11), 2127-2130.
- 132) Maraval, V.; Duhayon, C.; Coppel, Y.; Chauvin, R. *Eur. J. Org. Chem.* **2008**, *30*, 5144-5156.
- 133) Cho, E. J.; Kim, M.; Lee, D. *Org. Lett.* **2006**, *8* (23), 5413-5416.
- 134) Trost, B. M.; Chan, V. S.; Yamamoto, D. *J. Am. Chem. Soc.* **2010**, *132*, 5186-5192.
- 135) Hansch, C.; Unger, S. H.; Forsythe, A. B. *J. Med. Chem.* **1973**, *16* (11), 1217-1222.
- 136) Silverman, R. B. *The Organic Chemistry of Drug Design and Action*, 2nd ed.; Elsevier Academic Press: Burlington, 2004.
- 137) Mitsunobu, O.; Yamada, Y. *Bull. Chem. Soc. Japan* **1967**, *40*, 2380-2382.
- 138) Temperini, A.; Tiecco, M.; Testaferri, L.; Terlizzi, R. *Lett. Org. Chem.* **2009**, *6*, 22-24.
- 139) Padwa, A.; Dean, D. C.; Fairfax, D. J.; Xu, S. L. *J. Org. Chem.* **1993**, *58*, 4646-4655.

- 140) Neabo, J. R.; Tohoundjona, K. I. S.; Morin, J. F. *Org. Lett.* **2011**, *13* (6), 1358-1361.
- 141) Metaferia, B. B.; Fetterolf, B. J.; Shazad-ul-Hussan, S.; Moravec, M.; Smith, J. A.; Ray, S.; Gutierrez-Lugo, M. T.; Bewley, C. A. *J. Med. Chem.* **2007**, *50* (25), 6326-6336.
- 142) Mordant, C.; Dunkelmann, P.; Ratovelomanana-Vidal, V.; Genet, J. P. *Eur. J. Org. Chem.* **2004**, *14*, 3017-3026.
- 143) Verardo, G.; Geatti, P.; Pol, E.; Giumanini, A. G. *Can. J. Chem.* **2002**, *80* (7), 779-788.
- 144) Dohme, A. R. L.; Cox, E. H.; Miller, E. The Preparation of the Acyl and Alkyl Derivatives of Resorcinol. *J. Am. Chem. Soc.* **1926**, *48*, 1688-1693.
- 145) Topliss, J. G. A Manual Method for Applying the Hansch Approach to Drug Design. *J. Med. Chem.* **1977**, *20* (4), 463-469.
- 146) Richard, J. V.; Werbovetz, K. A. New AntiLeishmanial Candidates and Lead Compounds. *Curr. Opin. Chem. Biol.* **2010**, *14* (4), 447-455.
- 147) Kapou, A.; Benetis, N. P.; Avlonitis, N.; Calogeropoulou, T.; Koufaki, M.; Scoulica, E.; Nikolaropoulos, S. S.; Mavromoustakos, T. 3D-Quantitative Structure-Activity Relationships of Synthetic AntiLeishmanial Ring-Substituted Ether Phospholipids. *Bioorg. Med. Chem.* **2007**, *15*, 1252-1265.
- 148) Calogeropoulou, T.; Angelou, P.; Detsi, A.; Fragiadaki, I.; Scoulica, E. Design and Synthesis of Potent AntiLeishmanial Cycloalkyldiene-Substituted Ether Phospholipid Derivatives. *J. Med. Chem.* **2008**, *51*, 897-908.
- 149) Cruz, L. J.; Luque-Ortega, J. R.; Rivas, L.; Albericio, F. Kahalalide F, an Antitumor Depsipeptide in Clinical Trials, and Its Analogues as Effective AntiLeishmanial Agents. *Molecular Pharmaceutics* **2009**, *6* (3), 813-824.
- 150) Slade, D.; Galal, A. M.; Gul, W.; Radwan, M. M.; Ahmed, S. A.; Khan, S. I.; Tekwani, B. L.; Jacob, M. R.; Ross, S. A.; and ElSohly, M. A. Antiprotozoal, anticancer, and antimicrobial activities of dihydroartemisinin acetal dimers and monomers. *Bioorg. Med. Chem.* **2009**, *17*, 7949-7957.
- 151) Denny, W. A. Acridine Derivatives as Chemotherapeutic Agents. *Current Medicinal Chemistry* **2002**, *9* (18), 1655-1665.
- 152) Andrzejewska, M.; Yopez-Mulia, L.; Cedillo-Rivera, R.; Tapia, A.; Vilpo, L.; Vilpo, J.; Kazimierczuk, Z. Synthesis, antiprotozoal and anticancer activity of substituted 2-trifluoromethyl- and 2-pentafluoroethylbenzimidazoles. *Eur. J. Med. Chem.* **2002**, *37*, 973-978.
- 153) Riaz, M.; van Jaarsveld, M. T. M.; Hollestelle, A.; Prager-van der Smissen, W. J. C.; Heine, A. A. J.; Boersma, A. W. M.; Liu, J.; Helmijr, J.; Ozturk, B.; Smid, M.; Wiemer, E. A.; Foekens, J. A.; Martens, J. W. M. miRNA expression profiling of 51 human breast cancer cell lines reveals subtype and driver mutation-specific miRNAs. *Breast Cancer Research* **2013**, *15* (R33), 1-17.
- 154) American Type Culture Collection. [www.atcc.org](http://www.atcc.org) (accessed July 29, 2013)
- 155) Cell Biolabs, Inc. <http://www.cellbiolabs.com/> (accessed August 5, 2013)

- 156) Center for Cancer Research, National Cancer Institute.  
<http://strap.nci.nih.gov/main.php> (accessed August 6, 2013).
- 157) EZ Biosystems. <http://ezbiosystems.com/> (accessed April 7, 2014)
- 158) Carroll, A.G.; Voeller, H.J.; Sugars, L.; Gelmann, E.P. p53 Oncogene Mutations in Three Human Prostate Cancer Cell Lines. *Prostate* 1993, 23(2), 123-134.
- 159) Kaighn, M.E.; Narayan, K.S.; Ohnuki, Y.; Lechner, J.F.; Jones, L.W. Establishment and Characterization of a Human Prostatic Carcinoma Cell Line (PC-3). *Invest. Urol.* 1979, 17(1), 16-23.
- 160) Stone, K.R., Mickey, D.D.; Wunderli, H., Mickey, G.H.; Paulson, D.F. Isolation of a Human Prostate Carcinoma Cell Line (DU 145). *Int. J. Cancer* 1978, 21(3), 274-281.
- 161) Isaacs, W.B.; Carter, B.S.; Ewing, C.M. Wild-Type p53 Suppresses Growth of Human Prostate Cancer Cells Containing Mutant p53 Alleles. *Cancer Res.*, 1991, 51, 4716-4720.
- 162) Russell, P.J.; Kingsley, E.A. Human Prostate Cancer Cell Lines. In *Prostate Cancer Methods and Protocols*; Russell, P.J.; Jackson, P.; Kingsley, E.A., Ed.; Humana Press: New York, 2003; 21-39.
- 163) Sanlioglu, A.D.; Koksall, I.T.; Karacay, B.; Baykara, M., Luleci, G.; Sanlioglu, S. Adenovirus-Mediated IKK $\beta$ KA Expression Sensitizes Prostate Carcinoma Cells to TRAIL-Induced Apoptosis. *Cancer Gene Therapy* 2006, 13, 21-31.
- 164) Hartung, F.; Stuhmer, W.; Pardo, L.A. Tumor Cell-Selective Apoptosis Induction through Targeting of Kv10.1 via Bifunctional TRAIL Antibody. *Molecular Cancer* 2011, 10:109, 1-15.
- 165) TRAIL. <http://en.wikipedia.org/wiki/TRAIL> (accessed on July 29, 2013)
- 166) Ikediobi, O.N.; Davies, H.; Bignell, G.; Edkins, S.; Stevens, C.; O'Meara, S.; Santarius, T.; Avis, T.; Barthorpe, S.; Brackenberry, L.; Buck, G.; Butler, A.; Clements, J.; Cole, J.; Dicks, E.; Forbes, S.; Gray, K.; Halliday, K.; Harrison, R.; Hills, K.; Hinton, J.; Hunter, C.; Jenkinson, A.; Jones, D.; Kosmidou, V.; Lugg, R.; Menzies, A.; Mironenko, T.; Parker, A.; Perry, J.; Raine, K.; Richardson, D.; Shepherd, R.; Small, A.; Smith, R.; Solomon, H.; Stephens, P.; Teague, J.; Tofts, C.; Varian, J.; Webb, T.; West, S.; Widaa, S.; Yates, A.; Reinhold, W.; Weinstein, J.N.; Stratton, M.R.; Futreal, P.A.; Wooster, R. Mutation Analysis of 24 Known Cancer Genes in the NCI-60 Cell Line Set. *Mol. Cancer Ther.* 2006, 5, 2606-2612.
- 167) O'Connor, P.M.; Jackman, J.; Bae, I.; Myers, T.G.; Fan, S.; Mutoh, M.; Scudiero, D.A.; Monks, A.; Sausville, E.A.; Weinstein, J.; Friend, S.; Fornace Jr., A.J.; Kohn, K.W. Characterization of the p53 Tumor Suppressor Pathway in Cell Lines of the National Cancer Institute Anticancer Drug Screen and Correlations with the Growth-Inhibitory Potency of 123 Anticancer Agents. *Cancer Research* 1997, 57, 4285-4300.
- 168) Stinson, S.F.; Alley, M.C.; Kopp, W.C.; Fiebig, H.H.; Mullendore, L.A.; Pittman, A.F.; Kenney, S.; Keller, J.; Boyd, M.R. Morphological and Immunocytochemical Characteristics of Human Tumor Cell Lines for Use in a Disease-Oriented Anticancer Drug Screen. *Anticancer Res.* 1992, 12(4), 1035-1053.

- 169) Sokilde, R.; Kaczkowski, B.; Podolska, A.; Cirera, S.; Gorodkin, J.; Moller, S.; Litman, T. Global microRNA Analysis of the NCI-60 Cancer Cell Panel. *Mol. Cancer Ther.* 2011, 10(3), 375-384.
- 170) Liscovitch, M.; Ravid, D. A Case Study in Misidentification of Cancer Cell Lines: MCF-7/AdrR cells (re-designated NCI/ADR-RES) are Derived from OVCAR-8 Human Ovarian Carcinoma Cells. *Cancer Lett.* 2007, 245(1-2), 350-352.
- 171) Xu, X.; Veenstra, T.D. Concentration of Endogenous Estrogens and Estrogen Metabolites in the NCI-60 Human Tumor Cell Lines. *Genome Medicine* 2012, 4(31), 1-11.
- 172) Domcke, S.; Sinha, R.; Levine, D.A.; Sander, C.; Schultz, N. Evaluating Cell Lines as Tumour Models by Comparison of Genomic Profiles. *Nature Communications*, 2013, 4:2126, 1-10.
- 173) Vaughan, S.; Coward, J.I.; Bast Jr., R.C.; Berchuck, A.; Berek, J.S.; Brenton, J.D.; Coukos, G.; Crum, C.C.; Drapkin, R.; Etemadmoghadam, D.; Friedlander, M.; Gabra, H.; Kaye, S.B.; Lord, C.J.; Lengyel, E.; Levine, D.A.; McNeish, I.A.; Menon, U.; Mills, G.B.; Nephew, K.P.; Oza, A.M.; Sook, A.K.; Stronach, E.A.; Walczak, H.; Bowtell, D.D.; Balkwill, F.R. Rethinking Ovarian Cancer: Recommendations for Improving Outcomes. *Nat. Rev. Cancer* 2011, 11(10), 719-725.
- 174) Wu, L.; Smythe, A.M.; Stinson, S.F.; Mullendore, L.A.; Monks, A.; Scudiero, D.A.; Paull, K.D.; Koutsoukos, A.D.; Rubinstein, L.V.; Boyd, M.R.; Shoemaker, R.H. Multidrug-resistant Phenotype of Disease-oriented Panels of Human Tumor Cell Lines Used for Anticancer Drug Screening. *Cancer Res.* 1992, 52, 3029-30.

